



CANCERRESEARCHWALES
YMCHWILCANSERCYMRU



The Role of RUNX3 in Acute Myeloid Leukaemia and Normal Human Haematopoietic Development

Doctor of Philosophy in Medicine

2020

Ana Catarina Menezes

Acknowledgments

I would like to express my deepest gratitude to my supervisors Prof Alex Tonks and Prof Richard Darley for their guidance and support throughout my PhD studies. Your valuable knowledge, stimulating discussions, immense patience and continuous encouragement helped me to grow as a scientist and as a person, providing me with important tools for the future. I would like to acknowledge my mentor Dr Steven Knapper and express my thanks for your precious support in the clinical aspects of my project.

A considerable part of this study could not have been possible without the technical support provided by Dr Catherine Naseriyan and Dr Ann Kift-Morgan from Central Biotechnology Services (CBS) at Cardiff University. I appreciate everything you did for me, including your guidance and patience. I will miss our talks (almost) every Friday.

I would also like to thank the colleagues within the Department of Haematology that accompanied and assisted me during the course of this study, including Dr Mandy Gilkes, Rachael Nicholson, Sara Davies, Dr Namrata Rastogi and Dr Paul Hole.

Special thanks to Prof Alan Parker and Prof Rachel Errington for your precious support and feedback that drove me in the right direction.

A huge thanks to my Fiancé Dan for always being by my side during this process and incredible patience for listening to my endless updates about RUNX3. To all my family and friends, thank you for your constant support and for encouraging me to always pursue my dreams.

This study would not have been possible without the generosity of Cancer Research Wales funding. My sincerest thanks to everyone involved in helping raising awareness and funds to ultimately beat cancer.

Abstract

The t(8;21)(q22;q22) is a common abnormality in acute myeloid leukaemia (AML). This translocation encodes the RUNX1-ETO fusion protein which blocks the differentiation of human CD34⁺ haematopoietic stem and progenitor cells (HSPC) and promotes their self-renewal, hallmarks of AML. Transcriptional repression of RUNX3 by RUNX1-ETO has been identified in t(8;21) AML but is strongly expressed in AML without core binding factor abnormalities. This study examines RUNX3 expression during normal and malignant human haematopoiesis and the consequences of increased and reduced RUNX3 expression for erythroid and myeloid cell development.

Analysis of transcriptomic data showed that *RUNX3* mRNA expression is downregulated during normal haematopoietic development. In AML, variable *RUNX3* expression across different subtypes was observed, with core binding factor AML being associated with *RUNX3* downregulation whilst AML patients with complex cytogenetics overexpressed *RUNX3* compared to normal karyotype. The impact of altering RUNX3 expression on haematopoiesis was determined by transducing human HSPC with RUNX3 overexpression or shRNA knockdown vectors. RUNX3 overexpression inhibited both erythroid and myeloid growth and differentiation. Colony forming ability was also reduced but accompanied by increased self-renewal of progenitors. Reduced RUNX3 expression negatively impacted the survival of erythroid cells but did not cause significant effects in erythropoiesis and myelopoiesis. Attempts were also made to show whether RUNX3 could rescue the suppression of haematopoietic development seen in RUNX1-ETO-expressing cells. Further RNA-sequencing analysis showed that RUNX3 overexpression dysregulates the HSPC transcriptome, characterised by the repression of important erythroid-related genes, including *KIT* and *LMO2*. Differentiation markers *GYP A*, *CD36* and *ITGAM* were also downregulated by RUNX3, validating the RUNX3-induced phenotypic changes during erythroid and myeloid development. In addition, cross-regulation among RUNX proteins was observed, as RUNX3 overexpression downregulated *RUNX1* and *RUNX2* levels in HSPC.

In conclusion, this study shows that downregulation of RUNX3 expression is important for normal human erythroid and myeloid development. The ability of RUNX3 overexpression to inhibit differentiation suggest that RUNX3 could be a driver of leukaemogenesis.

Table of Contents

1	Introduction	1
1.1	Normal human haematopoiesis.....	1
1.1.1	<i>Haematopoietic stem cells</i>	2
1.1.2	<i>Hierarchical organisation of haematopoiesis</i>	6
1.1.3	<i>Haematopoietic cytokine network</i>	9
1.1.4	<i>Transcription regulation of haematopoietic development</i>	10
1.2	Acute Myeloid Leukaemia	15
1.2.1	<i>Molecular pathogenesis and classification system of AML</i>	16
1.2.2	<i>Epidemiology, diagnosis, and prognosis of AML</i>	20
1.2.3	<i>Treatment for AML</i>	23
1.2.4	<i>The 8;21 translocation in AML</i>	25
1.3	RUNX family of transcription factors.....	32
1.3.1	<i>RUNX structure and functions</i>	33
1.3.2	<i>Transcriptional regulation by RUNX proteins</i>	36
1.3.3	<i>Interplay of RUNX transcription factors</i>	40
1.3.4	<i>RUNX transcription factors in normal haematopoiesis</i>	41
1.3.5	<i>Role of RUNX in AML</i>	44
1.4	RUNX3	47
1.4.1	<i>Role of RUNX3 in the haematopoietic system</i>	48
1.4.2	<i>Multifunctionality of RUNX3 in carcinogenesis</i>	49
1.5	Aims and objectives	56
2	Materials and Methods.....	58
2.1	Materials.....	58
2.1.1	<i>General reagents</i>	58
2.1.2	<i>Antibodies</i>	61
2.2	Recombinant DNA techniques	62
2.2.1	<i>Source and structure of plasmids</i>	62
2.2.2	<i>Subcloning of RUNX3 cDNA into the PINCO DsRed vector</i>	62
2.2.3	<i>Transformation of competent E. coli with plasmid DNA</i>	65
2.2.4	<i>Preparation and thawing of glycerol stocks</i>	65
2.2.5	<i>Extraction and quantitation of amplified plasmid DNA</i>	65
2.2.6	<i>Restriction enzyme digestion and DNA sequencing</i>	66
2.3	Cell culture	67

2.3.1	<i>Source of primary material and cell lines</i>	67
2.3.2	<i>Culture of primary cells and cell lines</i>	67
2.3.3	<i>Cell counting using a haemocytometer</i>	69
2.3.4	<i>Cryopreservation and thawing of cells</i>	69
2.3.5	<i>Colony assay</i>	70
2.3.6	<i>Assessment of cell morphology</i>	70
2.4	<i>Isolation of human CD34⁺ haematopoietic stem and progenitor cells</i>	71
2.4.1	<i>Isolation of mononuclear cells from cord blood by density gradient centrifugation</i>	71
2.4.2	<i>Isolation of human haematopoietic stem and progenitor cells from mononuclear cells</i>	71
2.5	<i>Transduction of cell lines and primary cells</i>	72
2.5.1	<i>Generation of recombinant virus by cationic lipid transfection</i>	72
2.5.2	<i>Generation of recombinant virus by calcium phosphate transfection</i>	73
2.5.3	<i>Viral infection of cells</i>	73
2.5.4	<i>Selection of infected cells</i>	75
2.6	<i>Flow cytometry</i>	75
2.6.1	<i>Assessment of cell proliferation</i>	75
2.6.2	<i>Estimation of CD34⁺ cells in human cord blood</i>	76
2.6.3	<i>Fluorescence activated cell sorting of live cells</i>	76
2.6.4	<i>Immunophenotyping and differentiation analysis</i>	76
2.6.5	<i>Migration assay</i>	78
2.7	<i>Western blotting</i>	79
2.7.1	<i>Generation of protein extracts from whole cells</i>	79
2.7.2	<i>Generation of fractionated cytosolic and nuclear extracts</i>	79
2.7.3	<i>Protein quantitation using Bradford assay</i>	80
2.7.4	<i>Protein electrophoresis and electroblotting</i>	80
2.7.5	<i>Chemiluminescence detection of proteins</i>	81
2.8	<i>Transcriptome analysis</i>	82
2.8.1	<i>Total RNA extraction</i>	82
2.8.2	<i>Quantitative reverse-transcription polymerase chain reaction</i>	83
2.8.3	<i>RNA-sequencing</i>	84
2.9	<i>Data and statistical analysis</i>	88
2.9.1	<i>Publicly available databases and datasets</i>	88
2.9.2	<i>RNA-sequencing data analysis</i>	89
3	RUNX3 Supresses Normal Erythroid Development of Human CD34⁺ HSPC92	

3.1	Introduction	92
3.2	Aims and objectives	93
3.3	Results	94
	3.3.1 <i>Expression of RUNX3 declines during human terminal erythroid development</i>	94
	3.3.2 <i>Overexpression of RUNX3 supresses human erythroid development</i>	96
	3.3.3 <i>Knockdown of RUNX3 does not impair human erythroid development</i>	115
3.4	Discussion and conclusion	128
	3.4.1 <i>RUNX3 overexpression in human HSPC inhibits their normal erythroid development</i>	129
	3.4.2 <i>Knockdown of RUNX3 in HSPC does not affect their normal erythroid development</i>	131
4	RUNX3 Inhibits Normal Myeloid Development of Human CD34⁺ HSPC ...	134
4.1	Introduction	134
4.2	Aims and objectives	135
4.3	Results	136
	4.3.1 <i>Expression of RUNX3 mRNA decreases during early human myeloid development and increases towards terminal monocytic differentiation</i>	136
	4.3.2 <i>RUNX3 is variably expressed across AML and its expression is associated with poorer overall survival of patients</i>	138
	4.3.3 <i>Overexpression of RUNX3 inhibits human myeloid development</i>	140
	4.3.4 <i>Knockdown of RUNX3 does not affect myeloid growth and development</i>	150
	4.3.5 <i>RUNX3 overexpression failed to rescue the phenotype of RUNX1-ETO-expressing HSPC</i>	160
4.4	Discussion and conclusion	174
	4.4.1 <i>Increased RUNX3 expression is associated with poor outcome of AML patients</i>	175
	4.4.2 <i>RUNX3 overexpression in HSPC inhibits their myeloid growth and development</i>	176
	4.4.3 <i>Knockdown of RUNX3 does not impact the myeloid development of HSPC</i>	179
	4.4.4 <i>RUNX3 overexpression does not rescue the phenotype of RUNX1-ETO-expressing HSPC during myeloid development</i>	180
5	RUNX3 Overexpression Dysregulates the Human Haematopoietic Progenitor Cells Transcriptome	182
5.1	Introduction	182
5.2	Aims and objectives	183
5.3	Results	184

5.3.1	<i>Generation of HSPC overexpressing RUNX3 for RNA-seq analysis</i>	184
5.3.2	<i>QC analysis of RNA-seq data and quantification of gene expression</i>	188
5.3.3	<i>DE analysis determines the transcriptional dysregulation imposed by RUNX3 overexpression in human HSPC</i>	192
5.3.4	<i>RUNX3 overexpression downregulates key haematopoietic genes in human HSPC</i>	204
5.3.5	<i>Identification of upstream regulators associated with the transcriptional changes mediated by RUNX3 in HSPC</i>	210
5.3.6	<i>RUNX3 has an essential regulatory function in cellular processes</i>	212
5.3.7	<i>Expression of RUNX3 in AML patients is significantly correlated with the expression of dysregulated genes identified in this study</i>	219
5.4	Discussion and conclusion	219
5.4.1	<i>RUNX3 overexpression imposes a significant transcriptional dysregulation in human HSPC</i>	222
5.4.2	<i>RUNX3-mediated dysregulation of HSPC and erythroid-related transcriptional profiles</i>	225
5.4.3	<i>Potential master regulators cooperating with RUNX3 to induce transcriptional dysregulation in haematopoietic cells</i>	229
5.4.4	<i>Comparison analysis between RUNX3 and RUNX1-ETO-induced dysregulation of HSPC transcriptome</i>	230
6	Conclusion and Future Directions	232
6.1	Future directions	237
	Appendix	240
	References	243

Summary of Figures

Figure 1-1 – Hierarchical representation of human haematopoietic development in the BM.....	7
Figure 1-2 – Transcriptional regulation of myeloid development.	11
Figure 1-3 – Mechanisms of transcriptional regulation by RUNX1-ETO.....	26
Figure 1-4 – Structural representation of the three mammalian RUNX genes and proteins.....	34
Figure 1-5 – Relationship between RUNX proteins and important signalling pathways and cellular processes.....	46
Figure 1-6 – Tumour suppressor activity of RUNX3.	52
Figure 2-1 – Plasmid DNA structures used in this study.....	63
Figure 2-2 – Sample preparation prior to Illumina RNA sequencing.....	85
Figure 2-3 – Analysis workflow for RNA-sequencing data of transcriptional changes associated with high expression of <i>RUNX3</i> in HSPC.	87
Figure 2-4 – Strategy employed for DE gene analysis to study the effects of <i>RUNX3</i> overexpression in human HSPC.	91
Figure 3-1 – mRNA expression levels of RUNX3 in normal haematopoiesis.	95
Figure 3-2 – Plasmid cDNA sequencing confirms subcloning of <i>RUNX3</i> into PINCO.	97
Figure 3-3 – Control and RUNX3 plasmids are successfully transfected into Nx cells.	98
Figure 3-4 – Expression of control DsRed and RUNX3 in human HSPC cells.....	100
Figure 3-5 – RUNX3 is successfully expressed in human HSPC cells.	101
Figure 3-6 – RUNX3 expression inhibits erythroid colony formation and promotes self-renewal after an initial replating of colony forming cells.....	102
Figure 3-7 – RUNX3 induces a modest early erythroid growth suppression during the EPO-independent phase of differentiation.....	104
Figure 3-8 – Gating strategy used to follow the erythroid differentiation of HSPC by flow cytometry.....	105
Figure 3-9 – RUNX3 downregulates CD36 expression in HSPC during the EPO-independent erythroid differentiation.	106
Figure 3-10 – CD34 expression is downregulated in both control and RUNX3-expressing cells during the EPO-independent erythroid differentiation.	108
Figure 3-11 – RUNX3 overcome growth suppression during the EPO-dependent phase of differentiation.....	109
Figure 3-12 – RUNX3 induces abnormalities in CD36 expression during the EPO-dependent phase of differentiation.	110
Figure 3-13 – RUNX3 suppresses GlyA expression during the EPO-dependent phase of differentiation.....	112

Figure 3-14 – RUNX3 impairs cell size reduction in the EPO-dependent phase of differentiation..... 113

Figure 3-15 – RUNX3 impairs cell size reduction in the EPO-dependent phase of differentiation..... 114

Figure 3-16 – RUNX3 expression affects the morphology of cells during erythropoiesis. 116

Figure 3-17 – RUNX3 shRNA constructs successfully reduced the endogenous levels of RUNX3 in OCI-AML-5 cell line. 117

Figure 3-18 – Knockdown of RUNX3 was successful in human HSPC cells..... 119

Figure 3-19 – Knockdown of RUNX3 supresses erythroid colony formation of HSPC. 120

Figure 3-20 – Knockdown of RUNX3 did not affect significantly early erythroid growth during the EPO-independent phase of differentiation..... 121

Figure 3-21 – Knockdown of RUNX3 did not affect significantly CD36 (MFI) and CD34 (%) expression in HSPC during the EPO-independent erythroid differentiation. 122

Figure 3-22 – Effect of RUNX3 knockdown on late erythroid growth during the EPO-dependent phase of differentiation. 124

Figure 3-23 – Knockdown of RUNX3 does not affect CD36 and GlyA expression in HSPC during the EPO-dependent erythroid differentiation..... 125

Figure 3-24 – Knockdown of RUNX3 causes no effects on cell size reduction in the EPO-dependent phase of differentiation..... 126

Figure 3-25 – RUNX3 knockdown does not affect the morphology of cells during erythropoiesis..... 127

Figure 4-1 – *RUNX3* mRNA expression in different myeloid cell subpopulations..... 137

Figure 4-2 – *RUNX3* mRNA expression levels are variable in AML subtypes. 139

Figure 4-3 – Overexpression of RUNX3 is associated with poor overall survival of AML patients..... 141

Figure 4-4 – Increased *RUNX3* expression is associated with complex cytogenetics and poor prognosis in AML..... 142

Figure 4-5 – Overexpression of RUNX3 inhibits myeloid colony formation in human HSPC. 144

Figure 4-6 – Gating strategy used for the analysis of myeloid growth and differentiation of HSPC by flow cytometry..... 145

Figure 4-7 – Overexpression of RUNX3 inhibits erythroid and granulocytic growth during myeloid development..... 146

Figure 4-8 – Overexpression of RUNX3 disrupts the balance between monocytic and granulocytic populations in culture during myeloid development of HSPC. 148

Figure 4-9 – Overexpression of RUNX3 downregulates the expression of CD11b and CD14 in monocytic cells. 149

Figure 4-10 – RUNX3 expression disturbs granulocytic development by downregulating CD11b expression..... 151

Figure 4-11 – Overexpression of RUNX3 affects the morphology of cells during myeloid development..... 152

Figure 4-12 – Knockdown of RUNX3 does not disrupt the myeloid colony formation of HSPC. 154

Figure 4-13 – Knockdown of RUNX3 impairs the growth of erythroid cells in culture. 155

Figure 4-14 – Knockdown of RUNX3 does not affect the lineage balance of cells. .. 156

Figure 4-15 – Knockdown of RUNX3 does not significantly disturb the monocytic differentiation of HSPC..... 157

Figure 4-16 – Knockdown of RUNX3 does not significantly affect the granulocytic differentiation of HSPC..... 158

Figure 4-17 – Knockdown of RUNX3 does not affect cell morphology during myeloid differentiation..... 159

Figure 4-18 – RUNX1-ETO significantly downregulated the expression of *RUNX3* in HSPC. 161

Figure 4-19 – Expression of RUNX3 and RUNX1-ETO in human HSPC..... 162

Figure 4-20 – Expression of RUNX1-ETO as a single abnormality or in combination with RUNX3 suppresses erythroid colony formation..... 164

Figure 4-21 – Expression of RUNX1-ETO as a single abnormality or in combination with RUNX3 inhibits myeloid colony formation..... 165

Figure 4-22 – Expression of RUNX1-ETO as a single abnormality or in combination with RUNX3 does not significantly affect the growth of myeloid cells. 167

Figure 4-23 – Expression of RUNX1-ETO as a single abnormality or in combination with RUNX3 does not significantly affect the lineage-specific growth of cells..... 168

Figure 4-24 – RUNX1-ETO itself and in combination with RUNX3 overexpression did not impact significantly the lineage balance in HSPC..... 169

Figure 4-25 – RUNX3 overexpression dysregulates CD11b expression and exhibits normal CD14 upregulation during monocytic development of RUNX1-ETO-expressing cells. 170

Figure 4-26 – Abnormal granulocytic development observed in cells expressing RUNX1-ETO alone or in combination with RUNX3 overexpression..... 172

Figure 4-27 – RUNX3 overexpression promotes morphological changes associated with intermediate to later stages of development in RUNX1-ETO cells. 173

Figure 5-1 – Experimental design of RNA-seq analysis of transcriptional changes associated with RUNX3 overexpression in HSPC..... 185

Figure 5-2 – Successful expression and enrichment of GFP in human HSPC..... 186

Figure 5-3 – Pre-alignment QC and filtering of raw reads for a control RNA sample. 189

Figure 5-4 – Analysis of global gene expression among samples..... 194

Figure 5-5 – Three-dimensional PCA of control and RUNX3 RNA-seq data..... 195

Figure 5-6 – Hierarchical clustering of control and RUNX3 RNA-seq data..... 196

Figure 5-7 – *RUNX3* mRNA is overexpressed in human HSPC cells..... 198

Figure 5-8 – *RUNX3* overexpression induces transcriptional dysregulation in human HSPC. 199

Figure 5-9 – Haematopoiesis is the most significantly dysregulated process in human HSPC overexpressing *RUNX3*. 202

Figure 5-10 – *RUNX3* overexpression did not significantly impact cell migration of HSPC in response to SDF-1 exposure..... 205

Figure 5-11 – *RUNX3* overexpression dysregulate important genes involved in human haematopoiesis. 206

Figure 5-12 – Overexpression of *RUNX3* significantly downregulates key haematopoietic genes in human HSPC..... 208

Figure 5-13 – Network analysis of *RUNX3* dysregulated genes involved in the haematopoietic development of human HSPC..... 209

Figure 5-14 – Pathways and functions comparative analysis of increased and reduced *RUNX3* expression levels in human HSPC. 213

Figure 5-15 – Differentially expressed genes comparison analysis of increased and reduced *RUNX3* expression levels in human HSPC. 215

Figure 5-16 – Pathways and functions comparative analysis of increased *RUNX3* and *RUNX1-ETO* expression in human HSPC..... 217

Figure 5-17 – Differentially expressed genes comparison analysis of increased *RUNX3* and *RUNX1-ETO* expression in human HSPC..... 218

Figure 6-1 – Graphical abstract summarising the main findings on the role of *RUNX3* in normal human haematopoietic development and AML. 239

Summary of Tables

Table 1-1 – WHO classification of cytogenetically and molecularly defined subtypes of AML (2016 revision).	17
Table 1-2 – Genetic risk stratification of AML according to 2017 ELN recommendations.	22
Table 1-3 – Summary of post-translational modifications of RUNX factors.	38
Table 1-4 – Summary of RUNX KO mouse models in normal haematopoiesis.....	42
Table 2-1 – Summary of general reagents with supplier used in this study.....	58
Table 2-2 – Summary of antibodies used in flow cytometry and western blotting studies.	61
Table 2-3 – Summary of all retro- and lentiviral systems used for overexpression and KD studies.....	64
Table 2-4 – Summary of primers used to validate the DNA plasmid structures used in this study.	66
Table 2-5 – Different combinations and concentrations of growth factors used for the growth and development of human primary HSPC.	68
Table 2-6 – Subculturing conditions for all cell lines used in this study.	69
Table 2-7 – Summary of transduced HSPC cultures generated in this study.	74
Table 2-8 – Cell surface markers used in the multiparameter analysis of the development of human myeloid subpopulations grown <i>in vitro</i> culture.....	78
Table 2-9 – Summary of transcriptomic datasets used in this study.....	90
Table 5-1 – QC assessment of RNA samples.	187
Table 5-2 – Pre-alignment quality control and filtering of raw reads for control and RUNX3 RNA samples.	190
Table 5-3 – Alignment status and QC of control and RUNX3 RNA samples against a human reference genome.	191
Table 5-4 – Distribution of gene expression levels among samples.....	193
Table 5-5 – Top 10 genes dysregulated by RUNX3 overexpression in human HSPC.	200
Table 5-6 – Protein function enrichment analysis of genes dysregulated by RUNX3 overexpression in human HSPC.	203
Table 5-7 – Upstream and master gene regulators predicted to be influencing the transcriptomic changes caused by RUNX3 overexpression in human HSPC.	211
Table 5-8 – Summary list of dysregulated genes and potential upstream regulators significantly co-expressed with RUNX3 in AML patients from TCGA dataset.....	220

List of Abbreviations

ALL	Acute lymphoblastic leukaemia
APC	Allophycocyanin
AML	Acute myeloid leukaemia
APL	Acute promyelocytic leukaemia
Ara-C	Cytarabine
BFU-E	Burst-forming units-erythroid
BM	Bone marrow
β -ME	β -mercaptoethanol
BSA	Bovine serum albumin
CB	Cord blood
CBF	Core binding factor
CDK	Cyclin-dependent kinase
cDNA	Complementary DNA
CDS	Coding sequence
CFU	Colony-forming units
ChIP-seq	Chromatin immunoprecipitation sequencing
CLP	Common lymphoid progenitor
CMP	Common myeloid progenitor
c-MPL	Myeloproliferative leukaemia virus
CR	Complete remission
DC	Dendritic cell
DE	Differential expression/ed
DMEM	Dulbecco's Modified Eagle Medium
DNase	Deoxyribonuclease
DsRed	<i>Discosoma</i> red fluorescent protein
EFS	Event-free survival
ELN	European Leukaemia Network
EPO	Erythropoietin
ETS	E26 transformation-specific
FAB	French-American-British
FACS	Fluorescence activated cell sorting
FBS	Foetal bovine serum
FDA	US Food and Drug Administration
FDR	False discovery rate
FLT3	Fms-like tyrosine kinase 3
FLT3L	Fms-like tyrosine kinase 3-ligand
FPKM	Fragments per kilobase of transcript per million
FSC	Forward scatter

G-CSF	Granulocyte colony-stimulating factor
GFP	green fluorescent protein
GlyA	Glycophorin A
GM-CSF	Granulocyte-macrophage colony-stimulating factor
GMP	Granulocyte-monocyte progenitor
GO	Gene Ontology
HDAC	Histone deacetylase
HRP	Horseradish peroxidase
HSC	Haematopoietic stem cell
HSCT	Haematopoietic stem cell transplantation
HSPC	Haematopoietic stem and progenitor cell
IL	Interleukin
IMDM	Iscove's Modified Dulbecco's Medium
IPA	Ingenuity Pathway Analysis
ITD	Internal tandem duplication
KD	Knockdown
KEGG	Kyoto Encyclopaedia of Genes and Genomes
KO	Knockout
LMPP	Lymphoid-primed multipotent progenitor
log ₂ FC	Logarithmic (base 2) fold change
LSC	Leukaemia stem cell
LT-HSC	Long-term multipotent HSC
M	Million
MACS	Magnetic-activated cell sorting
MDP	Monocyte-dendritic cell progenitor
MDS	Myelodysplastic syndrome
MEM	Minimum Essential Medium Eagle
MEP	Megakaryocyte-erythrocyte progenitor
MFI	Mean fluorescence intensity
MILE	Microarray Innovations in Leukaemia
MLL	Mixed lineage leukaemia
MNC	Mononuclear cells
MPD	Myeloproliferative disorder
MPP	Multipotent progenitor
NEB	New England BioLabs
NGS	Next-generation sequencing
NHR	Nervy homology regions
NK	Natural killer
Nx	Phoenix
OS	Overall survival
PB	Pacific blue

padj	Adjusted p-value
PB	Peripheral blood
PBS	Phosphate-buffered saline
PCA	Principal component analysis
PE	Phycoerythrin
PRMT	Protein arginine N-methyltransferase
Puro	Puromycin
QC	Quality control
qRT-PCR	Quantitative reverse transcription polymerase chain reaction
RIN	RNA integrity number
RNase	Ribonuclease
RNA-seq	RNA-sequencing
RPMI	Roswell Park Memorial Institute
RT	Room temperature
SCF	Stem cell factor
SDF-1	Stromal cell derived factor 1
shRNA	Short hairpin RNA
scRNA-seq	Single-cell RNA sequencing
SSC	Side scatter
TBS	Tris-buffered saline
TCGA	The Cancer Genome Atlas
TF	Transcription factor
TGF- β	Transforming growth factor β
TPO	Thrombopoietin
WHO	World Health Organisation

Publications and Presentations

Oral presentations:

- Menezes AC, Darley RL, Tonks A. Overexpression or knockdown of RUNX3 supresses human blood cell development. 34th Annual Schools of Medicine and Dentistry Postgraduate Research Symposium. Cardiff, UK 2020
- Menezes AC, Darley RL, Tonks A. RUNX3 Expression Inhibits Normal Human Erythroid Development. RUNX Meeting 2019. Seoul, South Korea 2019
- Menezes AC, Darley RL, Tonks A. The Role of RUNX3 in Acute Myeloid Leukaemia and Normal Human Haematopoietic Development. Division of Cancer and Genetics Postgraduate Symposium. Cardiff, UK 2018
- Divisional and Departmental Seminars

Poster presentations:

- Menezes AC, Knapper S, Darley RL, Tonks A. Overexpression or Deficiency of RUNX3 Results in Defective Normal Human Hematopoietic Development Similar to RUNX1-ETO Expression in AML. Blood 2019, 134 (Supplement_1): 2527

Awards:

- 2nd place for best oral presentation at the Division of Cancer and Genetics Postgraduate Symposium. Cardiff, UK 2018

Dedication

This work is dedicated to you, Mum.

You taught me to never give up and follow my dreams.

1 Introduction

1.1 Normal human haematopoiesis

Blood is characterised as a highly regenerative and diverse tissue, and the constant production of blood cells is called haematopoiesis. In early days, a unitarian theory for haematopoiesis defined a common precursor for the origin of all blood cells, the haematopoietic stem cell (HSC) (Doulatov *et al.* 2012). The existence of HSC was further supported during the atomic era where a bone marrow (BM) failure in radiation exposed recipients could be rescued using BM or spleen cells from non-exposed donors (Lorenz *et al.* 1951). A major breakthrough in this field happened when Till and McCulloch developed a clonal *in vivo* repopulation assay to assess the regenerative potential of HSC, supporting their multipotency capacity (Till and McCulloch 1961). Over the years, the concept of haematopoietic development has been refined into a more detailed cellular hierarchy with multipotent HSC sitting atop and mature differentiated cells on the bottom. Single-cell RNA sequencing (scRNA-seq) is a powerful tool that has helped defining the cellular heterogeneity associated with haematopoiesis. HSC are characterised by their self-renewal capacity as well as ability to differentiate into intermediate progenitor cells, the haematopoietic stem and progenitor cells (HSPC), and later to mature blood cells of all haematopoietic lineages (Doulatov *et al.* 2012).

During embryogenesis, haematopoiesis occurs in successive temporally and spatially different waves producing specific haematopoietic progenitors: primitive and definitive haematopoiesis. The primitive wave takes place in the yolk sac where precursors give rise to primitive erythroid progenitor cells, which in turn differentiate into primitive erythrocytes, macrophages and megakaryocytes (Jagannathan-Bogdan and Zon 2013; Lacaud and Kouskoff 2017). Definitive haematopoiesis takes place later in development and starts with the emergence of erythroid-myeloid progenitors, responsible for the production of definitive erythrocytes and most myeloid lineages (Lacaud and Kouskoff 2017). B and T lymphoid progenitors are further generated, preceding the emergence of long-term multipotent HSC (LT-HSC) that will ultimately reside in the BM throughout adult life (Lacaud and Kouskoff 2017).

1.1.1 Haematopoietic stem cells

HSC are the only cells within the haematopoietic system with multipotency and self-renewal potential, being able to differentiate into all functional haematopoietic cells while maintaining the HSC pool (Seita and Weissman 2010). The current understanding of normal and malignant haematopoiesis comes from mouse studies. The obvious differences between mouse and human basic biology and haematology drove the development of genetic tools and *in vivo* repopulation assays to study human HSC (Doulatov *et al.* 2012). The discovery of colony-forming units (CFU) in the spleen of transplanted mice (Till and McCulloch 1961) instigated the first studies of human colony-forming progenitors using *in vitro* CFU assays (Pike and Robinson 1970; Gartner and Kaplan 1980; Sutherland *et al.* 1989). In addition, engraftment of primary human HSC into immunocompromised mice prompted the development of different humanised mouse models that have helped characterise HSC (Bosma *et al.* 1983; McCune *et al.* 1988; Shultz *et al.* 1995; Shultz *et al.* 2005; Rongvaux *et al.* 2011). Isolation of human HSC requires characterisation of different cell surface markers such as CD34, the first marker found to define human HSC as well as progenitor cells (Civin *et al.* 1984). Further studies identified human HSC by expression of CD90 (Thy1) and absence of lineage markers (Lin⁻) (Baum *et al.* 1992; Craig *et al.* 1993). Surface marker CD38 was also identified in most of the CD34⁺ cells (90-99%), and early progenitors were found to reside in the CD38⁻CD90⁺ fraction (Huang and Terstappen 1994; Hao *et al.* 1996; Uchida *et al.* 1998; Miller *et al.* 1999). Together, human HSC are found within the Lin⁻CD34⁺CD38⁻CD90⁺ fraction of haematopoietic cells. This fraction can be further divided into three subpopulations based on the expression of CD90 and CD45RA: CD90⁺CD45RA⁻ subpopulation containing HSC, CD90⁻CD45RA⁻ containing multipotent progenitors (MPP), and a less primitive CD90⁻CD45RA⁺ subpopulation (Majeti *et al.* 2007).

At the cellular level, the transcriptional profile of HSC is defined by unique properties that are not intuitively and directly associated with multipotency. Curiously, around 70% of all transcriptional changes between HSC and progenitors are independent of lineage fate. HSC are characterised by a quiescent, autophagy-dependent, and glycolytic state defined by reduced mitochondrial activity and tightly regulated protein synthesis (Laurenti and Gottgens 2018). Conversely, early progenitor cells are highly proliferative and metabolically active compared to HSC. The

HSC state and its characteristics are not absolute and an understanding of the mechanisms that regulate self-renewal and lineage programming are still necessary.

1.1.1.1 Self-renewal potential of haematopoietic stem cells

The heterogeneity of the HSC pool is intimately related with self-renewal, as distinct subpopulations differ in their repopulation capacity. Self-renewal potential of haematopoietic cells can be determined by *in vivo* transplantation experiments using immunocompromised mice (Ema *et al.* 2005). LT-HSC reside in the BM and are characterised by a sustained self-renewal capacity of more than 16 weeks post-transplantation (reviewed by (Laurenti and Gottgens 2018)). On the other hand, cells that differentiate into all other haematopoietic cell types and transiently engraft in primary transplants are called short-term HSC or MPP (Laurenti and Gottgens 2018; Zhang *et al.* 2018). MPP have a higher differentiation potential and absent self-renewal capacity compared to HSC. The need to discriminate between these populations within the heterogenous HSC pool prompted the identification of additional markers, such as CD49f that differently characterises HSC and MPP (Notta *et al.* 2011) (1.1.1). An extensive and defined characterisation of such closely related cell types is essential for the understanding of the processes behind the loss of stem cell function.

The differences in self-renewal capacity observed within the HSC pool are closely associated with their quiescent state. Previous studies have shown a direct relationship between the dormancy state and repopulation capacity of HSC (Wilson *et al.* 2008; Takizawa *et al.* 2011; Bernitz *et al.* 2016). In particular, increased repopulation capacity is correlated with lower frequency of cell divisions as well as slower quiescence exit (Laurenti *et al.* 2015). The precise control of cyclin-dependent kinase 6 (CDK6) expression during quiescent exit has been found important for the dynamics of the HSC pool (Laurenti *et al.* 2015). Low MYC activity and reduced protein synthesis are examples of additional factors associated with HSC quiescence (Laurenti *et al.* 2008; Cabezas-Wallscheid *et al.* 2017). Based on the previous observations, different cell cycle dynamics between HSC subpopulations reflects their inherent functions.

1.1.1.2 The haematopoietic stem cell niche

Although HSC are in a quiescent state during homeostasis, extracellular signals can lead to their activation and subsequent cell proliferation and differentiation (Mendelson and Frenette 2014). These extracellular signals are regulated by a strict local environment within the BM called 'niche', initially proposed more than 40 decades ago (Schofield 1978). Over the years, advances in imaging techniques and the identification of additional markers for the different cellular constituents have improved the characterisation of the HSC niche (Pinho and Frenette 2019). Most of the current knowledge of the HSC niche is based on transgenic mouse models, allowing the identification of distinct cell types, niche factors and their receptors (Pinho and Frenette 2019). An osteoblastic niche population able to regulate HSC expansion has been suggested by previous studies (Taichman and Emerson 1994; Taichman *et al.* 1996; Calvi *et al.* 2003; Zhang *et al.* 2003). In particular, production of angiopoietin-1, osteopontin and thrombopoietin (TPO) by osteoblasts was previously shown to influence HSC maintenance (Arai *et al.* 2004; Stier *et al.* 2005; Yoshihara *et al.* 2007). However, the role of osteoblasts in HSC function is highly controversial. Expression of N-cadherin, proposed to mediate the interaction between osteoblasts and HSC, was found dispensable for HSC niche function in mice (Kiel *et al.* 2009; Bromberg *et al.* 2012; Greenbaum *et al.* 2012). In addition, 3D imaging of HSC localisation revealed that these cells are not significantly associated with osteoblasts (Kunisaki *et al.* 2013; Nombela-Arrieta *et al.* 2013).

In addition to the endosteal region, HSC were also shown to localise in perivascular niches. This complex vascular network is responsible for the efficient removal of waste products and the delivery of oxygen, nutrients, growth factors, hormones, and neurotransmitters to different locations in the BM (Pinho and Frenette 2019). The oxygenated arterial blood is associated with an extensive network of sinusoids, with sinusoidal endothelial cells representing the bulk of the BM endothelium (Pinho and Frenette 2019). Endothelial cells secrete several niche factors, including stromal cell derived factor 1 (SDF-1 or CXCL12), stem cell factor (SCF), and Notch ligands to regulate HSC function and regeneration (Butler *et al.* 2010; Ding *et al.* 2012; Greenbaum *et al.* 2013; Guo *et al.* 2017). Concomitantly, perivascular cells account for all BM mesenchymal stem cells and have also been shown to express high levels of SDF-1 and SCF (Sacchetti *et al.* 2007; Méndez-Ferrer

et al. 2010; Pinho *et al.* 2013). These cells are characterised by their repopulating capacity and can give rise to different of cells that form the skeleton and BM stroma (Frenette *et al.* 2013). Several studies have described their important role in the organisation and maintenance of the HSC niche (Sacchetti *et al.* 2007; Chan *et al.* 2009). Adipo-osteogenic progenitors CXCL12-abundant reticular (CAR) stromal cells and leptin receptor (LEPR) cells are mainly distributed around sinusoids (reviewed in (Pinho and Frenette 2019)). On the other hand, periarteriolar cells were found to express both the pericyte the marker neural–glial antigen 2 (NG2) and the type VI intermediate filament protein nestin (NES), or the smooth muscle marker myosin heavy chain 11 (MYH11) (reviewed in (Wei and Frenette 2018; Pinho and Frenette 2019)). 3D imaging analysis uncovered that a subset of quiescent HSC was favourably localised near the arterioles, which in turn are more abundant in the endosteal region (Wei and Frenette 2018). Perivascular and endothelial cells are intimately connected by molecular pathways that modulate their function within the BM. For instance, Notch signalling in endothelial cells increases the numbers of platelet-derived growth factor receptor β positive perivascular cells, mesenchymal stem cells and HSC frequency, as well as SCF expression (Kusumbe *et al.* 2016). Sympathetic and sensory nerves have also been shown to support haematopoiesis within the BM (Mach *et al.* 2002), highlighting the importance of a vascular niche for HSC. HSC mobilisation during steady state is tightly controlled by the circadian secretion of noradrenaline, which in turn regulates the expression of SDF-1 (Katayama *et al.* 2006; Mendez-Ferrer *et al.* 2008). In addition, nonmyelinating Schwann cells promote HSC quiescence by regulating the transforming growth factor β (TGF- β) signalling pathway (Yamazaki *et al.* 2011).

Besides stromal cells, haematopoietic cells are also capable of regulating HSC activity within the BM, including megakaryocytes and macrophages. HSC quiescence is controlled by megakaryocytes through CXCL4 and TPO secretion, as well as TGF- β signalling (Bruns *et al.* 2014; Nakamura-Ishizu *et al.* 2014; Zhao *et al.* 2014a). On the other hand, macrophages are involved in HSC retention within the BM (Winkler *et al.* 2010; Chow *et al.* 2011). Understanding the complexity of the BM niche and its influence on HSC activity is important for the improvement of treatment options for haematological malignancies.

1.1.2 Hierarchical organisation of haematopoiesis

The haematopoietic system comprises numerous different types of mature blood cells, including erythrocytes, megakaryocytes and platelets, granulocytes, monocytes and macrophages, mast cells, T and B lymphocytes, dendritic cells (DC), and natural killer (NK) cells (reviewed by (Seita and Weissman 2010)). Cell surface protein analysis by flow cytometry is widely used to define and study haematopoietic subpopulations. Immunophenotyping of haematopoietic cells hinted the existence of a hierarchical organisation in haematopoiesis, where multipotent HSC differentiate into unipotent mature blood cells and are generally represented by a tree-like branched roadmap (Akashi *et al.* 2000; Reya *et al.* 2001). [Figure 1-1](#) shows a commonly accepted representation of normal human haematopoiesis. Initially, HSC differentiate into MPP, which in turn give rise to different progenitor cells: the common myeloid progenitor (CMP) and the lymphoid-primed multipotent progenitor (LMPP) followed by the common lymphoid progenitor (CLP).

These individual progenitor cells further differentiate into mature cells of all haematopoietic lineages. For instance, CMP give rise to both megakaryocyte-erythrocyte progenitors (MEP) and granulocyte-monocyte progenitors (GMP). As progenitor cells differentiate, cell numbers increase whilst their proliferative potential declines. The formation of granulocytes within the BM is termed granulopoiesis, and it develops for over 4 to 6 days starting at the myeloblast phase (reviewed by (Lawrence *et al.* 2018)). Granulocyte precursors including myeloblasts, promyelocytes and early myelocytes retain their proliferative potential, whereas committed metamyelocytes are post-mitotic (Lawrence *et al.* 2018). Granulocytic development is characterised by the gradual appearance of granules within the cells and culminates with the nucleus assuming a band-like shape that is segmented in mature neutrophils (Lawrence *et al.* 2018). Human CD15 expression is limited to terminally differentiated myeloid cells, in particular mature granulocytes (eosinophils and neutrophils) and, to some extent, monocytes (Gooi *et al.* 1983; Tao *et al.* 2004). On the other hand, monopoiesis leads to the development of mature monocytes, which in turn can give rise to a subset of macrophages and inflammatory DC in tissues. Discrete human monocytic populations were initially identified by differential expression of CD14 and CD16 cell surface markers (Passlick *et al.* 1989).

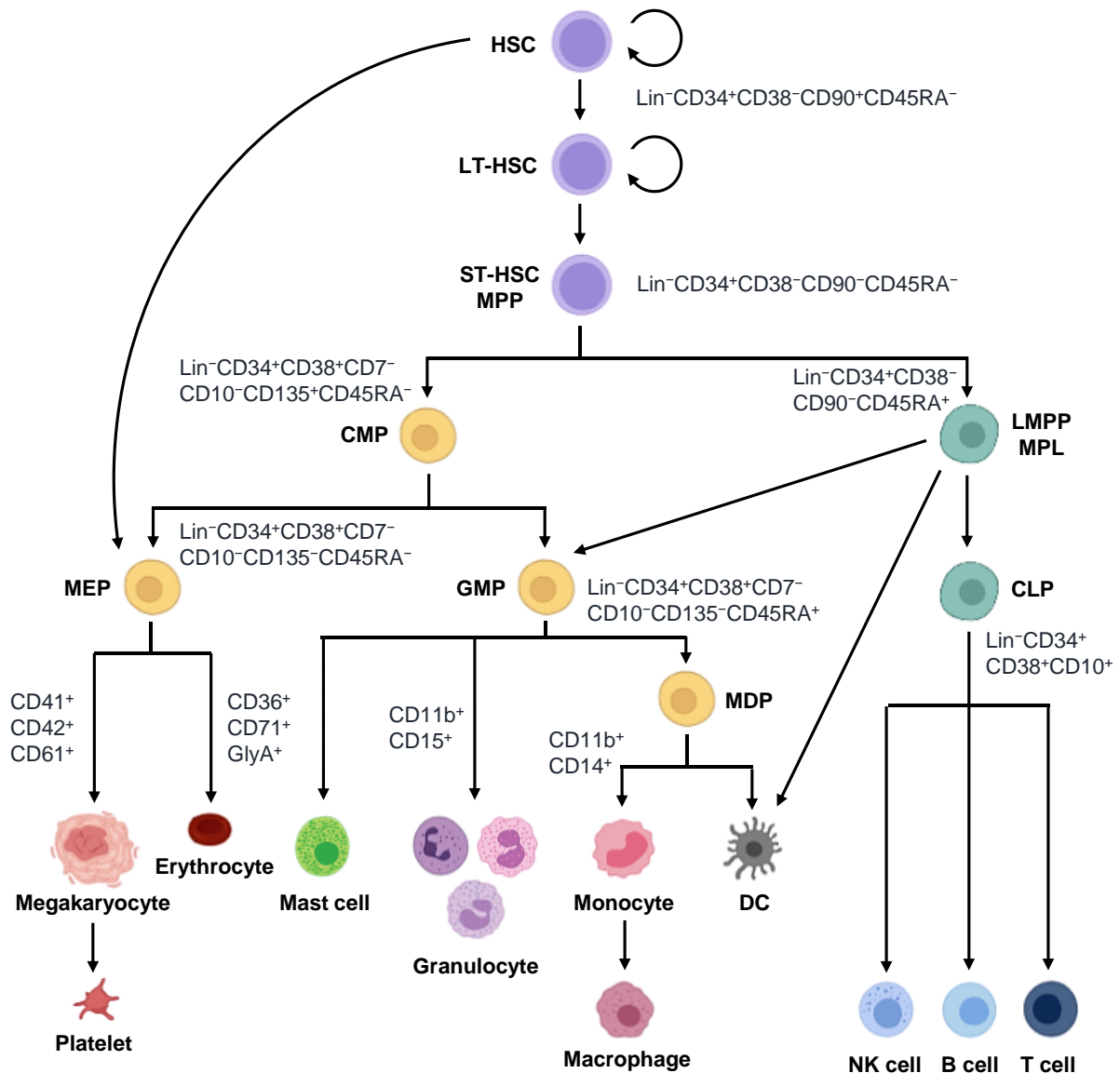


Figure 1-1 – Hierarchical representation of human haematopoietic development in the BM.

HSC – Haematopoietic stem cell; LT-HSC – Long-term haematopoietic stem cell; ST-HSC – Short-term haematopoietic stem cell; MPP – Multipotent progenitor; CMP – Common myeloid progenitor; LMPP – Lymphoid-primed multipotent progenitor; MLP – Multi-lymphoid progenitor; CLP – Common lymphoid progenitor; MEP – Megakaryocyte-erythrocyte progenitor; GMP – Granulocyte-monocyte progenitor; MDP – Monocyte-dendritic cell progenitor; DC – Dendritic cell; GlyA – Glycophorin A (or CD235a). Haematopoietic progenitor subpopulations were defined according to (Pellin *et al.* 2019). Adapted from (Doulatov *et al.* 2012; Weiskopf *et al.* 2016; Guilliams *et al.* 2018; Ulirsch *et al.* 2019).

Current hierarchical models of haematopoiesis propose that monocytes, macrophages, and DC arise from progenitors with myeloid-restricted differentiation potential called monocyte/DC progenitors (MDP) (reviewed by (Guilliams *et al.* 2018)). This population is believed to produce either common DC precursors or unipotent common monocyte progenitors (Guilliams *et al.* 2018).

Erythropoiesis is the process by which immature erythroid-committed progenitors identified as the burst-forming units-erythroid (BFU-E) fully mature into erythrocytes, the most abundant cell type in adult blood with an average life span of 120 days (reviewed by (Dzierzak and Philipsen 2013)). BFU-E give rise to large colonies of haemoglobinised cells that can be detected in methylcellulose cultures after 5 to 8 days or 10 to 14 days for mouse or human cells, respectively (Dzierzak and Philipsen 2013). CFU-Erythroid represent the next step of erythroid development and these small colonies are detected in methylcellulose culture after 2 to 3 days or 5 to 8 days for mouse and human cells, respectively (Dzierzak and Philipsen 2013). Late erythroid progenitor cells are more abundant in the BM compared to BFU-E, where they stay under normal conditions. Pro-erythroblasts develop into reticulocytes in four/five rapid division steps, progressively gaining erythroid characteristics, such as expression of glycophorin A (GlyA or CD235a) and reducing in size. In fact, erythroid cells expel their nucleus, mitochondria, and endoplasmic reticulum at later stages of differentiation, losing their proliferative potential (Dzierzak and Philipsen 2013). Some common erythroid cell surface proteins include CD36, CD71 and CD105 in early stages of development, and GlyA in late erythroid maturation (Edelman *et al.* 1986; Okumura *et al.* 1992; Mori *et al.* 2015).

Integration of flow cytometry with scRNA-seq has allowed an improved understanding of human haematopoiesis by studying transcriptional single-cell states (Velten *et al.* 2017; Pellin *et al.* 2019). An alternative view challenging the rigid classical tree proposed that unilineage-restricted cells arise from a 'continuum of low-primed undifferentiated haematopoietic stem and progenitor cells' (CLOUD-HSPC) (Velten *et al.* 2017). Further studies have supported instead the idea of a structured hierarchy, exposing a continuous and heterogenous regulatory landscape of human haematopoiesis (Buenrostro *et al.* 2018; Karamitros *et al.* 2018; Pellin *et al.* 2019).

1.1.3 Haematopoietic cytokine network

Haematopoiesis is a tightly controlled process that involves intricate regulatory pathways mediated by several factors, including cytokines and their receptors. Key haematopoietic cytokines include colony-stimulating factors (CSF), interleukins (IL), SCF, erythropoietin (EPO), and TPO. While some of these cytokines stimulate the proliferation and differentiation of several myeloid lineages, such as IL-3, others influence specific lineages, such as EPO in erythroid development. Early erythroid progenitor growth depends on cytokines including TPO, IL-3, fms-like tyrosine kinase 3 (FLT3)-ligand or SCF. SCF binds to its tyrosine kinase receptor c-KIT and, at later stages of development, acts synergically with EPO to support late erythroid growth and expansion. Regarded as the main regulator of erythropoiesis, EPO also plays an essential role in the response to hypoxic stress, increasing the rate of erythroid production. Additional factors shown to contribute to this response, include bone morphogenic protein 4 (BMP4) or SCF/KIT signalling (Perry *et al.* 2007). On the other hand, growth factors such as granulocyte-macrophage and granulocyte-CSF (GM- and G-CSF, respectively), SCF, and IL-3 were shown to act synergically to induce myeloid differentiation of human progenitor cells (McNiece *et al.* 1991).

Knockout (KO) mice studies have provided critical insights into the cytokine-mediated control of haematopoiesis. Absence of EPO signalling resulted in reduced primitive erythropoiesis with midgestational death due to lack of foetal liver definitive erythropoiesis (Wu *et al.* 1995; Kieran *et al.* 1996; Lin *et al.* 1996). Despite being important for definitive erythroid growth and survival, EPO signalling is not required for erythroid lineage commitment (Wu *et al.* 1995; Lin *et al.* 1996). Moreover, TPO and its receptor myeloproliferative leukaemia virus (c-MPL) were found to stimulate proliferation and terminal maturation of erythroid progenitors (Kieran *et al.* 1996). These studies suggest that cytokines are not the primary drivers of lineage commitment. Loss of TPO and c-MPL results in reduced platelet and megakaryocyte numbers as well as HSC, which suggests an important role in the development of megakaryocytes and a non-redundant activity in HSC (Gurney *et al.* 1994; Alexander *et al.* 1996; Solar *et al.* 1998). Alternatively, mice lacking G-CSF signalling exhibit defective granulopoiesis with chronic neutropenia (Lieschke *et al.* 1994; Liu *et al.* 1996; Semerad *et al.* 2002). However, the existence of compensatory mechanisms regulating granulopoiesis in the absence of G-CSF/R was suggested (Liu *et al.* 1996).

Although cytokines and their receptors provide important signals for the proliferation and development of multipotent and mature haematopoietic cells, transcription factors (TF) seem to be the major drivers of haematopoiesis.

1.1.4 Transcription regulation of haematopoietic development

The hierarchical structure of the haematopoietic system is intimately related to a complex network of TFs responsible for cell proliferation and fate decisions (Figure 1-2). Next generation and chromatin immunoprecipitation sequencing (NGS and ChIP-seq, respectively) have allowed a more comprehensive study of the transcriptional regulation of haematopoiesis. Accordingly, gene profiling of each haematopoietic subpopulation, from HSC to terminally differentiated cells, revealed the presence of distinct and intricate regulatory circuits (Novershtern *et al.* 2011). HSPC, mature erythroid cells, granulocytes/monocytes, B and T cells were shown to be defined by a group of significantly and differently expressed genes particular to each lineage (Novershtern *et al.* 2011). In addition, multiple lineages express similar gene sets at different levels. For instance, PU.1 (or SPI1) is expressed in both monocytic and B cell development (Dakic *et al.* 2005; Iwasaki *et al.* 2005; Houston *et al.* 2007), as well as growth-factor independent 1 (GFI1) for HSC self-renewal and granulopoiesis (Hock *et al.* 2004; Horman *et al.* 2009).

At the HSC level, TFs such as RUNX1 (Runt-related TF, also known as AML1) or stem cell leukaemia (SCL/TAL1) are crucial for the production of foetal HSC (Shivdasani *et al.* 1995; Okuda *et al.* 1996). However, conditional ablation of these factors showed that they are dispensable for HSC maintenance in the BM during adult haematopoiesis (Mikkola *et al.* 2003; Ichikawa *et al.* 2004b; Growney *et al.* 2005). Further studies showed that RUNX1 deletion failed to significantly reduce HSC or LT-HSC numbers in foetal liver, whereas loss of its binding partner core binding factor β (CBF β) dramatically compromised LT-HSC (Cai *et al.* 2011; Tober *et al.* 2013). These results suggest that the other members of the RUNX family, RUNX2 and RUNX3, are likely involved in the maintenance of HSC (1.3.4). Conversely, lineage-specific effects were observed in RUNX1- or SCL-deficient mice, including suppression of megakaryocytic and T/B cell development, reduction of CLP and platelet production, and defective maturation of megakaryocytic and erythroid progenitors (Mikkola *et al.* 2003; Ichikawa *et al.* 2004b; Growney *et al.* 2005).

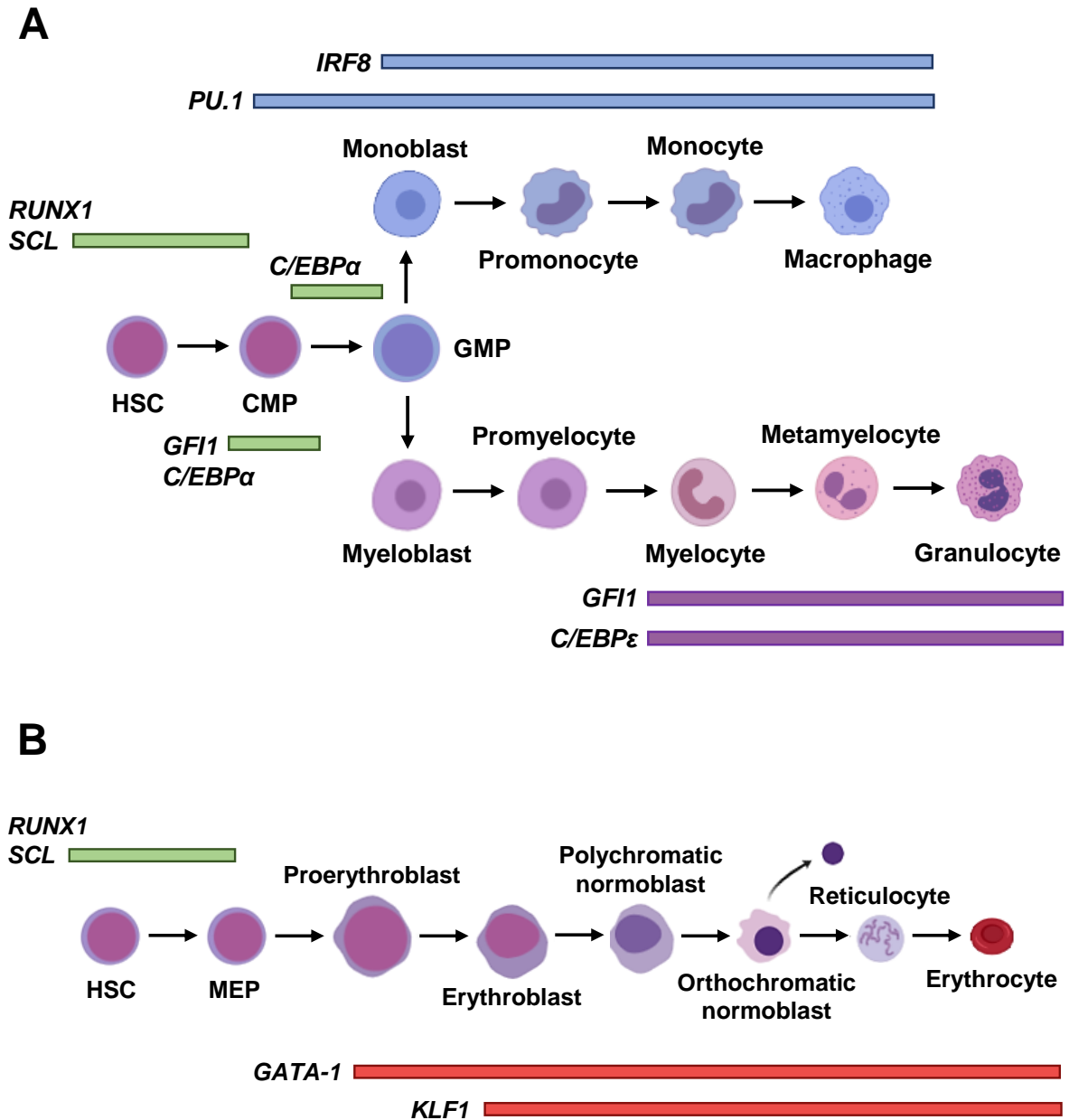


Figure 1-2 – Transcriptional regulation of myeloid development.

Developmental phases and transcriptional regulation of monocytic and granulocytic **(A)** and erythroid **(B)** maturation. HSC – Haematopoietic stem cell; GMP – Granulocyte-monocyte progenitor; MEP – Megakaryocyte-erythrocyte progenitor. RUNX1 (or AML1) and stem cell leukaemia (SCL) are essential for the generation of HSC. Growth-factor independent 1 (GFI1) and CCAAT/enhancer binding protein α (C/EBP α) are important for HSC self-renewal, as well as different steps in myeloid differentiation (along with C/EBP ϵ). Monocytic development depends on PU.1 (also known as SPI1) and interferon-regulatory factor 8 (IRF8). Bars represent the expression of different TFs during haematopoietic development, with different colours indicating distinct developmental phases/lineages. Adapted from (Rosenbauer and Tenen 2007).

In addition, loss of RUNX1 led to a mild myeloproliferative disorder (MPD) (Growney *et al.* 2005). Expression of PU.1 or CCAAT/enhancer binding protein α (C/EBP α) has been found necessary for the maintenance of the HSC pool (Iwasaki *et al.* 2005; Ye *et al.* 2013).

A combination of positive and negative signals from major transcriptional regulators drives lineage specification. The earliest haematopoietic branchpoint is primarily regulated by PU.1 and GATA-1 (Arinobu *et al.* 2007; Hoppe *et al.* 2016). Downregulation of GATA-1 directs haematopoiesis towards the myeloid lineage, whereas absence of PU.1 expression has the opposite effect (Rhodes *et al.* 2005). Additional examples of antagonism between TFs in haematopoiesis include friend leukaemia integration 1 (FLI1) and erythroid Krüppel-like factor KLF1 (also known as EKLF) for the erythroid versus megakaryocytic decision (Starck *et al.* 2003), and GFI1 and PU.1 for monocytic and granulocytic cell fates (Dahl *et al.* 2007). Developmental unidirectionality has been questioned in haematopoiesis, and lineage reprogramming has been found to happen in certain situations (Xie *et al.* 2004; Iwasaki *et al.* 2006; Laiosa *et al.* 2006). Upregulation of GATA-1 in GMP and CLP was shown to redirect these cells into a MEP fate (Iwasaki *et al.* 2003). A precise regulation of the transcriptional networks that govern self-renewal and cell fate decisions is of utmost importance to avoid leukaemic transformation. Numerous key haematopoietic TFs were initially identified in chromosomal abnormalities observed in leukaemia: RUNX1 in RUNX1-ETO (also known as AML1-ETO or RUNX1-RUNX1T1) t(8;21) acute myeloid leukaemia (AML) (1.2.4), Lim domain only 2 (LMO-2) in t(11;14) T cell acute lymphoblastic leukaemia (ALL), and SCL in t(1;14) T-ALL (Begley *et al.* 1989; Boehm *et al.* 1991; Miyoshi *et al.* 1991). RUNX1-ETO fusion protein has been extensively studied in AML, and it is primarily considered to have a dominant negative effect over RUNX1 (reviewed by Lin *et al.* 2017)) (1.2.4.1). Recent studies have revealed a more complex relationship between native RUNX1 and RUNX1-ETO (Ptasinska *et al.* 2014; Mandoli *et al.* 2016).

1.1.4.1 Transcription control of monocytic and granulocytic development

Granulocytic and monocytic differentiation is orchestrated by master regulators such as PU.1, C/EBP α , C/EBP β and C/EBP ϵ , GFI1, and interferon-regulatory factor 8 (IRF8), among others (reviewed by (Rosenbauer and Tenen 2007)). PU.1 is a member

of the E26 transformation-specific (ETS) family of TFs, and it is expressed in several haematopoietic lineages, from HSC to terminally differentiated myeloid cells (Back *et al.* 2005; Nutt *et al.* 2005). Loss of PU.1 disrupts the commitment and differentiation of myeloid and lymphoid lineages (Dakic *et al.* 2005; Iwasaki *et al.* 2005; Pang *et al.* 2018), and is fatal in mice characterised by the lack of mature macrophages and B cells (McKercher *et al.* 1996). Increased expression of PU.1 was shown to favour the production of macrophages, whereas its absence enhanced granulopoiesis (Dahl *et al.* 2003; Dakic *et al.* 2005; Ghani *et al.* 2011). A positive feedback between PU.1 and cell cycle has been demonstrated during myeloid development, where early macrophages were shown to increase PU.1 level by lengthening their cell cycle (Kueh *et al.* 2013). Together, these results suggest that PU.1 has an important role in the normal transition through the CMP and CLP phases and, in contrast, inhibits granulocytic development.

C/EBP α is a basic-region leucine zipper TF expressed by HSC, myeloid progenitor cells and differentiating granulocytes (Radomska *et al.* 1998). Induced expression of C/EBP α promotes neutrophilic differentiation whilst inhibiting monopoiesis (Radomska *et al.* 1998). Conversely, defective levels of C/EBP α result in the absence of GMP and granulocytic-committed cells but normal CMP numbers, which suggests that C/EBP α is involved in the CMP to GMP differentiation step (Zhang *et al.* 1997; Zhang *et al.* 2004). Furthermore, C/EBP α expression was shown to be dispensable in terminal granulocytic development (Zhang *et al.* 2004). Family members C/EBP β and C/EBP ϵ are also important for the normal programme of myeloid differentiation, in particular for the maturation of neutrophils and macrophages (Akagi *et al.* 2010). Terminal maturation of myelocytes to granulocytes requires GFI1 and C/EBP ϵ TFs. GFI1 is expressed by HSC, neutrophils, and T/B precursor cells, and has an important role in lymphocytic differentiation and last stages of granulopoiesis revealed by KO studies (Karsunky *et al.* 2002; Hock *et al.* 2003; Hock *et al.* 2004). Similarly, absence of C/EBP ϵ causes a defect in neutrophilic development beyond the promyelocyte stage (Yamanaka *et al.* 1997).

The switch between granulocytic and monocytic differentiation involves additional TFs, such as IRF8. This transcriptional regulator is expressed in several haematopoietic lineages (Driggers *et al.* 1990), and in the GMP compartment its expression pattern distinguishes monocytic (high IRF8 expression) from granulocytic

progenitors (low IRF8 expression) (Wang *et al.* 2014b). IRF8 was shown to direct monocytic differentiation whilst preventing myeloid cell growth and granulopoiesis (Tamura *et al.* 2000; Sontag *et al.* 2017). Importantly, loss of IRF8 in mice leads to a myeloproliferative syndrome resembling chronic myeloid leukaemia, characterised by an abnormal expansion of neutrophils at the expense of monocytes and macrophages (Holtschke *et al.* 1996; Scheller *et al.* 1999; Tsujimura *et al.* 2002). Myeloid development was also shown to depend on additional TFs, including KLF4 and GATA-2 (Feinberg *et al.* 2007; Rodrigues *et al.* 2008).

1.1.4.2 Transcription control of erythroid development

Erythroid and megakaryocytic development are finely regulated by a complex transcriptional network that involves members of different families: GATA-binding TFs GATA-1 and GATA-2; ETS factors FLI1 and GABP α ; Krüppel-containing factors KLF1 and leukaemia/lymphoma-related factor (LRF); basic helix-loop-helix factor SCL/TAL1; transcriptional regulators such as friend of GATA-1 (FOG-1) and LIM domain binding 1 (LDB1), among others (reviewed by (Dore and Crispino 2011)). GATA-1 is one of the most extensively studied TFs involved in haematopoiesis. Expression of GATA-1 is essential for the terminal development of erythrocytes, megakaryocytes, eosinophils and mast cells (Weiss and Orkin 1995; Shivdasani *et al.* 1997; Yu *et al.* 2002; Migliaccio *et al.* 2003), and absence of either GATA-1 or GATA-2 in mice results in embryonic death associated with anaemia (Pevny *et al.* 1991; Tsai *et al.* 1994). GATA-2 is expressed in megakaryocytes and erythroid cells, and its overexpression was shown to shift erythroid to megakaryocytic development (Ikonomi *et al.* 2000). During erythropoiesis, GATA-2 expression is downregulated as GATA-1 is activated (Welch *et al.* 2004) and enforced GATA-2 expression inhibits erythroid development (Persons *et al.* 1999), possibly by interfering with GATA-1 regulatory mechanism. Transcriptional activation and repression by GATA-1 in erythroid cells involves different target genes and binding partners, including FOG-1. This partnership is important for globin expression and downregulation of c-KIT in mature erythroid cells (Vakoc *et al.* 2005; Jing *et al.* 2008). SCL is an additional GATA-1 target gene critical for HSC generation as well as lineage specification, and the cause of embryonic death when absent in mice (Robb *et al.* 1995; Shivdasani *et al.* 1995; Porcher *et al.* 1996). Furthermore, both erythroid and megakaryocytic development are significantly

disrupted in SCL-deficient mice (Mikkola *et al.* 2003). Other members of the GATA-nucleated complex include LMO-2, E2A (also known as TCF3), LDB1 and CBFA2T3 (or MTG16/ETO2) (Fujiwara *et al.* 2009).

KLF1 is of great importance for later stages of erythroid development, and its expression was shown to be confined to the erythroid lineage fate (Southwood *et al.* 1996). KLF1 interacts with GATA-1 and the BMP4/SMAD pathway in erythroid cells (Merika and Orkin 1995; Adelman *et al.* 2002; Tallack *et al.* 2010). Loss of KLF1 results in foetal death due ineffective definitive erythropoiesis and anaemia in mice (Nuez *et al.* 1995; Perkins *et al.* 1995). Mutations in human KLF1 have also been associated with anaemias, some of which displaying abnormal terminal maturation (Arnaud *et al.* 2010). ChIP-seq and NGS technologies have revealed the vast repertoire of KLF1 target genes associated with cell cycle, haemoglobin production, transcription, apoptosis, among others (Tallack *et al.* 2010; Tallack *et al.* 2012; Magor *et al.* 2015). Further studies show that KLF1 regulates cell cycle exit and is functionally important for enucleation (Gnanapragasam *et al.* 2016). Therefore, haematopoiesis requires not only an ordered succession of lineage-specific TFs, but also fine-tuning of their expression levels to coordinate normal development.

1.2 Acute Myeloid Leukaemia

AML is a type of malignancy characterised by the aberrant growth and development of HSC, leading to the accumulation of immature myeloid cells in the BM and peripheral blood (PB). AML is the most common type of acute leukaemia in adults, with more than 3,000 new AML cases being diagnosed in the United Kingdom every year (Cancer Research UK). Clinical outcome is poorer for AML patients over 60 years old compared to younger patients, however survival rates have improved substantially over the past 30 years with advances in healthcare systems and treatments (Derolf *et al.* 2009; Sant *et al.* 2014). In particular, 1-year survival has increased for all age groups, whereas 5- and 10-year survival was more significant in AML patients under 60 years old (Derolf *et al.* 2009). Poor survival in elderly AML patients is usually associated with the presence of more comorbidities in this age group that prevent curative regimens (Sant *et al.* 2014). Symptoms initially appear in only a few weeks, and the clinical presentation at diagnosis is variable. Typical symptoms of AML associated with BM failure include fatigue, persistent infections and haemorrhage due

to anaemia, neutropaenia, and thrombocytopaenia, respectively (Khwaja *et al.* 2016). Diagnosis is based on the percentage of myeloid blasts present in the BM and PB coupled with immunophenotyping and cytogenetic/molecular characterisation of myeloid blasts (1.2.2).

AML is classified into seven main subtypes in terms of genetic, morphological and cytochemical criteria according to the World Health Organisation (WHO) latest system (Arber *et al.* 2016) (1.2.1). Currently, newly diagnosed AML patients are genetically tested according to the European Leukaemia Network (ELN) recommendations (Dohner *et al.* 2017), which is usually performed by reverse transcription polymerase chain reaction (qRT-PCR). Mutational and cytogenetic profiling by NGS, which allows cost-effective sequencing of several genes or whole exome/genome in a short period of time, has led to changes in classification, risk stratification, treatment options and response assessment in AML (Leisch *et al.* 2019). Although NGS has opened new perspectives of individualised diagnosis and treatments of AML patients, its clinical value needs to be further defined (Bacher *et al.* 2018).

1.2.1 Molecular pathogenesis and classification system of AML

Cytogenetic analysis and genome profiling of AML have been incorporated and refined over the years to improve prognosis and treatment for AML (1.2.3). Two main classification systems have been used to stratify AML into different subtypes, the French-American-British (FAB) system and the most recent WHO classification system (Table 1-1). The FAB classification was devised in the 1970s based only on cellular morphology and cytochemistry, classifying AML into M0 (undifferentiated acute myeloblastic leukaemia) to M7 (acute megakaryoblastic leukaemia) subtypes (Bennett *et al.* 1976). To account for cytogenetics, the WHO classification system was developed and subsequently updated in 2016, stratifying AML into seven main groups (Arber *et al.* 2016). Representing approximately 20% of all AML cases, t(8;21)(q22;q22.1) and inv(16)(p13.1q22) are classified as core binding factor (CBF) AML, and form the RUNX1-ETO and CBF β -MYH11 fusion proteins, respectively (Sood *et al.* 2016). Both abnormalities cause the disruption of genes encoding the subunits of the heterodimeric TF CBF (i.e. RUNX1 and CBF β), which are required for normal haematopoiesis (Okuda *et al.* 1996; Wang *et al.* 1996b).

Table 1-1 – WHO classification of cytogenetically and molecularly defined subtypes of AML (2016 revision).APL – Acute promyelocytic leukaemia; NOS – not otherwise specified. Adapted from (Arber *et al.* 2016).**AML and related neoplasms**

AML with recurrent genetic abnormalities
AML with t(8;21)(q22;q22.1); <i>RUNX1-RUNX1T1</i>
AML with inv(16)(p13.1q22) or t(16;16)(p13.1;q22); <i>CBFB-MYH11</i>
APL with <i>PML-RARA</i>
AML with t(9;11)(p21.3;q23.3); <i>MLLT3-KMT2A</i>
AML with t(6;9)(p23;q34.1); <i>DEK-NUP214</i>
AML with inv(3)(q21.3q26.2) or t(3;3)(q21.3;q26.2); <i>GATA2, MECOM</i>
AML (megakaryoblastic) with t(1;22)(p13.3;q13.3); <i>RBM15-MKL1</i>
Provisional entity: AML with <i>BCR-ABL1</i>
AML with mutated <i>NPM1</i>
AML with biallelic mutations of <i>CEBPA</i>
Provisional entity: AML with mutated <i>RUNX1</i>
AML with myelodysplasia-related changes
Therapy-related myeloid neoplasms
AML, NOS
AML with minimal differentiation
AML without maturation
AML with maturation
Acute myelomonocytic leukaemia
Acute monoblastic/monocytic leukaemia
Pure erythroid leukaemia
Acute megakaryoblastic leukaemia
Acute basophilic leukaemia
Acute panmyelosis with myelofibrosis
Myeloid sarcoma
Myeloid proliferations related to Down syndrome
Transient abnormal myelopoiesis (TAM)
Myeloid leukaemia associated with Down syndrome

In general, CBF AML patients have a favourable prognosis, with more than 85% achieving complete remission (CR) (Sood *et al.* 2016) (1.2.2). An additional recurring abnormality in AML is the t(15;17)(q22;q21), which generates the PML-RARA fusion protein and defines acute promyelocytic leukaemia (APL) (10-15% of AML cases) (Bassi and Rego 2012). APL is a biologically and clinically different subtype of AML, previously associated with a poor prognosis, is currently highly curable with success rates of approximately 90-95% CR (Lo-Coco *et al.* 2013; Sanz *et al.* 2019) (1.2.3).

FLT3 is one of the most mutated genes found in AML patients (30% of total AML cases (Daver *et al.* 2019)), accompanied by nucleophosmin (*NPM1*, 30% (Lachowiez *et al.* 2020)) and DNA methyltransferase 3A (*DNMT3A*, 20% (Park *et al.* 2020)). *NPM1* mutations are usually associated with a favourable prognosis, whereas *FLT3*-internal tandem duplication (ITD) confers a poor prognosis to AML patients (Daver *et al.* 2019; Lachowiez *et al.* 2020). These cooperating mutations and others have been described and classified in AML according to functional groups, including TFs, epigenetic modifiers, activated signalling pathways, and spliceosome or cohesin complex mutations (Khwaja *et al.* 2016). Although the combination of mutations is variable in AML, certain cooperating mutations are specific, such as *GATA2* and *CEBPA* mutations, implying a functional cooperation between both TFs (Greif *et al.* 2012a).

In addition to well established AML subtypes, new heterogenous groups were defined including AML with mutated *RUNX1* or AML with *BCR-ABL1*. Genetic profiling of a large cohort of AML patients revealed additional heterogenous genomic classes: AML with mutations in chromatin and RNA splicing genes; AML with *TP53* mutations; and AML with isocitrate dehydrogenase 2 IDH2^{R172} mutations (Papaemmanuil *et al.* 2016). Further characterisation of the genomic landscape of AML, with significant contributions from The Cancer Genome Atlas (TCGA) genomic programme (Cancer Genome Atlas Research *et al.* 2013), have expanded the current knowledge of genes associated with leukaemia. Common mutations in AML, such as *DNMT3A*, *CEBPA* or *RUNX1*, were shown to be mutually exclusive of TF fusions, which implies similar functions to fusion genes in the initiation of AML (Cancer Genome Atlas Research *et al.* 2013). Furthermore, a few AML patients with a complex cytogenetic profile (poor risk) were significantly associated with tumour protein p53 (*TP53*) mutations. Overall,

this study provided a better understanding of AML pathogenesis governed by genetic abnormalities.

1.2.1.1 Leukaemia stem cells

AML is a rapidly evolving disease characterised by the accumulation of clonal myeloid progenitor cells incapable of differentiate into mature haematopoietic cells. Similar to normal haematopoiesis, AML is organised hierarchically with self-renewing leukaemia stem cells (LSC) driving the disease long-term in immunocompromised mice (Lapidot *et al.* 1994; Bonnet and Dick 1997). In terms of their immunophenotype in CD34⁺ AML (~ 75%), LSC were shown to mainly reside in the CD34⁺CD38⁻ fraction resembling LMPP, and occasionally in the CD34⁺CD38⁺ population resembling GMP (Goardon *et al.* 2011). Both populations were shown to coexist in around 80% of patients in a hierarchical manner with LMPP-like LSC giving rise to GMP-like LSC, but not the contrary (Goardon *et al.* 2011). An additional MPP-like LSC population within the CD34⁺CD38⁻ fraction was also observed in 10 to 15% of cases. Furthermore, gene expression profiling showed that these LSC populations were more similar to their normal counterpart progenitors than normal HSC, suggesting that LSC could arise from a self-renewing progenitor rather than stem cells (Goardon *et al.* 2011).

Understanding the properties of human LSC is of utmost importance for the development of targeted therapies for AML. Several studies have shown that LSC are quiescent in nature, a mechanism involved in LSC intrinsic resistance to conventional therapies (Hope *et al.* 2004; Ishikawa *et al.* 2007; Saito *et al.* 2010). Considering that quiescence cells have low energy requirements, LSC were shown to have low reactive oxygen stress suggestive of a reduced oxidative metabolism (Lagadinou *et al.* 2013). Further studies have revealed an increase in LSC frequency between diagnosis and relapse and have identified a significant change in the physiology of LSC following chemotherapy and upon relapse (Ho *et al.* 2016). Therefore, it is imperative that the increase in complexity and heterogeneity of LSC observed at relapse be considered in the design and evaluation of new therapeutic strategies.

Advanced genomic technologies have allowed the identification of pre-leukaemic cells in AML patients that possess early competitive driver mutations, usually in epigenetic regulator genes, and are capable of non-leukaemic differentiation (Jan *et al.* 2012). The driver mutations observed in pre-LSC are preserved in AML

blasts, implicating them as initiating events and establishing clonal expansion as the initial step in leukaemogenesis (Shlush *et al.* 2014). As opposed to AML blasts, pre-LSC resist chemotherapy and remain in the BM at remission, supporting a possible leukaemic transformation (Corces-Zimmerman *et al.* 2014; Shlush *et al.* 2014). Therefore, pre-LSC should be considered in future targeted therapies to prevent relapse (1.2.3).

Early evidence for the accumulation of serial mutations and/or epigenetic events in self-renewing HSC arose from studies in t(8;21) AML, suggesting that RUNX1-ETO is acquired in pre-leukemic HSC. *RUNX1-ETO* transcripts are detected in most t(8;21) patients in long-term remission, and its expression was previously found in a fraction of myeloid colony-forming cells in t(8;21) AML remission marrow (Miyamoto *et al.* 1996; Miyamoto *et al.* 2000). Further, RUNX1-ETO was shown to remain stable at relapse, whereas additional mutations were highly dynamic (Krauth *et al.* 2014). Conditional knock-in mouse studies showed that RUNX1-ETO alone is insufficient to induce leukaemia, but RUNX1-ETO-expressing cells exhibited enhanced in vitro replating efficiency suggestive of enhanced self-renewal capacity (Higuchi *et al.* 2002). Induction of cooperating mutations in the presence of RUNX1-ETO resulted in the efficient development of leukaemia (Higuchi *et al.* 2002) (1.2.4). Together, the previous findings support the concept that initiating mutations confer a competitive advantage to pre-LSC without causing transformation of progenitor cells.

1.2.2 Epidemiology, diagnosis, and prognosis of AML

AML is considerably more common in male adults and the median age at diagnosis is 68 years old (Khwaja *et al.* 2016; Short *et al.* 2018). The incidence of AML has increased by 29% since the early 1990s in the U.K. (Cancer Research UK). Increasing prevalence of therapy-related AML could explain, to some extent, the rising incidence of AML (Short *et al.* 2018). These rates have varied among different age groups, with elderly patients (> 80 years old) registering the highest increase in AML incidence of 72% during the same period (Cancer Research UK). In addition, AML is strongly associated with ethnicity, with lower incidence rates reported in Hispanics, blacks and Asian/Pacific Islanders compared to whites (Kirtane and Lee 2017). Nevertheless, some minority groups exhibit worse survival. There is no predisposing risk factor in most AML cases (Short *et al.* 2018). However, exposure to DNA-

damaging agents, such as ionising radiation, benzene, or cytotoxic chemotherapy, can increase the risk of developing AML or another haematological malignancy (Khwaja *et al.* 2016). Relatives of AML patients and specific inherited disorders, including Down syndrome or Fanconi anaemia, are also associated with an increased risk of AML (Alter *et al.* 2010; Bhatnagar *et al.* 2016). Curiously, myeloid leukaemia of Down syndrome is rarely associated with the t(8;21) abnormality (Bhatnagar *et al.* 2016). In terms of survival, 70-80% of younger patients (< 60 years) should achieve CR following one or two induction treatments, which represents a significant improvement over the past years (Burnett *et al.* 2011). On the other hand, older patients receiving the same chemotherapy fail to respond the same way, and although 40% to 65% enters CR, 85% of AML patients over 60 years old relapses within 2 to 3 years (Burnett *et al.* 2011). Increased awareness of the genomic landscape of AML as a result of the rapid growth of affordable genome sequencing has contributed to the recent progress in AML therapy (DiNardo and Perl 2019). The approval of new target therapies provides increasingly effective treatment strategies for risk groups that until now were difficult to treat (1.2.3).

AML is diagnosed with the detection of 20% or more myeloid blasts, including myeloblasts, monoblasts or megakaryoblasts, within the BM or PB. However, there are exceptions to this requirement in which AML can be diagnosed based on the cytogenetics alone, namely t(8;21), inv(16) and t(15;17) AML (Dohner *et al.* 2017). Immunophenotyping and cytogenetic/mutational analysis are also used to further characterise AML and facilitate its categorisation into the different subtypes (1.2.1). Cell surface and cytoplasmic markers used for the diagnosis of AML include precursor markers, such as CD34, CD117 or CD13, and granulocytic and monocytic markers such as cytoplasmic myeloperoxidase and CD14, respectively (Dohner *et al.* 2017). Cytogenetics and molecular mutations are of utmost importance not only for the diagnosis of AML, but also for its prognosis and treatment options. In fact, cytogenetic and molecular analysis can also be used for risk stratification of AML patients into three categories: favourable, intermediate, and adverse risk/outcome (Table 1-2).

Table 1-2 – Genetic risk stratification of AML according to 2017 ELN recommendations.* Without adverse-risk genetic lesions. Adapted from (Dohner *et al.* 2017).

Risk category	Genetic abnormality
<i>Favourable</i>	t(8;21)(q22;q22.1); <i>RUNX1-RUNX1T1</i> inv(16)(p13.1q22) or t(16;16)(p13.1;q22); <i>CBFB-MYH11</i> Mutated <i>NPM1</i> without <i>FLT3-ITD</i> or with <i>FLT3-ITD</i> ^{low} (allelic ratio < 0.5) Biallelic mutated <i>CEBPA</i>
<i>Intermediate</i>	Mutated <i>NPM1</i> and <i>FLT3-ITD</i> ^{high} (allelic ratio ≥ 0.5) Wild-type <i>NPM1</i> without <i>FLT3-ITD</i> or with <i>FLT3-ITD</i> ^{low} * t(9;11)(p21.3;q23.3); <i>MLLT3-KMT2A</i> Cytogenetic abnormalities not classified as favourable or adverse
<i>Adverse</i>	t(6;9)(p23;q34.1); <i>DEK-NUP214</i> t(v;11q23.3); <i>KMT2A</i> rearranged t(9;22)(q34.1;q11.2); <i>BCR-ABL1</i> inv(3)(q21.3q26.2) or t(3;3)(q21.3;q26.2); <i>GATA2, MECOM</i> -5 or del(5q); -7; -17/abn(17p) Complex karyotype (≥ 3 abnormalities), monosomal karyotype Wild-type <i>NPM1</i> and <i>FLT3-ITD</i> ^{high} Mutated <i>RUNX1</i> (if not co-occurring with favourable AML subtypes) Mutated <i>ASXL1</i> (if not co-occurring with favourable AML subtypes) Mutated <i>TP53</i>

For instance, t(15;17) and CBF AML are associated with a good prognosis, whereas cytogenetically complex patients (three or more chromosomal abnormalities), inv(3) or t(6;9) AML have a poor prognosis in terms of clinical presentation and outcome (Dohner *et al.* 2017). Nonetheless, the prognostic value of several cytogenetic and molecular abnormalities is context-dependent and could vary with the presence or absence of other abnormalities (Dohner *et al.* 2017).

1.2.3 Treatment for AML

Management of AML is gradually changing with the approval of new therapies, the identification of new prognostic factors that influence treatment choices, and the expanding knowledge of leukaemogenesis and discovery of promising targets. Conventional treatment for AML can be divided into three different phases: induction, consolidation, and maintenance. An important factor to consider when choosing the best treatment option and dose intensity is age, which is usually associated with comorbidities. During the remission induction phase, AML patients are given standard chemotherapy involving a combination of cytarabine and an anthracycline, commonly daunorubicin or idarubicin (Khwaja *et al.* 2016; Short *et al.* 2018). This is usually followed by cycles of high dose cytarabine during the consolidation phase for favourable-risk patients (Khwaja *et al.* 2016). Allogeneic haematopoietic stem cell transplantation (HSCT) generally improves the outcome of intermediate and poor-risk AML patients, and requires profound considerations in terms of patient selection, donor, and optimal regimen (Short *et al.* 2018). The benefits of allogeneic HSCT in intermediate-risk patients are lower compared to the high-risk group, given their heterogeneity and better responses to standard chemotherapy compared high-risk AML patients (Koreth *et al.* 2009; Stelljes *et al.* 2014). Treatment options according to risk stratification of AML are associated with cure rates of approximately 35-45% for patients under 60 years old (Short *et al.* 2020). Comprising the majority of those diagnosed with AML, older patients (≥ 60 years) exhibit cure rates lower than 15% with this approach due to their poor tolerance to intensive treatment with increased mortality and higher predominance of adverse-risk genetic abnormalities (Short *et al.* 2020). Older patients unfit for intensive treatment have limited options, with low dose cytarabine or demethylation therapy providing only modest improvements (Burnett *et al.* 2007; Dombret *et al.* 2015). However, these treatment approaches are associated

with a median survival of 6 to 10 months, and therefore new effective therapies are needed for older AML patients (Short *et al.* 2020).

One of the greatest advances in the management of AML was the treatment of APL, which was associated with poor clinical outcome associated with fatal haemorrhages at diagnosis (Tomita *et al.* 2013). Currently, *all-trans* retinoic acid and arsenic trioxide are used for APL treatment, and act by inducing PML-RARA degradation and cell differentiation (reviewed in (Tomita *et al.* 2013)). This approach has significantly improved the outcome of APL patients, which achieve CR by almost 100% and a long-term survival of more than 98% (Lo-Coco *et al.* 2013; Burnett *et al.* 2015). Recent advances in the general understanding of AML pathogenesis resulted in the discovery and approval by the US Food and Drug Administration (FDA) of eight new promising targeted therapies for AML (reviewed in (Short *et al.* 2020)). These include inhibitors of mutant *FLT3*, *IDH1* and *IDH2*, *KRAS* and *NRAS*, *KIT* and *TP53*, resulting in improved outcomes for AML patients harbouring mutations in those genes. Mutant *FLT3* is constitutively activated, inducing cell proliferation whilst suppressing differentiation (Meshinchi and Appelbaum 2009). First-generation *FLT3* inhibitors (e.g. midostaurin) have a broad activity on non-*FLT3* targets, while second-generation (e.g. gilteritinib) have a more specific activity and thus less off-target effects (Short *et al.* 2020). For instance, midostaurin has shown significant improvement of overall survival (OS) in all *FLT3*-mutated patients (Stone *et al.* 2017) and was approved by FDA in April 2017 in combination with induction and consolidation therapies. Midostaurin is a multikinase inhibitor that also targets c-KIT, and mutations in its gene are present in approximately 25% of CBF AML patients, conferring a worse prognosis when compared to wild-type *KIT* patients (Cairolì *et al.* 2006). Introducing *KIT* inhibitors to induction and consolidation therapies of these patients has shown strong improvements in their clinical outcome (Paschka *et al.* 2018). Additional therapies have been developed to target the intrinsic apoptotic pathway involved in chemotherapy resistance and AML maintenance, including BCL-2, MCL1, and MDM2 inhibitors that can be used in patients with or without targetable mutations (Short *et al.* 2020). In late 2018, FDA approved the combination of the selective BCL-2 inhibitor venetoclax with either low dose cytarabine or demethylation therapy for older (≥ 75 years) or unfit AML patients following successful clinical trials (DiNardo *et al.* 2019; Wei *et al.* 2019). Despite improvements in remission rates and OS, primary and

adaptive resistance to targeted therapies constitute significant challenge in the management of AML (DiNardo *et al.* 2020). *FLT3*-ITD and *TP53* defects were shown to correlate with adaptive resistance to venetoclax alone as well as in combination with other therapies (DiNardo *et al.* 2020). Upregulation of MCL1 is another mechanism of resistance to venetoclax, and MCL1 inhibitors are currently being investigated in early clinical trials (Kadia *et al.* 2019). Conversely, mutations in *NPM1* or *IDH2* were associated with better response rates and prolonged remissions (DiNardo *et al.* 2020). These studies highlight the importance of genomic profiling for guiding future treatment options. Besides targeted therapies, immune-based strategies have also been developed and are currently in clinical trials, such as anti-CD33 antibody-drug conjugate, checkpoint inhibitors, or cellular therapies (reviewed in (Short *et al.* 2020)). Although these novel AML therapies have shown exciting improvements in clinical trials, they are only an option for a minority of patients.

1.2.4 The 8;21 translocation in AML

The t(8;21)(q22;q22.1) is one of the most common chromosomal abnormalities in AML, accounting for 12% of all AML cases (Lam and Zhang 2012). This cytogenetic group of patients present granulocytic maturation of AML blasts characterised by the expression of the cell surface markers CD13, CD19, CD34 and CD56 (reviewed by (Lin *et al.* 2017)). Early studies reported the molecular rearrangements of the *RUNX1* gene located on chromosome 21q22 with the *ETO* gene (eight twenty one, also known as *MTG8* or *RUNX1T1*) on chromosome 8q22, generating the RUNX1-ETO fusion protein (Miyoshi *et al.* 1991; Miyoshi *et al.* 1993) (Figure 1-3, 1.3.5). *ETO* is a member of the myeloid translocation gene family of transcriptional corepressors. An alternative fusion gene *ETO-RUNX1* is also generated by the t(8;21); however, absence of *ETO-RUNX1* mRNA expression in t(8;21) AML centred research on RUNX1-ETO (Peterson *et al.* 2007a). The causes of such rearrangements remain unclear. A previous study has found that Wnt signaling promotes the expression and the genomic proximity of *RUNX1* and *ETO* genes and could be involved in the generation of RUNX1-ETO (Ugarte *et al.* 2015). Although t(8;21) AML patients are generally associated with good prognosis, the heterogeneity of this subtype explains the 40% relapse rate of patients (Qin *et al.* 2017).

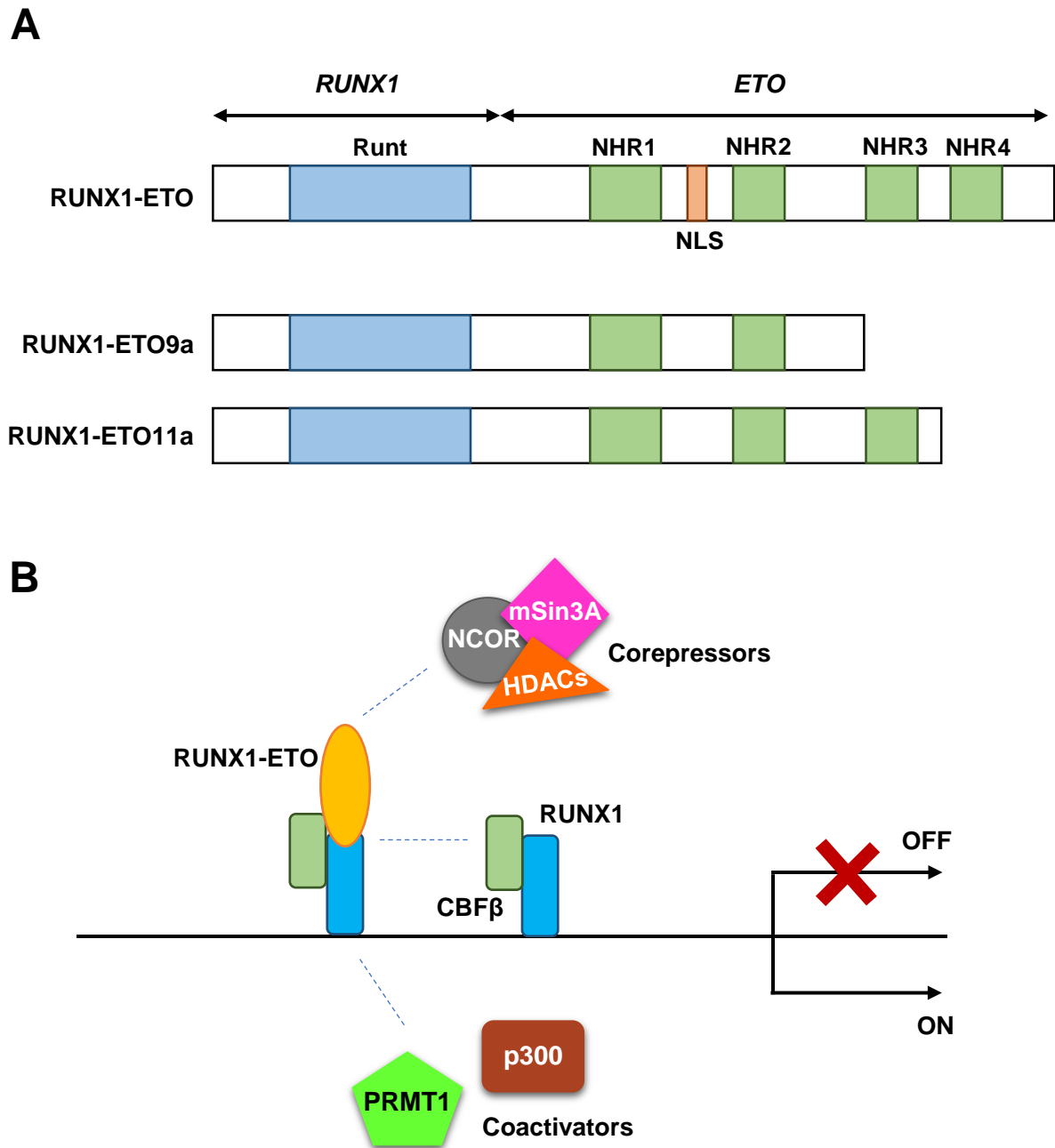


Figure 1-3 – Mechanisms of transcriptional regulation by RUNX1-ETO.

(A) Protein structure of full-length RUNX1-ETO and isoforms. RUNX1-ETO possesses the Runt domain (blue) and four Nerve homology regions (NHR1-4, green). The Runt domain is responsible for DNA binding and heterodimerisation with CBF β , whereas the NHR domains are involved in RUNX1-ETO leukaemogenesis. The nuclear localisation signal (NLS) is also represented in its structure (orange). Shorter isoforms RUNX1-ETO9a and 11a lack some of the NHR domain in the ETO regions. **(B)** Transcriptional repression and activation of genes by RUNX1-ETO involving the recruitment of corepressors and coactivators. Transcriptional repression of genes by RUNX1-ETO is represented by 'OFF', whereas activation is represented by 'ON'. Adapter from (Lin *et al.* 2017).

RUNX1-ETO transcript levels are used to monitor minimal residual disease in t(8;21) AML, with a < 3-log reduction in *RUNX1-ETO* between diagnosis and 12 months post-HSCT and/or < 4-log reduction for more than 12 months generally predicting relapse (Qin *et al.* 2017).

Expression of *RUNX1-ETO* in mice results in midgestational death due to the absence of foetal liver definitive haematopoiesis (Yergeau *et al.* 1997; Okuda *et al.* 1998), a result previously observed for *RUNX1*-deficient mice (Okuda *et al.* 1996; Wang *et al.* 1996a). In addition, *RUNX1-ETO* embryos exhibited abnormal monocytes or progenitors with enhanced self-renewal capacity (Yergeau *et al.* 1997; Okuda *et al.* 1998), which suggested that this fusion protein not only affects *RUNX1* native function, but also induces abnormal cell proliferation. Further, conditional knock-in mouse models showed that *RUNX1-ETO* fails to completely block differentiation of adult haematopoietic cells, and instead promotes their self-renewal capacity *in vitro* (Rhoades *et al.* 2000; Higuchi *et al.* 2002; Fenske *et al.* 2004). Similar results were observed using transplantation mouse models (de Guzman *et al.* 2002; Basecke *et al.* 2005). In human CD34⁺ HSPC, ectopic expression of *RUNX1-ETO* was shown to suppress erythroid and granulocytic development, with increasing self-renewal of progenitors (Mulloy *et al.* 2002; Tonks *et al.* 2003; Tonks *et al.* 2004). Recently, *RUNX1-ETO* expression in human embryonic stem cells was reported to block myeloid differentiation, inducing cell growth arrest, and interfere with *RUNX1* chromatin binding (Nafria *et al.* 2020). Although *RUNX1-ETO* plays an important role in leukaemogenesis by disrupting normal haematopoiesis, numerous studies have shown that *RUNX1-ETO* expression alone is incapable of inducing leukaemia in both mice and human cells (Rhoades *et al.* 2000; Yuan *et al.* 2001; Higuchi *et al.* 2002; Mulloy *et al.* 2003; Tonks *et al.* 2004). In the presence of additional genetic abnormalities, *RUNX1-ETO* was shown to promote leukemogenesis in different cell models (Schessl *et al.* 2005; Wang *et al.* 2011b; Zhao *et al.* 2014b; Goyama *et al.* 2016) (1.2.1.1). The collaborative abnormalities include chromosomal aberrations (loss of sex chromosomes, del(9q), trisomy 8), mutations in signalling pathways (*KIT*, *K/NRAS*, *FLT3-ITD/TKD*, *JAK2* and *CBL*), and mutations in epigenetic genes (*ASXL1/2* and *IDH1/2*) (reviewed by (Lin *et al.* 2017)). For instance, *KIT* mutations are commonly found in t(8;21) patients (Boissel *et al.* 2006; Krauth *et al.* 2014), and are associated with increased relapse rates following chemotherapy (Paschka *et al.* 2006)

(1.2.3). The combination of RUNX1-ETO expression with a specific *KIT* mutation (D816) was shown to have adverse impact on OS and event-free survival (EFS) (Schnittger *et al.* 2006; Krauth *et al.* 2014). Oncogenic cooperation between RUNX1-ETO and mutated *KIT* has been previously described in mice and human cells (Wang *et al.* 2011b; Nick *et al.* 2012; Wichmann *et al.* 2015). Although the majority of t(8;21) patients attain complete remission following induction therapy, further risk stratification based on additional genetic alterations may improve the outcome of these patients.

1.2.4.1 Mechanisms of leukaemogenesis by RUNX1-ETO

RUNX1-ETO structure encompasses the N-terminal region of RUNX1 and the majority of the ETO protein. The RUNX1 region includes the Runt homology domain, which is responsible for DNA binding and heterodimerisation with CBF β (1.3). ETO, on the other hand, comprises four evolutionarily conserved domains, the Nervy homology regions 1 to 4 (NHR1-4) (Lin *et al.* 2017) (Figure 1-3). NHR2 domain, in particular, was shown to promote the oligomerisation of RUNX1-ETO, which in turn contributes to leukaemic events (Liu *et al.* 2006; Yan *et al.* 2009). Conversely, disruption of NHR4 domain in RUNX1-ETO structure resulted in a rapid induction of leukaemogenesis, suggesting that NHR4 has important inhibitory effects in this process (Ahn *et al.* 2008). This domain along with NHR3 are absent in the truncated variant RUNX1-ETO9a, a fusion protein present in t(8;21) AML that was shown to induce leukaemia in mice (Ming *et al.* 2004; Yan *et al.* 2006; Yan *et al.* 2009). C-terminal truncated RUNX1-ETO9a has therefore been widely used in mouse models to study RUNX1-ETO leukaemogenesis (Link *et al.* 2016). RUNX1-ETO variants including RUNX1-ETO9a have been shown to equally transform human CD34⁺ HSPC compared with the full-length fusion protein (Wichmann *et al.* 2015; Link *et al.* 2016). RUNX1-ETO11a is an additional spliced isoform of RUNX1-ETO lacking the NHR4 domain that has been found co-expressed with full-length RUNX1-ETO in t(8;21) patients (Kozu *et al.* 2005), but no role in leukaemogenesis has been revealed.

Transcriptional regulation by RUNX1-ETO and binding partners

Several binding partners of RUNX1-ETO have been described in the literature over the last decades. (Assi *et al.* 2019). One of those partners is CBF β , as RUNX1-ETO retains the ability to heterodimerise with CBF β via Runt domain. The role of CBF β in RUNX1-ETO-mediated leukaemogenesis remains elusive, as it was shown to be

critical for RUNX1-ETO function by promoting DNA binding (Roudaia *et al.* 2009), but also dispensable for its oncogenic activity (Kwok *et al.* 2009). RUNX1-ETO is primarily considered to have repressive activity by cooperating with multiple corepressors, such as nuclear receptor corepressor/silencing mediator of retinoic acid and thyroid hormone (N-CoR/SMRT), histone deacetylases (HDAC) 1-3 and mammalian SIN3A (mSIN3A), and ultimately having a dominant negative effect over wild-type RUNX1 (Lutterbach *et al.* 1998; Wang *et al.* 1998; Amann *et al.* 2001; Zhang *et al.* 2001). These interactions were shown to result in the formation of a stable complex that mediates the repression of genes. This behaviour was further confirmed in ChIP-seq and transcriptomic analysis of t(8;21) transcriptional network, revealing that RUNX1-ETO complex preferentially recruits corepressors (Ptasinska *et al.* 2014). Genome-wide studies revealed that RUNX1-ETO cooperates preferentially with N-CoR than with the coactivator p300, and RUNX1-ETO/N-CoR co-occupancy establishes the leukaemic phenotype in t(8;21) cells (Trombly *et al.* 2015). Epigenetic regulators such as DNMT1 were also shown to interact with RUNX1-ETO and lead to transcriptional repression of genes (Liu *et al.* 2005).

Besides its important role in gene silencing, RUNX1-ETO is also involved in the transcriptional activation of several genes by interacting with epigenetic regulators, including p300 and protein arginine N-methyltransferase 1 (PRMT1) (Wang *et al.* 2011a; Shia *et al.* 2012). Acetylation of RUNX1-ETO promotes transcriptional activation and is important for leukaemic self-renewal and transformation promoted by RUNX1-ETO (Wang *et al.* 2011a). Arginine methyltransferase PRMT1 was identified as a binding partner of RUNX1-ETO9a, with loss of PRMT1 affecting the transcriptional activation of RUNX1-ETO9a target genes (Shia *et al.* 2012). In addition to epigenetic factors, a RUNX1-ETO/RUNX1 complex was shown to recruit activator protein 1 (AP-1) on chromatin to transactivate gene expression. p300 and PRMT1 were previously identified as important regulators of AP-1 (Albanese *et al.* 1999; Davies *et al.* 2013), suggesting that these three factors may participate together in the RUNX1-ETO/RUNX1 complex. Recently, transcriptional networks associated with different AML subtypes were established and AP-1 family was shown to be of high regulatory relevance among all (Assi *et al.* 2019).

In human t(8;21) cells, RUNX1-ETO was further shown to reside in an endogenous stable complex along with CBF β , E proteins HEB and E2A, LYL1, LMO2

and its binding partner LDB1 (Sun *et al.* 2013). This transcriptional complex was shown to regulate gene expression in leukaemia cells, and therefore contributes to leukaemogenesis (Sun *et al.* 2013). The ETS family members FLI1 and ERG were also shown to occupy similar genomic loci as RUNX1-ETO in these cells, and further found to regulate RUNX1-ETO transcription and facilitate its binding to DNA (Martens *et al.* 2012). Additional studies have demonstrated the indirect association of RUNX1-ETO with several haematopoietic regulators, such as C/EBP α , PU.1 and GATA-1 (Pabst *et al.* 2001; Vangala *et al.* 2003; Choi *et al.* 2006). RUNX1-ETO was shown to indirectly downregulate C/EBP α expression and PU.1 transcriptional activity (Pabst *et al.* 2001; Vangala *et al.* 2003), as well as preventing acetylation of GATA-1 which abrogates erythroid development (Choi *et al.* 2006). Together, the multiple functional interactions of RUNX1-ETO provide opportunities for its recruitment to several target genes and transcriptional regulation of key haematopoietic genes.

An unexpected partner of RUNX1-ETO in leukaemogenic transformation is RUNX1, which was initially believed to be inhibited by RUNX1-ETO as a central mechanism of t(8;21) AML. Indeed, RUNX1-ETO has been found to repress RUNX1 target genes by establishing a corepressor complex with multiple factors (Meyers *et al.* 1995; Wang *et al.* 1998; Amann *et al.* 2001; Zhang *et al.* 2001) and induce similar haematopoietic defects compared to RUNX1-deficiency in mice (Yergeau *et al.* 1997; Okuda *et al.* 1998). On the other hand, RUNX1 was found critical for the survival of t(8;21) cells through a delicate balance between its native function and RUNX1-ETO (Ben-Ami *et al.* 2013; Goyama *et al.* 2013). Mechanistically, this balance was characterised by an opposite transcriptional regulation of common target genes by RUNX1-ETO and RUNX1 (Ben-Ami *et al.* 2013). Further genome-wide studies in t(8;21) patient samples and cell lines revealed that 60% of RUNX1-ETO binding sites are shared with RUNX1, and highlighted the existence of a dynamic equilibrium between both complexes competing for equal genomic sites (Ptasinska *et al.* 2012; Ptasinska *et al.* 2014). In addition, wild-type RUNX1 was shown to form a complex with RUNX1-ETO on chromatin by binding to adjacent separate motifs and interacting via the Runt domain (Li *et al.* 2016). The relative binding signals of RUNX1-ETO and RUNX1 and recruitment of cofactors determine the transcriptional activation or repression of genes by RUNX1-ETO (Li *et al.* 2016). Clinical data shows that inactivating mutations of RUNX1 are frequently identified in multiple AML subtypes

apart from t(8;21) and inv(16) patients (Tang *et al.* 2009b; Schnittger *et al.* 2011), suggesting that native RUNX1 may support RUNX1-ETO-mediated leukaemogenesis. Moreover, the variant with a stronger leukaemogenic potential RUNX1-ETO9a showed attenuated repression of RUNX1 target genes compared to full-length RUNX1-ETO (DeKelver *et al.* 2013). Together, these findings suggest a complex relationship between RUNX1 and RUNX1-ETO in the development of AML.

Molecular mechanisms of RUNX1-ETO leukaemia

Over the years, gain and loss of function studies have provided valuable insights into the molecular mechanisms associated with the initiation and progression of leukaemia by RUNX1-ETO (Mulloy *et al.* 2003; Tonks *et al.* 2007; Ptasinska *et al.* 2012; Ben-Ami *et al.* 2013; Ptasinska *et al.* 2014; Mandoli *et al.* 2016; Martinez-Soria *et al.* 2018; Ptasinska *et al.* 2019). Loss of RUNX1-ETO in t(8;21) AML cells results in a complex but reversible change in chromatin structure, RUNX1 binding sites and gene expression (Ptasinska *et al.* 2012). Moreover, transcriptional programmes associated with proliferation, self-renewal, cell cycle dynamics, DNA synthesis, and myeloid development were disrupted by RUNX1-ETO absence (Ptasinska *et al.* 2012). RUNX1-ETO-deficient cells were characterised by a reduction in the CD34⁺CD38⁻ leukaemogenic cell population, along with enhanced proliferation and myeloid differentiation, with cells overcoming the RUNX1-ETO differentiation block (Ptasinska *et al.* 2012; Ben-Ami *et al.* 2013). Expression of C/EBP α was also upregulated following RUNX1-ETO depletion from t(8;21) AML cells, leading to a shift in the transcriptional network associated with myeloid differentiation (Ptasinska *et al.* 2014). A recent study identified cyclin D2 as a critical gene in RUNX1-ETO-driven leukaemogenesis (Martinez-Soria *et al.* 2018). Similar to previous RUNX1-ETO KD studies (Martinez *et al.* 2004), absence of cyclin D2 in t(8;21) cells suppressed cell proliferation characterised by a G0/G1 cell cycle arrest, suggesting that RUNX1-ETO promotes leukaemic growth and cell cycle progression by regulating cyclin D2 expression (Martinez-Soria *et al.* 2018). POU domain class 4 transcription factor 1 (POU4F1) was also shown to be significantly correlated with the t(8;21) AML transcriptional network, and KD studies revealed that loss of POU4F1 expression inhibits the proliferation of t(8;21) cells supporting previous results (Dunne *et al.* 2010; Assi *et al.* 2019).

Besides dysregulating the expression of important haematopoietic factors (Tonks *et al.* 2007), RUNX1-ETO has been shown to repress known tumour suppressor genes such as cyclin-dependent kinase inhibitor 2A (p14^{ARF} or *CDKN2A*) (Linggi *et al.* 2002). Interestingly, RUNX3, another member of the RUNX family of TFs and a putative tumour suppressor in solid tumours, has been found downregulated in t(8;21) AML (Cheng *et al.* 2008b) (1.4). Conversely, cyclin-dependent kinase inhibitor 1A (*CDKN1A*/p21^{WAF1}) expression is upregulated in t(8;21) AML (Peterson *et al.* 2007b). Disruption of important cellular processes such as proliferation, apoptosis, cell cycle progression, and differentiation by RUNX1-ETO suggests that this fusion protein modulates the expression of multiple genes involved in specific signalling pathways. RUNX1-ETO was shown to block the response to TGF- β 1 and given the relevance of this signalling pathway in growth and differentiation of cells, disruption of TGF- β signalling may contribute to leukaemogenesis (Jakubowiak *et al.* 2000). TPO/MPL signalling was shown to be upregulated in t(8;21) AML, leading to increased expression of the anti-apoptotic protein Bcl-xL important for the cell survival and self-renewal (Chou *et al.* 2012; Pulikkan *et al.* 2012). In addition, this signalling pathway was shown to provide a survival advantage to t(8;21) cells by activating the phosphatidylinositol 3-kinase (PI3K)/protein kinase B (PKB or AKT) axis (Pulikkan *et al.* 2012). Furthermore, RUNX1-ETO was found to activate Wnt signalling by upregulation of γ -catenin (Muller-Tidow *et al.* 2004; Tonks *et al.* 2007) and COX-2 (Zhang *et al.* 2013). Additional pathways have been associated with RUNX1-ETO-induced leukaemia, including the nuclear factor NF- κ B or the JAK-STAT pathway (Nakagawa *et al.* 2011; Lo *et al.* 2012).

Overall, increasing evidence shows that RUNX1-ETO promotes leukaemic transformation by cooperating with a multitude of transcriptional and epigenetic regulators in stable complexes to regulate transcriptional activation or repression of genes. The continuous technological advances will aid the development of targeted therapies to such complexes and pathways.

1.3 RUNX family of transcription factors

RUNX proteins belong to a family of TFs that plays an important role in the regulation of different developmental processes, such as proliferation, apoptosis, differentiation, and cell lineage determination (Mevel *et al.* 2019). Named after the

discovery of the developmental regulatory gene *runt* in *Drosophila melanogaster* (Nusslein-Volhard and Wieschaus 1980; Gergen and Butler 1988), the members of this family are evolutionarily old with extensive structural similarities (Levanon *et al.* 2003). RUNX1 was the first member identified as a nuclear factor binding to the Moloney murine leukaemia virus and polyomavirus enhancers, and it was originally named core binding factor α (CBF α) and polyoma enhancer binding protein 2 (PEBP2), respectively (Speck and Baltimore 1987; Kamachi *et al.* 1990). The gene was later found rearranged in t(8;21) AML patients and cloned on chromosome 21, and was designated *AML1* (Miyoshi *et al.* 1991). In mammals there are three RUNX genes with different tissue-specific expression patterns: *RUNX1*, localised on human chromosome 21q22, *RUNX2* (also known as *AML3*) on 6p21, and *RUNX3* (*AML2*) on 1p36 (Levanon *et al.* 1994). RUNX factors bind to the same DNA motif and function as transcriptional activators or repressors (Levanon and Groner 2004) involved in major developmental pathways, including TGF- β (Yano *et al.* 2006; Liu *et al.* 2015), Wnt (Ito *et al.* 2008), Notch (Burns *et al.* 2005; Nishina *et al.* 2011), and receptor tyrosine kinases (RTK) signalling pathways (Huang *et al.* 2012b), among others. The expression of each RUNX factor is tightly regulated by two distinct promoters (1.3.1), and misregulation of their expression or function by epigenetic modifications (1.3.2.1) contributes to the pathogenesis of numerous types of cancer (1.3.5).

1.3.1 RUNX structure and functions

A similar genomic structure is shared among the three mammalian RUNX genes (Figure 1-4). Their expression is finely regulated by a distal P1 and a proximal P2 promoter containing multiple RUNX binding sites, which suggests cross-regulation between distinct RUNX members (Rini and Calabi 2001; Levanon and Groner 2004). The P1 and P2 promoters regions vary in terms of their GC content as well as binding sites for different transcription factors (Bangsow *et al.* 2001). *RUNX1* is the largest member of the family containing 11 exons (Levanon *et al.* 2001b), whereas *RUNX3* is the smallest gene with 6 exons, all of which are conserved within the RUNX family (Bangsow *et al.* 2001). In addition, *RUNX3* gene possesses the highest level of the ancient Mammalian-wide interspersed repeat, supporting the idea that *RUNX3* is the evolutionary founder of the mammalian RUNX family (Bangsow *et al.* 2001).

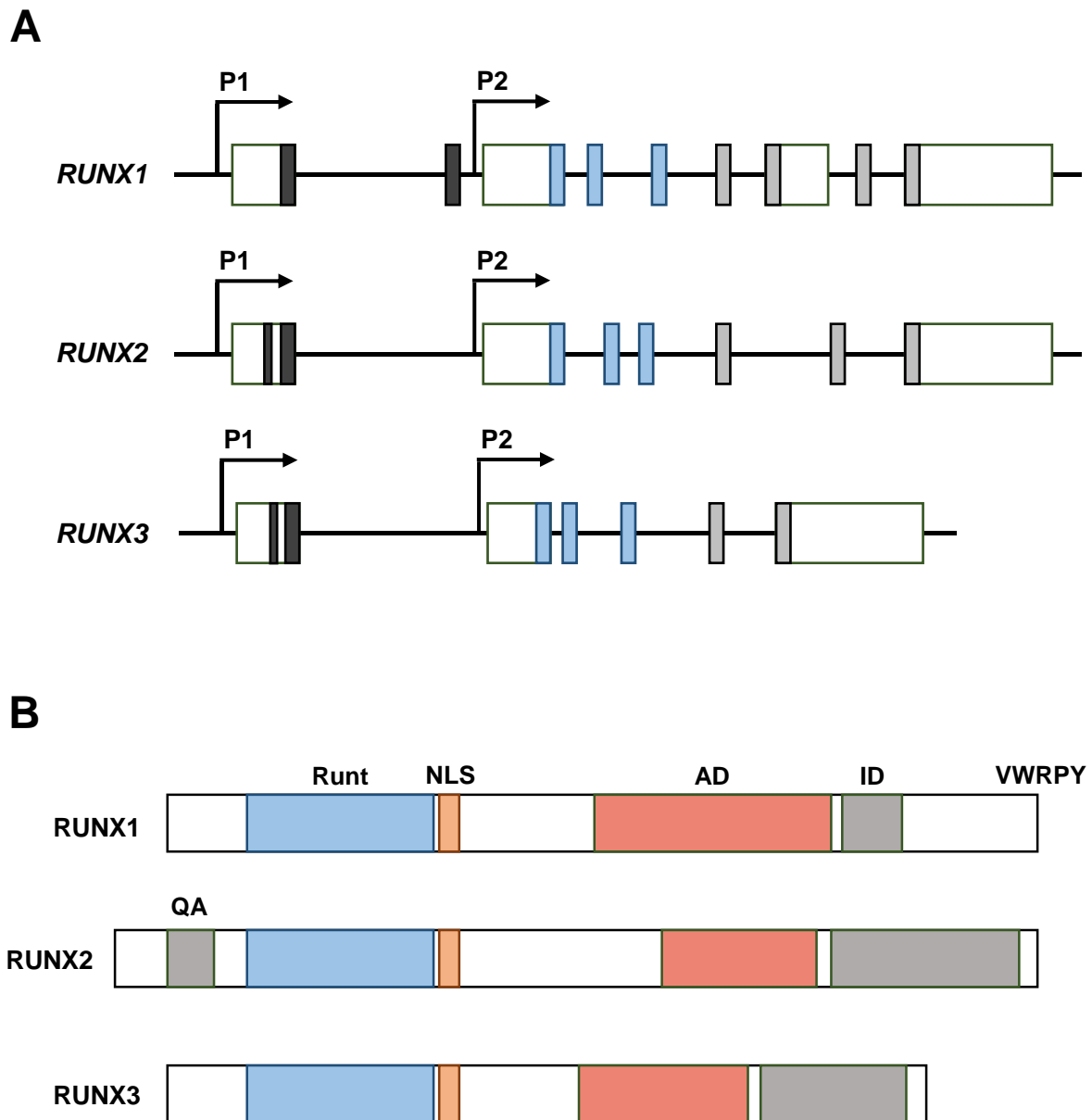


Figure 1-4 – Structural representation of the three mammalian RUNX genes and proteins.

(A) Conserved genomic structure of RUNX1 (Entrez Gene ID: 861), RUNX2 (Entrez Gene ID: 860), and RUNX3 (Entrez Gene ID: 864). Exons coding for the Runt domain are represented in blue, and exons coding for the transactivation domains are shown in grey. Untranslated regions are shown in white; **(B)** Structures of human RUNX1 (NP_001001890), RUNX2 (NP_001265407), and RUNX3 (NP_004341) proteins including the RUNX2-specific glutamine/alanine rich sequence (QA), Runt domain, nuclear localisation signal (NLS), activation domain (AD), inhibitory domain (ID) and the VWRPY motif. Adapted from (Mével *et al.* 2019).

Each promoter is induced at different developmental stages to generate RUNX isoforms with distinct N-terminal amino acid sequences (Ghozi *et al.* 1996; Fujiwara *et al.* 1999; Drissi *et al.* 2000; Bangsow *et al.* 2001). The combination of multiple promoters and alternative splicing results in a vast number of protein isoforms with diverse biological functions (Bae *et al.* 1994; Miyoshi *et al.* 1995; Tanaka *et al.* 1995; Stewart *et al.* 1997; Bangsow *et al.* 2001). RUNX1 has three protein isoforms: the truncated isoform RUNX1a and the most abundant RUNX1b both generated from the P2 promoter, and the rare RUNX1c isoform transcribed from the P1 promoter (Miyoshi *et al.* 1995). RUNX1a isoform has been shown to favour the expansion of the HSC compartment, whereas full-length RUNX1b and RUNX1c were shown to induce cell differentiation (Tsuzuki *et al.* 2007; Tsuzuki and Seto 2012). At least two isoforms with distinct N-terminus have been reported for RUNX2, type I (also known as PEBP2 α A or p56) transcribed from the P2 promoter, and type II (TIL-1, p57) generated from the P1 promoter (Fujiwara *et al.* 1999). Although both isoforms have been detected in chondrocytes and osteoblasts, *RUNX2* expression in osteoblasts was found to be mainly under the P1 promoter (Enomoto *et al.* 2000; Park *et al.* 2001). In RUNX3 case, P1 promoter generates the 46 kDa (RUNX3/p46), 33 kDa (RUNX3/p33), and the 27 kDa (RUNX3/p27) isoforms, while P2 promoter produces the 44 kDa (RUNX3/p44) isoform with an alternative N-terminus (Bangsow *et al.* 2001; Puig-Kroger and Corbi 2006; Puig-Kroger *et al.* 2010). The various RUNX isoforms have been shown to retain enhanced or reduced transactivation activities (Bae *et al.* 1994; Bangsow *et al.* 2001; Telfer and Rothenberg 2001). Furthermore, differences in the 5' and 3' untranslated regions of RUNX isoforms have an impact in their stability and translation efficiency (Pozner *et al.* 2000).

A highly conserved DNA binding Runt domain is present in each RUNX protein, consisting of a 128 amino acid sequence located near the N terminus (Figure 1-3) (Kagoshima *et al.* 1993). This critical domain is responsible for DNA binding at the consensus motif 'PuACCPuCA' (Kamachi *et al.* 1990), interactions with proteins (Meyers *et al.* 1993; Nagata *et al.* 1999), and their nuclear localisation (Osato *et al.* 1999; Michaud *et al.* 2002). The C-terminus is less conserved and has both inhibitory and activation domains responsible for the functional diversity of the RUNX proteins (Ito *et al.* 2015). In addition, the presence of a five amino acid sequence (VWRPY) is essential for the recruitment of the Groucho/transducing-like enhancer of split (TLE)

family of corepressors (Levanon *et al.* 1998; Yarmus *et al.* 2006). A conserved nuclear matrix-targeting signal sequence important for the nuclear localisation and regulation of RUNX activity can also be found in this region (Zeng *et al.* 1998; Zaidi *et al.* 2001).

The role of RUNX proteins in different systems has been explored over the years using KO mice. Early studies showed that deletion of either RUNX gene significantly impacted survival and uncovered important functions for each protein: RUNX1 is important for definitive haematopoiesis (Okuda *et al.* 1996; Wang *et al.* 1996a); RUNX2 is involved in skeletal development (Komori *et al.* 1997; Otto *et al.* 1997); and RUNX3 is essential for neurogenesis, thymopoiesis and gastric epithelium growth (Levanon *et al.* 2002; Li *et al.* 2002; Woolf *et al.* 2003).

1.3.2 Transcriptional regulation by RUNX proteins

RUNX factors represent the α subunit of a heterodimeric complex formed with their main partner CBF β (Figure 1-3) (Kamachi *et al.* 1990; Ogawa *et al.* 1993; Wang *et al.* 1993). Binding to CBF β through the Runt domain causes a localised conformational change and increases the affinity of this domain for DNA (Tang *et al.* 2000a; Tang *et al.* 2000b; Bravo *et al.* 2001). This complex is involved in the transcriptional regulation of several target genes through the recruitment of different coactivators and corepressors, as RUNX proteins are considered weak transcriptional regulators on their own (Chuang *et al.* 2013). RUNX factors have been shown to interact with multiple TFs, including C/EBP α , GATA-1, ETS, AP-1, SOX9, STAT5, and CDK9, among others (Elagib *et al.* 2003; Fujimoto *et al.* 2007; Ogawa *et al.* 2008; Wilson *et al.* 2010; Pencovich *et al.* 2011; Gilmour *et al.* 2018). Genome-wide studies have identified a cooperation between eight TFs critical for HSPC function that included RUNX1 along with SCL, PU.1, ERG, GATA-2, LMO-2, LYL1, MEIS1, FLI-1 and GFI1B (Wilson *et al.* 2010). A smaller transcriptional network including RUNX1, FLI1 and NF-E2 has been reported during terminal megakaryocyte development (Zang *et al.* 2016). Further studies showed that RUNX1 recruits CDK9, BRD4, LDB1 and the Mediator complex to RUNX1 binding sites of target genes during endothelial-haematopoietic transition (Gilmour *et al.* 2018). Cooperation between RUNX3 and GATA-3 has been demonstrated in T cell development (Kohu *et al.* 2009; Yagi *et al.* 2010). Physical interaction between the TCF-LEF family member TCF-1 and RUNX3 was also reported in CD4 silencing (Steinke *et al.* 2014). Overall, these interactions

usually occur through the Runt domain, and the different combinations of TF binding translate in the broad functions of RUNX factors (Chuang *et al.* 2013).

Despite being considered weak TFs alone, RUNX proteins have been suggested to act as pioneer factors able to interact with condensed chromatin and facilitate its opening, promoting the recruitment of other co-regulators (Hoogenkamp *et al.* 2009). In particular, RUNX1 is essential for transient chromatin remodelling during haematopoiesis (Hoogenkamp *et al.* 2009; Lichtinger *et al.* 2012), and RUNX3 was shown to open chromatin structure during cell cycle progression (Lee *et al.* 2019). Their important role as transcriptional activators or repressors is complex and tightly regulated. Indeed, RUNX1 can promote the expression of PU.1 in myeloid and B cells, while repressing its expression in T cells and megakaryocytes (Huang *et al.* 2008).

1.3.2.1 Post-translation modifications

Post-translation modifications of RUNX proteins are essential to regulate their transcriptional activity by modulating their stability, DNA binding, localisation, and protein-protein interactions (Table 1-3) (Blumenthal *et al.* 2017). The transcriptional activity of RUNX factors is usually associated with the recruitment of coactivators that possess histone acetyltransferase activity, such as the members of the lysine acetyltransferase family p300/CBP and MOZ (Kitabayashi *et al.* 2001; Jin *et al.* 2004). Acetylation of RUNX1 by p300 stimulates DNA binding (Yamaguchi *et al.* 2004), whereas acetylated RUNX2 and RUNX3 show enhanced transcriptional activity and protein stability, respectively (Jin *et al.* 2004; Jeon *et al.* 2006). Acetylated RUNX3 has been shown to interact with bromodomain-containing protein 2 (BRD2), inducing the transcription of p21^{WAF1} and p14^{ARF} (Lee *et al.* 2013). Deacetylation of RUNX3 during cell cycle progression results in the replacement of RUNX3-BRD2 complex by the RUNX3-HDAC4 complex and suppression of p21^{WAF1} and p14^{ARF} transcription. Therefore, RUNX3 plays an essential role in sensing aberrant proliferation signals, and its inactivation might contribute to uncontrolled cell cycle progression (Lee *et al.* 2013).

Table 1-3 – Summary of post-translational modifications of RUNX factors.Adapted from (Ito *et al.* 2015; Blumenthal *et al.* 2017).

RUNX	Enzyme	Modification	Transcriptional regulation	References
RUNX1	p300	Lysine acetylation	Activation	(Yamaguchi <i>et al.</i> 2004)
	MOZ	Lysine acetylation	Activation	(Kitabayashi <i>et al.</i> 2001)
	PRMT1	Arginine methylation	Activation	(Zhao <i>et al.</i> 2008)
	PRMT4	Arginine methylation	Repression	(Vu <i>et al.</i> 2013)
	PRMT6	Arginine methylation	Repression	(Herglotz <i>et al.</i> 2013)
	MLL	Lysine methylation	Activation	(Huang <i>et al.</i> 2011; Koh <i>et al.</i> 2013)
	ERK	Serine and threonine phosphorylation	Activation	(Tanaka <i>et al.</i> 1996; Yoshimi <i>et al.</i> 2012)
	PIM-1	Serine and threonine phosphorylation	Activation	(Aho <i>et al.</i> 2006)
	CDK	Serine and threonine phosphorylation	Activation	(Biggs <i>et al.</i> 2006; Zhang <i>et al.</i> 2008)
	HDAC	Deacetylation	Repression	(Lutterbach <i>et al.</i> 2000; Guo and Friedman 2011)
SRC	Tyrosine phosphorylation	Repression	(Huang <i>et al.</i> 2012b)	
RUNX2	p300	Lysine acetylation	Activation	(Sierra <i>et al.</i> 2003)
	MOZ	Lysine acetylation	Activation	(Pelletier <i>et al.</i> 2002)
	HDAC	Deacetylation	Repression	(Jeon <i>et al.</i> 2006)
	ERK	Serine and threonine phosphorylation	Activation	(Qiao <i>et al.</i> 2004)
RUNX3	p300	Lysine acetylation	Activation	(Jin <i>et al.</i> 2004)
	SMURF	Ubiquitination	Repression	(Jin <i>et al.</i> 2004)
	HDAC	Deacetylation	Repression	(Jin <i>et al.</i> 2004)
	SRC	Tyrosine phosphorylation	Repression	(Goh <i>et al.</i> 2010; Liu <i>et al.</i> 2012)
	PIM-1	Serine and threonine phosphorylation	Repression	(Kim <i>et al.</i> 2008b; Liu <i>et al.</i> 2020)
	MDM2	Ubiquitination	Repression	(Chi <i>et al.</i> 2009)

Methyltransferases are a group of histone modifying enzymes that regulate RUNX transcriptional activity, and can either enhance DNA binding (Zhao *et al.* 2008), or induce transcriptional repression (Herglotz *et al.* 2013; Vu *et al.* 2013). Mixed lineage leukaemia (MLL) lysine methyltransferase helps stabilise RUNX1 by inhibiting its poly-ubiquitination (Huang *et al.* 2011), whereas PRMT1 disrupts the association between RUNX1 and the corepressor SIN3A and promotes its transcriptional activity (Zhao *et al.* 2008). RUNX1-ETO and its truncated form RUNX1-ETO9a are also methylated by PRMT1, which in turn affects their regulatory functions (Shia *et al.* 2012).

Serine and threonine phosphorylation of RUNX factors by kinase signalling cascades can also promote their transcriptional activity in different cellular contexts (Imai *et al.* 2004; Aikawa *et al.* 2006; Kim *et al.* 2008b; Wee *et al.* 2008). Phosphorylation of RUNX1 by extracellular signal-regulated kinases ERK1 and ERK2 following cytokine stimulation enhances its transactivation activity (Tanaka *et al.* 1996), concomitant with the disruption of RUNX1-SIN3A interaction (Imai *et al.* 2004). Interestingly, the region containing ERK phosphorylation sites is absent in RUNX3, which suggests a differential regulation by ERK of RUNX3 protein (Bae and Lee 2006). RUNX1 phosphorylation status varies during cell cycle progression due to its phosphorylation by CDK1 and CDK6, which affects its ability to activate transcription as well as its stability (Biggs *et al.* 2006; Zhang *et al.* 2008). Similarly, RUNX2 is phosphorylated by cyclin D1-CDK4 (Shen *et al.* 2006). Moreover, phosphorylation by proto-oncogene PIM-1 results in enhanced transactivation properties of RUNX1 (Aho *et al.* 2006), as well as increased RUNX3 protein stability and cytoplasmic localisation (Kim *et al.* 2008b). Given the involvement of PIM-1 and the RAS-ERK pathway in cancer, misregulation of RUNX transcriptional activity by these proteins could contribute to tumourigenesis.

Repressive activity of the RUNX family members is also controlled by covalent modifications, including deacetylation by HDAC complexes (Amann *et al.* 2001; Westendorf *et al.* 2002), methylation (Herglotz *et al.* 2013; Vu *et al.* 2013), and phosphorylation processes (Goh *et al.* 2010; Huang *et al.* 2012b). For instance, transcriptional repression by RUNX proteins is important for normal haematopoiesis, with RUNX1 and RUNX3 being involved in CD4 silencing required for cytotoxic T cell development (Woolf *et al.* 2003). Several members of HDAC complexes have been

shown to interact with RUNX1, such as HDAC1, SIN3A and Gro/TLE (Levanon *et al.* 1998; Imai *et al.* 2004). Interestingly, an enhanced recruitment of corepressors was observed for RUNX1 fusion proteins compared to wild-type RUNX1, in particular TEL-RUNX1 and its higher affinity for SIN3A (Blumenthal *et al.* 2017). Moreover, HDAC4 and 5 have been shown to reverse RUNX2 acetylation and inhibit osteoblast differentiation (Jeon *et al.* 2006), while HDAC SIRT2 deacetylates RUNX3 and promotes its ubiquitination and subsequent degradation (Jin *et al.* 2004; Kim *et al.* 2011).

Methylation of RUNX1 can also lead to transcriptional repression. PRMT4 methyltransferase is highly expressed in haematopoietic stem cells and responsible for the formation of an inhibitory complex affecting myeloid differentiation (Vu *et al.* 2013). In addition, PRMT6 forms a corepressor complex with RUNX1 to regulate gene expression preceding megakaryocytic differentiation (Herglotz *et al.* 2013). This same developmental process is also impaired by RUNX1 tyrosine phosphorylation. Phosphorylation of RUNX1 by c-Src was shown to reduce RUNX1 interaction with CBF β , GATA-1 and FLI1 (Huang *et al.* 2012b). Similar to RUNX1, serine phosphorylation of RUNX2 disrupts its binding with CBF β and leads to its proteolytic degradation (Wee *et al.* 2002). Understanding how post-translational modifications influence RUNX function as tumour suppressors or oncogenes might contribute to novel approaches in cancer treatment.

1.3.3 Interplay of RUNX transcription factors

The presence of consensus RUNX binding sites in P1 and P2 promoters suggests an auto-regulatory mechanism by all RUNX members (Ghozi *et al.* 1996). RUNX1 has been found to regulate its own expression in haematopoietic cells (Martinez *et al.* 2016), while RUNX2 auto-regulation was shown in bone formation (Drissi *et al.* 2000). Cross-regulation of RUNX1 by RUNX3 has been demonstrated in human B lymphoid cells, resulting in the inhibition of RUNX1 transcription (Brady *et al.* 2009). Functional redundancy between RUNX proteins has been exposed previously, with some studies suggesting that expression of RUNX2 or RUNX3 is able to rescue haematopoietic development in RUNX1 deficient cells (Goyama *et al.* 2004; Fukushima-Nakase *et al.* 2005). Furthermore, RUNX1 and RUNX3 double KO mice studies implied a redundant function between these two RUNX members in the

Fanconi anaemia DNA repair pathway independent of their transcriptional role (Wang *et al.* 2014a; Tay *et al.* 2018). Functional overlap between family members can be seen in bone development with requirement of all RUNX members (Liakhovitskaia *et al.* 2010; Bauer *et al.* 2015), as well as in leukaemia (Morita *et al.* 2017). In recent studies, overexpression of RUNX3 in a TET2-deficient myelodysplastic syndrome (MDS) mouse model was shown to significantly repress RUNX1 expression and its target genes, including *Cebpa* and *Csf1r* (Yokomizo-Nakano *et al.* 2020).

Non-redundant functions between RUNX proteins are also described in the literature, explained in part by their specific spatiotemporal expression and requirements in different cellular and developmental contexts (Levanon *et al.* 2001a). For instance, the phenotype of RUNX2 and RUNX3 double KO mice in teeth development is different from the phenotype observed for single RUNX2 KO with no obvious compensatory mechanism between the two members (Wang *et al.* 2005). Furthermore, RUNX1 and RUNX3 are both expressed in mature T cells where they act sequentially to silence CD4 (Taniuchi *et al.* 2002). New technologies such as scRNA-seq should help elucidate the expression of all RUNX factors in specific cellular contexts and highlight their crucial and non-redundant functions.

1.3.4 RUNX transcription factors in normal haematopoiesis

RUNX factors are key players in normal haematopoiesis, essential for the ontogeny of the haematopoietic system and involved in critical processes in the lymphocytic and myeloid lineages (Mevel *et al.* 2019) (1.1). The functions of all three RUNX proteins in different systems using KO mouse models are summarised in Table 1-4. Expression of RUNX1 occurs in all developmental stages, and it is present in all haematopoietic cells apart from mature erythrocytes (North *et al.* 1999; North *et al.* 2002). Depletion of RUNX1 leads to midgestational lethality with a complete absence of foetal liver haematopoiesis (Okuda *et al.* 1996; Wang *et al.* 1996a). A similar effect was observed in CBF β -deficient mice, highlighting the importance of this complex for normal haematopoiesis (Wang *et al.* 1996b). Absence of RUNX1 in adult mice leads to a stronger expansion of the HSPC compartment with reduced apoptosis and ribosome biogenesis, inducing a pre-leukaemic condition (Ichikawa *et al.* 2004b; Growney *et al.* 2005; Jacob *et al.* 2010; Cai *et al.* 2011; Cai *et al.* 2015).

Table 1-4 – Summary of RUNX KO mouse models in normal haematopoiesis.

Gene	Phenotype	References
<i>Runx1</i>	Embryonic death with absence of definitive HSC	(Okuda <i>et al.</i> 1996; Wang <i>et al.</i> 1996a)
	Abnormal megakaryocyte and T/B cell development. Mild MPD with mild HSPC expansion and myeloid growth in aged mice	(Taniuchi <i>et al.</i> 2002; Ichikawa <i>et al.</i> 2004a; Gowney <i>et al.</i> 2005; Egawa <i>et al.</i> 2007; Seo <i>et al.</i> 2012)
	HSC expansion followed by their exhaustion	(Motoda <i>et al.</i> 2007; Jacob <i>et al.</i> 2010)
	Decreased proliferation and apoptosis with a minimal impact in the LT-HSC numbers	(Cai <i>et al.</i> 2011)
	Reduced HSPC growth, metabolism, and ribosome biogenesis. Increased stress resistance	(Cai <i>et al.</i> 2015)
<i>Runx3</i>	Embryonic, neonatal, and postnatal death. Impaired T cell development	(Taniuchi <i>et al.</i> 2002; Woolf <i>et al.</i> 2003; Brenner <i>et al.</i> 2004; Egawa <i>et al.</i> 2007; Ebihara <i>et al.</i> 2015; Milner <i>et al.</i> 2017)
	MPD with enhanced HSPC expansion	(Wang <i>et al.</i> 2013)
<i>Runx1/Runx3</i>	Lethality induced by BM failure, with abnormal Fanconi anaemia DNA-repair pathways and reduced haematopoietic mature cells	(Wang <i>et al.</i> 2014a)

In addition, RUNX1 deficiency impaired lymphoid development, and decreased platelet production (Ichikawa *et al.* 2004b; Gowney *et al.* 2005). Moreover, RUNX1 expression was shown to influence megakaryopoiesis (Kuvardina *et al.* 2015; Behrens *et al.* 2016) and to interact with AP-1, p300, GATA and ETS factors, among others (Elagib *et al.* 2003; Pencovich *et al.* 2011; Pencovich *et al.* 2013). The disruption of RUNX1 and CBF β interaction was shown to enhance myeloid differentiation, highlighting its importance for normal haematopoiesis (Illendula *et al.* 2016).

Although not as established as RUNX1 in haematopoietic development, RUNX3 is highly expressed in HSPC and its deletion in aged mice causes mild HSPC expansion and myeloid proliferation similar to RUNX1 conditional KO phenotype (Wang *et al.* 2013). An interplay between RUNX1 and RUNX3 has been found in a RUNX1/RUNX3 double KO model, with mice dying as a result of either bone marrow failure or MPD (Wang *et al.* 2014a). These contradictory phenotypes resemble Fanconi anaemia caused by defective DNA repair in which RUNX1 and RUNX3 are critical (Wang *et al.* 2014a; Tay *et al.* 2018). Moreover, bone marrow failure could be attributed to a decrease in all mature haematopoietic lineage compartments. In recent studies, RUNX3 downregulation was found to be associated with aging and abrogation of erythroid differentiation (Balogh *et al.* 2020). Overexpression of RUNX3 was recently shown to induce TET2-deficient MDS in mice, characterised by a disruption of cancer-related pathways and RUNX1-mediated haematopoiesis (Yokomizo-Nakano *et al.* 2020). Overall, these studies support an important role of RUNX3 in haematopoietic development, with misregulation of its expression contributing to the pathogenesis of different haematological malignancies.

RUNX factors have been associated with different immune cell subsets, with RUNX1 and RUNX3 being important for peripheral and thymic T cell differentiation (Taniuchi *et al.* 2002; Woolf *et al.* 2003; Sato *et al.* 2005; Egawa *et al.* 2007). Lineage determination between T helper CD4⁺ and cytotoxic CD8⁺ T cells is another process highly dependent on RUNX factors, as RUNX1 is crucial for the repression of CD4 transcription in thymocytes and RUNX3 in cytotoxic T cells (Taniuchi *et al.* 2002; Collins *et al.* 2011; Steinke *et al.* 2014). In addition, CD8 expression is induced by RUNX3 in the cytotoxic T cell fate (Kohu *et al.* 2005; Hassan *et al.* 2011).

1.3.5 Role of RUNX in AML

The oncogenic potential of the RUNX factors was first observed in animal models where they act as targets for transcriptional activation by murine leukaemia viruses (Stewart *et al.* 1997; Vaillant *et al.* 1999). RUNX proteins are known to have a dualistic role in cancer, being able to toggle between oncogene and tumour suppressor in different contexts (reviewed by (Blyth *et al.* 2005)). The importance of RUNX proteins in major biological processes explains its involvement in tumourigenesis (Figure 1-5). RUNX1 was identified as a tumour suppressor in prostate and lung cancers (Takayama *et al.* 2015; Ramsey *et al.* 2018), as well as an oncogene in skin and ovarian cancers (Scheitz *et al.* 2012; Keita *et al.* 2013). Contradictory roles for RUNX1 have been suggested in breast cancer: while RUNX1 downregulation has been extensively reported in breast cancer tissues (Ramaswamy *et al.* 2003; Kadota *et al.* 2010), recently identified RUNX1 mutations were considered to drive breast cancer progression (Pereira *et al.* 2016; Kas *et al.* 2017). An oncogenic behaviour of RUNX2 was observed in osteosarcoma where increased levels of RUNX2 were associated with early tumourigenesis and poor treatment response (Sadikovic *et al.* 2010; Martin *et al.* 2011). A pro-metastatic activity of RUNX2 was also found in breast and prostate cancer (Pratap *et al.* 2008; Akech *et al.* 2010). RUNX3 is generally accepted as a tumour suppressor in a variety of solid tumours where its inactivation arises mainly by epigenetic modifications (Ku *et al.* 2004; Wada *et al.* 2004; Ito *et al.* 2005; Kim *et al.* 2005; Lau *et al.* 2006; Sato *et al.* 2006). Mutations in the RUNX3 gene are rare, nonetheless reported in bladder and gastric cancers (Li *et al.* 2002; Kim *et al.* 2005). In fact, R122C mutant RUNX3 expression promoted tumour growth in gastric cells, conferring RUNX3 an oncogenic activity (Li *et al.* 2002). Similarly, RUNX3 overexpression in ovarian (Lee *et al.* 2011), head and neck carcinoma (Tsunematsu *et al.* 2009) and basal cell carcinoma (Salto-Tellez *et al.* 2006) is associated with malignancy.

RUNX1 is one of the most common targets for mutations and chromosomal abnormalities in haematological diseases, including AML, ALL, MDS, and Familial platelet disorder/AML (reviewed by (Mangan and Speck 2011)). In addition to RUNX1-ETO fusion protein generated by t(8;21) in AML (1.2), more than 50 chromosomal translocations involving RUNX1 have been reported (De Braekeleer *et al.* 2011). These include t(12;21) in paediatric ALL and t(3;21) in therapy-related AML and MDS

which form ETV6-RUNX1 (also known as TEL-RUNX1) and RUNX1-MECOM (MDS1 and EVI1 complex locus) fusion proteins, respectively (Nucifora *et al.* 1994; Golub *et al.* 1995). In addition, several mutations in RUNX1 have been reported over the years (Song *et al.* 1999; Preudhomme *et al.* 2000; Matsuno *et al.* 2003), representing approximately 3% of paediatric and 15% of adult *de novo* AML (Tang *et al.* 2009b; Greif *et al.* 2012b; Mendler *et al.* 2012; Skokowa *et al.* 2014). These mutations correlate with poor prognosis, older age and male gender compared to AML with wild-type RUNX1 (Tang *et al.* 2009b; Greif *et al.* 2012b; Mendler *et al.* 2012) (1.2.2). Moreover, RUNX1 mutations are frequently associated with FLT3-ITD or mutations in other driver genes (Gaidzik *et al.* 2011; Schnittger *et al.* 2011; Greif *et al.* 2012b; Mendler *et al.* 2012). These additional mutations support the growth of haematopoietic progenitor cells with abnormal development due to mutated RUNX1, inducing leukaemogenesis (Sood *et al.* 2017). Normal RUNX1 also plays an essential role in the development of leukaemia, being involved in RUNX1-ETO, CBF β -MYH11 and MLL fusion protein leukaemogenesis (Ben-Ami *et al.* 2013; Goyama *et al.* 2013) (1.2.4.1).

The oncogenic synergy between the RUNX factors and MYC has been demonstrated in lymphoma where RUNX2 was identified as a common target of retroviral insertional activation (Stewart *et al.* 1997; Vaillant *et al.* 1999). Further studies suggest that dysregulation of RUNX2 expression synergises with CBF β -MYH11 in AML (Castilla *et al.* 2004; Kuo *et al.* 2009). On the other hand, RUNX3 expression was shown to be an independent prognostic factor in childhood AML, with increased RUNX3 levels being associated with a shortened EFS (Cheng *et al.* 2008b). Furthermore, RUNX3 expression was found downregulated in prognostically favourable CBF-AML (Cheng *et al.* 2008b) (1.2.4.1). Downregulation of RUNX3 expression in *inv(16)* AML has been reported in different expression profiling studies (Debernardi *et al.* 2003; Guteerrez *et al.* 2005), further associated with RUNX3 hypermethylation in this particular subtype of AML (Estecio *et al.* 2015). No inactivating mutations of RUNX3 have been detected in AML (Otto *et al.* 2003). A more detailed summary of RUNX3 role in AML can be found in 1.4.2.3.

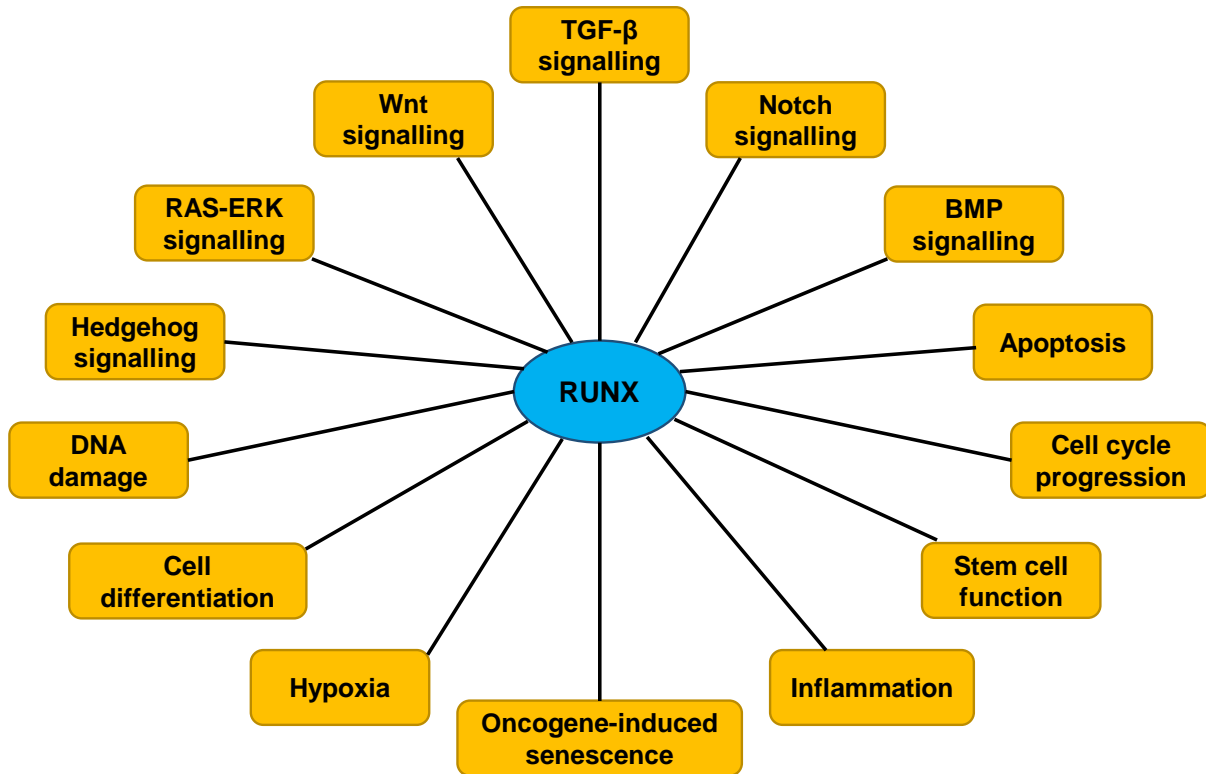


Figure 1-5 – Relationship between RUNX proteins and important signalling pathways and cellular processes.

RUNX proteins are involved in major biological processes in several tissues, and when their expression or function is disturbed it could lead to tumour initiation and progression. Figure adapted from (Ito *et al.* 2015).

1.4 RUNX3

RUNX3, the evolutionary founder of the mammalian RUNX gene family, was initially cloned based on RUNX1 and found to be located on human chromosome 1p36 (Levanon *et al.* 1994). RUNX3 is expressed in the haematopoietic system (Levanon *et al.* 1994; Meyers *et al.* 1996; Le *et al.* 1999; Levanon *et al.* 2001a), peripheral nervous system (Levanon *et al.* 2001a; Levanon *et al.* 2002; Chen *et al.* 2006; Kramer *et al.* 2006), epidermal appendages (Levanon *et al.* 2001a; Raveh *et al.* 2005), teeth (Yamashiro *et al.* 2002; Zheng *et al.* 2007), and skeleton (Levanon *et al.* 2001a; Yamashiro *et al.* 2002; Yoshida *et al.* 2004) (1.3.1).

KO studies in mice have shown the critical role of RUNX3 in different systems. For instance, RUNX3 KO mice develop sensory limb ataxia (Levanon *et al.* 2002), delayed chondrocyte maturation and severe congenital osteopenia (Yoshida *et al.* 2004; Bauer *et al.* 2015), and numerous defects in immunity and inflammation processes (Taniuchi *et al.* 2002; Woolf *et al.* 2003; Brenner *et al.* 2004; Fainaru *et al.* 2004; Levanon *et al.* 2014; Ebihara *et al.* 2015). RUNX3 is essential for the transcriptional regulation of genes related with growth, survival, and differentiation by participating in several signalling pathways (Chi *et al.* 2005; Ito *et al.* 2008; Nishina *et al.* 2011; Kim *et al.* 2020). Deregulation of such processes can lead to malignant events, with RUNX3 being implicated in gastric (Li *et al.* 2002; Ito *et al.* 2005), colorectal (Soong *et al.* 2009; Kim *et al.* 2020), breast (Lau *et al.* 2006; Huang *et al.* 2012a), and lung cancers (Sato *et al.* 2006; Lee *et al.* 2010), among others (1.3.5).

RUNX3 plays an important role regarding the development of sensory neurons (Inoue *et al.* 2002), and both RUNX1 and RUNX3 are believed to be downstream targets of the neurogenesis regulator Brn3a (Levanon *et al.* 2002). In addition, RUNX3 KO studies suggest that RUNX3 is a positive regulator of tropomyosin-receptor-kinase A (TrkA) and TrkC expression (Levanon *et al.* 2002; Nakamura *et al.* 2008). In cartilage and bone formation, RUNX3 was shown to be part of a regulatory cascade together with EGR1 and SOX9B TFs, which is associated with TGF- β /BMP signalling in zebrafish (Dalcq *et al.* 2012). The interaction of RUNX3 with SMAD proteins and therefore its involvement with the TGF- β and BMP signalling pathways has been extensively reported in the literature (Hanai *et al.* 1999; Jin *et al.* 2004; Chi *et al.* 2005; Yano *et al.* 2006).

1.4.1 Role of RUNX3 in the haematopoietic system

RUNX3 is predominantly expressed in cells of haematopoietic origin, including myeloid, B and T cell lineages, mature DC, spleen, thymus, BM, PB, and several normal and malignant haematopoietic cell lines (Meyers *et al.* 1996; Le *et al.* 1999; Levanon *et al.* 2001a; Taniuchi *et al.* 2002; Puig-Kroger *et al.* 2003; Woolf *et al.* 2003; Fainaru *et al.* 2004). Functional evidence implicating RUNX3 in haematopoiesis revealed that RUNX3 is selectively regulated by the retinoic acid receptor α signalling pathway (Le *et al.* 1999). In addition, RUNX3 expression can be induced by Epstein-Barr Virus infection (Spender *et al.* 2002) and by TGF- β 1 in B lymphoid cells (Shi and Stavnezer 1998). RUNX3 expression was shown to be upregulated during DC maturation and mediates their response to TGF- β (Fainaru *et al.* 2004). Within the CD8 T cell lineage, RUNX3 is considered a master regulator of their differentiation process as it is responsible for the silencing of CD4 and induction of CD8 expression (Woolf *et al.* 2003; Grueter *et al.* 2005; Sato *et al.* 2005; Yarmus *et al.* 2006). Moreover, RUNX3 is necessary for the induction of CD103 expression in T cells (Grueter *et al.* 2005; Yarmus *et al.* 2006; Woolf *et al.* 2007), and plays an important role in FOXP3 upregulation triggered by TGF- β (Klunker *et al.* 2009). A partnership between RUNX3 and T-BET was also uncovered in T cells, where RUNX3 is firstly induced by T-BET followed by a cooperation between both TFs to repress IL-4 and activate IFN- γ (Djuretic *et al.* 2007). Further studies showed that IFN- γ production induced by RUNX3 is actively suppressed by GATA-3 (Yagi *et al.* 2010). The expression of additional adhesion molecules and chemokine receptors associated with cell migration were shown to be regulated by RUNX3 in myeloid cells, such as CD11a, CD11c, CD49d, CCR7 and CD36 (Puig-Kroger *et al.* 2003; Fainaru *et al.* 2004; Dominguez-Soto *et al.* 2005; Fainaru *et al.* 2005; Puig-Kroger *et al.* 2006). Therefore, RUNX3 seems to be an important regulator of the adhesion molecules profile in haematopoietic cells.

In zebrafish, RUNX3 positively regulates the proliferation of primitive haematopoietic progenitors and participates in the development of definitive haematopoiesis (Kalev-Zylinska *et al.* 2003). RUNX3 role in haematopoiesis was further consolidated by RUNX3 KO studies showing that aged RUNX3 KO mice develop a MPD with a modest HSPC expansion (Wang *et al.* 2013). In addition, loss of RUNX3 led to hypersensitivity to G-CSF, promoting cell proliferation and mobilisation. Together, these results showed that RUNX3 *per se* is important for

haematopoiesis and possibly has distinct roles to RUNX1 in regulating the HSC behaviour (Wang *et al.* 2013). Furthermore, loss of both RUNX1 and RUNX3 in mice promoted the development of BM failure and MPD, accompanied by DNA damage response defects (Wang *et al.* 2014a). Recently, RUNX3 expression was confirmed in HSC and shown to decline with aging (Balogh *et al.* 2020). Elderly unexplained anaemia patients showed reduced RUNX3 levels associated with decreased erythroid colony forming ability. These results were further confirmed in KD studies, where loss of RUNX3 disrupted erythroid differentiation in human progenitor cells and dysregulated genes included key erythroid factors such as *KLF1* and *GATA1* (Balogh *et al.* 2020). Previously, RUNX3 has been suggested as a direct target of SCL, a key haematopoietic TF (Landry *et al.* 2008). The current findings suggest that RUNX3 is important for the maintenance of a lineage balance of haematopoietic progenitors within the BM.

1.4.2 Multifunctionality of RUNX3 in carcinogenesis

Since loss of RUNX3 expression due to hemizygous deletion and promoter hypermethylation was associated with gastric cancer (Li *et al.* 2002), RUNX3 has emerged primarily as a tumour suppressor for a variety of neoplasms. In these setting, defective levels of RUNX3 are mainly caused by promoter hypermethylation, inactivating mutations, protein mislocalisation and/or gene deletions (Ku *et al.* 2004; Xiao and Liu 2004; Ito *et al.* 2005; Kim *et al.* 2005; Lau *et al.* 2006). However, the role of RUNX3 in carcinogenesis is ambiguous, and its transcriptional activation suggests that RUNX3 has oncogenic potential (Tsunematsu *et al.* 2009; Lee *et al.* 2011; Selvarajan *et al.* 2017). Further investigations around the factors controlling RUNX3 function and its downstream targets are needed to understand such contrasting mechanisms.

1.4.2.1 Tumour suppressor activity of RUNX3

RUNX3 is located on human chromosome 1p36, a region frequently deleted in numerous types of cancer and thus associated with tumour suppressor activity (Bagchi and Mills 2008). RUNX3 silencing has been often associated with a poor prognosis of gastric (Wei *et al.* 2005; Hsu *et al.* 2009), oesophageal (Sakakura *et al.* 2007),

colorectal (Soong *et al.* 2009), lung (Li *et al.* 2004; Yanagawa *et al.* 2007), and bladder cancer (Kim *et al.* 2005; Kim *et al.* 2008a).

Hemizygous deletions of RUNX3 were previously found in gastric cancer tissues (Li *et al.* 2002), as well as lung, pancreatic and bile duct cell lines (Wada *et al.* 2004; Yanada *et al.* 2005). Other forms of RUNX3 inactivation have been reported in solid tumours over the years, such as hypermethylation of the CpG island at the RUNX3 promoter. Hypermethylation of RUNX3 was observed in gastric (Li *et al.* 2002; Kim *et al.* 2004; Oshimo *et al.* 2004; Chen *et al.* 2010), lung (Li *et al.* 2004; Yanada *et al.* 2005; Sato *et al.* 2006), breast (Lau *et al.* 2006; Subramaniam *et al.* 2009a), pancreatic (Wada *et al.* 2004; Nomoto *et al.* 2008), brain (Mueller *et al.* 2007), bladder (Kim *et al.* 2005; Kim *et al.* 2008a), colorectal (Ku *et al.* 2004; Soong *et al.* 2009), and hepatocellular carcinoma (Xiao and Liu 2004; Park *et al.* 2005). In fact, RUNX3 methylation status was proposed as one of five new markers to classify a subset of colorectal tumours (Weisenberger *et al.* 2006). Moreover, promoter hypermethylation of RUNX3 has shown potential as prognostic marker in lung (Yanagawa *et al.* 2007) and bladder cancers (Kim *et al.* 2008a; Yan *et al.* 2012). Enhancer of Zeste Homologue 2 (EZH2)-mediated histone methylation is an additional epigenetic mechanism that can lead to RUNX3 silencing (Fujii *et al.* 2008). This oncogene is essential for stem cell pluripotency and self-renewal and targets key developmental regulators such as RUNX3 (Lee *et al.* 2006). Other reported sources of RUNX3 hypermethylation include hypoxia (Lee *et al.* 2009), *Helicobacter pylori* (Katayama *et al.* 2009), and oestrogen exposure (Cheng *et al.* 2008a). Therefore, different environmental contexts can result in abnormal epigenetic silencing of RUNX3 and influence tumour progression.

Cytoplasmic sequestration of RUNX3 is another common event in tumorigenesis (Ito *et al.* 2005; Lau *et al.* 2006; Subramaniam *et al.* 2009a). Examples of well-established tumour suppressors that are also sequestered to the cytoplasm in cancer cells include *p27^{KIP}*, *BRCA1* and *pRb1* (Chuang and Ito 2010). RUNX3 cytoplasmic expression has been shown to increase with advancing colorectal tumour stage (Soong *et al.* 2009) and is associated with increased tumorigenicity of gastric epithelial cells in mice (Ito *et al.* 2005). This phenomenon might be attributed to post-translational modifications or other intracellular environmental events (Chuang and Ito 2010). Jun-activation domain-binding protein 1 (Jab1/CSN5) has been found to induce

nuclear exclusion and degradation of RUNX3 (Kim *et al.* 2009), a scenario equally promoted by oncoproteins MDM2 E3 ubiquitin ligase (Chi *et al.* 2009) and Src kinase (Goh *et al.* 2010). Moreover, hypoxia-induced upregulation of G9a histone methyltransferase and HDAC1 prevents nuclear translocation of RUNX3 (Lee *et al.* 2009). Overall, inactivation of RUNX3 is a significant risk factor for tumour progression and supports its tumour suppressive function.

Molecular mechanisms associated with RUNX3 tumour suppressive function

The tumour suppressor function of RUNX3 involves multiple mechanisms, including the transcriptional regulation of growth genes and/or disruption of DNA binding capacities of oncoproteins (Chuang *et al.* 2017) (Figure 1-6). RUNX3 has been shown to regulate cell proliferation and death by apoptosis (Chi *et al.* 2005; Yamamura *et al.* 2006; Yano *et al.* 2006; Kim *et al.* 2019), interact with DNA repair proteins (Tanaka *et al.* 2007), inhibit angiogenesis (Peng *et al.* 2006), and regulate cell adhesion and invasion (Sakakura *et al.* 2005). During TGF- β -mediated apoptotic cell death, RUNX3 interacts with SMAD proteins to directly upregulate the transcription of pro-apoptotic *BIM1* and enhance the expression of the cyclin-dependent kinase inhibitor *p21^{WAF1}* in gastric cancer cells (Chi *et al.* 2005; Yano *et al.* 2006; Yamada *et al.* 2010). TGF- β pathway has been found to stimulate the nuclear translocation of RUNX3 (Ito *et al.* 2005). These results suggest that RUNX3 is a downstream effector of the TGF- β signalling pathway. Furthermore, cooperation between RUNX3 and the Forkhead box O3a (FoxO3a), a key regulator of apoptosis and cell cycle, has been found to induce apoptosis by activating Bim and may represent an important tumour suppressive mechanism in gastric cancer (Yamamura *et al.* 2006). Loss of RUNX3 compromises TGF- β signalling, leading to increased proliferation in the gastric epithelia caused by reduced apoptosis and sensitivity to TGF- β 1 (Li *et al.* 2002). In addition, RUNX3 exerts its tumour suppressor activity by negatively regulating the oncogenic YAP and the YAP-TEAD complex, a nuclear effector of the Hippo signalling pathway (Qiao *et al.* 2016; Kulkarni *et al.* 2018).

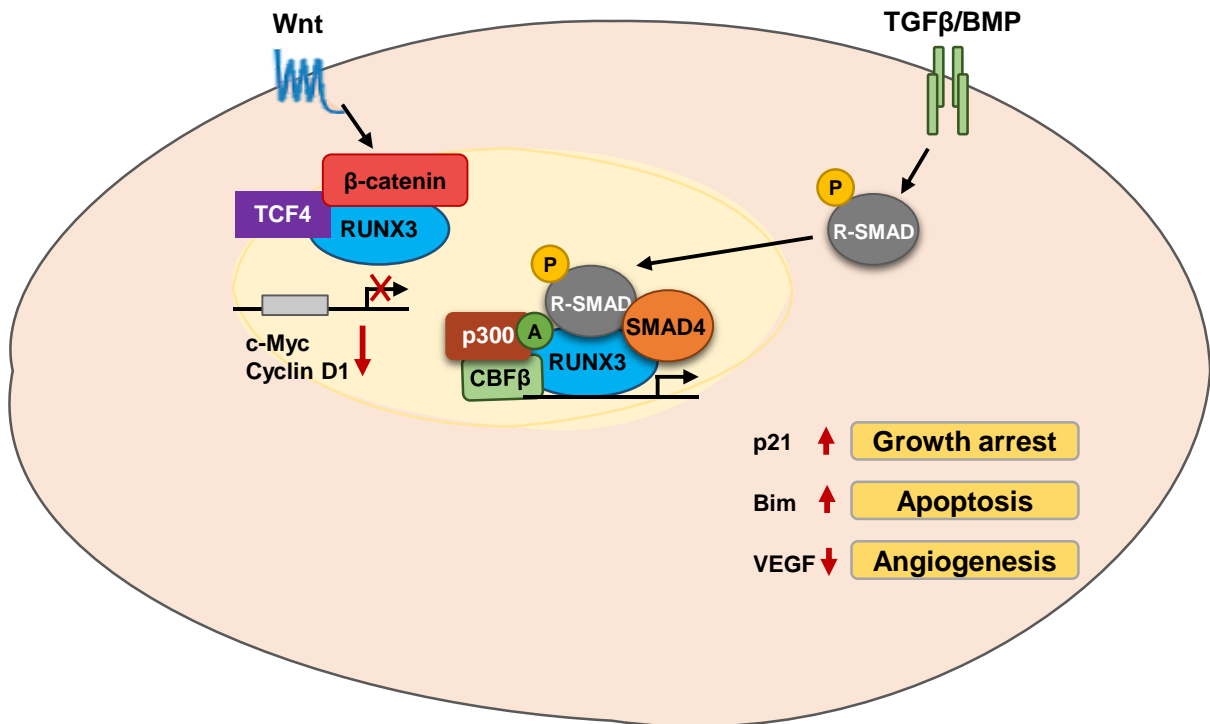


Figure 1-6 – Tumour suppressor activity of RUNX3.

Transcriptional regulation mediated by RUNX3 in cooperation with regulators and signalling pathways during tumourigenesis. RUNX3 suppresses the oncogenic Wnt pathway by recruiting the TCF4-β-catenin complex and blocking its binding to promoter sites, including c-MYC and cyclin D1. RUNX3 also interacts with SMAD to activate TGF-β-dependent growth arrest and apoptosis by induction of p21^{WAF1} and Bim, respectively. Figure adapted from (Chuang and Ito 2010; Chuang *et al.* 2017).

Intestinal epithelia of RUNX3-deficient mice exhibit enhanced Wnt signalling activity and upregulated expression of Wnt targets, such as c-MYC and cyclin D1 (Ito *et al.* 2008). Moreover, RUNX3 was shown to form a ternary complex with β -catenin/TCF4, attenuating the Wnt signalling activity (Ito *et al.* 2008; Sun *et al.* 2018). Whether RUNX3 activates or inhibits the Wnt signalling is however context dependent (Chuang *et al.* 2017).

In lung cancer RUNX3 has been found to protect against oncogenic *KRAS* by cooperating with co-activator BRD2 to induce the p53-p14^{ARF} pathway (Lee *et al.* 2013). RUNX proteins are able to act upstream of p53, with both RUNX1 and RUNX3 being capable of directly inducing p14^{ARF}, which functions to stabilise the p53 protein and possesses RUNX binding sites in its promoter (Linggi *et al.* 2002; Lee *et al.* 2013). Together, these studies provide evidence of an important tumour suppressive mechanism associated with RUNX3.

Restoring RUNX3 tumour suppressive function in cancer cells

Suppression of tumour cell migration and invasion is one of the main effects arising from restored RUNX3 expression in cancer cells and it has been reported in hepatocellular carcinoma (Gou *et al.* 2017), renal cell carcinoma (Chen *et al.* 2013), glioma (Sun *et al.* 2018), gastric (Liu *et al.* 2014a; Yu *et al.* 2017), and breast cancer (Chen *et al.* 2007). In addition, RUNX3 overexpression was shown to repress cancer cell migration, invasion and stemness properties by inactivating matrix metalloproteinase-2 (MMP-2) and MMP-9 expression, reducing vascular endothelial growth factor (VEGF) secretion, and suppressing Hedgehog signalling (Chen *et al.* 2011; Chen *et al.* 2014; Kim *et al.* 2016; Kim *et al.* 2020).

An additional mechanism implicating RUNX3 in carcinogenesis was revealed as a RUNX3-mediated pro-apoptotic pathway in response to DNA damage involving functional interaction between RUNX3 and p53. Forced expression of RUNX3 induced phosphorylation of p53 and proteolytic cleavage of PARP, enhancing the transcriptional and pro-apoptotic functions of p53 (Yamada *et al.* 2010). Ectopic expression of RUNX3 in gastric cancer cells was shown to suppress cell proliferation by inducing apoptosis, dysregulating the expression of apoptosis-related genes (Sakakura *et al.* 2005; Nagahama *et al.* 2008; Liu *et al.* 2014b). This was accompanied by an inhibition of peritoneal metastasis and transcriptional dysregulation of genes related to cell

adhesion, signal transduction, apoptosis, and immune responses (Sakakura *et al.* 2005). Furthermore, RUNX3 deficiency correlated with upregulation of VEGF expression and thus angiogenesis, which was suppressed by restoring RUNX3 expression in gastric cancer cells (Peng *et al.* 2006). Interestingly, overexpression of RUNX3 in a mouse model of adoptive T cell therapy for melanoma led to a delay in tumour growth with improved survival (Milner *et al.* 2017). A link between RUNX3 and proto-oncogene *MYCN* has also been established in neuroblastoma, with RUNX3 overexpression leading to reduced growth, migration activity and MYC stability. This study suggests that RUNX3 could overcome the oncogenic function of MYC and thus contributing to a favourable outcome in neuroblastoma patients (Yu *et al.* 2014). Overall, restoring RUNX3 expression in cancer cells has helped in elucidating the molecular mechanisms underlying RUNX3 tumour suppressive activity as well as potential therapeutic applications.

1.4.2.2 RUNX3 as an oncogene

RUNX proteins regulate important cellular processes by participating in important developmental signalling pathways, including TGF- β , Wnt, Notch, Hedgehog, Hippo, and RTK (Ito *et al.* 2015) (1.3). RUNX3 is silenced in numerous solid tumours (1.4.2.1), whereas its overexpression is observed in basal cell carcinoma where RUNX3 is considered to be a universal downstream effector of the Sonic Hedgehog pathway (Salto-Tellez *et al.* 2006). RUNX3 oncogenic function was also described in ovarian cancer (Nevadunsky *et al.* 2009; Lee *et al.* 2011), head and neck squamous carcinoma (Tsunematsu *et al.* 2009), and Ewing sarcoma (Bledsoe *et al.* 2014), with RUNX3 overexpression promoting cell growth and tumourigenesis. RUNX factors were first considered as oncogenes by retroviral insertional mutagenesis screens that showed a cooperation between all three murine Runx genes and the Myc oncogene in promoting leukaemogenesis (Stewart *et al.* 1997; Stewart *et al.* 2002; Wotton *et al.* 2002). Together, these findings suggest that RUNX3 has a dualistic role in cancer, acting as a tumour suppressor or oncogene in a cellular context-dependent manner (1.3.5).

Transcriptomic data showed that RUNX3 expression is upregulated in extranodal NK/T cell lymphoma nasal type cells compared to normal NK cells (Ng *et al.* 2011). Further, KD studies supported the role of RUNX3 as an oncogene in this type of lymphoma by showing an increase in apoptosis and a reduction in cell proliferation in

the absence of RUNX3 (Selvarajan *et al.* 2017). Targeted inhibition of MYC led to its downregulation as well as of RUNX3, followed by an enhanced apoptosis and growth arrest, which suggests that MYC may be a key upstream driver of RUNX3 upregulation in extranodal NK/T cell lymphoma (Selvarajan *et al.* 2017). Recently, RUNX3 overexpression was reported to induce the transcription of MYC target genes, disrupting haematopoiesis to facilitate the development of MDS (Yokomizo-Nakano *et al.* 2020).

Regulation of RUNX3 expression in pancreatic cancer is highly complex. SMAD4 dosage has been shown to regulate RUNX3 expression in a biphasic manner, with absence of SMAD4 expression being associated with increased RUNX3 levels as well as enhanced metastatic potential (Whittle *et al.* 2015). Concomitantly, RUNX3 induced p21^{WAF1} expression and inhibited proliferation of cells, suggestive of a dualistic role in pancreatic cancer and possibly mediated by TGF- β and p53 (Whittle *et al.* 2015). The oncogenic behaviour of RUNX3 can also arise from its cytoplasmic mislocalisation via PIM-1 serine/threonine kinase, a well-known oncoprotein (Aho *et al.* 2006; Kim *et al.* 2008b), resulting in the absence of nuclear partners of RUNX3 (Kim *et al.* 2008b). Overall, precise expression of RUNX3 is critical for normal cell growth and an oncogenic activity of RUNX3 seems to occur when its overexpression is combined with other critical growth abnormalities or interaction with additional oncogenes (Subramaniam *et al.* 2009b).

1.4.2.3 RUNX3 in leukaemogenesis

Although RUNX1 is the family member most extensively studied in leukaemogenesis, RUNX3 has also shown to be associated with this malignant process. A previous study showed that RUNX3 overexpression in BCR-ABL cells protected these cells from imatinib-induced apoptosis, suggesting that RUNX3 is involved in disease persistence in CML (Miething *et al.* 2007). In childhood AML, the correlation between RUNX3 expression and FLT3 mutations status remains unclear, with contrasting observations (Lacayo *et al.* 2004; Cheng *et al.* 2008b) (1.3.5). On the other hand, RUNX3 was shown to act as a tumour suppressor in cutaneous T cell lymphoma where RUNX3 expression is indirectly downregulated by TOX (Haider *et al.* 2016; Dulmage *et al.* 2019).

RUNX3 expression in AML is highly heterogeneous. Increased levels of RUNX3 were reported in t(15;17) APL patients, whereas decreased RUNX3 expression was

associated with CBF AML (Debernardi *et al.* 2003; Gutierrez *et al.* 2005; Cheng *et al.* 2008b) (1.3.5). Furthermore, RUNX1-ETO and CBF β -MYH11 fusion proteins were shown to repress RUNX3 via the conserved RUNX binding sites in the P1 promoter, with absence of P2 promoter methylation (Cheng *et al.* 2008b). Furthermore, RUNX3 was shown to be repressed by RUNX1-ETO via direct binding to its promoter, whereas CBF β -MYH11 cooperated with RUNX1 to downregulate RUNX3 (Cheng *et al.* 2008b). A later study showed that RUNX3 hypermethylation was highly frequent in inv(16) patients compared to other AML subtypes, as well as in ALL patients (Estecio *et al.* 2015) (1.3.5). RUNX3 silencing was reversed in cell lines by treatment with decitabine, a hypomethylating agent (Estecio *et al.* 2015). Together, these results suggest that RUNX3 expression might be useful to stratify prognostically distinct CBF-AML subtypes for future therapeutic approaches.

1.5 Aims and objectives

RUNX proteins play an important role in haematopoietic development and is therefore unsurprising that their dysregulation is associated with several malignancies including leukaemic transformation. The t(8;21) is one of the most common genetic abnormalities in AML and leads to the formation of the RUNX1-ETO fusion protein. Expression of RUNX1-ETO has been shown to induce severe transcriptional dysregulation of key haematopoietic genes, disrupting RUNX1 native function. Repression of RUNX3 is observed in prognostically favourable AML subtypes involving disruption of the CBF complex. However, half of these patients still relapse. Furthermore, increased RUNX3 levels are observed in non-CBF AML. RUNX3 is one of the least studied RUNX members, and its role in normal human haematopoiesis and leukaemia remains unclear. Therefore, this study aims to determine the impact of RUNX3 expression in normal human haematopoiesis and its involvement in RUNX1-ETO-induced abnormal phenotype of human HSPC. To achieve this, the following objectives will be addressed:

1. Determining the mRNA expression of *RUNX3* during normal haematopoiesis and its association with AML

Analysis of publicly available transcriptomic datasets using different human and murine haematopoietic subpopulations will be performed to establish *RUNX3* expression during haematopoietic development. Publicly available transcriptomic data

will also be analysed to determine *RUNX3* mRNA expression in different AML subtypes, including patients harbouring t(8;21).

2. Determine the effects of *RUNX3* overexpression or KD on normal human erythroid, monocytic and granulocytic development.

Transduced human HSPC will be cultured in bulk liquid culture and clonal conditions to assess the growth and differentiation of erythroid and myeloid cells (specifically monocytes and granulocytes).

3. Determining whether co-expression of *RUNX3* and *RUNX1-ETO* rescues the developmental block and colony forming ability of erythroid and myeloid *RUNX1-ETO*-expressing cells.

Human HSPC will be co-transduced with both *RUNX3* and *RUNX1-ETO* retroviruses and their growth and differentiation will be evaluated as above.

4. Determining the transcriptional dysregulation associated with abnormal haematopoiesis induced by *RUNX3* expression.

Total RNA will be extracted from human *RUNX3*-expressing HSPC and controls and transcriptomic (RNA-seq) data analysed to establish the transcriptional dysregulation associated with *RUNX3* overexpression in HSPC.

2 Materials and Methods

2.1 Materials

2.1.1 General reagents

General reagents used in this study are alphabetically listed below.

Table 2-1 – Summary of general reagents with supplier used in this study.

NEB – New England BioLabs; Cambridge Bio – Cambridge Biosciences.

Reagent	Supplier
0.05% w/v Trypsin-EDTA	Fisher Scientific, Loughborough, UK
1 kb DNA Ladder	NEB, Hitchin, UK
α -Minimum Essential Medium Eagle (MEM)	Merck Life Science, Gillingham, UK
β -Mercaptoethanol (β -ME, 14.3 M)	Merck Life Science, Gillingham, UK
AG [®] 501-X8(D) Mixed Bed Resin	Bio-Rad, Hertfordshire, UK
Amersham [™] ECL [™] Prime Western Blotting Detection Reagent	Cytiva, Little Chalfont, UK
Ampicillin (100 mg/mL)	Merck Life Science, Gillingham, UK
<i>Bam</i> HI-HF [®] (20,000 U/mL)	NEB, Ipswich, UK
BD FACS [™] Lysing Solution	BD Biosciences, Wokingham, UK
Benzonase Nuclease (25 U/mL)	Merck Life Science, Gillingham, UK
<i>Bgl</i> III (10,000 U/mL)	NEB, Hitchin, UK
Biovision Nuclear/Cytosol Fractionation Kit	Cambridge Bio., Cambridge, UK
Bovine Serum Albumin (BSA)	Biosera Europe, Nuaille, France
Calcium Phosphate Transfection Kit	Fisher Scientific, Loughborough, UK
Chloroquine	Merck Life Science, Gillingham, UK
CutSmart [®] Buffer (10X)	NEB, Hitchin, UK
Deoxyribonuclease (DNase) I from Bovine Pancreas	Merck Life Science, Gillingham, UK
Dimethyl Sulfoxide (DMSO)	Merck Life Science, Gillingham, UK
Dulbecco's Modified Eagle Medium (DMEM)	Merck Life Science, Gillingham, UK
<i>Eco</i> RI-HF [®] (20,000 U/mL)	NEB, Hitchin, UK
EDTA-free Protease Inhibitor Cocktail	Merck Life Science, Gillingham, UK
Egtazic Acid (EGTA, 0.5 M)	Merck Life Science, Gillingham, UK

Ethanol 99.8%	Merck Life Science, Gillingham, UK
Ethylenediaminetetraacetic Acid (EDTA, 0.5 M)	Merck Life Science, Gillingham, UK
Ficoll®-Paque Premium	Merck Life Science, Gillingham, UK
Foetal Bovine Serum (FBS)	Biosera Europe, Nuaille, France
Gel Loading Dye, Purple (6X)	NEB, Hitchin, UK
Gentamicin (50 mg/mL)	Fisher Scientific, Loughborough, UK
Hanks' Balanced Salt Solution (HBSS)	Fisher Scientific, Loughborough, UK
Heparin Sodium (1000 U/mL)	Wockhardt, Wrexham, UK
HEPES (1 M)	Merck Life Science, Gillingham, UK
High-Capacity cDNA Reverse Transcription Kit	Fisher Scientific, Loughborough, UK
HiSpeed® Plasmid Maxi Kit	Qiagen, Manchester, UK
Indirect CD34 MicroBead Kit, Human	Miltenyi Biotec, Bisley, UK
Iscove's Modified Dulbecco's Medium (IMDM)	Fisher Scientific, Loughborough, UK
IMDM Powder	Fisher Scientific, Loughborough, UK
Isopropanol 99.5%	Merck Life Science, Gillingham, UK
LB Broth	Merck Life Science, Gillingham, UK
LB Broth with Agar	Merck Life Science, Gillingham, UK
L-Glutamine (200 mM)	Fisher Scientific, Loughborough, UK
Lipofectamine™ 3000 Transfection Kit	Fisher Scientific, Loughborough, UK
MagicMark™ XP Western Protein Standard	Fisher Scientific, Loughborough, UK
Magnesium Acetate (1 M)	Merck Life Science, Gillingham, UK
Magnesium Chloride (MgCl ₂)	Merck Life Science, Gillingham, UK
Methanol 99.8%	Merck Life Science, Gillingham, UK
NEBuffer™ 3.1 (10X)	NEB, Hitchin, UK
NuPAGE™ Antioxidant	Fisher Scientific, Loughborough, UK
NuPAGE™ LDS Sample Buffer (4X)	Fisher Scientific, Loughborough, UK
NuPAGE™ MOPS SDS Running Buffer (20X)	Fisher Scientific, Loughborough, UK
NuPAGE™ Sample Reducing Agent (10X)	Fisher Scientific, Loughborough, UK
NuPAGE™ Transfer Buffer (20X)	Fisher Scientific, Loughborough, UK
One Shot™ Stbl3™ Chemically Competent <i>E. coli</i>	Fisher Scientific, Loughborough, UK
Opti-MEM™ I Reduced Serum Medium	Fisher Scientific, Loughborough, UK
Penicillin-Streptomycin (10,000 U/mL)	Fisher Scientific, Loughborough, UK
PeqGREEN DNA/RNA Dye	Peglab, Shanghai, China
Phosphatase Inhibitor Cocktail	Merck Life Science, Gillingham, UK
Phosphate-buffered Saline (PBS, 10X)	Fisher Scientific, Loughborough, UK
Poly-D-Lysine	Merck Life Science, Gillingham, UK
Ponceau S solution 0.1 % w/v in 5% Acetic Acid	Merck Life Science, Gillingham, UK
Protease Inhibitor Cocktail	Merck Life Science, Gillingham, UK
Puromycin	Merck Life Science, Gillingham, UK

QIAquick® Gel Extraction Kit	Qiagen, Manchester, UK
Recombinant Human EPO	BioLegend, London, UK
Recombinant Human FLT3 Ligand (FLT3L)	BioLegend, London, UK
Recombinant Human G-CSF	BioLegend, London, UK
Recombinant Human GM-CSF	BioLegend, London, UK
Recombinant Human IL-3	BioLegend, London, UK
Recombinant Human IL-6	BioLegend, London, UK
Recombinant Human SCF	BioLegend, London, UK
RetroNectin® (1 mg/mL)	Takara, Paris, France
Ribonuclease (RNase) A from Bovine Pancreas	Merck Life Science, Gillingham, UK
RNeasy® Plus Mini Kit	Qiagen, Manchester, UK
Roswell Park Memorial Institute (RPMI) 1640	Fisher Scientific, Loughborough, UK
SeaKem® GTG™ Agarose	Lonza, Slough, UK
S.O.C. Medium	Fisher Scientific, Loughborough, UK
Sodium Bicarbonate 7.5% Solution	Fisher Scientific, Loughborough, UK
Sodium Chloride (NaCl)	Merck Life Science, Gillingham, UK
Sodium Dodecyl Sulfate (SDS)	Merck Life Science, Gillingham, UK
Sodium Orthovanadate	Merck Life Science, Gillingham, UK
Recombinant Human SDF-1 α (CXCL12)	PeproTech, London, UK
Sucrose (1 M)	Merck Life Science, Gillingham, UK
T4 DNA Ligase (2,000,000U/mL)	NEB, Hitchin, UK
T4 DNA Ligase Buffer (10X)	NEB, Hitchin, UK
TaqMan™ Fast Advanced Master Mix	Fisher Scientific, Loughborough, UK
Transferrin (Human, 30 mg/mL)	Merck Life Science, Gillingham, UK
Triethylammonium Bicarbonate Buffer (TEAB, 1 M)	Merck Life Science, Gillingham, UK
Tris-Acetate-EDTA Buffer	Merck Life Science, Gillingham, UK
Tris-Borate-EDTA Buffer	Merck Life Science, Gillingham, UK
Triton™ X-100	Merck Life Science, Gillingham, UK
TO-PRO™-3 Iodide (1 mM)	Fisher Scientific, Loughborough, UK
Tris Hydrochloride (HCl)	Merck Life Science, Gillingham, UK
TWEEN® 20	Merck Life Science, Gillingham, UK
UltraPure™ Agarose	Fisher Scientific, Loughborough, UK
XhoI (20,000 U/mL)	NEB, Hitchin, UK

2.1.2 Antibodies

Antibodies used in flow cytometry (2.6) and western blotting (2.7) procedures are alphabetically listed below.

Table 2-2 – Summary of antibodies used in flow cytometry and western blotting studies.

NA – Not applicable; Cambridge Bio – Cambridge Biosciences; CST – Cell Signaling Technology; SCBT – Santa Cruz Biotechnology.

Antibody	Clone	Dilution	Supplier
Flow cytometry antibodies			
Anti-Human CD11b-Pacific Blue™ (PB)	ICRF44	1/17	BioLegend, London, UK
Anti-Human CD13-Allophycocyanin (APC)	WM15	1/17	BioLegend, London, UK
Anti-Human CD14-PB	HCD14	1/17	BioLegend, London, UK
Anti-Human CD15-PB	W6D3	1/17	BioLegend, London, UK
Anti-Human CD34-PB	581	1/17	BioLegend, London, UK
Anti-Human CD34-Phycoerythrin (PE)	581	1/10	BioLegend, London, UK
Anti-Human CD36-Biotin	NA	1/100	Cambridge Bio., Cambridge, UK
Anti-Human CD45-APC	2D1	1/20	BioLegend, London, UK
Anti-Human CD235a-PB	HI264	1/17	BioLegend, London, UK
Mouse IgG1-PB	MOPC-21	1/17	BioLegend, London, UK
Mouse IgG1-PE	MOPC-21	1/10	BioLegend, London, UK
PerCP-Cy™5.5 Streptavidin	NA	1/100	BD Biosciences, Wokingham, UK
Western blot antibodies			
GAPDH Mouse mAb	6C5	12500	SCBT, Heidelberg, Germany
Histone 1 Mouse mAb	AE-4	1/2500	Bio-Rad, Hertfordshire, UK
Mouse IgG Horseradish Peroxidase (HRP) conjugate	NA931	1/5000	Fisher Scientific, Loughborough, UK
Rabbit IgG HRP conjugate	NA934	1/5000	Fisher Scientific, Loughborough, UK
RUNX3/AML2 Rabbit mAb	D6E2	1/5000	CST, London, UK

2.2 Recombinant DNA techniques

2.2.1 Source and structure of plasmids

Overexpression of RUNX3 and RUNX1-ETO in human primary HSPC was successfully achieved by using a recombinant PINCO retroviral system harbouring the complementary DNA (cDNA) of either *RUNX3* or *RUNX1-ETO* and co-expressing a selectable marker (Figure 2-1A). The selectable markers used in this study were *Discosoma* red fluorescent protein (DsRed) for the RUNX3 overexpressing vector, and green fluorescent protein (GFP) for either RUNX1-ETO or RUNX3 overexpressing PINCO vectors. Similar PINCO DsRed or GFP vectors lacking *RUNX3* or *RUNX1-ETO* cDNA were used as control. A pLV-EGFP-T2A-Puro-EF1A lentiviral vector was used to overexpress RUNX3 in AML cell lines. This lentiviral vector was purchased from VectorBuilder (Guangzhou, China).

Knockdown (KD) of RUNX3 in human primary HSPC and AML cell lines was performed by using short hairpin RNA (shRNA) lentiviral vectors co-expressing GFP and puromycin and targeting different regions in RUNX3 sequence (Figure 2-1B). shRNA lentiviral vectors were purchased from VectorBuilder (Guangzhou, China). Table 2-3 summarises the viral systems used in this study.

2.2.2 Subcloning of *RUNX3* cDNA into the PINCO DsRed vector

A retroviral vector co-expressing RUNX3 and DsRed was generated by directional cloning of RUNX3 (NM_001031680.2) into *Bam*HI/*Eco*RI sites of PINCO vector (Grignani *et al.* 1998). In addition, a control vector with a non-coding DNA fragment subcloned into PINCO DsRed was generated. PINCO DsRed vector (10 µg) was initially prepared by enzyme digestion with 50U *Bam*HI and 50U *Eco*RI for 1 hour at 37°C. Following incubation, the successful digestion was confirmed by performing a qualitative gel using 1% w/v Seakem gel agarose stained with 1 µL PeqGreen (25,000X). To purify the insert, electrophoresis was performed using 1% w/v Seakem gel agarose and 96 µL DNA digest with 20 µL gel loading dye was loaded into the well. Electrophoresis was performed at 5 V/cm until separation between the digested fragment 'insert' and remaining plasmid was achieved (40 V for 8 cm of gel).

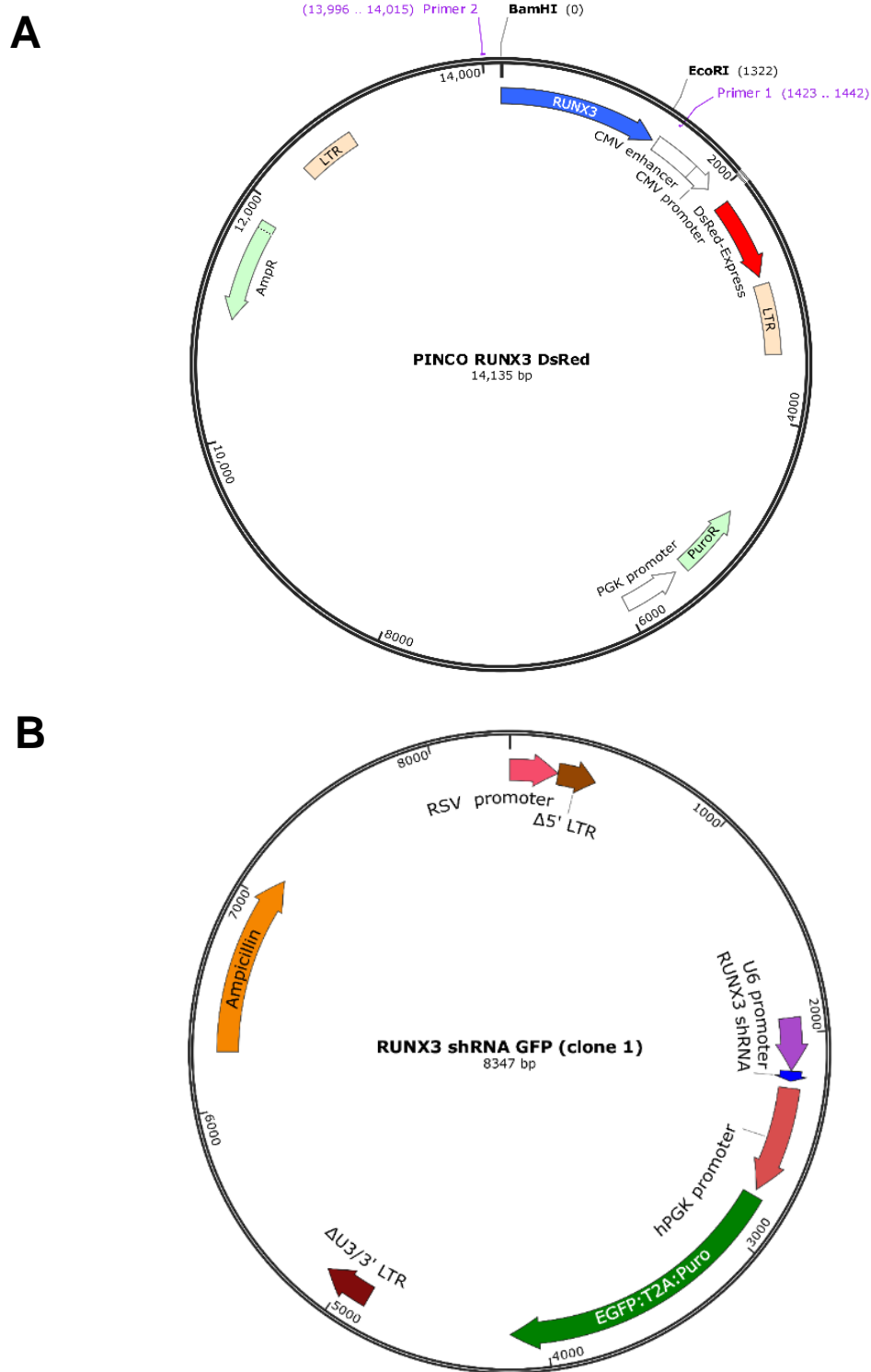


Figure 2-1 – Plasmid DNA structures used in this study.

(A) Representation of PINCO-RUNX3 DsRed vector created using SnapGene software (GSL Biotech LLC, USA). **(B)** Representation of RUNX3 shRNA GFP vector for shRNA 1 (TRCN0000235675). This vector includes the ampicillin resistance gene; Rous sarcoma virus (RSV) promoter; long terminal repeat (LTR); U6 type III RNA polymerase promoter; the RUNX3 shRNA sequence; human phosphoglycerate kinase (hPGK) promoter; and EGFP:T2A:Puro sequence that confers both green fluorescence and resistance to puromycin.

Table 2-3 – Summary of all retro- and lentiviral systems used for overexpression and KD studies.

All vectors include the ampicillin resistance gene. psPAX2 is a 2nd generation lentiviral packaging plasmid expressing HIV-1 gag, pol, rev and tat genes, and pMD2.G is a vesicular stomatitis virus (VSV-G) envelope expressing plasmid. Stuffer fragment – Non-coding DNA fragment; Puro – Puromycin; NM Number – National Center for Biotechnology Information (NCBI) reference sequence (RefSeq) database transcript accession number; TRCN Number – The RNAi Consortium shRNA Clone ID number.

Plasmid	Gene/Target sequence	Selectable marker
PINCO	Empty	DsRed
PINCO	Stuffer fragment	DsRed
PINCO	RUNX3 [NM_001031680.2]	DsRed
PINCO	Stuffer fragment	GFP
PINCO	RUNX1-ETO (Tonks <i>et al.</i> 2003)	GFP
PINCO	RUNX3 [NM_001031680.2]	GFP
pLV	Empty	GFP/Puro
pLV	RUNX3 [NM_001031680.2]	GFP/Puro
pLV	Scramble shRNA	GFP/Puro
pLV	RUNX3 shRNA 1 [TRCN0000235676]	GFP/Puro
pLV	RUNX3 shRNA 3 [TRCN0000235675]	GFP/Puro
pLV	RUNX3 shRNA 4 [TRCN0000235672]	GFP/Puro
psPAX2	Empty	–
pMD2.G	VSV-G	–

Following electrophoresis, the agarose gel was stained with 10 μ L PeqGreen (20,000X) and the band corresponding to the insert was excised from the gel and weighed. DNA was extracted using the QIAquick[®] Gel Extraction Kit and quantitated using NanoDrop[™] (Fisher Scientific UK Ltd, Loughborough, UK). Ligation of the purified insert to the PINCO DsRed vector was achieved by incubation using a target insert:vector molar ratio of 10, for approximately 2 hours at room temperature (RT), followed by heat inactivation at 65°C for 10 minutes to stop the reaction. The resulting vector was posteriorly transformed into Stbl3 *E. coli* cells (2.2.3).

2.2.3 Transformation of competent *E. coli* with plasmid DNA

Efficient transformation of Stbl3 competent cells was performed by mixing 6 μL DNA with competent cells and incubating on ice for 30 minutes. After incubation, the mixture was transferred to the water bath and incubated for exactly 30 seconds at 42°C, followed by a 2-minute incubation on ice. Cells were then mixed with 250 μL pre-warmed sterile S.O.C. medium and placed in a shaking incubator at 37°C and 225 rpm for 1 hour. Following incubation, 50 and 200 μL of the transformed cells were spread on selective agar plates and grown overnight at 37°C. Single colonies were selected the following day and grown in LB broth for glycerol stocks (2.2.4), DNA extraction (2.2.5), and validation purposes, such as digestion and sequencing (2.2.6).

2.2.4 Preparation and thawing of glycerol stocks

To prepare glycerol stocks for each plasmid, 150 μL glycerol was added to 850 μL of bacterial culture in LB broth, mixed and transferred to appropriate cryovials. Glycerol stocks were kept at – 80°C. To recover a glycerol stock, the vial was placed on dry ice and, using a sterile inoculation loop, cells were spread onto an appropriate selective agar plate.

2.2.5 Extraction and quantitation of amplified plasmid DNA

To extract plasmid DNA, a bacterial culture was initiated by selecting a single colony grown overnight and inoculated into 5 mL sterile LB broth with ampicillin (100 mg/mL). For a Qiagen Maxiprep, the bacterial culture was grown overday at 37°C and 225 rpm, and subsequently diluted by transferring 150 μL culture into 150 mL LB broth supplemented with ampicillin and left shaking overnight at 37°C. The next day, cells were harvested by centrifugation at 6,000 $\times g$ for 15 minutes at 4°C. DNA extraction was performed using the HiSpeed® Plasmid Maxi Kit according to manufacturer's instructions. Briefly, the bacterial supernatant was discarded, and the pellet was resuspended in 10 mL Buffer P1 in the presence of ethanol. Next, 10 mL Buffer P2 was added and the cell suspension was gently mixed. Following a 5-minute incubation, 10 mL of Buffer N3 was added, the lysate mixed, poured into a QIAfilter cartridge, and incubated for 10 minutes. The lysate was subsequently filtered into a pre-equilibrated HiSpeed Maxi Tip and allowed to enter the resin by gravity flow. HiSpeed Maxi Tip was further washed with 60 mL Buffer QC and DNA was eluted with 15 mL Buffer QF.

Precipitation of DNA was achieved by adding 10.5 mL isopropanol to the eluted DNA, followed by a 5-minute incubation. The eluate-isopropanol mixture was then transferred into a 30 mL syringe with a QIAprecipitator Maxi Module attached and filtered using constant pressure. DNA was washed with 2 mL 70% v/v ethanol and the membrane dried by pressing air through the QIAprecipitator. DNA was eluted in 500 μ L of water and the concentration was determined using NanoDrop™. Extracted DNA was stored at – 20°C for further use.

2.2.6 Restriction enzyme digestion and DNA sequencing

Restriction digestion was performed to quickly assess clones harbouring RUNX3. To set up a digestion reaction, 1 μ g DNA was mixed with 1 μ L of the appropriate enzymes (10-20 units/ μ g DNA) in a total volume of 10 μ L and incubated at 37°C for 1 hour. Following incubation, 2 μ L of gel loading dye was added to the digest and electrophoresed using a 0.8% w/v agarose gel containing 1 μ L PeqGreen (25,000X) at 80 V constant for 1 to 2 hours. NEB 1 Kb ladder was used to determine the fragments size. An additional DNA sequencing step was performed by combining 15 μ L of DNA (concentration between 50-100 ng/ μ L) to 2 μ L of each forward or reverse primers (12 μ M) and sent to Eurofins for sequencing (Table 2-4).

Table 2-4 – Summary of primers used to validate the DNA plasmid structures used in this study.

Primers were used at a final concentration of 12 μ M. CDS – Coding sequence. Human RUNX3 CDS corresponds to NM_001031680.2 transcript variant.

Ref.	Direction	Target	Sequence
P1	Reverse	Flanking <i>Bam</i> HI/ <i>Eco</i> RI cloning site	5' TTA TGT AAC GCG GAA CTC CA 3'
P2	Forward	Flanking <i>Bam</i> HI/ <i>Eco</i> RI cloning site	5' TAG AAC CTC GCT GGA AAG GA 3'
P5	Forward	Human RUNX3 CDS	5' GAA CTG GTG AGA ACC GAC AG 3'
P6	Forward	Human RUNX3 CDS	5' CCC AAG CGG CAC AAG CAT TTC 3'
P18	Forward	Human RUNX3 CDS	5' ACT GAA CCC ATT CTC CGA CC 3'
P21	Forward	Human RUNX3 CDS	5' CCT TCA AGG TGG TGG CAT TG 3'

2.3 Cell culture

2.3.1 Source of primary material and cell lines

Primary human HSPC were obtained by a 2-step isolation protocol (2.3.5) from human neonatal cord blood (CB) collected from the Maternity Unit of the University Hospital of Wales (Cardiff). Informed consent of mothers undertaking caesarean sections was approved by the research ethics committee in accordance with the 1964 Declaration of Helsinki. CB was also bought from the NHS CB Bank (London/Bristol, UK). AML cell lines used in this study KASUMI-1, OCI-AML-5 and SKNO-1 were obtained from ATCC (LGC Standards, Middlesex, UK) and DSMZ (Braunschweig, Germany).

2.3.2 Culture of primary cells and cell lines

All cells were cultured according to the supplier standard cell culture guidelines, under aseptic conditions and grown at 37°C in a 5% CO₂ humidified incubator.

Human HSPC were cultured in IMDM containing 20% *v/v* FBS, 1% *v/v* BSA, human transferrin (30 mg/mL), β -ME (9 mM), gentamicin (20 μ g/mL), and supplemented with different combinations of cytokines depending on cell lineage and fate (Table 2-5). The subculturing conditions of all cell lines used in this study are summarised in Table 2-6. Unless otherwise stated, all cell culture centrifugation steps were performed at 200 x *g* for 5 or 10 minutes for volumes below or above 5 mL, respectively. Cell density was determined by cell counting using a haemocytometer (2.3.3) or flow cytometry with a viability dye (2.6.1).

Adherent cell lines were subcultured by adding 0.05% *w/v* trypsin-EDTA (3 mL for T25; 5 mL for T75) to the cell layer and leaving for 3 minutes at RT. Detached cells were transferred to a universal container (UC) and an equal volume of pre-warmed complete DMEM (Table 2-6) was added before centrifugation. Supernatant was discarded and cells were resuspended in fresh growth medium and subcultured according to Table 2-6.

Table 2-5 – Different combinations and concentrations of growth factors used for the growth and development of human primary HSPC.

Human HSPC were cultured in IMDM supplemented with 20% v/v FBS, 1% v/v BSA, human transferrin (30 mg/mL), β -ME (9 mM), gentamicin (20 μ g/mL). Different combinations of cytokines were added to the growth medium according to cell fate (erythroid/myeloid).

Growth factor	Final concentration (ng/mL)
36S^{high} (Day 0 – 3)	
FLT3L	50
G-CSF	25
GM-CSF	25
IL-3	50
IL-6	25
SCF	50
36S^{low} (Day 3 – 10)	
IL-3	5
IL-6	5
SCF	5
36S^{low} + EPO (Day 10 – 22)	
EPO	5
IL-3	5
IL-6	5
SCF	5
3S^{low}G/GM (Day 3 – 17)	
G-CSF	5
GM-CSF	5
IL-3	5
SCF	5

Table 2-6 – Subculturing conditions for all cell lines used in this study.

Growth media was supplemented with either 10% or 20% v/v FBS, 1% v/v L-Glutamine, and 20 µg/mL gentamicin. Subculture regime and normal working range cell densities are according to ATCC and DSMZ guidelines.

Cell line	Complete growth medium	Subculture regime (every 3 days)	Optimal cell density
HEK 293T	DMEM + 10% v/v FBS	1:6	$2 \times 10^5 - 1 \times 10^6$
Phoenix	DMEM + 10% v/v FBS	1:6	$2 \times 10^5 - 1 \times 10^6$
KASUMI-1	RPMI + 20% v/v FBS	1:2	$3 \times 10^5 - 1 \times 10^6$
OCI-AML-5	MEM + 20% v/v FBS + 10 ng/ml GM-CSF	1:4	$1 \times 10^5 - 1 \times 10^6$
SKNO-1	RPMI + 10% v/v FBS + 10 ng/ml GM-CSF	1:3	$2 \times 10^5 - 1 \times 10^6$

2.3.3 Cell counting using a haemocytometer

Cell counting was performed using an improved Neubauer haemocytometer counting chamber. The coverslip was moistened beforehand and securely placed over the haemocytometer chamber. Approximately 10 µL of culture was transferred directly to the edge of the coverslip and allowed to enter the chamber. Viable cells (refractile) were counted under a phase contrast microscope in four large corner squares of the haemocytometer. Cell density per mL was determined by multiplying the average cell count of the four quadrants by 1×10^4 .

2.3.4 Cryopreservation and thawing of cells

For cryopreservation, confluent cells (1×10^6 cells/mL) were harvested, centrifuged, and resuspended in the appropriate growth medium (Table 2-6). An equal volume of freezing medium (IMDM with 30% v/v FBS and 20% v/v DMSO) was added to the cells and 1 mL of culture was aliquoted into 1.8 mL cryovials. CoolCell® LX (Biocision, LLC, Larkspur, CA, USA) freezing container was used to cool the cells at a rate of 1°C/minute in a – 80°C freezer, after which the vials were transferred to liquid nitrogen for long-term storage.

Cryopreserved cells were recovered by rapidly thawing cells with 1 mL FBS in a 37°C water bath, transferred to a UC, and slowly diluted by adding dropwise 5 mL of the appropriate growth medium. Cultures were centrifuged gently at 200 x *g* for 5 minutes, followed by resuspension of cells in 5 mL fresh pre-warmed medium (Table 2-6) and subcultured in T25 flasks.

2.3.5 Colony assay

To assess the colony forming ability of DsRed/GFP⁺ HSPC (2.6.3), colony assays were performed on day 3 of culture by limiting dilution in 96-U plates (0.3 cells/well) in growth medium and incubated at 37°C with 5% CO₂. Following 7 days of growth, individual colonies (> 50 cells) and clusters (> 5 cells) were counted and scored. To assess their self-renewal potential, colonies were harvested, replated at higher density (1 cell/well), and cultured for an additional week.

2.3.6 Assessment of cell morphology

Examination of cell morphology was achieved by transferring 70-100 µL of culture (30,000 cells) to a pre-assembled cytopsin sample chamber with glass slide and centrifuging it at 60 x *g* for 5 minutes using a Cytospin 3 (Fisher Scientific, Loughborough, UK). Slides were further stained with May–Grünwald–Giemsa for morphology examination and scanned using Zeiss Axioscan Z1 slide scanner (Carl Zeiss, Cambridge, UK) at 20X magnification. Differential counts were performed using Zen Lite software (Carl Zeiss, Cambridge, UK) to determine the number of cells in separate developmental stages. For the erythroid studies, cells in an early, intermediate, and late phase of development were defined as proerythroblasts, erythroblasts and normoblasts, respectively. For the myeloid studies, granulocytic cells in an early, intermediate, and late phase of development were defined as myeloblasts/promyelocytes, myelocytes/metamyelocytes and band/segmented cells, respectively.

2.4 Isolation of human CD34⁺ haematopoietic stem and progenitor cells

2.4.1 Isolation of mononuclear cells from cord blood by density gradient centrifugation

Initially, an aliquot of human CB was immunophenotyped for CD34 positivity by flow cytometry to estimate the percentage of CD34⁺ cells present in the sample (2.6.2). CB was then diluted 1:1 with HBSS containing 20 µg/mL gentamicin and 10 mg/mL heparin to isolate the mononuclear cells (MNC) fraction. Ficoll-Paque™ was added to multiple UC and 8-9 mL of CB was layered on top of 5 mL Ficoll before centrifuging at 400 x g for 40 minutes. Following density gradient separation of the different blood cell types, MNC were aspirated from the interface between the plasma and Ficoll layers into several UC containing 15 mL of wash medium (RPMI with 5% v/v FBS, 20 µg/mL gentamicin, and 10 mg/mL heparin). Cells were washed 2 to 3 times until the supernatant was completely clear (free of platelet contamination). MNC were counted under the microscope using a haemocytometer (2.3.3), followed by resuspension in RPMI with 10% v/v FBS and aliquoted into cryovials (5x10⁷ cells/vial) for cryopreservation in liquid nitrogen (2.3.4). The number of MNC and the percentage of CD34⁺ cells were important for planning future experiments, as it gives an estimation of the number of HSPC present in each processed human CB sample.

2.4.2 Isolation of human haematopoietic stem and progenitor cells from mononuclear cells

An additional isolation step was necessary to enrich CD34⁺ HSPC from the MNC fraction previously isolated (2.4.1). Magnetic-Activated Cell Sorting (MACS) of CD34⁺ cells was performed using the MiniMACS™ Separator (Miltenyi Biotec, Woking, UK), and the Indirect CD34 MicroBeads Kit, according to the manufacturer's instructions. Briefly, MNC were rapidly thawed as previously described (2.3.4) and transferred to a separate UC. An equal volume of PBS with 5 mM MgCl₂ at RT was added dropwise to the culture over 3 minutes, with this step being repeated twice so the volume of the culture doubled a total of 3 times (8 mL final volume if starting from 1 mL cell culture). Cells were gently centrifuged, and 10 µL DNase (10 mg/mL) was added to the cell pellet and mixed. Subsequent volumes were determined per 1x10⁸

cells based on previous cell counts (2.4.1). The pellet was then resuspended in 400 μL of cold column buffer (PBS containing 1% v/v BSA and 5 mM MgCl_2) and 100 μL of A1 and A2 reagents were added. At the end of a 15-minute incubation at 4°C, 5 mL column buffer was added, and cells were centrifuged. Supernatant was carefully discarded, and cells were resuspended in 400 μL column buffer followed by addition of 100 μL reagent B. After a second 15-minute incubation at 4°C, 5 mL column buffer was added, and the cell suspension was strained and centrifuged. The cell pellet was finally resuspended in 500 μL of buffer and transferred to a pre-equilibrated MS column (Miltenyi Biotec, Woking, UK), Once the column flow stopped, four washes of 500 μL buffer were performed, and the $\text{CD}34^+$ enriched population was eluted in 1 mL buffer. The eluted fraction was transferred to a second column and the previous steps were repeated to improve the purity of the culture. At the end, eluted cells were counted (2.3.3) and subcultured at 2×10^5 cells/mL in appropriate medium (Table 2-5). Isolation of HSPC is defined as 'day 0' in growth and differentiation experiments (2.3, 2.5, 2.6, 2.8).

2.5 Transduction of cell lines and primary cells

Retro- and lentivirus were generated by transient transfection of Phoenix (Nx) or HEK 293T packaging cells, respectively. Recombinant virus was mainly obtained by cationic lipid transfection (2.5.1) or in some cases by calcium phosphate transfection (2.5.2) of packaging cells.

2.5.1 Generation of recombinant virus by cationic lipid transfection

Cationic lipid transfection was achieved using Lipofectamine™ 3000 Transfection Kit according to manufacturer's instructions. Initially, flasks were pre-treated with 5 mL poly-D-lysine for 30 minutes at RT, followed by a wash with PBS. Approximately 15×10^6 of HEK 293T or Nx cells were seeded in pre-treated flasks and, on the following day, lipid-DNA complexes were prepared by mixing 24 μg of retro- or lentiviral plasmid DNA with 4 mL Opti-MEM, 48 μL P3000™ Enhancer Reagent and 57 μL Lipofectamine 3000™ Reagent (values adjusted for T75). For lentiviral production, 6.6 μg of pMD2.G envelope plasmid and 4 μg of psPAX2 packaging plasmid (Table 2-3) were added to the previous solution. Following incubation for 15-20 minutes, medium in each T75 flask was reduced to 6 mL and the lipid-DNA complex

was carefully added to the cells. HEK 293T or Nx packaging cells were incubated for 6 hours at 37°C and 5% CO₂, followed by medium change. Harvesting of retrovirus was performed 48 and 72 hours later, with cell medium being changed in between harvests and viral supernatant being centrifuged and aliquoted each day. On the other hand, harvesting of lentivirus was performed 24 and 48 hours later, with the viral supernatant being pooled, centrifuged and aliquoted on the final day. Viruses were stored at – 80°C until further use. Validation of GFP/DsRed expression was performed by flow cytometry and Nx cells transfected with RUNX3 retrovirus were used occasionally as positive controls for western blotting (2.7.4).

2.5.2 Generation of recombinant virus by calcium phosphate transfection

Improved transduction efficiencies in human primary cells were shown for RUNX1-ETO and control retroviruses produced using the Calcium Phosphate Transfection Kit according to manufacturer's instructions. Briefly, 8x10⁶ Nx cells were initially seeded in a T75 flask and left to grow for a day. On the following morning, growth medium was replaced by 14 mL of fresh pre-warmed medium and by the afternoon 45 µg of DNA was mixed with tissue culture grade sterile water, 54 µL CaCl₂ (2.5 M) and added dropwise to 450 µL 2X HEPES buffered saline whilst the solution was bubbled with a pipette. The mixture was immediately vortexed for 4 seconds and incubated for 20 minutes. Five minutes prior to the transfection, 14 µL chloroquine (25 µM) was added to the cultures, followed by the dropwise addition of DNA to the medium and incubation at 37°C and 5% CO₂ until the next day. Growth medium was changed 24 hours later, and the incubator temperature was lowered to 33°C to maximise retroviral stability. Viral supernatant was harvested 48 and 72 hours later as previously described (2.5.1).

2.5.3 Viral infection of cells

Normal human HSPC were isolated and transduced in 36S^{high} medium as previously described (Tonks *et al.* 2003) (2.4.2). To infect normal human HSPC, retro- or lentivirus were centrifuged for 120 minutes at room temperature in 24-well plates pre-coated with RetroNectin® (30 µg/mL) (Tonks *et al.* 2005). Following centrifugation, the retroviral supernatant was removed and the HSPC were added to the wells, as previously described (Tonks *et al.* 2003; Tonks *et al.* 2005). The infection procedure

was repeated on the following day to improve the transduction efficiency. All HSPC cultures generated during this study are summarised below.

Table 2-7 – Summary of transduced HSPC cultures generated in this study.

Mock transduced cells were generated using the same infection approach and Nx supernatant with no retro- or lentivirus.

Culture name	Description
RUNX3 overexpression	
Mock	–
Control	DsRed (or GFP)
RUNX3	RUNX3 DsRed (or GFP)
RUNX3 KD	
Mock	–
shRNA control	shRNA GFP
shRNA 1	RUNX3 shRNA 1 GFP
shRNA 3	RUNX3 shRNA 3 GFP
shRNA 4	RUNX3 shRNA 4 GFP
RUNX1-ETO and RUNX3 overexpression	
Control	GFP
RUNX1-ETO	RUNX1-ETO GFP
Control GFP/DsRed	GFP and DsRed
RUNX1-ETO/RUNX3	RUNX1-ETO GFP and RUNX3 DsRed

For KD experiments (Table 2-7), HSPC were only transduced once with shRNA vectors 24 hours following their isolation, as these vectors gave higher titre and infection efficiency due to their smaller size compared to the overexpression vectors. On day 2 of cultures, cells were kept in the incubator growing until the next day. Following infection (day 3 of culture), cells were harvested, counted, and cultured in appropriate growth medium (Table 2-5) depending on downstream experiments (2.6.3).

For AML cell lines, only one round of infection was performed, and for overexpression systems was similar to the HSPC protocol. Briefly, viral supernatants were added to pre-coated 24-well plates and centrifuged as before. Following spin-infection, viruses were discarded, and cells were plated at an appropriate density into the wells (Table 2-6). Conversely, for KD studies, 300 μ L of the viral supernatant was directly added to 700 μ L of culture plated at a suitable density depending on the cell line and respective doubling time. For both protocols, 24 hours after the infection was performed, cells were harvested, washed, resuspended in 1 mL of fresh pre-warmed cell medium and plated in new 24-well plates.

2.5.4 Selection of infected cells

Puromycin (puro) resistance was used as a drug selectable marker. This allowed enrichment for infected cells by adding the aminonucleoside antibiotic puro to the cell medium. Cells that are not transduced die due to inhibition of protein synthesis, whereas the infected population should continue to proliferate. Uninfected cells should be used alongside as a killing control to inform when the selection is completed. Following infection of AML cells and wash (2.5.3), cells were resuspended in 1 mL growth media and 10 μ L of puro was added (10 μ g/mL). Cells were cultured in 24-well plates (1 mL/well) along with the killing control, and selection of infected cells happened approximately over a week (depending on doubling times).

2.6 Flow cytometry

2.6.1 Assessment of cell proliferation

Cultures were counted by flow cytometry using a viability discriminator dye (permeable to dead cells), such as DNA binding 7-Aminoactinomycin D or TO-PRO-3 stains, allowing the appropriate gating of viable cells. Cell proliferation was measured by transferring 99 μ L of cell culture into mini-flow tubes and adding 1 μ L TO-PRO-3 (5 nM). BD Accuri™ C6 Plus flow cytometer was used to acquire events within 10 μ L of sample at a medium flow rate. Following data analysis (2.9), cell density was determined, and the cumulative fold expansion was plotted over time.

2.6.2 Estimation of CD34⁺ cells in human cord blood

The percentage of CD34⁺ cells in human CB samples was determined by staining 100 μ L of blood with 10 μ L CD34-PE and 5 μ L CD45-APC and incubating for 30 minutes at 4°C. An additional sample was stained with IgG1-PE and CD45-APC as control. At the end of the incubation, 5mL 1X FACS Lysis buffer was added to each tube and incubated for 10 minutes at RT. To stop the lysis, 5 mL PBS was added, and the cells were centrifuged at 200 x g for 5 minutes. Finally, the cell pellet was resuspended in residual buffer and analysed by flow cytometry.

2.6.3 Fluorescence activated cell sorting of live cells

Following the infection of HSPC over two days (2.5.3), cells were harvested, counted, and prepared for fluorescence activated cell sorting (FACS). For the erythroid studies (Tonks *et al.* 2003), cultures were incubated at RT with 10 μ L CD13-APC for 30 minutes, after which 2 mL PBS containing 1% v/v BSA and IL-3 (5 ng/mL) was added to stop the staining reaction. Stained cells were centrifuged and resuspended in the same buffer at 2×10^6 cells/mL. Erythroid-committed cells are negative for CD13, a myeloid marker, and so transduced erythroid cells (DsRed⁺CD13⁻) were enriched by FACS using Aria II (BD Biosciences, Wokingham, UK). Sorted cells were subsequently used in colony assays (2.3.5), morphology assessment (2.3.6) or grown in bulk liquid culture for growth and differentiation assessment by flow cytometry (2.6.4). For myeloid studies, day 3 cultures were sorted for DsRed or GFP positivity for colony assays or morphology slides.

HSPC co-expressing RUNX1-ETO and RUNX3 (Table 2-7) and respective controls were sorted for both GFP and DsRed positivity on day 3 of culture for colony assays and morphology assessment of myeloid cells. For erythroid studies, the same cultures were pre-stained with CD13-APC for 30 minutes at RT to enrich for erythroid-committed cells by FACS. GFP⁺DsRed⁺CD13⁻ cells were index sorted into 96-U plates containing 36S^{low} + EPO medium at a density of 1 cell/well and left to grow for one week at 37°C with 5% CO₂. Colonies and clusters were counted and scored (2.3.5).

2.6.4 Immunophenotyping and differentiation analysis

The role of RUNX3 in human primary HSPC growth and differentiation was monitored over time, with cultures counted and immunophenotyped every two days.

To study the effects of increased and reduced RUNX3 expression on erythroid differentiation, cultures were enriched for erythroid-committed cells on day 3 (2.6.3) and maintained in erythroid growth medium (36S^{low}). On day 10, cultures were supplemented with EPO (36S^{low} + EPO) and grown for a further twelve days. Transduced cultures were analysed by flow cytometry using BD FACSCanto™ (BD Biosciences, Wokingham, UK) at different time points using a panel of cell surface markers (Table 2-8) as previously described (Tonks *et al.* 2003). CD13-APC in combination with CD36-biotin was used for lineage discrimination, and streptavidin PerCP-Cy™5.5 was used for second-step labelling. In addition, cells were incubated with one of the following Pacific Blue (PB)-labelled differentiation markers: glycophorin A (GlyA) and CD34. To measure the expression of the different cell surface markers, 0.5-1x10⁵ cells were washed and resuspended in cold staining buffer (1X PBS containing 0.5% v/v BSA and 0.02% v/v sodium azide), with volumes depending on the number of markers to be analysed. Antibodies were added to the sides of separate wells in a 96-well plate (Table 2-2), followed by the addition of 15 µL cell suspension to each well. The plate was then briefly centrifuged, cells resuspended and left at 4°C for 30 minutes. At the end of the incubation, 150 µL of staining buffer was added to each well and the contents were transferred to the corresponding mini flow tube. Samples were centrifuged at 200 x g for 5 minutes and the supernatant discarded. Samples previously stained with CD36-biotin were incubated with PerCP-Cy™5.5 Streptavidin for another 30 minutes, and the previous steps were repeated after incubation. Cells were resuspended in 100 µL of staining buffer and analysed by flow cytometry. Reactions were controlled with the appropriate isotype-matched irrelevant antibody. Reagent concentrations were as recommended by the manufacturer. Morphology was assessed on day 20 of culture as previously described (Tonks *et al.* 2003) (2.3.6).

The effects of RUNX3 overexpression and KD on myeloid development were assessed over 3 to 17 days. On day 3, cultures were resuspended in 3S^{low}G/GM. Immunophenotyping was performed as described above using the same lineage discriminator cell surface markers. However, myeloid differentiation was assessed with the following panel of PB-labelled cell markers: CD11b, CD14, CD15 and CD34 (Table 2-8). Morphology was assessed on day 17 of culture (2.3.6). In terms of double infection studies (RUNX3 and RUNX1-ETO), a similar approach was taken.

Table 2-8 – Cell surface markers used in the multiparameter analysis of the development of human myeloid subpopulations grown *in vitro* culture.

	Erythroid	Monocytic/Granulocytic
Lineage discriminators		CD13
		CD36
Developmental markers	CD34	CD11b
		CD14
	GlyA	CD15
		CD34

2.6.5 Migration assay

The Transwell® cell migration assay measures the capacity of cell motility towards a chemoattractant gradient (e.g. stromal cell-derived factor 1, SDF-1) (Justus *et al.* 2014). Initially, the transwell 24-well plate was pre-incubated with serum free growth medium or chemotaxis medium (IMDM containing 1% v/v BSA) by adding 600 µL medium to each lower chamber and 100 µL to the top of the filter membrane or transwell insert. In addition, serial dilutions of SDF-1 were prepared in chemotaxis medium at final concentrations of 0.36, 1.2, 3.6, and 12 µg/mL. Transduced HSPC (day 6) were counted and 1×10^5 cells were washed and resuspended in 590 µL (1.7×10^5 cells/mL) of chemotaxis medium. The medium in each transwell insert was then replaced by 100 µL of cell suspension and 5 µL of SDF-1 at final concentrations of 3, 10, 30 and 100 ng/mL was added to the lower chambers. Cells were incubated at 37°C and 5% CO₂ for 4 hours, after which the number of migrated cells was counted by flow cytometry. A negative control to account for spontaneous migration was included by replacing the addition of SDF-1 for chemotaxis medium. To measure cell migration, 50 µL of cell suspension was harvested from each transwell insert and transferred to mini-flow tubes. The contents of each lower chamber were collected, centrifuged, resuspended in residual medium (approximately 100 µL), and transferred to mini-flow tubes. 7-Aminoactinomycin D was added to each tube at a final concentration of 1 µg/mL and samples were acquired on analysed on BD Accuri™ C6 Plus. The percentage of cell migration was calculated based on the number of cells

present in the lower chamber in relation to the total number of cells measured in both compartments. For unsorted cultures, the previous calculations need to account for the percentage of DsRed⁺ cells in culture.

2.7 Western blotting

2.7.1 Generation of protein extracts from whole cells

Total cell proteins were extracted from 1×10^6 cells that were washed with 10 mL of cold tris-buffered saline (TBS, prepared with 2.5 M Tris HCl, 5 M NaCl, and distilled water), followed by snap freezing of the cell pellet in liquid nitrogen to break the cell membrane and release the protein contents. The cell pellet was then thawed in the presence of 1 μ L DNase (1 mg/mL), and 50 μ L of homogenisation buffer (0.25 M sucrose, 10 mM HEPES, 1 mM magnesium acetate, 0.5 mM EDTA, 0.5 mM EGTA, 10 mM β -ME, 200 mM sodium orthovanadate, protease inhibitor cocktail, 1% v/v Triton-X100) was added to the sample and incubated for 30 minutes on ice with occasional vortexing to promote solubilisation. When the incubation elapsed, the total extract was transferred to an Eppendorf tube and centrifuged at 10,000 x *g* for 5 minutes at 4°C. The supernatant was collected to a fresh chilled tube and the volume was recorded for protein quantification (2.7.3).

2.7.2 Generation of fractionated cytosolic and nuclear extracts

Cytosolic and nuclear proteins were extracted from cells using the Biovision Nuclear/Cytosol fractionation Kit following manufacturer's instructions. Briefly, 5×10^6 HSPC or $2\text{-}3 \times 10^6$ AML cells were pelleted and washed with 20 mL of cold TBS, followed by sequential incubations with extraction buffers on ice. After the last incubation, cells were vortexed on the highest setting and centrifuged at 10,000 x *g* for 8 minutes at 4°C. The cytosolic fraction present in the supernatant was transferred to a fresh pre-chilled tube and the pellet was washed with 500 μ L of PBS with 5 mM MgCl₂. Following centrifugation for 3 minutes, the supernatant was discarded, and the pellet was snap frozen with liquid nitrogen. The cytosolic fractions and nuclear pellets were stored at – 80°C until further use. Subsequently, nuclear pellets were quickly thawed and re-frozen in the vapour phase of liquid nitrogen for 1 minute. Pellets were once again thawed and 2 additional series of freeze thaws were performed, allowing

the rupture of the nuclear membrane. Benzonase was further added to the nuclear pellets (2 $\mu\text{L}/1 \times 10^6$ cells) followed by a 30-minute incubation on ice and occasionally mixing. Following incubation, 100 or 50 μL of TEAB was added per 1×10^6 HSPC or AML cells, respectively, and the samples were left on ice for another 30 minutes with constant vortexing. Cell lysates were centrifuged at $10,000 \times g$ for 10 minutes at 4°C and the nuclear fraction in the supernatant was collected to a fresh tube. Quantification of cytosolic and nuclear proteins was performed using the Bradford assay (2.7.3).

2.7.3 Protein quantitation using Bradford assay

Total protein extracts were initially diluted 1:50 in distilled water, whereas cytosolic and nuclear extracts were diluted 1:100 in water. For each diluted sample, 10 μL were transferred in duplicate to individual wells in a 96-well plate. Protein standards of increasing concentrations of BSA (0, 10, 40, 70 and 100 $\mu\text{g}/\text{mL}$) were also prepared in water and added to separate well in duplicate. Bradford's reagent at RT was next diluted 1:1 in distilled water and 190 μL of this solution was added to each well containing either samples or standards. Following a 5-minute incubation in the dark at RT, absorbance was measured at 595 nm using Hidex Chameleon Microplate Reader (LabLogic ScienceTec, Courtaboeuf, France). Protein concentration was determined using the following equation:

$$\text{Concentration } (\mu\text{g}/\text{mL}) = \frac{\text{Abs}_{595} - b}{m}$$

Where,

Abs_{595} = Absorbance of the sample at 595 nm

b = Y-axis intersection

m = Slope of the linear regression

Equation 2-1 – Linear regression equation used to calculate the protein concentration in a sample.

2.7.4 Protein electrophoresis and electroblotting

Western blotting was performed as previously described (Hole *et al.* 2010) using the NuPAGE[®] electrophoresis system (Fisher Scientific, Loughborough, UK). Briefly, protein samples were thawed on ice and prepared for SDS-PAGE electrophoresis by adding the appropriate volumes of LDS, reducing agent and water according to protein concentration and sample volume. Prepared samples were vortexed and placed for 10

minutes in a water bath at 70°C to denature the proteins. NuPAGE™ 4 to 12%, Bis-Tris, 1.0 mm, Mini Protein Gel were rinsed with water and the wells were washed with 1X NuPAGE MOPS SDS Running Buffer before being placed in the XCell SureLock™ Mini-Cell Electrophoresis System. The inner chamber of the tank was filled with 200 mL of running buffer containing 500 µL of NuPAGE antioxidant, and the reduced samples were added onto the wells. A MagicMark XP Western Standard protein ladder was used to determine protein molecular weight. The outer chamber was then filled with 600 µL of running buffer and electrophoresis was performed at 200 V for 50 minutes. During electrophoresis, 1X NuPAGE Transfer Buffer with 1 mL of NuPAGE antioxidant and 10% v/v methanol (20% v/v if transferring 2 gels) was prepared and used to pre-soak blotting pads, membrane, and filter paper.

Following electrophoresis, the gel was removed from the tank and placed in between a pre-soaked 0.45 µm nitrocellulose membrane and filter paper (Fisher Scientific, Loughborough, UK). An additional filter paper was placed on top of the membrane making sure that bubbles were removed, before placing the previous assembly in between layers of pre-soaked blotting pads and into an XCell II™ Blot Module. The module was filled with the remaining transfer buffer and the outside of the tank with 600 µL of distilled water. Electroblotting was performed at 30 V for 1 hour.

2.7.5 Chemiluminescence detection of proteins

Detection of protein expression was determined using Amersham ECL Advance Western Blotting Detection Kit according to the manufacturer's instructions. The membrane was initially washed and stained with Ponceau S for 30 seconds to assess transfer efficiency across lanes. A 2.5% w/v skimmed milk powder blocking solution was prepared in TBS-TWEEN® 20 and 10 mL were used to block the membrane for 45 minutes on a shaker at RT. Following a 15-minute wash and three 5-minute washes with TBS-T, the membrane was incubated in 10 mL of blocking solution with the chosen primary antibody (Table 2-2) overnight in a shaker at 4°C. The following day, the membrane was washed as before and incubated with a HRP conjugated anti-mouse or anti-rabbit secondary antibody prepared in 10 mL of 1% w/v milk powder for 1 hour in a shaker at RT. The membrane was washed once again before the next step.

Chemiluminescence detection of proteins was achieved by combining reagent A and B at 1:1 ratio and evenly applying the substrate solution to the membrane

surface. The reaction was developed over 5 minutes at RT and protected from light. LAS-3000 Imaging System (Fujifilm, Bedford, UK) was used to capture digital images of the chemiluminescence reaction and detect proteins over 30-second to 30-minute exposure time. Equal protein loading was further assessed using GAPDH or Histone 1 antibodies for total/cytosolic or nuclear protein extracts (Table 2-2). Densitometry was performed using ImageJ v1.8 software (<https://imagej.nih.gov/ij/>) by plotting a histogram of peak intensity for each band. The peak area was used as an arbitrary intensity value to estimate the fold changes in protein expression.

2.8 Transcriptome analysis

2.8.1 Total RNA extraction

Total RNA was extracted from cells using the RNeasy[®] Plus Mini Kit, following manufacturer's instructions. Briefly, approximately $0.5-1 \times 10^5$ HSPC were pelleted and resuspended in 350 μ L RLT Plus containing β -ME (10 μ L/mL) for cell lysis. A QIAshredder spin column (QIAGEN, Manchester, UK) was used to further homogenise the cell lysate by pipetting the sample directly into the column and centrifuging at 10,000 $\times g$ for 2 minutes. DNA removal was achieved by transferring the homogenised lysate to a gDNA Eliminator spin column and centrifuging it at 8,000 $\times g$ for 30 seconds. One volume (approximately 350 μ L) of 70% v/v ethanol was further added to the flow-through recovered in the previous step, followed by mixing and transferring the sample into a RNeasy spin column. Following centrifugation at 8,000 $\times g$ for 15 seconds, the flow-through was discarded and 700 μ L of Buffer RW1 was added to the RNeasy spin column. Centrifugation was repeated with the same conditions as before and the flow-through was discarded. Next, 500 μ L Buffer RPE containing ethanol was added to the RNeasy spin column, followed by centrifugation as before and removal of the flow-through. The previous step was repeated, centrifuging the column for 2 minutes to ensure no ethanol carryover. An optional step was performed by centrifuging the empty spin column in a new collection tube at full speed for 1 minute. Lastly, 30 μ L RNase-free water was added directly to the centre of the spin column membrane and the column was centrifuged at 8,000 $\times g$ for 1 minute to elute the RNA. RNA concentration and purity were assessed using NanoDrop[™] and the purified RNA was used in downstream applications (2.8.2, 2.8.3).

2.8.2 Quantitative reverse-transcription polymerase chain reaction

A two-step quantitative reverse-transcription polymerase chain reaction (qRT-PCR) and TaqMan[®] Expression Assays were chosen to quantify the expression of target genes. The first step started with the reverse transcription of total RNA extracted from primary human cells (2.8.1) into cDNA using the High Capacity cDNA Reverse Transcription Kit (Fisher Scientific, Loughborough, UK) according to manufacturer's instructions. The kit components were first allowed to thaw on ice, and a 2X reverse transcription mix was prepared by calculating the volumes of each component according to the number of reactions (20 µL reaction volume). To prepare the reverse transcription reactions, 10 µL of 2X reverse transcription master mix were added to each tube followed by the addition of 10 µL of RNA sample and mixing. A control reaction was established by adding the reverse transcription mix to 10 µL of water (blank). An additional control was prepared by substituting the MultiScribe[™] reverse transcriptase in the mix with water and adding it to a sample (reverse transcription minus). The tubes were briefly centrifuged to spin down the contents and remove air bubbles and finally placed in the PCR System 9700 thermal cycler (Fisher Scientific, Loughborough, UK). The optimised conditions to use with this kit consisted of four steps: 25°C for 10 minutes; 37°C for 120 minutes; 85°C for 5 minutes; and 4°C indefinitely. At the end of the thermal cycler run, samples were stored at – 20°C until further use.

RUNX3 mRNA expression was determined using TaqMan[®] Fast Advanced Master Mix and gene expression assay (Hs00231709_m1, Fisher Scientific UK Ltd, Loughborough, UK). *GAPDH* was used as reference gene (Hs02786624_g1). Before starting, the number of reactions was determined and included a gene expression assay for each cDNA sample in triplicate and a no-template control for each assay. After thawing on ice, the kit components were mixed using the calculated volumes and briefly centrifuged to bring down the contents and remove any air bubbles in the tube. To prepare the PCR reaction plate, 18 µL of PCR reaction mix were added to separate wells in a 96-well plate, followed by the addition of 2 µL of cDNA template (or nuclease-free water for the no-template control) to each well. The reaction plate was then sealed with optical adhesive film and briefly centrifuged. Gene expression was assessed using QuantStudio[™] 5 real-time PCR system (Fisher Scientific UK Ltd, Loughborough, UK) and the optimal conditions used with this kit were as follow: uracil N-glycosylase

incubation step at 50°C for 2 minutes; polymerase activation at 95°C for 2 minutes; denaturation PCR step at 95°C for 1 second; and annealing/extending PCR step at 60°C for 1 second. The number of cycles was set as 40 and the fast run mode was selected according to manufacturer's instructions.

2.8.3 RNA-sequencing

RNA-sequencing platform performed by NGS specialist Novogene Co. (Cambridge, UK) was selected to identify early transcriptomic changes caused by overexpression of RUNX3 in human primary HSPC. Briefly, CD34⁺ HSPC cells were isolated, infected with a recombinant RUNX3 retrovirus co-expressing GFP, and sorted for GFP positivity on day 3 of culture (2.6.3). Although the previous overexpression studies were performed using a retroviral vector co-expressing RUNX3 and DsRed, GFP was chosen as selectable marker for these experiments due to its increased brightness. Five independent experiments were performed for this study (control vs RUNX3), given the variability associated with human CB from different donors. After confirming the sort for GFP enrichment by flow cytometry, cells were resuspended in Buffer RLT and total RNA was extracted (2.8.1) (Figure 5-1).

To guarantee the reliability of the sequencing data, a quality control (QC) assessment of every step was performed. A total of 10 RNA samples were shipped to Novogene, for library preparation, addition of adaptors, and sequencing (Figure 2-2A). Total RNA sample QC was performed using NanoDrop™ to assess RNA purity, agarose gel electrophoresis to assess RNA degradation and potential contamination, and Agilent 2100 to check RNA integrity. Agilent 2100 BioAnalyzer measures RNA concentration and integrity by capillary electrophoresis (Panaro *et al.* 2000). An RNA integrity number (RIN) ≥ 6.8 was required by Novogene for library preparation and sequencing.

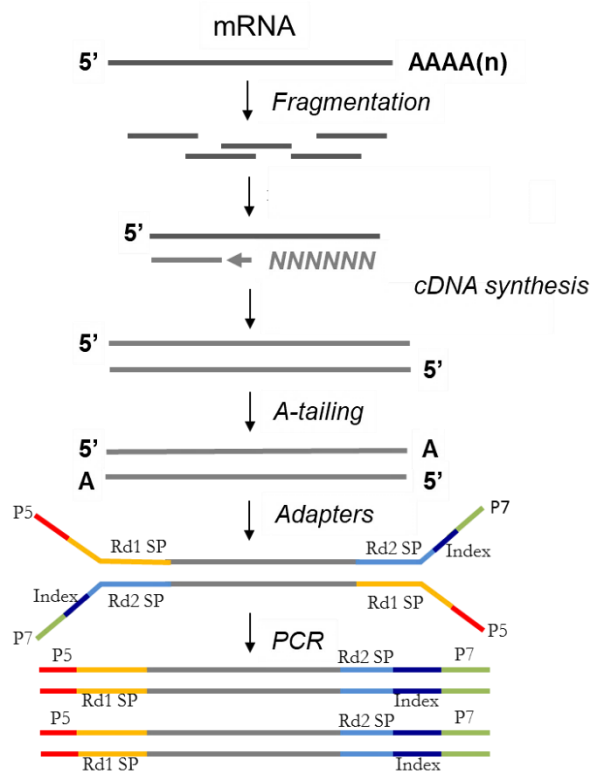
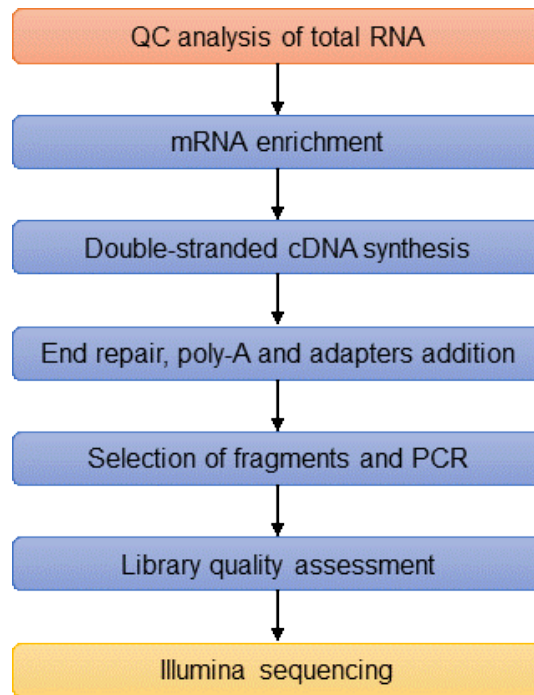


Figure 2-2 – Sample preparation prior to Illumina RNA sequencing.

(A) Workflow detailing the general steps to prepare a cDNA library ready to be sequenced from total RNA samples. Workflow adapted from Novogene Co. **(B)** Representation of cDNA library preparation preceding sequencing of samples. Figure adapted from Novogene Co.

Following QC of RNA samples, mRNA was enriched using oligo(dT) beads, fragmented randomly in buffer, and the first strand of cDNA was synthesised using random hexamers and reverse transcriptase. A custom second-strand buffer from Illumina was next added with dNTPs, RNase H and *E. coli* polymerase I to synthesise the second strand by nick-translation. The next steps included purification, terminal repair, A-tailing, addition of sequencing adapters, size selection and PCR enrichment, generating a cDNA library ready for sequencing (Figure 2-2B). An additional QC procedure was performed by determining library concentration using Qubit 2.0 fluorometer, and insert size using Agilent 2100 and qRT-PCR.

Illumina NovaSeq 6000 was used to sequence the cDNA library with a read length of 150bp paired-end, 20 million (M) reads per sample and a sequencing quality score for a given base ($Q \geq 80\%$). This last parameter can be calculated using the following equation: $Q = -10\log_{10}E$, where E represents the base calling error rate. Raw data was analysed by Novogene bioinformatics team according to the workflow shown in Figure 2-3 and an analysis report was provided. Raw sequencing data from Illumina was initially transformed to sequence reads by base calling, producing FASTQ files that contained sequence information (reads) and the corresponding sequencing quality information. QC assessment of raw reads was firstly performed by determining the error rate for each base (using Q score) and it is influenced by the sequencer, samples, and reagent availability. GC content distribution was also assessed to identify potential AT/GC separation that ultimately affects gene expression quantification. Raw reads were then filtered to discard the reads with low quality, adapter contamination or uncertain nucleotides, and only clean reads were used for downstream analysis. The next step was performed using HISAT2 algorithm to map the reads to the human reference genome (hg19).

Quantification of gene expression was determined by transcript abundance and estimated by counting the reads that align to genes or exons. Fragments Per Kilobase of transcript per Million mapped reads (FPKM) was used as normalised estimation method of gene expression as it considers the effects of sequencing depth and gene length, essential for comparisons between different genes and samples. HTSeq package was used to determine gene expression levels using the union mode. Moreover, an FPKM value of 1 was set as the threshold for determining whether the gene was expressed or not.

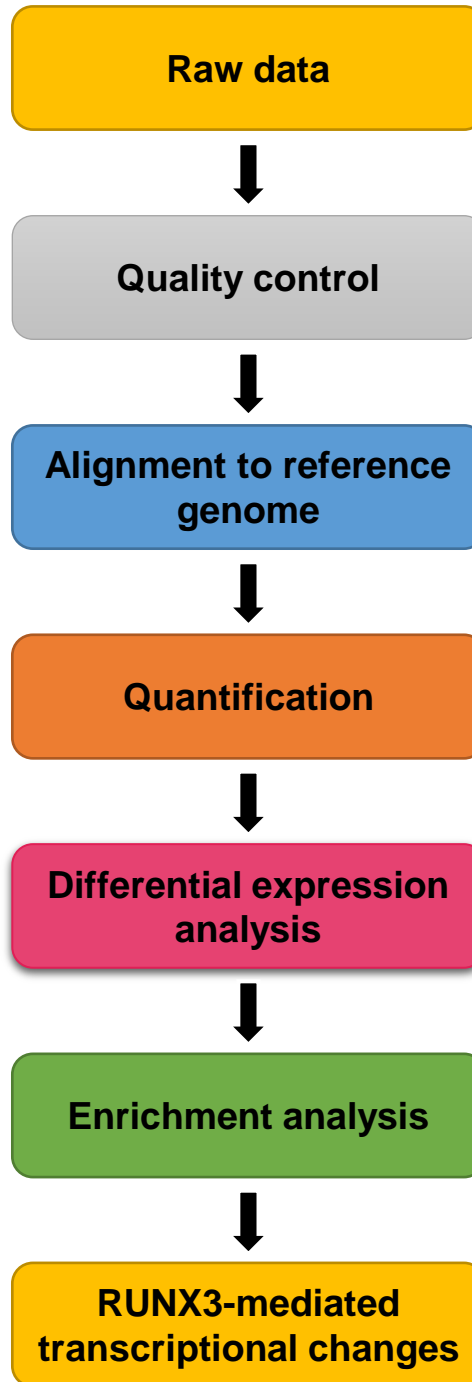


Figure 2-3 – Analysis workflow for RNA-sequencing data of transcriptional changes associated with high expression of *RUNX3* in HSPC.

Bioinformatic analysis workflow of control and *RUNX3* RNA-seq data from raw reads to elucidation of *RUNX3*-mediated transcriptional changes in human HSPC.

To identify transcriptomic changes induced by RUNX3 overexpression in HSPC, differential expression (DE) analysis was performed in three steps: normalisation of read counts using DESeq2, p-value estimation following a negative binomial distribution model, and false discovery rate (FDR) estimation based on Benjamini-Hochberg method. An initial cut-off for DE gene screening was set as $p < 0.05$. Volcano plots were used to visualise the DE genes that were up- or downregulated by RUNX3. Enrichment analysis of DE genes is essential to identify dysregulated biological functions of pathways associated with the dataset. KEGG (Kyoto Encyclopaedia of Genes and Genomes) enrichment analysis was part of the bioinformatic analysis performed by Novogene.

2.9 Data and statistical analysis

Data obtained by flow cytometry were analysed using FCS Express v6 (De Novo Software, Pasadena, CA, USA). The threshold for GFP/DsRed positivity was defined using identically treated mock transduced cultures. Approximately 20,000 events were recorded for each sample at a medium flow rate. Debris was excluded from all analyses based on a viability dye and/or light scatter. Gene expression data was analysed using QuantStudio™ Design and Analysis software v1.5.1 (Fisher Scientific, Loughborough, UK) and the Comparative C_T ($\Delta\Delta C_T$) method. Control samples were used as reference and GAPDH as endogenous control.

For statistical analysis purposes, three or more independent experiments or biological replicates (n) were used during this study. Statistical analysis was performed using a paired sample t-test, or one-way ANOVA with Tukey's post hoc test for multiple comparisons. Significance of difference was considered for $p < 0.05$. Minitab 18 software (Minitab LLC, State College, Pennsylvania, USA) was used for all statistical analyses.

2.9.1 Publicly available databases and datasets

mRNA expression data for *RUNX3* and additional genes of interest in different haematopoietic cells and AML subtypes was obtained from BloodSpot database (www.bloodspot.eu). This database allows quick access to transcriptomic data using different haematopoietic cell types and leukaemic blasts (Bagger *et al.* 2019). *RUNX3* expression data from AML patients was obtained from the TCGA AML dataset (Cancer

Genome Atlas Research *et al.* 2013) and analysed using cBioPortal (www.cbioportal.org). This platform provides interactive exploration of several cancer genomic datasets, including TCGA AML, allowing quick access to clinical attributes and molecular profiles from these studies (Cerami *et al.* 2012).

Additional databases used in this study include the NCBI Gene database (www.ncbi.nlm.nih.gov/gene) to obtain information on RUNX3 transcript variants, isoforms, CDS, among others. The Human Protein Atlas (www.proteinatlas.org) to find information regarding tissue expression and cell type specificity, splice variants, protein function, among others. Cancer Cell Line Encyclopaedia (www.broadinstitute.org/ccle) was used to obtain information on *RUNX3* mRNA expression in different AML cells lines. GeneCards[®] Human Gene Database (www.genecards.org) was used to investigate promoters and enhancers of different gene targets. Web-based tool Morpheus (www.software.broadinstitute.org/morpheus) was used to generate expression heat maps of relevant genes in control and RUNX3-expressing HSPC.

The different transcriptomic datasets used during this study are summarised in Table 2-9. RNA-seq data from RUNX3 KD HSPC (#2 dataset) and erythroid progenitors (#3 dataset) (Balogh *et al.* 2020), as well as RUNX1-ETO HSPC (#4 dataset) (Tonks *et al.* 2007) were used for a comparison analysis performed in IPA[®] with the data generated in this study (#1 dataset) (5.3.6).

2.9.2 RNA-sequencing data analysis

Assessment of RNA-seq data variability was performed using Partek[®] Flow[®] software (St. Louis, MO, USA). Following read quantification, Principal Component Analysis (PCA) and hierarchical clustering of RNA-seq data were achieved using the Partek[®] E/M algorithm. An independent DE analysis was performed using the sequencing data obtained from Novogene, and different software was used for this analysis, including MetaCore[™] (Clarivate[™] Analytics, Philadelphia, PA, USA) and Ingenuity[®] Pathway Analysis (IPA[®], QIAGEN, Manchester, UK) (Figure 2-4). To reduce and filter the DE gene list for further analysis, a cut-off was established of fold changes ≥ 1.5 and an adjusted p-value (p_{adj}) < 0.05 . The 'Interactome' feature was used in MetaCore[™] to identify proteins interacting with the proteins associated with the DE gene list. Interactions can be categorised by protein class or TFs only, among others. In addition, an enrichment analysis was performed according to Gene Ontology (GO)

processes and molecular functions. In IPA®, a ‘Core Analysis’ was performed using the same DE gene list and settings. This analysis includes different algorithms, such as ‘Canonical Pathways’, ‘Upstream Analysis’, ‘Diseases and Functions’ and ‘Networks’, among others. To compare two or more datasets, a ‘Comparison Analysis’ was performed using the same algorithms. In addition, the BioProfiler tool was used to further investigate important haematopoietic genes dysregulated by RUNX3, and the Molecular Activity Predictor algorithm was used to predict interactions according to the Ingenuity Knowledge Base.

Table 2-9 – Summary of transcriptomic datasets used in this study.

HSPC – Haematopoietic stem and progenitor cells; KD – Knockdown. *RUNX3* mRNA expression data from microarray studies obtained using 204197_s_at.

Cell model	Cell type	Observations	Accession number
Normal mRNA expression during haematopoiesis			
Human	Haematopoietic cells	Cells analysed at different stages of haematopoietic development	GSE24759
Mouse			GSE60101
Human			GSE17054 GSE19599 GSE11864 E-MEXP-1242
Human			GSE42519
Human			BLUEPRINT
mRNA expression in AML			
Human	AML patient samples	2096 samples	MILE study
		200 samples	TCGA
Human HSPC studies for comparison analysis – Chapter 5			
Human	HSPC	RUNX3 KD	GSE119264
	Erythroid progenitors		
	HSPC	RUNX1-ETO	E-MEXP-583

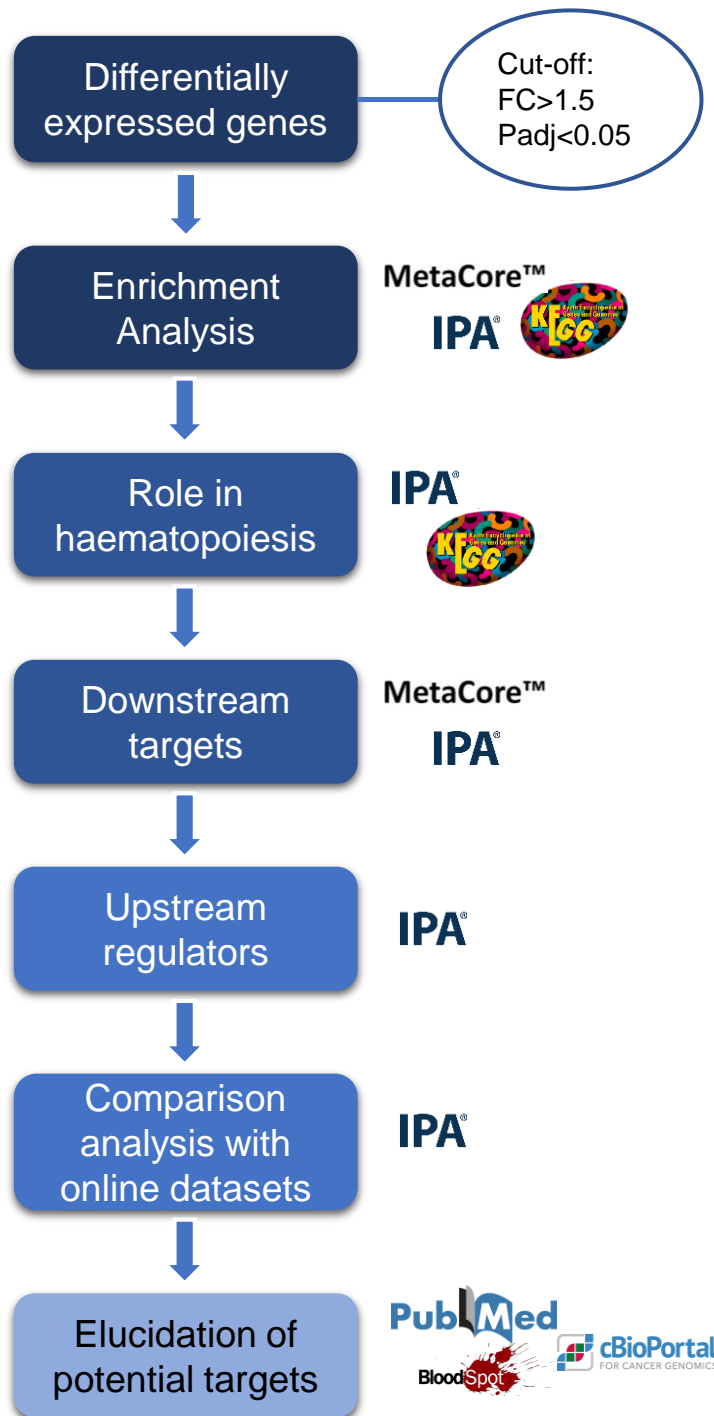


Figure 2-4 – Strategy employed for DE gene analysis to study the effects of *RUNX3* overexpression in human HSPC.

Diagram illustrating the strategy employed in the study of *RUNX3* overexpression effects on HSPC for DE gene analysis. Results were filtered using Fold Change > 1.5 and $p_{adj} < 0.05$ as cut-off values. Enrichment analysis was performed using MetaCore™, IPA® and KEGG databases. Downstream targets of *RUNX3* were obtained using both MetaCore™ and IPA® knowledge databases. Upstream regulator analysis was performed using a causal analytic algorithm available by IPA®.

3 RUNX3 Suppresses Normal Erythroid Development of Human CD34⁺ HSPC

3.1 Introduction

Several intracellular signalling proteins and TFs play an important role on the establishment of haematopoietic lineages by regulating not only the survival and proliferation of HSPC, but also cell fate decisions and differentiation (Zhu and Emerson 2002) (1.1). Disruption of these processes can lead to changes in haematopoietic differentiation and the subsequent development of haematopoietic malignancies. Chromosomal translocations involving TFs are a hallmark of AML with the t(8;21) encoding RUNX1-ETO, representing around 12% of all AML cases (1.2.4) (Peterson and Zhang 2004; Ptasinska *et al.* 2012). Despite being associated with a more favourable clinical outcome, the role of RUNX1-ETO in the pathogenesis of AML is poorly understood. This fusion protein has primarily been recognised as a dominant-negative regulator of RUNX1, nonetheless some studies suggest that RUNX1-ETO has other properties that may be important in its ability to promote leukemogenesis (Lam and Zhang 2012; Lin *et al.* 2017) (1.2.4.1).

Previous studies have shown that expression of RUNX1-ETO is capable of suppressing both human erythroid and myeloid differentiation whilst promoting the self-renewal of progenitor cells (Tonks *et al.* 2003; Tonks *et al.* 2004). In addition, RUNX1-ETO expression as a single abnormality caused a severe dysregulation of human HSPC transcriptome (Tonks *et al.* 2007). Interestingly, expression of RUNX1-ETO in HSPC leads to the repression of *RUNX3* mRNA, a member of the RUNX family of TFs (4.3.5). On the other hand, increased *RUNX3* expression has been associated with poorer survival rates in AML patients with the FLT3 mutation (Lacayo *et al.* 2004). In recent studies, *RUNX3* mRNA expression levels were associated with clinicopathological features, with mortality being more frequent among patients with a higher *RUNX3* expression level (Krygier *et al.* 2018; Sun *et al.* 2019). However, the role of RUNX3 in haematopoietic development is not well understood, with most studies using non-human models. One study demonstrated that aged *RUNX3* KO mice exhibited enhanced myeloproliferation and an expanded HSPC compartment,

suggesting that RUNX3 *per se* has an important role in haematopoiesis (Wang *et al.* 2013). Previous studies in murine models demonstrated that RUNX3 can rescue a haematopoietic defect due to RUNX1 deficiency, implying redundancy among RUNX proteins in murine haematopoiesis (Goyama *et al.* 2004; Fukushima-Nakase *et al.* 2005).

Considering that RUNX3 was shown to be dysregulated by RUNX1-ETO expression in HSPC, and that RUNX1-ETO leads to abnormal erythroid development of these cells, this Chapter seeks to establish the role of RUNX3 expression on normal human erythropoiesis. Further studies will investigate the effects of RUNX3 expression on the myeloid development (Chapter 4).

3.2 Aims and objectives

This study hypothesises that changes in the expression of RUNX3 will affect the development of normal human primary erythroid cells. The main aim of this Chapter is to understand the normal expression of RUNX3 and its role on erythroid development using a normal human primary HSPC model. To achieve this aim, this Chapter has the following objectives:

- **Determine the expression level of *RUNX3* during normal erythroid development.**

Analysis of publicly available transcriptomic datasets will be performed to determine *RUNX3* mRNA expression levels in both mouse and human CD34⁺ HSPC subsets.

- **Determine the effect of *RUNX3* overexpression/knockdown on human erythroid colony forming ability and self-renewal.**

Limiting-dilution colony forming assays will be performed using control and RUNX3-expressing human HSPC previously enriched for erythroid progenitors. This will be followed by serial replating to assess the self-renewal potential of cells.

- **Determine the effect of RUNX3 overexpression/knockdown on the growth and differentiation of erythroid cells.**

Transduced human HSPC will be grown in bulk liquid culture and changes in their erythroid growth and differentiation will be assessed by analysis of lineage and developmental cell surface markers coupled with multicolour flow cytometry.

3.3 Results

3.3.1 Expression of *RUNX3* declines during human terminal erythroid development

To elucidate the impact of RUNX3 expression on human erythroid differentiation it was necessary to understand the normal expression level of RUNX3 during this process. Analysis of publicly available transcriptomic datasets using human CB purified cells and different haematopoietic cell subsets (Novershtern *et al.* 2011) shows that *RUNX3* mRNA expression significantly decrease during erythropoiesis. In particular, this reduction occurs as cells mature from pro-erythroblasts towards reticulocytes (Figure 3-1A). RNA-seq data from multiple murine haematopoietic cell types (Lara-Astiaso *et al.* 2014) show a similar reduction in *RUNX3* levels with differentiation, especially in the erythroid lineage (Figure 3-1B). Further, microarray data was analysed for *RUNX3* mRNA expression in normal human CD34⁺ HSPC cultured towards different lineages (Tonks *et al.* 2007). As shown in Figure 3-1C, an expected decrease in *RUNX3* mRNA expression was observed for erythroid-committed cells in comparison with HSPC.

Taken together, these data suggest that RUNX3 is expressed at the mRNA level in HSPC and its expression is gradually reduced as cells differentiate into mature human erythrocytes.

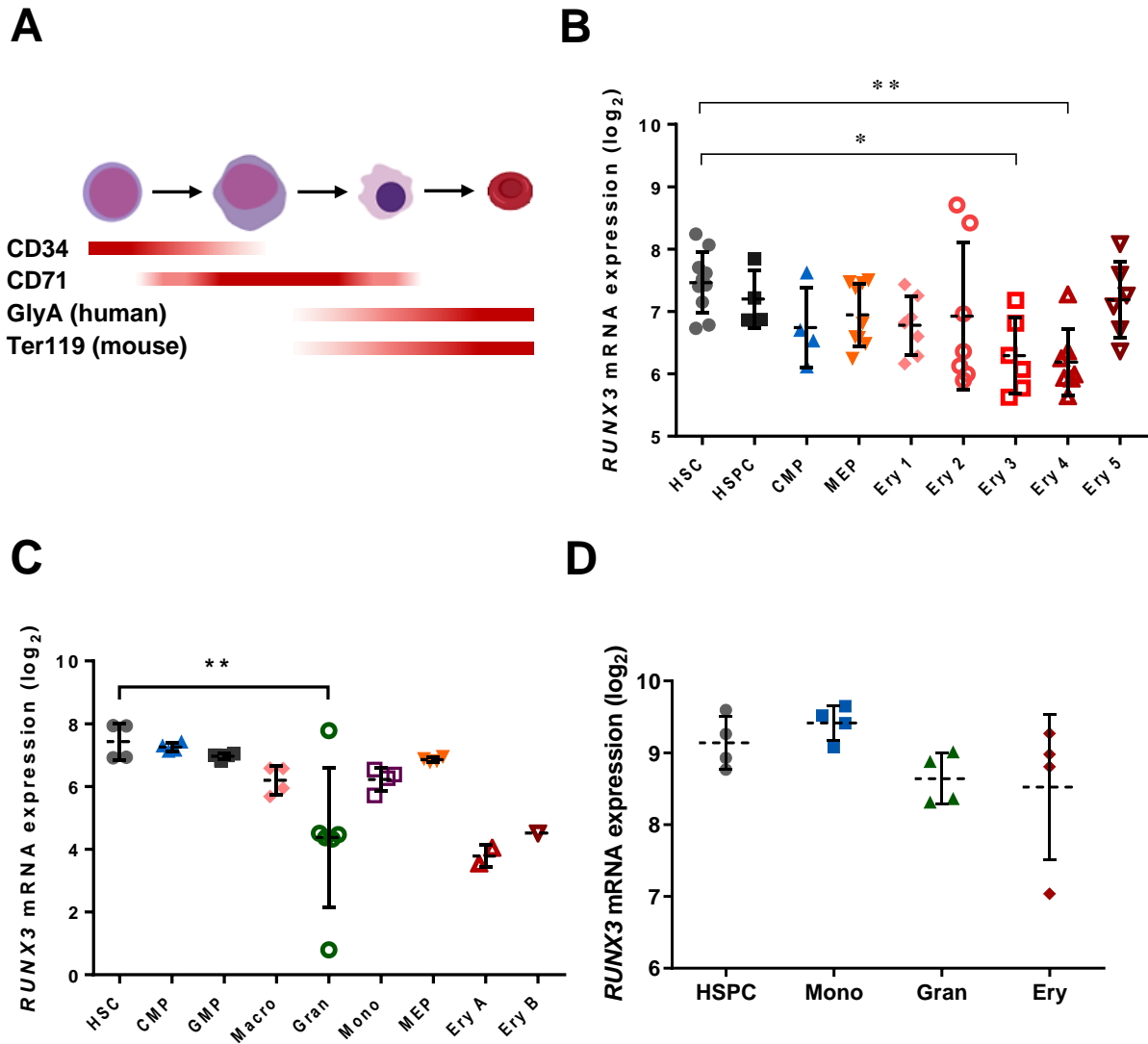


Figure 3-1 – mRNA expression levels of RUNX3 in normal haematopoiesis.

(A) Expression of stage-specific cell surface markers during erythroid development. **(B)** *RUNX3* mRNA expression in distinct haematopoietic cell subsets based on cell surface marker expression. HSC – Haematopoietic stem cell CD133⁺CD34^{dim}; HPC – Haematopoietic progenitor cell CD38⁺CD34⁺; CMP – Common myeloid progenitor; MEP – Megakaryocyte/erythroid progenitor; Ery 1 –Erythroid CD34⁺CD71⁺GlyA⁻; Ery 2 – Erythroid CD34⁻CD71⁺GlyA⁻; Ery 3 – Erythroid CD34⁻CD71⁺GlyA⁺; Ery 4 – Erythroid CD34⁻CD71^{low}GlyA⁺; Ery 5 – Erythroid CD34⁻CD71⁻GlyA⁺. Data obtained from GSE24759 using 204197_s_at probeset (Novershtern *et al.* 2011). Data indicate mean ± 1SD (n≥4). **(C)** *RUNX3* mRNA expression across different murine haematopoietic cell types. GMP – Granulocyte-monocyte progenitor; Macro – Bone marrow macrophages; Gran – Granulocytes; Mono – Monocytes; Ery A – Erythrocytes B220⁻CD3⁻Ter119⁺CD71⁺; Ery B – Erythrocytes B220⁻CD3⁻Ter119⁺CD71⁻. Data obtained from GSE60101 (Lara-Astiaso *et al.* 2014). Data indicate mean ± 1SD (n≥2). Data from both sets indicate mean ± 1SD of at least four independent experiments. Statistical analysis was performed using ANOVA with Tukey’s multiple comparison test, **p*<0.05; ***p*<0.01 vs HSC. **(D)** *RUNX3* mRNA expression in human CB derived CD34⁺ HSPC, monocytic, granulocytic and erythrocytic-enriched populations. Data obtained from e-mexp-583 using 204197_s_at probeset (Tonks *et al.* 2007). HSPC – Haematopoietic stem and progenitor cells (CD34⁺); Mono – Monocyte-committed cells (CD34⁻CD13⁺CD36⁺); Gran – Granulocyte-committed cells (CD34⁻CD13⁺CD36⁻); Ery – Erythroid-committed cells (CD34⁻CD13⁻CD36⁺).

3.3.2 Overexpression of RUNX3 suppresses human erythroid development

As *RUNX3* expression naturally decreases with erythroid maturation, this study first sought to investigate the effect of RUNX3 overexpression on erythroid growth, development, and self-renewal. To achieve this, RUNX3 was ectopically expressed as a single abnormality (co-expressing DsRed as a selectable marker) in an *in vitro* model of human haematopoiesis. To study erythropoiesis in detail, two different phases of erythroid growth, controlled by the absence/presence of EPO in the culture media, were examined.

3.3.2.1 Generation of RUNX3 overexpressing HSPC

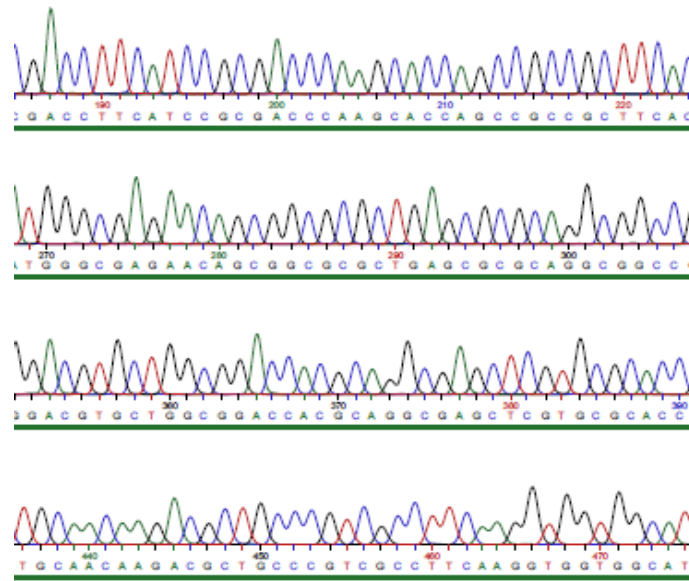
Validation of subcloning RUNX3 cDNA into a retroviral plasmid

A retroviral vector based on PINCO backbone (Grignani *et al.* 1998) harbouring RUNX3 and co-expressing DsRed as a selectable marker was kindly provided by Dr Tonks (Cardiff University). The *RUNX3* transcript variant associated with this vector encodes the p46 isoform transcribed from the P1 promoter (1.3.1, 2.2.1). Since this vector had not been used or validated previously, it was necessary to confirm the successful subcloning of *RUNX3* into the PINCO plasmid (2.2.6). PINCO-RUNX3 plasmid cDNA was sequenced using primers flanking the *Bam*HI and *Eco*RI cloning site (Figure 3-2). Using Clustal Omega, a 100% sequence alignment was observed using primers 1 (reverse) and 2 (forward) with the published CDS of RUNX3 (NM_001031680.2). These data demonstrated that the *RUNX3* sequence was subcloned into the vector correctly with no mutations, and therefore could be used for subsequent studies.

RUNX3 and DsRed protein expression is observed in Phoenix cells transfected with plasmid cDNA

Having generated and validated the cDNA sequence of control (expressing DsRed alone) and RUNX3 expressing retroviral plasmids, Nx packaging cells were transiently transfected with cDNA to generate retrovirus (2.5). As shown in Figure 3-3A, over 90% of control and RUNX3 transfected Nx cells expressed DsRed. To determine the ectopic expression of RUNX3 protein in these cells, a western blot was performed.

A



B

Primer2	GTTTCACCTGACCATCACTGTGTTACCAACCCACCAAGTGGCGACCTACCACCGAG	660
RUNX3NCBI	gtttcacctgaccatcactgtgttcaccaacccccaccaagtgccgacctaccaccgag	547
Primer1	-----ACCATCACTGTGTTACCAACCCACCAAGTGGCGACCTACCACCGAG	49
PINCO-RUNX3	GTTTCACCTGACCATCACTGTGTTACCAACCCACCAAGTGGCGACCTACCACCGAG	578

Primer2	CCATCAAGGTGACCGTGGACGGACCCGGGAGCCAGACGGCACCGGACAGAAAGCTGGAGG	720
RUNX3NCBI	ccatcaaggtgaccgtggacggacccccgggagccagacggcaccggcagaagctggagg	607
Primer1	CCATCAAGGTGACCGTGGACGGACCCGGGAGCCAGACGGCACCGGACAGAAAGCTGGAGG	109
PINCO-RUNX3	CCATCAAGGTGACCGTGGACGGACCCGGGAGCCAGACGGCACCGGACAGAAAGCTGGAGG	638

Primer2	ACCAGACCAAGCGTTCCTGACCGCTTGGGGACCTGGAACGGCTGCGCATGCGGGTGA	780
RUNX3NCBI	accagaccaagcgttccctgaccgcttggggacctggaacggctgcatgcccgggtga	667
Primer1	ACCAGACCAAGCGTTCCTGACCGCTTGGGGACCTGGAACGGCTGCGCATGCGGGTGA	169
PINCO-RUNX3	ACCAGACCAAGCGTTCCTGACCGCTTGGGGACCTGGAACGGCTGCGCATGCGGGTGA	698

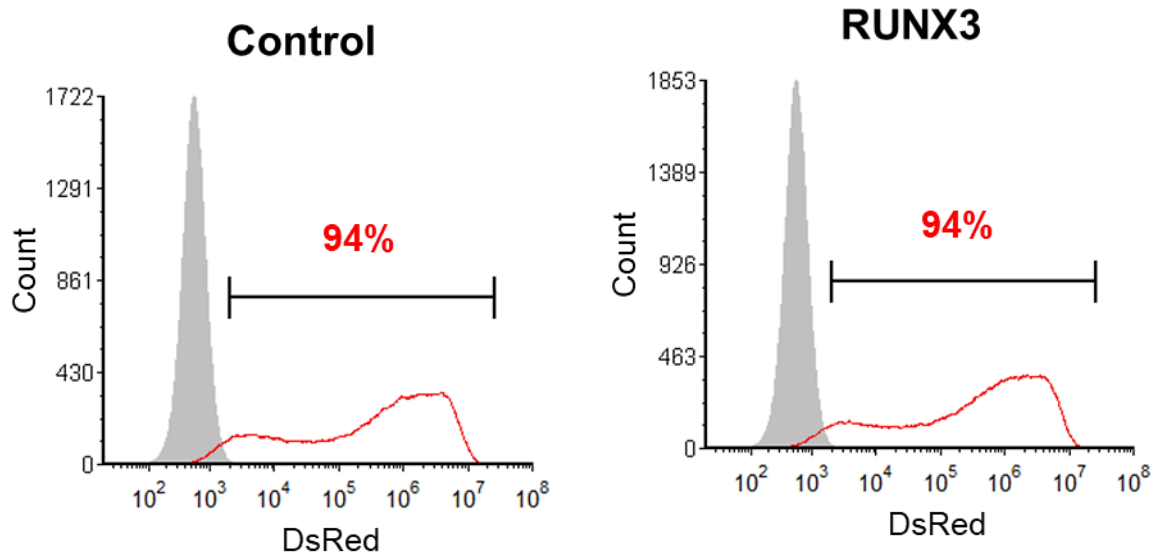
Primer2	CACCGAGCACACCCAGCCCCGAGGCTCACTCAGCACCACAAGCCACTTCAGCAGCCAGC	840
RUNX3NCBI	caccgagcacaccagccccgaggctcactcagcaccacaagccacttcagcagccagc	727
Primer1	CACCGAGCACACCCAGCCCCGAGGCTCACTCAGCACCACAAGCCACTTCAGCAGCCAGC	229
PINCO-RUNX3	CACCGAGCACACCCAGCCCCGAGGCTCACTCAGCACCACAAGCCACTTCAGCAGCCAGC	758

Primer2	CCCAGACCCCAATCCAAGGCACCTCGGAACCTGAACC-----	876
RUNX3NCBI	cccagaccccaatccaaggcacctcggaaactgaaccattctccgacccccgagtttg	787
Primer1	CCCAGACCCCAATCCAAGGCACCTCGGAACCTGAACCCATTCTCCGACCCCGCCAGTTTG	289
PINCO-RUNX3	CCCAGACCCCAATCCAAGGCACCTCGGAACCTGAACCCATTCTCCGACCCCGCCAGTTTG	818

Figure 3-2 – Plasmid cDNA sequencing confirms subcloning of *RUNX3* into PINCO.

(A) Example partial DNA sequencing trace chromatogram of RUNX3 DsRed plasmid (C – Cytosine, blue; A – Adenine, green; T – Thymine, red; G – Guanine, black). The green bar below chromatogram represents high confidence scores. (B) Sequence alignment between primers 1 and 2, the theorised sequence of PINCO-RUNX3 plasmid and the published coding sequence of RUNX3 (NM_001031680.2). Stars show perfect alignment between all sequences, and numbers represent nucleotide positions.

A



B

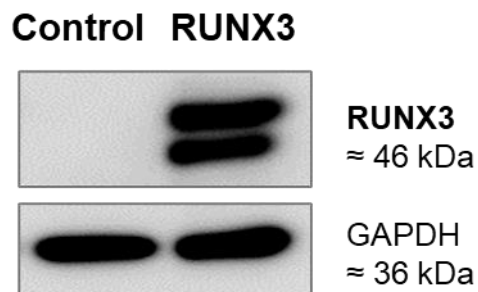


Figure 3-3 – Control and RUNX3 plasmids are successfully transfected into Nx cells.

(A) Example flow cytometric histogram showing the percentage of Nx cells transfected with control or PINCO-RUNX3 expressing DsRed vectors. Untransfected Nx cells – grey; Transfected Nx cells – Red. Representative data. **(B)** Representative western blot of RUNX3 protein in control and RUNX3 expressing Nx cells. GAPDH was used as a loading control.

Figure 3-3B shows RUNX3 protein expressed in Nx cells transfected with PINCO-RUNX3 whilst absent in control cultures. A double band was observed for RUNX3 protein which could be explained by post-translational modifications such as phosphorylation (1.3.2.1). These data demonstrate that in the context Nx cells, transfection of these vectors is functional in terms of DsRed and RUNX3 expression.

Expression of control DsRed and RUNX3 in human HSPC cells

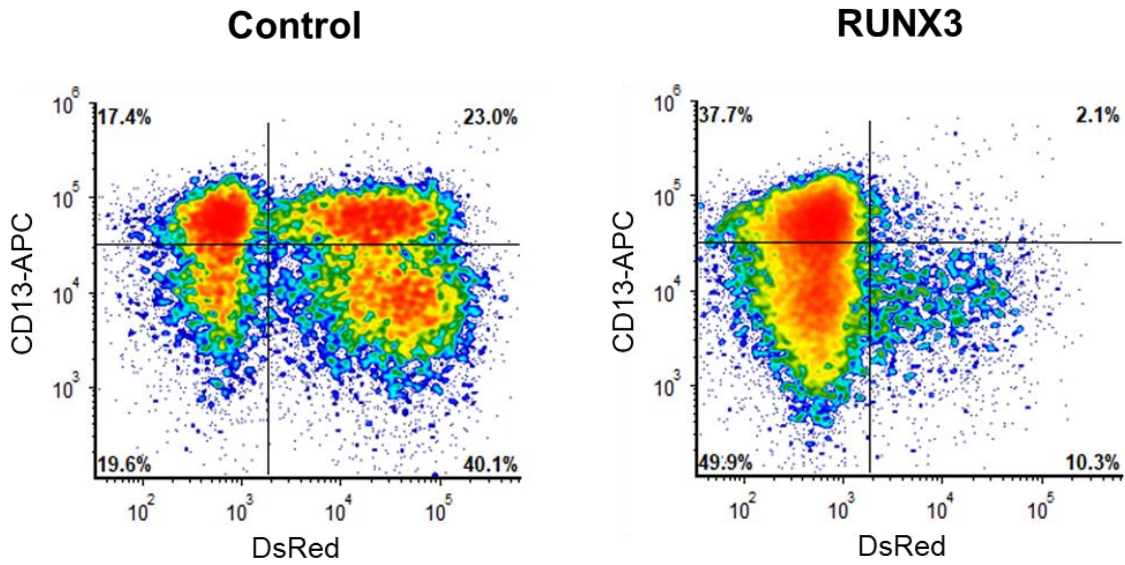
In order to determine the effects of RUNX3 expression on human erythroid development, normal human CB derived CD34⁺ HSPC were infected with a recombinant retrovirus derived from the vectors described above. Following infection, cultures were enriched for DsRed⁺CD13⁻ cells (on day 3 of culture) by FACS in order to aid the analysis of the retrovirally transduced erythroid population (CD13⁻CD36⁺) (Figure 3-4A). Pre- and post-FACS analysis showed an enrichment of DsRed⁺ cells to more than 90% (Figure 3-4B). Infection efficiencies for both control and RUNX3 retrovirus in HSPC cells are summarised in Figure 3-5A.

Induced expression of RUNX3 in HSPC was validated by qRT-PCR and western blot on day 3 and 6 of culture, respectively. As shown in Figure 3-5B and C, RUNX3 was successfully overexpressed at the mRNA level by 16.8 ± 4.9 -fold and at the protein levels by 4.4-fold in cells infected with RUNX3 vector compared with empty vector. Furthermore, the distribution of RUNX3 bands is similar to endogenous levels in control cells. This result also provides confirmation of RUNX3 nuclear localisation.

3.3.2.2 RUNX3 expression inhibits erythroid colony formation and promotes self-renewal

Having generated and validated the overexpression of RUNX3 in human HSPC, the effects on erythroid colony forming capacity and self-renewal were examined under clonal conditions. Primitive erythroid cells (predominantly DsRed⁺CD34⁺CD13⁻) were seeded by limiting dilution in 96-well plates and cultured in the presence of IL-3, SCF, IL-6 and EPO. Under these conditions, the colony forming efficiency of RUNX3-expressing cells was 1.7 ± 0.7 -fold lower when compared with control (Figure 3-6A). Self-renewal potential was subsequently assessed by serial replating of colony forming cells. RUNX3-expressing cells were able to form 2.7 ± 0.6 -fold more erythroid colonies than the control (Figure 3-6B).

A



B

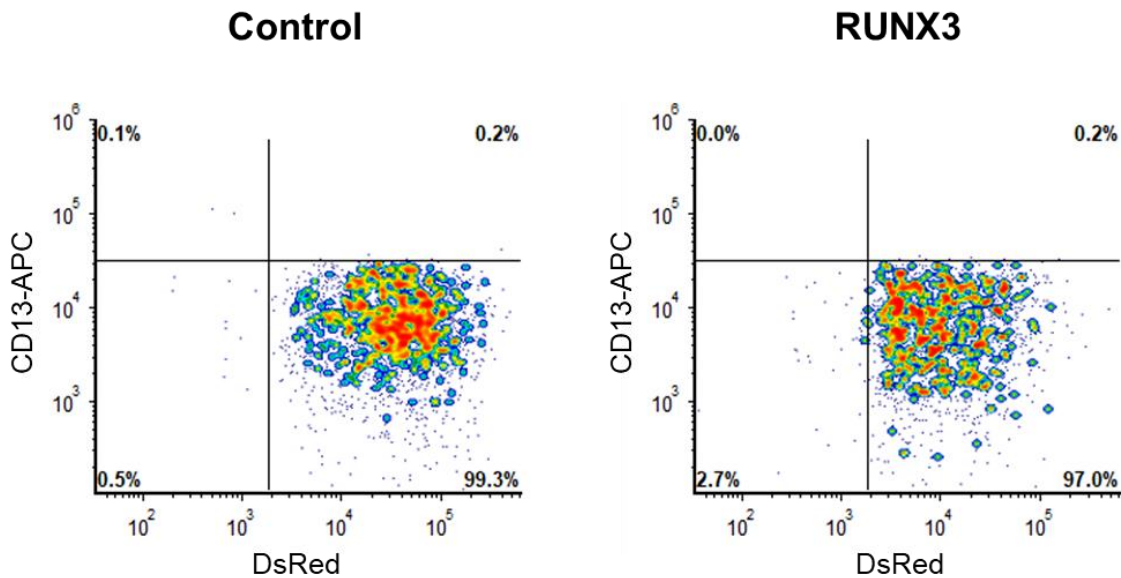


Figure 3-4 – Expression of control DsRed and RUNX3 in human HSPC cells.

(A) Representative bi-variate density plots of CD13 expression vs DsRed in control and RUNX3 cultures (day 3) pre-sorting for CD13-DsRed⁺ erythroid population. **(B)** Representative bi-variate density plots of CD13 expression vs DsRed in control and RUNX3 cultures (day 3) post-sorting for CD13-DsRed⁺ erythroid-committed cells. An initial gating on viable cells was applied on all plots based on light scatter.

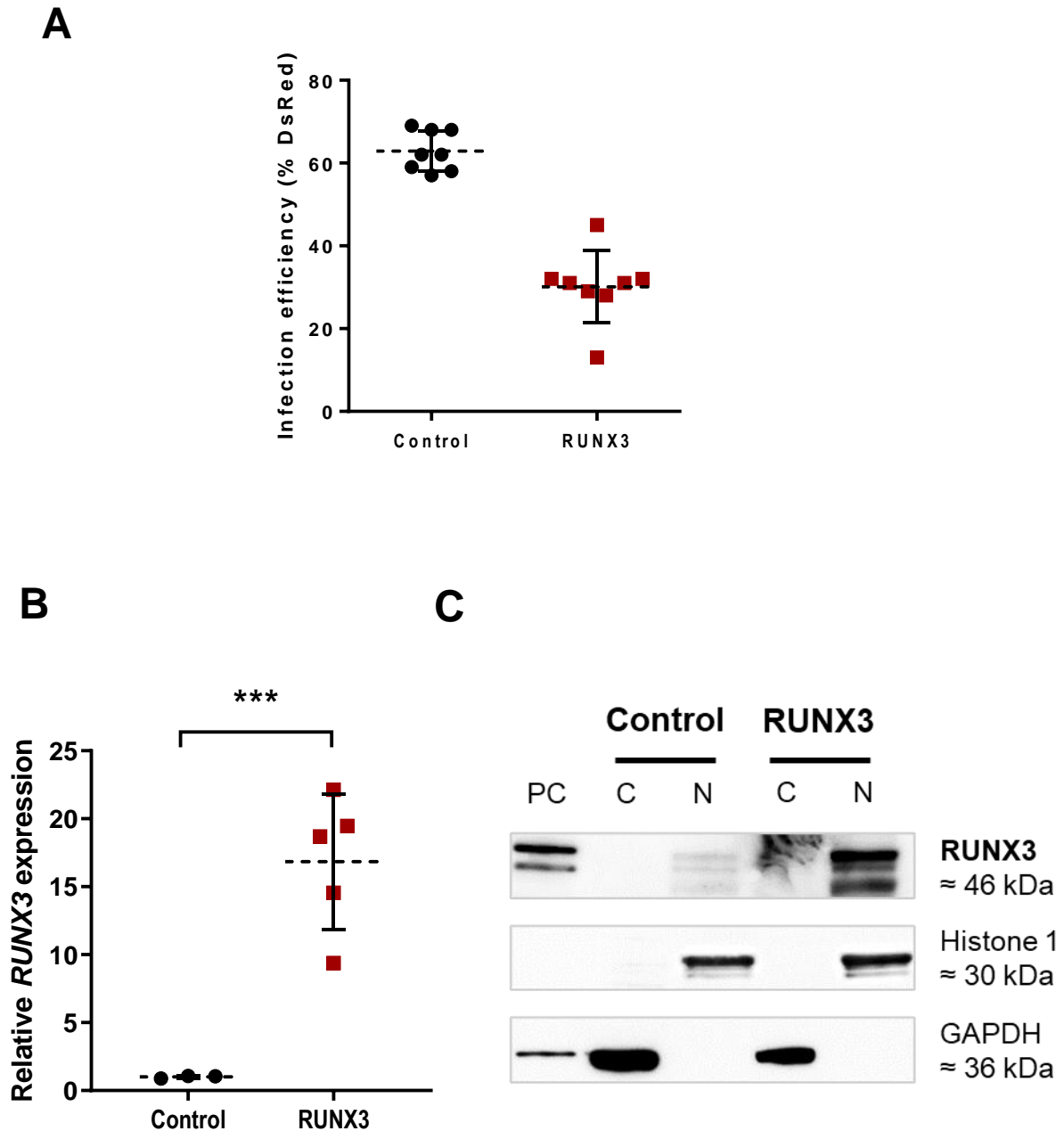
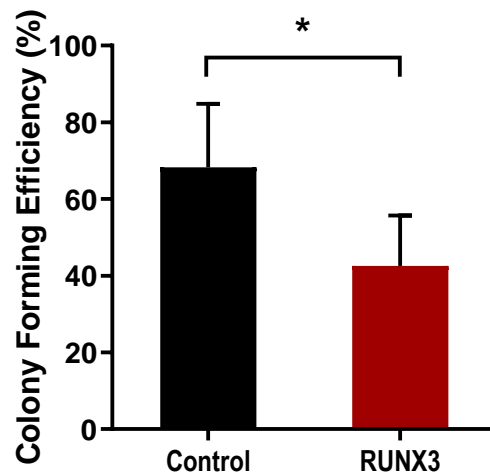


Figure 3-5 – RUNX3 is successfully expressed in human HSPC cells.

(A) Summary data of percentages of DsRed⁺ cells in control and RUNX3 cultures. Data indicate mean ± 1SD of eight independent experiments. (B) Relative *RUNX3* mRNA levels in control and RUNX3 GFP⁺ cells on day 3 of culture. Total RNA extracts obtained from Chapter 5 RNA-seq studies. Data indicate mean ± 1SD of at least three independent experiments. GAPDH was used as endogenous control. Relative expression calculated using the Comparative C_T ($\Delta\Delta C_T$) method (2.8.2). Significant difference of RUNX3-expressing cells from controls was analysed by two-sample t test, *** $p < 0.001$. (C) Example western blot analysis of RUNX3 protein levels in the cytosol and nucleus of control and RUNX3 unsorted HSPC cells (day 6 of culture). Nx expressing RUNX3 were used as a positive control (total extract) and GAPDH/Histone 1 as loading controls. PC – Positive control; C – Cytosol; N – Nucleus.

A



B

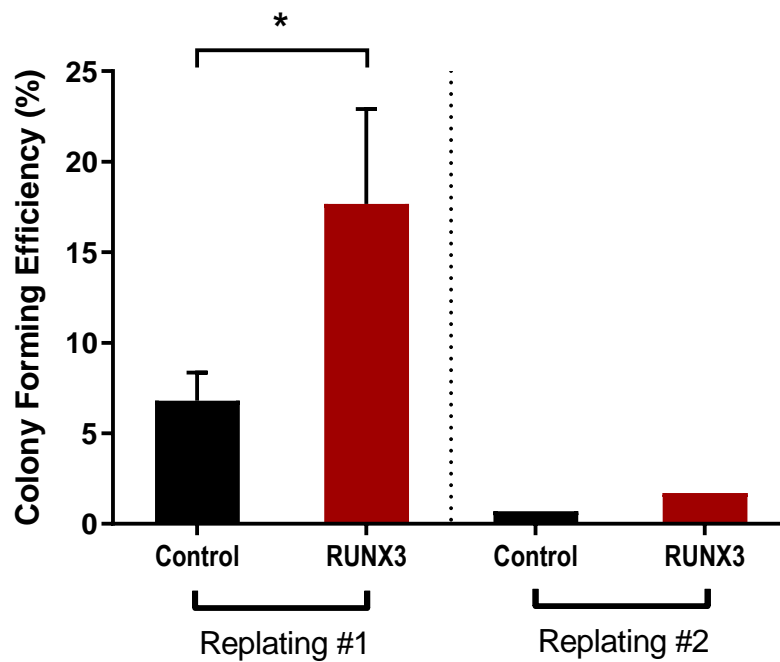


Figure 3-6 – RUNX3 expression inhibits erythroid colony formation and promotes self-renewal after an initial replating of colony forming cells.

(A) Colony forming efficiency of control and RUNX3-expressing cultures following 7 days of growth in liquid culture containing IL-3, IL-6, SCF, and EPO (2.3.5). Data indicate mean \pm 1SD of at least three independent experiments. **(B)** Self-renewal potential assessed by 2 replating rounds of control and RUNX3 cultures in the same conditions as previously. Replating #1 data indicate mean \pm 1SD of three independent experiments. Significant difference of RUNX3-expressing cells from controls was analysed by paired t test, $*p < 0.05$. Replating #2 data was obtained from a single experiment.

This difference was lessened in a subsequent replating, as cells approached senescence. Taken together, these data indicate that expression of RUNX3 impairs erythroid colony formation, but these cells have a higher self-renewal potential following an initial replating of colony forming cells.

3.3.2.3 RUNX3 expression disturbs early erythroid differentiation

Erythroid differentiation can be divided into an early developmental stage which occurs independently of EPO (EPO-independent phase, 1.1.3) and a late developmental stage that depends on the presence of this cytokine (Wu *et al.* 1995). Having generated a population of retrovirally transduced cells enriched for primitive erythroid cells (DsRed⁺CD34⁺CD13⁻), the effects of RUNX3 overexpression on EPO-independent erythroid development was first determined. Growth and differentiation were assessed within the CD13⁻CD36⁺ erythroid-committed population. RUNX3 expressing erythroid-committed cells exhibited a slower growth compared to control cells during the EPO-independent stage of development, though it did not reach significance (Figure 3-7). This finding suggests that RUNX3 does not impair significantly erythroid growth in early stage of development.

To determine the effects of RUNX3 overexpression in the differentiation of erythroid cells during the EPO-independent phase, cell surface protein expression was analysed over time by flow cytometry. The lineage discriminators CD13 and CD36 were used to discriminate erythroid-committed cells (CD13⁻CD36⁺) from other lineages. Within this population a panel of developmental markers including CD34 and GlyA were used to determine their differentiation status. Phenotypic changes associated with normal early erythropoiesis are characterised by an increase of CD36 expression with a simultaneous loss of CD34, the HSPC marker (van Schravendijk *et al.* 1992; Darley *et al.* 1997; Ziegler *et al.* 1999). The gating strategy used to follow the erythroid differentiation of cells over time is shown in Figure 3-8. As shown in Figure 3-9A and B, abnormalities in the pattern of CD36 expression were observed as a result of RUNX3 overexpression. The proportion of CD13⁻CD36⁺ erythroid-committed cells was lower for cells expressing RUNX3 (19% vs 30% on day 6), as exemplified in Figure 3-9A. Within this population, RUNX3 expressing cells exhibited a 1.2 ± 0.1 -fold significant downregulation of CD36 expression compared to control cells (day 6, Figure 3-9B).

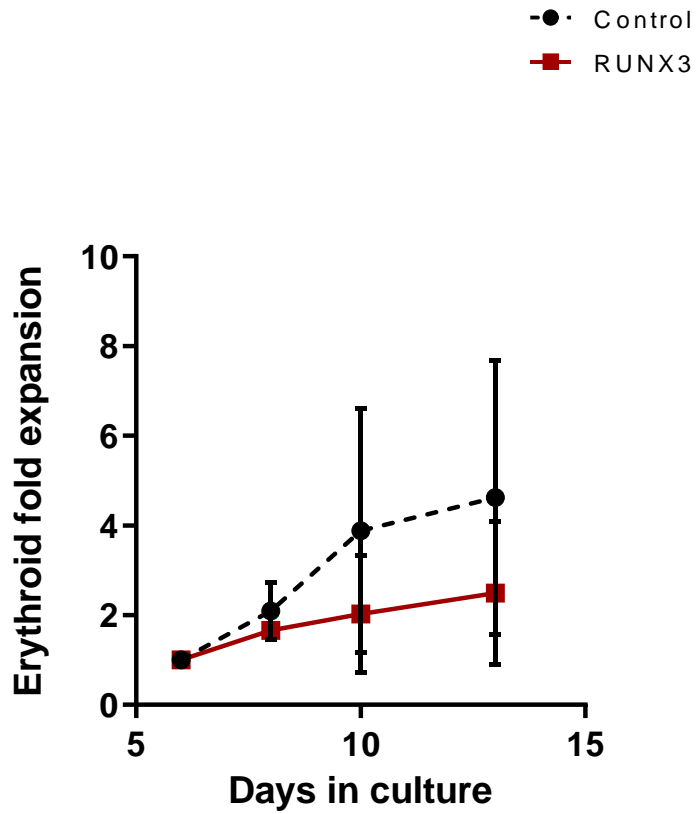


Figure 3-7 – RUNX3 induces a modest early erythroid growth suppression during the EPO-independent phase of differentiation.

Cumulative fold expansion of CD13-CD36⁺ erythroid-committed cells during the EPO-independent phase of growth. Cells were grown in media supplemented with IL-3, IL-6 and SCF for their first 13 days of culture. Data indicate mean \pm 1SD of at least three independent experiments.

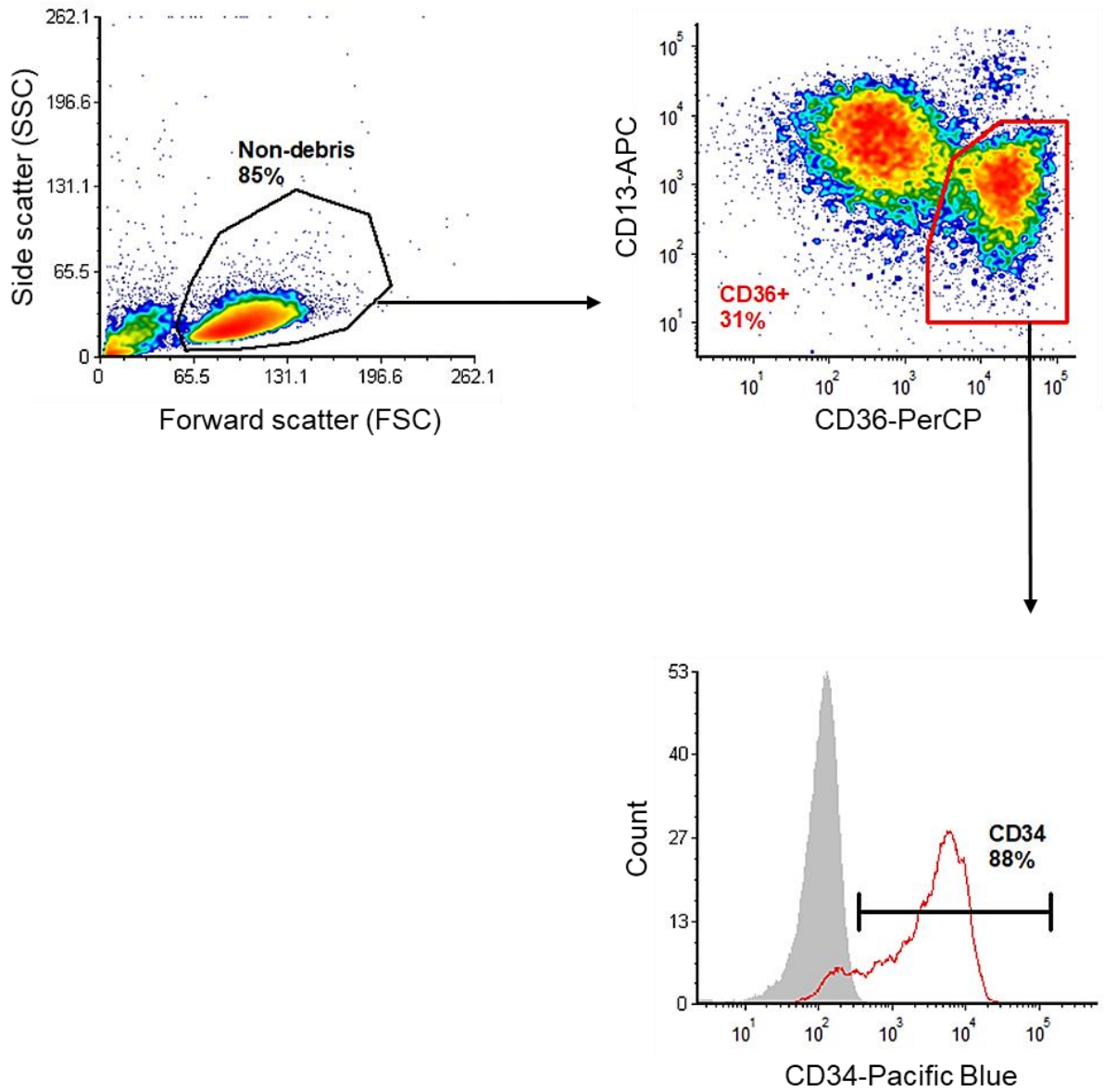


Figure 3-8 – Gating strategy used to follow the erythroid differentiation of HSPC by flow cytometry.

Representative density plots and flow cytometry histograms of erythroid progenitor cells on day 3 of differentiation. Non-debris – Gate used to exclude all debris from the analysis. CD36+ – Gate to analyse the differentiation of erythroid committed cells CD13–CD36+; IgG-Pacific Blue HSPC cells – grey.

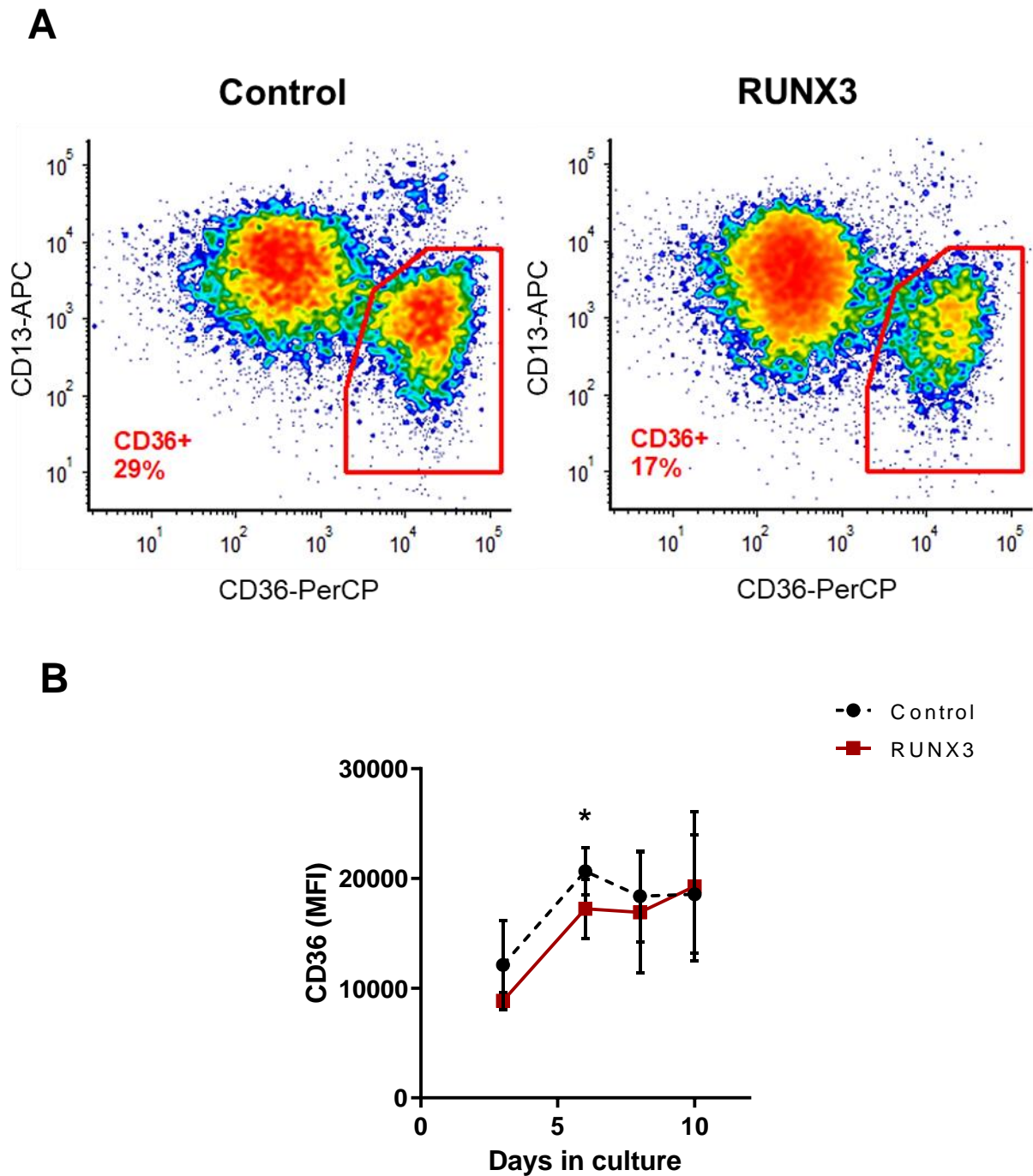


Figure 3-9 – RUNX3 downregulates CD36 expression in HSPC during the EPO-independent erythroid differentiation.

(A) Example density plots of control and RUNX3 cultures labelled with the lineage discriminators markers CD13 and CD36 (Day 6 of differentiation). **(B)** Summary data of CD36 expression (mean fluorescence intensity, MFI) in CD13-CD36⁺ erythroid-committed cells over time. Data indicate mean \pm 1SD of at least four independent experiments. Significant difference of RUNX3-expressing cells from controls was analysed by paired t test, * $p < 0.05$.

Taken together, increased expression of RUNX3 led to a reduced frequency of CD13⁻CD36⁺ erythroid-committed cells, which implies a reduced erythroid commitment by these cells. In terms of differentiation, an example of CD34 histograms for both cultures on day 8 of differentiation is shown in [Figure 3-10A](#). The erythroid-committed population for both control and RUNX3 transduced cells exhibited a similar reduction of CD34 expression over time ([Figure 3-10B](#)).

In summary, overexpression of RUNX3 in human HSPC induces abnormalities in the expression of lineage-specific markers suggestive of a suppression of early erythroid development.

3.3.2.4 RUNX3 expression disturbs EPO-dependent growth and development

Data above suggests that ectopic expression of RUNX3 delays early erythropoiesis. This study subsequently analysed the effects of RUNX3 on the EPO-dependent phase of erythroid development. Cell differentiation is tightly coordinated with cell cycle exit and is characterised by the growth arrest of terminally differentiated erythroid cells (Hsieh *et al.* 2000). As shown in [Figure 3-11](#), controls expanded in the presence of EPO and, as expected, the net proliferation of these cells decelerated as cells became more mature over time ceasing by day 17. Furthermore, RUNX3 transduced cells overcame the growth suppression observed in the early stages of development and enhanced their proliferation by 7.0 ± 4.7 -fold on day 20 compared to control cells. These data indicate that RUNX3-expressing cells may be less differentiated than controls given their higher proliferative capacity.

Given that RUNX3 expressing cells proliferated more than controls, this study next examined whether differentiation was normal. As erythroid cells terminally differentiate, there is a reduction in cell size and upregulation of GlyA (Darley *et al.* 2002; Tonks *et al.* 2003). Accordingly, their size decreased with time and levels of CD36 follow the same trend (Dzierzak and Philipsen 2013; Mao *et al.* 2016).

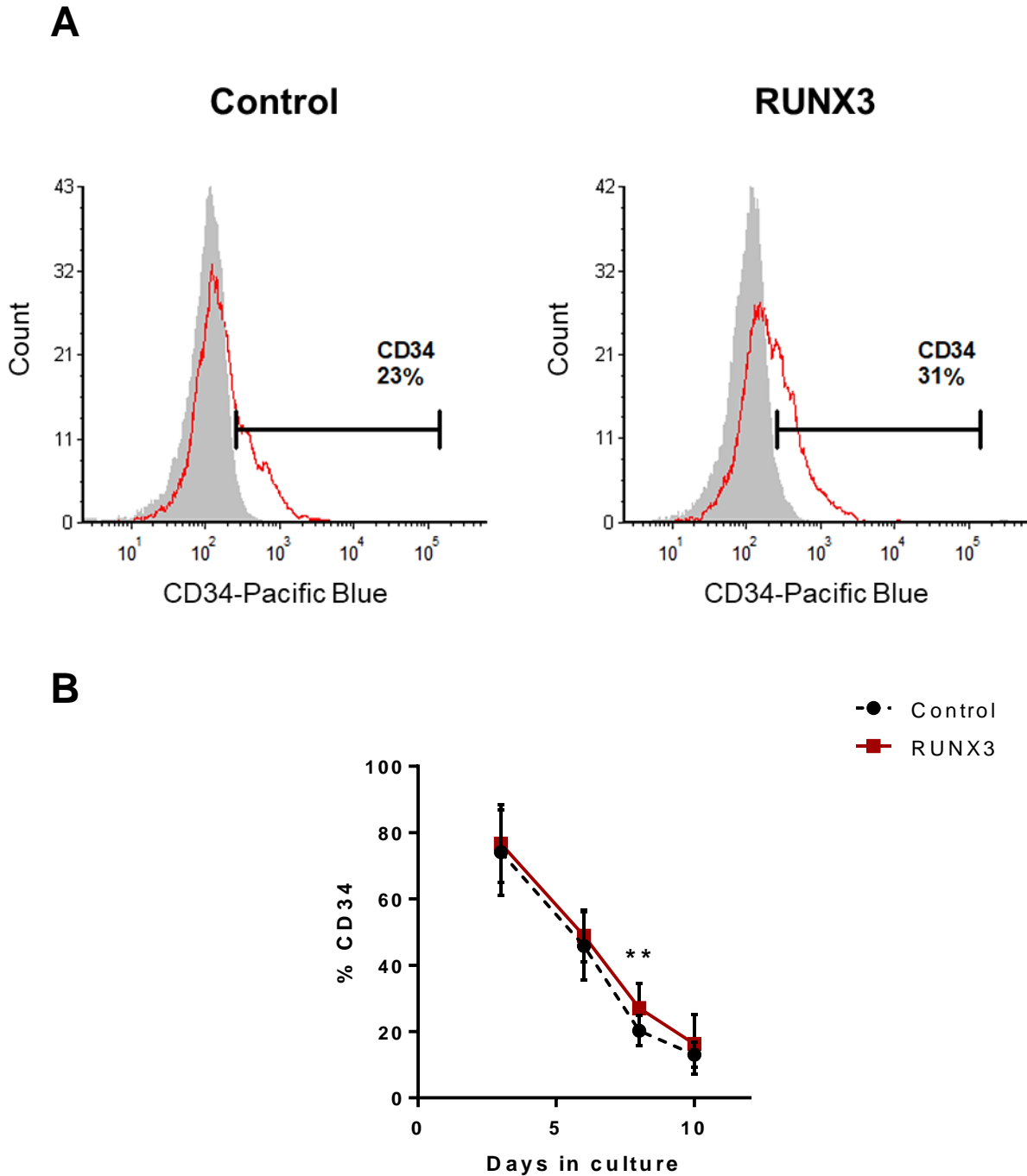


Figure 3-10 – CD34 expression is downregulated in both control and RUNX3-expressing cells during the EPO-independent erythroid differentiation.

(A) Example histograms of control and RUNX3 cultures labelled with the HSPC marker CD34 (Day 8 of differentiation). IgG-Pacific Blue stained HSPC cells – grey. **(B)** Summary data showing CD34 expression in terms of percentage in DsRed⁺ CD13⁻CD36⁺ cells over time. Data indicate mean \pm 1SD of at least four independent experiments. Significant difference of RUNX3-expressing cells from controls was analysed by paired t test, ** $p < 0.01$.

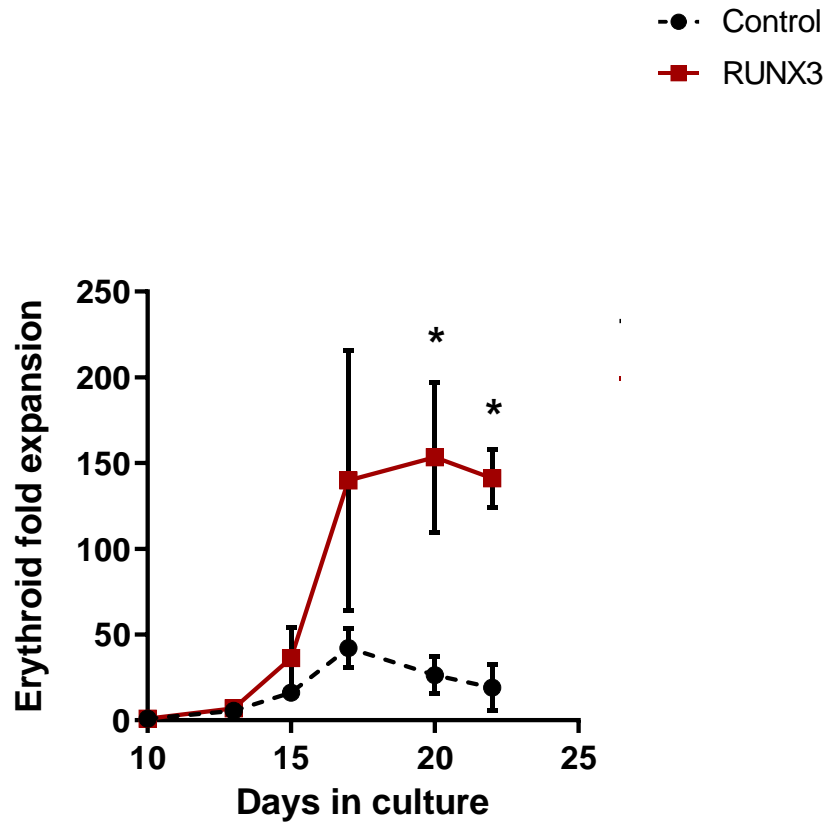


Figure 3-11 – RUNX3 overcome growth suppression during the EPO-dependent phase of differentiation.

Cumulative fold expansion of CD13-CD36⁺ erythroid-committed cells during the EPO-dependent phase of growth. Cells were grown in media supplemented with IL-3, IL-6, SCF and EPO from day 10 to day 22 of differentiation. Data indicate mean \pm 1SD of at least four independent experiments. Significant difference of RUNX3-expressing cells from controls was analysed by paired t test, * $p < 0.05$.

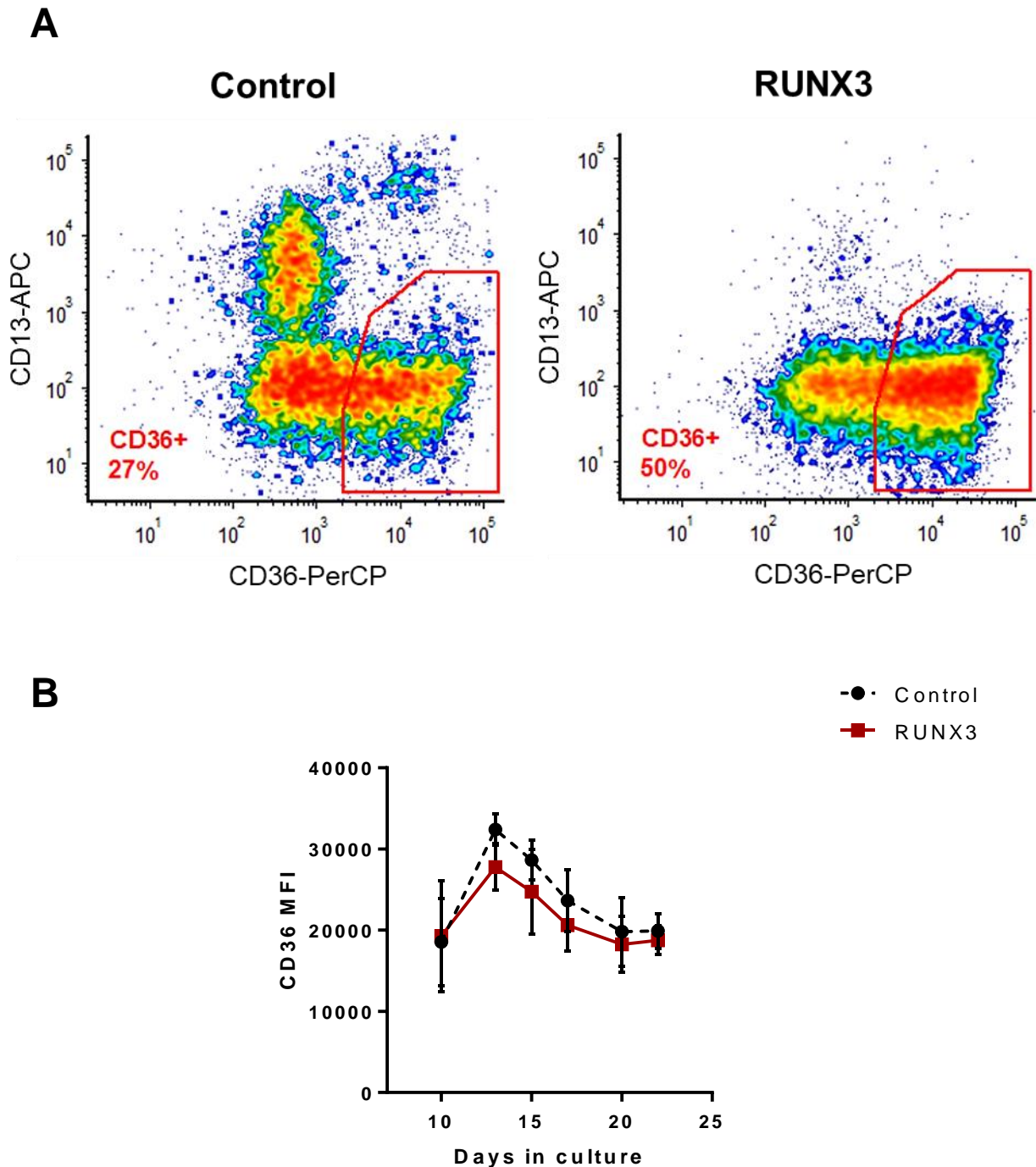


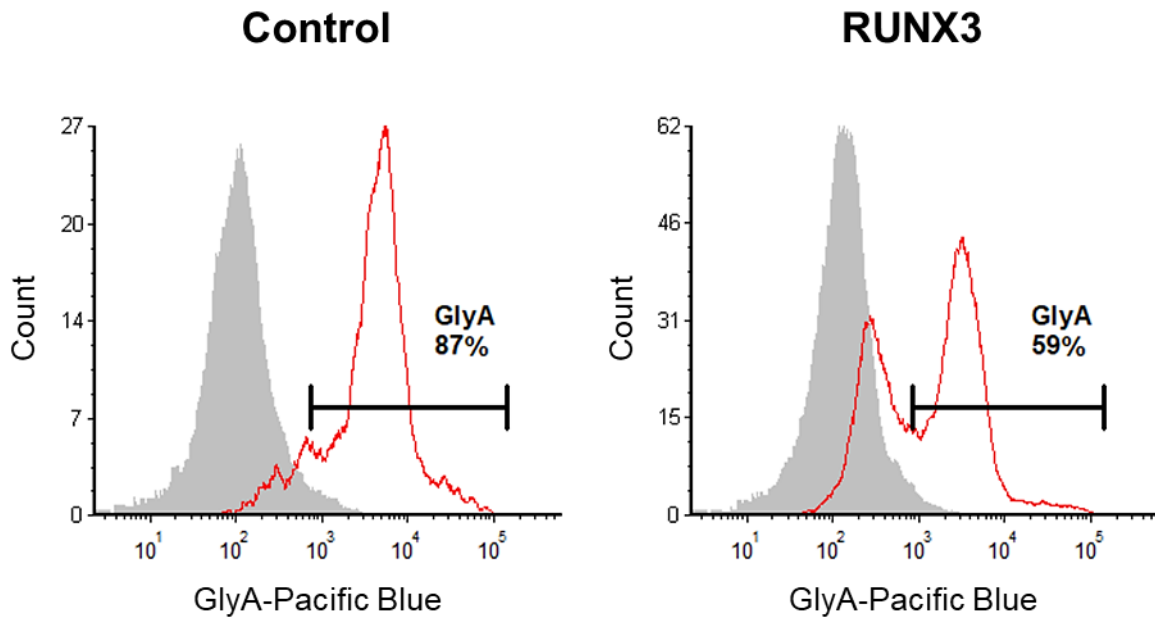
Figure 3-12 – RUNX3 induces abnormalities in CD36 expression during the EPO-dependent phase of differentiation.

(A) Example density plots of control and RUNX3 cultures labelled with the lineage discriminator markers CD13 and CD36 (Day 22 of differentiation). The effects of RUNX3 overexpression on monocytic and granulocytic cells (CD13⁺) are described in 4.3.3. **(B)** Summary data of CD36 expression profile in terms of MFI in CD13⁺CD36⁺ cells over time. Data indicate mean \pm 1SD of at least four independent experiments.

Although the percentage of CD36⁺ cells was higher in RUNX3 culture compared to controls (Figure 3-12A), within this erythroid population the intensity of CD36 expression was reduced by 1.2 ± 0.1 -fold compared to control cells and close to significance on day 13 of culture (Figure 3-12B). Together, these data indicate that RUNX3-expressing cells maintain lower levels of CD36 expression upon exposure to EPO compared to control cells.

Furthermore, aberrant expression of GlyA was observed in RUNX3 cells, with 59% vs 87% GlyA⁺ compared to control, respectively (day 22, Figure 3-13A). The expected upregulation of GlyA expression was reduced by 1.6 ± 0.1 -fold in RUNX3-expressing cells compared to controls (day 22, Figure 3-13B). To determine the cell size, changes in forward scatter (FSC) for both cultures were assessed by flow cytometry following addition of EPO to the growth medium. The expected reduction of FSC was delayed by 1.2 ± 0.1 -fold in RUNX3-expressing erythroid cells compared to control at day 22, suggesting that RUNX3 cells were significantly bigger than controls (Figure 3-14). In order to discriminate between populations in different stages of erythroid development, three gating markers were established according to FSC changes and the proportion of cells in each region were determined (Figure 3-15A). Cells within marker 1 (M1) are smallest in size, with highest levels of GlyA and are in a late stage of differentiation. Cells within marker 2 (M2) have an intermediate size and high levels of GlyA, and cells within marker 3 (M3) are largest have low levels of GlyA and are in relatively early stages of erythroid development. As shown in Figure 3-15B, there was an expected increase in the proportion of cells in M1 with development, as well as a decrease in the number of cells in M3. However, the percentage of cells in M1 was significantly lower for the RUNX3 culture in the last day of development. In addition, the proportion of cells in M3 was consistently higher in the RUNX3 culture compared to control throughout development. These data imply that RUNX3 transduced cultures have their erythroid differentiation suppressed in comparison with control cultures and their full maturation was impaired.

A



B

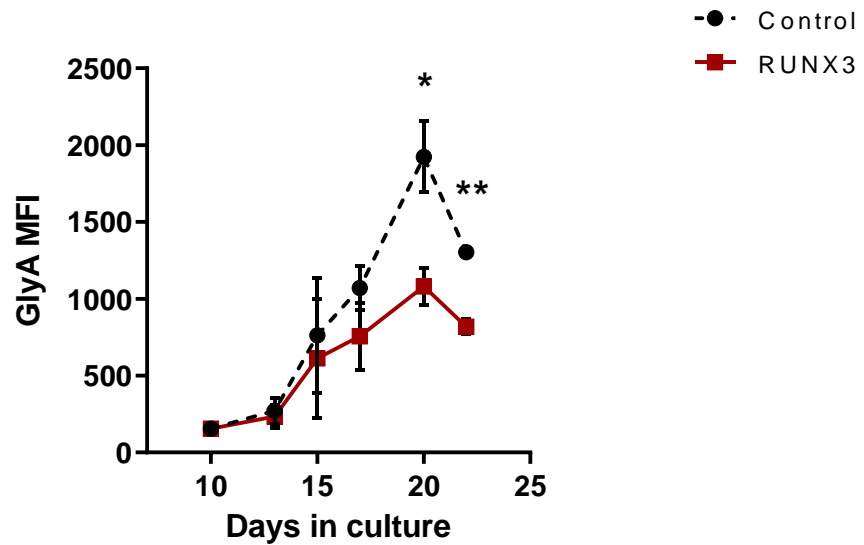


Figure 3-13 – RUNX3 suppresses GlyA expression during the EPO-dependent phase of differentiation.

(A) Example density plots of control and RUNX3 cultures labelled with the erythroid differentiation marker GlyA (Day 22 of differentiation). IgG-Pacific Blue stained HSPC cells – grey. **(B)** Summary data showing GlyA expression in terms of MFI in DsRed⁺CD13⁺CD36⁺ cells over time. Data indicate mean ± 1SD of at least four independent experiments. Significant difference of RUNX3-expressing cells from controls was analysed by paired t test, * $p < 0.05$, ** $p < 0.01$.

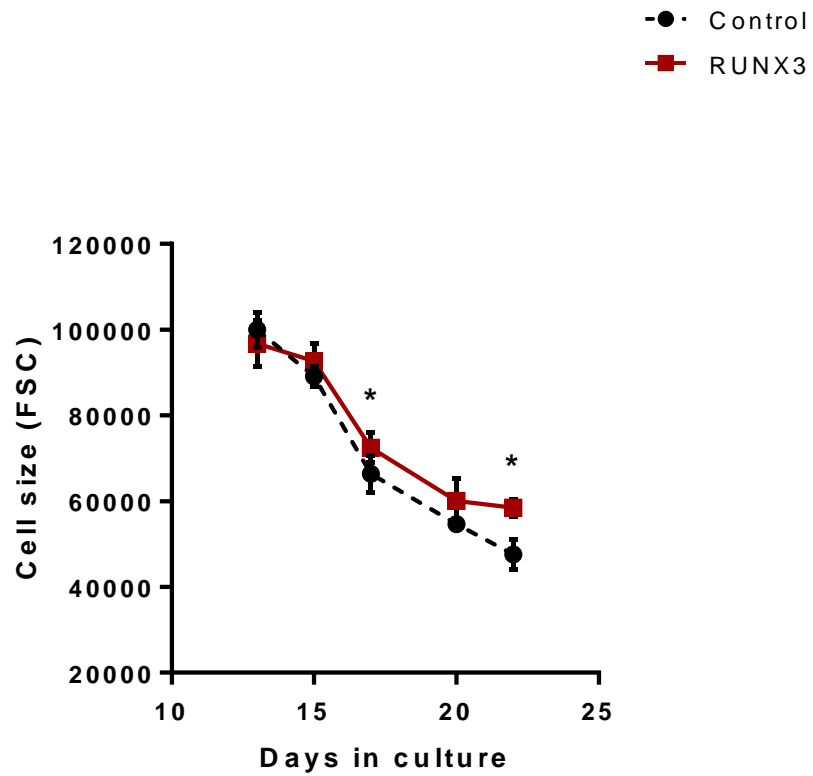


Figure 3-14 – RUNX3 impairs cell size reduction in the EPO-dependent phase of differentiation.

Summary plot showing cell size changes in terms of forward scatter (FSC) for control and RUNX3 cultures analysed by flow cytometry. Data indicate mean \pm 1SD of at least four independent experiments. Significant difference of RUNX3-expressing cells from controls was analysed by paired t test, * $p < 0.05$.

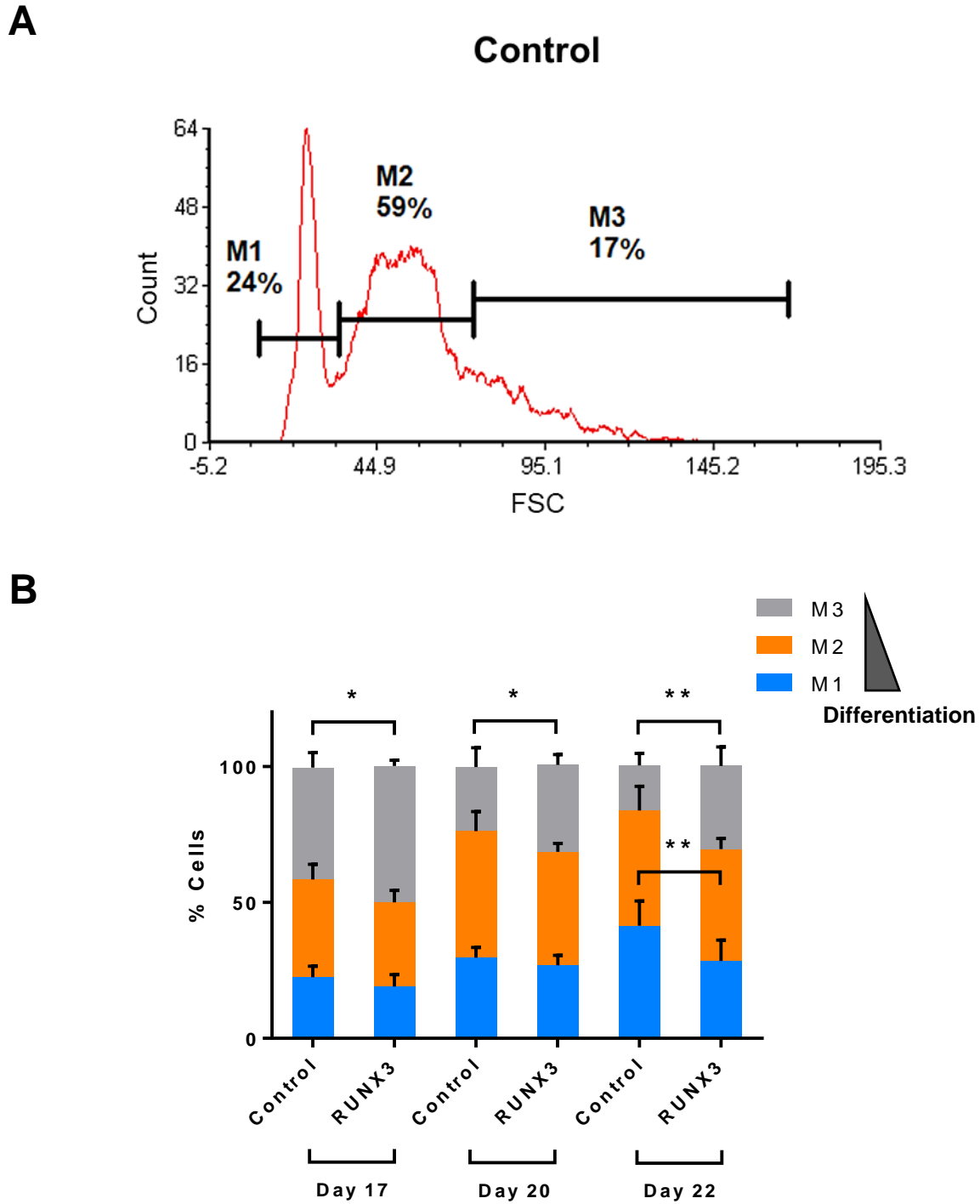


Figure 3-15 – RUNX3 impairs cell size reduction in the EPO-dependent phase of differentiation.

(A) Example histogram plot discriminating between populations with different FSC within control and RUNX3 cultures (Day 22 of differentiation). M1 – Cells with a low FSC; M2 – Cells with an intermediate FSC; M3 – Cells with a high FSC. **(B)** Summary plot showing differences in the proportion of cells within M1, M2 and M3 depending on their FSC on day 17, 20 and 22 of erythroid differentiation. Data indicate mean \pm 1SD of at least three independent experiments. Significant difference of RUNX3-expressing cells from controls was analysed by paired t test, * $p < 0.05$, ** $p < 0.01$.

To support the previous results suggesting that RUNX3 overexpression inhibits terminal erythroid differentiation, morphologic features of May-Grünwald-Giemsa stained cells were analysed. As shown in [Figure 3-16A](#), control cells exhibited a mature morphology, whereas RUNX3-expressing cells were associated intermediate morphological features. However, significance was not reached in terms of differential counts ([Figure 3-16B](#)).

Taken together, RUNX3 overexpression inhibited normal human erythropoiesis, particularly at later stages of development, with RUNX3-expressing cells failing to upregulate GlyA retaining their size compared to controls.

3.3.3 Knockdown of RUNX3 does not impair human erythroid development

The above data show that RUNX3 overexpression in HSPC disrupted erythroid differentiation of these cells, characterised by the abnormal terminal maturation of erythroid cells. This study next sought to examine the effects of reducing endogenous levels of RUNX3 on human erythroid development.

3.3.3.1 Selection and validation of RUNX3 shRNA constructs

In order to reduce RUNX3 expression in normal human HSPC and determine its effects on erythroid growth and differentiation, lentiviral vectors encoding different RUNX3 shRNA were employed ([2.2.1](#)). To optimise and validate this approach, the AML cell line OCI-AML-5 was used due to their relatively high endogenous RUNX3 expression. Three shRNA sequences complementary to RUNX3 and encoding puromycin resistance as well as GFP were lentivirally infected into OCI-AML-5 cells and the successful KD of RUNX3 was confirmed by western blot ([Figure 3-17A](#)). Variable KD efficiencies among the different RUNX3 shRNA constructs were observed in OCI-AML-5 cells, with shRNA 1 being the most effective shRNA to KD RUNX3 expression in these cells (7.7-fold vs shRNA control, [Figure 3-17B](#)).

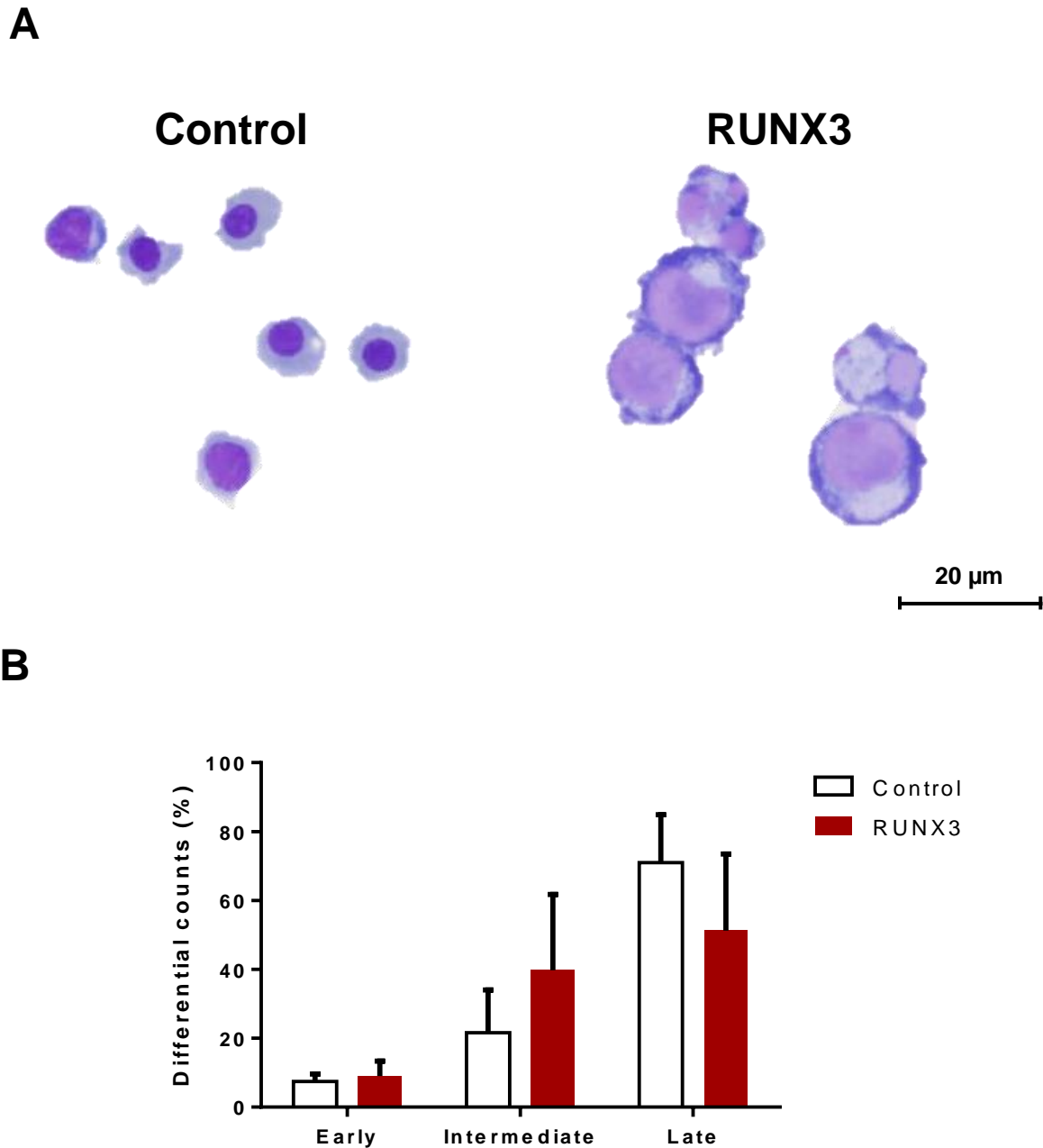


Figure 3-16 – RUNX3 expression affects the morphology of cells during erythropoiesis.

(A) Control and RUNX3-expressing cells analysed on day 20 of differentiation with May-Grünwald-Giemsa. **(B)** Differential counts of both cultures with morphology categorised into early (proerythroblasts), intermediate (erythroblasts) and late phase (normoblasts). Data indicate mean \pm 1SD of three independent experiments.

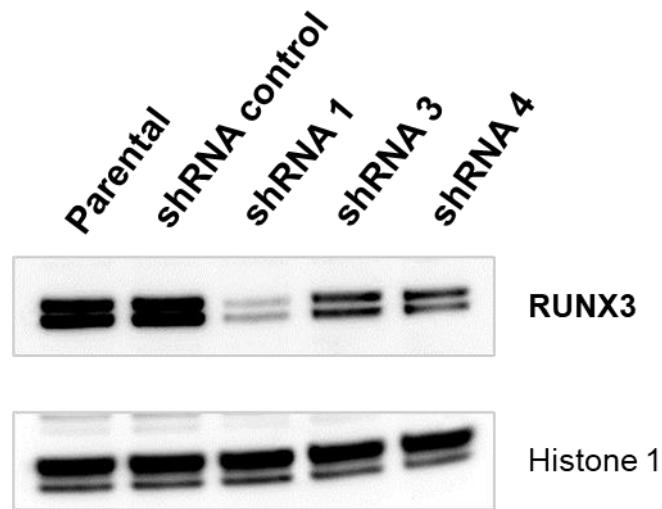
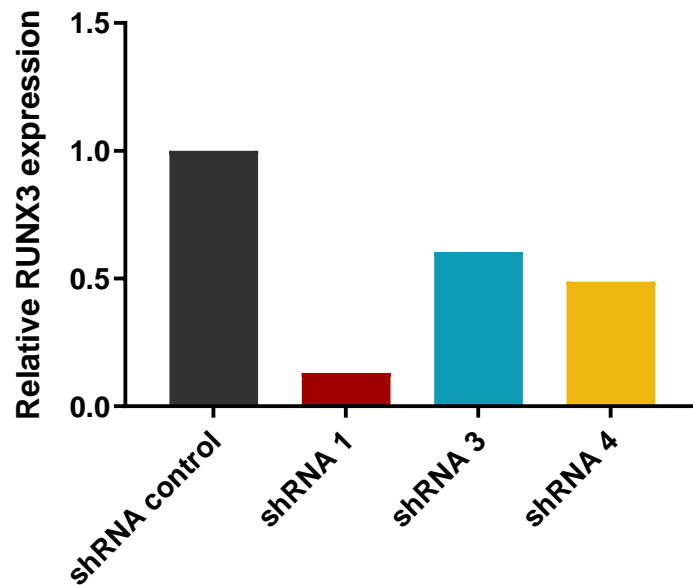
A**B**

Figure 3-17 – RUNX3 shRNA constructs successfully reduced the endogenous levels of RUNX3 in OCI-AML-5 cell line.

(A) Example western blot analysis of RUNX3 total protein levels in OCI-AML-5 cells infected with a scramble shRNA (control) and different RUNX3 shRNA constructs. OCI-AML-5 parental cells were used as positive control and Histone 1 as a loading control. shRNA TCRN numbers in the 2.2.1 section. **(B)** Relative RUNX3 endogenous expression in OCI-AML-5 cells infected with different RUNX3 shRNA constructs. Data was corrected for loading and normalised against shRNA control.

HSPC were transduced at a more than 50% efficiency for the different shRNA clones and at around 33% for the shRNA control (Figure 3-18A), resulting in the specific downregulation of RUNX3. To validate the efficient KD of *RUNX3* in HSPC, qRT-PCR was performed. As shown in Figure 3-18B, *RUNX3* expression was reduced by approximately 50% for all three shRNA clones in comparison with control cells.

3.3.3.2 Knockdown of *RUNX3* inhibits erythroid colony formation

Using the above shRNA constructs, the effects of RUNX3 KD on normal HSPC erythroid colony forming capacity and self-renewal potential were examined under clonal conditions in GFP⁺CD13⁻ cells as described above (3.3.2.2). Following one week of growth, RUNX3 KD in these cells led to a significant decrease in erythroid colony forming efficiency (Figure 3-19A). More specifically, RUNX3 shRNA 1 suppressed erythroid colony formation by 1.2 ± 0.1 -fold, RUNX3 shRNA 3 by 1.5 ± 0.4 -fold and RUNX3 shRNA 4 by 1.9 ± 0.8 -fold compared with control. To evaluate the self-renewal potential of these cells, serial replating assays in liquid culture were performed. RUNX3 KD cells showed a similar colony forming efficiency compared to control, showing that reduced RUNX3 expression does not affect the self-renewal potential of these cells (Figure 3-19B). Overall, these data suggest that KD of RUNX3 impairs the survival of erythroid cells but does not affect their self-renewal potential.

3.3.3.3 Knockdown of *RUNX3* does not suppress erythroid growth and development

To study in detail the effects of reducing RUNX3 expression in HSPC on growth and differentiation of erythroid cells, the EPO-independent phase of development was initially analysed. GFP⁺CD34⁺CD13⁻ cells were generated as described in section 3.3.2. KD of RUNX3 in these cells failed to induce a significant growth suppression during early stages of development (Figure 3-20). To assess the early erythroid differentiation of cells in bulk liquid culture, multi-parameter flow cytometry of lineage and differentiation markers was performed similar to the strategy outlined in Figure 3-8. RUNX3 KD erythroid cells exhibited a modest reduction in CD36 expression during this early phase of development, though no significance was obtained for these changes (Figure 3-21A). Further, RUNX3 KD had no effect on the expression of CD34 (Figure 3-21B).

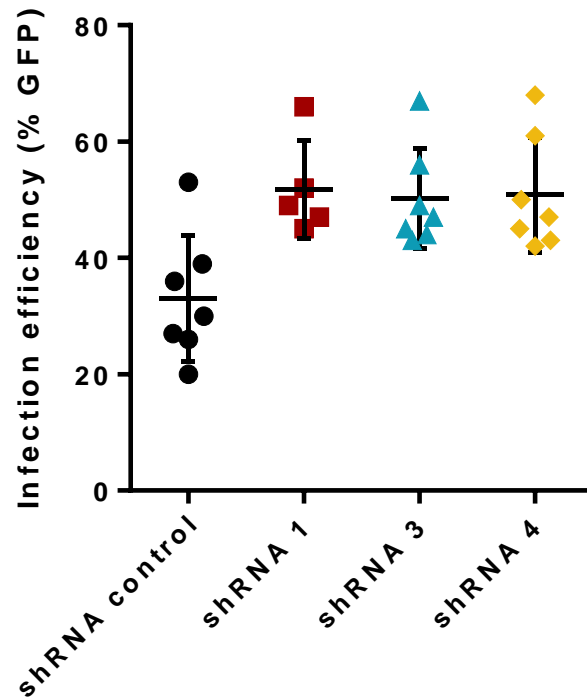
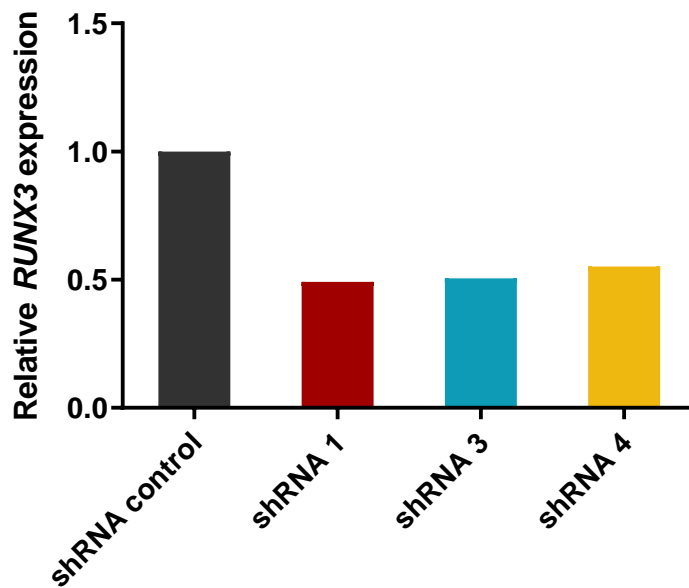
A**B**

Figure 3-18 – Knockdown of RUNX3 was successful in human HSPC cells.

(A) Summary data of percentages of GFP⁺ cells in control and RUNX3 KD HSPC cultures. Data indicate mean \pm 1SD of at least five independent experiments. **(B)** qRT-PCR analysis of *RUNX3* mRNA levels in control and RUNX3 KD HSPC on day 3 of culture sorted for GFP positivity (representative data). GAPDH was used as endogenous control. Relative expression calculated using the Comparative C_T ($\Delta\Delta C_T$) method (2.8.2).

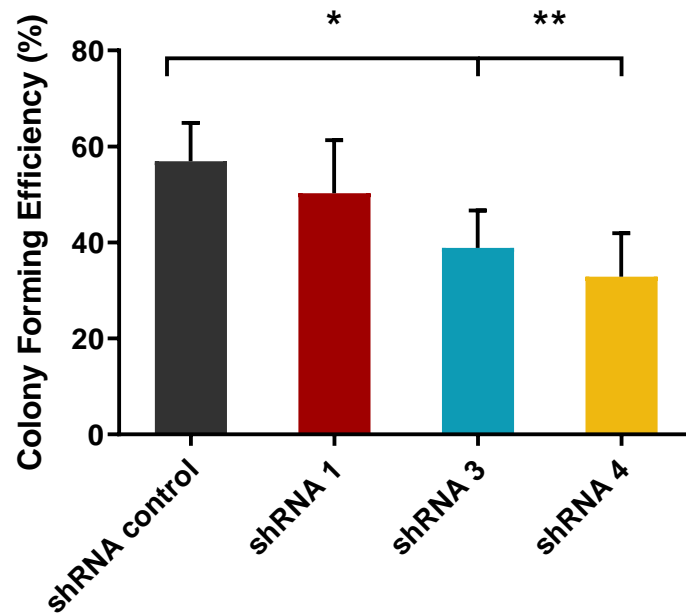
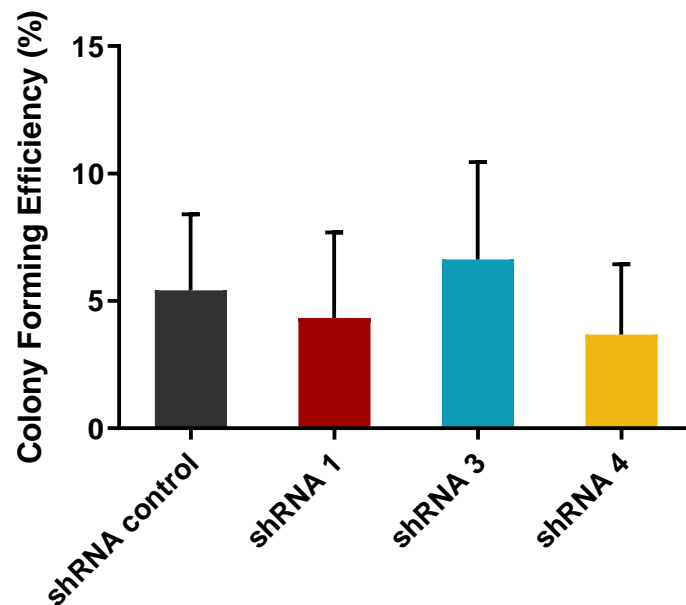
A**B**

Figure 3-19 – Knockdown of RUNX3 suppresses erythroid colony formation of HSPC.

(A) Colony forming efficiency of control and RUNX3 KD cultures after 7 days of growth in liquid culture containing IL-3, IL-6, SCF, and EPO. **(B)** Self-renewal potential assessed by a single replating round of control and RUNX3 KD cultures in the same conditions as previously. Data indicate mean \pm 1SD of at least three independent experiments. Significant difference of RUNX3 shRNA 3 and 4 from control was analysed by one-way ANOVA using Tukey's test, * $p < 0.05$, ** $p < 0.01$.

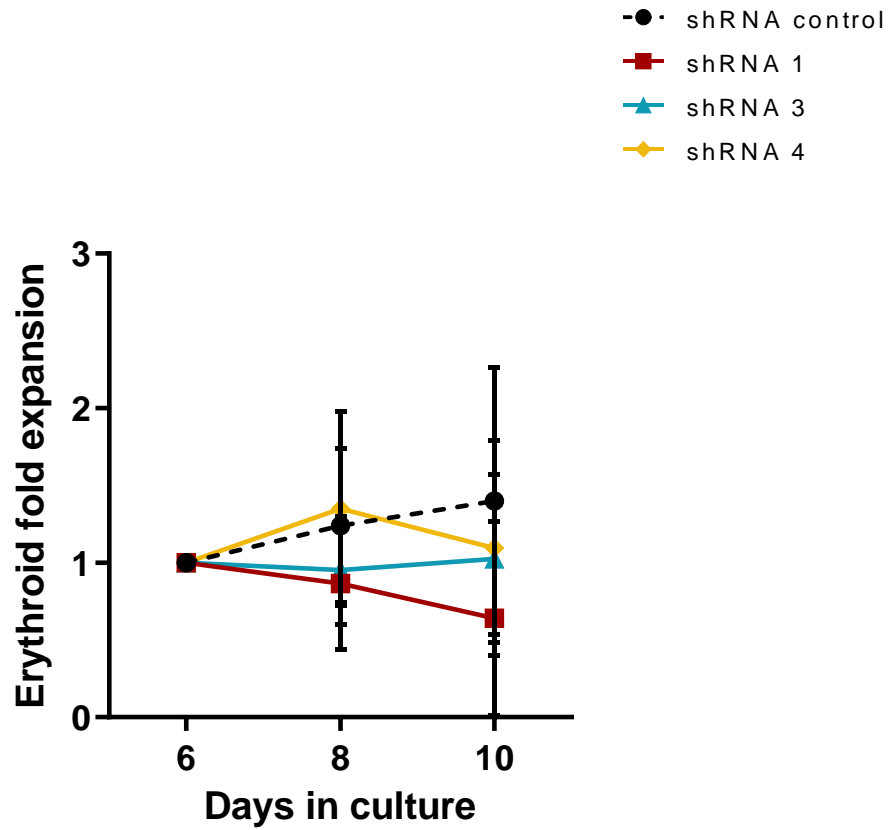


Figure 3-20 – Knockdown of RUNX3 did not affect significantly early erythroid growth during the EPO-independent phase of differentiation.

Cumulative expansion of CD13-CD36⁺ erythroid progenitors in control and RUNX3 KD cultures during the EPO-independent phase of growth. Cells were grown in media supplemented with IL-3, IL-6 and SCF for their first 10 days of differentiation. Data indicate mean \pm 1SD of at least four independent experiments.

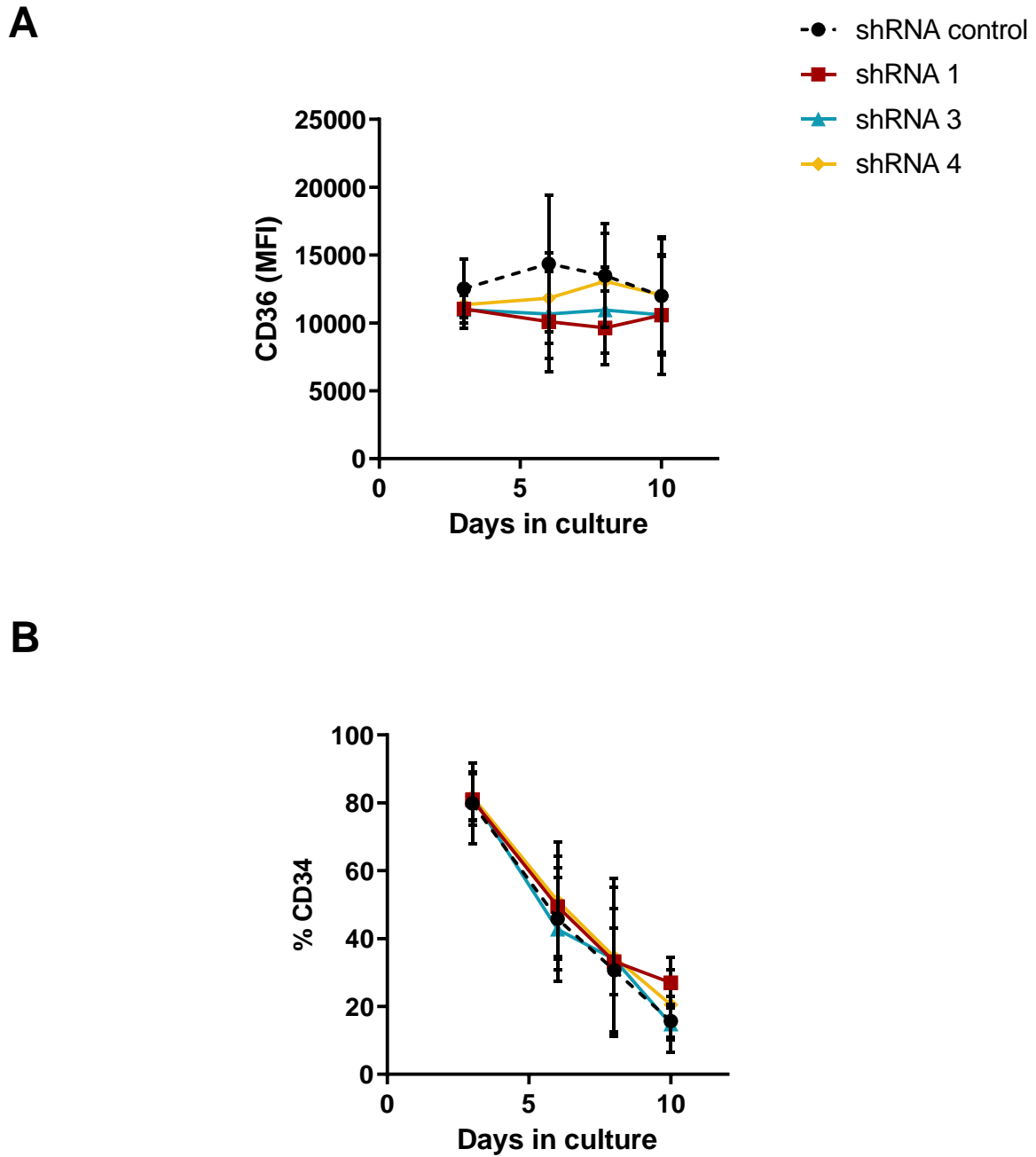


Figure 3-21 – Knockdown of RUNX3 did not affect significantly CD36 (MFI) and CD34 (%) expression in HSPC during the EPO-independent erythroid differentiation.

(A) Summary data of CD36 expression profile in terms of MFI in GFP⁺CD13⁻CD36⁺ cells over time. Data indicate mean \pm 1SD of at least four independent experiments. **(B)** Summary data showing CD34 expression in terms of percentage in GFP⁺ CD13⁻CD36⁺ cells throughout the EPO-independent phase of development. Data indicate mean \pm SD of at least four independent experiments.

Taken together, these results suggest that reduced RUNX3 expression does not significantly impair the early differentiation of erythroid cells.

To investigate the later stages of erythroid development in RUNX3 KD cells, EPO was added to the growth medium and changes in growth and maturation of cells were monitored over time. As shown in [Figure 3-22](#), RUNX3 shRNA cultures disrupted the late erythroid expansion at different levels. Nevertheless, and apart from shRNA 3, no significance was observed in erythroid growth for RUNX3 KD cells during late erythropoiesis. RUNX3 shRNA 3 cells exhibited a significant increased expansion by 2.3 ± 0.7 -fold compared to shRNA control on day 20 of culture. However, western blot validation suggests that shRNA 3 is the least efficient clone at reducing RUNX3 protein levels in OCI-AML-5 ([Figure 3-17](#)), and therefore the results observed could be due to off-target effects. Overall, these results suggest that the KD of RUNX3 in HSPC does not inhibit their late erythroid growth.

As mentioned in section 3.3.2.4, during the EPO-dependent phase of development, CD36 expression is upregulated simultaneously with GlyA upon exposure to EPO, followed by CD36 downregulation and a reduction in cell size during the last days of differentiation. A similar trend in CD36 expression was observed among control and RUNX3 shRNA cultures ([Figure 3-23A](#)). No significant changes were observed in terms of upregulation of GlyA in RUNX3 shRNA cultures compared to controls during late erythroid development ([Figure 3-23B](#)). Furthermore, cell size was unaffected by RUNX3 KD in erythroid cells ([Figure 3-24A](#)). The proportion of cells in each marker discriminating cells according to their size was also similar between all cultures ([Figure 3-24B](#)). Morphologic features of cells were assessed on day 20 of differentiation to support the previous data and confirm the normal maturation of cells. As shown in [Figure 3-25](#), all cultures were predominantly in a late stage of erythroid differentiation characterised by the abundance of orthochromatic erythroblasts in the slides.

Taken together, KD of RUNX3 impairs the colony forming ability of erythroid cells compared to controls but fails to induce similar effects on erythroid growth and development in bulk liquid culture. The effect of RUNX3 KD differs from its overexpression in HSPC as no obvious developmental defect was observed.

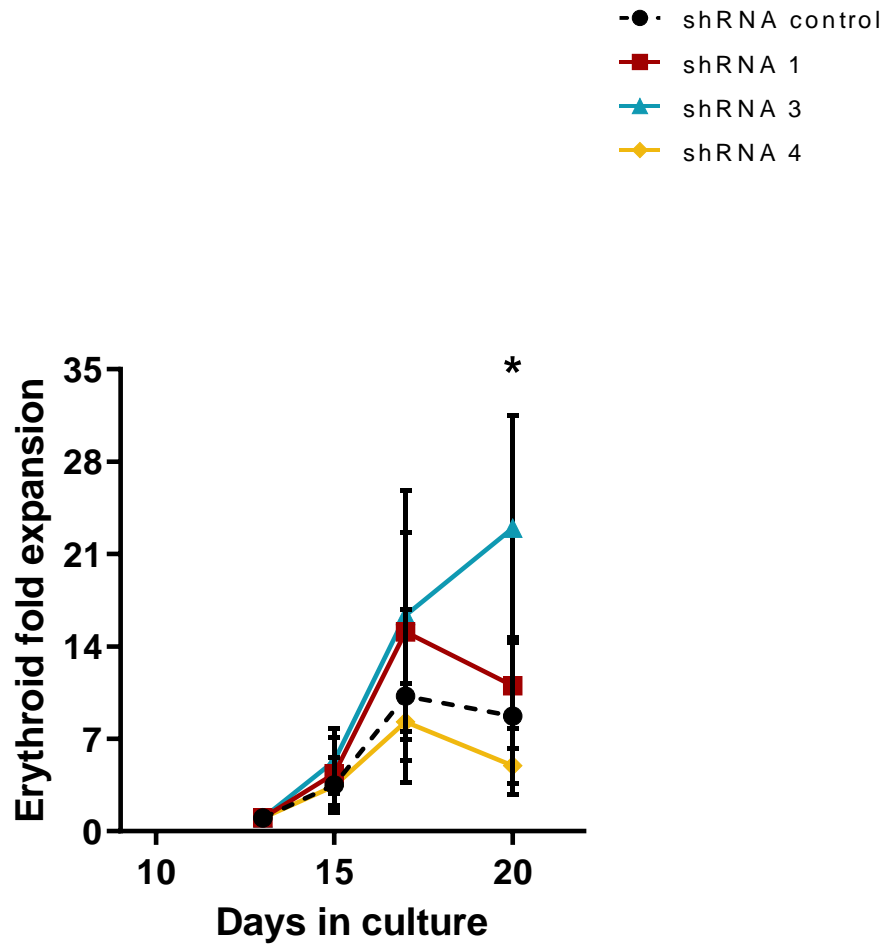
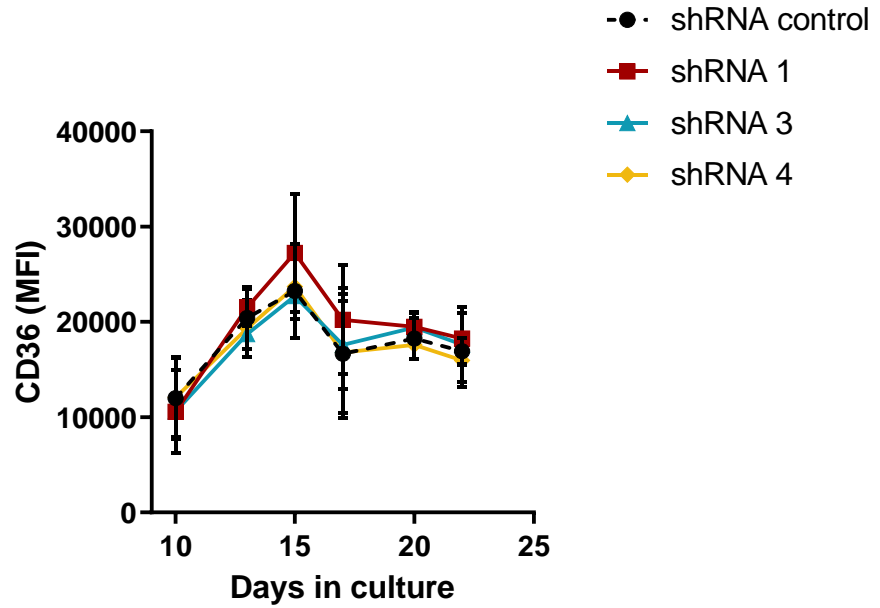


Figure 3-22 – Effect of RUNX3 knockdown on late erythroid growth during the EPO-dependent phase of differentiation.

Cumulative expansion of erythroid progenitors in control and RUNX3 KD cultures during the EPO-dependent phase of growth. Cells were grown in media supplemented with IL-3, IL-6, SCF and EPO from day 10 of differentiation. Data indicate mean \pm 1SD of at least three independent experiments. Significant difference of RUNX3 shRNA 3 from controls was analysed by one-way ANOVA using Tukey's test, * $p < 0.05$.

A



B

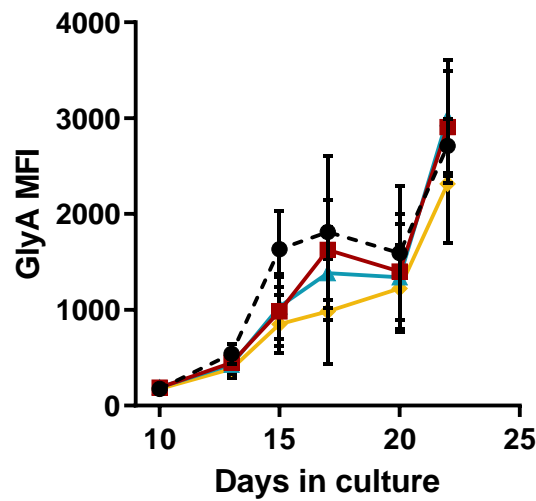


Figure 3-23 – Knockdown of RUNX3 does not affect CD36 and GlyA expression in HSPC during the EPO-dependent erythroid differentiation.

(A) Summary data of CD36 expression profile in terms of MFI in GFP⁺CD13⁻CD36⁺ cells over time. Data indicate mean \pm 1SD of at least four independent experiments. **(B)** Summary data showing GlyA expression in terms of MFI in GFP⁺ CD13⁻CD36⁺ cells over time. Data indicate mean \pm 1SD of at least four independent experiments.

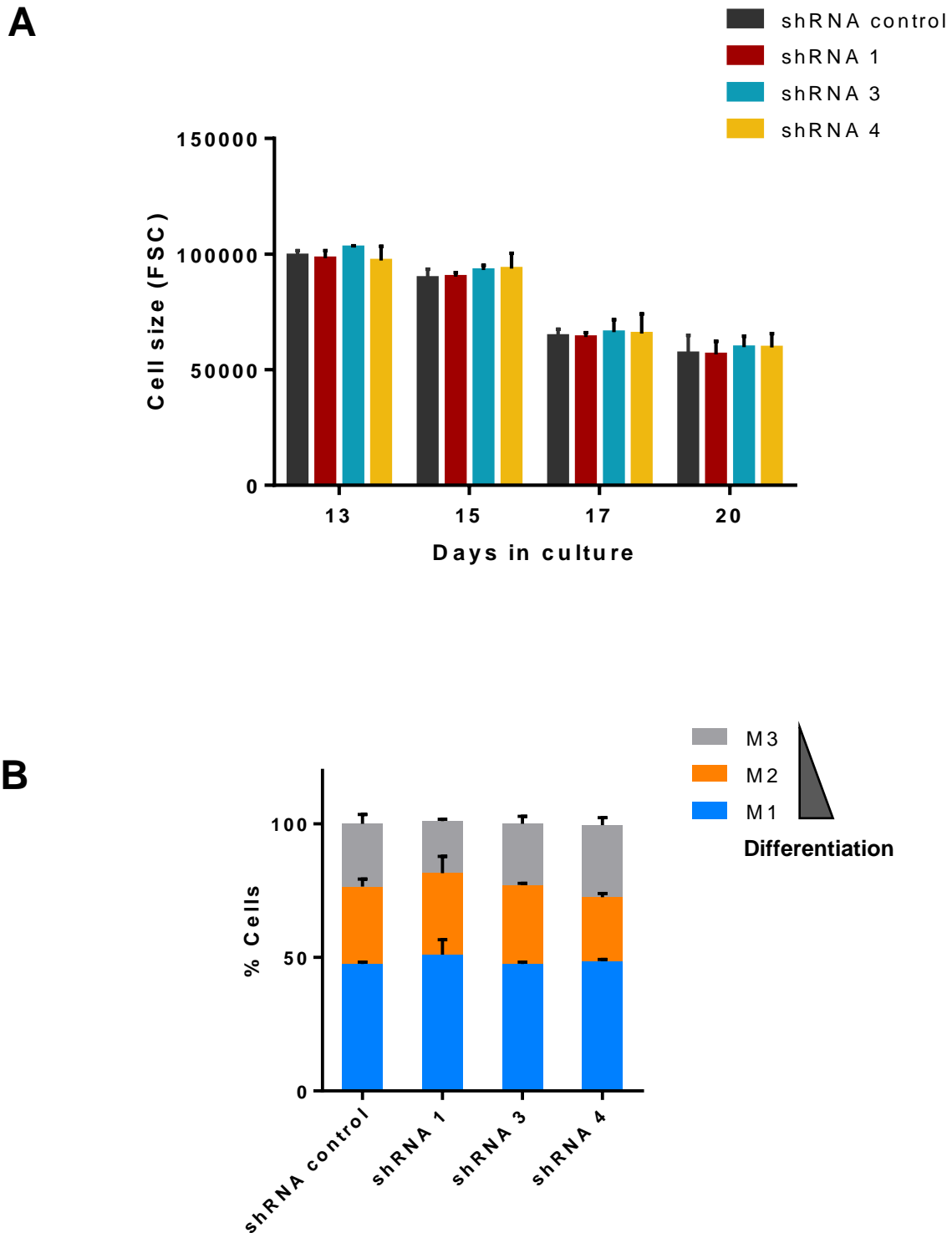


Figure 3-24 – Knockdown of RUNX3 causes no effects on cell size reduction in the EPO-dependent phase of differentiation.

(A) Summary plot showing cell size changes in terms of FSC for control and RUNX3 KD cultures. Data indicate mean \pm 1SD of at least four independent experiments. **(B)**. Summary plot showing differences in the proportion of cells within M1, M2 and M3 depending on their FSC on day 22 of erythroid differentiation. M1 – Cells with a low FSC; M2 – Cells with an intermediate FSC; M3 – Cells with a high FSC. Data indicate mean \pm 1SD of at least three independent experiments.

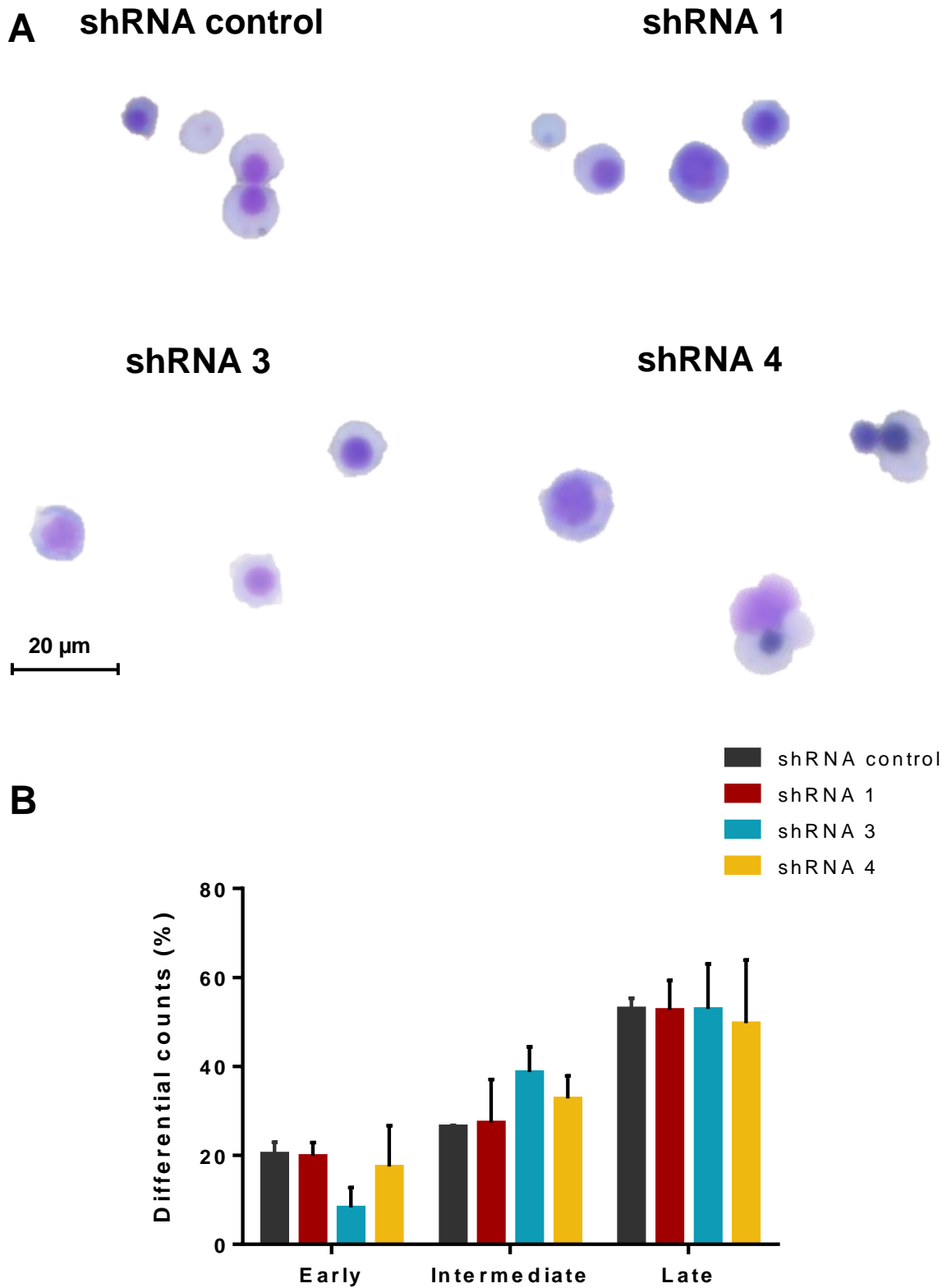


Figure 3-25 – RUNX3 knockdown does not affect the morphology of cells during erythropoiesis.

Differential counts of all cultures with morphology categorised into early (proerythroblasts), intermediate (erythroblasts) and late phase (normoblasts) on day 20 of differentiation. Data indicate mean \pm 1SD of three independent experiments.

3.4 Discussion and conclusion

RUNX3 (located at 1p36, a chromosomal region often deleted in several types of cancer) has a major role in the development of gastro-intestinal tract, neurogenesis and thymopoiesis (Cheng *et al.* 2008b; Chuang and Ito 2010) (1.4). Whilst this TF has also been shown to be crucial during haematopoiesis in non-human models, there remains a paucity of studies regarding its role in normal human haematopoiesis and in leukaemia development (1.4.1, 1.4.2.3). This study describes the normal expression of RUNX3 and its role on human erythroid development using a human primary cell model. Overexpression of RUNX3 in HSPC significantly inhibited the growth and differentiation of normal human erythroid progenitors. Overall, RUNX3 overexpressing cells exhibited a more immature phenotype and morphology, as well as a higher self-renewal potential. In terms of RUNX3 KD, and although some RUNX3 shRNA cultures exhibited changes in their growth and differentiation during erythropoiesis, no significance was observed. These results could be explained by a modest KD of RUNX3 in HSPC. Taken together, this study suggests that the downregulation of RUNX3 expression during normal human erythroid development is important for their full maturation.

To understand any pathological role RUNX3 may have on leukaemia development, it is important to understand its expression level during normal haematopoiesis. In CB derived HSPC, *RUNX3* mRNA expression levels gradually decrease as cells differentiate into mature red blood cells (3.3.1). The increase in mRNA observed at a later stage of maturation is unlikely to have functional relevance as erythroid cells expel their nucleus as part of their terminal differentiation, and RUNX3 function and localisation is nuclear. Mouse RNA-seq data revealed a similar trend, with erythroid cells having the lowest expression of *RUNX3* compared to HSPC and between different cell types from distinct lineages. *RUNX1* expression has been shown to decrease during erythroid development in adult mice, particularly after the proerythroblast stage (North *et al.* 2004). In a more recent study, *RUNX3* expression in HSPC was shown to decline with aging in humans and mice (Balogh *et al.* 2020). HSPC from elderly patients with unexplained anaemia presented a greater reduction in RUNX3 expression (Balogh *et al.* 2020). These observations suggest that RUNX3 is expressed throughout erythropoiesis with its highest levels in HSPC.

3.4.1 RUNX3 overexpression in human HSPC inhibits their normal erythroid development

Having generated an enriched population of retrovirally transduced primitive erythroid cells (predominantly DsRed⁺CD34⁺CD13⁻) expressing RUNX3, this study initially determined the effects of RUNX3 overexpression on erythropoiesis. Under clonal conditions, RUNX3 significantly suppressed erythroid colony formation, suggesting that RUNX3 expression affects the proliferative capacity and survival of these cells (3.3.2.2). Subsequently, in a serial replating strategy, RUNX3 cells were able to form more erythroid colonies than controls, implying that RUNX3 overexpressing cells maintained a more immature phenotype and have an increased self-renewal potential. Interestingly, this data parallels the effect of RUNX1-ETO expression on erythroid colony formation in HSPC cells (Tonks *et al.* 2003). In this study, Tonks *et al.* showed that expression of the fusion protein almost completely abrogated erythroid colony forming ability. Considering that RUNX3 overexpression was shown to downregulate *RUNX1* in HSPC (5.3.4), and RUNX1-ETO dysregulates the expression of RUNX1 target genes (1.2.4.1), dysregulation of RUNX1 could help explaining these results. Previous studies have shown that loss of RUNX1 increases the numbers of HSPC and their replating capacity (Ichikawa *et al.* 2004a). Overall, these findings show that increased RUNX3 expression inhibits erythroid colony formation whilst promoting self-renewal of erythroid progenitors.

The first erythroid-committed progenitors require SCF but not EPO for their proliferation (Gautier *et al.* 2016). The consequences of RUNX3 overexpression as a single abnormality on early erythroid development in the absence of EPO was next examined. RUNX3 imposed a modest reduction in erythroid growth (3.3.2.3). Phenotypically, HSPC-derived erythroblasts mature by downregulating CD34 on their surface, which in turn is followed by the upregulation of GlyA. CD36 is co-expressed with GlyA when cells are committed to the erythroid lineage. Expression of CD36 is then gradually downregulated during the terminal maturation stage on enucleated erythroid cells (Mao *et al.* 2016). RUNX3-expressing cells exhibited a slower upregulation of the erythroid lineage discriminator CD36 (thrombospondin receptor) compared to controls. This result is supported by a previous study in which RUNX3 was shown to directly downregulate CD36 expression in myeloid cells (Puig-Kroger *et al.* 2006). RUNX3 overexpression was also shown to induce important transcriptome changes in HSPC,

including the reduced expression of CD36 at day 3 of culture (5.3.4). Taken together, data suggest a suppression of early erythroid development for RUNX3 transduced cells and a potential role for RUNX3 in the initial activation of erythroid-specific genes.

EPO is absolutely required for the survival and proliferation of the late erythroid progenitors and for their terminal differentiation (Gautier *et al.* 2016). During this process, the size of the cells gradually decreases, and at the end of terminal erythroid differentiation cells expel their nucleus and complete their maturation in the bloodstream (Gautier *et al.* 2016). To determine whether addition of EPO to the cultures above could overcome the abnormal erythroid development and induce terminal maturation, the EPO-dependent phase of growth was analysed. Interestingly, there was a partial differentiation response, but cells were unable to terminally develop into mature erythroid cells. RUNX3 cultures overcame the slower growth and proliferated faster than controls when cultured with EPO (3.3.2.4). This effect is consistent with RUNX3 expressing cells being less differentiated and retaining more proliferative potential. Further, RUNX3 expressing cells were unable to complete terminal erythroid differentiation; they had decreased upregulation of GlyA, reduced CD36 expression and increased cell size compared to controls (3.3.2.4). RNA-seq data confirmed the inhibition of GlyA gene expression (*GYPA*) and *CD36* by RUNX3 overexpression in HSPC (5.3.4). Additional erythroid-related genes, including *KIT* and *LMO2*, were significantly downregulated by RUNX3 overexpression in the same context. Assessment of morphology supported the cell surface protein expression analysis. As mentioned previously, downregulation of RUNX1 could contribute to the abrogation of erythroid development by RUNX3 overexpression in HSPC. RUNX1 is a crucial TF in the early stages of definitive haematopoiesis (Dzierzak and Philipsen 2013) and it plays a central role during lineage fate decision at the megakaryocyte/erythroid branching point (Kuvardina *et al.* 2015). In *RUNX1* KO embryos, yolk sac erythropoiesis is normal but foetal liver haematopoiesis is absent (Okuda *et al.* 1996; Wang *et al.* 1996a). Furthermore, definitive erythropoiesis and myelopoiesis is absent in *RUNX1* KO mice embryos, and disruption of one copy of *RUNX1* significantly reduces the number of progenitors for erythroid and myeloid cells (Wang *et al.* 1996a). RUNX1 expression has also been shown to affect primitive erythropoiesis (Yokomizo *et al.* 2008; Ghanem *et al.* 2018). In addition, RUNX1-ETO was previously shown to increase the numbers of immature erythroblasts along with the induction of self-renewal (Tonks *et al.* 2003).

The previous findings show that RUNX3 overexpression in human HSPC induce severe abnormalities in the normal programme of erythroid differentiation at a later phase upon addition of EPO to the culture medium. Further RNA-seq data support this observation, as RUNX3 overexpression at an early stage of development (day 3 of culture) led to a significant downregulation of late erythroid-specific genes, including *GYPA*, *HBA1* or *HBA2* (5.3.4). Moreover, reduced levels of RUNX3 in human HSPC were previously shown to negatively influence the expression of several globin-encoding genes, as well as downstream erythroid genes *GYPA* and *EPOR* (Balogh *et al.* 2020). EPO signalling has been proved important for erythroid maturation and heme biosynthesis (Grover *et al.* 2014; Chung *et al.* 2017). Therefore, these results highlighting the importance of RUNX3 downregulation during erythroid maturation.

Overall, ectopic expression of RUNX3 in HSPC induces important abnormalities in normal erythroid development supported by the dysregulation of key erythroid genes (5.3.4). Nevertheless, it is important to consider that RUNX3 was overexpressed in HSPC at higher levels than seen in patients (Sun *et al.* 2019) (4.3.2).

3.4.2 Knockdown of RUNX3 in HSPC does not affect their normal erythroid development

To investigate whether reduced RUNX3 expression has any effect on erythroid development, an enriched population lentivirally infected with a scrambled shRNA control or RUNX3 shRNA (GFP⁺CD34⁺CD13⁻) was generated. KD of RUNX3 significantly inhibited erythroid colony formation but was not associated with increased self-renewal. These results suggest that reduced RUNX3 expression does not promote the retention of an immature phenotype but has an adverse effect on survival of erythroid cells. A similar inhibition of erythroid colony formation was recently shown in RUNX3 KD human HSPC (Balogh *et al.* 2020). The effects of RUNX3 KD in erythroid development were next studied in bulk liquid culture in the absence of EPO. In this early stage of development, RUNX3 KD did not significantly affect the early growth of erythroid cells, and expression of cell surface proteins suffered minimal impact during early erythropoiesis. Although RUNX3 shRNA cultures exhibited modest reduction of CD36 expression compared to controls, their normal programme of early differentiation seemed unperturbed with similar expression levels of CD34 compared to controls.

Taken together, the previous findings imply that reduction of RUNX3 expression in human HSPC does not impair their early erythroid development in bulk liquid culture.

Late erythropoiesis was further studied upon addition of EPO to the culture medium of cells. In terms of erythroid growth, KD of RUNX3 by different shRNA constructs led to contrasting effects but no significant disruption of cell growth was observed in the EPO-independent phase of development. The increased expansion of RUNX3 shRNA 3 cells during late erythroid development might be explained by off-target effects instead of RUNX3 KD, as the other KD cultures did not exhibit the same behaviour. Regarding their differentiation status, RUNX3 KD did not significantly affect the expression of erythroid markers. In terms of cell size, RUNX3 shRNA cultures behaved similarly to controls characterised by a reduction in their size throughout differentiation. These data contrast with recently published data showing that compromised RUNX3 expression abrogates erythroid differentiation, with abnormal GlyA expression (Balogh *et al.* 2020). RUNX3 KD in HSPC was shown to downregulate the expression of genes required for erythroid development, such as *KLF1* and *GATA1*. Furthermore, this study concluded that RUNX3 KD restricts erythropoiesis at commitment and later stages, therefore implying an important role for RUNX3 in the maintenance of BM lineage balance (Balogh *et al.* 2020). However, it is important to consider the differences between both studies, as Balogh *et al.* assessed viability and GlyA expression of RUNX3 KD HSPC cultured in erythroid medium for 3 days. In addition, the results obtained in this study were solely based on one RUNX3 shRNA construct, and therefore, did not consider possible off-target effects. In a different study, RUNX1-ETO has been found capable of impeding the earliest steps of erythroid lineage commitment by repressing GATA-1, a key TF of erythroid differentiation (Choi *et al.* 2006). Functional redundancy between RUNX1 and RUNX3 could potentially explain the full erythroid development of RUNX3 KD cells (Brady and Farrell 2009; Wong *et al.* 2011; Yokomizo-Nakano *et al.* 2020). In addition, loss of both RUNX1 and RUNX3 has been shown to block murine erythroid differentiation (Wang *et al.* 2014a). Together, these findings indicate that RUNX3 KD does not significantly impair erythroid development, with cells attaining terminal maturation in the presence of EPO. However, this study is unable to conclude that RUNX3 expression is dispensable for human erythropoiesis, as the KD efficiencies achieved in HSPC were only modest.

In summary, RUNX3 expression decreases with erythroid maturation in human HSPC and its ectopic expression leads to an impairment of normal erythropoiesis with increased self-renewal potential, a hallmark of a potential leukaemogenic change. KD of RUNX3 had a modest impact on proliferation and survival of erythroid cells. Further studies determined the role of RUNX3 expression in human myeloid development, revealing that RUNX3 downregulation is equally important for this process.

4 RUNX3 Inhibits Normal Myeloid Development of Human CD34⁺ HSPC

4.1 Introduction

Malignant transformation of haematopoietic cells can lead to AML of varying subtypes depending on the molecular abnormalities that drive this process and the differentiation stage at which it occurs (Rosenbauer and Tenen 2007) (1.2). AML is an aggressive BM malignancy with uncontrolled clonal expansion of immature myeloid cells coupled with a block in differentiation. Functional changes of key differentiation-inducing TFs are a major driving force of AML, exemplified by the t(8;21) encoding the RUNX1-ETO fusion oncogene (Rosenbauer and Tenen 2007) (1.2.4). Expression of RUNX1-ETO in normal human HSPC leads to a block in erythroid and myeloid development (particularly affecting granulocytes), as well as self-renewal of progenitor cells (Tonks *et al.* 2003; Tonks *et al.* 2004). Furthermore, expression of RUNX1-ETO was shown to induce transcription dysregulation in HSPC (Tonks *et al.* 2007). Analysis of RUNX1-ETO-mediated gene expression changes in these cells shows that this fusion protein is associated with downregulation of *RUNX3*, which has also demonstrated in t(8;21) AML patients (Cheng *et al.* 2008b) (1.2.4.1).

Genetically engineered mouse models lacking RUNX3 have demonstrated the importance of this TF in a variety of physiological processes including neurogenesis, thymopoiesis, and DC functional maturation (Levanon *et al.* 2002; Woolf *et al.* 2003; Fainaru *et al.* 2004) (1.4). Loss of RUNX3 was shown to cause a mild expansion of HSC and myeloid cells in aged mice (Wang *et al.* 2013), whereas disruption of both RUNX1 and RUNX3 leads to BM failure and MPD characterised by DNA repair defects (Wang *et al.* 2014a). Recently, RUNX3 was found essential for the lineage balance of human haematopoietic progenitors within the BM (Balogh *et al.* 2020). Furthermore, increased RUNX3 expression was shown to inhibit the normal programme of erythroid development of human HSPC (3.3.2).

Considering its important role in a multitude of developmental processes, abnormal RUNX3 expression and/or function may lead to tumorigenesis. RUNX3 has an ambiguous role in cancer, and is primarily considered a tumour suppressor in

gastric, colorectal, lung and bladder cancers, among others (Li *et al.* 2002; Li *et al.* 2004; Kim *et al.* 2008a; Soong *et al.* 2009) (1.4.2). Conversely, RUNX3 behaves as an oncogene in ovarian cancer, head and neck squamous carcinoma, and NK/T cell lymphoma (Tsunematsu *et al.* 2009; Lee *et al.* 2011; Ng *et al.* 2011). In AML, *RUNX3* mRNA expression is highly heterogenous and downregulation of this TF was previously shown in good prognosis CBF AML (Gutierrez *et al.* 2005; Cheng *et al.* 2008b) (1.3.5). Expression of RUNX3 has been associated with chemoresistance of leukaemic cells and worse EFS in childhood AML (Cheng *et al.* 2008b). Understanding the contribution of RUNX3 for the pathogenesis of AML would potentially benefit risk stratification of AML patients and future therapeutic strategies.

This Chapter aims to examine the impact of RUNX3 expression on normal human myelopoiesis. In addition, given the downregulation of RUNX3 by RUNX1-ETO, the expression of RUNX3 will be restored in RUNX1-ETO-expressing HSPC and its effects further determined. Together with Chapter 3, this study discloses the importance of RUNX3 on human haematopoiesis and its contribution to the pathogenesis of AML.

4.2 Aims and objectives

This study hypothesises that RUNX3 expression levels are important for normal myeloid development of human HSPC. The main aim of this Chapter is to determine the role of RUNX3 in normal human myelopoiesis, as well as the impact of its expression in RUNX1-ETO-expressing HSPC. To achieve this aim, this Chapter has the following objectives:

- **Determine the expression of *RUNX3* during normal human myeloid development.**

Publicly available transcriptomic datasets will be analysed to determine *RUNX3* mRNA expression in different human myeloid haematopoietic cells subsets.

- **Determine the expression level of RUNX3 and associated clinical attributes in t(8;21) and non-t(8;21) AML patient derived blasts.**

Publicly available transcriptomic data will be analysed to establish *RUNX3* expression levels across different AML subtypes, including patients harbouring t(8;21).

- **Determine the effects of RUNX3 overexpression/knockdown on the colony forming ability, growth, and differentiation of myeloid cells.**

Colony forming ability of transduced human HSPC will be assessed by limiting-dilution assay. Serial replating of these colonies will be performed to investigate the self-renewal potential of cells. Concomitantly, transduced cells will be grown in bulk liquid culture and changes in growth and differentiation of these cells will be assessed by analysis of lineage and developmental cell surface markers coupled with multicolour flow cytometry.

- **Assess whether co-expression of RUNX3 and RUNX1-ETO reverts the differentiation block and colony forming ability of erythroid and myeloid RUNX1-ETO expressing cells.**

Human HSPC will be co-transduced with RUNX3 and RUNX1-ETO overexpression viral vectors and their growth and differentiation will be assessed as above. Colony forming ability of these cells will also be determined by limiting-dilution assay.

4.3 Results

4.3.1 Expression of *RUNX3* mRNA decreases during early human myeloid development and increases towards terminal monocytic differentiation

RUNX3 mRNA expression was previously shown to decrease during normal human erythroid development (3.3.1). Microarray-based gene expression profiling of normal human haematopoietic cells shows that *RUNX3* expression decreases significantly during granulocytic development, particularly in promyelocytes, myelocytes and polymorphonuclear cells (Figure 4-1A) (Hu *et al.* 2008; Wildenberg *et al.* 2008; Majeti *et al.* 2009; Andersson *et al.* 2010).

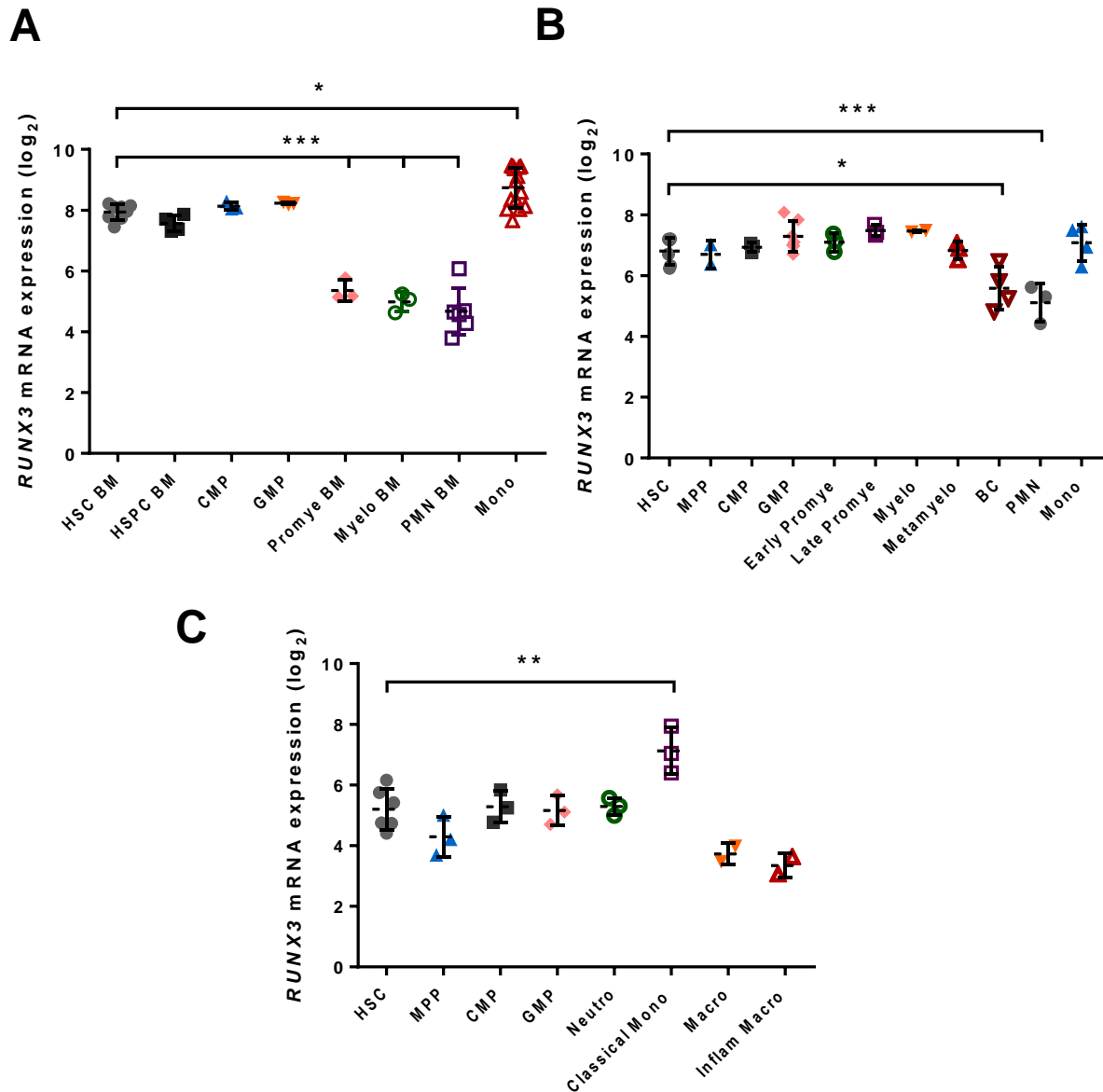


Figure 4-1 – RUNX3 mRNA expression in different myeloid cell subpopulations.

(A) RUNX3 mRNA expression in distinct human haematopoietic cell subsets based on cell surface marker expression. HSC BM – Bone marrow haematopoietic stem cell; HPC BM – Bone marrow haematopoietic stem and progenitor cell; CMP – Common myeloid progenitor; GMP – Granulocyte-monocyte progenitor; Promye BM – Bone marrow promyelocyte; Myelo BM – Bone marrow myelocyte; PMN BM – Bone marrow polymorphonuclear cell; Mono – CD14⁺ Monocyte. Human HSC are from GSE17054; Human GMP are from GSE19599; Human monocytes are from GSE11864 and E-MEXP-1242 (Hu *et al.* 2008; Wildenberg *et al.* 2008; Majeti *et al.* 2009; Andersson *et al.* 2010). 204197_s_at probeset used. Data indicate mean \pm 1SD (n \geq 3). Statistical analysis was performed using ANOVA with Tukey's multiple comparisons test, * p <0.05; *** p <0.001 vs HSC BM. **(B)** RUNX3 mRNA expression in different human haematopoietic cell subtypes. MPP – Multipotent progenitor cell; Metamyelo – Metamyelocyte; BC – Band cell. Data obtained from GSE42519 (Rapin *et al.* 2014; Svendsen *et al.* 2016). Data indicate mean \pm 1SD (n \geq 2). Statistical analysis was performed using ANOVA with Tukey's multiple comparisons test, * p <0.05; *** p <0.001 vs HSC. **(C)** RUNX3 mRNA expression within distinct human haematopoietic cell subsets. Neutro – Neutrophil; Classical Mono – CD14⁺CD16⁻ Monocyte; Macro – Macrophage; Inflam Macro – Inflammatory macrophage. Data obtained from the BLUEPRINT study (www.blueprint-epigenome.eu). Data indicate mean \pm 1SD (n \geq 2). Statistical analysis was performed using ANOVA with Tukey's multiple comparisons test, ** p <0.01 vs HSC.

A similar trend was observed in an additional transcriptomic dataset (Figure 4-1B) (Rapin *et al.* 2014; Svendsen *et al.* 2016). In terms of monocytic differentiation, *RUNX3* mRNA levels increase in mature monocytes compared to HSC (Figure 4-1A). Furthermore, human RNA-seq data from the BLUEPRINT study (www.blueprint-epigenome.eu) reveal a similar upregulation of *RUNX3* in classical monocytes (CD14⁺CD16⁻) (Figure 4-1C). Overall, these data demonstrate that *RUNX3* is differently expressed during normal myeloid development and suggest different roles for *RUNX3* during monocytic and granulocytic differentiation.

4.3.2 *RUNX3* is variably expressed across AML and its expression is associated with poorer overall survival of patients

AML is a heterogeneous malignancy in terms of cytogenetic and molecular characteristics, as previously detailed in 1.2. In order to determine an association between the mRNA expression levels of *RUNX3* and different AML subtypes, publicly available transcriptomic datasets were analysed. As shown in Figure 4-2, *RUNX3* expression is highly variable across AML. Expression data from healthy BM and AML patient samples were obtained from the Microarray Innovations in Leukaemia (MILE) study (Figure 4-2A) (Kohlmann *et al.* 2008; Haferlach *et al.* 2010). A significant downregulation of *RUNX3* by 1.7- and 1.4-fold fold was observed in inv(16) and t(8;21) AML patients, respectively. CBF-AML, comprising both inv(16) and t(8;21) subtypes, is associated with a good prognosis of AML patients (1.2.2).

TCGA is a genomics programme that characterised over 20,000 normal and cancer patient samples, including AML (www.cancer.gov/tcga). TCGA RNA-seq data from 173 AML patients (Cancer Genome Atlas Research *et al.* 2013) confirms the data from the MILE study regarding *RUNX3* mRNA expression. As shown in Figure 4-2B, there was a significant downregulation of *RUNX3* levels in inv(16) and t(8;21) AML by 1.3- and 1.2-fold, respectively, compared to AML with normal karyotype. In addition, *RUNX3* expression was significantly upregulated in AML patients with complex cytogenetics compared to normal karyotype patients. This observation associates increased *RUNX3* levels with a subtype of AML that is mainly characterised by poor prognosis and survival of patients.

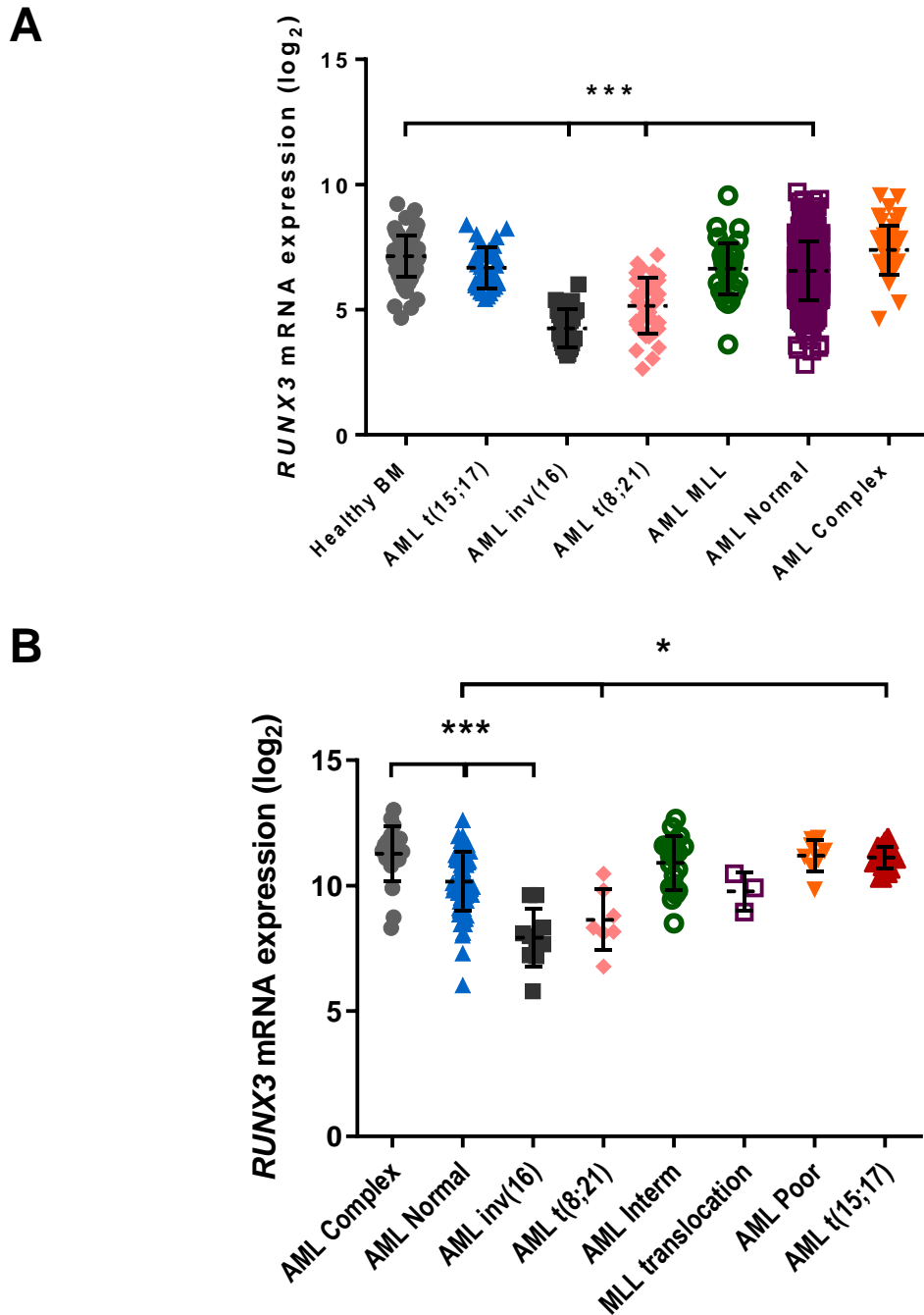


Figure 4-2 – RUNX3 mRNA expression levels are variable in AML subtypes.

(A) RUNX3 mRNA expression in healthy BM cells and in distinct AML subtypes based on cytogenetics of patients. BM – Bone marrow; AML Normal – AML with normal karyotype; AML complex – AML with a complex karyotype. Data obtained from GSE13159 (Kohlmann *et al.* 2008; Haferlach *et al.* 2010) using 204197_s_at probeset. Data indicate mean \pm 1SD ($n \geq 28$). Statistical analysis was performed using ANOVA with Tukey’s multiple comparisons test, *** $p < 0.001$ vs Healthy BM. **(B)** RUNX3 mRNA expression in different AML subtypes. AML Interm – AML with intermediate cytogenetic risk; AML Poor – AML with poor cytogenetic risk. RNA-seq data obtained from TCGA (Cancer Genome Atlas Research *et al.* 2013). Data indicate mean \pm 1SD ($n \geq 3$). Statistical analysis was performed using ANOVA with Tukey’s multiple comparisons test, * $p < 0.05$; *** $p < 0.001$ vs AML Normal.

To further investigate the association between RUNX3 levels and AML subtypes, patient data was stratified according to *RUNX3* expression in upper and lower quartiles and survival curves were plotted using the Kaplan-Meier estimator (Figure 4-3). AML patients with increased *RUNX3* expression showed a significant worse clinical outcome compared to patients with lower *RUNX3* levels. Taken together, these data suggest that RUNX3 expression is significantly associated with prognosis and OS of AML patients.

To further understand the relationship between *RUNX3* expression and OS of AML patients, cBioPortal was used to analyse the TCGA AML dataset. The following clinical attributes were significantly correlated with *RUNX3* expression in AML patients: white blood cell count (WBC) > molecular risk > cytogenetic code > tumour histological subtype > cytogenetic risk > fraction of altered genome > PB blast percentage > OS status and diagnosis age. As shown in Figure 4-4A and B, increased *RUNX3* expression was associated with complex cytogenetics, poor and intermediate risk AML cases, which in turn relate to poor prognosis. On the other hand, lower *RUNX3* expression was found in normal karyotype and CBF AML patients, which are associated with intermediate and good prognosis, respectively. Lower WBC and later diagnosis age are additional clinical attributes found significantly correlated *RUNX3* overexpression in AML patients, and therefore worse prognosis (Figure 4-4C and D). Taken together, these findings suggest that both up- and downregulation of RUNX3 may contribute to the pathogenesis of AML, but it is not clear from this data whether RUNX3 is a driver of disease.

4.3.3 Overexpression of RUNX3 inhibits human myeloid development

Considering that RUNX3 was shown overexpressed in different subtypes of AML, and its important role in murine haematopoiesis (Wang *et al.* 2013), this study sought to explore the effect of RUNX3 overexpression on myeloid growth and differentiation using an *in vitro* HSPC model (3.3.2).

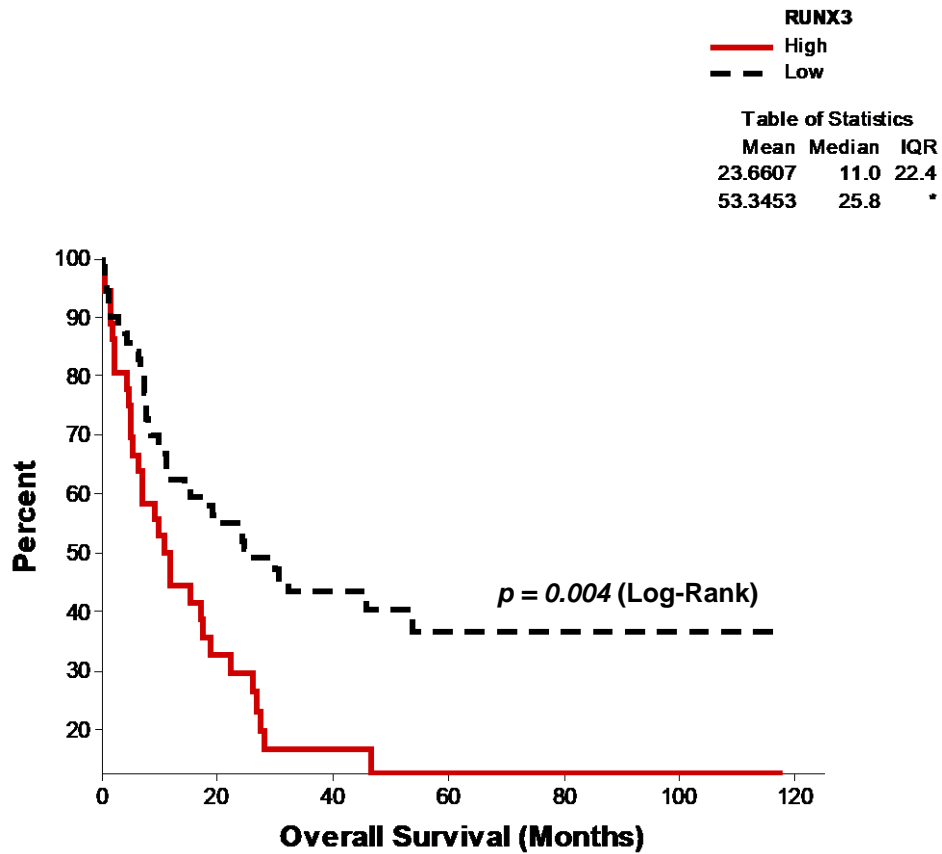


Figure 4-3 – Overexpression of RUNX3 is associated with poor overall survival of AML patients.

Kaplan-Meier survival curve for AML patients stratified according to upper and lower *RUNX3* mRNA expression quartiles. Data obtained from TCGA (Cancer Genome Atlas Research *et al.* 2013) using cBioPortal (www.cbioportal.org). *RUNX3* upper quartile (n=36); *RUNX3* lower quartile (n=70). Untreated patients were excluded from this analysis, along with t(15;17) AML patients that have a different treatment regimen compared to all other AML subtypes. Statistical analysis of survival curves was performed using the Long-Rank test between high and low *RUNX3* expression groups. IQR – Difference between the first (Q1) and third (Q3) quartiles. * is displayed when the survival probability cannot be found.

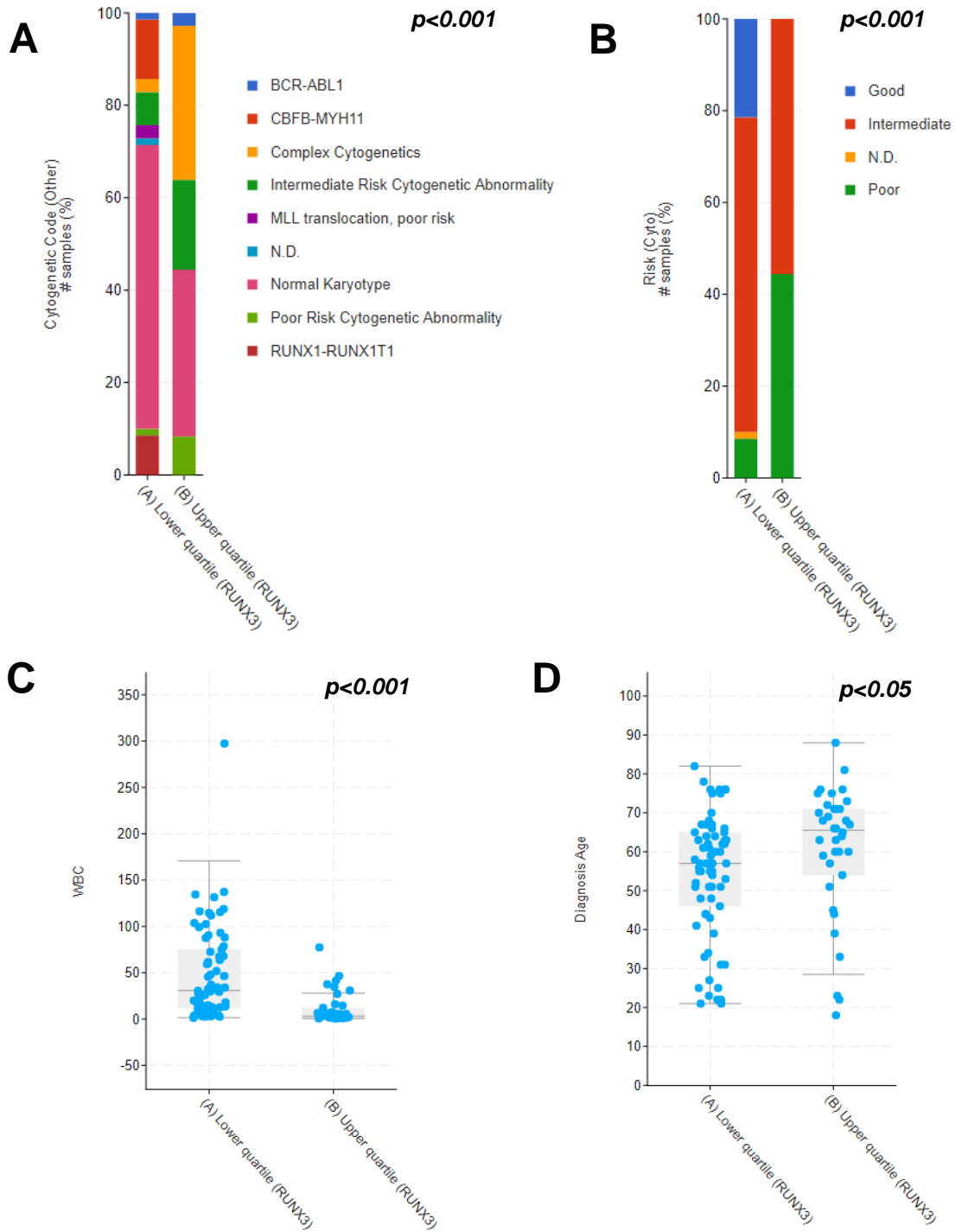


Figure 4-4 – Increased *RUNX3* expression is associated with complex cytogenetics and poor prognosis in AML.

Relationship between increased and reduced *RUNX3* expression and different clinical attributes of AML patients. Data obtained from TCGA (Cancer Genome Atlas Research *et al.* 2013). *RUNX3* upper quartile (n=36); *RUNX3* lower quartile (n=70). **(A)** Cytogenetic code of AML patients according to *RUNX3* expression. Statistical analysis performed using the Chi-squared test. **(B)** Cytogenetic risk of AML patients according to *RUNX3* expression. Statistical analysis performed using the Chi-squared test. **(C)** White blood cell (WBC) count of AML patients according to *RUNX3* expression. Statistical analysis performed using the Kruskal Wallis test. **(D)** Diagnosis age of AML patients according to *RUNX3* expression. Statistical analysis performed using the Kruskal Wallis test.

4.3.3.1 RUNX3 expression inhibits myeloid colony formation

The effects of RUNX3 overexpression on myeloid colony forming ability and self-renewal capacity of progenitor cells were initially evaluated. Transduced HSPC were sorted by FACS for DsRed expression on day 3 (2.6.3) and cultured by limiting dilution in 96-well plates in the presence of IL-3, SCF, G-CSF and GM-CSF. As shown in Figure 4-5A, RUNX3 overexpression in HSPC led to a significant reduction in colony forming efficiency by 1.5 ± 0.4 -fold compared to control cells. Self-renewal potential of these cells was further determined by serial replating of colony forming cells. RUNX3-expressing cells formed 3.7 ± 4.6 -fold more myeloid colonies than controls, though it did not reach significance (Figure 4-5B). Taken together, these results show that overexpression of RUNX3 reduces myeloid colony formation, suggesting that increase RUNX3 levels affect the survival of myeloid cells.

4.3.3.2 RUNX3 overexpression suppresses the growth of myeloid cells

Having showed that RUNX3 overexpression impairs the formation of myeloid colonies, the growth and differentiation of HSPC in liquid culture supplemented with IL-3, SCF, G-CSF and GM-CSF were followed over 13 days. The gating strategy employed for the myeloid studies is shown in Figure 4-6. RUNX3 overexpression caused a modest suppression of proliferation during myeloid development of cells (Figure 4-7A). To assess the growth of cells committed to different lineages, CD13 and CD36 cell surface markers were used to discriminate between the erythroid, monocytic and granulocytic populations. As expected, erythroid-committed cells (CD13⁻CD36⁺) overexpressing RUNX3 grew significantly slower than controls (2.5 ± 0.8 -fold on day 13) (Figure 4-7B). Conversely, the growth of monocytic cells (CD13⁺CD36⁺) was not significantly affected by RUNX3 overexpression in these cells (Figure 4-7C). In addition, granulocytes overexpressing RUNX3 (CD13^{-/+}CD36⁺) grew slower than control cells by 1.4 ± 0.1 -fold on day 13 of culture (Figure 4-7D). These results indicate that RUNX3 overexpression affects the growth of myeloid cells, especially the cells committed to the erythroid and granulocytic lineages.

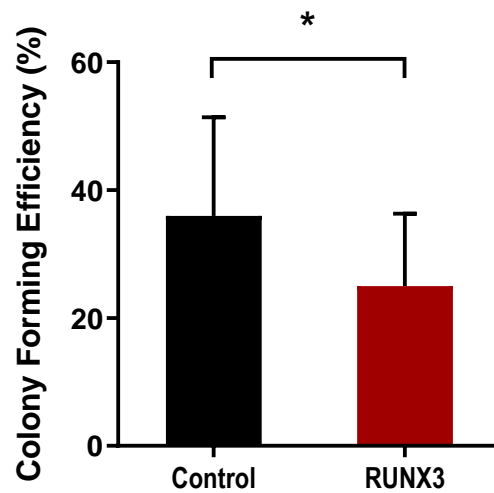
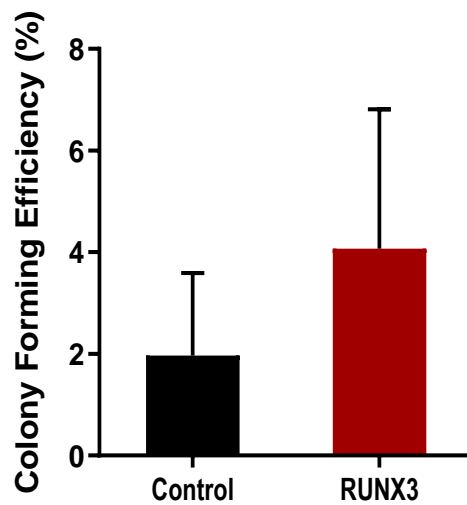
A**B**

Figure 4-5 – Overexpression of RUNX3 inhibits myeloid colony formation in human HSPC.

(A) Summary data of colony forming efficiency for control and RUNX3-expressing cultures following 7 days of growth in liquid culture containing IL-3, SCF, G-CSF and GM-CSF. Data indicate mean \pm 1SD of six independent experiments. Significant difference of RUNX3-expressing cells from controls was analysed by paired t test, $*p < 0.05$. **(B)** Self-renewal potential assessed by a single replating round of control and RUNX3 cultures in the same conditions as previously. Data indicate mean \pm 1SD of three independent experiments.

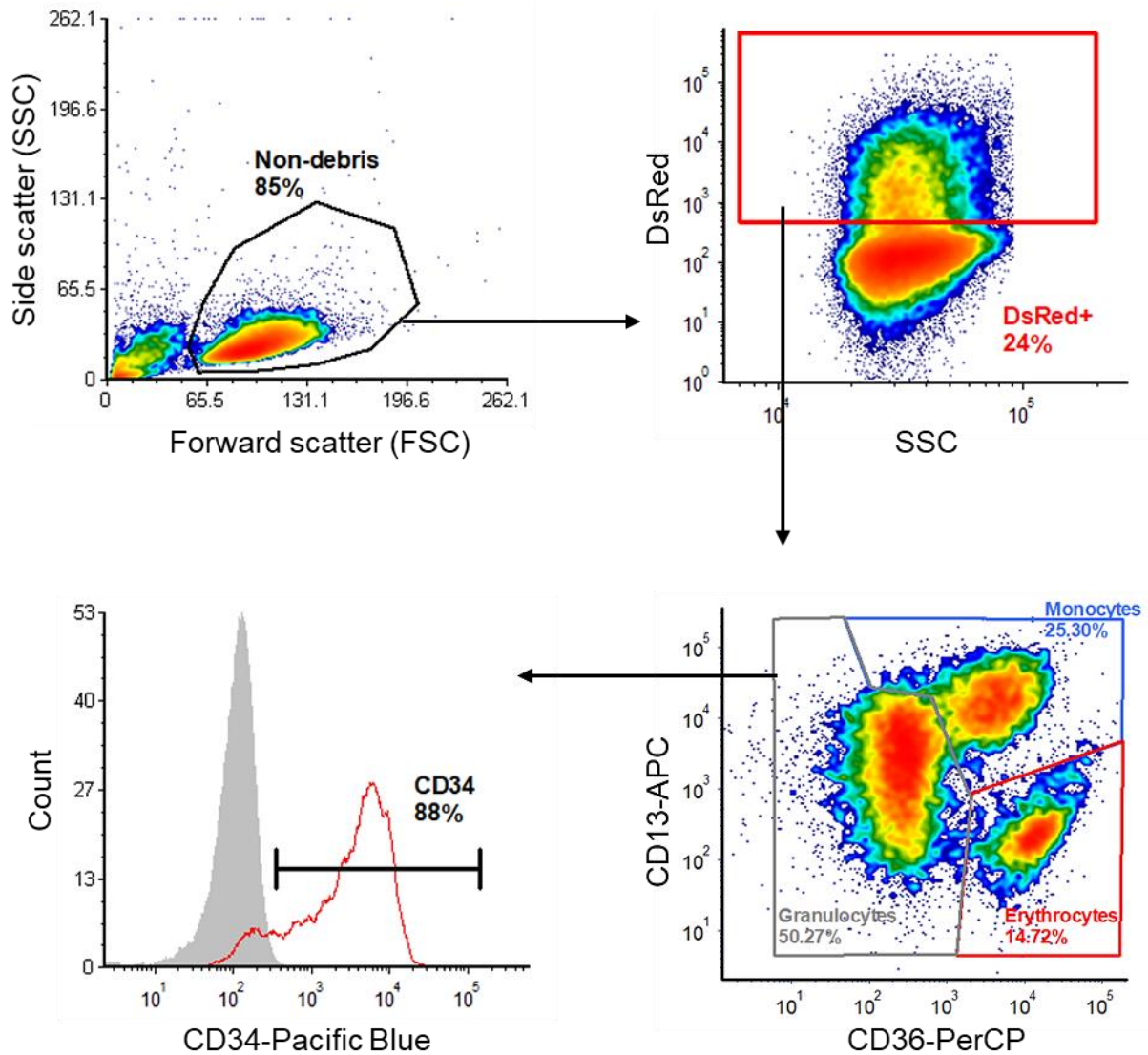


Figure 4-6 – Gating strategy used for the analysis of myeloid growth and differentiation of HSPC by flow cytometry.

Representative density plots and flow cytometry histograms of transduced HSPC on day 6 of culture. Non-debris – Gate used to exclude all debris from the analysis. DsRed⁺ – Gate used to analyse transduced HSPC. Granulocytes – Gate used to analyse the growth and differentiation of granulocytic cells (CD13^{-/+}CD36⁺); Monocytes – Gate used to analyse the growth and differentiation of monocytic cells (CD13⁺CD36⁺); Erythrocytes – Gate used to assess the growth and percentage of erythroid-committed cells (CD13⁻CD36⁺) in culture (Figure 3-8). IgG-Pacific Blue HSPC cells – grey.

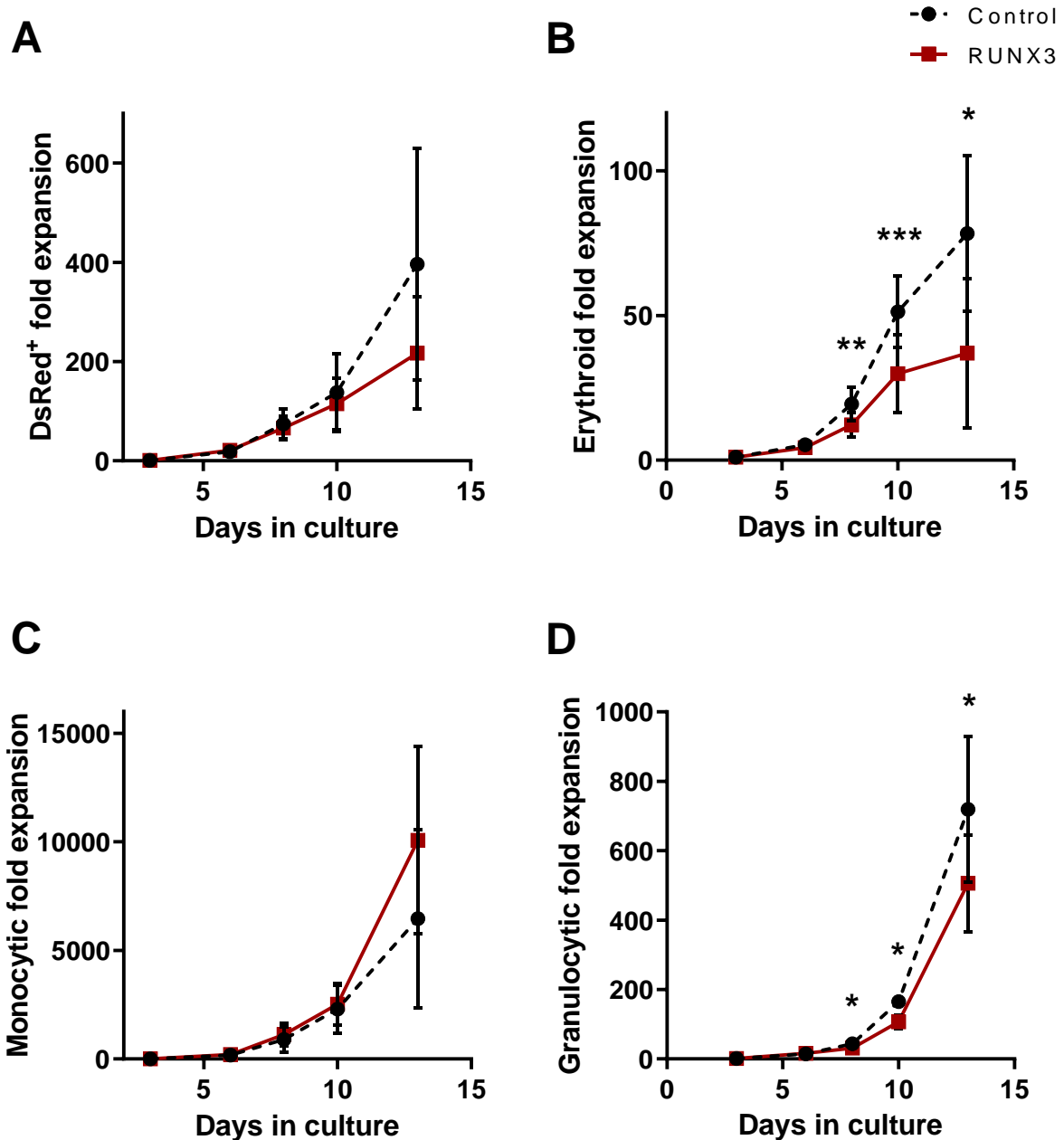


Figure 4-7 – Overexpression of RUNX3 inhibits erythroid and granulocytic growth during myeloid development.

(A) Cumulative fold expansion of DsRed⁺ cells for both control and RUNX3 myeloid cultures grown over 13 days in culture medium containing IL-3, SCF, G-CSF and GM-CSF. Data indicate mean \pm 1SD of at least four independent experiments. **(B)** Cumulative fold expansion of erythroid-committed cells (CD13⁻CD36⁺) for both control and RUNX3 cultures (3.3.2). Data indicate mean \pm 1SD of at least three independent experiments. Significant difference of RUNX3-expressing cells from controls was analysed by paired t test, * $p < 0.05$, ** $p < 0.01$, *** $p < 0.001$. **(C)** Cumulative fold expansion of monocytic cells (CD13⁺CD36⁺) for both control and RUNX3 cells. Data indicate mean \pm 1SD of at least three independent experiments. **(D)** Cumulative fold expansion of granulocytic cells (CD13^{-/+}CD36⁻) for both control and RUNX3 cells. Data indicate mean \pm 1SD of at least three independent experiments. Significant difference of RUNX3-expressing cells from controls was analysed by paired t test, * $p < 0.05$.

4.3.3.3 *RUNX3 overexpression inhibits myeloid differentiation*

To determine the impact of RUNX3 overexpression on myeloid development, expression of differentiation cell surface markers was analysed over time by flow cytometry. Using the lineage discrimination markers CD13 and CD36, development of distinct lineages was assessed in combination with CD11b, CD14, CD15 and CD34 (Figure 4-6). Normal myeloid differentiation is characterised by the rapid loss of CD34 expression and upregulation of CD11b (Egeland *et al.* 1991; Tonks *et al.* 2004). Monocytic cells are expected to upregulate CD14 during development, whereas granulocytic cells upregulate CD15 expression (Egeland *et al.* 1991; Tonks *et al.* 2004). As shown in Figure 4-8A, RUNX3 overexpression led to a 1.5 ± 0.3 -fold reduction in the percentage of erythroid cells in culture compared to control (day 3). The proportion of monocytic cells overexpressing RUNX3 was 1.5 ± 0.3 -fold higher than controls by day 13 (Figure 4-8B). In contrast, a 1.1 ± 0.1 -fold reduction in the percentage of granulocytic-committed cells in RUNX3 culture compared with controls was observed on the same day (Figure 4-8C). Overall, these data indicate that RUNX3 affected the balance between different lineages in culture by reducing the number of granulocytic cells in favour of monocytes during normal myeloid development of human HSPC.

Having assessed the proportion of cells committed to each lineage for both control and RUNX3 cultures, the effect of RUNX3 overexpression on the normal differentiation of monocytes and granulocytes was further determined. As shown in Figure 4-9, increased expression of RUNX3 in HSPC led to a disruption of the normal programme of monocytic differentiation. Upregulation of CD11b expression was significantly impaired in RUNX3 cells throughout development, and by day 8 was 2.3 ± 0.4 -fold lower compared to controls (Figure 4-9A). CD14 upregulation was also impacted by RUNX3 expression, though to a lesser extent. On day 6, CD14 expression was significantly reduced by 1.5 ± 0.2 -fold in differentiating cells overexpressing RUNX3 (Figure 4-9B). Expression of CD34 did not change significantly between conditions and its expected downregulation over time was observed during monocytic development (Figure 4-9C).

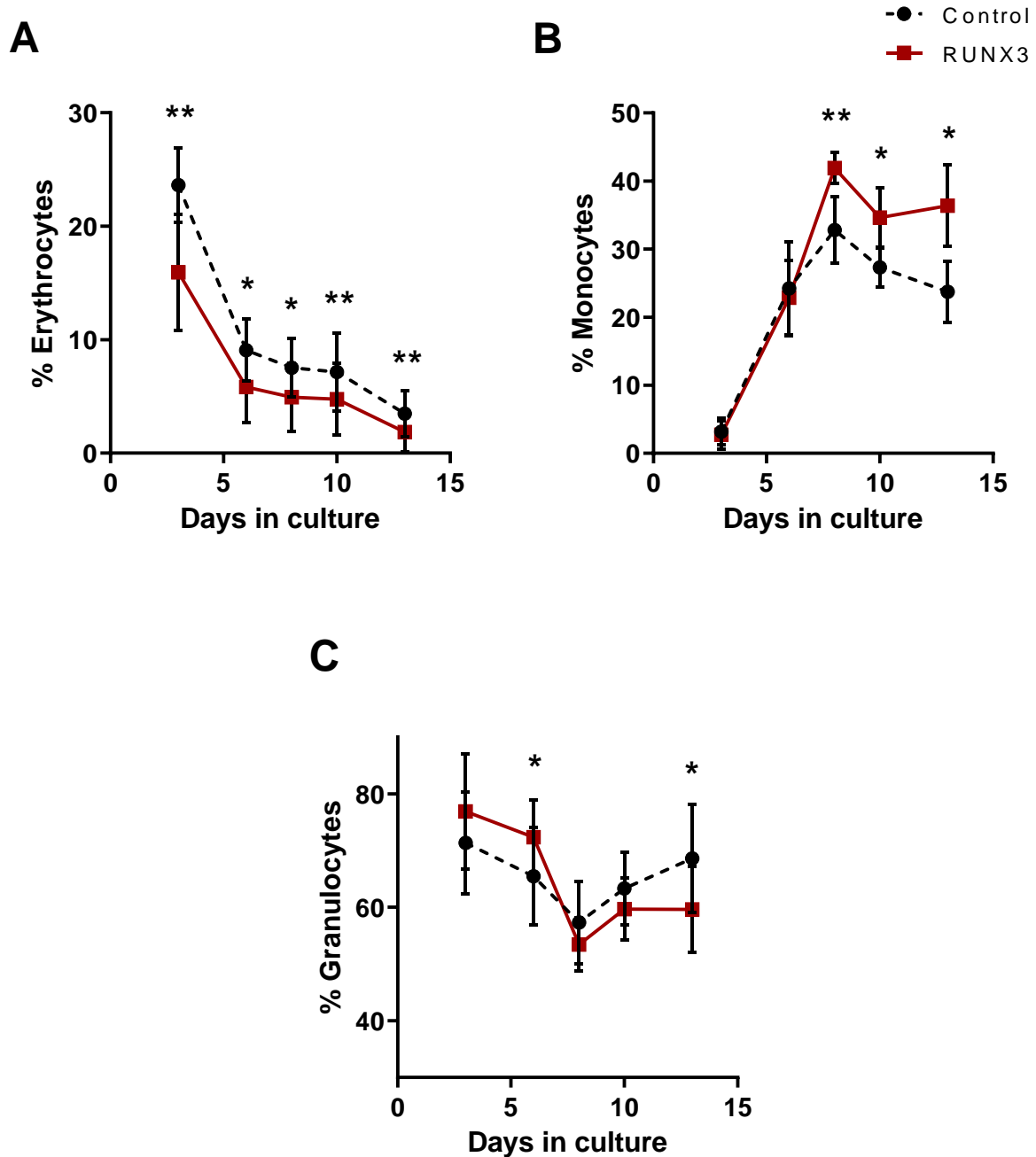


Figure 4-8 – Overexpression of RUNX3 disrupts the balance between monocytic and granulocytic populations in culture during myeloid development of HSPC.

(A) Summary data of erythroid committed cells (CD13⁺CD36⁺) in terms of percentage for both control and RUNX3 cultures (3.3.2). Data indicate mean \pm 1SD of at least four independent experiments. Significant difference of RUNX3-expressing cells from controls was analysed by paired t test, * $p < 0.05$, ** $p < 0.01$. **(B)** Summary data of the percentage of monocytic cells (CD13⁺CD36⁺) in control and RUNX3 cultures. Data indicate mean \pm 1SD of at least four independent experiments. Significant difference of RUNX3-expressing cells from controls was analysed by paired t test, * $p < 0.05$, ** $p < 0.01$. **(C)** Summary data of the percentage of granulocytic cells (CD13⁺CD36⁻) in control and RUNX3 cultures. Data indicate mean \pm 1SD of at least five independent experiments. Significant difference of RUNX3-expressing cells from controls was analysed by paired t test, * $p < 0.05$.

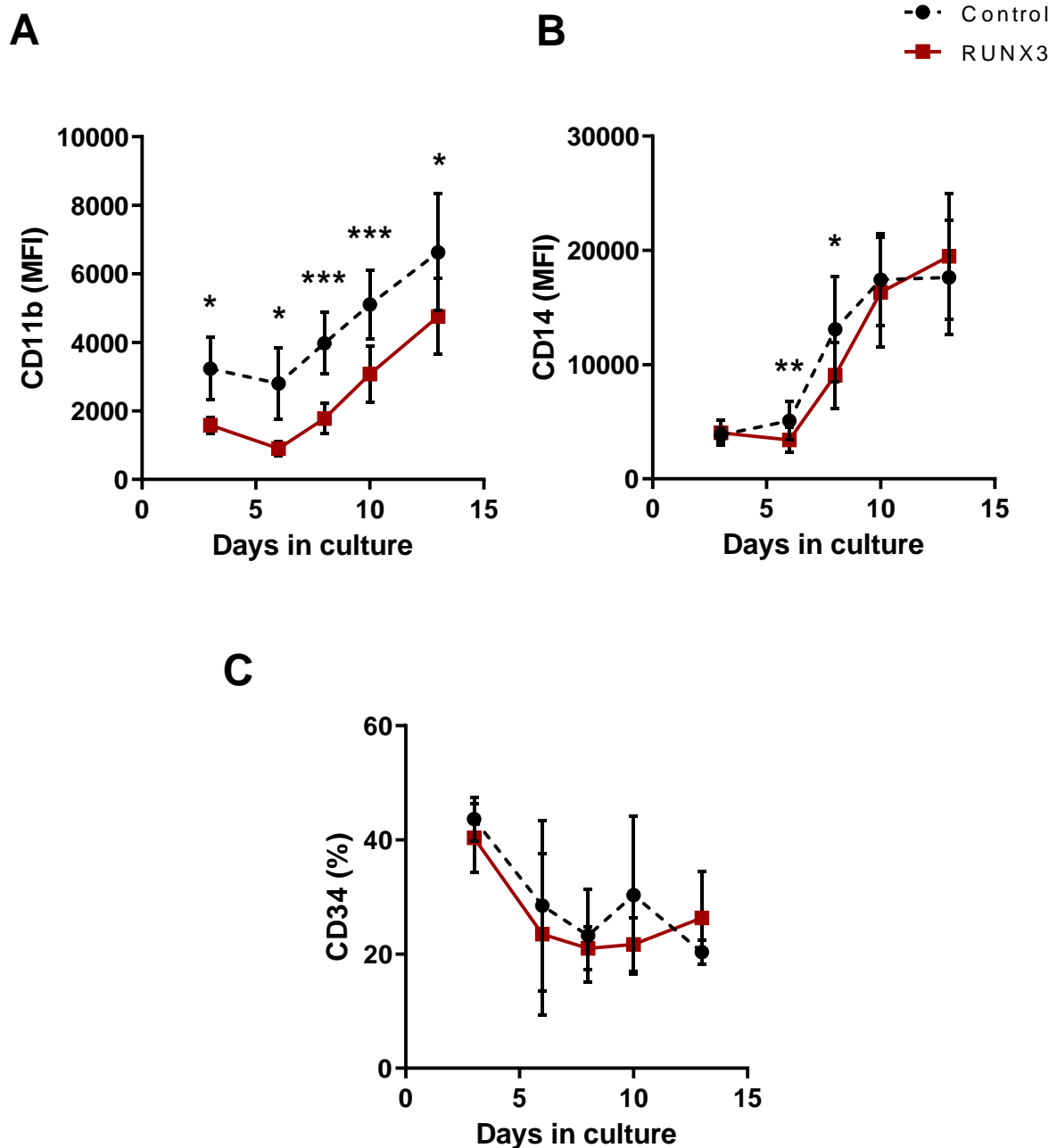


Figure 4-9 – Overexpression of RUNX3 downregulates the expression of CD11b and CD14 in monocytic cells.

(A) Summary data of CD11b expression in terms of MFI in monocytic-committed cells (CD13⁺CD36⁺) over time for both control and RUNX3 cultures. Data indicate mean \pm 1SD of at least four independent experiments. Significant difference of RUNX3-expressing cells from controls was analysed by paired t test, * $p < 0.05$, *** $p < 0.001$. **(B)** Summary data of CD14 expression (MFI) for control and RUNX3 monocytic cells over time. Data indicate mean \pm 1SD of at least four independent experiments. Significant difference of RUNX3-expressing cells from controls was analysed by paired t test, * $p < 0.05$, ** $p < 0.01$. **(C)** Summary data of CD34 expression in terms of percentage for monocytic cells in both control and RUNX3 cultures over time. Data indicate mean \pm 1SD of at least three independent experiments.

In terms of granulocytic differentiation, RUNX3 expression suppressed the normal development of granulocytes in culture by reducing upregulation of CD11b expression by 2.8 ± 0.8 -fold compared to controls (Figure 4-10A). Although CD15 expression was reduced in RUNX3-expressing cells over 13 days, these changes were not significant (Figure 4-10B). No changes were observed in CD34 expression between control and RUNX3 cultures (Figure 4-10C). Interestingly, there was a 1.2 ± 0.05 -fold significant reduction in the granularity (SSC) of granulocytic cells overexpressing RUNX3 on the last day of culture, which might suggest that these cells were more immature than controls (Figure 4-10D). Morphological assessment of May-Grünwald-Giemsa stained cells was performed to further consolidate the immunophenotypic data. As shown in Figure 4-11A, controls were defined predominantly as band/segment mature cells (late phase granulocytic development), and myelocytes/metamyelocytes (intermediate phase). Overexpression of RUNX3 retained the cells in an intermediate phase of development by 1.2 ± 0.01 -fold compared to control (Figure 4-11A and B). Concomitantly, there was a significant reduction in the number of mature cells expressing RUNX3 compared to controls by 1.4 ± 0.1 -fold. Taken together, these results suggest that RUNX3 expression suppresses the terminal differentiation of myeloid cells.

In summary, these data suggest that overexpression of RUNX3 in human HSPC favours the expansion of monocytes over granulocytes while inhibiting the development of both myeloid lineages in culture.

4.3.4 Knockdown of RUNX3 does not affect myeloid growth and development

Overexpression of RUNX3 in human HSPC was shown to inhibit normal myeloid development by suppressing granulocytic growth and the terminal maturation of both monocytic and granulocytic cells. These observations prompted the study of RUNX3 KD and its effects on myeloid growth and differentiation of HSPC using the same shRNA constructs as before (3.3.3).

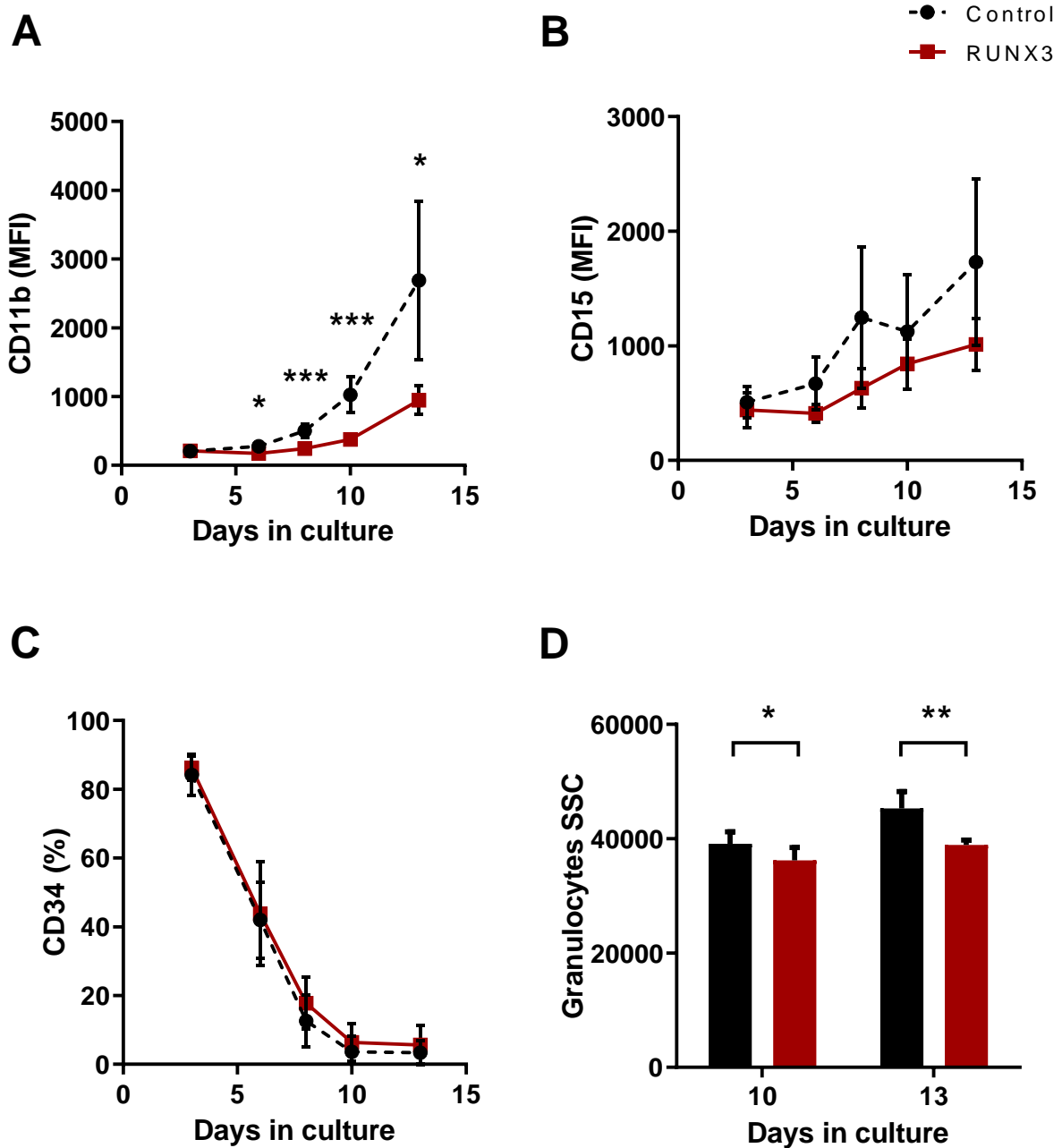


Figure 4-10 – RUNX3 expression disturbs granulocytic development by downregulating CD11b expression.

(A) Summary data of CD11b expression in terms of MFI in granulocytic-committed cells CD13^{-/+}CD36⁻ over time for both control and RUNX3 cultures. Data indicate mean \pm 1SD of at least five independent experiments. Significant difference of RUNX3-expressing cells from controls was analysed by paired t test, * $p < 0.05$, *** $p < 0.001$. **(B)** Summary data of CD15 expression (MFI) for control and RUNX3 granulocytic cells over time. Data indicate mean \pm 1SD of at least three independent experiments. **(C)** Summary data of CD34 expression in terms of percentage for granulocytic cells in both control and RUNX3 cultures over time. Data indicate mean \pm 1SD of at least five independent experiments. **(D)** Complexity of granulocytic cells measured by changes in SSC for both control and RUNX3 cells on days 10 and 13 of myeloid differentiation. Data indicate mean \pm 1SD of at least four independent experiments. Significant difference of RUNX3-expressing cells from controls was analysed by paired t test, * $p < 0.05$, ** $p < 0.01$.

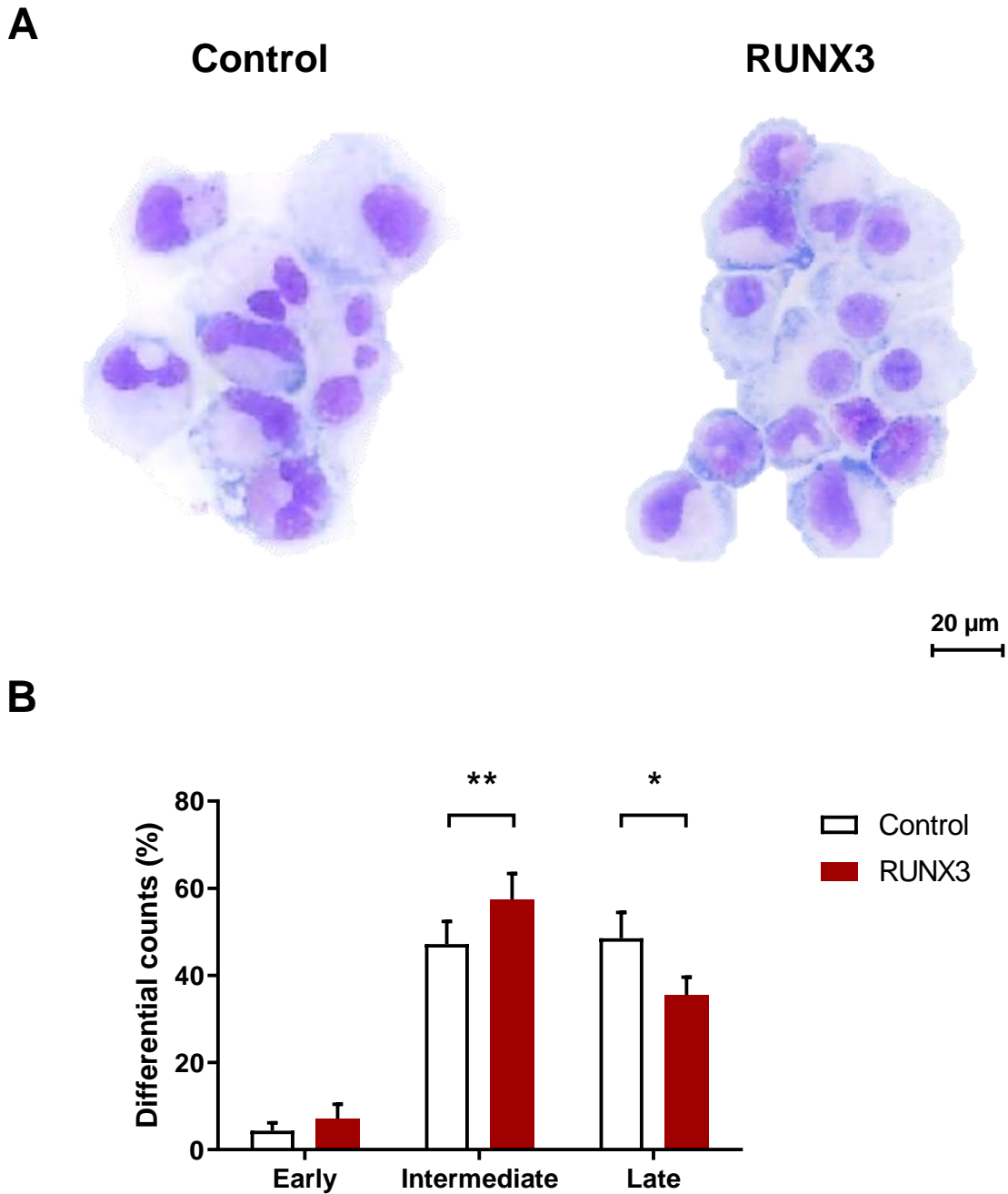


Figure 4-11 – Overexpression of RUNX3 affects the morphology of cells during myeloid development.

(A) Control and RUNX3-expressing cells analysed on day 17 of differentiation with May-Grünwald-Giemsa staining. **(B)** Differential counts of both cultures with morphology categorised into early (myeloblasts/promyelocytes), intermediate (myelocytes/metamyelocytes) and late phase (band/segmented granulocytic cells). Data indicate mean \pm 1SD of three independent experiments. Significant difference of RUNX3-expressing cells from controls was analysed by paired t test, * $p < 0.05$, ** $p < 0.01$.

To determine the effects of RUNX3 KD on colony formation ability of myeloid cells, sorted GFP⁺ HSPC were plated by limiting dilution as previously described (4.3.3.1). Following one week of growth, all three RUNX3 KD cultures formed less myeloid colonies compared to control (Figure 4-12), though these differences did not reach significance. No effect was observed in the self-renewal capacity of these cells (data not shown). Taken together, reduction of RUNX3 levels did not affect significantly the colony forming ability of cells during normal human myeloid development.

In order to assess the growth of myeloid cells with reduced RUNX3 levels, HSPC were cultured as above (4.3.3.2). As shown in Figure 4-13A, RUNX3 KD did not induce significant changes in the growth of myeloid cells. In terms of lineage-specific growth, there was a significant reduction in erythroid growth by 4.9 ± 1.0 - and 4.6 ± 1.6 -fold for RUNX3 shRNA 1 and 4 cultures, respectively, on the last day of differentiation (Figure 4-13B), supporting previous results (3.3.3). Regarding monocytic and granulocytic growth, no significant changes in growth were observed compared to shRNA control cells (Figure 4-13C and D). Taken together, these data indicate that KD of RUNX3 does not impair the growth of myeloid cells, apart from erythroid-committed cells in culture.

A similar approach as described above was used to determine the effects of RUNX3 KD on myeloid development of cells (4.3.3.3). No significant changes were observed in terms of lineage balance in RUNX3 KD cells compared to control cells (Figure 4-14). The same was observed regarding their differentiation status, with no significant changes identified in the expression pattern of specific cell surface markers during monocytic (Figure 4-15) and granulocytic development (Figure 4-16). Morphological assessment of control and RUNX3 KD cells on day 17 of culture supported the full maturation of myeloid cells observed for all cultures (Figure 4-17).

Taken together, these data suggest no strong requirement of RUNX3 expression during normal human myeloid development. Nevertheless, and similarly to RUNX3 KD in erythroid development (3.3.3), this study cannot conclude that RUNX3 expression is completely redundant for myelopoiesis given that a complete loss of RUNX3 was not observed in these cells.

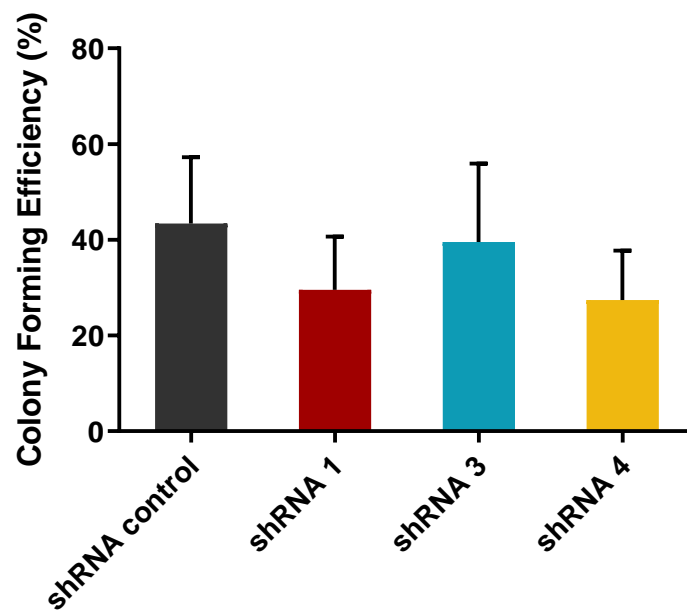


Figure 4-12 – Knockdown of RUNX3 does not disrupt the myeloid colony formation of HSPC.

(A) Colony forming efficiency of control and RUNX3 KD cultures after 7 days of growth in liquid culture containing IL-3 SCF, G-CSF and GM-CSF. Data indicate mean \pm 1SD of three independent experiments.

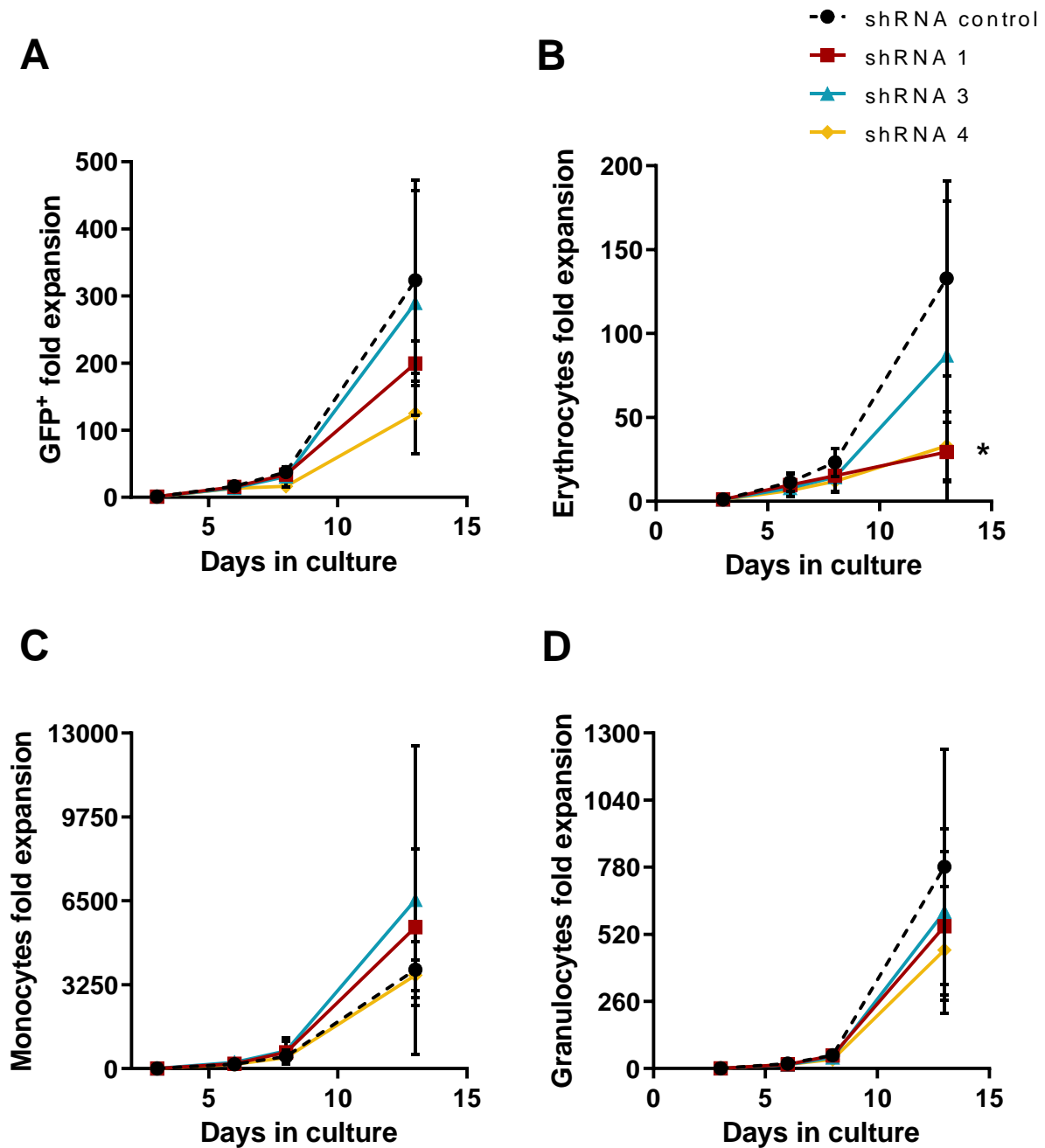


Figure 4-13 – Knockdown of RUNX3 impairs the growth of erythroid cells in culture.

(A) Cumulative fold expansion of GFP⁺ cells in liquid culture for both control and RUNX3 shRNA cultures over 13 days in myeloid medium containing IL-3, SCF, G-CSF and GM-CSF. Data indicate mean \pm 1SD of at least three independent experiments. (B) Cumulative fold expansion of erythroid-committed cells for control and RUNX3 KD cultures (3.3.3). Data indicate mean \pm 1SD of at least three independent experiments. Significant difference between control and each shRNA cultures was analysed by one-way ANOVA using Tukey's multiple comparisons test, * $p < 0.05$ shRNA 1 or 4 vs shRNA control. (C) Cumulative fold expansion of control and RUNX3 KD monocytic cells. Data indicate mean \pm 1SD of at least three independent experiments. (D) Cumulative fold expansion of control and RUNX3 KD granulocytic cells. Data indicate mean \pm 1SD of at least three independent experiments.

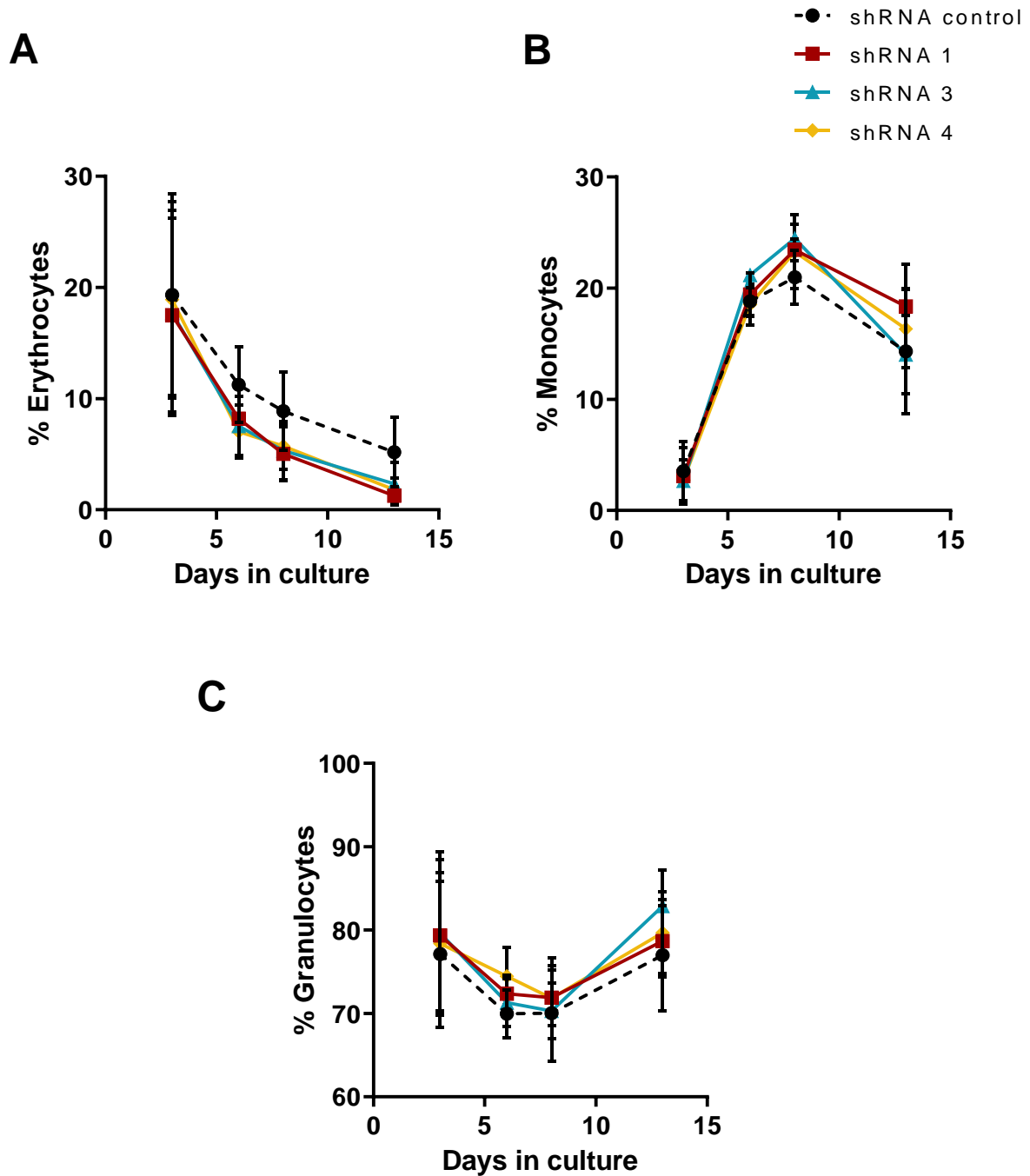


Figure 4-14 – Knockdown of RUNX3 does not affect the lineage balance of cells.

(A) Summary data of erythroid-committed cells in terms of percentage for control and RUNX3 shRNA cultures (3.3.3). Data indicate mean \pm 1SD of at least three independent experiments. **(B)** Summary data of the percentage of monocytic cells in culture for control and RUNX3 KD cells. Data indicate mean \pm 1SD of at least three independent experiments. **(C)** Summary data of granulocytic cells percentages for control and RUNX3 KD cells. Data indicate mean \pm 1SD of at least three independent experiments.

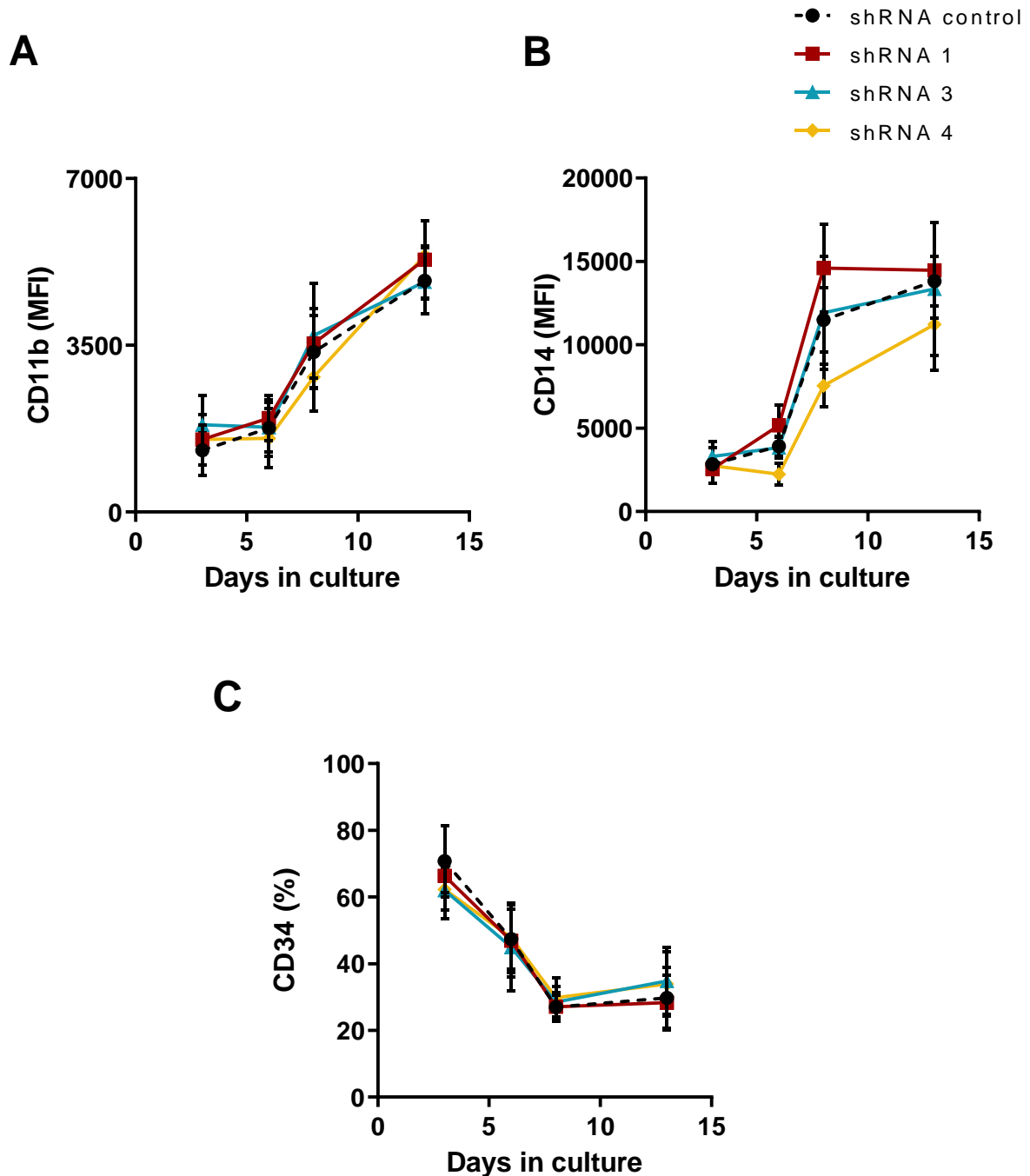


Figure 4-15 – Knockdown of RUNX3 does not significantly disturb the monocytic differentiation of HSPC.

(A) Summary data of CD11b expression in terms of MFI in monocytic-committed cells over time for control and RUNX3 shRNA cultures. Data indicate mean \pm 1SD of at least three independent experiments. (B) Summary data of CD14 expression in MFI for control and RUNX3 KD monocytic cells over time. Data indicate mean \pm 1SD of at least three independent experiments. (C) Summary data of CD34 expression in terms of percentage for monocytic cells in control and RUNX3 KD cultures over time. Data indicate mean \pm 1SD of at least three independent experiments.

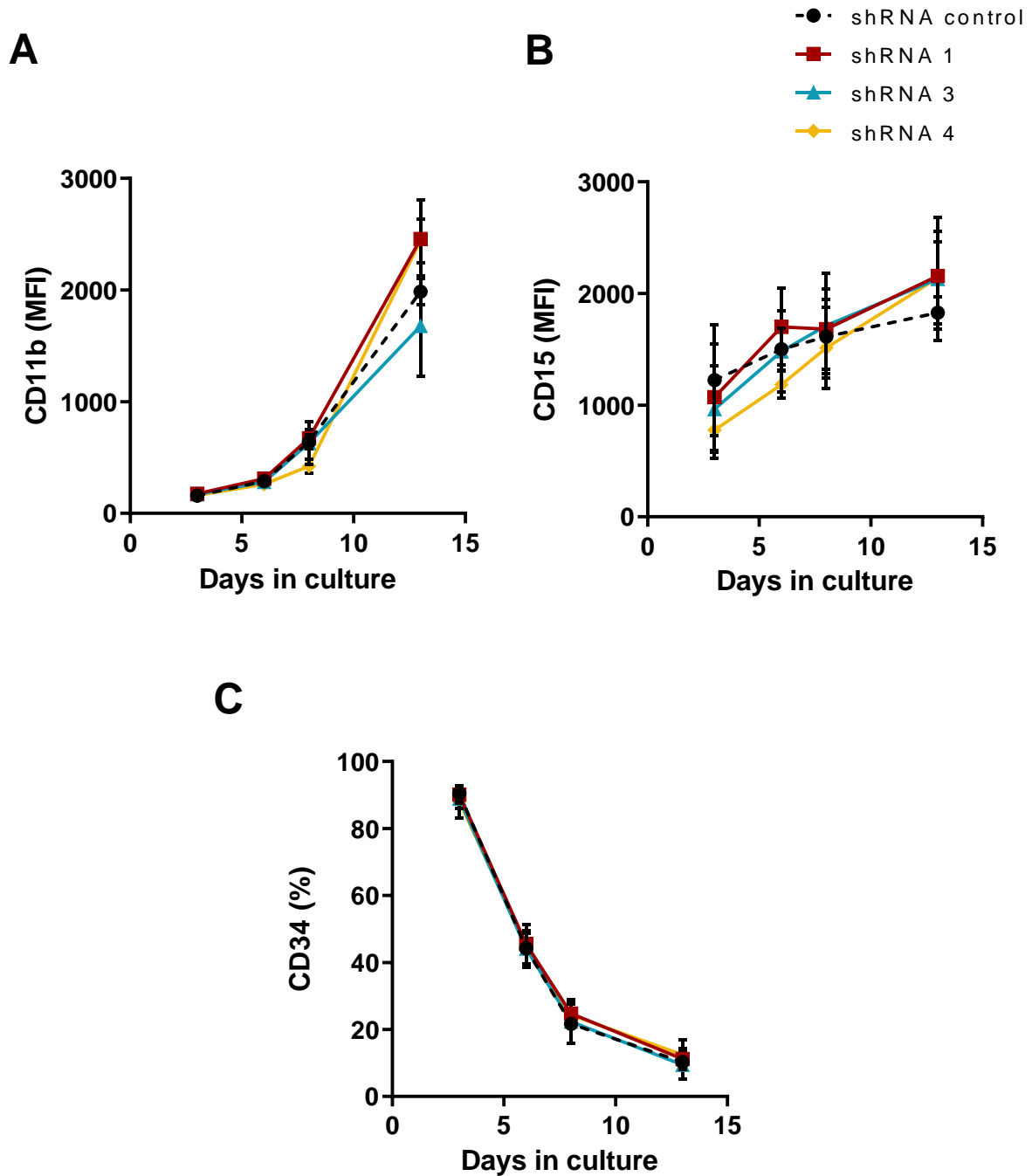


Figure 4-16 – Knockdown of RUNX3 does not significantly affect the granulocytic differentiation of HSPC.

(A) Summary data of CD11b expression in terms of MFI in granulocytic-committed cells over time for control and RUNX3 shRNA cultures. Data indicate mean \pm 1SD of at least three independent experiments. (B) Summary data of CD15 expression in MFI for control and RUNX3 KD granulocytic cells over time. Data indicate mean \pm 1SD of at least three independent experiments. (C) Summary data of CD34 expression in terms of percentage for granulocytic cells in control and RUNX3 KD cultures over time. Data indicate mean \pm 1SD of at least three independent experiments.

4.3.5 RUNX3 overexpression failed to rescue the phenotype of RUNX1-ETO-expressing HSPC

Overexpression of RUNX3 in HSPC was shown to inhibit myeloid growth and induce developmental abnormalities in both monocytic and granulocytic differentiation (4.3.3). Conversely, no significant effects were observed in RUNX3 KD cells during myeloid development (4.3.4). Interestingly, the phenotype of RUNX3-expressing cells resembles RUNX1-ETO-mediated inhibition of myeloid and erythroid development (Tonks *et al.* 2003; Tonks *et al.* 2004). Given that downregulation of *RUNX3* expression was evidenced in t(8;21) AML patients (Cheng *et al.* 2008b), this study next sought to determine whether overexpression of RUNX3 could rescue the phenotype of RUNX1-ETO-expressing cells.

4.3.5.1 RUNX1-ETO downregulated RUNX3 expression in human HSPC

In order to determine whether the repression of RUNX3 reported in t(8;21) AML cells was observed in RUNX1-ETO-expressing human HSPC *in vitro*, transcriptomic data from a previous study was analysed (Tonks *et al.* 2007). A similar methodology was used in this study (2.4, 2.5), with RNA being extracted from HSPC on day 3 of culture, and subsequently on day 6 from erythroid, monocytic and granulocytic progenitors. As shown in Figure 4-18, RUNX1-ETO significantly downregulated *RUNX3* mRNA expression by 2.1 ± 0.6 -fold on day 3 of culture compared to control cells. This repression was not sustained on day 6 in committed progenitors (data not shown).

4.3.5.2 Generation of RUNX1-ETO and RUNX3 expressing HSPC

Having determined the magnitude of *RUNX3* downregulation in RUNX1-ETO-expressing cells, two vectors harbouring different selectable markers were used for the subsequent experiments: RUNX1-ETO-GFP and RUNX3-DsRed (2.5.3). HSPC were infected with 'single' vectors alone or in combination 'double'. Following infection, double transduced HSPC were analysed for growth and differentiation by using a gate defining the GFP⁺DsRed⁺ cells, as shown in Figure 4-19A. Infection efficiencies are summarised in Figure 4-19B. Single infected cells were used as 'positive control' in these experiments as their effects have been previously established (Tonks *et al.* 2003; Tonks *et al.* 2004) (4.3.3).

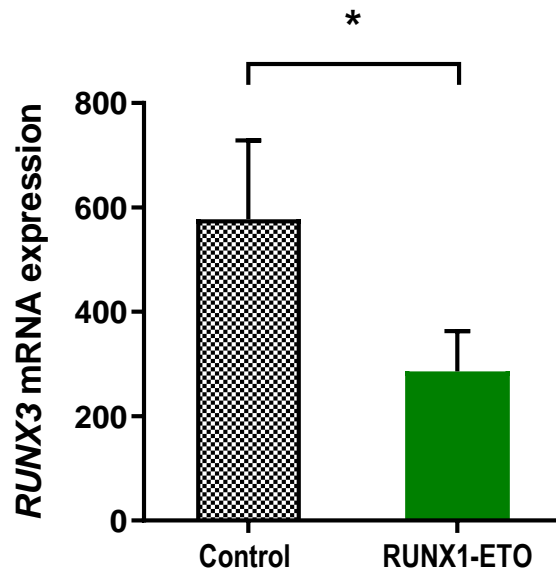


Figure 4-18 – RUNX1-ETO significantly downregulated the expression of *RUNX3* in HSPC.

Summary data of relative *RUNX3* mRNA expression in human CB derived control and RUNX1-ETO-expressing HSPC on day 3 of culture. Data indicate mean \pm 1SD of four independent experiments. Significant difference of RUNX1-ETO-expressing cells from controls was analysed by paired t test, * $p < 0.05$.

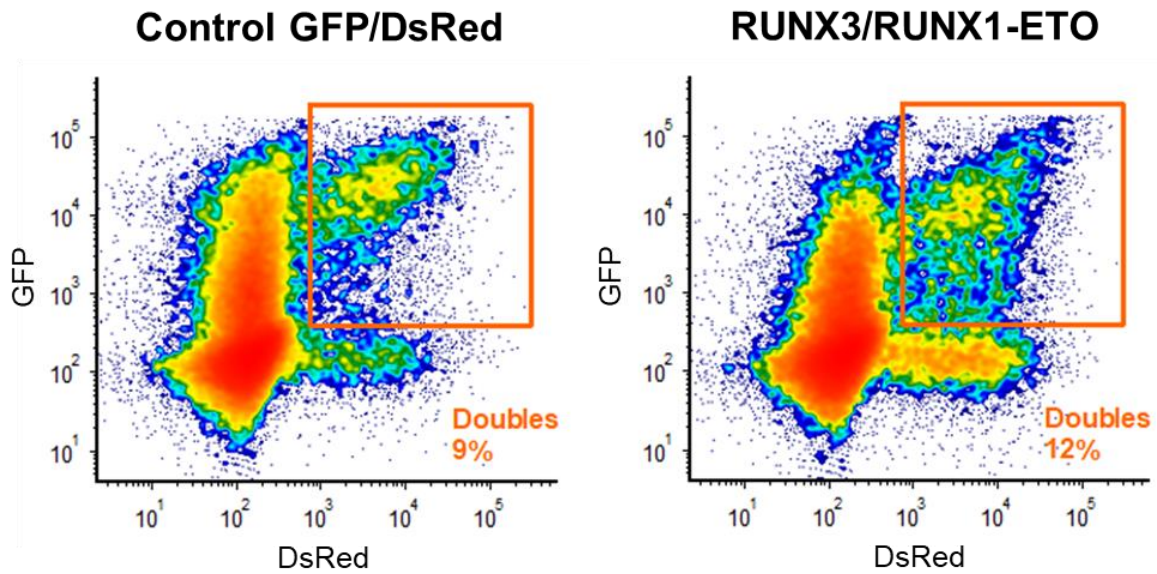
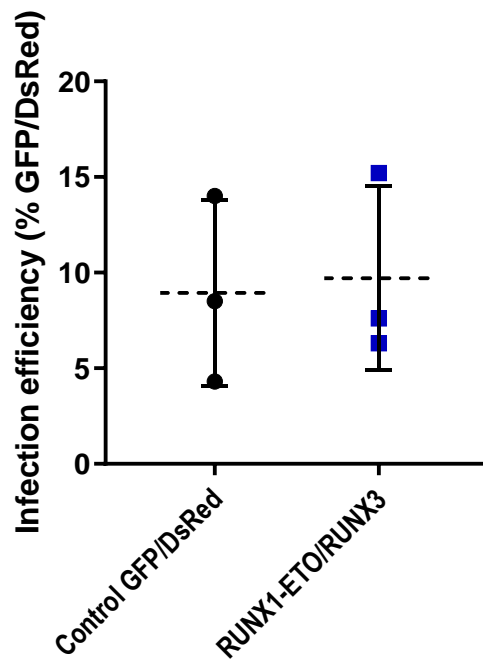
A**B**

Figure 4-19 – Expression of RUNX3 and RUNX1-ETO in human HSPC.

(A) Summary data of percentages of GFP⁺ cells in control and RUNX1-ETO cultures. Data indicate mean \pm 1SD of three independent experiments. **(B)** Example density plots of control GFP/DsRed and RUNX1-ETO/RUNX3 cultures on day 3 showing the double transduced HSPC populations. RUNX3 was overexpressed using a DsRed vector (4.3.3), whereas RUNX1-ETO was expressed using a GFP vector (Tonks *et al.* 2003). Doubles – Gate used to analyse the double transduced (GFP⁺DsRed⁺) cells.

4.3.5.3 RUNX3 overexpression does not rescue the colony formation ability of RUNX1-ETO-expressing cells

RUNX1-ETO and RUNX3 expressed as single abnormalities in normal human HSPC inhibit the colony forming ability of erythroid cells (Tonks *et al.* 2003) (3.3.2). To assess whether overexpression of RUNX3 could rescue the erythroid colony formation ability of RUNX1-ETO-expressing cells, HSPC were transduced with the vectors above and subsequently sorted by FACS to enrich for transduced erythroid population (GFP⁺CD13 or GFP⁺DsRed⁺CD13⁻) (2.6.3). As expected, HSPC expressing RUNX1-ETO exhibited a 11.2 ± 6.5 -fold lower colony forming efficiency compared to control cells (Figure 4-20A). Similarly, RUNX3 expression induced a 2.1 ± 1.1 -fold reduction in erythroid colony formation compared with controls, a result previously observed (3.3.2.2). However, double transduced cells formed 10.0 ± 3.2 -fold less erythroid colonies compared to controls (Figure 4-20B). Given that RUNX3 overexpression failed to restore the colony forming ability of RUNX1-ETO-expressing erythroid cells, the effects of co-expressing RUNX3 and RUNX1-ETO on erythroid colony formation were not further pursued. Therefore, due to the limited number of repeats performed in this section, data were not significant. Overall, these data suggest that restoring RUNX3 expression in RUNX1-ETO cells does not alleviate the suppression of erythroid colony formation imposed by RUNX1-ETO.

The effects of RUNX1-ETO alone and in combination with RUNX3 expression on myeloid colony forming ability were also examined. Again as expected, under clonal conditions, RUNX1-ETO-expressing cells formed 3.6 ± 1.3 -fold less myeloid colonies when compared to control cells ($p=0.051$, Figure 4-21A) (Tonks *et al.* 2004). A similar trend was observed in HSPC expressing both RUNX1-ETO and RUNX3, with cells exhibiting 4.5 ± 2.3 -fold significantly lower colony forming ability compared to controls (Figure 4-21B). Taken together, these results indicate that RUNX3 overexpression was not able to revert the suppression of myeloid colony formation in RUNX1-ETO-expressing HSPC. Therefore, under clonal conditions, RUNX3 overexpression failed to rescue the survival of RUNX1-ETO-transduced myeloid cells.

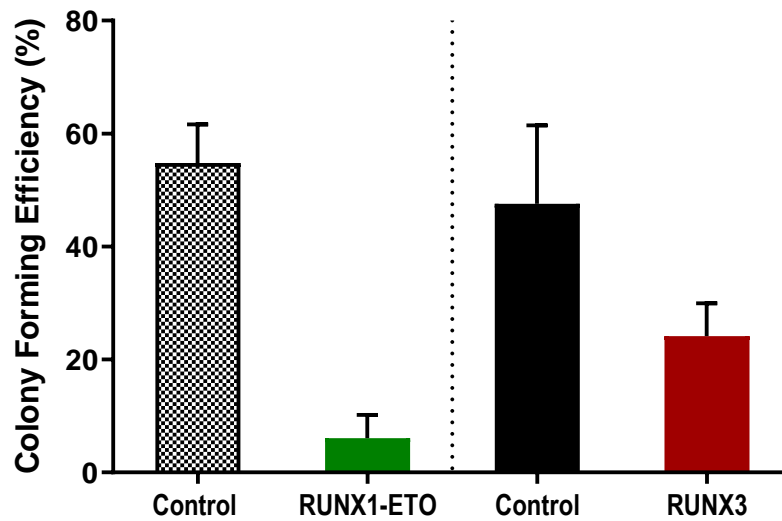
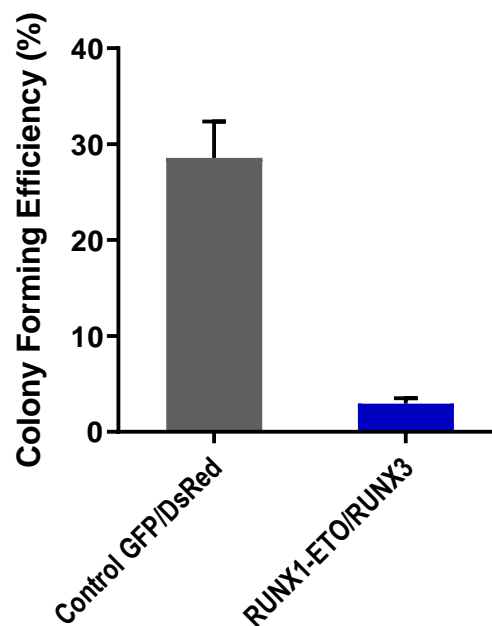
A**B**

Figure 4-20 – Expression of RUNX1-ETO as a single abnormality or in combination with RUNX3 suppresses erythroid colony formation.

(A) Summary data of colony forming efficiency for control and RUNX1-ETO cells, as well as control and RUNX3 cells following 7 days of growth in liquid culture containing IL-3, SCF, IL-6 and EPO. Data indicate mean \pm 1SD of two independent experiments. RUNX1-ETO cells and respective control were sorted for GFP positivity, whereas RUNX3 cells and respective controls were sorted for DsRed positivity on day 3 by FACS. **(B)** Colony forming efficiency of control and RUNX1-ETO and RUNX3-expressing cells following 7 days of growth in similar conditions. Data indicate mean \pm 1SD of two independent experiments. Double cultures were sorted for GFP and DsRed positivity on day 3 by FACS. In addition, all cultures were enriched for primitive erythroid cells (CD13⁻) on day 3 by FACS.

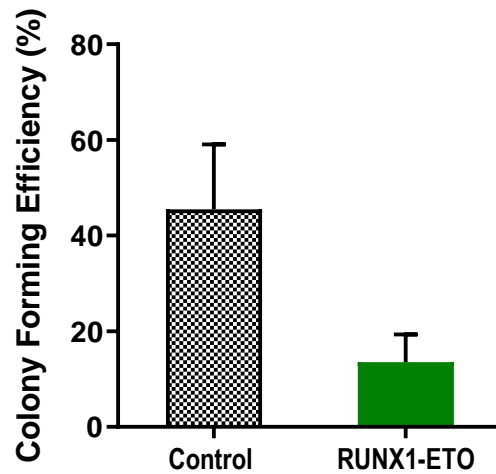
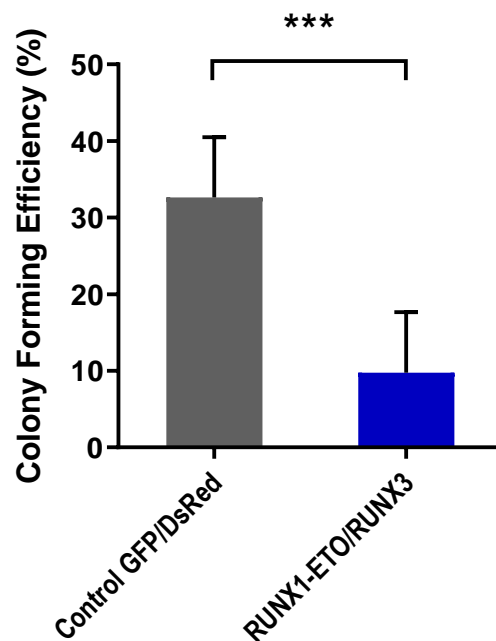
A**B**

Figure 4-21 – Expression of RUNX1-ETO as a single abnormality or in combination with RUNX3 inhibits myeloid colony formation.

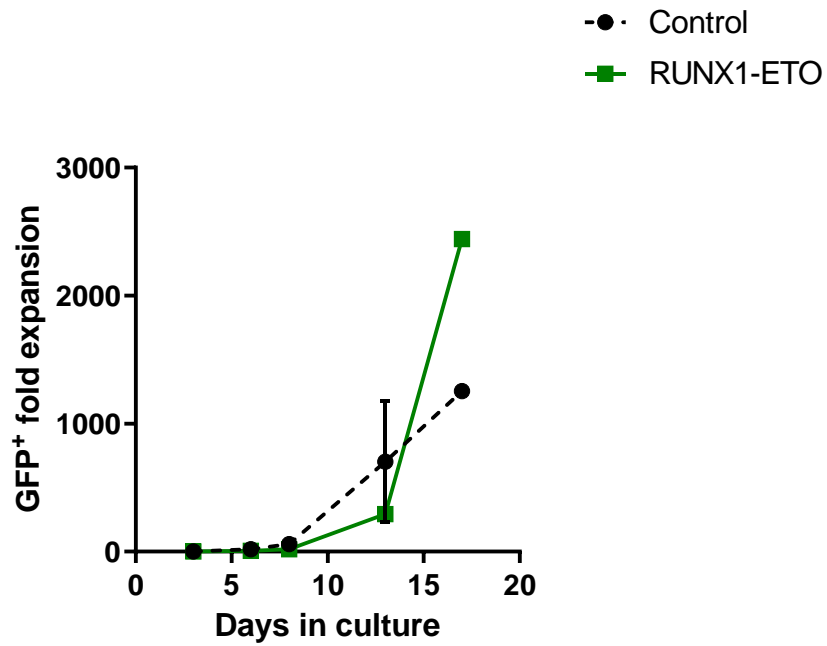
(A) Colony forming efficiency of control and RUNX1-ETO-expressing cells following 7 days of growth in liquid culture containing IL-3, SCF, G-CSF and GM-CSF. Cultures were sorted for GFP positivity on day 3 by FACS. Data indicate mean \pm 1SD of three independent experiments. **(B)** Colony forming efficiency of control and RUNX1-ETO and RUNX3-expressing cells following 7 days of growth in similar conditions. Cultures were sorted for GFP and DsRed positivity on day 3 by FACS. Data indicate mean \pm 1SD of three independent experiments. Significant difference of RUNX1-ETO and RUNX3-expressing cells from controls was analysed by paired t test, *** $p < 0.001$.

4.3.5.4 RUNX3 overexpression did not rescue the myeloid growth and differentiation of RUNX1-ETO-expressing cells

In order to study the effects of RUNX3 overexpression on the growth inhibition induced by RUNX1-ETO in HSPC, double transduced cells were cultured for 13 days. A similar gating strategy was used for these studies as shown previously in Figure 4-6. As shown in Figure 4-22A, no significant effects were observed in the myeloid growth of cells expressing RUNX1-ETO as a single abnormality or in combination with RUNX3 overexpression. As shown in Figure 4-22B, double transduced cells grew similarly to controls. Furthermore, no significant changes were observed in lineage-specific growth of either RUNX1-ETO alone or RUNX1-ETO/RUNX3 cultures (Figure 4-23), with the exception of granulocytic growth, an effect previously reported (Tonks *et al.* 2007). RUNX1-ETO-expressing granulocytic cells grew 1.9 ± 0.2 -fold slower than controls on day 8 of culture (Figure 4-23E). This growth inhibition was not sustained in double transduced granulocytic cells (Figure 4-23F). Overall, these data do not suggest that RUNX3 overexpression rescues the growth of RUNX1-ETO-expressing myeloid cells.

To determine whether RUNX3 overexpression could revert the abnormal phenotype of RUNX1-ETO-expressing cells during myeloid development, a similar approach was used as above (4.3.3.3). Expression of RUNX1-ETO did not induce significant changes in the proportion of erythroid, monocytic and granulocytic cells in culture compared to controls (Figure 4-24). A similar trend was observed for double transduced cells. In terms of monocytic differentiation, RUNX1-ETO did not induce significant changes in CD11b expression over time (Figure 4-25A). Conversely, a significant downregulation of CD11b expression by 1.7 ± 0.3 -fold was observed in RUNX1-ETO and RUNX3-expressing cells on day 6 compared to controls (Figure 4-25B). Furthermore, a significant downregulation of CD14 expression by 1.7 ± 0.4 -fold was identified on day 8 in RUNX1-ETO-expressing cells compared to control cells (Figure 4-25C). Interestingly, RUNX1-ETO and RUNX3-expressing cells upregulated CD14 expression similarly to controls over 13 days of development (Figure 4-25D). No changes were observed in CD34 expression over time among all cultures (Figure 4-25E and F). Taken together, these data show that double transduced cells have their granulocytic differentiation suppressed.

A



B

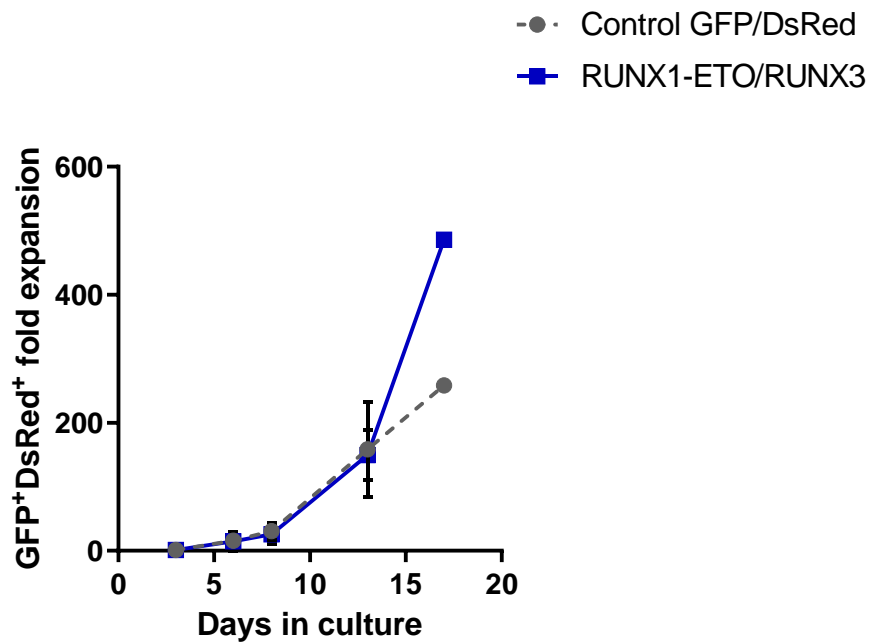


Figure 4-22 – Expression of RUNX1-ETO as a single abnormality or in combination with RUNX3 does not significantly affect the growth of myeloid cells.

(A) Cumulative fold expansion of GFP⁺ control and RUNX1-ETO cells and **(B)** GFP⁺DsRed⁺ control and RUNX1-ETO/RUNX3 cells during myeloid development over 17 days. Data indicate mean \pm 1SD of three independent experiments. Counts on day 17 are representative.

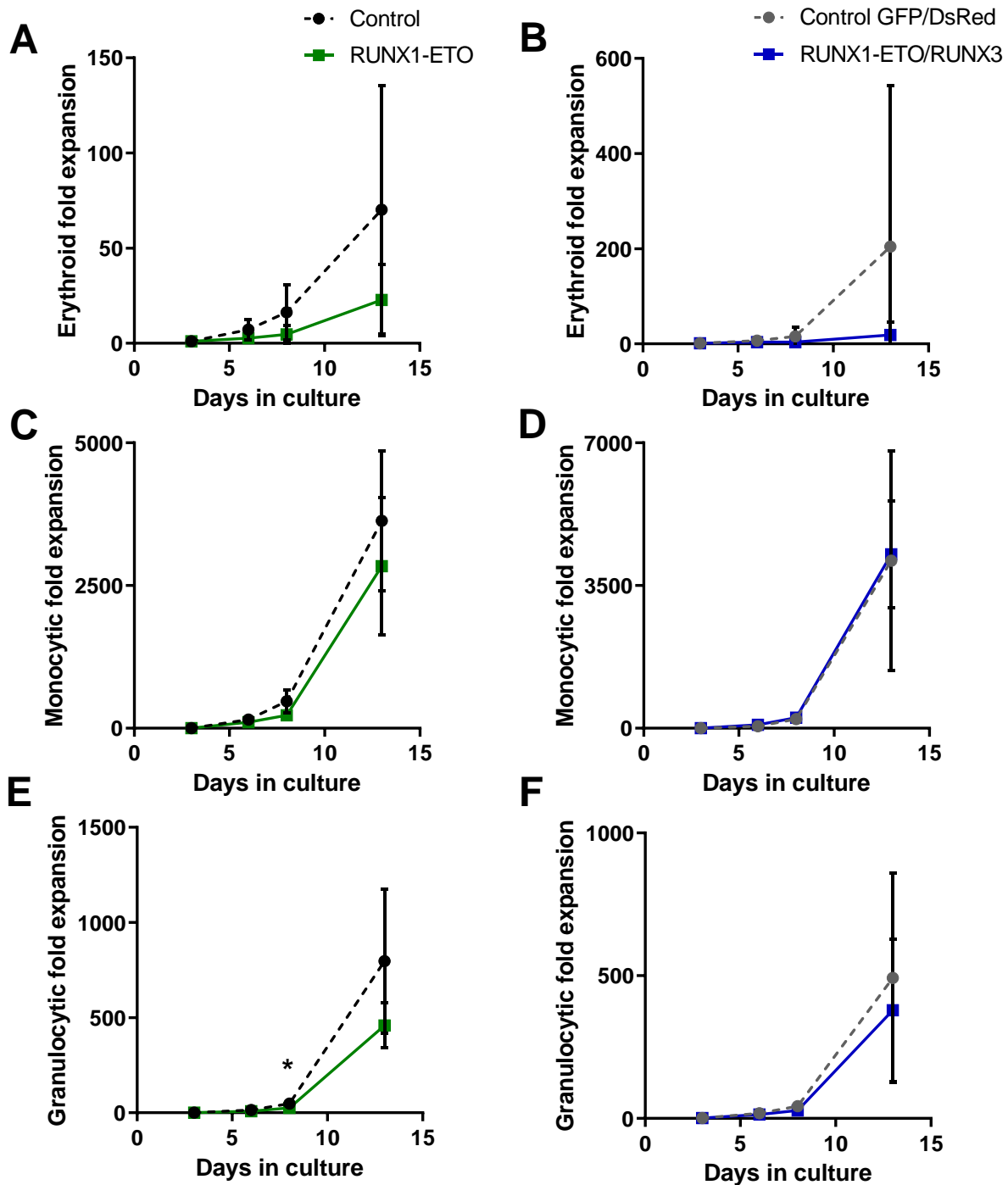


Figure 4-23 – Expression of RUNX1-ETO as a single abnormality or in combination with RUNX3 does not significantly affect the lineage-specific growth of cells.

(A) Cumulative fold expansion of erythroid-committed cells (CD13⁺CD36⁺) for both GFP⁺ control and RUNX1-ETO cells and **(B)** GFP⁺DsRed⁺ control and RUNX1-ETO/RUNX3 cells during myeloid development over 13 days. Data indicate mean \pm 1SD of at least three independent experiments. **(C)** Cumulative fold expansion of monocytic cells (CD13⁺CD36⁺) for both GFP⁺ control and RUNX1-ETO cells and **(D)** GFP⁺DsRed⁺ control and RUNX1-ETO/RUNX3 cells during myeloid development over 13 days. Data indicate mean \pm 1SD of at least three independent experiments. **(E)** Cumulative fold expansion of granulocytic-committed cells (CD13⁺CD36⁻) for both GFP⁺ control and RUNX1-ETO cells and **(F)** GFP⁺DsRed⁺ control and RUNX1-ETO/RUNX3 cells during myeloid development over 13 days. Data indicate mean \pm 1SD of at least three independent experiments. Significant difference of RUNX1-ETO-expressing cells vs controls was analysed by paired t test, * $p < 0.05$.

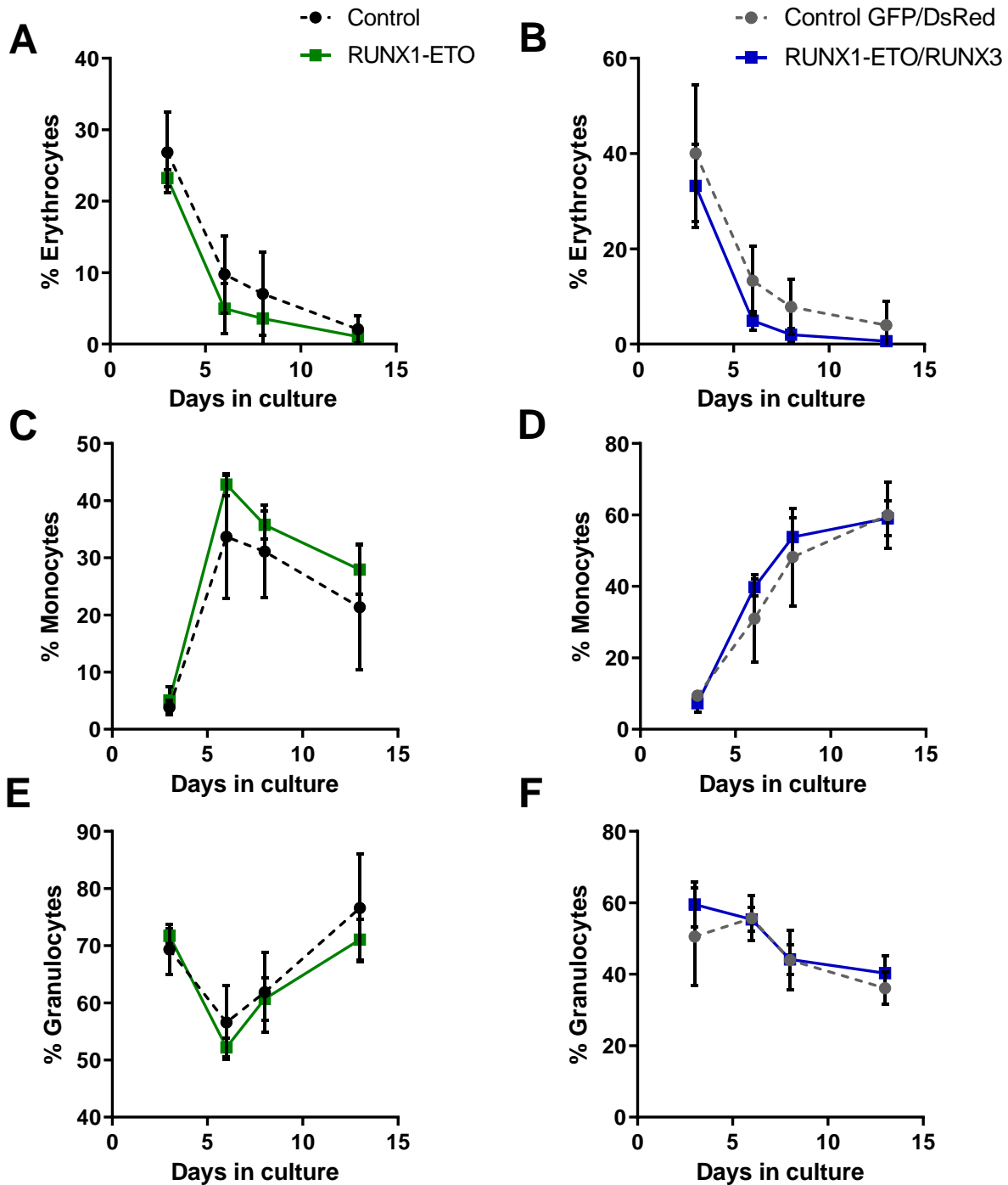


Figure 4-24 – RUNX1-ETO itself and in combination with RUNX3 overexpression did not impact significantly the lineage balance in HSPC.

(A) Summary data of erythroid cells (CD13⁺CD36⁺) in terms of percentage for both GFP⁺ control and RUNX1-ETO cultures, and **(B)** GFP⁺DsRed⁺ control and RUNX1-ETO/RUNX3 cells during myeloid development over 13 days. Data indicate mean \pm 1SD of at least three independent experiments. **(C)** Summary data of monocytic cells (CD13⁺CD36⁺) in terms of percentage for both GFP⁺ control and RUNX1-ETO cultures, and **(D)** GFP⁺DsRed⁺ control and RUNX1-ETO/RUNX3 cells during myeloid development in the same conditions. Data indicate mean \pm 1SD of at least three independent experiments. **(E)** Summary data of granulocytic cells (CD13⁺CD36⁺) in terms of percentage for both GFP⁺ control and RUNX1-ETO cultures, and **(F)** GFP⁺DsRed⁺ control and RUNX1-ETO/RUNX3 cells during myeloid development in similar conditions. Data indicate mean \pm 1SD of at least three independent experiments.

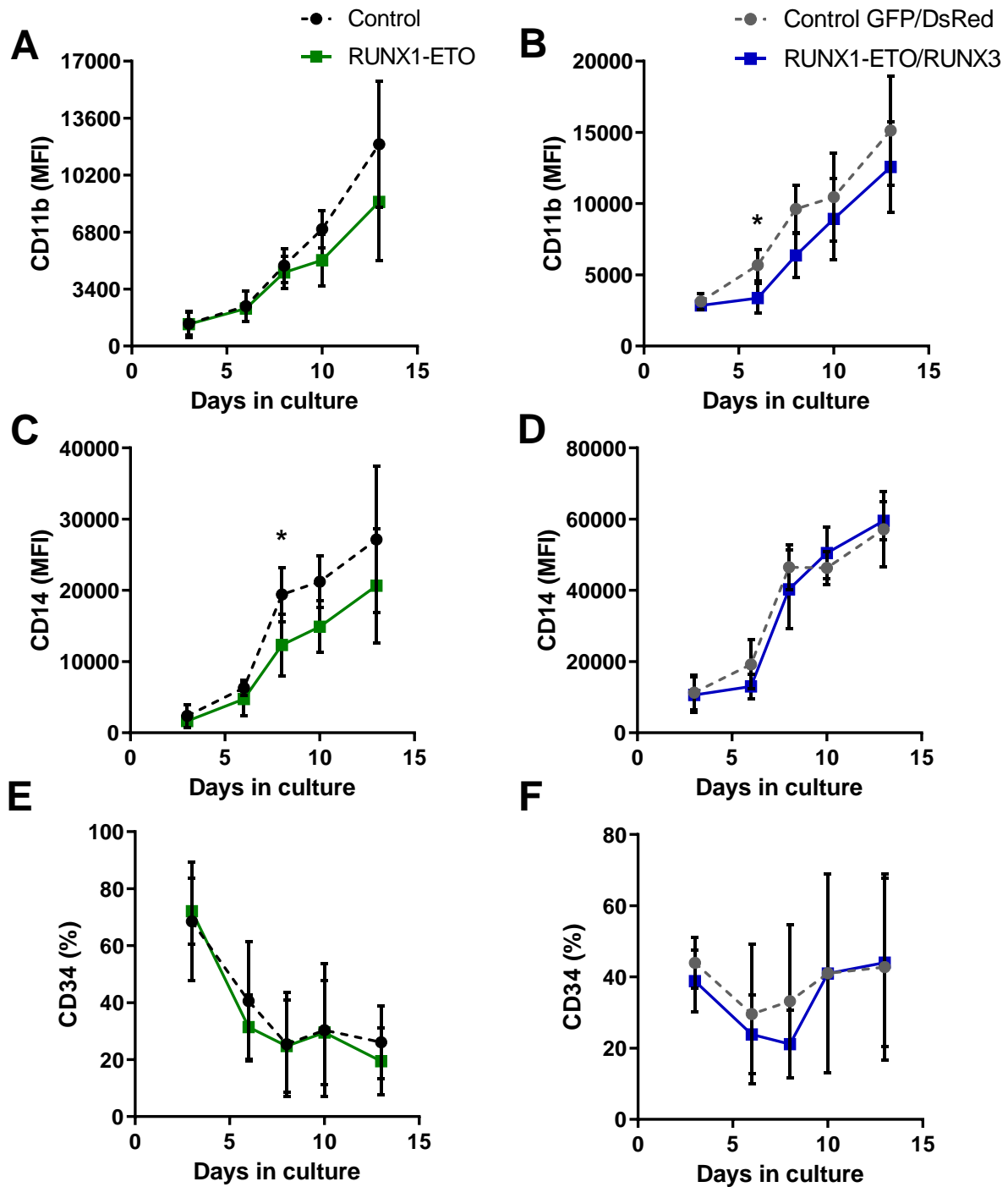


Figure 4-25 – RUNX3 overexpression dysregulates CD11b expression and exhibits normal CD14 upregulation during monocytic development of RUNX1-ETO-expressing cells.

(A) Summary data of CD11b expression in terms of MFI in monocytic-committed cells over time for GFP⁺ control and RUNX1-ETO cultures, and (B) GFP⁺DsRed⁺ control and RUNX1-ETO/RUNX3 cells. Data indicate mean ± 1SD of three independent experiments. Significant difference of RUNX1-ETO/RUNX3 cells vs GFP⁺DsRed⁺ controls was analysed by paired t test, **p*<0.05. (C) Summary data of CD14 expression in MFI for GFP⁺ control and RUNX1-ETO cultures, and (D) GFP⁺DsRed⁺ control and RUNX1-ETO/RUNX3 monocytic cells over time. Data indicate mean ± 1SD of three independent experiments. Significant difference of RUNX1-ETO cells vs GFP⁺ control was analysed by paired t test, **p*<0.05. (E) Summary data of CD34 expression in terms of percentage for monocytic cells in GFP⁺ control and RUNX1-ETO cultures, and (F) GFP⁺DsRed⁺ control and RUNX1-ETO/RUNX3 cells over time. Data indicate mean ± 1SD of three independent experiments.

Regarding granulocytic development, the expected CD11b upregulation was significantly reduced by 1.8 ± 0.1 -fold in RUNX1-ETO cells compared to controls (day 8, [Figure 4-26A](#)). Similarly, co-expression of RUNX3 and RUNX1-ETO led to a significant downregulation of CD11b expression by 2.6 ± 0.6 -fold on the same compared to control cells ([Figure 4-26B](#)). As shown in [Figure 4-26C](#), the expression of the granulocytic marker CD15 was comparable between control and RUNX1-ETO cells. Conversely, restoring RUNX3 expression in RUNX1-ETO cells resulted in a 1.5 ± 0.2 -fold significant reduction of CD15 expression by day 3 ([Figure 4-26D](#)). Furthermore, RUNX1-ETO-expressing cells exhibited a retention of CD34 expression by 1.6 ± 0.3 -fold on day 8 ([Figure 4-26E](#)), whereas double transduced cells downregulated CD34 similarly to controls with no significance observed ([Figure 4-26F](#)). Overall, these findings show that cells co-expressing RUNX1-ETO and RUNX3 have their granulocytic differentiation suppressed.

To support the phenotypic analysis, assessment of morphology was performed. Control cultures were associated primarily with a late and intermediate phase of development characterised by the presence of band/segmented cells and myelocytes/metamyelocytes, respectively ([Figure 4-27A](#)). Conversely, RUNX1-ETO-expressing cultures were predominantly myeloblasts/promyelocytes (early phase) as previously described (Tonks *et al.* 2004). RUNX1-ETO cells in an early phase of development significantly increased by 11.6 ± 5.4 -fold, whereas cells in a late phase decreased by 11.9 ± 5.0 -fold compared to controls ([Figure 4-27B](#)). An imbalance between cells in different developmental stages was also observed for the double transduced culture compared to the respective control. Cultures co-expressing RUNX1-ETO and RUNX3 were predominantly in an early phase of development, with an increase by 4.3 ± 2.8 -fold in myeloblasts and promyelocytes in culture compared to controls. However, no significance was observed in terms of the presence of mature double transduced cells in culture compared to controls, which suggests that RUNX3 overexpression positively affected the morphology of RUNX1-ETO-expressing cells.

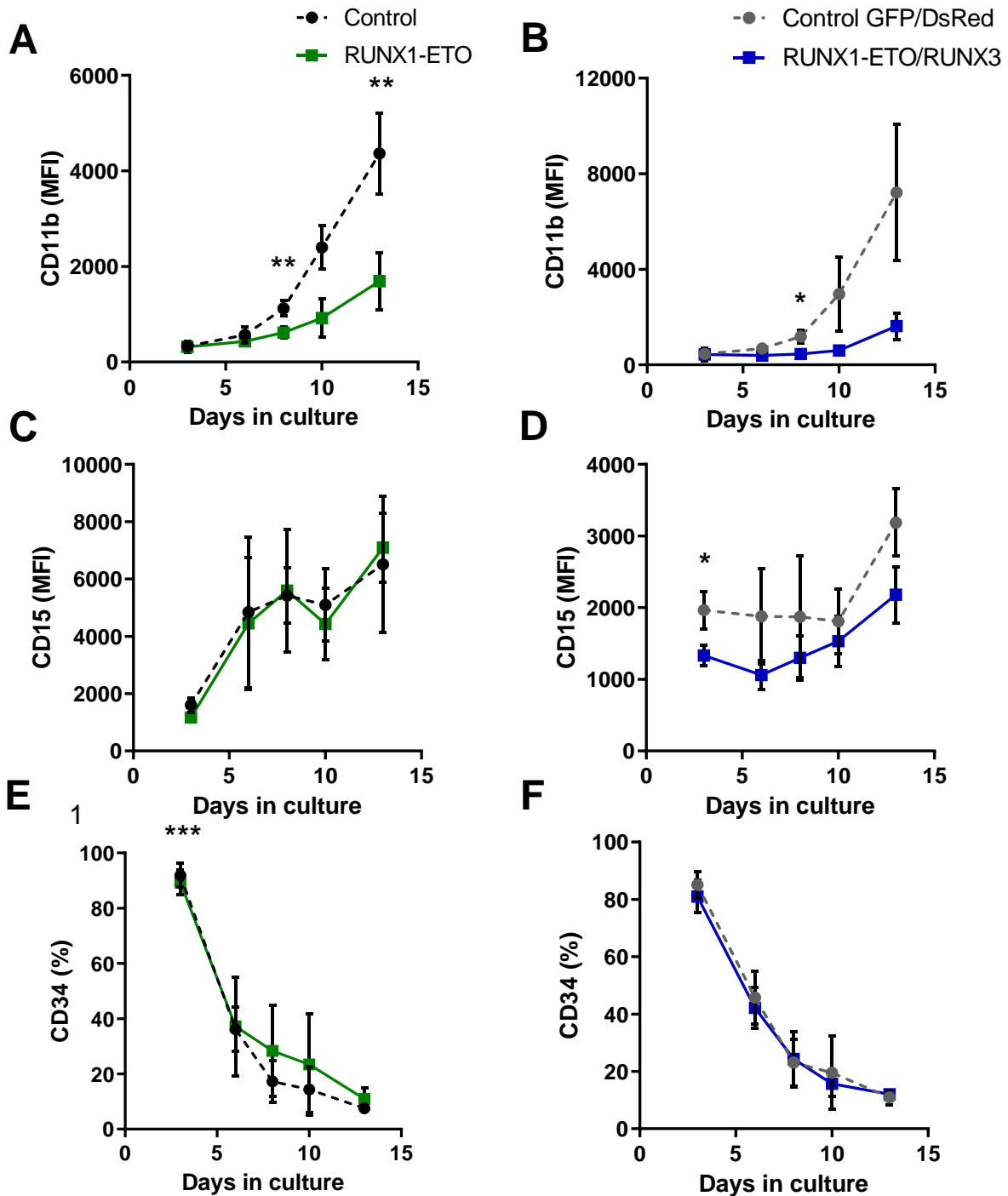


Figure 4-26 – Abnormal granulocytic development observed in cells expressing RUNX1-ETO alone or in combination with RUNX3 overexpression.

(A) Summary data of CD11b expression in terms of MFI in granulocytic cells over time for GFP⁺ control and RUNX1-ETO cultures, and (B) GFP⁺DsRed⁺ control and RUNX1-ETO/RUNX3 cells. Data indicate mean \pm 1SD of three independent experiments. (C) Summary data of CD15 expression in MFI for GFP⁺ control and RUNX1-ETO cultures, and (D) GFP⁺DsRed⁺ control and RUNX1-ETO/RUNX3 granulocytic cells over time. Data indicate mean \pm 1SD of three independent experiments. (E) Summary data of CD34 expression in terms of percentage for granulocytic cells in GFP⁺ control and RUNX1-ETO cultures, and (F) GFP⁺DsRed⁺ control and RUNX1-ETO/RUNX3 cells over time. Data indicate mean \pm 1SD of three independent experiments. Significant difference of RUNX1-ETO cells vs GFP⁺ control, and RUNX1-ETO/RUNX3-expressing cells vs GFP⁺DsRed⁺ controls was analysed by paired t test, * $p < 0.05$, ** $p < 0.01$, *** $p < 0.001$.

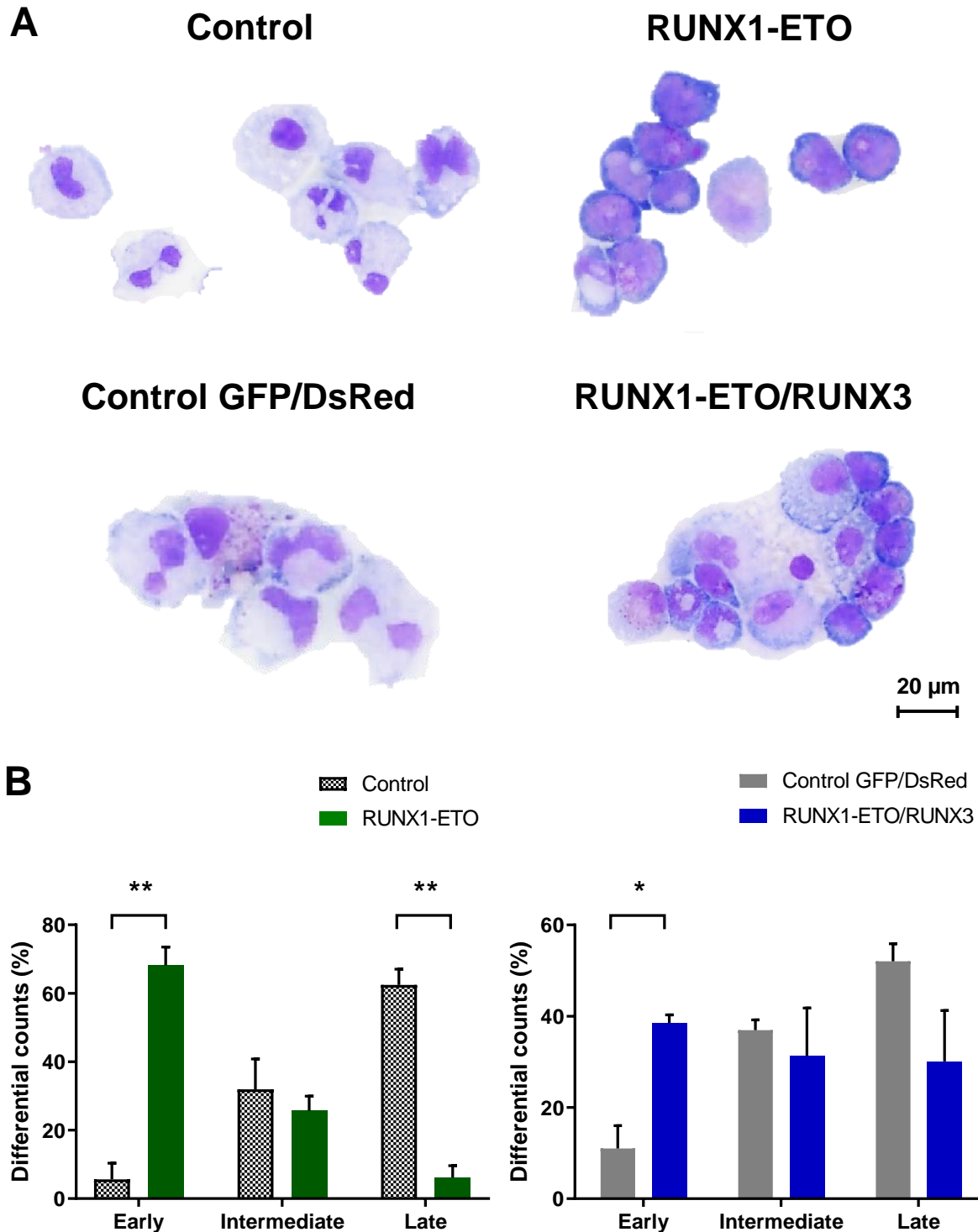


Figure 4-27 – RUNX3 overexpression promotes morphological changes associated with intermediate to later stages of development in RUNX1-ETO cells.

(A) Single and double transduced cells analysed on day 17 of differentiation with May-Grünwald-Giemsa staining. (B) Differential counts for all cultures with morphology categorised into early (myeloblasts/promyelocytes), intermediate (myelocytes/metamyelocytes) and late phase (band/segmented granulocytic cells). Data indicate mean \pm 1SD of three independent experiments. Significant difference of RUNX1-ETO cells vs GFP⁺ control, and RUNX1-ETO/RUNX3-expressing cells vs GFP⁺DsRed⁺ controls was analysed by paired t test, * $p < 0.05$, ** $p < 0.01$

4.4 Discussion and conclusion

RUNX3 has been shown to play a key role in haematopoiesis using different cell models, and its expression has been studied in the context of AML (Levanon *et al.* 2001a; Debernardi *et al.* 2003; Kaley-Zylinska *et al.* 2003; Gutierrez *et al.* 2005; Sun *et al.* 2007; Cheng *et al.* 2008b; Wang *et al.* 2013; Wang *et al.* 2014a; Estecio *et al.* 2015; Balogh *et al.* 2020). However, its role in human haematopoiesis and leukaemia remains poorly understood. Previously, RUNX3 expression was shown to inhibit normal human erythroid development (3.3.2), whereas reduced RUNX3 expression did not significantly affect this process (3.3.3). This study initially sought to determine the expression of RUNX3 in normal myeloid development using publicly available transcriptomic datasets. These data revealed that *RUNX3* is generally downregulated during myelopoiesis (4.3.1). Furthermore, analysis of TCGA AML patient data showed that *RUNX3* is significantly downregulated in prognostically favourable CBF AML and upregulated in patients with complex cytogenetics that are usually associated with a poor clinical outcome (4.3.2). To determine the role of RUNX3 in human myelopoiesis, RUNX3 expression level was modulated in human primary HSPC and its effects on myeloid growth and development were analysed *in vitro* (4.3.3, 4.3.4). Increased RUNX3 expression in HSPC led to an inhibition of both granulocytic and monocytic development, whereas RUNX3 KD failed to significantly impact myeloid growth and development. Considering its downregulation by RUNX1-ETO (Cheng *et al.* 2008b), RUNX3 was overexpressed in RUNX1-ETO cells to determine whether it could revert the developmental block imposed by RUNX1-ETO expression in these cells (Tonks *et al.* 2003; Tonks *et al.* 2004) (4.3.5). However, no significant role for RUNX3 expression in RUNX1-ETO leukaemogenesis was observed. Overall, this study supports a role for RUNX3 in human haematopoiesis and highlights a potential association between RUNX3 overexpression and AML pathogenesis.

To determine the importance of RUNX3 expression during normal human myeloid development, published transcriptomic data was analysed. *RUNX3* mRNA expression is sustained in CB derived HSPC and early stages of myeloid differentiation, but different trends are observed when cells mature into the granulocytic and monocytic lineages (4.3.1). Whereas mature monocytes seem to

upregulate *RUNX3*, cells in different stages of granulocytic differentiation (promyelocytes, myelocytes and band cells) show decreased *RUNX3* expression compared to early progenitors. *RUNX3* overexpression has been shown in both monocytes and macrophages, and its expression was shown to be tightly regulated during differentiation and activation of myeloid cells (Puig-Kroger and Corbi 2006; Puig-Kroger *et al.* 2006). An additional study using HL-60 cells as a model for granulocytic and monocytic differentiation suggested that *RUNX3* might be initially involved in myeloid development but reverts to basal levels during terminal maturation of granulocytes or monocytes (Muller *et al.* 2008). These findings are supported by a recent study showing that *RUNX3* participates in erythroid rather than granulocytic development of human HSPC (Balogh *et al.* 2020). Taken together, these results suggest that *RUNX3* expression has a role in early myeloid differentiation, with its involvement diminishing as cells fully mature into monocytes or granulocytes.

4.4.1 Increased *RUNX3* expression is associated with poor outcome of AML patients

In order to explore the association between *RUNX3* expression and leukaemogenesis, different transcriptomic datasets were analysed (4.3.2). MILE study microarray data (Kohlmann *et al.* 2008; Haferlach *et al.* 2010) shows that *RUNX3* mRNA expression is highly variable between different AML subtypes and could be associated with distinct prognosis. Indeed, *RUNX3* mRNA is significantly downregulated in both t(8;21) and inv(16) AML patients compared to normal human BM. Both abnormalities involve the heterodimeric protein complex CBF and are considered to have relatively good prognosis compared to other leukaemic subtypes (1.2.2). On the other hand, AML patients with complex cytogenetics have significantly higher levels of *RUNX3* and are associated with a poor outcome. RNA-seq data obtained from the TCGA AML dataset confirm the previous trend (Cancer Genome Atlas Research *et al.* 2013). To determine how *RUNX3* expression influences different clinical attributes, AML patients were stratified according to *RUNX3* expression in upper and lower quartiles. OS is significantly affected by *RUNX3* expression, with patients in the upper quartile having a poorer outcome than low *RUNX3* AML patients. Clinically, WBC, risk (both molecular and cytogenetic), PB blast percentage and diagnosis age, among others, are the most significant attributes between both groups.

In terms of risk and cytogenetics, lower expression of *RUNX3* is associated with good prognosis AML cases, which mainly comprise *inv(16)* and *t(8;21)* AML subtypes. Conversely, increased *RUNX3* expression is associated with poor prognosis of AML, which mainly include complex cytogenetic cases. These results are supported by numerous other studies in the literature (Debernardi *et al.* 2003; Gutierrez *et al.* 2005; Sun *et al.* 2007). Cheng *et al.* showed that reduced *RUNX3* expression is associated with better EFS and is overrepresented by *t(8;21)* and *inv(16)* AML patients (Cheng *et al.* 2008b). Most importantly, *RUNX3* downregulation was caused by direct binding of RUNX1-ETO to its promoter, whereas for *inv(16)* cases *RUNX3* downregulation resulted from a cooperation between CBF β -MYH11 and RUNX1 (Cheng *et al.* 2008b) (1.4.2.3). An additional study suggests that *RUNX3* downregulation in *inv(16)* patients is caused by promoter methylation (Estecio *et al.* 2015). Furthermore, this study implies that epigenetic dysregulation of *RUNX3* is likely an important event in CBF leukaemogenesis. *RUNX3* expression was found to be an independent prognostic factor in childhood AML and increased *RUNX3* was associated with worse EFS independent of the *FLT3* mutations status (Estecio *et al.* 2015). Conversely, Lacayo *et al.* found that *RUNX3* overexpression among childhood AML patients with mutated *FLT3* had an inferior outcome (Lacayo *et al.* 2004). Interestingly, *FLT3*-ITD has been found to induce *RUNX3* expression, resulting in Ara-C resistance in leukaemic cells (Damdinsuren *et al.* 2015) though the mechanisms underlying this event are unclear. In addition, repression of *RUNX3* in CBF AML has been associated with a good response to Ara-C treatment (Cheng *et al.* 2008b). Taken together, these studies support *RUNX3* potential as a prognostic marker in AML. Additionally, these results give insight into the close relationship between *RUNX3* expression and AML pathogenesis. Further studies including more patients and a multivariate analysis would help establish whether *RUNX3* is a potential prognostic marker for AML.

4.4.2 RUNX3 overexpression in HSPC inhibits their myeloid growth and development

Considering the association between *RUNX3* expression and poor prognosis of AML patients, the effects of *RUNX3* overexpression on myeloid development of human HSPC were next determined. Following one week of growth and under clonal conditions, *RUNX3* overexpression negatively affected the colony formation capacity

of myeloid cells (4.3.3.1). Previous studies have shown that RUNX1-ETO expression selectively inhibits granulocytic colony formation in human HSPC (Tonks *et al.* 2004). RUNX3 overexpression was previously found to inhibit the formation of erythroid colonies whilst promoting the self-renewal of progenitors (3.3.2.2). Overall, these findings suggest that increased RUNX3 expression negatively affects the survival of cells under clonal conditions.

Having observed abnormalities in the colony formation ability of myeloid cells, this study next sought to determine the effects of RUNX3 overexpression on myeloid growth and development in bulk liquid culture. RUNX3-expressing cells grew slower than controls characterised by a suppression of erythroid growth, supporting previous results (3.3.2), as well as granulocytic growth (4.3.3.2). RNA-seq data of HSPC overexpressing RUNX3 shows a dysregulation in genes enriched for apoptosis and proliferation pathways (5.3.3). For instance, *KIT* mRNA expression was significantly downregulated in RUNX3-transduced cells compared to controls. c-Kit ligand or SCF has been shown previously to enhance the proliferation of both myeloid and lymphoid haematopoietic progenitor cells (Hoffman *et al.* 1993). Furthermore, SCF-KIT pathway is thought to promote survival of progenitors by suppressing apoptosis (Bashamboo *et al.* 2006; Zhang and Lodish 2008). In addition, RNA-seq results revealed a downregulation of *RUNX1* expression, and, to a lesser extent *RUNX2*, by RUNX3 overexpression in HSPC (5.3.4), which can help explain the growth inhibition observed here. Reduction of RUNX1 expression was found to substantially inhibit the growth of both CB derived and AML cells (Goyama *et al.* 2013). In a different setting, cells harbouring a RUNX1 mutation maintain a progenitor phenotype with monocytic characteristics and show repression of only granulocytic genes (Gerritsen *et al.* 2019). These results suggest that RUNX1 mutations primarily affect granulocytic development. Moreover, the suppression of granulocytic growth parallels the growth inhibition imposed by RUNX1-ETO in the granulocytic lineage (Tonks *et al.* 2004). Taken together, increased RUNX3 expression impairs myeloid growth, which could be mainly due to abnormalities within the erythroid and granulocytic lineages.

The growth suppression caused by RUNX3 overexpression in myeloid cells was accompanied by a lineage imbalance (4.3.3.2), as well as an aberrant programme of myeloid differentiation (4.3.3.3). Monopoiesis develops from the monoblast to the circulating monocyte, which is typically characterised by the expression of CD11b,

CD14, CD16, HLA-DR and CD33 (Friedman 2002; Gustafson *et al.* 2015). On the other hand, granulocytes are characterised by CD11b, CD15, CD33 and CD66b (Gustafson *et al.* 2015). RUNX3 significantly downregulated cell surface expression of CD11b and CD14 during monocytic development. Further RNA-seq results support the abnormal phenotype observed for RUNX3-expressing cells (5.3.4). *ITGAM*, also known as CD11b, was the 6th most downregulated by RUNX3 overexpression in HSPC. The close relationship between RUNX3 and CD11b has been previously described in DC using RUNX3-deficient mouse models (Dicken *et al.* 2013). RUNX3 was shown to occupy the genomic loci of *Itgam* and its loss led to increased expression of CD11b in mouse DC. In terms of CD14 expression, RUNX3 has been considered a potential regulator of monocyte differentiation due to its involvement with the TGF- β signalling pathway in DC and its crucial role in the generation of Langerhans cells (Sanchez-Martin *et al.* 2011). Moreover, it was shown that primary blood monocytes secrete the chemokine CXCL12 to modulate differentiation through downregulation of RUNX3, which in turn leads to an increase of CD14 expression (Sanchez-Martin *et al.* 2011). These studies suggest that a precise balance of RUNX3 expression is important during myeloid development.

Regarding granulocytic differentiation, RUNX3 expression similarly inhibited this process by significantly downregulating the expression of CD11b and, to a lesser extent, the granulocytic marker CD15. This abnormal phenotype was accompanied by reduction in granularity in RUNX3-expressing granulocytes at later days, and further supported by morphology assessment of cells (4.3.3.3). RUNX1-ETO has been shown to disrupt myeloid differentiation, delaying the upregulation of CD11b and CD15 in human HSPC (Tonks *et al.* 2004). This process can be restored by silencing this oncogene in t(8;21) AML cell lines (Heidenreich *et al.* 2003). The abnormal differentiation of RUNX3 overexpressing cells could be explained in part by the downregulation of *RUNX1* in these cells (5.3.4). An additional study suggests that RUNX1 acts as a tumour suppressor in CB derived cells by inducing myeloid development, and loss of this differentiation capacity is a common feature of leukaemogenic RUNX1 mutants (Goyama *et al.* 2013). Furthermore, RUNX1 deficiency blocked myeloid differentiation in HSPC and RUNX1-ETO cells. Overall, RUNX3 expression inhibits both monocytic and granulocytic differentiation of cells.

4.4.3 Knockdown of RUNX3 does not impact the myeloid development of HSPC

Given the downregulation of *RUNX3* expression observed in CBF AML patients, and to fully assess its importance in normal human myeloid development, the effects of RUNX3 KD in cell growth and differentiation were further determined. In terms of colony formation ability, no significant changes were observed in RUNX3 KD cells compared to controls (4.3.4). Recently, RUNX3 KD in HSPC was shown to block erythroid colony formation with no relevant effect on myeloid colonies (Balogh *et al.* 2020). Taken together, these data suggest that reduced RUNX3 expression does not affect the survival of myeloid cells under clonal conditions.

In bulk liquid culture, KD of RUNX3 induced a modest reduction in the myeloid growth of cells mainly due to a significant suppression of erythroid growth compared to control cells (4.3.4). Conversely, no significant growth inhibition was observed in RUNX3 KD monocytic and granulocytic cells during their development. RUNX3 KD progenitors cultured in expansion medium supplemented with SCF, IL-3, TPO, and FLT3L preserved normal proliferation and almost all viability (Balogh *et al.* 2020). The same was not observed for progenitors cultured in erythroid medium. Overall, RUNX3 KD in HSPC does not inhibit myeloid growth, nonetheless it shows a clearer impact on erythroid growth. This might be due to a more prominent role for RUNX3 in erythroid development rather than myeloid.

In terms of myeloid development, monocytic and granulocytic cells managed to fully mature with reduced RUNX3 expression (4.3.4). Reduced RUNX3 levels have been associated with enhanced CD11b expression in HSPC and shown to cause minimal changes in granulocytic differentiation measured by CD15 levels (Balogh *et al.* 2020). This study suggested that the retention of myeloid differentiation capacity and GMP markers by RUNX3 KD cells is associated with an additional role for RUNX3 in lineage resolution. Overall, RUNX3 KD did not affect the normal programme of myeloid differentiation of human HSPC. Nevertheless, combined loss of RUNX1 and RUNX3 has been shown to inhibit the maturation of granulocytes at a relatively late stage of development in mice (Wang *et al.* 2014a). Additionally, a blockage in lymphocyte, megakaryocyte and erythrocyte maturation was observed at early stages of development.

4.4.4 RUNX3 overexpression does not rescue the phenotype of RUNX1-ETO-expressing HSPC during myeloid development

Having observed a downregulation of *RUNX3* expression in t(8;21) AML patient data from TCGA dataset (4.3.2) and in human HSPC expressing RUNX1-ETO as a single abnormality (4.3.5), RUNX3 was overexpressed in RUNX1-ETO HSPC and its effects were further determined. Overexpression of RUNX3 in t(8;21) KASUMI-1 and SKNO-1 cell lines was also attempted, but no interpretable outcomes were obtained (data not shown). Under clonal conditions, RUNX3 expression failed to rescue the erythroid and myeloid colony forming capacity of RUNX1-ETO-expressing HSPC (4.3.5.3). RUNX1-ETO mainly affects the differentiation of granulocytic cells (Tonks *et al.* 2004). In bulk liquid culture, RUNX1-ETO itself induced a significant downregulation of CD11b compared with control cells (4.3.5.4). These abnormalities were sustained in double transduced cells, which suggests that both RUNX1-ETO and RUNX3 are capable of repress the transcription of *ITGAM*. As mentioned previously, CD11b is a putative target of RUNX3 and it was one of the most downregulated genes by RUNX3 overexpression in HSPC (Dicken *et al.* 2013). Morphological examination suggest that RUNX1-ETO-expressing cells were retained in an early stage of development characterised by the increased presence of myeloblasts and promyelocytes in culture compared to controls. Similar results were previously reported (Tonks *et al.* 2004). Similarly, double transduced cells were associated with immature morphological features compared to control cells. However, there was an increase in the proportion of cells in a later stage of development in these cultures compared to the effect of RUNX1-ETO alone. Recently, cyclin D2 was identified as an important element of RUNX1-ETO leukaemia (Martinez-Soria *et al.* 2018). KD of cyclin D2 in t(8;21) cells inhibited their proliferation and induced a cell cycle arrest; however, it failed to alleviate the myeloid differentiation block imposed by RUNX1-ETO (Martinez-Soria *et al.* 2018). Taken together, these findings do not support a rescue of phenotypic changes by RUNX3 in RUNX1-ETO-expressing cells during myeloid development.

Although RUNX3 overexpression did not induce the myeloid differentiation of RUNX1-ETO-expressing cells, the functional requirement of RUNX3 in t(8;21) AML should be further addressed by KD studies. For instance, *ZEB1* was recently shown to be downregulated in AML, and its KO in *MLL-AF9* and *Meis1a/Hoxa9*-driven AML mouse models led to a rapid disease progression (Almotiri *et al.* 2021). The

association between RUNX3 and the RUNX1/RUNX1-ETO complex has been previously identified (Mandoli *et al.* 2016), as well as its specific downregulation in CBF AML (1.4.2.3). Therefore, further reduction of RUNX3 expression in RUNX1-ETO HSPC could provide novel insights regarding its functional and potential tumour suppressive role in CBF AML.

In conclusion, this study shows that increased expression of RUNX3 in human HSPC inhibits normal myeloid development. A similar result was not observed in RUNX3 KD cells, which supports a possible role in leukaemogenesis. In addition, restoration of RUNX3 expression in RUNX1-ETO-expressing HSPC does not support a significant role for RUNX3 in RUNX1-ETO leukaemogenesis. Nevertheless, it is important to consider possible caveats associated with this study, including the fact that RUNX3 was overexpressed at supra-physiological levels in these cells. Further studies are needed to elucidate the mechanisms associated with RUNX3 expression and AML pathogenesis.

5 RUNX3 Overexpression Dysregulates the Human Haematopoietic Progenitor Cells Transcriptome

5.1 Introduction

RUNX3 is one of three mammalian Runt-domain TFs and was initially cloned based on its similarity to RUNX1 (Levanon *et al.* 1994). Overexpression and KO studies in mice have demonstrated a role for RUNX3 in the normal function of several important organs (Levanon *et al.* 2001a; Levanon *et al.* 2002; Kaley-Zylinska *et al.* 2003; Yoshida *et al.* 2004; Kohu *et al.* 2005; Bauer *et al.* 2015; Wang *et al.* 2018a) (1.4). Amongst the many impacts arising from loss of RUNX3 expression are a variety of defects in the adaptive and innate immune system. These include impaired proliferation and differentiation of activated cytotoxic CD8⁺ T cells, helper Th1 cells and NK cells (Djuretic *et al.* 2007; Cruz-Guilloty *et al.* 2009; Levanon *et al.* 2014). Besides its important role in controlling immunity and inflammation, RUNX3 is also essential for the maintenance of HSC in adults (Wang and Stifani 2017) (1.4.1). Both RUNX1 and RUNX3 are able to directly inhibit cell cycle progression as well as maintain stem cells in their quiescent state, thereby influencing the HSC population size (Wang and Stifani 2017). A recent study showed that increased RUNX3 expression suppressed the expression of RUNX1, compromising haematopoiesis and leading to the development of MDS in mice (Yokomizo-Nakano *et al.* 2020). RUNX3 expression has also been shown to inhibit both erythroid and myeloid development of human HSPC (3.3.2, 4.3.3). Further, abrogation of erythropoiesis by loss of RUNX3 was shown previously in human HSPC with RUNX3 controlling key erythroid TFs, such as *KLF1* and *GATA1* (Balogh *et al.* 2020). Taken together, these studies show that dysregulation of RUNX3 expression can contribute to impaired development of haematopoietic cells.

The role of RUNX3 in tumour initiation and progression is ambiguous, with RUNX3 exhibiting both tumour-promoting and suppressive behaviours in a context-dependent manner (Li *et al.* 2002; Cheng *et al.* 2008b; Tsunematsu *et al.* 2009; Lee *et al.* 2011; Huang *et al.* 2012a; Lee *et al.* 2013) (1.4.2). As demonstrated in 4.3.2, *RUNX3* mRNA expression is variable in AML. FLT3-ITD AML which is associated with

poor prognosis, induces *RUNX3* mRNA expression resulting in Ara-C resistance (Damdinsuren *et al.* 2015). Furthermore, increased *RUNX3* mRNA expression was associated with a shortened EFS and OS among childhood AML patients (Cheng *et al.* 2008b) (1.3.5). Interestingly, *RUNX3* mRNA expression was found to be repressed in the prognostically favourable CBF-AML subgroup (harbouring the fusion proteins, RUNX1-ETO or CBF β -MYH11), which are associated with good responses to Ara-C treatment (Cheng *et al.* 2008b).

Understanding the involvement of RUNX in leukaemia development and the balance between their tumour suppressive and oncogenic functions may lead to new therapeutic possibilities (Ito *et al.* 2015). RUNX TFs interact with essential signalling pathways, including apoptosis, hypoxia, inflammation, DNA damage responses, stem cell functions, Wnt, TGF- β , BMP, Notch and RAS-ERK signalling, amongst others (reviewed by (Ito *et al.* 2015)). Nonetheless, RUNX3 is the least studied member of its family and its regulatory function has been mainly explored in mice models and/or different cellular contexts other than haematopoietic cells. RUNX3 overexpression was shown to inhibit human haematopoietic development *in vitro* (3.3.2, 4.3.3) and is associated with poor clinical outcome of AML patients (4.3.2). Therefore, this Chapter aims to identify the transcriptional changes induced by RUNX3 overexpression in human HSPC.

5.2 Aims and objectives

This study hypothesises that overexpression of RUNX3 leads to transcriptomic changes that may affect haematopoietic growth and development. The main aim of this Chapter is to analyse the transcriptomic profile of cells overexpressing RUNX3 and identify dysregulated pathways influencing haematopoiesis and other related processes. This Chapter has the following objectives:

- **Determine the transcriptomic changes associated with RUNX3 overexpression in haematopoietic cells**

Total RNA will be extracted from human HSPC overexpressing RUNX3 and controls (expressing GFP alone). Following Qc assessment of RNA integrity, samples will be shipped to Novogene for library preparation and RNA-seq.

Sequencing data will be analysed to establish DE genes between control and RUNX3 overexpressing HSPC.

- **Determine which pathways and networks are dysregulated by RUNX3 overexpression in HSPC**

Using the DE gene list (above), an enrichment analysis will be performed to establish the transcriptional dysregulation imposed by RUNX3 ectopic expression in human HSPC. For this analysis, MetaCore™, IPA® and KEGG databases will be used.

- **Establish the genes regulated by RUNX3 in HSPC including a comparative analysis of data above with publicly available mRNA expression datasets**

To further understand the genes and pathways dysregulated by RUNX3 expression in HSPC, a comparative analysis will be performed between the RNA-seq data obtained in this study and publicly available datasets. These datasets include RNA-seq data from RUNX3-deficient human HSPC and erythroid progenitors (Balogh *et al.* 2020), and microarray data from RUNX1-ETO-expressing human HSPC (Tonks *et al.* 2007).

5.3 Results

5.3.1 Generation of HSPC overexpressing RUNX3 for RNA-seq analysis

Overexpression of RUNX3 in human HSPC was shown to inhibit both erythroid and myeloid differentiation (3.3.2, 4.3.3). To determine the transcriptional changes associated with increased RUNX3 expression, RNA-seq of RUNX3 transduced HSPC was performed. The experimental design for this study is shown in Figure 5-1. Following infection, transduced cultures were enriched for GFP expression by FACS (>98% GFP⁺) and subsequently processed for total RNA extraction (Figure 5-2). Table 5-1 shows each sample with a 260/280 ratio ~2.0 indicating RNA with no significant contamination by proteins, phenol or other contaminants that absorb near 280 nm. To support this, RNA concentration and integrity were also assessed using Agilent 2100 Bioanalyzer (Schroeder *et al.* 2006). All RNA samples were of high quality represented by a RIN of 10 (Table 5-1).

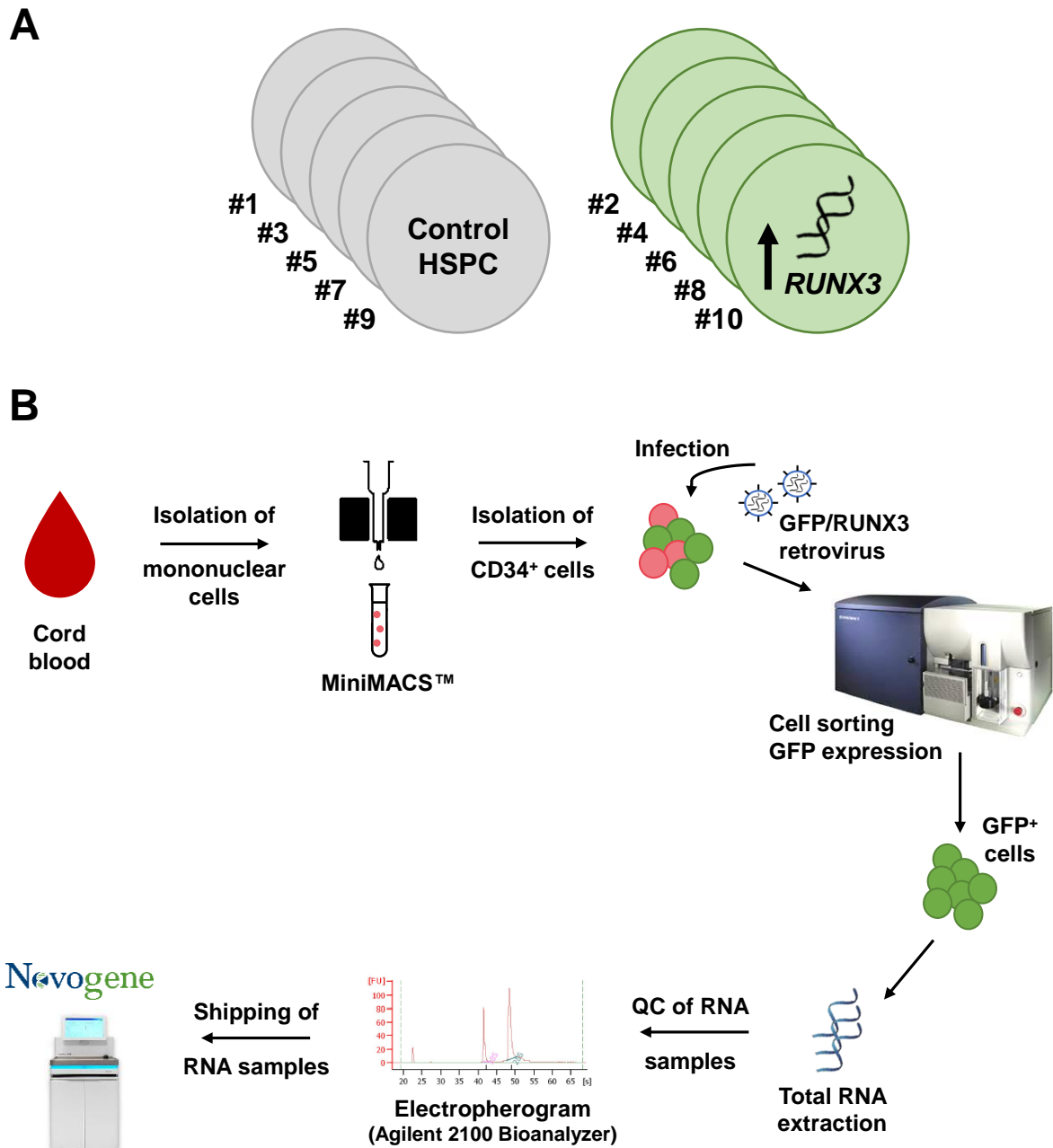


Figure 5-1 – Experimental design of RNA-seq analysis of transcriptional changes associated with RUNX3 overexpression in HSPC.

(A) Control and RUNX3 HSPC (5 independent experiments; samples #1 to #10) were analysed by RNA-seq as in (B). **(B)** CB derived HSPC were isolated using the MiniMACS™ magnetic sorting system for CD34 positivity and subsequently infected with control (PINCO GFP) or RUNX3 GFP retrovirus (as described in 2.6.3). Following enrichment for GFP expression by FACS, total RNA was extracted using the RNeasy Plus Mini Kit and RNA integrity was assessed using Agilent 2100 Bioanalyzer. Samples with a RIN above 8 were deemed to be high quality and shipped to Novogene for RNA-seq.

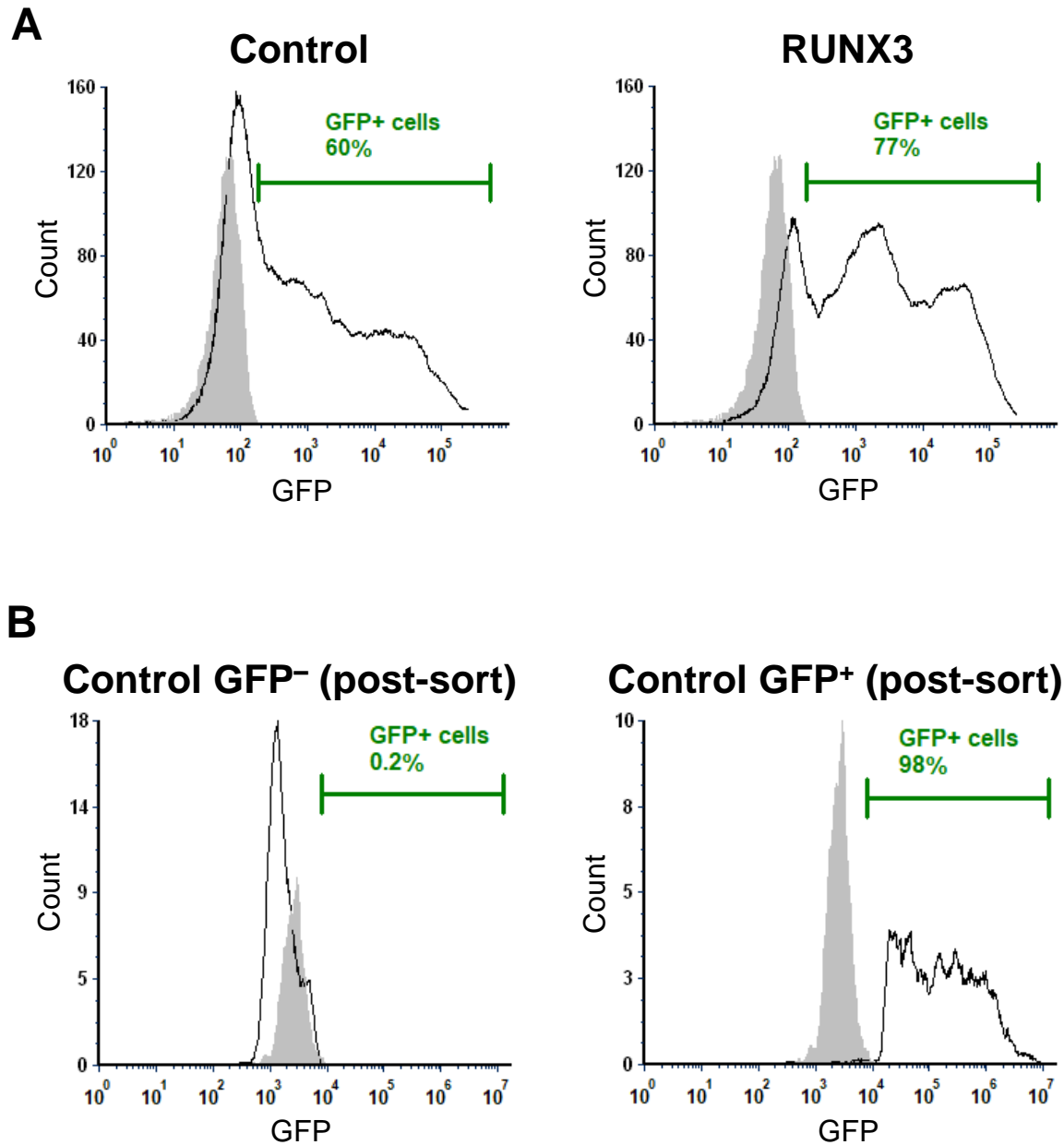


Figure 5-2 – Successful expression and enrichment of GFP in human HSPC.

(A) Representative flow cytometric histograms of GFP expression for control and RUNX3 infected cells (pre-sorted cultures day 3). GFP⁺ gate delimits the sorted population and was defined using mock infected control cells (GFP⁻). Data obtained using BD FACSAria™ II cytometer. **(B)** Representative histograms for control culture post-sorting for GFP⁻ and GFP⁺ cells. Data obtained using BD Accuri™ C6 Plus cytometer. Mock HSPC – grey; Transduced HSPC – black.

Table 5-1 – QC assessment of RNA samples.

Summary data of five independent experiments (control vs RUNX3-expressing HSPC) showing RNA concentration, purity, and RIN. Data was obtained using NanoDrop™ spectrophotometer and Agilent 2100 Bioanalyzer. N – independent experimental number; RIN – RNA Integrity Number; QC – Quality control. Example densitometry plots and electropherograms generated using Agilent 2100 Bioanalyzer and are represented in [Appendix 1](#).

Sample #	Condition	N	NanoDrop™			Agilent 2100 Bioanalyzer (Cardiff)		Novogene				
			RNA (ng/μL)	A260/A280	A260/A230	RNA (ng/μL)	RIN	RNA (ng/μL)	Volume (μL)	Total amount (μg)	RIN	QC Result
1	Control	1	120.1	2.09	1.75	156	10	54	18	0.97	10	Pass
2	RUNX3		159.9	2.09	1.78	185	10	45	18	0.81	10	Pass
3	Control	2	106.2	2.10	1.61	155	10	67	18	1.21	10	Pass
4	RUNX3		178.3	2.02	1.95	208	10	53	18	0.95	10	Pass
5	Control	3	102.1	2.07	1.81	119	10	59	18	1.06	10	Pass
6	RUNX3		138.8	2.10	1.59	164	10	69	18	1.24	10	Pass
7	Control	4	57.4	2.01	1.93	65	10	52	19	0.99	9.8	Pass
8	RUNX3		65.2	2.09	1.98	84	10	56	18	1.01	10	Pass
9	Control	5	60.7	2.05	1.63	80	10	54	18	0.97	9.8	Pass
10	RUNX3		88.3	2.10	1.85	113	10	51	18	0.92	10	Pass

Taken together, these data demonstrate that both quantity and quality of total RNA were according to recommendations for downstream sequencing applications.

5.3.2 QC analysis of RNA-seq data and quantification of gene expression

RNA-seq is a high-throughput sequencing technology that combines the aspects of gene discovery and quantification (Conesa *et al.* 2016). RNA-seq data analysis followed five steps: pre-alignment QC, read alignment, quantification of gene expression, QC analysis of the study, and DE gene analysis.

5.3.2.1 Quality control of RNA sequencing and alignment to a reference genome

To assess the overall quality of sequencing, raw reads were analysed using R software. Examples of QC plots for a control sample (sample #1) are shown in [Figure 5-3](#). A summary of the pre-alignment QC and filtering process of raw reads is shown in [Table 5-2](#). Control and *RUNX3* RNA samples generated more than 20 million (M) raw reads. More than 93% of bases were assigned a Q score of 30 for all samples, suggesting that the probability of a correct base call is 99.9% ([Table 5-2](#)). All RNA samples had a similar GC content of approximately 48%, which corresponds to the expected %GC for humans (Romiguier *et al.* 2010). Taken together, these results suggest that library preparation and sequencing of samples were successful and high-quality data was produced for downstream analysis.

Following pre-alignment QC of raw reads, a mapping step was necessary to perform alignments of reads to a reference genome. Reads from each sample were mainly exonic (>96%), and only these reads were considered informative for downstream analysis (data not shown). An overview of mapping status for all aligned samples is shown in [Table 5-3](#). More than 96% of reads from each sample was successfully mapped to the reference genome. Moreover, most of these reads mapped uniquely to the genome and not to multiple locations. Overall, the alignment step was successful for all samples.

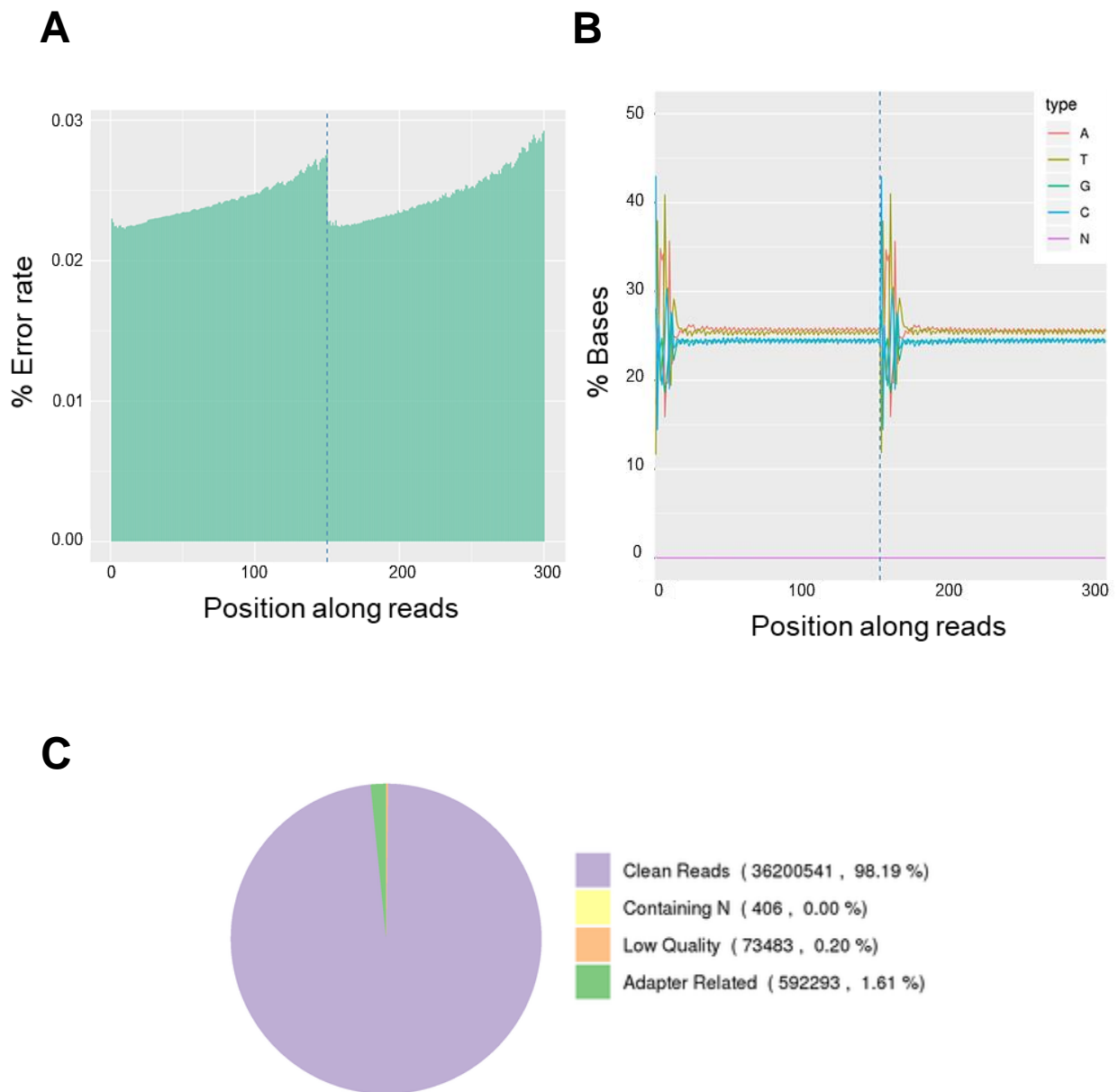


Figure 5-3 – Pre-alignment QC and filtering of raw reads for a control RNA sample.

(A) Representative plot of error base distribution along each sequencing read for control (Sample #1). **(B)** Representative plot describing the percentage of each base per read for control 1 sample. Each base is represented by a different colour. A – Adenine; T –Thymine; G – Guanine; C – Cytosine; N – Unknown base. **(C)** Representative pie chart of different raw reads classes for sample #1. Raw reads are classified in clean reads, reads containing uncertain nucleotides (N), low quality reads and reads with adapter contamination. Only clean reads are used for downstream analysis.

Table 5-2 – Pre-alignment quality control and filtering of raw reads for control and RUNX3 RNA samples.

Summary data of pre-alignment QC and filtering of raw reads following the sequencing process from five independent experiments (control vs RUNX3 overexpression in HSPC). N – independent experimental number; Raw reads – The original read counts; Clean Reads – Number of reads after filtering; Error rate – Average sequencing error rate calculated by Qphred = $-10\log_{10}(e)$; Q20 – Percentages of bases whose correct base recognition rates are greater than 99% in total bases; Q30 – Percentages of bases whose correct base recognition rates are greater than 99.9% in total bases; GC content – Percentages of G and C in total bases.

Sample #	Condition	N	Raw reads	Clean reads	Error rate (%)	Q20 (%)	Q30 (%)	GC content (%)
1	Control	1	36866723	36200541	0.02	98.19	94.71	48.8
2	RUNX3		27382265	26899743	0.03	97.85	93.94	48.62
3	Control	2	30492731	29917692	0.03	97.60	93.44	48.82
4	RUNX3		28256123	27795916	0.03	97.71	93.64	48.88
5	Control	3	37996460	37332931	0.03	97.73	93.69	48.94
6	RUNX3		24754387	24271004	0.03	97.56	93.33	49.04
7	Control	4	26070810	25564030	0.03	97.62	93.45	48.70
8	RUNX3		28333713	27853512	0.03	97.60	93.40	48.79
9	Control	5	34710508	34144813	0.03	97.73	93.68	48.74
10	RUNX3		26630049	26210326	0.03	97.87	93.99	48.88

Table 5-3 – Alignment status and QC of control and RUNX3 RNA samples against a human reference genome.

Summary data of alignment results and QC parameters of control and RUNX3 samples against hg19 human reference genome. N – independent experimental number; Total reads – Total number of filtered reads (clean data); Total mapped – Total number of reads mapped to the reference genome; Multiple mapped – Number of reads mapped to multiple sites in the reference genome; Uniquely mapped – Number of reads mapped to single locations in the reference genome. Clean reads were aligned to GRCh37 (hg19, UCSC version) human reference genome using HISAT2 alignment programme.

Sample #	Condition	N	Total reads	Total mapped	Multi mapped	Uniquely mapped
1	Control	1	72401082	70348316 (97.16%)	1902493 (2.63%)	68445823 (94.54%)
2	RUNX3		53799486	52189544 (97.01%)	1373751 (2.55%)	50815793 (94.45%)
3	Control	2	59835384	57931902 (96.82%)	1562663 (2.61%)	56369239 (94.21%)
4	RUNX3		55591832	53928114 (97.01%)	1482248 (2.67%)	52445866 (94.34%)
5	Control	3	74665862	72327561 (96.87%)	2042808 (2.74%)	70284753 (94.13%)
6	RUNX3		48542008	46928673 (96.68%)	1271049 (2.62%)	45657624 (94.06%)
7	Control	4	51128060	49485080 (96.79%)	1316289 (2.57%)	48168791 (94.21%)
8	RUNX3		55707024	54002812 (96.94%)	1446733 (2.60%)	52556079 (94.34%)
9	Control	5	68289626	66283436 (97.06%)	1792099 (2.62%)	64491337 (94.44%)
10	RUNX3		52420652	50908611 (97.12%)	1333061 (2.54%)	49575550 (94.57%)

5.3.2.2 Quantification of gene expression in control and RUNX3-expressing HSPC

Having aligned the raw reads to a reference genome and assessed alignment quality (5.3.2.1), gene expression levels were quantified using the HTSeq package (2.8.3). Table 5-4 summarises the number and percentage of genes with different gene expression levels across all samples. Approximately 74% of genes are below 1 FPKM, representing genes that are likely to be by-products of biological or experimental noise. The smaller percentage of highly expressed genes correspond to the functional transcriptome of HSPC. These results are also represented in terms of FPKM distribution using diagrams and violin plots in Figure 5-4A and B. Data indicate that there was a similar gene expression distribution between control and RUNX3 overexpression samples for all biological replicates.

5.3.3 DE analysis determines the transcriptional dysregulation imposed by RUNX3 overexpression in human HSPC

5.3.3.1 Assessment of RNA-seq data variability and relationships

An examination of sample relations can expose the inherent variability of the study. To investigate sample relationships, Principal Component Analysis (PCA) and hierarchical clustering methods were used. Using PCA, Figure 5-5 shows that 'biological replicate' is the dominant factor separating gene expression differences rather than experimental condition (e.g. group: control vs RUNX3). However, there are differences between control and RUNX3-expressing cells. This analysis is supported by hierarchical clustering (Figure 5-6) where samples cluster with the 'replicate' rather than the experimental condition. Taken together, these data suggest that the variation between replicates is bigger than the variation caused by RUNX3 overexpression in each paired sample and this should be an important consideration in statistical analyses.

Table 5-4 – Distribution of gene expression levels among samples.

Summary data of gene expression levels represented by FPKM for control and RUNX3 samples stratified according to interval of expression value. Gene expression was measured using FPKM normalisation method, which removes biases such as gene length and sequencing depth (Conesa *et al.* 2016). N – independent experimental number; 0-1 – Interval of expression levels between 0 and 1 FPKM; 1-3 – Interval of expression levels between 1 and 3 FPKM; 3-15 – Interval of expression levels between 3 and 15 FPKM; 15-60 – Interval of expression levels between 15 and 60 FPKM; >60 – Interval of expression levels above 60 FPKM.

Sample #	Condition	N	0-1 FPKM	1-3 FPKM	3-15 FPKM	15-60 FPKM	>60 FPKM
1	Control	1	35806 (74.34%)	1917 (3.98%)	3726 (7.74%)	4163 (8.64%)	2550 (5.29%)
2	RUNX3		35840 (74.42%)	1939 (4.03%)	3680 (7.64%)	4139 (8.59%)	2564 (5.32%)
3	Control	2	35959 (74.66%)	2006 (4.17%)	3795 (7.88%)	3958 (8.22%)	2444 (5.07%)
4	RUNX3		36024 (74.8%)	1987 (4.13%)	3796 (7.88%)	3881 (8.06%)	2474 (5.14%)
5	Control	3	35853 (74.44%)	1954 (4.06%)	3971 (8.25%)	3942 (8.18%)	2442 (5.07%)
6	RUNX3		35879 (74.5%)	1969 (4.09%)	3848 (7.99%)	3995 (8.29%)	2471 (5.13%)
7	Control	4	35896 (74.53%)	1953 (4.06%)	3743 (7.77%)	4102 (8.52%)	2468 (5.12%)
8	RUNX3		35998 (74.74%)	1937 (4.02%)	3649 (7.58%)	4060 (8.43%)	2518 (5.23%)
9	Control	5	35885 (74.51%)	1969 (4.09%)	3773 (7.83%)	4076 (8.46%)	2459 (5.11%)
10	RUNX3		35846 (74.43%)	1970 (4.09%)	3771 (7.83%)	4071 (8.45%)	2504 (5.2%)

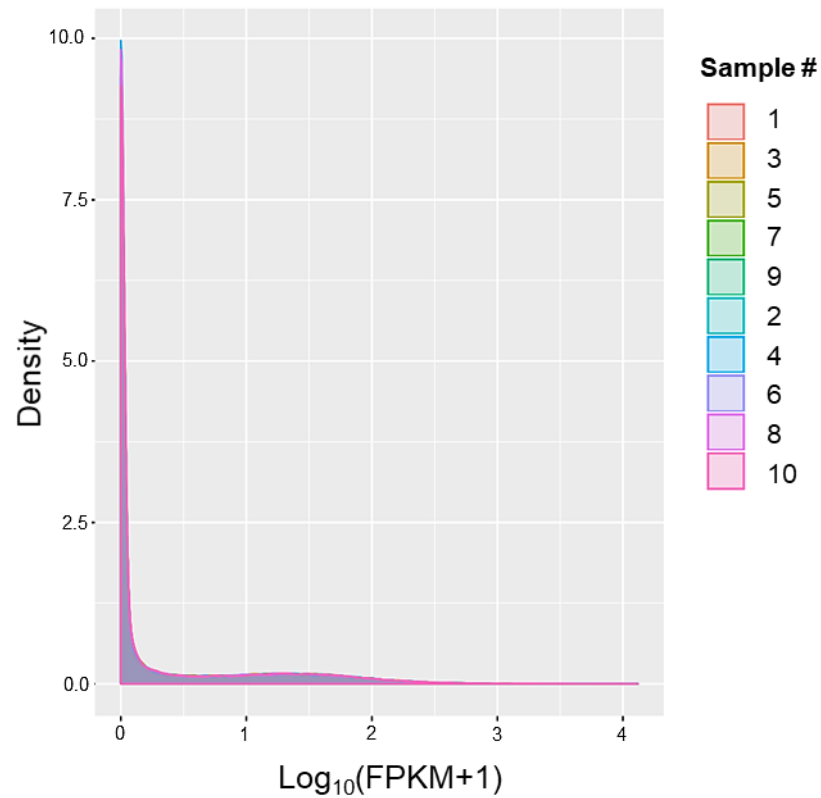
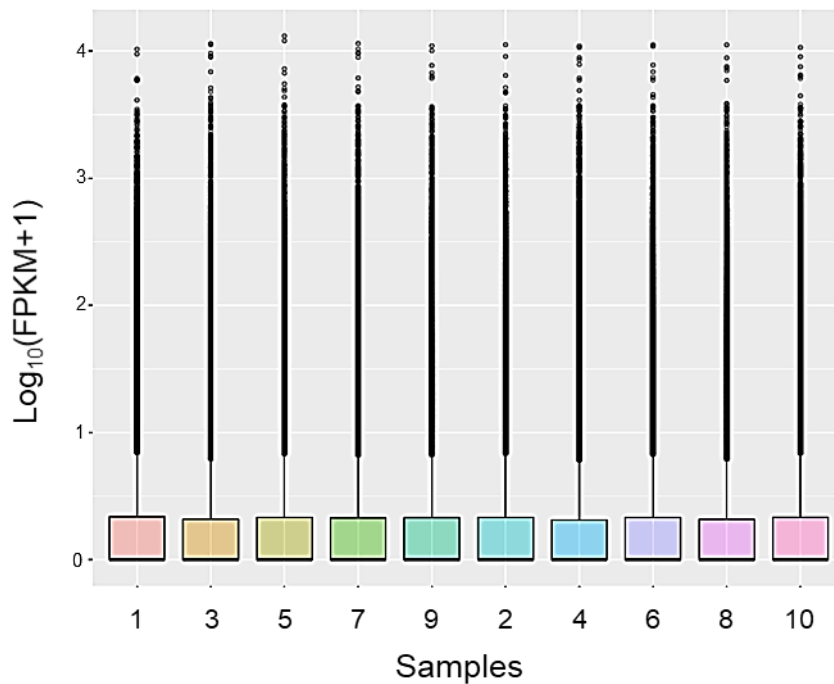
A**B**

Figure 5-4 – Analysis of global gene expression among samples.

Distribution of gene expression levels in FPKM among samples. **(A)** Representative plot of FPKM density distribution for control and RUNX3 biological replicate samples. **(B)** Representative box plot describing the different sample FPKM distributions. Sample # and label is described in Table 5-4. Samples #1, 3, 5, 7 and 9 – Control HSPC; Samples #2, 4, 6, 8, 10 – RUNX3-expressing HSPC.

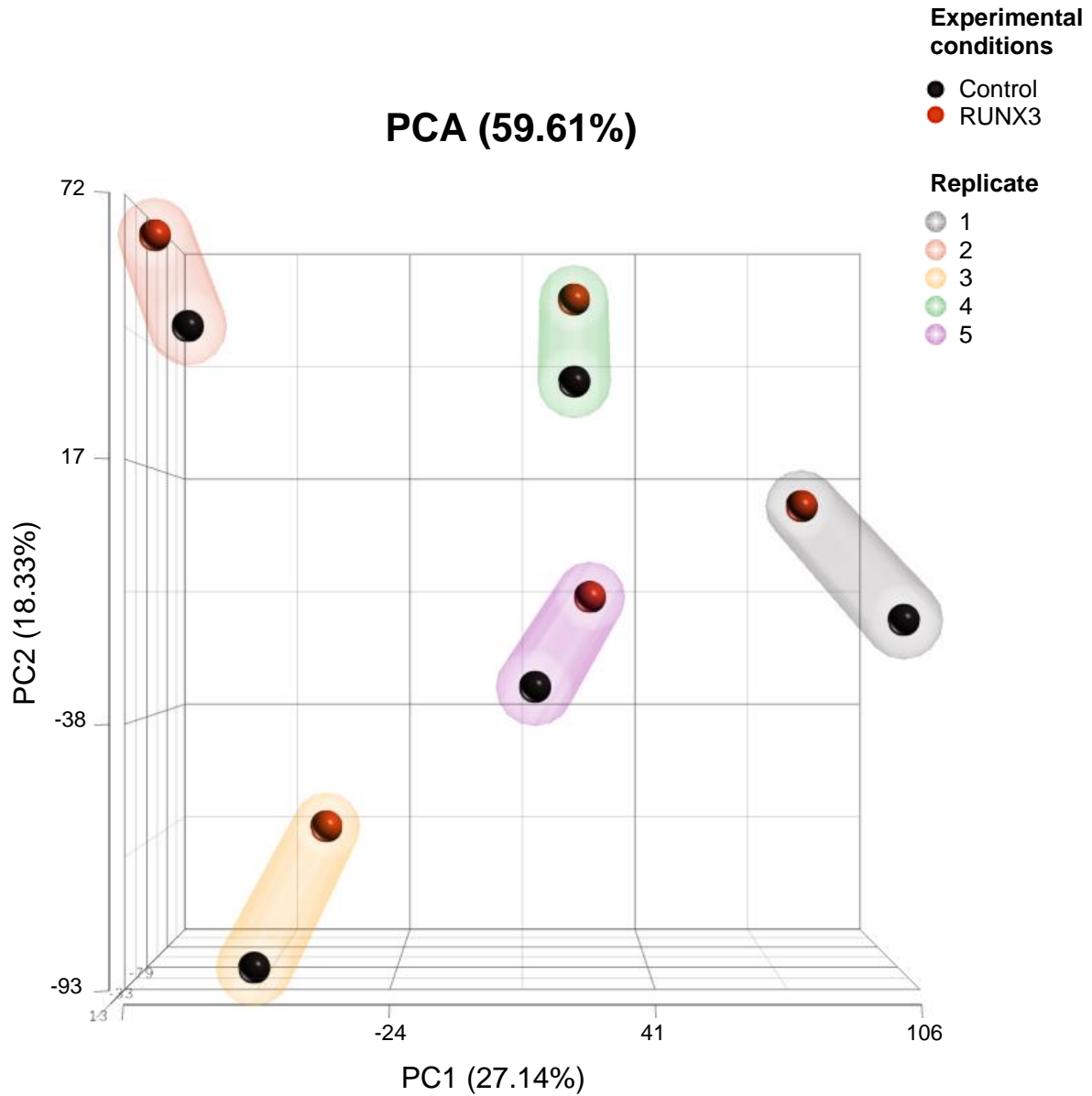


Figure 5-5 – Three-dimensional PCA of control and RUNX3 RNA-seq data.

PCA plot representing PC1 vs PC2 of control and RUNX3 human HSPC biological replicates. Percentages indicate the variation between samples. PCA plot generated following read quantification using the Partek® E/M algorithm.

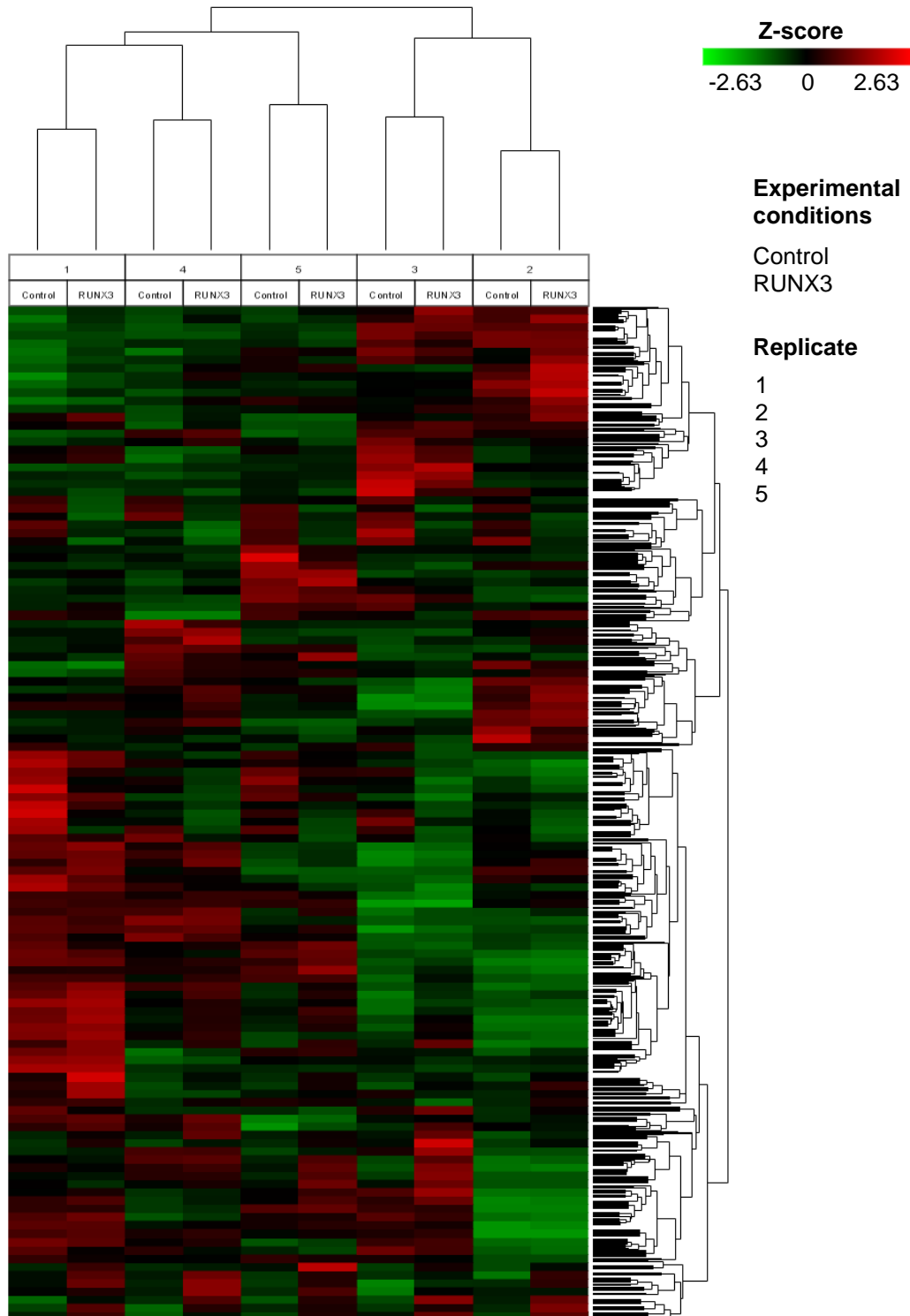


Figure 5-6 – Hierarchical clustering of control and RUNX3 RNA-seq data.

Heat map of control and RUNX3-expressing HSPC biological replicates samples. Columns represent sample number (defined by experimental condition and replicate number) and rows represent genes. Colours are based on z-score standardised expression values (green – low expression; red – high expression). Z-score hierarchical clustering of samples and genes was performed using the average linkage for cluster distance metric and the Pearson correlation for point distance metric. Dendrogram trees show the hierarchy of clusters for both samples and genes. Hierarchical clustering heat map generated using the Partek® Flow® algorithm.

5.3.3.2 *RUNX3 is successfully overexpressed in human HSPC*

The ectopic expression of *RUNX3* mRNA in HSPC was further validated using the RNA-seq data. As shown in [Figure 5-7](#), *RUNX3* expression was 4.1 ± 1.1 -fold significantly higher in *RUNX3* transduced HSPC compared to control cells. Increased *RUNX3* mRNA expression in HSPC was previously confirmed by qRT-PCR ([3.3.2](#)). These results demonstrate that *RUNX3* mRNA was successfully overexpressed in HSPC and further validates the experimental model for downstream RNA-seq analysis.

5.3.3.3 *RUNX3 overexpression favours transcriptional repression and disrupts cell communication and immunity related processes in human HSPC*

To identify DE genes as result of increased *RUNX3* expression in human HSPC, DESeq2 package was used. Overexpression of *RUNX3* in normal human HSPC resulted in 607 DE genes when compared to control; 154 genes were upregulated, and 453 genes were downregulated compared to control ([Figure 5-8](#)). The top 10 dysregulated genes are shown in [Table 5-5](#). Downregulated genes are primarily involved in key cell signalling and metabolic processes in HSPC. A more detailed summary table showing logarithmic fold change (\log_2FC), p-values and adjusted p-values (*padj*) for each DE gene can be found in [Appendix 2](#).

Increased expression of *RUNX3* in HSPC upregulated *KLRB1* (NKR-P1A or CD161), a cell surface protein involved in NK function (Kurioka *et al.* 2018), as well as *PCSK5* (PC5), a protein essential for cleavage of protein precursors generating active products such as growth factors and hormones, among others (Essalmani *et al.* 2008). Examples of downregulated genes include *PDPK1* (PDK1), a master kinase in the phosphoinositide 3-kinase (PI3K)/Akt pathway playing essential roles in cell growth, metabolism, proliferation, and survival (Hinton *et al.* 2004; Baracho *et al.* 2014); *C5AR1* (C5A receptor or CD88), a complement system receptor important for immunomodulatory responses and expressed in several haematopoietic cells (Ricklin *et al.* 2016; Lubbers *et al.* 2017); and *ITGAM* (CD11b or CR3), involved in cellular adhesion, migration and inflammatory responses (Springer 1990; Han *et al.* 2010; Kumar *et al.* 2012; Ling *et al.* 2014).

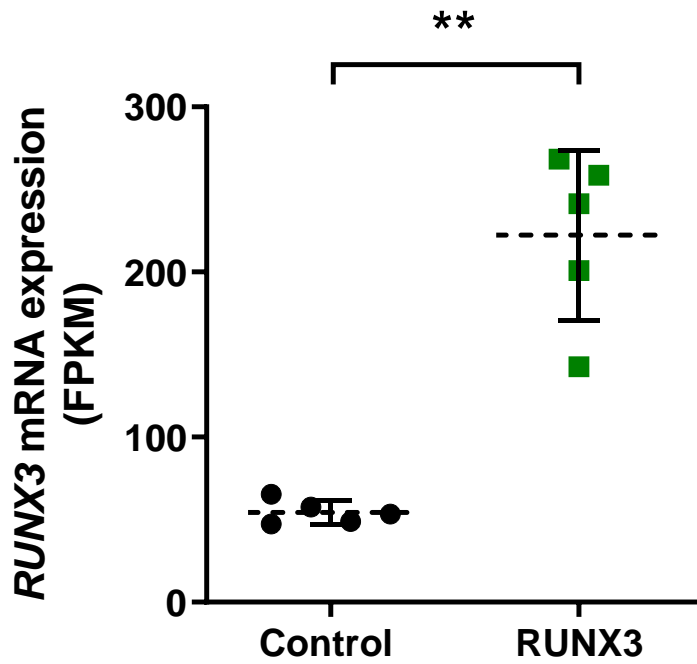


Figure 5-7 – *RUNX3* mRNA is overexpressed in human HSPC cells.

Summary data of *RUNX3* mRNA expression (FPKM) for control and *RUNX3* overexpressing HSPC obtained using the HTSeq package. Dotted line indicates mean \pm 1SD of five independent experiments. Significant difference of *RUNX3* overexpressing cells compared to controls was analysed by paired t-test, ** $p < 0.01$.

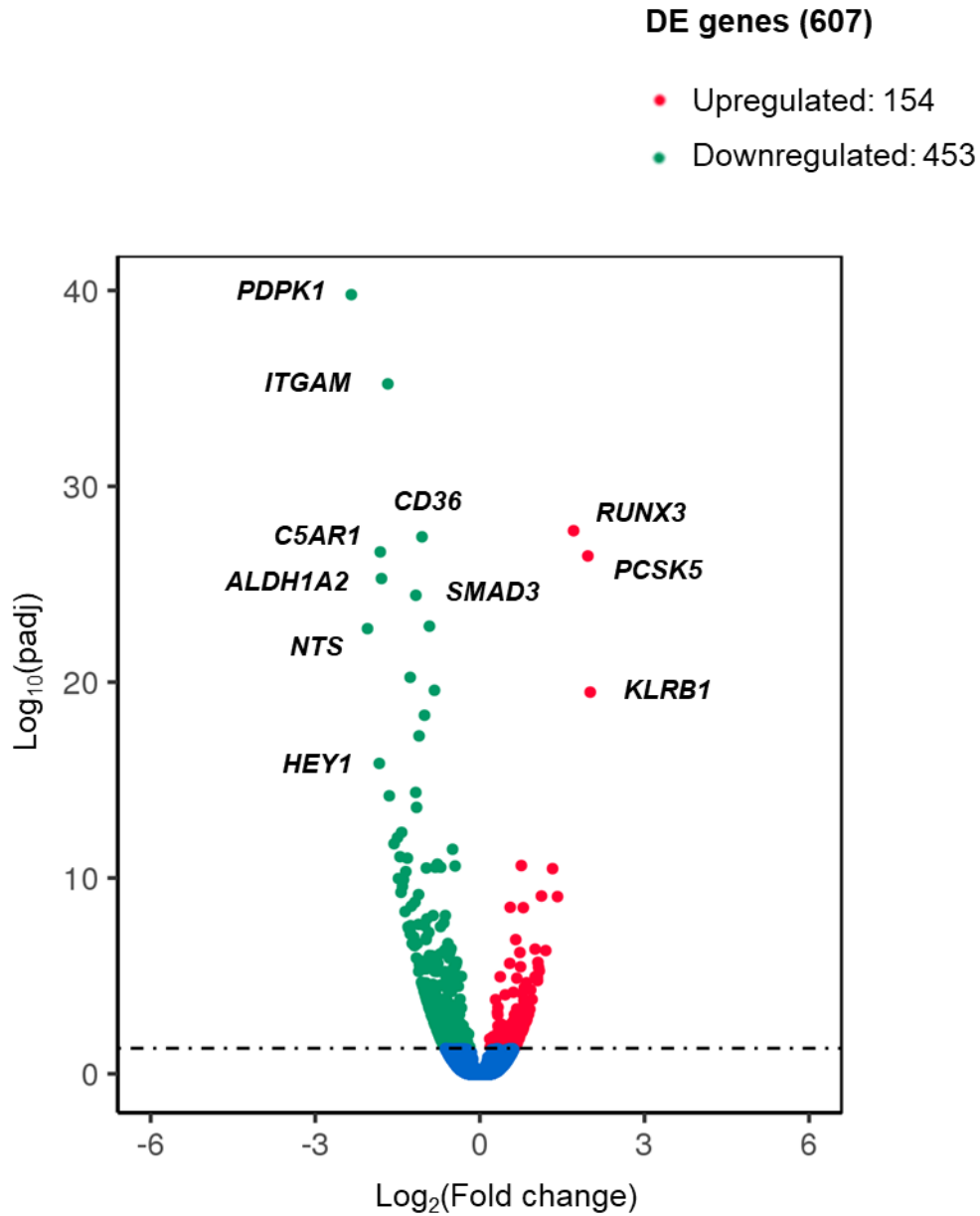


Figure 5-8 – RUNX3 overexpression induces transcriptional dysregulation in human HSPC.

Volcano plot identifying DE genes between control and RUNX3 HSPC (five independent experiments). $\text{padj} < 0.05$ and $\log_2\text{Fold Change} > 1$ were used as threshold. Statistically significantly up- and downregulated genes are highlighted in red and green, respectively. Genes that were not DE between control and RUNX3 samples are highlighted in blue.

Table 5-5 – Top 10 genes dysregulated by RUNX3 overexpression in human HSPC.

Summary data of the 10 most dysregulated genes in HSPC due to RUNX3 ectopic expression. Values are expressed as the logarithmic (base 2) fold change of differentially expressed genes compared to control with the respective adjusted p-value (padj). A negative \log_2FC value represents downregulation (green shade), whereas a positive value represents upregulation (red shade) compared to control. Ensembl ID is a unique number assigned to each gene according to the Ensembl database (www.ensembl.org).

Ensembl ID	Gene symbol	Class	Log ₂ FC	padj
ENSG00000140992	<i>PDPK1</i>	Kinase	-2.34	1.63E-40
ENSG00000133636	<i>NTS</i>	Ligand	-2.05	1.85E-23
ENSG00000111796	<i>KLRB1</i>	Receptor	2.01	3.25E-20
ENSG00000099139	<i>PCSK5</i>	Protease	1.97	3.60E-27
ENSG00000164683	<i>HEY1</i>	TF	-1.83	1.42E-16
ENSG00000197405	<i>C5AR1</i>	Receptor	-1.82	2.24E-27
ENSG00000128918	<i>ALDH1A2</i>	Enzyme	-1.79	5.12E-26
ENSG00000020633	<i>RUNX3</i>	TF	1.71	1.85E-28
ENSG00000169896	<i>ITGAM</i>	Receptor	-1.68	5.86E-36
ENSG00000148468	<i>FAM171A1</i>	Protein	-1.65	6.41E-15

Only one TF was present in the top 10 dysregulated genes, *HEY1* (HERP2) a member of the Notch signalling pathway that has been shown to interact with RUNX2 (Sharff *et al.* 2009). Notch signalling has been implicated in diverse functions, such as stem cell maintenance, lineage determination, cell proliferation and apoptosis (reviewed in (Suresh and Irvine 2015)). Despite being considered an oncogenic pathway in a variety of malignancies, a tumour suppressor role for Notch signalling has been recently explored in AML (Kannan *et al.* 2013; Lobry *et al.* 2013; Ye *et al.* 2016). Taken together, overexpression of RUNX3 in HSPC favoured the downregulation of genes, suggesting that RUNX3 has an influential role on human HSPC transcriptome and possibly their function.

To identify enriched biological processes and functions dysregulated by RUNX3, an enrichment analysis for biological pathways was performed using KEGG knowledge database. KEGG is a compilation of manually drawn pathway maps frequently used for enrichment analysis of gene lists (Kanehisa and Goto 2000). [Figure 5-9](#) shows that the most significantly enriched KEGG pathway dysregulated by RUNX3 overexpression involves the 'Haematopoietic cell lineage'. This observation is supported by previous studies ([3.3.2](#), [4.3.3](#)), where increased RUNX3 levels were shown to disrupt the normal development of erythroid and myeloid progenitors in culture. Furthermore, RUNX3 overexpression dysregulated genes involved with cell communication (e.g., 'Chemokine signalling pathway' and 'Cytokine-cytokine receptor interaction'); cell adhesion and movement (e.g., 'Focal adhesion', 'Regulation of actin cytoskeleton'; and 'Cell adhesion molecules'); and immune-related processes (e.g., 'T cell receptor signalling pathway'), amongst others. An enrichment analysis by protein function using MetaCore™ identified 'Receptors' as the main dysregulated protein class, followed by 'Ligands' and 'Kinases' ([Table 5-6](#)).

Overall, these data imply that RUNX3 overexpression disrupts important biological processes in cells, including haematopoiesis, cell communication, and cell adhesion and movement. A significant transcriptional dysregulation of genes encoding receptors by RUNX3 overexpression in HSPC further support these observations.

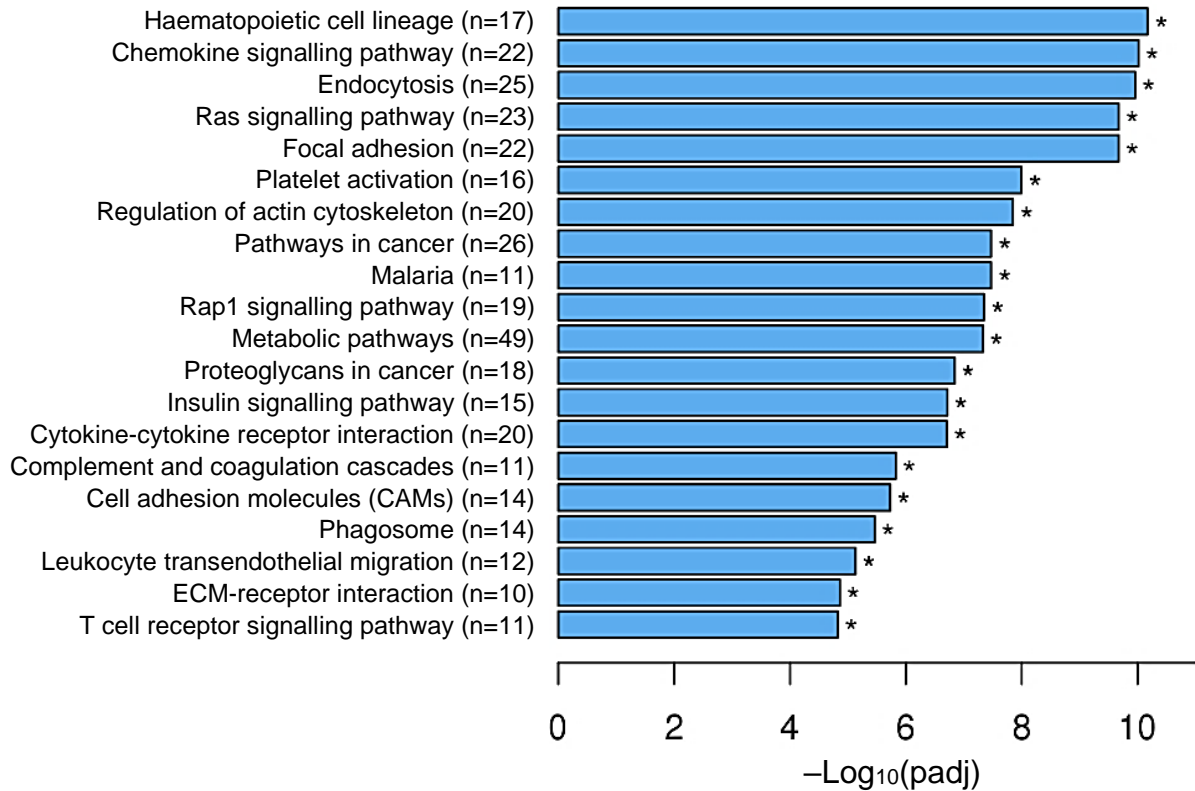


Figure 5-9 – Haematopoiesis is the most significantly dysregulated process in human HSPC overexpressing RUNX3.

Bar plot showing the enrichment scores in terms of negative logarithm of the adjusted p-value (padj) of enriched terms using KEGG Pathway Analysis (www.genome.jp/kegg/pathway.html). KEGG terms with padj < 0.05 are significantly enriched. n indicates the number of DE genes included in each KEGG pathway.

Table 5-6 – Protein function enrichment analysis of genes dysregulated by RUNX3 overexpression in human HSPC.

Summary data of the enrichment analysis performed by protein function using MetaCore™. A cut-off of $\log_2FC > 0.58$ (equating to $FC > 1.5$) and $padj < 0.05$ was applied for this analysis. 'Actual' column represents the number of genes in the dataset for a given protein class. P-value represents the probability to have the given value of the Actual column or higher (or lower for negative z-score. Z-score represents the degree of over- and under-connectivity between objects in the dataset.

Protein class	Actual	p-value	z-score
Receptors	63	1.23E-13	8.87
Ligands	24	5.64E-07	6.20
Kinases	19	2.72E-03	3.26
Proteases	15	2.10E-02	2.37
Transcription factors	26	2.01E-02	2.29
Phosphatases	7	4.49E-02	2.12
Enzymes	48	7.30E-02	1.56
Other	228	3.55E-21	-10.05

Cell migration is not affected by RUNX3 overexpression in human HSPC

Having identified a significant dysregulation of cell movement and adhesion processes by enrichment analysis, the effects of RUNX3 overexpression on cell migration were further determined in these cells. Following transduction of HSPC with RUNX3 (or control) (4.3.3), cells were cultured in a transwell system with 3S^{low}G/GM supplemented with increasing concentrations of SDF-1. The chemokine SDF-1 and its receptor CXCR4 have a pivotal role in cell migration (Doitsidou *et al.* 2002). Spontaneous migration was measured by culturing control and RUNX3-expressing HSPC in the absence of SDF-1. As shown in Figure 5-10, RUNX3 overexpression induced a modest increase in cell migration of HSPC towards an SDF-1 gradient. However, such increase was not significant, suggesting that RUNX3 overexpression does not affect cell migration of HSPC. These findings contrast the predictions of pathway analysis, which highlights the importance of further validating these results.

5.3.4 RUNX3 overexpression downregulates key haematopoietic genes in human HSPC

Overexpression of RUNX3 in HSPC was previously shown to inhibit erythroid and myeloid development (3.3.2, 4.3.3). Further, KEGG analysis (Figure 5-9) shows that the most significantly disrupted pathway by RUNX3 is related to haematopoiesis. This study next sought to explore in detail the ‘Haematopoietic Cell Lineage’ KEGG pathway shown in Figure 5-11 to identify transcriptional changes in important cell surface proteins that could support the results obtained in previous chapters. In early haematopoiesis, *FLT3* expression was significantly upregulated in RUNX3-expressing cells. This receptor plays a critical role in the maintenance of haematopoietic homeostasis and is a common target for leukaemic transformation (Kikushige *et al.* 2008). Expression of myeloid cell surface markers *CD33* and *ITGAM* (CD11b) were significantly downregulated by RUNX3 overexpression, indicating abnormalities in the normal programme of myeloid differentiation (4.3.3). In addition, several of the observed transcriptional changes were in genes related to the megakaryocytic and erythroid lineages, supporting the inhibition of erythroid differentiation by RUNX3 overexpression (3.3.2). In particular, increased RUNX3 expression in HSPC led to a significant downregulation of the erythroid-related developmental genes *KIT* (CD117), *CD36*, *GYP A* (GlyA/CD235a), *CR1* (CD35) and *CD55*.

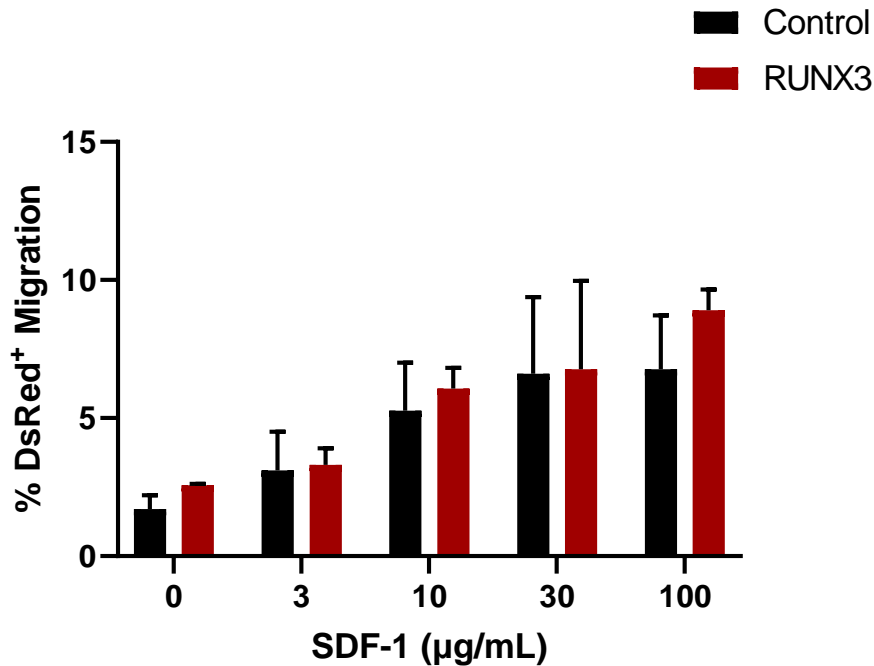


Figure 5-10 – RUNX3 overexpression did not significantly impact cell migration of HSPC in response to SDF-1 exposure.

Summary data of the percentage of migration for control and RUNX3 DsRed⁺ transduced HSPC in response to SDF-1 exposure. Unsorted HSPC (control and RUNX3) on day 6 of culture were cultured in a transwell system with increasing concentrations of SDF-1 (0, 3, 10, 30 and 100 ng/mL) and incubated for 4 hours (2.6.5). Percentage of migration was calculated based on the number of DsRed⁺ cells present in the lower compartment compared to the top compartment. Data indicates mean \pm 1SD of three independent experiments.

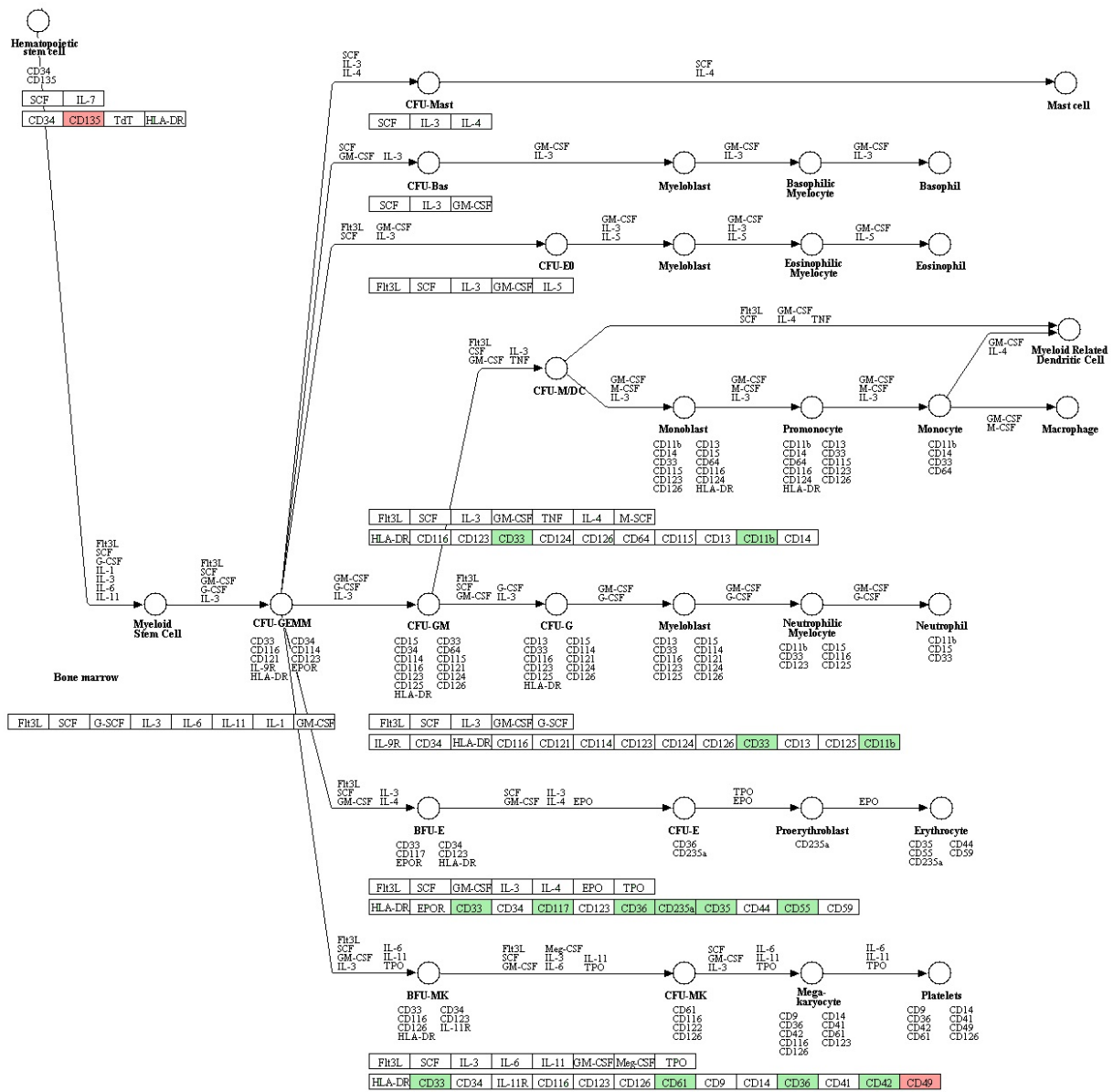


Figure 5-11 – RUNX3 overexpression dysregulate important genes involved in human haematopoiesis.

Representation of the human Hematopoietic Cell Lineage KEGG pathway map (hsa04640). Cellular stages are identified by the specific expression of genes, which are highlighted in red for upregulation and green for downregulation associated with RUNX3 overexpression in HSPC. The lymphoid arm of haematopoiesis was removed from this pathway, as it is not the focus of this study.

IPA[®] leverages the Ingenuity Knowledge Base containing more than 7.2M findings (Kramer et al. 2014). To further identify dysregulated genes associated with haematopoietic development due to RUNX3 overexpression, IPA[®] BioProfiler tool was used. As shown in [Figure 5-12](#), RUNX3 overexpression downregulated important haematopoietic genes in HSPC associated with different developmental stages, highlighting its relevance for haematopoiesis. Important genes for HSPC maintenance and function were significantly downregulated by RUNX3 overexpression, including *RUNX1*, *KIT* and *MPL*. These findings support previous observations that RUNX3 overexpression negatively impacts the proliferation and survival of progenitor cells (3.3.2, 4.3.3). On the other hand, *FLT3* and *ITGA6* (CD49f) were upregulated by RUNX3 expression in HSPC. In terms of the myeloid lineage, increased levels of RUNX3 downregulated genes associated with cell migration, survival, and inflammation (e.g., *C5AR1*, *CCL2*, *TIMP1*). Furthermore, RUNX3 overexpression significantly repressed the expression of important TFs that regulate erythropoiesis, including *LMO2* and *LYL1*, supporting previous observations (3.3.2) A similar transcriptional repression by RUNX3 was observed for megakaryocytic-related genes. Interestingly, several lymphoid-related genes such as *CD7* or *GNLY* were upregulated by RUNX3, which supports previous observations and a central role for RUNX3 in lymphoid development (Lotem *et al.* 2013; Levanon *et al.* 2014; Ebihara *et al.* 2015). A network summarising known interactions between some of these molecules is shown in [Figure 5-13](#). Development of haematopoietic system is one of the most significantly enriched function associated with these molecules and predicted to be inhibited by RUNX3 overexpression in HSPC.

Taken together, these data suggest that RUNX3 expression has an important role in the regulation of human haematopoiesis and its downregulation during erythroid and myeloid development is essential for the expression of genes that ultimately ensure terminal maturation of cells.

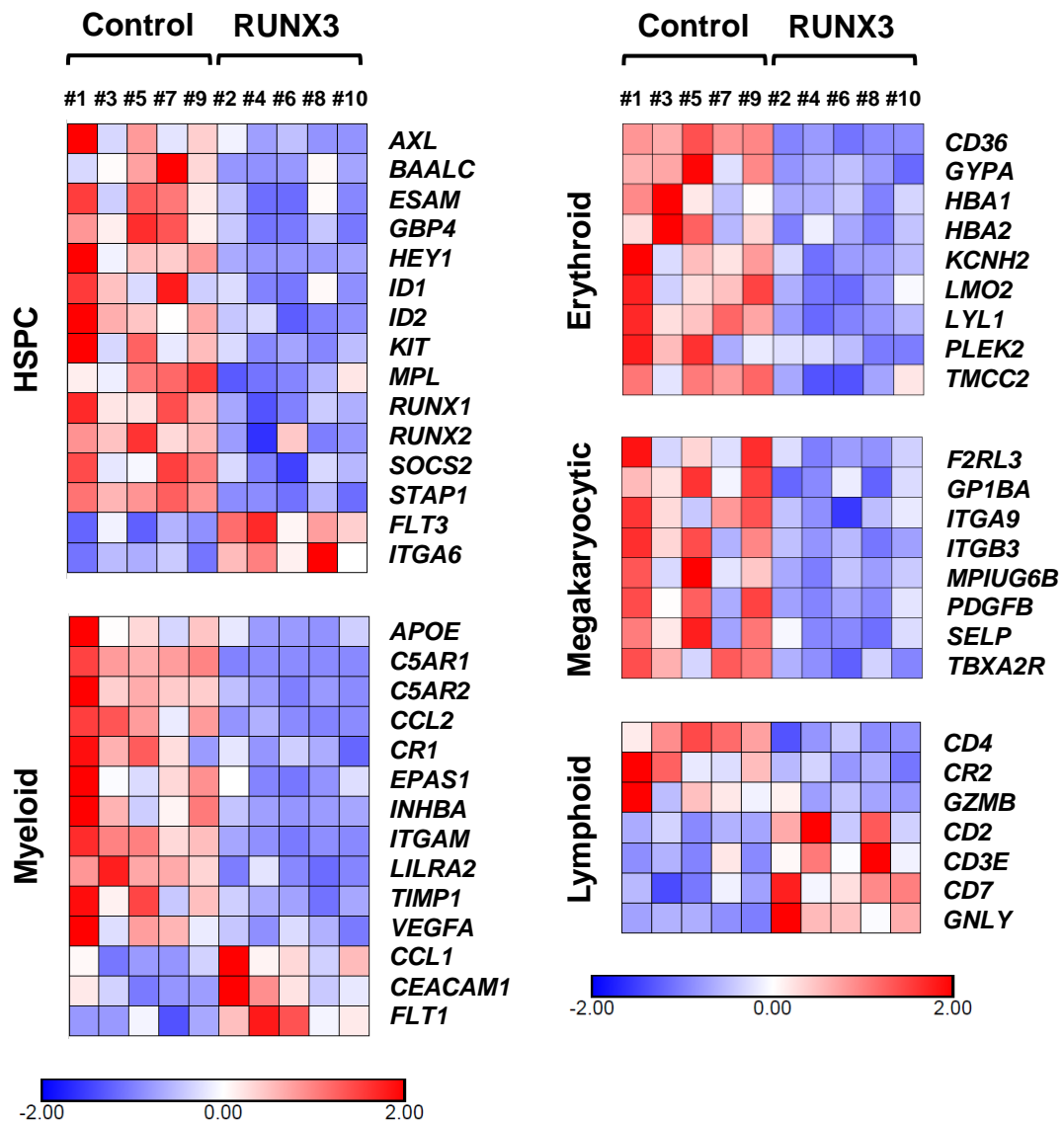


Figure 5-12 – Overexpression of RUNX3 significantly downregulates key haematopoietic genes in human HSPC.

Heat map representing the changes in expression levels of genes related to HSPC, myeloid, erythroid, megakaryocytic, and lymphoid compartments in control and RUNX3 human HSPC. BioProfiler in IPA® was used to identify genes associated with human haematopoiesis. Control samples - #1, 3, 5, 7, and 9; RUNX3 samples - #2, 4, 6, 8, and 10. Data indicate transformed FPKM expression values (subtracted row mean, divided by row SD); box colour is determined by low (blue) or high (red) gene expression levels. Each column represents an independent experiment. Heat map generated using Morpheus software (<https://software.broadinstitute.org/morpheus/>).

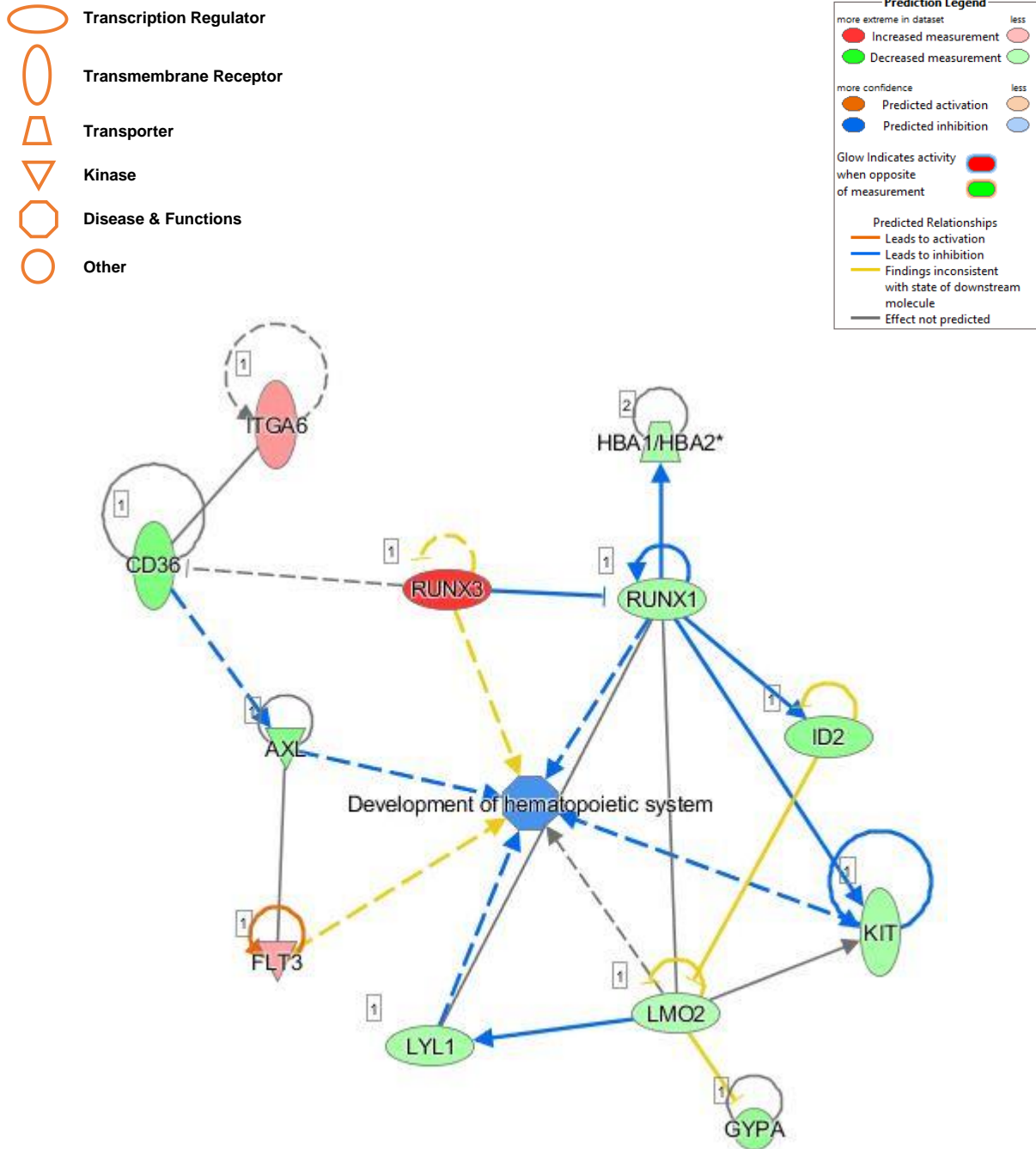


Figure 5-13 – Network analysis of RUNX3 dysregulated genes involved in the haematopoietic development of human HSPC.

Network with predicted interactions between key genes dysregulated by RUNX3 overexpression that are involved in haematopoietic differentiation of human HSPC (Figure 5-12). The majority of interactions between this set of dysregulated genes have been reported in the literature, denoted by blue lines in case of repression or orange for transactivation (arrow heads indicate direction and effect). Interactions reported for other species other than human were included in this analysis. RUNX3 interactions and function in haematopoiesis are scarce in the literature as evidenced in this network. Network generated using IPA® software and the Molecular Activity Predictor algorithm.

5.3.5 Identification of upstream regulators associated with the transcriptional changes mediated by RUNX3 in HSPC

Upstream regulator analysis and Causal network analysis are analytic algorithms available in IPA[®] that were used to identify upstream regulators connected to RUNX3 overexpression gene changes in HSPC (Kramer *et al.* 2014). As expected, most potential upstream gene regulators are TFs (Table 5-7). Furthermore, several of these upstream regulators are predicted to be inhibited, suggesting that RUNX3 overexpression is associated with potential inhibition of key TFs and proteins in these cells. *TGFB1* (TGF- β 1) is the most significant upstream gene regulator and predicted to be inhibited in this context (\log_2 FC -0.33; z-score -3.53). The relationship between TGF- β and RUNX3 has been previously studied and identifies RUNX3 as a downstream effector of the TGF- β signalling pathway (Chi *et al.* 2005; Yano *et al.* 2006). Moreover, essential haematopoietic TFs in megakaryocytic and erythroid differentiation are present in the upstream regulators list, such as *RUNX1*, *GATA1* or *GATA2*. GATA-1 is responsible for the transcriptional activation of several erythroid-specific genes, such as α - and β -globin, erythroid membrane proteins and heme biosynthesis enzymes (reviewed in (Ferreira *et al.* 2005)). Downregulation of such genes (e.g., *HBA1* and *HBA2*) by RUNX3 overexpression in HSPC highlights a potential network involving RUNX3 and GATA-1 in erythroid development.

Causal network analysis uncovers causal relationships associated with the dataset by expanding the previous analysis to include novel master upstream regulators that are not directly connected to the experimental data. This IPA[®] algorithm identified important master regulators associated with AML and upstream regulators that could explain the transcriptional changes induced by RUNX3. Interestingly, the most significant master regulator in this context, *CBFA2T3*, is predicted to be activated and it is a CBF-related gene. *CBFA2T3* (MTG16 or ETO2) is a master transcriptional coregulator in haematopoiesis and has a role in leukaemogenesis (Goardon *et al.* 2006; Chyla *et al.* 2008; Hamlett *et al.* 2008; Steinauer *et al.* 2019).

Table 5-7 – Upstream and master gene regulators predicted to be influencing the transcriptomic changes caused by RUNX3 overexpression in human HSPC.

Summary data of upstream and master regulators predicted by IPA® that are associated with the transcriptional changes caused by RUNX3 overexpression in HSPC. The 10 most significant regulators are shown for each analysis. DE genes in the dataset include their associated logarithmic (base 2) fold change. Activation z-score infers the activation states of predicted transcriptional regulators. A gene is considered inhibited when z-score < -2 and activated when z-score > 2. P-value of overlap measures whether the overlap between the dataset genes and the genes that are regulated by a transcriptional regulator is statistically significant. A negative log₂FC value represents downregulation (green shade), whereas a positive value represents upregulation (red shade). Data obtained using the Upstream Regulator Analysis and the Causal network analysis algorithms in IPA®.

Gene symbol	Log ₂ FC	Molecule type	Predicted Activation State	Activation z-score	p-value of overlap
<i>Upstream regulators</i>					
<i>TGFB1</i>	-0.33	Growth factor	Inhibited	-3.53	3.35E-17
<i>TNF</i>		Cytokine	Inhibited	-2.52	7.95E-17
<i>RUNX1</i>	-0.76	Transcription regulator	Inhibited	-2.28	6.95E-14
<i>GATA1</i>		Transcription regulator	Inhibited	-2.47	1.23E-12
<i>SP1</i>		Transcription regulator	Inhibited	-3.12	7.00E-12
<i>KLF2</i>		Transcription regulator		0.69	8.25E-11
<i>ZBTB16</i>		Transcription regulator		-0.15	1.06E-10
<i>GATA2</i>		Transcription regulator	Inhibited	-2.00	1.12E-10
<i>IFNG</i>		Cytokine	Inhibited	-2.56	9.68E-10
<i>SMAD4</i>		Transcription regulator		-1.23	1.82E-09
<i>Master regulators</i>					
<i>CBFA2T3</i>		Transcription regulator	Activated	3.62	3.61E-21
<i>HOXA3</i>		Transcription regulator		0.80	7.77E-20
<i>GATA1</i>		Transcription regulator	Inhibited	-3.58	2.82E-19
<i>VEGFA</i>	-0.78	Growth factor	Inhibited	-4.43	6.86E-19
<i>RLIM</i>		Enzyme		-1.84	6.56E-18
<i>NRL</i>		Transcription regulator		-0.12	6.80E-18
<i>TAT</i>		Enzyme	Inhibited	-3.00	2.07E-17
<i>CSF1</i>		Cytokine	Inhibited	-3.29	2.45E-17
<i>LMO2</i>	-0.62	Transcription regulator		0.75	3.33E-17
<i>TNF</i>		Cytokine	Inhibited	-2.29	5.30E-17

Other important master regulators are involved in haematopoietic development, including *GATA1*, *LMO2*, *SPI1*, and *KLF10*, which reinforces the idea that RUNX3 expression is relevant for normal haematopoiesis.

In conclusion, upstream and master regulator analysis identified key regulators of haematopoiesis that are associated with the RUNX3-mediated expression changes in HSPC.

5.3.6 RUNX3 has an essential regulatory function in cellular processes

To determine the main pathways and genes that are dysregulated or influenced by RUNX3 expression in human HSPC it is imperative to study not only its overexpression, but also the biological consequences of *RUNX3* loss in these cells. In addition, the possible functional redundancy between the RUNX proteins raises the question about a negative dominant effect of RUNX3 overexpression over RUNX1, similar to RUNX1-ETO. To address this, different comparative analyses were performed between RUNX3 overexpression transcriptional dysregulation and RUNX3 KD and RUNX1-ETO HSPC transcriptomic datasets.

5.3.6.1 Modulation of RUNX3 expression in progenitor cells support an important role for RUNX3 in cell signalling

In order to further substantiate the dysregulated pathways and genes mediated by RUNX3 expression in HSPC, a comparison between data obtained in this study regarding RUNX3 overexpression in human HSPC (Dataset #1) and RUNX3 KD in human HSPC (Dataset #2; GSE119264) and normal human erythroid precursor cells (Dataset #3; GSE119264) (Balogh *et al.* 2020) was performed (2.9.1). As shown in Figure 5-14A, several signalling pathways were predicted to be activated in erythroid precursors with low RUNX3 expression and, in some cases, inhibited when RUNX3 levels are elevated, such as integrin signalling. Furthermore, CXCR4 signalling was predicted to be differentially regulated by RUNX3 expression, with RUNX3 KD being associated with its increased activation. Comparing diseases and functions, platelet-related functions, including aggregation of cells and haemostasis, were predicted to be inhibited in both scenarios, which supports the relevance of RUNX3 in platelet function (Figure 5-14B).

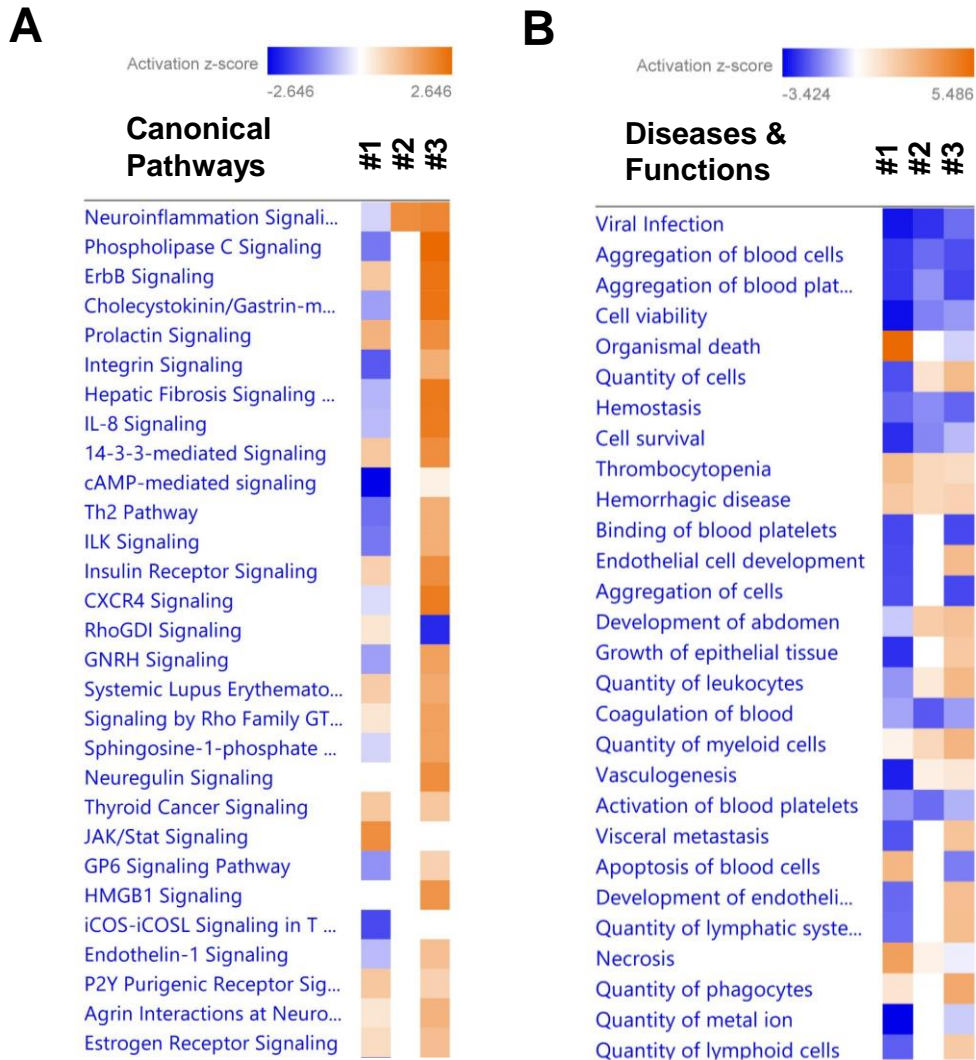


Figure 5-14 – Pathways and functions comparative analysis of increased and reduced RUNX3 expression levels in human HSPC.

Comparison analysis by IPA® between RUNX3 overexpression and KD datasets. **(A)** Heat maps representing dysregulated canonical pathways and **(B)** diseases and functions between increased and reduced RUNX3 expression HSPC datasets. Heat maps list terms according to the predicted activation z-score which infers the activation states of pathways and functions. Dataset numbers are identified by #1 – RUNX3 overexpressing HSPC; #2 – RUNX3 KD HSPC; #3 – RUNX3 KD erythroid progenitor cells.

In addition, apoptosis was significantly associated with increased RUNX3 levels rather than reduced RUNX3 expression. Overall, the comparison between RUNX3 overexpression and KD induced changes suggest that RUNX3 expression is important for the regulation of cell proliferation and survival, previously shown to have a functional correlation (3.3.2, 4.3.3).

To gain more insights on RUNX3-mediated transcriptional dysregulation and downstream effects, a comparison analysis between the DE genes of each dataset was performed (Figure 5-15). Common to RUNX3-expressing HSPC and RUNX3 KD undifferentiated and erythroid progenitors were 55 DE genes, representing 15% of all genes considered. This implies that the mechanism(s) of developmental disruption in RUNX3 overexpressing cells and KD are different. Furthermore, of these 55 genes, 36 are dysregulated concordantly representing 65% of the common DE genes. The six genes commonly dysregulated between datasets include *CCL2*, *GP1BA*, *HGD*, *LGALS1*, *MPL* and *TUBB1*. Only *CCL2* was coordinately dysregulated between RUNX3 overexpression and KD in HSPC. *CCL2* or monocyte chemoattractant protein-1 (MCP-1) is a chemokine involved in the activation of important downstream signalling cascades (e.g., JAK2/STAT3, MAPK, or PI3K signalling) to ultimately promote cell migration, among other processes (reviewed in (Gschwandtner *et al.* 2019)).

The above data suggests that RUNX3 expression is important for the transcriptional regulation of commonly DE genes, such as *CCL2*. Nevertheless, this analysis has some caveats, namely the fact that the #2 dataset is only associated with 67 DE genes ($p_{adj} > 0.05$) and #3 dataset is erythroid focused, which hinders the comparative analysis.

Datasets

- #1 – RUNX3-expressing HSPC
- #2 – RUNX3 KD HSPC
- #3 – RUNX3 KD erythroid progenitors

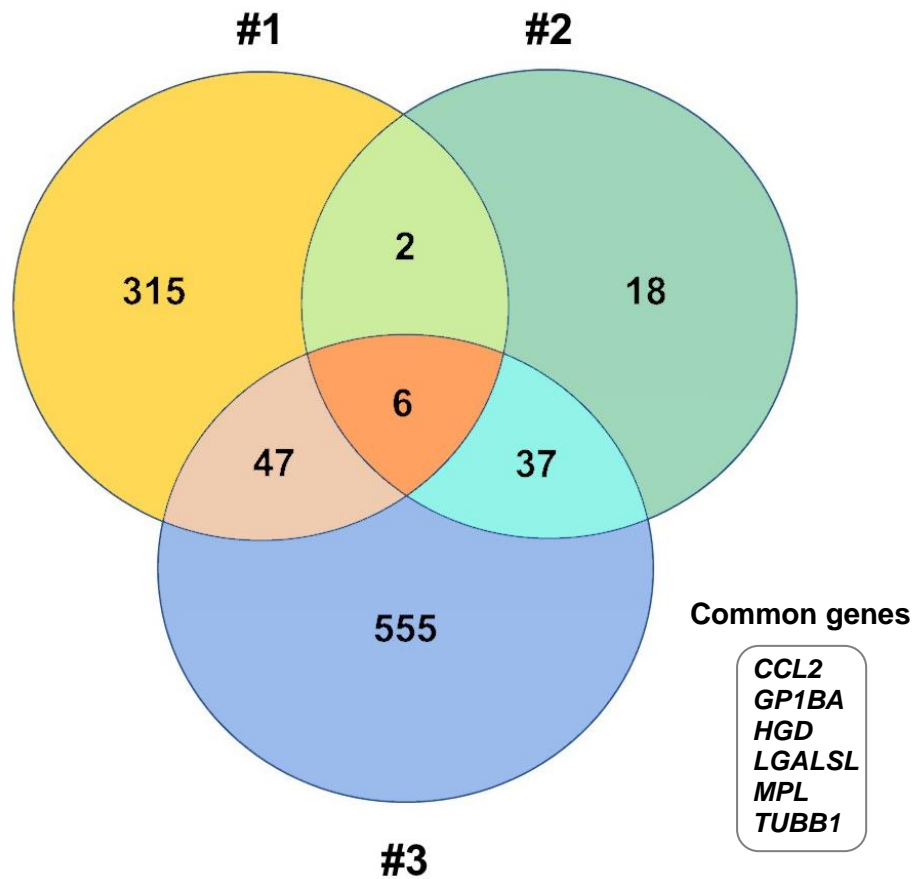


Figure 5-15 – Differentially expressed genes comparison analysis of increased and reduced RUNX3 expression levels in human HSPC.

Venn diagrams representing DE genes between increased and reduced *RUNX3* expression HSPC datasets, including the names of the genes commonly dysregulated between all three datasets.

5.3.6.2 Overexpression of *RUNX3* disrupts important biological processes by different mechanisms other than a dominant negative effect over *RUNX1*

Ectopic expression of RUNX1-ETO in HSPC downregulates *RUNX3* mRNA expression (4.3.5). To determine the transcriptional similarities and/or differences between the *RUNX3* overexpression dataset and a RUNX1-ETO expressing HSPC microarray dataset (Dataset #4; e-mexp-583) (2.9.1), a Comparison Analysis in IPA® was performed. As shown in Figure 5-16A, signalling pathways, such as Gβγ and Gαi signalling, are predicted to be differentially regulated in these contexts (inhibited by increased *RUNX3* levels and activated by RUNX1-ETO expression), which could indicate that *RUNX3* expression regulates such processes. G protein-coupled receptors signalling is intimately related to cell movement of haematopoietic cells and certain members of this large family are found highly expressed in AML (reviewed in (Selheim *et al.* 2019)). Furthermore, AML signalling is predicted to be activated in both scenarios. In terms of dysregulated functions, platelets activity and haematopoiesis are processes predicted to be inhibited in both high *RUNX3* and RUNX1-ETO contexts, which explains their association with leukaemogenesis (Figure 5-16B).

Given the similarities between *RUNX3* and RUNX1-ETO disruption of human haematopoietic development (Tonks *et al.* 2003; Tonks *et al.* 2004) (3.3.2, 4.3.3), a comparison analysis of their transcriptional dysregulation in HSPC (i.e. DE genes) was performed. As shown in Figure 5-17, 38 genes including *RUNX3* were commonly dysregulated between datasets, which represents only 10% of all DE genes. This comparison analysis suggest that the transcriptional changes caused by high levels of *RUNX3* arise from a different regulatory mechanism compared to RUNX1-ETO changes and mechanism. In part, this was expected given that RUNX1-ETO can recruit activating and inhibitory complexes to regulate transcription of RUNX1 target genes. In terms of common DE genes, 42% are concordant in terms of expression change and could be targets of both *RUNX3* and *RUNX1* (functional redundancy). The remaining common DE genes (58%) that present contrasting directions of expression change could be exclusive targets of *RUNX1* or *RUNX3*. Interestingly, some of the common DE genes are important for haematopoietic development, such as *RUNX1*, *CD36*, *ITGA6* and *ID2* (5.3.4). Together, these findings explain the phenotypic similarities of *RUNX3* and RUNX1-ETO-expressing HSPC (3.3.2, 4.3.3).

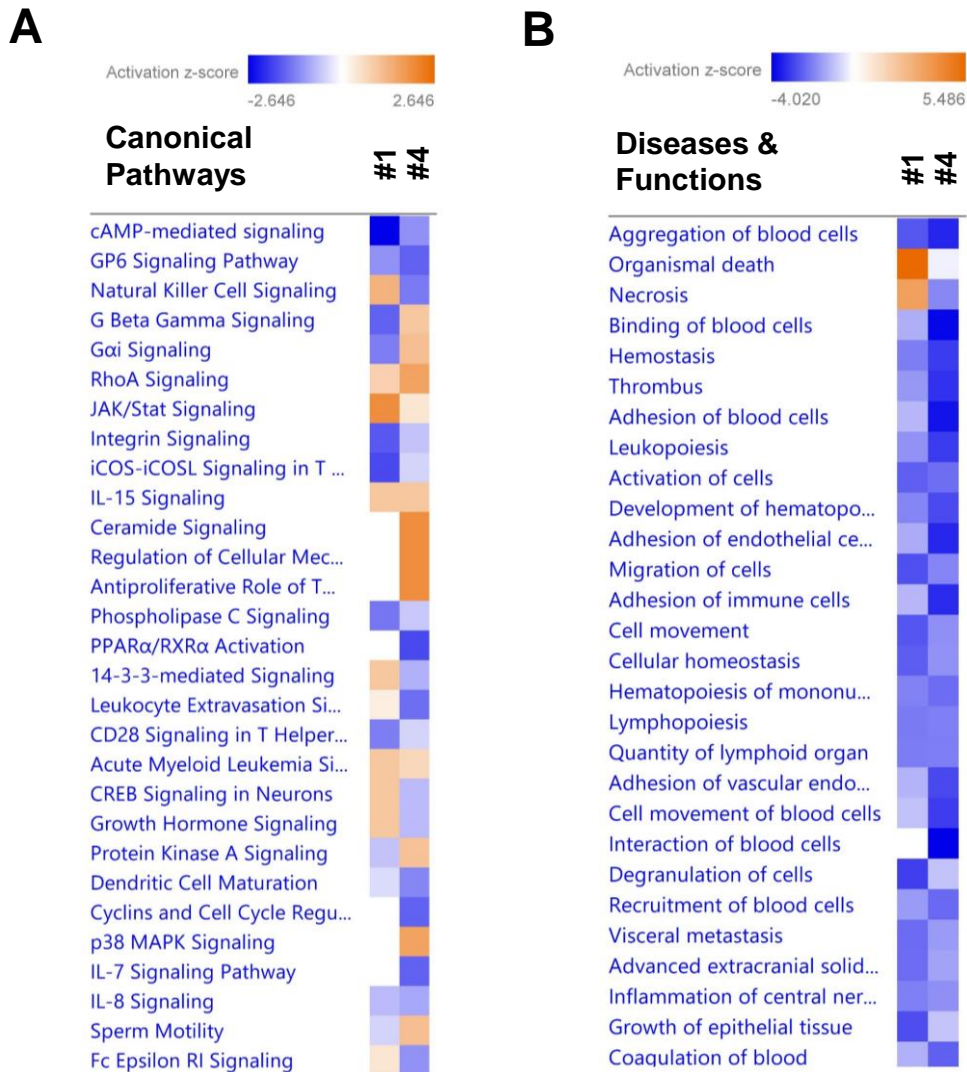


Figure 5-16 – Pathways and functions comparative analysis of increased RUNX3 and RUNX1-ETO expression in human HSPC.

Comparison analysis by IPA® between RUNX3 overexpression and RUNX1-ETO datasets. **(A)** Heat maps representing dysregulated canonical pathways and **(B)** diseases and functions between increased RUNX3 and RUNX1-ETO expression HSPC datasets. Heat maps list terms according to the predicted activation z-score which infers the activation states of pathways and functions. #1 – RUNX3-expressing HSPC; #4 – RUNX1-ETO-expressing HSPC. Annotations are ordered by

Datasets

- #1 – RUNX3-expressing HSPC
- #4 – RUNX1-ETO HSPC

Common genes

- APOE*
- CA2*
- CCL2*
- CD244*
- CD36*
- CEACAM1*
- CH25H*
- COCH*
- CRHBP*
- CYP51A1*
- DEPTOR*
- ECM1*
- EHD3*
- FUT7*
- HBA1*
- ID1*
- ID2*
- IGFBP4*
- ITGA6*
- KCNH2*
- LILRA2*
- LTB*
- MAGEF1*
- NID1*
- NTS*
- P2RX5*
- PLAT*
- PLCH1*
- PLXNC1*
- PMP22*
- PRG2*
- RMND5B*
- RUNX1*
- RUNX3*
- S1PR1*
- SLC2A3*
- SOCS2*
- TGFB11*
- TM4SF1*

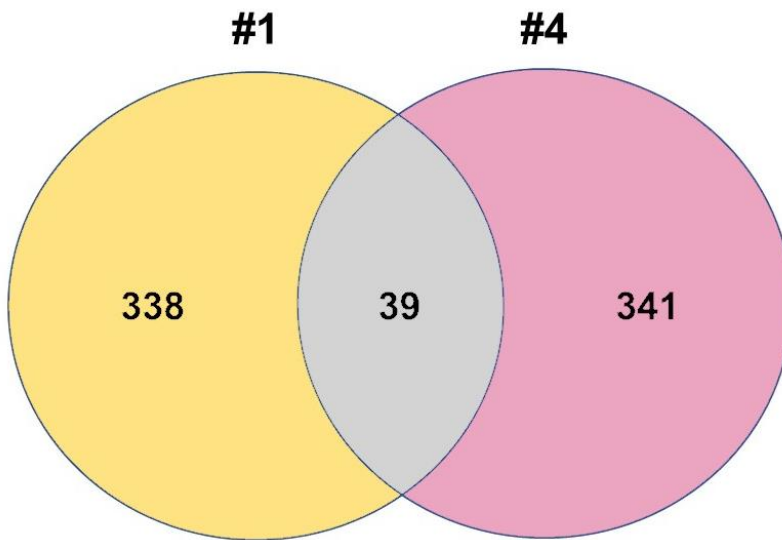


Figure 5-17 – Differentially expressed genes comparison analysis of increased *RUNX3* and *RUNX1*-ETO expression in human HSPC.

Venn diagrams representing DE genes between increased *RUNX3* and *RUNX1*-ETO expression HSPC datasets, including the names of the genes commonly dysregulated between the datasets.

Overall, this analysis suggests that RUNX3 and RUNX1-ETO expression appear to inhibit important cell functions and have some opposing effects in certain canonical cellular pathways, which could be due to different mechanisms other than a dominant negative effect over RUNX1.

5.3.7 Expression of RUNX3 in AML patients is significantly correlated with the expression of dysregulated genes identified in this study

To validate the transcriptional dysregulation imposed by RUNX3 overexpression in human HSPC and identify the genes that are significantly co-expressed with RUNX3 in blasts from AML patients, analysis of the TCGA dataset was performed (Cancer Genome Atlas Research *et al.* 2013). Only the top dysregulated genes and genes associated with significantly enriched pathways were investigated. A significant correlation between expression levels was considered when $p_{adj} < 0.05$. As shown in [Table 5-8](#), several receptors and TFs were dysregulated by RUNX3 overexpression in HSPC and this change is associated with expression in AML patient blasts. These genes might be interesting molecules for further investigation into the contribution of RUNX3 for AML pathogenesis.

5.4 Discussion and conclusion

Previous Chapters show that overexpression of RUNX3 in HSPC have a significant effect on haematopoietic development ([3.3.2](#), [4.3.3](#)). Therefore, this study next sought to determine the transcriptional dysregulation imposed by RUNX3 overexpression in human HSPC. Increased RUNX3 expression induced a significant dysregulation in HSPC transcriptome, favouring the downregulation of genes. RUNX3-mediated transcriptional dysregulation was associated with predicted changes in cell signalling, inflammation and cell movement arising from the fact that ‘Receptors’ was the main protein class affected by RUNX3 expression in HSPC ([5.3.3.3](#)). Dysregulation of key TFs, including *HEY1*, *RUNX1* or *LMO2* were also observed in HSPC overexpressing RUNX3, highlighting RUNX3 importance in the regulation of signalling pathways (e.g., Notch pathway) and human haematopoiesis ([5.3.4](#)). Moreover, CBFA2T3 was identified as a TF that might cooperate with RUNX3 to induce the observed transcriptional changes in these cells (see below) ([5.3.5](#)).

Table 5-8 – Summary list of dysregulated genes and potential upstream regulators significantly co-expressed with RUNX3 in AML patients from TCGA dataset.

Summary data of dysregulated genes and additional upstream regulators that are significantly co-expressed with RUNX3 in AML patients (Cancer Genome Atlas Research *et al.* 2013). From this list, only the genes with significant co-expression with RUNX3 in and concordant effect on their expression level (downregulation/upregulation) in AML patients are shown here. DE genes in the different datasets include their associated logarithmic (base 2) fold change. #1 – RUNX3-expressing HSPC; #3 – RUNX3 KD erythroid progenitor cells; #4 – RUNX1-ETO-expressing HSPC. Activation z-score infers the activation states of predicted transcriptional regulators. A gene is considered inhibited when z-score < -2 and activated when z-score > 2. Co-expression values obtained using Spearman's correlation with the respective adjusted p-value (padj). A negative log₂FC value represents downregulation (green shade), whereas a positive value represents upregulation (red shade) compared to controls. Data analysed using cBioPortal (www.cbioportal.org/).

Gene symbol	Log ₂ FC			Activation z-score	Co-expression with RUNX3	padj
	RUNX3 #1	RUNX3 KD #3	RUNX1-ETO #4			
<i>KLRB1</i>	2.01	1.19			0.383	5.643E-6
<i>CEACAM1</i>	0.78		4.47		0.341	6.902E-5
<i>GNLY</i>	1.41				0.460	2.270E-8
<i>RUNX1</i>	-0.76		1.91		-0.226	1.290E-2
<i>ITGA6</i>	0.86		-1.66		0.235	9.026E-3
<i>CD2</i>	0.77				0.333	1.089E-4
<i>CD7</i>	0.74				0.545	9.480E-12
<i>CD3E</i>	0.65				0.454	3.690E-8
<i>TCF7</i>				-0.054	0.443	8.830E-8
<i>CBFA2T3</i>				3.615	0.478	5.770E-9
<i>B3GNT7</i>	1.32	1.78			0.356	2.965E-5
<i>FAM43A</i>	0.72	0.70			0.269	2.371E-3
<i>FUT7</i>	0.70	1.09	-2.26		0.335	1.753E-4
<i>NTN1</i>	0.68	-0.74			0.186	4.500E-2
<i>SPOCK1</i>	-1.19	1.58			-0.326	1.591E-4
<i>UBXN10</i>	0.64	-0.80			0.268	2.490E-3
<i>LTB</i>	1.01		-1.65		0.431	1.350E-7
<i>CD244</i>	0.67		-1.72		0.209	2.2280E-2
<i>RASD1</i>	0.78				0.478	1.720E-8
<i>TBX21</i>	1.01				0.461	8.290E-9

A comparison analysis between RUNX3 overexpression and KD changes in human HSPC identified potential downstream targets of RUNX3, such as CCL2 (5.3.6). Further, transcriptional dysregulation imposed by RUNX3 or RUNX1-ETO expression in HSPC was compared and suggested different deregulatory mechanism of important cell functions and pathways. Overall, this study supports an important role for RUNX3 in human haematopoiesis and unveils the main pathways and genes dysregulated by RUNX3 in HSPC.

To examine the transcriptome in HSPC, a GFP vector harbouring *RUNX3* cDNA (or control) was selected for these studies given GFP fluorescence intensity is higher compared to DsRed, making it a better selectable marker for cell sorting. Following GFP enrichment and total RNA extraction, a preliminary QC assessment of samples was performed to assess RNA integrity, as sample quality directly impacts RNA sequencing and subsequent bioinformatics analysis. RNA concentration and integrity were determined using Agilent 2100 Bioanalyzer, where RNA is considered of high quality when the ratio of 28S:18S ribosomal RNA species is about 2.0 and higher (Schroeder *et al.* 2006). The limitations on using ribosomal ratio for RNA quality assessment fuelled the development of a tool to standardise RNA QC, the RIN algorithm (Schroeder *et al.* 2006). Total RNA present in all control and RUNX3 samples was sufficient for library preparation and sequencing, and the RNA quality and integrity were of high standard for downstream applications (5.3.1).

QC is one of the most disregarded aspects of RNA-seq data analysis and it is of major importance for the success of RNA-seq experiments (Sheng *et al.* 2017). Conducting QC for RNA-seq is important and should follow these perspectives: RNA quality, raw read data, alignment, and gene quantification (Sheng *et al.* 2017). More than 20M raw reads were generated for each sample which, according to the literature, is sufficient for successful gene expression profiling (Sheng *et al.* 2017). This parameter is also the easiest and most intuitive approach to detect problems with the sequencing process. Raw reads were filtered to remove reads with adapter contamination, uncertain nucleotides (N), and low quality of nucleotides. Only 'clean' reads were used for downstream analysis and mapped to the human reference genome. Mapped reads were mainly exonic, as expected. Read mapping to intron regions could indicate the presence of immature transcripts or alternative splicing events, while reads mapped to intergenic regions could be due to weak annotation of

the reference genome (van Bakel *et al.* 2010; Ameer *et al.* 2011). In terms of mapping status, 'clean' reads can map uniquely when they are assigned to a single position in the reference or could be multiple mapped and should not be discarded (Conesa *et al.* 2016). A high percentage of reads was successfully and uniquely mapped to the human genome, which provided confidence in the RNA-seq data (5.3.2.1).

Following alignment of reads to the genome, a quantification step was performed, and gene expression was estimated. Raw read counts alone are not adequate to compare gene expression levels between samples, and thus gene length and sequencing depth need to be considered as well. This process is essential in current RNA-seq protocols because of the several intrinsic biases and limitations, such as nucleotide composition bias, GC bias and PCR bias (Wang *et al.* 2012). Distribution of gene expression was similar between both control and RUNX3 HSPC transcriptome, an expected outcome given that the only difference between groups is the ectopic expression of RUNX3. To understand the major sources of variation in the data and identification of outlying samples, which may compromise DE analysis, PCA and hierarchical clustering was performed (5.3.3.1). The PCA plots identified batch effects associated with the experimental design of this study, which were considered during the DE modelling analysis. Sources of variation associated with the experimental design primarily arose from the inherent variability of CB samples in terms of genetic and progenitor composition, among other factors. Therefore, the statistical model used for DE analysis was adjusted to consider these variations within the data and a multifactorial pairwise comparison was favoured.

5.4.1 RUNX3 overexpression imposes a significant transcriptional dysregulation in human HSPC

Overexpression of RUNX3 led to a significant dysregulation of HSPC transcriptome, characterised by expression changes in 607 genes: 154 genes were upregulated, and 453 genes were downregulated compared to control (5.3.3.3). Enrichment analysis showed a significant correlation between these changes and important biological processes, such as immunity, cell communication, haematopoiesis, cell movement and proliferation. The predicted regulation of cell movement and migration by RUNX3 was further determined in HSPC. Although RUNX3 overexpression increased the general motility of haematopoietic cells, the

differences compared to controls were not significant and did not validate the enrichment analysis results. RUNX3 expression has been primarily shown to inhibit cell migration in different settings (Fainaru *et al.* 2005; Mei *et al.* 2011; Chen *et al.* 2013; Gou *et al.* 2017). Nevertheless, RUNX3 expression has also been found to promote this process depending on cellular context (Whittle *et al.* 2015). Previous studies in different cell systems have shown that RUNX3, along with RUNX1 and RUNX2, regulates the transcription of adhesion molecules (Dominguez-Soto *et al.* 2005; Fainaru *et al.* 2005; Puig-Kroger *et al.* 2006; Wotton *et al.* 2008; Estecha *et al.* 2012). Interestingly, murine HSPC expressing RUNX1-ETO have enhanced migration *in vitro*, and RUNX1-ETO silencing in t(8;21) AML cells resulted in a reduced motility of cells (Saia *et al.* 2016). Taken together, these results suggest that RUNX3 expression is important for the regulation of haematopoiesis and cell proliferation, previously shown to have a functional correlation (3.3.2, 4.3.3).

Receptors were the main protein class dysregulated by RUNX3 overexpression in HSPC, with the top 5 dysregulated receptors being significantly downregulated by RUNX3, except for CD161 upregulation. This receptor is mainly expressed in lymphoid cells, particularly NK cells (Maggi *et al.* 2010; Afzali *et al.* 2013; Pesenacker *et al.* 2013; Ussher *et al.* 2014; Kurioka *et al.* 2018), and its expression has been shown in murine DCs and along monocyte differentiation in the BM and thymus (Poggi *et al.* 1997). However, no evidence of its expression in myeloid human cells was found in the literature. ChIP-seq analysis showed that RUNX1 binds to *KLRB1* promoter in pre-B cells (Debaize *et al.* 2018), and RUNX3 was shown to regulate the expression of *Klrb1b* in IL-15-activated NK cells (Levanon *et al.* 2014). Although RUNX3 was shown to upregulate CD161 in HSPC, its contribution to RUNX3-mediated inhibition of erythroid and myeloid development should be minimal. Nevertheless, AML patient data from the TCGA dataset shows a significant positive correlation between RUNX3 and CD161 expression (Cancer Genome Atlas Research *et al.* 2013). A subset of drug-effluxing memory T cells expressing CD161 were shown to help preserving antiviral immunity in AML patients undergoing chemotherapy (Alsuliman *et al.* 2017). This study highlights the potential of CD161-expressing memory T cells for adoptive therapy against viruses and cancer.

PDPK1 was the most dysregulated gene in RUNX3-expressing HSPC (\log_2FC of -2.34). Its encoded protein PDK1 is a master kinase essential for cell survival and

development in many species (Hu *et al.* 2017). Conditional deletion of PDK1 in mice impairs the reconstitution capacity of HSC during foetal liver haematopoiesis (Hu *et al.* 2017; Wang *et al.* 2018b). In addition, PDK1 was shown to contribute to HSC function partially via regulating reactive oxygen species levels (Hu *et al.* 2017), and to regulate apoptosis and cell cycle activation of HSC and progenitor cells, suggesting an important role for PDK1 in HSC survival (Wang *et al.* 2018b). RUNX3-induced PDK1 downregulation in HSPC supports some of the deleterious effects of RUNX3 in growth and survival of these cells (3.3.2, 4.3.3). Loss of PDK1 was also shown to impair erythroid and myeloid colony formation and the terminal differentiation of embryonic cells, implying that PDK1 expression is required for haematopoietic development (Bone and Welham 2007). PDK1 overexpression in human HSPC has been found to promote their monocytic colony formation (Pearn *et al.* 2007). Downregulation of PDK1 by RUNX3 could therefore explain the inhibition of both erythroid and myeloid colony formation exhibited by RUNX3-expressing HSPC. PI3K pathway has been implicated in erythroid development and survival of erythroid precursors (Haseyama *et al.* 1999; Xie *et al.* 2019). Furthermore, PDK1 overexpression is a common feature of several types of cancers, and its increased levels were showed in myelomonocytic AML (FAB M4 and M5) and is associated with poor clinical outcome with survival of AML blasts (Zabkiewicz *et al.* 2014). Taken together, the significant downregulation of PDK1 by RUNX3 could explain some of the observed abnormalities in growth and differentiation of cells overexpressing RUNX3 described in Chapter 3 and 4.

RUNX3 overexpression in HSPC led to the downregulation of *NTRK1*, a tyrosine kinase receptor for nerve growth factor that plays an important role in the nervous system and its alteration has been associated to cancer (Alberti *et al.* 2003). Expression of *NTRK1* at the mRNA and protein levels was found upregulated by RUNX1-ETO in t(8;21) cell lines and in human HSPC expressing this fusion protein (Mulloy *et al.* 2005), which are associated to RUNX3 downregulation (Cheng *et al.* 2008b). Interestingly, inv(16) cells were also shown to upregulate this receptor (Mulloy *et al.* 2005), which suggests that RUNX3 expression could be important for the transcriptional regulation of *NTRK1* in this context. Upregulation of *NTRK1* in RUNX1-ETO cells was suggested to provide an important growth advantage to these cells, as NGF is secreted by stromal cells within the BM microenvironment (Mulloy *et al.* 2005). Although this signalling pathway is not relevant for the effects of RUNX3 or RUNX1-

ETO on human HSPC *in vitro*, downregulation of NTRK1 by RUNX3 overexpression could remove the growth advantage of t(8;21) cells *in vivo*.

5.4.2 RUNX3-mediated dysregulation of HSPC and erythroid-related transcriptional profiles

In terms of its effect in human haematopoiesis, RUNX3 overexpression was shown to induce significant changes in the transcription signatures related to HSPC function and maintenance, and erythroid development, among others (5.3.4). For instance, additional RUNX family members, *RUNX1* and *RUNX2*, were also significantly downregulated by RUNX3 overexpression in HSPC. RUNX1 is required for HSC emergence (North *et al.* 1999; Cai *et al.* 2000), as well as definitive haematopoiesis resulting in midgestational death of RUNX1-deficient mice (Okuda *et al.* 1996; Wang *et al.* 1996a). Further studies showed that loss of RUNX1 increases the numbers of HSPC and their replating capacity (Ichikawa *et al.* 2004a), which could support the increase in self-renewal observed in RUNX3-expressing HSPC under clonal conditions (3.3.2.2). Expression of RUNX1 was shown predominantly in haematopoietic progenitors, and to a lesser extent in several lineages including myeloid cells (Lorsbach *et al.* 2004; North *et al.* 2004) (1.3.4). Conversely, RUNX1 is weakly expressed in erythroid progenitors, and its expression is downregulated during erythropoiesis (Lorsbach *et al.* 2004; North *et al.* 2004), a pattern previously observed for RUNX3 (3.3.1). Absence of RUNX1 in mice leads to abnormal primitive erythropoiesis, with reduced KLF1 and GATA-1 expression (Yokomizo *et al.* 2008). Recently, RUNX3 overexpression in TET2-deficient mice was shown to significantly inhibit RUNX1 expression, as well as its target genes *Cebpa* and *Csf1r* (Yokomizo-Nakano *et al.* 2020). In addition, AML patient samples from the TCGA dataset show a significant negative correlation between RUNX3 and RUNX1 expression (Cancer Genome Atlas Research *et al.* 2013). Considering these evidences, and the possible redundancy between both TFs previously described in the literature (Goyama *et al.* 2004; Wang *et al.* 2014a; Morita *et al.* 2017), RUNX3-induced suppression of erythroid and myeloid developmental might be in part due to the downregulation of RUNX1 and dysregulation of its target genes. Nevertheless, their intricate spatiotemporal regulation supports essential and non-redundant functions of each RUNX member (Levanon *et al.* 2001a).

Downregulation of Inhibitor of DNA binding 1 and 2 (ID1 and ID2, respectively) by RUNX3 was also observed in HSPC. ID1 and ID2 are members of a family of four proteins known to suppress the activity of the E protein helix-loop-helix TFs by limiting their ability to bind DNA, and thus regulating cell proliferation and fate determination (Jankovic *et al.* 2007). Expression of ID proteins is enriched in HSC, especially ID2, playing important roles in the control of HSC transcriptional state (Mercer *et al.* 2011; van Galen *et al.* 2014). Reducing ID2 expression in CB HSC was shown to increase lymphoid potential, whereas its overexpression biased myeloerythroid differentiation (van Galen *et al.* 2014). Overexpression of ID2 was previously found to promote erythroid development, with its absence impairing erythropoiesis in mice by modulating PU.1 and GATA-1 functions (Ji *et al.* 2008). In addition, upregulation of ID2 expression during granulopoiesis was found to be required for the maturation of human HSPC, with granulocyte development being suppressed when ID2 expression was reduced in these cells (Buitenhuis *et al.* 2005). Downregulation of ID2 by RUNX proteins has been reported in 3T3 fibroblasts, with RUNX3 exhibiting the strongest repressive effect (Wotton *et al.* 2008). Therefore, downregulation of ID2 by RUNX3 overexpression could be negatively influencing erythroid as well as myeloid development (3.3.2, 4.3.3).

As opposed to the previous changes, RUNX3 overexpression was shown to upregulate the expression of *ITGA6* and *FLT3*. Integrin $\alpha 6$ or CD49f is among the cell surface markers that have been identified in different HSC populations (1.1.1). CD49f expression in human HSC was shown to demarcate HSC and MPP populations, with CD49f⁺ cells being highly efficient at generating long-term multilineage grafts as opposed to CD49f⁻ MPP (Notta *et al.* 2011). Therefore, the upregulation of CD49f by RUNX3 in HSPC might explain previous findings, such as increased self-renewal of progenitors (3.3.2.2). On the other hand, FLT3 is a type III RTK selectively expressed during early stages of haematopoiesis, with BM and CB derived human HSPC exhibiting FLT3 expression, as well as CMP and GMP populations (Kikushige *et al.* 2008). Interestingly, FLT3L was shown to reduce early erythroid progenitors when injected in mice, suggesting that FLT3 signalling negatively regulates erythropoiesis (Tsapogas *et al.* 2014). *FLT3* genomic loci has been shown to be occupied by RUNX3 in splenic DCs (Dicken *et al.* 2013). Therefore, upregulation of FLT3 receptor by RUNX3 overexpression could contribute to the erythroid defects observed in these

cells (3.3.2). In addition, approximately 30% of AML patients present activating *FLT3* mutations which lead to constitutive FLT3 receptor signalling and ultimately promote leukaemic proliferation and survival (Larrosa-Garcia and Baer 2017). Notch signalling was reported to have a tumour suppressive role by downregulating the expression of FLT3 (Kato *et al.* 2015). These findings suggest a link between the Notch signalling pathway and FLT3 expression, and therefore negative regulation of Notch signalling by RUNX3 (*HEY1* downregulation) may contribute to the upregulation of FLT3 in HSPC.

Having shown that RUNX3 overexpression inhibits erythroid development of human HSPC, this study sought to determine the association of transcriptional changes behind that effect. Uniquely, downregulation of the *HEY1*, a downstream target of the canonical Notch signalling pathway which plays important roles in cellular growth, differentiation and fate choices, was the only change in TFs present in the top 10 DE genes (Weber and Calvi 2010). Notch signalling has been shown to promote erythroid differentiation of CD34⁺ human cells (Sugimoto *et al.* 2006), and a connection between this pathway and SCF signalling during erythropoiesis has been previously reported (Zeuner *et al.* 2011). Expression of HEY1 has been demonstrated in HSC and committed myeloid progenitors, which suggests an important role in haematopoiesis (Mercher *et al.* 2008; Cheng *et al.* 2016). In particular, HEY1 showed the highest expression in MEP, intermediate in CMP and lowest in the GMP population (Mercher *et al.* 2008). *Hey1* KO zebrafish showed significantly decreased mature erythroid cells and diminished expression of *runx1*, which suggests this TF is required for definitive haematopoiesis and plays a critical role in the emergence of HSC (Cheng *et al.* 2016). A negative correlation between RUNX3 and HEY1 expression levels has been shown previously in hepatocellular carcinoma and osteoblasts (Nishina *et al.* 2011; Bauer *et al.* 2015), whereas a positive correlation between these TFs has been shown in microvascular endothelial cells (Fu *et al.* 2011). Taken together, downregulation of HEY1 by RUNX3 overexpression in HSPC could contribute to the abnormal erythroid development of cells.

c-KIT is an additional type III RTK essential for the proliferation and survival of early progenitors and shown to be downregulated by RUNX3 overexpression in HSPC. KIT-deficient mice exhibit severe erythroid abnormalities characterised by reduced erythroid progenitors and midgestational death due to anaemia (reviewed in (Broudy

1997)). c-KIT expression was shown to promote the expansion of early erythroid precursors, with its downregulation allowing terminal erythroid maturation (Muta *et al.* 1995). In human CD34⁺ HSPC, promyelocytic leukaemia zinc-finger protein (PLZF) was reported to have similar effects on c-KIT expression as RUNX3 in this study. Accordingly, PLZF overexpression induced c-KIT downregulation in HSPC, inhibiting early erythroid proliferation and differentiation of cells (Spinello *et al.* 2009). Taken together, these findings suggest that regulation of c-KIT expression is mediated by RUNX3 in human HSPC and erythroid development.

Another downregulated RTK by RUNX3 expression in HSPC, AXL was isolated from patients with chronic myelogenous leukaemia and shown to be expressed in CD34⁺ early myeloid progenitors (O'Bryan *et al.* 1991; Neubauer *et al.* 1994). KO mice studies have shown that AXL and Mer RTK, cooperate to regulate erythroid development (Tang *et al.* 2009a), haemostasis, megakaryopoiesis and platelet function (Wang *et al.* 2007). Inhibition of erythropoiesis by loss of AXL and Mer occurred at the transition from erythroid progenitors to proerythroblasts and involved downregulation of GATA-1 and EPO receptor expression (Tang *et al.* 2009a). Therefore, RUNX3-mediated downregulation of AXL expression in HSPC could be implicated in the suppression of erythroid development caused by RUNX3 expression described in 3.3.2.

LMO2 encodes a LIM domain protein that has been found essential for yolk sac erythropoiesis in mice (Warren *et al.* 1994) that was significantly downregulated by RUNX3 expression in HSPC. Loss of function studies in mice and zebrafish have demonstrated important functions for LMO-2 in the establishment of primitive and definitive haematopoiesis during embryonic development (Warren *et al.* 1994; Yamada *et al.* 1998; Patterson *et al.* 2007). Expression of PML-RARA in human HSPC resulted in the suppression of EPO-induced erythroid development by directly targeting LMO-2 repression (Yang *et al.* 2018). Further, LMO-2 was shown to interact with additional TFs, including SCL, LDB1, GATA-1 and E2A, to induce erythroid development by regulating the expression of α -globin genes, GlyA and KLF1 (Wadman *et al.* 1997) (1.1). Overexpression of LMO-2 was able to partially rescue defective erythropoiesis caused by c-MYB loss (Bianchi *et al.* 2010), further highlighting its importance in erythroid development. Lymphoblastic leukaemia 1 (LYL1) was also downregulated by RUNX3 overexpression in HSPC. This TF is

broadly expressed in myeloid and B cell lineages as well as HSC (Souroullas *et al.* 2009), and it is a paralog of the key haematopoietic TF SCL (Chan *et al.* 2007). Loss of function studies showed that LYL1 is involved in erythroid development (Capron *et al.* 2011; Chiu *et al.* 2018). RUNX1 participates in a transcriptional complex important for HSPC function that includes both LMO-2 and LYL1, among other TFs (Wilson *et al.* 2010). RUNX1-ETO was also shown to interact with these TFs in a stable complex identified in t(8;21) cells (Sun *et al.* 2013). Therefore, RUNX3 repression of RUNX1 in HSPC could affect the expression of binding partners LMO-2 and LYL1, and ultimately contribute to the abrogation of erythroid development.

Important cell surface markers associated with erythroid development were downregulated by increased RUNX3 expression in HSPC, namely GlyA and CD36. Reduced levels of RUNX3 in human HSPC were previously shown to inhibit the expression of GlyA and CD36 within the human CMP and MEP compartments (Balogh *et al.* 2020). Conversely, downregulation of CD36 by RUNX3 expression has been previously reported in myeloid cells (Puig-Kroger *et al.* 2006). In terms of myeloid development, RUNX3 overexpression downregulated the expression of CD11b in HSPC. RUNX3 has been found to occupy the genomic loci of *ITGAM* (Dicken *et al.* 2013), and reduced RUNX3 expression was found to upregulate the expression of CD11b in human CMP and MEP (Balogh *et al.* 2020).

Taken together, RUNX3 overexpression in HSPC led to important transcriptional dysregulation of potential erythroid drivers, such as LMO-2 and c-KIT, as well as erythroid cell surface markers, including GlyA and CD36. These findings unveil potential mechanisms behind the RUNX3-induced inhibition of erythropoiesis in HSPC described in 3.3.2.

5.4.3 Potential master regulators cooperating with RUNX3 to induce transcriptional dysregulation in haematopoietic cells

A comprehensive analysis of master regulators and downstream targets is essential for the understanding of leukemogenesis and improvement of current therapies. Most potential upstream gene regulators associated with RUNX3 transcriptional dysregulation are TFs predicted to be inhibited in HSPC (5.3.5). *CBFA2T3* was the most significant master regulator identified by Causal Network Analysis in IPA[®], which is associated with t(16;21) AML (Chyla *et al.* 2008). *CBFA2T3*,

similarly to ETO, is able to recruit corepressors such as N-CoR/SMRT, mSin3A/3B, and HDAC 1, 2 and 3 (Chyla *et al.* 2008). CBFA2T3 KO mice exhibit a bias toward the GM lineage and a reduction in MEP cells (Chyla *et al.* 2008). Furthermore, loss of CBFA2T3 impairs progenitors cell cycle progression accompanied by c-MYC expression (Chyla *et al.* 2008). CBFA2T3 was shown to participate in the Notch regulatory network, and absence of CBFA2T3 in haematopoietic progenitors leads to upregulation of Notch targets HES1 and NOTCH1 expression (Engel *et al.* 2010). Expression of CBFA2T3 is confined to early haematopoiesis (Lindberg *et al.* 2005) and it has been shown to negatively regulate erythropoiesis and megakaryopoiesis by participating in protein complexes containing master regulators of haematopoiesis, such as GATA-1, LDB1, SCL and LMO-2 (Schuh *et al.* 2005; Goardon *et al.* 2006; Meier *et al.* 2006; Cai *et al.* 2009; Soler *et al.* 2010). Some genes downregulated by RUNX3 overexpression in HSPC, such as *ID1*, were also shown to be repressed by CBFA2T3 (Lacombe *et al.* 2010). Furthermore, there are some similarities between the transcriptional dysregulation mediated by RUNX3 expression in HSPC and CBFA2T3 overexpression in K562 cells (Fujiwara *et al.* 2013). Curiously, *RUNX3* and *CBFA2T3* expression are significantly and positively correlated in AML patients according to TCGA dataset (Cancer Genome Atlas Research *et al.* 2013). Along with this correlation, there is also a positive correlation between some clinical attributes, such as cytogenetic risk and FAB, with high CBFA2T3 AML patients being associated with a poor prognosis. Considering the similar transcriptional dysregulation induced by RUNX3 and CBFA2T3 expression in erythropoiesis and their significant correlation in AML patients, RUNX3 and CBFA2T3 might cooperate in leukaemogenesis.

5.4.4 Comparison analysis between RUNX3 and RUNX1-ETO-induced dysregulation of HSPC transcriptome

A comparative analysis between different datasets was performed to investigate the transcriptional dysregulation induced by RUNX3 and RUNX1-ETO expression as single abnormalities in HSPC, which predicted activation of AML signalling in both contexts (5.3.6). This is expected for RUNX1-ETO-expressing cells, as it is a fusion protein resulting from a common translocation in AML patients. In terms of RUNX3, this observation is supportive of a role for RUNX3 in the pathogenesis of AML. Important biological processes including haematopoiesis, platelets function and

cell movement were all predicted to be inhibited in both scenarios, which could explain their association with AML pathogenesis. Furthermore, 38 genes including RUNX3 were commonly dysregulated between datasets, representing only 10% of all DE genes. It is important to consider the caveat of such analysis, with one dataset produced using RNA-seq technology that quantifies the expression of more than 48,000 genes and the other dataset using a microarray chip measuring around 14,500 genes. Comparison between datasets imply that the transcriptional dysregulation caused by RUNX3 and RUNX1-ETO expressions derive from different regulatory mechanisms. Furthermore, 58% of the common genes were dysregulated in opposite directions by RUNX3 and RUNX1-ETO and could therefore be exclusive targets of RUNX1 or RUNX1. Overall, RUNX3 and RUNX1-ETO expression inhibit critical biological processes and have opposite effects in relevant cellular pathways due to potential different mechanisms other than a dominant negative effect over RUNX1.

In summary, increased expression of RUNX3 in human HSPC led to a significant transcriptional repression of genes, which could be explained in part by cross-regulation between the RUNX members. In particular, HSPC and erythroid-related genes were significantly downregulated by RUNX3 expression, including *KIT*, *LMO2* or *HEY1*, which supports previous observations (3.3.2). Furthermore, *CBFA2T3* was predicted to be activated and act as a master regulator in RUNX3-induced transcriptional dysregulation in HSPC, which suggests a possible cooperation between both TFs in the pathogenesis of AML. Lastly, comparison between RUNX3 and RUNX1-ETO-mediated dysregulation of genes in human HSPC suggested distinct regulatory mechanisms, which suggests that downregulation of RUNX3 by RUNX1-ETO is not the main factor behind its disruption of haematopoiesis in human HSPC. Nevertheless, this study determined transcriptional changes in mixed progenitors, and therefore their impact was extrapolated to later phases of development. Transcriptional dysregulation of cell surface markers associated with terminal maturation, such as *GlyA*, could imply that these changes are sustained along differentiation. Taken together, this study provided novel insights into the transcriptional dysregulation mediated by RUNX3 in human HSPC and reinforced its importance in normal haematopoietic development, as well as in other relevant signalling pathways.

6 Conclusion and Future Directions

AML is the most common type of acute leukaemia in adults, with around 3,100 new cases being diagnosed every year in the U.K. (Cancer Research UK 2020). The incidence of AML increases with age, and the five-year relative survival rate is approximately 15% in the U.K. (Cancer Research UK 2020) (1.2). A common abnormality in AML, is the t(8;21) which results in the formation of the RUNX1-ETO fusion protein (1.2.4). Expression of RUNX1-ETO was shown previously to impair myeloid differentiation (Okuda *et al.* 1998; Pabst *et al.* 2001; Cabezas-Wallscheid *et al.* 2013; Regha *et al.* 2015; Nafria *et al.* 2020), and is essential for leukaemic propagation (Heidenreich *et al.* 2003; Martinez *et al.* 2004; Dunne *et al.* 2006; Ptasinska *et al.* 2012; Ptasinska *et al.* 2014) (1.2.4.1). In human HSPC, ectopic expression of RUNX1-ETO was shown to block erythroid and myeloid development, promote their self-renewal, and dysregulate mRNA expression (Mulloy *et al.* 2002; Tonks *et al.* 2003; Tonks *et al.* 2004; Tonks *et al.* 2007). A central mechanism behind such dysregulation arises from perturbations in RUNX1 native function (Meyers *et al.* 1993; Frank *et al.* 1995; Yergeau *et al.* 1997; Okuda *et al.* 1998). Reduced RUNX3 expression levels have previously correlated with CBF leukaemia (1.3.5), but its role in leukaemogenesis is not well defined. Although RUNX3 is known to be expressed in immune cells where it plays an important role (1.4.1), it is still the least studied member of its family and its function in haematopoiesis has been mainly studied using non-human models. The findings of this study are summarised in [Figure 6-1](#).

This study examined the association between *RUNX3* mRNA expression and AML pathogenesis and showed that *RUNX3* mRNA expression is highly variable between different AML subtypes (4.3.2). Downregulation of *RUNX3* was observed in prognostically favourable t(8;21) and inv(16) AML, whereas *RUNX3* upregulation was observed in patients with complex cytogenetics which are associated with a poor outcome ([Figure 6-1](#)). Indeed, *RUNX3* expression has been previously found repressed in CBF AML (Cheng *et al.* 2008b) or increased expression associated with a shortened EFS in childhood AML (Lacayo *et al.* 2004; Cheng *et al.* 2008b). These results are supported by several gene expression profiling of AML samples (Debernardi *et al.* 2003; Gutierrez *et al.* 2005; Sun *et al.* 2007; Cheng *et al.* 2008b), demonstrating the prognostic value for *RUNX3* expression in this malignancy.

In normal haematopoiesis, RUNX3 is expressed in haematopoietic cells of different lineages (Meyers *et al.* 1996; Le *et al.* 1999; Levanon *et al.* 2001a; Taniuchi *et al.* 2002; Puig-Kroger *et al.* 2003; Woolf *et al.* 2003; Fainaru *et al.* 2004). Initially, this study sought to determine the role of RUNX3 expression on the normal development of erythroid cells using a human primary HSPC model. *RUNX3* mRNA expression was shown to gradually decrease as human HSPC cells mature into erythrocytes (3.3.1). A similar expression pattern was previously shown for *RUNX1* where in adult mice its expression is gradually reduced following proerythroblast development (Lorsbach *et al.* 2004; North *et al.* 2004). KD of RUNX3 significantly impaired erythroid colony formation but had little effect on the self-renewal potential of these cells (3.3.3.2). Furthermore, no significant changes were observed during erythroid growth and differentiation of RUNX3 KD cells, which managed to complete their terminal maturation. Recently, human HSPC were shown to be influenced by RUNX3 expression, with its KD disrupting the normal programme of erythroid differentiation (Balogh *et al.* 2020). However, this study only assessed the impact of RUNX3 KD in erythropoiesis for three days and was solely based on one RUNX3 shRNA clone. Redundancy between RUNX1 and RUNX3 expression could help explain the full maturation of RUNX3 KD erythroid cells (Brady and Farrell 2009; Wong *et al.* 2011; Yokomizo-Nakano *et al.* 2020). The combined loss of RUNX1 and RUNX3 in mice blocked erythroid differentiation. (Wang *et al.* 2014a). Together, these results suggest that KD of RUNX3 affects the proliferative capacity and survival of erythroid cells, with cells attaining terminal maturation in the presence of EPO (Figure 6-1).

Given that increased RUNX3 levels are associated with a significant proportion of AML patients (see above), this study overexpressed RUNX3 as a single abnormality in CB derived CD34⁺ HSPC and determined its effects on erythroid growth and development. Under clonal conditions, erythroid-committed cells exhibited a significant inhibition of colony formation ability coupled with increased self-renewal of progenitor cells (3.3.2.2). In bulk liquid culture, and in the absence of EPO, RUNX3 expression induced a delay in erythroid development (3.3.2.3). Upon culture with EPO, RUNX3-expressing cells overcame the early growth suppression and proliferated more than controls, a behaviour associated with immature cells, failing to terminally differentiate. Further RNA-seq studies showed that RUNX3 overexpression significantly downregulated erythroid-related genes, including *KIT* and *LMO2* as

developmental drivers, and *GYPA* and *CD36* as developmental markers (5.3.4). Some of these genes have been shown to be directly targeted by RUNX3 (e.g. *CD36*) (Puig-Kroger *et al.* 2006). The importance of RUNX proteins in erythroid development has been previously shown in RUNX1 KD mice which exhibit defects in primitive and definitive erythropoiesis (Okuda *et al.* 1996; Wang *et al.* 1996a; Yokomizo *et al.* 2008; Ghanem *et al.* 2018). Considering the cross-regulation between RUNX genes (5.3.4), and the similar erythroid developmental block induced by RUNX1-ETO (Tonks *et al.* 2003), downregulation of RUNX1 by RUNX3 in human HSPC could also contribute to these observations. Together, these findings suggest that downregulation of RUNX3 during erythropoiesis is important for the normal development of cells. Furthermore, the ability of RUNX3 overexpression to inhibit differentiation and promote self-renewal (albeit in erythroid cells) would suggest that RUNX3 could be a driver of leukaemogenesis.

Chapter 4 focused on the relevance of RUNX3 expression and its dysregulation during myeloid development. Analysis of transcriptomic data revealed that *RUNX3* mRNA expression is sustained in HSPC and early myeloid progenitors (4.3.1). Mature monocytes showed upregulation of *RUNX3*, whereas granulocytic cells exhibited a reduction in *RUNX3* levels. *RUNX3* upregulation has been shown during monocytic differentiation to either macrophages or DC (Fainaru *et al.* 2004; Sanchez-Martin *et al.* 2011; Estecha *et al.* 2012). These findings suggest that *RUNX3* expression is downregulated during myeloid development, with important roles in macrophage and DC differentiation. *RUNX3* KD failed to significantly impact myeloid growth and development of HSPC (4.3.4). These data are supported by previous observations showing that *RUNX3* deficiency in HSPC does not affect myeloid growth and colony formation as opposed to erythroid development (Balogh *et al.* 2020). Functional redundancy with *RUNX1* could explain these results, as loss of both *RUNX1* and *RUNX3* expression has been shown to suppress granulopoiesis at a relatively late stage of development in mice (Wang *et al.* 2014a). Overall, these data suggest that, similarly to erythropoiesis, reduced expression of *RUNX3* does not impair the myeloid development of HSPC (Figure 6-1).

The impact of *RUNX3* overexpression on myeloid development was determined in human HSPC under clonal conditions and bulk liquid culture. *RUNX3*-expressing cells formed significantly less myeloid colonies than controls (4.3.3.1). In

bulk liquid culture, RUNX3 overexpression resulted in slower growth of myeloid (granulocytic) cells (4.3.3.2) and perturbed the normal myeloid differentiation programme (4.3.3.3). RNA-seq data showed a significant downregulation of CD11b by RUNX3-expressing HSPC (5.3.4), which is explained by previous observations showing that RUNX3 occupies the genomic loci of *ITGAM* (Dicken *et al.* 2013). *PDPK1* (encoding PDK1 protein) was the most significantly dysregulated gene by RUNX3 overexpression in HSPC. Considering that PDK1 expression has been found important for haematopoietic development (Bone and Welham 2007; Pearn *et al.* 2007), loss of PDK1 in RUNX3-expressing cells could be a factor influencing myelopoiesis. Furthermore, a similar disruption of myeloid differentiation has been shown previously in RUNX1-ETO-expressing cells, characterised by selective inhibition of granulocytic colony formation and delayed CD11b and CD15 upregulation in human HSPC (Tonks *et al.* 2004). Given that RUNX1-ETO has a dominant negative effect over RUNX1 native function, RUNX3-mediated loss of RUNX1 could also contribute to the observed phenotype (5.3.4). RUNX1 deficiency was found to substantially inhibit the growth and myeloid differentiation of CB derived HSPC, while its expression showed opposite effects (Goyama *et al.* 2013). RUNX1 mutations lead to a similar inhibition of granulocytic development in human *in vitro* cell models (Gerritsen *et al.* 2019). Overall, RUNX3 expression inhibits both monocytic and granulocytic differentiation, and together with the effects on erythropoiesis show that RUNX3 overexpression might be involved in AML pathogenesis (Figure 6-1).

To determine the importance of RUNX3 downregulation to the pathogenesis of t(8;21) AML, RUNX3 was overexpressed in RUNX1-ETO transduced HSPC. Under clonal conditions, RUNX3 overexpression failed to rescue the colony forming ability of erythroid and myeloid cells expressing RUNX1-ETO (4.3.5.3). In bulk liquid culture, a similar situation was observed with RUNX3 failing to rescue phenotypic changes induced by RUNX1-ETO during myeloid development (4.3.5.4). For both monocytic and granulocytic cells, RUNX3 expression did not rescue the negative impact of RUNX1-ETO in CD11b upregulation, which is explained by the fact that CD11b itself is a putative target of RUNX3 (Dicken *et al.* 2013) (5.3.4). Morphology examination supported the previous findings, though RUNX3 overexpression favoured changes associated with intermediate to later stages of development in RUNX1-ETO cells. Together, these data failed to support a significant role for RUNX3 in RUNX1-ETO

leukaemogenesis, with the caveat that RUNX3 overexpression in these cells might have missed the ideal balance to counteract the negative effects of RUNX1-ETO (Figure 6-1). Overall, this study reinforces the involvement of RUNX3 in human haematopoiesis and highlights the association between increased RUNX3 expression and leukaemogenesis.

To investigate the RUNX3-mediated transcriptional dysregulation in human HSPC that could explain the suppression of both erythroid and myeloid development by RUNX3 in these cells, RNA-seq was performed in Chapter 5. RUNX3 overexpression was shown to primarily repress the expression of genes, with immune responses, cell signalling and communication, and cell movement being significantly associated with these changes (5.3.3.3). Furthermore, significant changes were observed in the expression of *RUNX1* or *KIT* (5.3.4), supporting the RUNX3-mediated inhibition of both erythroid and myeloid development (3.3.2, 4.3.3). Furthermore, pathway analysis suggested CBFA2T3 as a potential upstream regulator of RUNX3-induced transcriptional changes in HSPC (5.3.5). Considering the similarities between RUNX3 and CBFA2T3 transcriptional dysregulation (Lacombe *et al.* 2010; Fujiwara *et al.* 2013), and their significant co-expression in AML patients (Cancer Genome Atlas Research *et al.* 2013), CBFA2T3 could be associated with RUNX3 expression in the pathogenesis of AML. Further comparison between RUNX3 overexpression and KD datasets in human HSPC identified potential downstream targets of RUNX3, such as *CCL2* (5.3.6.1). Transcriptional dysregulation imposed by RUNX3 or RUNX1-ETO expression in HSPC was also compared and suggested different deregulatory mechanism of important cell functions and pathways (5.3.6.2). Taken together, transcriptomic analysis highlights the important role of RUNX3 in human haematopoiesis, unveiling the main pathways and genes dysregulated by RUNX3 in HSPC (Figure 6-1).

In conclusion, this study showed the importance of RUNX3 downregulation during the normal programme of erythroid and myeloid development of human HSPC. Increased RUNX3 expression was shown to inhibit erythroid, monocytic and granulocytic differentiation of cells. On the other hand, reduced expression of RUNX3 failed to induce significant effects on cell differentiation, but survival was negatively impacted by RUNX3 KD in erythroid cells. This study also provided mechanistical insights into the RUNX3-mediated inhibition of haematopoietic development by

unveiling a significant dysregulation of HSPC transcriptome. Lastly, no significant evidence was obtained to support an important role for RUNX3 downregulation in RUNX1-ETO leukaemia.

6.1 Future directions

Although CBF AML is associated with a good prognosis, standard chemotherapy with high dose cytarabine combined with an anthracycline account for only 40 to 60% CR of these patients (Sinha *et al.* 2015). Treatment of CBF AML has remained unchanged for many years, and therefore further studies are needed to develop new therapies that ultimately improve the cure rate in these patients. As future work, additional experimental repeats should be performed for the study of RUNX3 re-expression in RUNX1-ETO transduced HSPC to determine whether there is a significant contribution of RUNX3 downregulation to RUNX1-ETO leukemogenesis. CHIP-seq analysis in these cells would determine chromatin co-occupancy of RUNX3 and RUNX1-ETO. Furthermore, RUNX3 KD in RUNX1-ETO-expressing cells should be pursued to assess its functional requirement in t(8;21) AML. Considering that RUNX3 expression is also repressed in inv(16) AML, similar studies should be performed in this context.

Given the functional redundancy between RUNX1 and RUNX3, analysis of RUNX1 targets should be performed to elucidate whether the changes observed are induced exclusively by RUNX3 or by interfering with RUNX1 native function. Previous studies have focused on the analysis of RUNX3 direct targets by ChIP-seq in T and NK cells, as well as DC (Yagi *et al.* 2010; Dicken *et al.* 2013; Lotem *et al.* 2013; Levanon *et al.* 2014; Hantisteanu *et al.* 2020). A recent study performed ChIP-seq analysis in murine HSPC overexpressing RUNX3 in the absence of TET2 to induce a MDS phenotype (Yokomizo-Nakano *et al.* 2020), but no study in human HSPC has been performed. ChIP-seq analysis will identify genomic-wide target sites for RUNX3, which would allow a more comprehensive study of RUNX3-mediated transcriptional regulation in these cells. Moreover, complete ablation of RUNX3 expression by using CRISPR-Cas9-gRNA system in human HSPC and AML cells would fully assess the impact of RUNX3 deficiency in haematopoietic development and leukaemic growth and survival.

Lastly, dysregulated genes by RUNX3 overexpression in HSPC significantly associated with RUNX3 levels in AML patients, such as *LTB* or *FUT7*, should be further explored to help elucidate the mechanism behind the possible contribution of RUNX3 to leukaemogenesis (5.3.7). Both genes were upregulated by RUNX3 in HSPC and downregulated by RUNX1-ETO in HSPC and in t(8;21) AML (Cancer Genome Atlas Research *et al.* 2013), which have reduced *RUNX3* levels. Furthermore, *LTB* and *FUT7* have been previously implicated as oncogenes in different types of cancer (Lukashev *et al.* 2006; Fernandes *et al.* 2015; Das *et al.* 2019; Jassam *et al.* 2019; Liu *et al.* 2019; Dai *et al.* 2020).

TCGA AML dataset

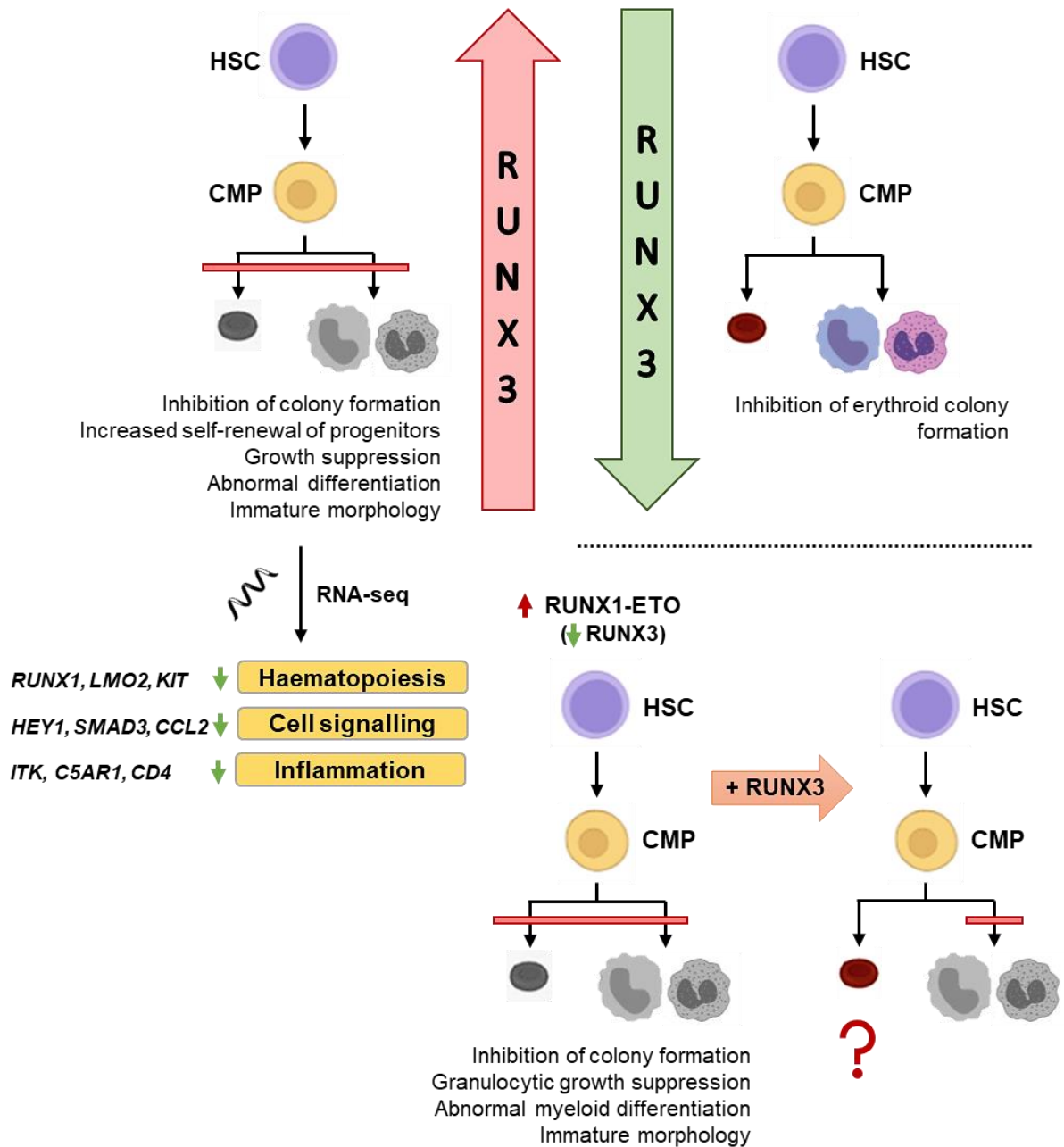
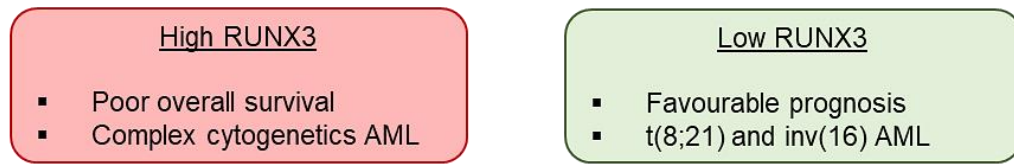
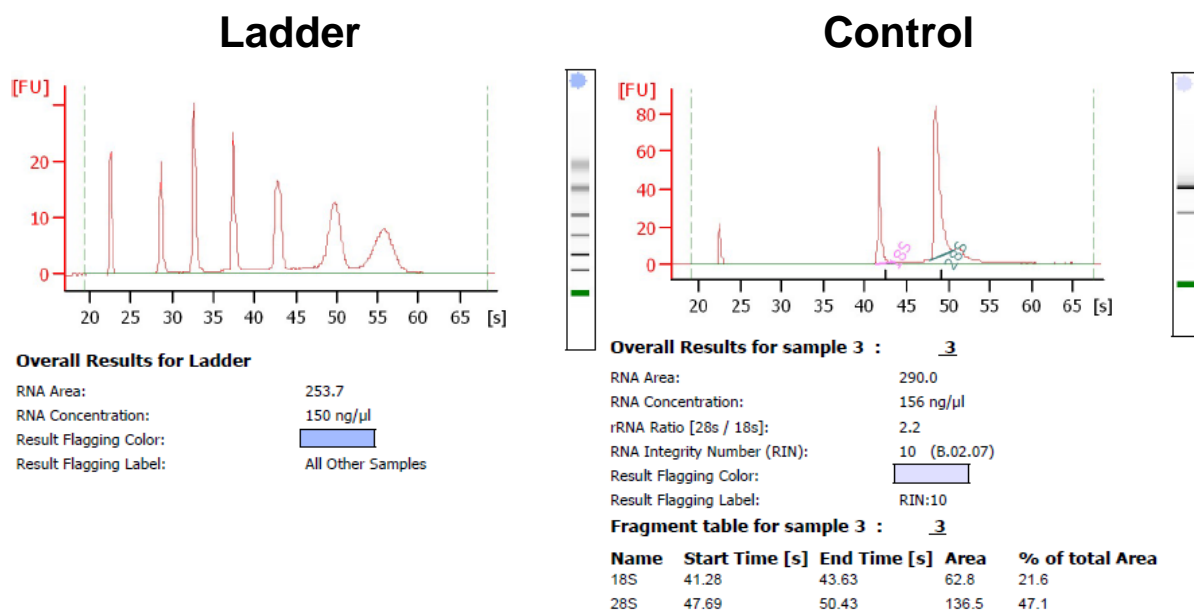


Figure 6-1 – Graphical abstract summarising the main findings on the role of RUNX3 in normal human haematopoietic development and AML.

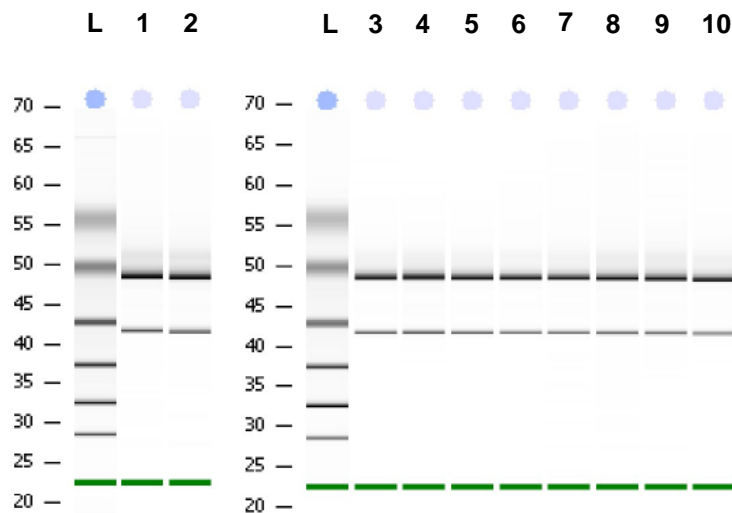
TCGA – The Cancer Genome Atlas Program (Cancer Genome Atlas Research *et al.* 2013); HSC – Haematopoietic stem cells; CMP – Common myeloid progenitor. The question mark represents unconfirmed effects by RUNX3 overexpression in RUNX1-ETO cells.

Appendix

A



B



Appendix 1– High quality total RNA was successfully extracted from control and RUNX3 HSPC.

(A) Representative electropherograms for the RNA ladder and control sample (Control 1) obtained using Agilent 2100 Bioanalyzer. Data is summarised in [Table 5-1](#). **(B)** Example densitometry plots (gel-like images) for the RNA ladder and 10 experimental samples. L – Ladder; Samples #1, 3, 5, 7 and 9 – Control HSPC; Samples #2, 4, 6, 8, 10 – RUNX3 overexpressing HSPC.

Appendix 2– Top 50 genes dysregulated by RUNX3 overexpression in human HSPC.

Summary data of the 50 most dysregulated genes in HSPC as a result of increased RUNX3 expression. Values are expressed as the logarithmic (base 2) fold change of differentially expressed genes compared to control with the respective adjusted p-value (padj). A negative log₂FC value represents downregulation (green shade), whereas a positive value represents upregulation (red shade). Ensembl ID is a unique number assigned to each gene according to the Ensembl database (www.ensembl.org).

Ensembl ID	Gene symbol	Log ₂ FC	padj
ENSG00000140992	<i>PDPK1</i>	-2.34	1.63E-40
ENSG00000133636	<i>NTS</i>	-2.05	1.85E-23
ENSG00000111796	<i>KLRB1</i>	2.01	3.25E-20
ENSG00000099139	<i>PCSK5</i>	1.97	3.60E-27
ENSG00000164683	<i>HEY1</i>	-1.83	1.42E-16
ENSG00000197405	<i>C5AR1</i>	-1.82	2.24E-27
ENSG00000128918	<i>ALDH1A2</i>	-1.79	5.12E-26
ENSG00000020633	<i>RUNX3</i>	1.71	1.85E-28
ENSG00000169896	<i>ITGAM</i>	-1.68	5.86E-36
ENSG00000148468	<i>FAM171A1</i>	-1.65	6.41E-15
ENSG00000167580	<i>AQP2</i>	-1.56	1.79E-12
ENSG00000181577	<i>C6orf223</i>	-1.50	8.70E-13
ENSG00000174358	<i>SLC6A19</i>	-1.49	1.06E-10
ENSG00000164199	<i>ADGRV1</i>	-1.46	8.27E-12
ENSG00000140279	<i>DUOX2</i>	-1.44	5.42E-10
ENSG00000134830	<i>C5AR2</i>	-1.43	4.70E-13
ENSG00000115523	<i>GNLY</i>	1.41	8.97E-10
ENSG00000083454	<i>P2RX5</i>	-1.41	2.68E-10
ENSG00000131409	<i>LRRC4B</i>	-1.39	1.21E-10
ENSG00000205918	<i>PDPK2P</i>	-1.36	5.22E-09
ENSG00000136040	<i>PLXNC1</i>	-1.35	4.71E-11
ENSG00000156966	<i>B3GNT7</i>	1.32	3.34E-11
ENSG00000198400	<i>NTRK1</i>	-1.32	9.79E-12
ENSG00000105509	<i>HAS1</i>	-1.31	3.16E-08
ENSG00000116833	<i>NR5A2</i>	-1.30	3.79E-08
ENSG00000138135	<i>CH25H</i>	-1.27	4.48E-08
ENSG00000145916	<i>RMND5B</i>	-1.27	5.70E-21
ENSG00000147081	<i>AKAP4</i>	-1.27	7.17E-08
ENSG00000122641	<i>INHBA</i>	-1.26	2.72E-08
ENSG00000079257	<i>LXN</i>	-1.25	2.76E-09
ENSG00000249992	<i>TMEM158</i>	-1.23	2.18E-07
ENSG00000111261	<i>MANSC1</i>	-1.20	1.03E-07
ENSG00000124212	<i>PTGIS</i>	1.20	5.10E-07

ENSG00000152377	<i>SPOCK1</i>	-1.19	2.90E-07
ENSG00000179604	<i>CDC42EP4</i>	-1.18	1.73E-09
ENSG00000100351	<i>GRAP2</i>	-1.17	4.30E-15
ENSG00000166949	<i>SMAD3</i>	-1.17	3.67E-25
ENSG00000137491	<i>SLCO2B1</i>	-1.16	1.22E-06
ENSG00000108691	<i>CCL2</i>	-1.15	2.50E-14
ENSG00000010610	<i>CD4</i>	-1.14	2.21E-07
ENSG00000120875	<i>DUSP4</i>	1.12	8.38E-10
ENSG00000092068	<i>SLC7A8</i>	-1.12	2.36E-08
ENSG00000075391	<i>RASAL2</i>	-1.12	7.05E-10
ENSG00000150510	<i>FAM124A</i>	-1.11	1.59E-06
ENSG00000101298	<i>SNPH</i>	-1.11	5.91E-06
ENSG00000162378	<i>ZYG11B</i>	-1.11	5.59E-18
ENSG00000116962	<i>NID1</i>	-1.10	2.78E-06
ENSG00000182580	<i>EPHB3</i>	1.08	5.56E-06
ENSG00000196220	<i>SRGAP3</i>	1.07	3.56E-06
ENSG00000127329	<i>PTPRB</i>	-1.06	2.12E-05

References

Adelman, C. A., Chattopadhyay, S. and Bieker, J. J. (2002). The BMP/BMPR/Smad pathway directs expression of the erythroid-specific EKLF and GATA1 transcription factors during embryoid body differentiation in serum-free media. *Development* **129**(2):539-549.

Afzali, B., Mitchell, P. J., Edozie, F. C., Povoleri, G. A., Dowson, S. E., Demandt, L. *et al.* (2013). CD161 expression characterizes a subpopulation of human regulatory T cells that produces IL-17 in a STAT3-dependent manner. *Eur J Immunol* **43**(8):2043-2054.

Ahn, E. Y., Yan, M., Malakhova, O. A., Lo, M. C., Boyapati, A., Ommen, H. B. *et al.* (2008). Disruption of the NHR4 domain structure in AML1-ETO abrogates SON binding and promotes leukemogenesis. *Proceedings of the National Academy of Sciences of the United States of America* **105**(44):17103-17108.

Aho, T. L., Sandholm, J., Peltola, K. J., Ito, Y. and Koskinen, P. J. (2006). Pim-1 kinase phosphorylates RUNX family transcription factors and enhances their activity. *Bmc Cell Biology* **7**.

Aikawa, Y., Nguyen, L. A., Isono, K., Takakura, N., Tagata, Y., Schmitz, M. L. *et al.* (2006). Roles of HIPK1 and HIPK2 in AML1- and p300-dependent transcription, hematopoiesis and blood vessel formation. *EMBO J* **25**(17):3955-3965.

Akagi, T., Thoennissen, N. H., George, A., Crooks, G., Song, J. H., Okamoto, R. *et al.* (2010). In vivo deficiency of both C/EBPbeta and C/EBPepsilon results in highly defective myeloid differentiation and lack of cytokine response. *PLoS One* **5**(11):e15419.

Akashi, K., Traver, D., Miyamoto, T. and Weissman, I. L. (2000). A clonogenic common myeloid progenitor that gives rise to all myeloid lineages. *Nature* **404**(6774):193-197.

Akech, J., Wixted, J. J., Bedard, K., van der Deen, M., Hussain, S., Guise, T. A. *et al.* (2010). Runx2 association with progression of prostate cancer in patients: mechanisms mediating bone osteolysis and osteoblastic metastatic lesions. *Oncogene* **29**(6):811-821.

Albanese, C., D'Amico, M., Reutens, A. T., Fu, M., Watanabe, G., Lee, R. J. *et al.* (1999). Activation of the cyclin D1 gene by the E1A-associated protein p300 through AP-1 inhibits cellular apoptosis. *J Biol Chem* **274**(48):34186-34195.

Alberti, L., Carniti, C., Miranda, C., Roccatò, E. and Pierotti, M. A. (2003). RET and NTRK1 proto-oncogenes in human diseases. *J Cell Physiol* **195**(2):168-186.

Alexander, W. S., Roberts, A. W., Nicola, N. A., Li, R. and Metcalf, D. (1996). Deficiencies in progenitor cells of multiple hematopoietic lineages and defective megakaryocytopoiesis in mice lacking the thrombopoietic receptor c-Mpl. *Blood* **87**(6):2162-2170.

Almotiri, A., Alzahrani, H., Menendez-Gonzalez, J. B., Abdelfattah, A., Alotaibi, B., Saleh, L. *et al.* (2021). Zeb1 modulates hematopoietic stem cell fates required for suppressing acute myeloid leukemia. *J Clin Invest* **131**(1).

Alsuliman, A., Muftuoglu, M., Khoder, A., Ahn, Y. O., Basar, R., Verneris, M. R. *et al.* (2017). A subset of virus-specific CD161(+) T cells selectively express the multidrug transporter MDR1 and are resistant to chemotherapy in AML. *Blood* **129**(6):740-758.

Alter, B. P., Giri, N., Savage, S. A., Peters, J. A., Loud, J. T., Leathwood, L. *et al.* (2010). Malignancies and survival patterns in the National Cancer Institute inherited bone marrow failure syndromes cohort study. *Br J Haematol* **150**(2):179-188.

Amann, J. M., Nip, J., Strom, D. K., Lutterbach, B., Harada, H., Lenny, N. *et al.* (2001). ETO, a target of t(8;21) in acute leukemia, makes distinct contacts with multiple histone deacetylases and binds mSin3A through its oligomerization domain. *Mol Cell Biol* **21**(19):6470-6483.

Ameur, A., Zaghlool, A., Halvardson, J., Wetterbom, A., Gyllenstein, U., Cavelier, L. *et al.* (2011). Total RNA sequencing reveals nascent transcription and widespread co-transcriptional splicing in the human brain. *Nat Struct Mol Biol* **18**(12):1435-1440.

Andersson, A., Eden, P., Olofsson, T. and Fioretos, T. (2010). Gene expression signatures in childhood acute leukemias are largely unique and distinct from those of normal tissues and other malignancies. *BMC Med Genomics* **3**:6.

Arai, F., Hirao, A., Ohmura, M., Sato, H., Matsuoka, S., Takubo, K. *et al.* (2004). Tie2/angiopoietin-1 signaling regulates hematopoietic stem cell quiescence in the bone marrow niche. *Cell* **118**(2):149-161.

Arber, D. A., Orazi, A., Hasserjian, R., Thiele, J., Borowitz, M. J., Le Beau, M. M. *et al.* (2016). The 2016 revision to the World Health Organization classification of myeloid neoplasms and acute leukemia. *Blood* **127**(20):2391-2405.

Arinobu, Y., Mizuno, S., Chong, Y., Shigematsu, H., Iino, T., Iwasaki, H. *et al.* (2007). Reciprocal activation of GATA-1 and PU.1 marks initial specification of hematopoietic stem cells into myeloerythroid and myelolymphoid lineages. *Cell Stem Cell* **1**(4):416-427.

Arnaud, L., Saison, C., Helias, V., Lucien, N., Steschenko, D., Giarratana, M. C. *et al.* (2010). A dominant mutation in the gene encoding the erythroid transcription factor KLF1 causes a congenital dyserythropoietic anemia. *Am J Hum Genet* **87**(5):721-727.

Assi, S. A., Imperato, M. R., Coleman, D. J. L., Pickin, A., Potluri, S., Ptasinska, A. *et al.* (2019). Subtype-specific regulatory network rewiring in acute myeloid leukemia. *Nature Genetics* **51**(1):151-162.

Bacher, U., Shumilov, E., Flach, J., Porret, N., Joncourt, R., Wiedemann, G. *et al.* (2018). Challenges in the introduction of next-generation sequencing (NGS) for diagnostics of myeloid malignancies into clinical routine use. *Blood Cancer J* **8**(11):113.

Back, J., Allman, D., Chan, S. and Kastner, P. (2005). Visualizing PU.1 activity during hematopoiesis. *Exp Hematol* **33**(4):395-402.

Bae, S. C. and Lee, Y. H. (2006). Phosphorylation, acetylation and ubiquitination: The molecular basis of RUNX regulation. *Gene* **366**(1):58-66.

Bae, S. C., Ogawa, E., Maruyama, M., Oka, H., Satake, M., Shigesada, K. *et al.* (1994). PEBP2 alpha B/mouse AML1 consists of multiple isoforms that possess differential transactivation potentials. *Mol Cell Biol* **14**(5):3242-3252.

Bagchi, A. and Mills, A. A. (2008). The quest for the 1p36 tumor suppressor. *Cancer Res* **68**(8):2551-2556.

Bagger, F. O., Kinalis, S. and Rapin, N. (2019). BloodSpot: a database of healthy and malignant haematopoiesis updated with purified and single cell mRNA sequencing profiles. *Nucleic Acids Res* **47**(D1):D881-D885.

Balogh, P., Adelman, E. R., Pluvinage, J. V., Capaldo, B. J., Freeman, K. C., Singh, S. *et al.* (2020). RUNX3 levels in human hematopoietic progenitors are regulated by aging and dictate erythroid-myeloid balance. *Haematologica* **105**(4):905-913.

Bangsow, C., Rubins, N., Glusman, G., Bernstein, Y., Negreanu, V., Goldenberg, D. *et al.* (2001). The RUNX3 gene - sequence, structure and regulated expression. *Gene* **279**(2):221-232.

Baracho, G. V., Cato, M. H., Zhu, Z., Jaren, O. R., Hobeika, E., Reth, M. *et al.* (2014). PDK1 regulates B cell differentiation and homeostasis. *Proc Natl Acad Sci U S A* **111**(26):9573-9578.

Basecke, J., Schwieger, M., Griesinger, F., Schiedlmeier, B., Wulf, G., Trumper, L. *et al.* (2005). AML1/ETO promotes the maintenance of early hematopoietic progenitors in NOD/SCID mice but does not abrogate their lineage specific differentiation. *Leukemia & Lymphoma* **46**(2):265-272.

Bashamboo, A., Taylor, A. H., Samuel, K., Panthier, J. J., Whetton, A. D. and Forrester, L. M. (2006). The survival of differentiating embryonic stem cells is dependent on the SCF-KIT pathway. *J Cell Sci* **119**(Pt 15):3039-3046.

Bassi, S. C. and Rego, E. M. (2012). Molecular basis for the diagnosis and treatment of acute promyelocytic leukemia. *Rev Bras Hematol Hemoter* **34**(2):134-139.

Bauer, O., Sharir, A., Kimura, A., Hantisteanu, S., Takeda, S. and Groner, Y. (2015). Loss of Osteoblast Runx3 Produces Severe Congenital Osteopenia. *Molecular and Cellular Biology* **35**(7):1097-1109.

Baum, C. M., Weissman, I. L., Tsukamoto, A. S., Buckle, A. M. and Peault, B. (1992). Isolation of a candidate human hematopoietic stem-cell population. *Proc Natl Acad Sci U S A* **89**(7):2804-2808.

Begley, C. G., Aplan, P. D., Davey, M. P., Nakahara, K., Tchorz, K., Kurtzberg, J. *et al.* (1989). Chromosomal translocation in a human leukemic stem-cell line disrupts the T-cell antigen receptor delta-chain diversity region and results in a previously unreported fusion transcript. *Proc Natl Acad Sci U S A* **86**(6):2031-2035.

Behrens, K., Triviai, I., Schwieger, M., Tekin, N., Alawi, M., Spohn, M. *et al.* (2016). Runx1 downregulates stem cell and megakaryocytic transcription programs that support niche interactions. *Blood* **127**(26):3369-3381.

Ben-Ami, O., Friedman, D., Leshkowitz, D., Goldenberg, D., Orlovsky, K., Pencovich, N. *et al.* (2013). Addiction of t(8;21) and inv(16) Acute Myeloid Leukemia to Native RUNX1. *Cell Reports* **4**(6):1131-1143.

Bennett, J. M., Catovsky, D., Daniel, M. T., Flandrin, G., Galton, D. A., Gralnick, H. R. *et al.* (1976). Proposals for the classification of the acute leukaemias. French-American-British (FAB) co-operative group. *Br J Haematol* **33**(4):451-458.

Bernitz, J. M., Kim, H. S., MacArthur, B., Sieburg, H. and Moore, K. (2016). Hematopoietic Stem Cells Count and Remember Self-Renewal Divisions. *Cell* **167**(5):1296-1309 e1210.

Bhatnagar, N., Nizery, L., Tunstall, O., Vyas, P. and Roberts, I. (2016). Transient Abnormal Myelopoiesis and AML in Down Syndrome: an Update. *Curr Hematol Malign Rep* **11**(5):333-341.

Bianchi, E., Zini, R., Salati, S., Tenedini, E., Norfo, R., Tagliafico, E. *et al.* (2010). c-myb supports erythropoiesis through the transactivation of KLF1 and LMO2 expression. *Blood* **116**(22):e99-110.

Biggs, J. R., Peterson, L. F., Zhang, Y., Kraft, A. S. and Zhang, D. E. (2006). AML1/RUNX1 phosphorylation by cyclin-dependent kinases regulates the degradation of AML1/RUNX1 by the anaphase-promoting complex. *Mol Cell Biol* **26**(20):7420-7429.

Bledsoe, K. L., McGee-Lawrence, M. E., Camilleri, E. T., Wang, X. K., Riester, S. M., van Wijnen, A. J. *et al.* (2014). RUNX3 Facilitates Growth of Ewing Sarcoma Cells. *Journal of Cellular Physiology* **229**(12):2049-2056.

Blumenthal, E., Greenblatt, S., Huang, G., Ando, K., Xu, Y. and Nimer, S. D. (2017). Covalent Modifications of RUNX Proteins: Structure Affects Function. *Runx Proteins in Development and Cancer* **962**:33-44.

Blyth, K., Cameron, E. R. and Neil, J. C. (2005). The RUNX genes: Gain or loss of function in cancer. *Nature Reviews Cancer* **5**(5):376-387.

Boehm, T., Feroni, L., Kaneko, Y., Perutz, M. F. and Rabbitts, T. H. (1991). The rhombotin family of cysteine-rich LIM-domain oncogenes: distinct members are involved in T-cell translocations to human chromosomes 11p15 and 11p13. *Proc Natl Acad Sci U S A* **88**(10):4367-4371.

Boissel, N., Leroy, H., Brethon, B., Philippe, N., de Botton, S., Auvrignon, A. *et al.* (2006). Incidence and prognostic impact of c-Kit, FLT3, and Ras gene mutations in core binding factor acute myeloid leukemia (CBF-AML). *Leukemia* **20**(6):965-970.

Bone, H. K. and Welham, M. J. (2007). Phosphoinositide 3-kinase signalling regulates early development and developmental haemopoiesis. *J Cell Sci* **120**(Pt 10):1752-1762.

Bonnet, D. and Dick, J. E. (1997). Human acute myeloid leukemia is organized as a hierarchy that originates from a primitive hematopoietic cell. *Nat Med* **3**(7):730-737.

Bosma, G. C., Custer, R. P. and Bosma, M. J. (1983). A severe combined immunodeficiency mutation in the mouse. *Nature* **301**(5900):527-530.

Brady, G. and Farrell, P. J. (2009). RUNX3-Mediated Repression of RUNX1 in B Cells. *Journal of Cellular Physiology* **221**(2):283-287.

Brady, G., Whiteman, H. J., Spender, L. C. and Farrell, P. J. (2009). Downregulation of RUNX1 by RUNX3 Requires the RUNX3 VWRPY Sequence and Is Essential for Epstein-Barr Virus-Driven B-Cell Proliferation. *Journal of Virology* **83**(13):6909-6916.

Bravo, J., Li, Z., Speck, N. A. and Warren, A. J. (2001). The leukemia-associated AML1 (Runx1)--CBF beta complex functions as a DNA-induced molecular clamp. *Nat Struct Biol* **8**(4):371-378.

Brenner, O., Levanon, D., Negreanu, V., Golubkov, O., Fainaru, O., Woolf, E. *et al.* (2004). Loss of Runx3 function in leukocytes is associated with spontaneously developed colitis and gastric mucosal hyperplasia. *Proceedings of the National Academy of Sciences of the United States of America* **101**(45):16016-16021.

Bromberg, O., Frisch, B. J., Weber, J. M., Porter, R. L., Civitelli, R. and Calvi, L. M. (2012). Osteoblastic N-cadherin is not required for microenvironmental support and regulation of hematopoietic stem and progenitor cells. *Blood* **120**(2):303-313.

Broudy, V. C. (1997). Stem Cell Factor and Hematopoiesis. *Blood* **90**(4):1345-1364.

Bruns, I., Lucas, D., Pinho, S., Ahmed, J., Lambert, M. P., Kunisaki, Y. *et al.* (2014). Megakaryocytes regulate hematopoietic stem cell quiescence through CXCL4 secretion. *Nat Med* **20**(11):1315-1320.

Buenrostro, J. D., Corces, M. R., Lareau, C. A., Wu, B., Schep, A. N., Aryee, M. J. *et al.* (2018). Integrated Single-Cell Analysis Maps the Continuous Regulatory Landscape of Human Hematopoietic Differentiation. *Cell* **173**(6):1535-1548 e1516.

Buitenhuis, M., van Deutekom, H. W., Verhagen, L. P., Castor, A., Jacobsen, S. E., Lammers, J. W. *et al.* (2005). Differential regulation of granulopoiesis by the basic helix-loop-helix transcriptional inhibitors Id1 and Id2. *Blood* **105**(11):4272-4281.

Burnett, A., Wetzler, M. and Lowenberg, B. (2011). Therapeutic advances in acute myeloid leukemia. *J Clin Oncol* **29**(5):487-494.

Burnett, A. K., Milligan, D., Prentice, A. G., Goldstone, A. H., McMullin, M. F., Hills, R. K. *et al.* (2007). A comparison of low-dose cytarabine and hydroxyurea with or without all-trans retinoic acid for acute myeloid leukemia and high-risk myelodysplastic syndrome in patients not considered fit for intensive treatment. *Cancer* **109**(6):1114-1124.

Burnett, A. K., Russell, N. H., Hills, R. K., Bowen, D., Kell, J., Knapper, S. *et al.* (2015). Arsenic trioxide and all-trans retinoic acid treatment for acute promyelocytic leukaemia in all risk groups (AML17): results of a randomised, controlled, phase 3 trial. *Lancet Oncol* **16**(13):1295-1305.

Burns, C. E., Traver, D., Mayhall, E., Shepard, J. L. and Zon, L. I. (2005). Hematopoietic stem cell fate is established by the Notch-Runx pathway. *Genes Dev* **19**(19):2331-2342.

Butler, J. M., Nolan, D. J., Vertes, E. L., Varnum-Finney, B., Kobayashi, H., Hooper, A. T. *et al.* (2010). Endothelial cells are essential for the self-renewal and repopulation of Notch-dependent hematopoietic stem cells. *Cell Stem Cell* **6**(3):251-264.

Cabezas-Wallscheid, N., Buettner, F., Sommerkamp, P., Klimmeck, D., Ladel, L., Thalheimer, F. B. *et al.* (2017). Vitamin A-Retinoic Acid Signaling Regulates Hematopoietic Stem Cell Dormancy. *Cell* **169**(5):807-823 e819.

Cabezas-Wallscheid, N., Eichwald, V., de Graaf, J., Lower, M., Lehr, H. A., Kreft, A. *et al.* (2013). Instruction of haematopoietic lineage choices, evolution of transcriptional landscapes and cancer stem cell hierarchies derived from an AML1-ETO mouse model. *Embo Molecular Medicine* **5**(12):1804-1820.

Cai, X., Gao, L., Teng, L., Ge, J., Oo, Z. M., Kumar, A. R. *et al.* (2015). Runx1 Deficiency Decreases Ribosome Biogenesis and Confers Stress Resistance to Hematopoietic Stem and Progenitor Cells. *Cell Stem Cell* **17**(2):165-177.

Cai, X., Gaudet, J. J., Mangan, J. K., Chen, M. J., De Obaldia, M. E., Oo, Z. *et al.* (2011). Runx1 loss minimally impacts long-term hematopoietic stem cells. *PLoS One* **6**(12):e28430.

Cai, Y., Xu, Z., Xie, J., Ham, A. J., Koury, M. J., Hiebert, S. W. *et al.* (2009). Eto2/MTG16 and MTGR1 are heteromeric corepressors of the TAL1/SCL transcription factor in murine erythroid progenitors. *Biochem Biophys Res Commun* **390**(2):295-301.

Cai, Z., de Bruijn, M., Ma, X., Dortland, B., Luteijn, T., Downing, R. J. *et al.* (2000). Haploinsufficiency of AML1 affects the temporal and spatial generation of hematopoietic stem cells in the mouse embryo. *Immunity* **13**(4):423-431.

Cairolì, R., Beghini, A., Grillo, G., Nadali, G., Elice, F., Ripamonti, C. B. *et al.* (2006). Prognostic impact of c-KIT mutations in core binding factor leukemias: an Italian retrospective study. *Blood* **107**(9):3463-3468.

Calvi, L. M., Adams, G. B., Weibrecht, K. W., Weber, J. M., Olson, D. P., Knight, M. C. *et al.* (2003). Osteoblastic cells regulate the haematopoietic stem cell niche. *Nature* **425**(6960):841-846.

Cancer Genome Atlas Research, N., Ley, T. J., Miller, C., Ding, L., Raphael, B. J., Mungall, A. J. *et al.* (2013). Genomic and epigenomic landscapes of adult de novo acute myeloid leukemia. *N Engl J Med* **368**(22):2059-2074.

Cancer Research UK. (2020). *Acute myeloid leukaemia (AML) incidence statistics*. Available at: <https://www.cancerresearchuk.org/health-professional/cancer-statistics/statistics-by-cancer-type/leukaemia-aml> [Accessed: 17/10/2020].

Capron, C., Lacout, C., Lecluse, Y., Wagner-Ballon, O., Kaushik, A. L., Cramer-Borde, E. *et al.* (2011). LYL-1 deficiency induces a stress erythropoiesis. *Exp Hematol* **39**(6):629-642.

Castilla, L. H., Perrat, P., Martinez, N. J., Landrette, S. F., Keys, R., Oikemus, S. *et al.* (2004). Identification of genes that synergize with Cbfb-MYH11 in the pathogenesis of acute myeloid leukemia. *Proc Natl Acad Sci U S A* **101**(14):4924-4929.

Cerami, E., Gao, J., Dogrusoz, U., Gross, B. E., Sumer, S. O., Aksoy, B. A. *et al.* (2012). The cBio cancer genomics portal: an open platform for exploring multidimensional cancer genomics data. *Cancer Discov* **2**(5):401-404.

Chan, C. K., Chen, C. C., Luppen, C. A., Kim, J. B., DeBoer, A. T., Wei, K. *et al.* (2009). Endochondral ossification is required for haematopoietic stem-cell niche formation. *Nature* **457**(7228):490-494.

Chan, W. Y., Follows, G. A., Lacaud, G., Pimanda, J. E., Landry, J. R., Kinston, S. *et al.* (2007). The paralogous hematopoietic regulators Lyl1 and Scl are coregulated by Ets and GATA factors, but Lyl1 cannot rescue the early Scl^{-/-} phenotype. *Blood* **109**(5):1908-1916.

Chen, A. I., de Nooij, J. C. and Jessell, T. M. (2006). Graded activity of transcription factor Runx3 specifies the laminar termination pattern of sensory axons in the developing spinal cord. *Neuron* **49**(3):395-408.

Chen, F. F., Bai, J., Li, W., Mei, P. J., Liu, H., Li, L. L. *et al.* (2013). RUNX3 Suppresses Migration, Invasion and Angiogenesis of Human Renal Cell Carcinoma. *Plos One* **8**(2).

Chen, F. F., Wang, M., Bai, J., Liu, Q. H., Xi, Y. G., Li, W. *et al.* (2014). Role of RUNX3 in Suppressing Metastasis and Angiogenesis of Human Prostate Cancer. *Plos One* **9**(1).

Chen, W., Salto-Tellez, M., Palanisamy, N., Ganesan, K., Hou, Q. S., Tan, L. K. *et al.* (2007). Targets of genome copy number reduction in primary breast cancers identified by integrative genomics. *Genes Chromosomes & Cancer* **46**(3):288-301.

Chen, W. C., Gao, N., Shen, Y. L. and Cen, J. N. (2010). Hypermethylation downregulates Runx3 gene expression and its restoration suppresses gastric epithelial cell growth by inducing p27 and caspase3 in human gastric cancer. *Journal of Gastroenterology and Hepatology* **25**(4):823-831.

Chen, Y., Wei, X. F., Guo, C. C., Jin, H. F., Han, Z. Y., Han, Y. *et al.* (2011). Runx3 suppresses gastric cancer metastasis through inactivation of MMP9 by upregulation of TIMP-1. *International Journal of Cancer* **129**(7):1586-1598.

Cheng, A. S. L., Culhane, A. C., Chan, M. W. Y., Venkataranm, C. R., Ehrich, M., Nasir, A. *et al.* (2008a). Epithelial progeny of estrogen-exposed breast progenitor cells display a cancer-like methylome. *Cancer Research* **68**(6):1786-1796.

Cheng, C. K., Li, L., Cheng, S. H., Lau, K. M., Chan, N. P. H., Wong, R. S. M. *et al.* (2008b). Transcriptional repression of the RUNX3/AML2 gene by the t(8;21) and inv(16) fusion proteins in acute myeloid leukemia. *Blood* **112**(8):3391-3402.

Cheng, H., Liu, Y., Jia, Q., Ma, S., Yuan, W., Jia, H. *et al.* (2016). Novel regulators in hematopoietic stem cells can be revealed by a functional approach under leukemic condition. *Leukemia* **30**(10):2074-2077.

Chi, X. Z., Kim, J., Lee, Y. H., Lee, J. W., Lee, K. S., Wee, H. *et al.* (2009). Runt-Related Transcription Factor RUNX3 Is a Target of MDM2-Mediated Ubiquitination. *Cancer Research* **69**(20):8111-8119.

Chi, X. Z., Yang, J. O., Lee, K. Y., Ito, K., Sakakura, C., Li, Q. L. *et al.* (2005). RUNX3 suppresses gastric epithelial cell growth by inducing p21(WAF1/Cip1) expression in cooperation with transforming growth factor beta-activated SMAD. *Molecular and Cellular Biology* **25**(18):8097-8107.

Chiu, S. K., Saw, J., Huang, Y., Sonderegger, S. E., Wong, N. C., Powell, D. R. *et al.* (2018). A novel role for Lyl1 in primitive erythropoiesis. *Development* **145**(19).

Choi, Y. J., Elagib, K. E., Delehanty, L. L. and Goldfarb, A. N. (2006). Erythroid inhibition by the leukemic fusion AML1-ETO is associated with impaired acetylation of the major erythroid transcription factor GATA-1. *Cancer Research* **66**(6):2990-2996.

Chou, F. S., Griesinger, A., Wunderlich, M., Lin, S., Link, K. A., Shrestha, M. *et al.* (2012). The thrombopoietin/MPL/Bcl-xL pathway is essential for survival and self-renewal in human preleukemia induced by AML1-ETO. *Blood* **120**(4):709-719.

Chow, A., Lucas, D., Hidalgo, A., Mendez-Ferrer, S., Hashimoto, D., Scheiermann, C. *et al.* (2011). Bone marrow CD169+ macrophages promote the retention of hematopoietic stem and progenitor cells in the mesenchymal stem cell niche. *J Exp Med* **208**(2):261-271.

Chuang, L. S., Ito, K. and Ito, Y. (2017). Roles of RUNX in Solid Tumors. *Adv Exp Med Biol* **962**:299-320.

Chuang, L. S. H., Ito, K. and Ito, Y. (2013). RUNX family: Regulation and diversification of roles through interacting proteins. *International Journal of Cancer* **132**(6):1260-1271.

Chuang, L. S. H. and Ito, Y. (2010). RUNX3 is multifunctional in carcinogenesis of multiple solid tumors. *Oncogene* **29**(18):2605-2615.

Chung, J., Wittig, J. G., Ghamari, A., Maeda, M., Dailey, T. A., Bergonia, H. *et al.* (2017). Erythropoietin signaling regulates heme biosynthesis. *Elife* **6**.

Chyla, B. J., Moreno-Miralles, I., Steapleton, M. A., Thompson, M. A., Bhaskara, S., Engel, M. *et al.* (2008). Deletion of Mtg16, a target of t(16;21), alters hematopoietic progenitor cell proliferation and lineage allocation. *Mol Cell Biol* **28**(20):6234-6247.

Civin, C. I., Strauss, L. C., Brovall, C., Fackler, M. J., Schwartz, J. F. and Shaper, J. H. (1984). Antigenic analysis of hematopoiesis. III. A hematopoietic progenitor cell surface antigen defined by a monoclonal antibody raised against KG-1a cells. *J Immunol* **133**(1):157-165.

Collins, A., Hewitt, S. L., Chaumeil, J., Sellars, M., Micsinai, M., Allinne, J. *et al.* (2011). RUNX transcription factor-mediated association of Cd4 and Cd8 enables coordinate gene regulation. *Immunity* **34**(3):303-314.

Conesa, A., Madrigal, P., Tarazona, S., Gomez-Cabrero, D., Cervera, A., McPherson, A. *et al.* (2016). A survey of best practices for RNA-seq data analysis. *Genome Biol* **17**:13.

Corces-Zimmerman, M. R., Hong, W. J., Weissman, I. L., Medeiros, B. C. and Majeti, R. (2014). Preleukemic mutations in human acute myeloid leukemia affect epigenetic regulators and persist in remission. *Proc Natl Acad Sci U S A* **111**(7):2548-2553.

Craig, W., Kay, R., Cutler, R. L. and Lansdorp, P. M. (1993). Expression of Thy-1 on human hematopoietic progenitor cells. *J Exp Med* **177**(5):1331-1342.

Cruz-Guilloty, F., Pipkin, M. E., Djuretic, I. M., Levanon, D., Lotem, J., Lichtenheld, M. G. *et al.* (2009). Runx3 and T-box proteins cooperate to establish the transcriptional program of effector CTLs. *Journal of Experimental Medicine* **206**(1):51-59.

Dahl, R., Iyer, S. R., Owens, K. S., Cuylear, D. D. and Simon, M. C. (2007). The transcriptional repressor GFI-1 antagonizes PU.1 activity through protein-protein interaction. *J Biol Chem* **282**(9):6473-6483.

Dahl, R., Walsh, J. C., Lancki, D., Laslo, P., Iyer, S. R., Singh, H. *et al.* (2003). Regulation of macrophage and neutrophil cell fates by the PU.1:C/EBPalpha ratio and granulocyte colony-stimulating factor. *Nat Immunol* **4**(10):1029-1036.

Dai, Y., Cheng, Z., Pang, Y., Jiao, Y., Qian, T., Quan, L. *et al.* (2020). Prognostic value of the FUT family in acute myeloid leukemia. *Cancer Gene Ther* **27**(1-2):70-80.

Dakic, A., Metcalf, D., Di Rago, L., Mifsud, S., Wu, L. and Nutt, S. L. (2005). PU.1 regulates the commitment of adult hematopoietic progenitors and restricts granulopoiesis. *J Exp Med* **201**(9):1487-1502.

Dalcq, J., Pasque, V., Ghaye, A., Larbuisson, A., Motte, P., Martial, J. A. *et al.* (2012). RUNX3, EGR1 and SOX9B Form a Regulatory Cascade Required to Modulate BMP-Signaling during Cranial Cartilage Development in Zebrafish. *Plos One* **7**(11).

Damdinsuren, A., Matsushita, H., Ito, M., Tanaka, M., Jin, G. L., Tsukamoto, H. *et al.* (2015). FLT3-ITD drives Ara-C resistance in leukemic cells via the induction of RUNX3. *Leukemia Research* **39**(12):1405-1413.

Darley, R. L., Hoy, T. G., Baines, P., Padua, R. A. and Burnett, A. K. (1997). Mutant N-RAS induces erythroid lineage dysplasia in human CD34+ cells. *J Exp Med* **185**(7):1337-1347.

Darley, R. L., Pearn, L., Omidvar, N., Sweeney, M., Fisher, J., Phillips, S. *et al.* (2002). Protein kinase C mediates mutant N-Ras-induced developmental abnormalities in normal human erythroid cells. *Blood* **100**(12):4185-4192.

Das, R., Coupar, J., Clavijo, P. E., Saleh, A., Cheng, T. F., Yang, X. *et al.* (2019). Lymphotoxin-beta receptor-NIK signaling induces alternative RELB/NF-kappaB2 activation to promote metastatic gene expression and cell migration in head and neck cancer. *Mol Carcinog* **58**(3):411-425.

Daver, N., Schlenk, R. F., Russell, N. H. and Levis, M. J. (2019). Targeting FLT3 mutations in AML: review of current knowledge and evidence. *Leukemia* **33**(2):299-312.

Davies, C. C., Chakraborty, A., Diefenbacher, M. E., Skehel, M. and Behrens, A. (2013). Arginine methylation of the c-Jun coactivator RACO-1 is required for c-Jun/AP-1 activation. *EMBO J* **32**(11):1556-1567.

De Braekeleer, E., Douet-Guilbert, N., Morel, F., Le Bris, M. J., Ferec, C. and De Braekeleer, M. (2011). RUNX1 translocations and fusion genes in malignant hemopathies. *Future Oncol* **7**(1):77-91.

de Guzman, C. G., Warren, A. J., Zhang, Z., Gartland, L., Erickson, P., Drabkin, H. *et al.* (2002). Hematopoietic stem cell expansion and distinct myeloid developmental abnormalities in a murine model of the AML1-ETO translocation. *Molecular and Cellular Biology* **22**(15):5506-5517.

Debaize, L., Jakobczyk, H., Avner, S., Gaudichon, J., Rio, A. G., Serandour, A. A. *et al.* (2018). Interplay between transcription regulators RUNX1 and FUBP1 activates an enhancer of the oncogene c-KIT and amplifies cell proliferation. *Nucleic Acids Res* **46**(21):11214-11228.

Debernardi, S., Lillington, D. M., Chaplin, T., Tomlinson, S., Amess, J., Rohatiner, A. *et al.* (2003). Genome-wide analysis of acute myeloid leukemia with normal karyotype reveals a unique pattern of homeobox gene expression distinct from those with translocation-mediated fusion events. *Genes Chromosomes Cancer* **37**(2):149-158.

DeKelder, R. C., Yan, M., Ahn, E. Y., Shia, W. J., Speck, N. A. and Zhang, D. E. (2013). Attenuation of AML1-ETO cellular dysregulation correlates with increased leukemogenic potential. *Blood* **121**(18):3714-3717.

Derolf, A. R., Kristinsson, S. Y., Andersson, T. M., Landgren, O., Dickman, P. W. and Bjorkholm, M. (2009). Improved patient survival for acute myeloid leukemia: a population-based study of 9729 patients diagnosed in Sweden between 1973 and 2005. *Blood* **113**(16):3666-3672.

Dicken, J., Mildner, A., Leshkowitz, D., Touw, I. P., Hantisteanu, S., Jung, S. *et al.* (2013). Transcriptional Reprogramming of CD11b(+)Esam(hi) Dendritic Cell Identity and Function by Loss of Runx3. *Plos One* **8**(10).

DiNardo, C. D. and Perl, A. E. (2019). Advances in patient care through increasingly individualized therapy. *Nat Rev Clin Oncol* **16**(2):73-74.

DiNardo, C. D., Pratz, K., Pullarkat, V., Jonas, B. A., Arellano, M., Becker, P. S. *et al.* (2019). Venetoclax combined with decitabine or azacitidine in treatment-naive, elderly patients with acute myeloid leukemia. *Blood* **133**(1):7-17.

DiNardo, C. D., Tiong, I. S., Quaglieri, A., MacRaid, S., Loghavi, S., Brown, F. C. *et al.* (2020). Molecular patterns of response and treatment failure after frontline venetoclax combinations in older patients with AML. *Blood* **135**(11):791-803.

Ding, L., Saunders, T. L., Enikolopov, G. and Morrison, S. J. (2012). Endothelial and perivascular cells maintain haematopoietic stem cells. *Nature* **481**(7382):457-462.

Djuretic, I. M., Levanon, D., Negreanu, V., Groner, Y., Rao, A. and Ansel, K. M. (2007). Transcription factors T-bet and Runx3 cooperate to activate Ifng and silence Il4 in T helper type 1 cells. *Nature Immunology* **8**(2):145-153.

Dohner, H., Estey, E., Grimwade, D., Amadori, S., Appelbaum, F. R., Buchner, T. *et al.* (2017). Diagnosis and management of AML in adults: 2017 ELN recommendations from an international expert panel. *Blood* **129**(4):424-447.

Doitsidou, M., Reichman-Fried, M., Stebler, J., Kopranner, M., Dorries, J., Meyer, D. *et al.* (2002). Guidance of primordial germ cell migration by the chemokine SDF-1. *Cell* **111**(5):647-659.

Dombret, H., Seymour, J. F., Butrym, A., Wierzbowska, A., Selleslag, D., Jang, J. H. *et al.* (2015). International phase 3 study of azacitidine vs conventional care regimens in older patients with newly diagnosed AML with >30% blasts. *Blood* **126**(3):291-299.

Dominguez-Soto, A., Relloso, M., Vega, M. A., Corbi, A. L. and Puig-Kroger, A. (2005). RUNX3 regulates the activity of the CD11a and CD49d integrin gene promoters. *Immunobiology* **210**(2-4):133-139.

Dore, L. C. and Crispino, J. D. (2011). Transcription factor networks in erythroid cell and megakaryocyte development. *Blood* **118**(2):231-239.

Doulatov, S., Notta, F., Laurenti, E. and Dick, J. E. (2012). Hematopoiesis: a human perspective. *Cell Stem Cell* **10**(2):120-136.

Driggers, P. H., Ennist, D. L., Gleason, S. L., Mak, W. H., Marks, M. S., Levi, B. Z. *et al.* (1990). An interferon gamma-regulated protein that binds the interferon-inducible enhancer element of major histocompatibility complex class I genes. *Proc Natl Acad Sci U S A* **87**(10):3743-3747.

Drissi, H., Luc, Q., Shakoori, R., Chuva De Sousa Lopes, S., Choi, J. Y., Terry, A. *et al.* (2000). Transcriptional autoregulation of the bone related CBFA1/RUNX2 gene. *J Cell Physiol* **184**(3):341-350.

Dulmage, B. O., Akilov, O., Vu, J. R., Falo, L. D. and Geskin, L. J. (2019). Dysregulation of the TOX-RUNX3 pathway in cutaneous T-cell lymphoma. *Oncotarget* **10**(33):3104-3113.

Dunne, J., Cullmann, C., Ritter, M., Soria, N. M., Drescher, B., Debernardi, S. *et al.* (2006). siRNA-mediated AML1/MTG8 depletion affects differentiation and proliferation-associated gene expression in t(8 ; 21)-positive cell lines and primary AML blasts. *Oncogene* **25**(45):6067-6078.

Dunne, J., Gascoyne, D. M., Lister, T. A., Brady, H. J. M., Heidenreich, O. and Young, B. D. (2010). AML1/ETO Proteins Control POU4F1/BRN3A Expression and Function in t(8;21) Acute Myeloid Leukemia. *Cancer Research* **70**(10):3985-3995.

Dzierzak, E. and Philipsen, S. (2013). Erythropoiesis: development and differentiation. *Cold Spring Harb Perspect Med* **3**(4):a011601.

Ebihara, T., Song, C., Ryu, S. H., Plougastel-Douglas, B., Yang, L. P., Levanon, D. *et al.* (2015). Runx3 specifies lineage commitment of innate lymphoid cells. *Nature Immunology* **16**(11):1124-1133.

Edelman, P., Vinci, G., Villeval, J. L., Vainchenker, W., Henri, A., Miglierina, R. *et al.* (1986). A monoclonal antibody against an erythrocyte ontogenic antigen identifies fetal and adult erythroid progenitors. *Blood* **67**(1):56-63.

Egawa, T., Tillman, R. E., Naoe, Y., Taniuchi, I. and Littman, D. R. (2007). The role of the Runx transcription factors in thymocyte differentiation and in homeostasis of naive T cells. *Journal of Experimental Medicine* **204**(8):1945-1957.

Egeland, T., Steen, R., Quarsten, H., Gaudernack, G., Yang, Y. C. and Thorsby, E. (1991). Myeloid differentiation of purified CD34+ cells after stimulation with recombinant

human granulocyte-monocyte colony-stimulating factor (CSF), granulocyte-CSF, monocyte-CSF, and interleukin-3. *Blood* **78**(12):3192-3199.

Elagib, K. E., Racke, F. K., Mogass, M., Khetawat, R., Delehanty, L. L. and Goldfarb, A. N. (2003). RUNX1 and GATA-1 coexpression and cooperation in megakaryocytic differentiation. *Blood* **101**(11):4333-4341.

Ema, H., Sudo, K., Seita, J., Matsubara, A., Morita, Y., Osawa, M. *et al.* (2005). Quantification of self-renewal capacity in single hematopoietic stem cells from normal and Lnk-deficient mice. *Dev Cell* **8**(6):907-914.

Engel, M. E., Nguyen, H. N., Mariotti, J., Hunt, A. and Hiebert, S. W. (2010). Myeloid translocation gene 16 (MTG16) interacts with Notch transcription complex components to integrate Notch signaling in hematopoietic cell fate specification. *Mol Cell Biol* **30**(7):1852-1863.

Enomoto, H., Enomoto-Iwamoto, M., Iwamoto, M., Nomura, S., Himeno, M., Kitamura, Y. *et al.* (2000). Cbfa1 is a positive regulatory factor in chondrocyte maturation. *J Biol Chem* **275**(12):8695-8702.

Essalmani, R., Zaid, A., Marcinkiewicz, J., Chamberland, A., Pasquato, A., Seidah, N. G. *et al.* (2008). In vivo functions of the proprotein convertase PC5/6 during mouse development: Gdf11 is a likely substrate. *Proc Natl Acad Sci U S A* **105**(15):5750-5755.

Estechea, A., Aguilera-Montilla, N., Sanchez-Mateos, P. and Puig-Kroger, A. (2012). RUNX3 regulates intercellular adhesion molecule 3 (ICAM-3) expression during macrophage differentiation and monocyte extravasation. *PLoS One* **7**(3):e33313.

Estecio, M. R. H., Maddipoti, S., Bueso-Ramos, C., DiNardo, C. D., Yang, H., Wei, Y. *et al.* (2015). RUNX3 promoter hypermethylation is frequent in leukaemia cell lines and associated with acute myeloid leukaemia inv(16) subtype. *British Journal of Haematology* **169**(3):344-351.

Fainaru, O., Shseyov, D., Hantisteanu, S. and Groner, Y. (2005). Accelerated chemokine receptor 7-mediated dendritic cell migration in Runx3 knockout mice and the spontaneous development of asthma-like disease. *Proceedings of the National Academy of Sciences of the United States of America* **102**(30):10598-10603.

Fainaru, O., Woolf, E., Lotem, J., Yarmus, M., Brenner, O., Goldenberg, D. *et al.* (2004). Runx3 regulates mouse TGF-beta-mediated dendritic cell function and its absence results in airway inflammation. *Embo Journal* **23**(4):969-979.

Feinberg, M. W., Wara, A. K., Cao, Z., Lebedeva, M. A., Rosenbauer, F., Iwasaki, H. *et al.* (2007). The Kruppel-like factor KLF4 is a critical regulator of monocyte differentiation. *EMBO J* **26**(18):4138-4148.

Fenske, T. S., Pengue, G., Mathews, V., Hanson, P. T., Hamm, S. E., Riaz, N. *et al.* (2004). Stem cell expression of the AML1/ETO fusion protein induces a myeloproliferative disorder in mice. *Proceedings of the National Academy of Sciences of the United States of America* **101**(42):15184-15189.

Fernandes, M. T., Ghezzi, M. N., Silveira, A. B., Kalathur, R. K., Pova, V., Ribeiro, A. R. *et al.* (2015). Lymphotoxin-beta receptor in microenvironmental cells promotes the development of T-cell acute lymphoblastic leukaemia with cortical/mature immunophenotype. *Br J Haematol* **171**(5):736-751.

Ferreira, R., Ohneda, K., Yamamoto, M. and Philipsen, S. (2005). GATA1 function, a paradigm for transcription factors in hematopoiesis. *Mol Cell Biol* **25**(4):1215-1227.

Frank, R., Zhang, J., Uchida, H., Meyers, S., Hiebert, S. W. and Nimer, S. D. (1995). The AML1/ETO fusion protein blocks transactivation of the GM-CSF promoter by AML1B. *Oncogene* **11**(12):2667-2674.

Frenette, P. S., Pinho, S., Lucas, D. and Scheiermann, C. (2013). Mesenchymal stem cell: keystone of the hematopoietic stem cell niche and a stepping-stone for regenerative medicine. *Annu Rev Immunol* **31**:285-316.

Friedman, A. D. (2002). Transcriptional regulation of granulocyte and monocyte development. *Oncogene* **21**(21):3377-3390.

Fu, Y. X., Chang, A. C. Y., Fournier, M., Chang, L., Niessen, K. and Karsan, A. (2011). RUNX3 Maintains the Mesenchymal Phenotype after Termination of the Notch Signal. *Journal of Biological Chemistry* **286**(13):11803-11813.

Fujii, S., Ito, K., Ito, Y. and Ochiai, A. (2008). Enhancer of zeste homologue 2 (EZH2) down-regulates RUNX3 by increasing histone H3 methylation. *Journal of Biological Chemistry* **283**(25):17324-17332.

Fujimoto, T., Anderson, K., Jacobsen, S. E., Nishikawa, S. I. and Nerlov, C. (2007). Cdk6 blocks myeloid differentiation by interfering with Runx1 DNA binding and Runx1-C/EBPalpha interaction. *EMBO J* **26**(9):2361-2370.

Fujiwara, M., Tagashira, S., Harada, H., Ogawa, S., Katsumata, T., Nakatsuka, M. *et al.* (1999). Isolation and characterization of the distal promoter region of mouse Cbfa1. *Biochim Biophys Acta* **1446**(3):265-272.

Fujiwara, T., Alqadi, Y. W., Okitsu, Y., Fukuhara, N., Onishi, Y., Ishizawa, K. *et al.* (2013). Role of transcriptional corepressor ETO2 in erythroid cells. *Exp Hematol* **41**(3):303-315 e301.

Fujiwara, T., O'Geen, H., Keles, S., Blahnik, K., Linnemann, A. K., Kang, Y. A. *et al.* (2009). Discovering hematopoietic mechanisms through genome-wide analysis of GATA factor chromatin occupancy. *Mol Cell* **36**(4):667-681.

Fukushima-Nakase, Y., Naoe, Y., Taniuchi, I., Hosoi, H., Sugimoto, T. and Okuda, T. (2005). Shared and distinct roles mediated through C-terminal subdomains, of acute myeloid leukemia/Runt-related transcription factor molecules in murine development. *Blood* **105**(11):4298-4307.

Gaidzik, V. I., Bullinger, L., Schlenk, R. F., Zimmermann, A. S., Rock, J., Paschka, P. *et al.* (2011). RUNX1 mutations in acute myeloid leukemia: results from a comprehensive genetic and clinical analysis from the AML study group. *J Clin Oncol* **29**(10):1364-1372.

Gartner, S. and Kaplan, H. S. (1980). Long-term culture of human bone marrow cells. *Proc Natl Acad Sci U S A* **77**(8):4756-4759.

Gautier, E. F., Ducamp, S., Leduc, M., Salnot, V., Guillonneau, F., Dussiot, M. *et al.* (2016). Comprehensive Proteomic Analysis of Human Erythropoiesis. *Cell Rep* **16**(5):1470-1484.

Gergen, J. P. and Butler, B. A. (1988). Isolation of the Drosophila segmentation gene runt and analysis of its expression during embryogenesis. *Genes Dev* **2**(9):1179-1193.

Gerritsen, M., Yi, G., Tijchon, E., Kuster, J., Schuringa, J. J., Martens, J. H. A. *et al.* (2019). RUNX1 mutations enhance self-renewal and block granulocytic differentiation in human in vitro models and primary AMLs. *Blood Adv* **3**(3):320-332.

Ghanem, L. R., Kromer, A., Silverman, I. M., Ji, X., Gazzara, M., Nguyen, N. *et al.* (2018). Poly(C)-Binding Protein Pcbp2 Enables Differentiation of Definitive Erythropoiesis by Directing Functional Splicing of the Runx1 Transcript. *Mol Cell Biol* **38**(16).

Ghani, S., Riemke, P., Schonheit, J., Lenze, D., Stumm, J., Hoogenkamp, M. *et al.* (2011). Macrophage development from HSCs requires PU.1-coordinated microRNA expression. *Blood* **118**(8):2275-2284.

Ghozi, M. C., Bernstein, Y., Negreanu, V., Levanon, D. and Groner, Y. (1996). Expression of the human acute myeloid leukemia gene AML1 is regulated by two promoter regions. *Proc Natl Acad Sci U S A* **93**(5):1935-1940.

Gilmour, J., Assi, S. A., Noailles, L., Lichtinger, M., Obier, N. and Bonifer, C. (2018). The Co-operation of RUNX1 with LDB1, CDK9 and BRD4 Drives Transcription Factor Complex Relocation During Haematopoietic Specification. *Sci Rep* **8**(1):10410.

Gnanapragasam, M. N., McGrath, K. E., Catherman, S., Xue, L., Palis, J. and Bieker, J. J. (2016). EKLF/KLF1-regulated cell cycle exit is essential for erythroblast enucleation. *Blood* **128**(12):1631-1641.

Goardon, N., Lambert, J. A., Rodriguez, P., Nissaire, P., Herblot, S., Thibault, P. *et al.* (2006). ETO2 coordinates cellular proliferation and differentiation during erythropoiesis. *EMBO J* **25**(2):357-366.

Goardon, N., Marchi, E., Atzberger, A., Quek, L., Schuh, A., Soneji, S. *et al.* (2011). Coexistence of LMPP-like and GMP-like leukemia stem cells in acute myeloid leukemia. *Cancer Cell* **19**(1):138-152.

Goh, Y. M., Cinghu, S., Hong, E. T. H., Lee, Y. S., Kim, J. H., Jang, J. W. *et al.* (2010). Src Kinase Phosphorylates RUNX3 at Tyrosine Residues and Localizes the Protein in the Cytoplasm. *Journal of Biological Chemistry* **285**(13):10122-10129.

Golub, T. R., Barker, G. F., Bohlander, S. K., Hiebert, S. W., Ward, D. C., Bray-Ward, P. *et al.* (1995). Fusion of the TEL gene on 12p13 to the AML1 gene on 21q22 in acute lymphoblastic leukemia. *Proc Natl Acad Sci U S A* **92**(11):4917-4921.

Gooi, H. C., Thorpe, S. J., Hounsell, E. F., Rumpold, H., Kraft, D., Forster, O. *et al.* (1983). Marker of peripheral blood granulocytes and monocytes of man recognized by two monoclonal antibodies VEP8 and VEP9 involves the trisaccharide 3-fucosyl-N-acetylglucosamine. *Eur J Immunol* **13**(4):306-312.

Gou, Y. L., Zhai, F. B., Zhang, L. and Cui, L. (2017). RUNX3 regulates hepatocellular carcinoma cell metastasis via targeting miR-186/E-cadherin/EMT pathway. *Oncotarget* **8**(37):61475-61486.

Goyama, S., Schibler, J., Cunningham, L., Zhang, Y., Rao, Y., Nishimoto, N. *et al.* (2013). Transcription factor RUNX1 promotes survival of acute myeloid leukemia cells. *Journal of Clinical Investigation* **123**(9):3876-3888.

Goyama, S., Schibler, J., Gasilina, A., Shrestha, M., Lin, S., Link, K. A. *et al.* (2016). UBASH3B/Sts-1-CBL axis regulates myeloid proliferation in human preleukemia induced by AML1-ETO. *Leukemia* **30**(3):728-739.

Goyama, S., Yamaguchi, Y., Imai, Y., Kawazu, M., Nakagawa, M., Asai, T. *et al.* (2004). The transcriptionally active form of AML1 is required for hematopoietic rescue of the AML1-deficient embryonic para-aortic splanchnopleural (P-Sp) region. *Blood* **104**(12):3558-3564.

Greenbaum, A., Hsu, Y.-M. S., Day, R. B., Schuettpelz, L. G., Christopher, M. J., Borgerding, J. N. *et al.* (2013). CXCL12 in early mesenchymal progenitors is required for haematopoietic stem-cell maintenance. *Nature* **495**(7440):227-230.

Greenbaum, A. M., Revollo, L. D., Woloszynek, J. R., Civitelli, R. and Link, D. C. (2012). N-cadherin in osteolineage cells is not required for maintenance of hematopoietic stem cells. *Blood* **120**(2):295-302.

Greif, P. A., Dufour, A., Konstandin, N. P., Ksienzyk, B., Zellmeier, E., Tizazu, B. *et al.* (2012a). GATA2 zinc finger 1 mutations associated with biallelic CEBPA mutations define a unique genetic entity of acute myeloid leukemia. *Blood* **120**(2):395-403.

Greif, P. A., Konstandin, N. P., Metzeler, K. H., Herold, T., Pasalic, Z., Ksienzyk, B. *et al.* (2012b). RUNX1 mutations in cytogenetically normal acute myeloid leukemia are associated with a poor prognosis and up-regulation of lymphoid genes. *Haematologica* **97**(12):1909-1915.

Grignani, F., Kinsella, T., Mencarelli, A., Valtieri, M., Riganelli, D., Grignani, F. *et al.* (1998). High-efficiency gene transfer and selection of human hematopoietic progenitor cells with a hybrid EBV/retroviral vector expressing the green fluorescence protein. *Cancer Res* **58**(1):14-19.

Grover, A., Mancini, E., Moore, S., Mead, A. J., Atkinson, D., Rasmussen, K. D. *et al.* (2014). Erythropoietin guides multipotent hematopoietic progenitor cells toward an erythroid fate. *J Exp Med* **211**(2):181-188.

Growney, J. D., Shigematsu, H., Li, Z., Lee, B. H., Adelsperger, J., Rowan, R. *et al.* (2005). Loss of Runx1 perturbs adult hematopoiesis and is associated with a myeloproliferative phenotype. *Blood* **106**(2):494-504.

Grueter, B., Petter, M., Egawa, T., Laule-Kilian, K., Aldrian, C. J., Wuerch, A. *et al.* (2005). Runx3 regulates integrin alpha(E)/CD103 and CD4 expression during development of CD4(-)/CD8(+) T cells. *Journal of Immunology* **175**(3):1694-1705.

Gschwandtner, M., Derler, R. and Midwood, K. S. (2019). More Than Just Attractive: How CCL2 Influences Myeloid Cell Behavior Beyond Chemotaxis. *Front Immunol* **10**:2759.

Guilliams, M., Mildner, A. and Yona, S. (2018). Developmental and Functional Heterogeneity of Monocytes. *Immunity* **49**(4):595-613.

Guo, H. and Friedman, A. D. (2011). Phosphorylation of RUNX1 by cyclin-dependent kinase reduces direct interaction with HDAC1 and HDAC3. *J Biol Chem* **286**(1):208-215.

Guo, P., Poulos, M. G., Palikuqi, B., Badwe, C. R., Lis, R., Kunar, B. *et al.* (2017). Endothelial jagged-2 sustains hematopoietic stem and progenitor reconstitution after myelosuppression. *J Clin Invest* **127**(12):4242-4256.

Gurney, A. L., Carver-Moore, K., de Sauvage, F. J. and Moore, M. W. (1994). Thrombocytopenia in c-mpl-deficient mice. *Science* **265**(5177):1445-1447.

Gustafson, M. P., Lin, Y., Maas, M. L., Van Keulen, V. P., Johnston, P. B., Peikert, T. *et al.* (2015). A method for identification and analysis of non-overlapping myeloid immunophenotypes in humans. *PLoS One* **10**(3):e0121546.

Gutierrez, N. C., Lopez-Perez, R., Hernandez, J. M., Isidro, I., Gonzalez, B., Delgado, M. *et al.* (2005). Gene expression profile reveals deregulation of genes with relevant functions in the different subclasses of acute myeloid leukemia. *Leukemia* **19**(3):402-409.

Gutierrez, N. C., Lopez-Perez, R., Hernandez, J. M., Isidro, I., Gonzalez, B., Delgado, M. *et al.* (2005). Gene expression profile reveals deregulation of genes with relevant functions in the different subclasses of acute myeloid leukemia. *Leukemia* **19**(3):402-409.

Haferlach, T., Kohlmann, A., Wiczorek, L., Basso, G., Kronnie, G. T., Bene, M. C. *et al.* (2010). Clinical utility of microarray-based gene expression profiling in the diagnosis and subclassification of leukemia: report from the International Microarray Innovations in Leukemia Study Group. *J Clin Oncol* **28**(15):2529-2537.

Haider, A., Steininger, A., Ullmann, R., Hummel, M., Dimitrova, L., Beyer, M. *et al.* (2016). Inactivation of RUNX3/p46 Promotes Cutaneous T-Cell Lymphoma. *Journal of Investigative Dermatology* **136**(11):2287-2296.

Hamlett, I., Draper, J., Strouboulis, J., Iborra, F., Porcher, C. and Vyas, P. (2008). Characterization of megakaryocyte GATA1-interacting proteins: the corepressor ETO2 and GATA1 interact to regulate terminal megakaryocyte maturation. *Blood* **112**(7):2738-2749.

Han, C., Jin, J., Xu, S., Liu, H., Li, N. and Cao, X. (2010). Integrin CD11b negatively regulates TLR-triggered inflammatory responses by activating Syk and promoting degradation of MyD88 and TRIF via Cbl-b. *Nat Immunol* **11**(8):734-742.

Hanai, J., Chen, L. F., Kanno, T., Ohtani-Fujita, N., Kim, W. Y., Guo, W. H. *et al.* (1999). Interaction and functional cooperation of PEBP2/CBF with Smads. Synergistic induction of the immunoglobulin germline Calpha promoter. *J Biol Chem* **274**(44):31577-31582.

Hantisteanu, S., Dicken, Y., Negreanu, V., Goldenberg, D., Brenner, O., Leshkowitz, D. *et al.* (2020). Runx3 prevents spontaneous colitis by directing the differentiation of anti-inflammatory mononuclear phagocytes. *PLoS One* **15**(5):e0233044.

Hao, Q. L., Thiemann, F. T., Petersen, D., Smogorzewska, E. M. and Crooks, G. M. (1996). Extended long-term culture reveals a highly quiescent and primitive human hematopoietic progenitor population. *Blood* **88**(9):3306-3313.

Haseyama, Y., Sawada, K., Oda, A., Koizumi, K., Takano, H., Tarumi, T. *et al.* (1999). Phosphatidylinositol 3-kinase is involved in the protection of primary cultured human erythroid precursor cells from apoptosis. *Blood* **94**(5):1568-1577.

Hassan, H., Sakaguchi, S., Tenno, M., Kopf, A., Boucheron, N., Carpenter, A. C. *et al.* (2011). Cd8 enhancer E8(I) and Runx factors regulate CD8 alpha expression in activated CD8(+) T cells. *Proceedings of the National Academy of Sciences of the United States of America* **108**(45):18330-18335.

Heidenreich, O., Krauter, J., Riehle, H., Hadwiger, P., John, M., Heil, G. *et al.* (2003). AML1/MTG8 oncogene suppression by small interfering RNAs supports myeloid differentiation of t(8;21)-positive leukemic cells. *Blood* **101**(8):3157-3163.

Herglotz, J., Kuvardina, O. N., Kolodziej, S., Kumar, A., Hussong, H., Grez, M. *et al.* (2013). Histone arginine methylation keeps RUNX1 target genes in an intermediate state. *Oncogene* **32**(20):2565-2575.

Higuchi, M., O'Brien, D., Kumaravelu, P., Lenny, N., Yeoh, E. J. and Downing, J. R. (2002). Expression of a conditional AML1-ETO oncogene bypasses embryonic lethality and establishes a murine model of human t(8;21) acute myeloid leukemia. *Cancer Cell* **1**(1):63-74.

Hinton, H. J., Alessi, D. R. and Cantrell, D. A. (2004). The serine kinase phosphoinositide-dependent kinase 1 (PDK1) regulates T cell development. *Nat Immunol* **5**(5):539-545.

Ho, T. C., LaMere, M., Stevens, B. M., Ashton, J. M., Myers, J. R., O'Dwyer, K. M. *et al.* (2016). Evolution of acute myelogenous leukemia stem cell properties after treatment and progression. *Blood* **128**(13):1671-1678.

Hock, H., Hamblen, M. J., Rooke, H. M., Schindler, J. W., Saleque, S., Fujiwara, Y. *et al.* (2004). Gfi-1 restricts proliferation and preserves functional integrity of haematopoietic stem cells. *Nature* **431**(7011):1002-1007.

Hock, H., Hamblen, M. J., Rooke, H. M., Traver, D., Bronson, R. T., Cameron, S. *et al.* (2003). Intrinsic requirement for zinc finger transcription factor Gfi-1 in neutrophil differentiation. *Immunity* **18**(1):109-120.

Hoffman, R., Tong, J., Brandt, J., Traycoff, C., Bruno, E., McGuire, B. W. *et al.* (1993). The in vitro and in vivo effects of stem cell factor on human hematopoiesis. *Stem Cells* **11 Suppl 2**:76-82.

Hole, P. S., Pearn, L., Tonks, A. J., James, P. E., Burnett, A. K., Darley, R. L. *et al.* (2010). Ras-induced reactive oxygen species promote growth factor-independent proliferation in human CD34+ hematopoietic progenitor cells. *Blood* **115**(6):1238-1246.

Holtschke, T., Lohler, J., Kanno, Y., Fehr, T., Giese, N., Rosenbauer, F. *et al.* (1996). Immunodeficiency and chronic myelogenous leukemia-like syndrome in mice with a targeted mutation of the ICSBP gene. *Cell* **87**(2):307-317.

Hoogenkamp, M., Lichtinger, M., Krysinska, H., Lancrin, C., Clarke, D., Williamson, A. *et al.* (2009). Early chromatin unfolding by RUNX1: a molecular explanation for differential requirements during specification versus maintenance of the hematopoietic gene expression program. *Blood* **114**(2):299-309.

Hope, K. J., Jin, L. and Dick, J. E. (2004). Acute myeloid leukemia originates from a hierarchy of leukemic stem cell classes that differ in self-renewal capacity. *Nature Immunology* **5**(7):738-743.

Hoppe, P. S., Schwarzfischer, M., Loeffler, D., Kokkaliaris, K. D., Hilsenbeck, O., Moritz, N. *et al.* (2016). Early myeloid lineage choice is not initiated by random PU.1 to GATA1 protein ratios. *Nature* **535**(7611):299-302.

Horman, S. R., Velu, C. S., Chaubey, A., Bourdeau, T., Zhu, J., Paul, W. E. *et al.* (2009). Gfi1 integrates progenitor versus granulocytic transcriptional programming. *Blood* **113**(22):5466-5475.

Houston, I. B., Kamath, M. B., Schweitzer, B. L., Chlon, T. M. and DeKoter, R. P. (2007). Reduction in PU.1 activity results in a block to B-cell development, abnormal myeloid proliferation, and neonatal lethality. *Exp Hematol* **35**(7):1056-1068.

Hsieh, F. F., Barnett, L. A., Green, W. F., Freedman, K., Matushansky, I., Skoultchi, A. I. *et al.* (2000). Cell cycle exit during terminal erythroid differentiation is associated with accumulation of p27(Kip1) and inactivation of cdk2 kinase. *Blood* **96**(8):2746-2754.

Hsu, P. I., Hsieh, H. L., Lee, J., Lin, L. F., Chen, H. C., Lu, P. J. *et al.* (2009). Loss of RUNX3 Expression Correlates with Differentiation, Nodal Metastasis, and Poor Prognosis of Gastric Cancer. *Annals of Surgical Oncology* **16**(6):1686-1694.

Hu, T., Li, C., Wang, L., Zhang, Y., Peng, L., Cheng, H. *et al.* (2017). PDK1 plays a vital role on hematopoietic stem cell function. *Sci Rep* **7**(1):4943.

Hu, X., Chung, A. Y., Wu, I., Foldi, J., Chen, J., Ji, J. D. *et al.* (2008). Integrated regulation of Toll-like receptor responses by Notch and interferon-gamma pathways. *Immunity* **29**(5):691-703.

Huang, B., Qu, Z., Ong, C. W., Tsang, Y. H. N., Xiao, G., Shapiro, D. *et al.* (2012a). RUNX3 acts as a tumor suppressor in breast cancer by targeting estrogen receptor alpha. *Oncogene* **31**(4):527-534.

Huang, G., Zhang, P., Hirai, H., Elf, S., Yan, X., Chen, Z. *et al.* (2008). PU.1 is a major downstream target of AML1 (RUNX1) in adult mouse hematopoiesis. *Nat Genet* **40**(1):51-60.

Huang, G., Zhao, X., Wang, L., Elf, S., Xu, H., Zhao, X. *et al.* (2011). The ability of MLL to bind RUNX1 and methylate H3K4 at PU.1 regulatory regions is impaired by MDS/AML-associated RUNX1/AML1 mutations. *Blood* **118**(25):6544-6552.

Huang, H., Woo, A. J., Waldon, Z., Schindler, Y., Moran, T. B., Zhu, H. H. *et al.* (2012b). A Src family kinase-Shp2 axis controls RUNX1 activity in megakaryocyte and T-lymphocyte differentiation. *Genes Dev* **26**(14):1587-1601.

Huang, S. and Terstappen, L. W. (1994). Lymphoid and myeloid differentiation of single human CD34+, HLA-DR+, CD38- hematopoietic stem cells. *Blood* **83**(6):1515-1526.

Ichikawa, M., Asai, T., Chiba, S., Kurokawa, M. and Ogawa, S. (2004a). Runx1/AML-1 ranks as a master regulator of adult hematopoiesis. *Cell Cycle* **3**(6):722-724.

Ichikawa, M., Asai, T., Saito, T., Yamamoto, G., Seo, S., Yamazaki, I. *et al.* (2004b). AML-1 is required for megakaryocytic maturation and lymphocytic differentiation, but not for maintenance of hematopoietic stem cells in adult hematopoiesis. *Nature Medicine* **10**(3):299-304.

Ikonomi, P., Rivera, C. E., Riordan, M., Washington, G., Schechter, A. N. and Noguchi, C. T. (2000). Overexpression of GATA-2 inhibits erythroid and promotes megakaryocyte differentiation. *Exp Hematol* **28**(12):1423-1431.

Illendula, A., Gilmour, J., Grembecka, J., Tirumala, V. S. S., Boulton, A., Kuntimaddi, A. *et al.* (2016). Small Molecule Inhibitor of CBFbeta-RUNX Binding for RUNX Transcription Factor Driven Cancers. *EBioMedicine* **8**:117-131.

Imai, Y., Kurokawa, M., Yamaguchi, Y., Izutsu, K., Nitta, E., Mitani, K. *et al.* (2004). The corepressor mSin3A regulates phosphorylation-induced activation, intranuclear location, and stability of AML1. *Mol Cell Biol* **24**(3):1033-1043.

Inoue, K., Ozaki, S., Shiga, T., Ito, K., Masuda, T., Okado, N. *et al.* (2002). Runx3 controls the axonal projection of proprioceptive dorsal root ganglion neurons. *Nature Neuroscience* **5**(10):946-954.

Ishikawa, F., Yoshida, S., Saito, Y., Hijikata, A., Kitamura, H., Tanaka, S. *et al.* (2007). Chemotherapy-resistant human AML stem cells home to and engraft within the bone-marrow endosteal region. *Nature Biotechnology* **25**(11):1315-1321.

Ito, K., Lim, A. C. B., Salto-Tellez, M., Motoda, L., Osato, M., Shyue, L. *et al.* (2008). RUNX3 attenuates beta-catenin/T cell factors in intestinal tumorigenesis. *Cancer Cell* **14**(3):226-237.

Ito, K., Liu, Q., Salto-Tellez, M., Yano, T., Tada, K., Ida, H. *et al.* (2005). RUNX3, a novel tumor suppressor, is frequently inactivated in gastric cancer by protein mislocalization. *Cancer Research* **65**(17):7743-7750.

Ito, Y., Bae, S. C. and Chuang, L. S. H. (2015). The RUNX family: developmental regulators in cancer. *Nature Reviews Cancer* **15**(2):81-95.

Iwasaki, H., Mizuno, S., Arinobu, Y., Ozawa, H., Mori, Y., Shigematsu, H. *et al.* (2006). The order of expression of transcription factors directs hierarchical specification of hematopoietic lineages. *Genes Dev* **20**(21):3010-3021.

Iwasaki, H., Mizuno, S., Wells, R. A., Cantor, A. B., Watanabe, S. and Akashi, K. (2003). GATA-1 converts lymphoid and myelomonocytic progenitors into the megakaryocyte/erythrocyte lineages. *Immunity* **19**(3):451-462.

Iwasaki, H., Somoza, C., Shigematsu, H., Duprez, E. A., Iwasaki-Arai, J., Mizuno, S. *et al.* (2005). Distinctive and indispensable roles of PU.1 in maintenance of hematopoietic stem cells and their differentiation. *Blood* **106**(5):1590-1600.

Jacob, B., Osato, M., Yamashita, N., Wang, C. Q., Taniuchi, I., Littman, D. R. *et al.* (2010). Stem cell exhaustion due to Runx1 deficiency is prevented by Evi5 activation in leukemogenesis. *Blood* **115**(8):1610-1620.

Jagannathan-Bogdan, M. and Zon, L. I. (2013). Hematopoiesis. *Development* **140**(12):2463-2467.

Jakubowiak, A., Pouponnot, C., Berguido, F., Frank, R., Mao, S., Massague, J. *et al.* (2000). Inhibition of the transforming growth factor beta 1 signaling pathway by the AML1/ETO leukemia-associated fusion protein. *J Biol Chem* **275**(51):40282-40287.

Jan, M., Snyder, T. M., Corces-Zimmerman, M. R., Vyas, P., Weissman, I. L., Quake, S. R. *et al.* (2012). Clonal evolution of preleukemic hematopoietic stem cells precedes human acute myeloid leukemia. *Sci Transl Med* **4**(149):149ra118.

Jankovic, V., Ciarrocchi, A., Boccuni, P., DeBlasio, T., Benezra, R. and Nimer, S. D. (2007). Id1 restrains myeloid commitment, maintaining the self-renewal capacity of hematopoietic stem cells. *Proc Natl Acad Sci U S A* **104**(4):1260-1265.

Jassam, S. A., Maherally, Z., Ashkan, K., Pilkington, G. J. and Fillmore, H. L. (2019). Fucosyltransferase 4 and 7 mediates adhesion of non-small cell lung cancer cells to brain-derived endothelial cells and results in modification of the blood-brain-barrier: in vitro investigation of CD15 and CD15s in lung-to-brain metastasis. *J Neurooncol* **143**(3):405-415.

Jeon, E. J., Lee, K. Y., Choi, N. S., Lee, M. H., Kim, H. N., Jin, Y. H. *et al.* (2006). Bone morphogenetic protein-2 stimulates Runx2 acetylation. *J Biol Chem* **281**(24):16502-16511.

Ji, M., Li, H., Suh, H. C., Klarmann, K. D., Yokota, Y. and Keller, J. R. (2008). Id2 intrinsically regulates lymphoid and erythroid development via interaction with different target proteins. *Blood* **112**(4):1068-1077.

Jin, Y. H., Jeon, E. J., Li, Q. L., Lee, Y. H., Choi, J. K., Kim, W. J. *et al.* (2004). Transforming growth factor-beta stimulates p300-dependent RUNX3 acetylation, which inhibits ubiquitination-mediated degradation. *Journal of Biological Chemistry* **279**(28):29409-29417.

Jing, H., Vakoc, C. R., Ying, L., Mandat, S., Wang, H., Zheng, X. *et al.* (2008). Exchange of GATA factors mediates transitions in looped chromatin organization at a developmentally regulated gene locus. *Mol Cell* **29**(2):232-242.

Justus, C. R., Leffler, N., Ruiz-Echevarria, M. and Yang, L. V. (2014). In vitro cell migration and invasion assays. *J Vis Exp* (88).

Kadia, T. M., Kantarjian, H. M. and Konopleva, M. (2019). Myeloid cell leukemia-1 dependence in acute myeloid leukemia: a novel approach to patient therapy. *Oncotarget* **10**(12):1250-1265.

Kadota, M., Yang, H. H., Gomez, B., Sato, M., Clifford, R. J., Meerzaman, D. *et al.* (2010). Delineating genetic alterations for tumor progression in the MCF10A series of breast cancer cell lines. *PLoS One* **5**(2):e9201.

Kagoshima, H., Shigesada, K., Satake, M., Ito, Y., Miyoshi, H., Ohki, M. *et al.* (1993). The Runt domain identifies a new family of heteromeric transcriptional regulators. *Trends Genet* **9**(10):338-341.

Kalev-Zylinska, M. L., Horsfield, J. A., Flores, M. V. C., Postlethwait, J. H., Chau, J. Y. M., Cattin, P. M. *et al.* (2003). Runx3 is required for hematopoietic development in zebrafish. *Developmental Dynamics* **228**(3):323-336.

Kamachi, Y., Ogawa, E., Asano, M., Ishida, S., Murakami, Y., Satake, M. *et al.* (1990). Purification of a mouse nuclear factor that binds to both the A and B cores of the polyomavirus enhancer. *J Virol* **64**(10):4808-4819.

Kanehisa, M. and Goto, S. (2000). KEGG: kyoto encyclopedia of genes and genomes. *Nucleic Acids Res* **28**(1):27-30.

Kannan, S., Sutphin, R. M., Hall, M. G., Golfman, L. S., Fang, W., Nolo, R. M. *et al.* (2013). Notch activation inhibits AML growth and survival: a potential therapeutic approach. *J Exp Med* **210**(2):321-337.

Karamitros, D., Stoilova, B., Aboukhalil, Z., Hamey, F., Reinisch, A., Samitsch, M. *et al.* (2018). Single-cell analysis reveals the continuum of human lympho-myeloid progenitor cells. *Nature Immunology* **19**(1):85-97.

Karsunky, H., Zeng, H., Schmidt, T., Zevnik, B., Kluge, R., Schmid, K. W. *et al.* (2002). Inflammatory reactions and severe neutropenia in mice lacking the transcriptional repressor Gfi1. *Nat Genet* **30**(3):295-300.

Kas, S. M., de Ruiter, J. R., Schipper, K., Annunziato, S., Schut, E., Klarenbeek, S. *et al.* (2017). Insertional mutagenesis identifies drivers of a novel oncogenic pathway in invasive lobular breast carcinoma. *Nat Genet* **49**(8):1219-1230.

Katayama, Y., Battista, M., Kao, W. M., Hidalgo, A., Peired, A. J., Thomas, S. A. *et al.* (2006). Signals from the sympathetic nervous system regulate hematopoietic stem cell egress from bone marrow. *Cell* **124**(2):407-421.

Katayama, Y., Takahashi, M. and Kuwayama, H. (2009). Helicobacter pylori causes runx3 gene methylation and its loss of expression in gastric epithelial cells, which is mediated by nitric oxide produced by macrophages. *Biochemical and Biophysical Research Communications* **388**(3):496-500.

Kato, T., Sakata-Yanagimoto, M., Nishikii, H., Ueno, M., Miyake, Y., Yokoyama, Y. *et al.* (2015). Hes1 suppresses acute myeloid leukemia development through FLT3 repression. *Leukemia* **29**(3):576-585.

Keita, M., Bachvarova, M., Morin, C., Plante, M., Gregoire, J., Renaud, M. C. *et al.* (2013). The RUNX1 transcription factor is expressed in serous epithelial ovarian carcinoma and contributes to cell proliferation, migration and invasion. *Cell Cycle* **12**(6):972-986.

Khwaja, A., Bjorkholm, M., Gale, R. E., Levine, R. L., Jordan, C. T., Ehninger, G. *et al.* (2016). Acute myeloid leukaemia. *Nat Rev Dis Primers* **2**:16010.

Kiel, M. J., Acar, M., Radice, G. L. and Morrison, S. J. (2009). Hematopoietic stem cells do not depend on N-cadherin to regulate their maintenance. *Cell stem cell* **4**(2):170-179.

Kieran, M. W., Perkins, A. C., Orkin, S. H. and Zon, L. I. (1996). Thrombopoietin rescues in vitro erythroid colony formation from mouse embryos lacking the erythropoietin receptor. *Proc Natl Acad Sci U S A* **93**(17):9126-9131.

Kikushige, Y., Yoshimoto, G., Miyamoto, T., Iino, T., Mori, Y., Iwasaki, H. *et al.* (2008). Human Flt3 is expressed at the hematopoietic stem cell and the granulocyte/macrophage progenitor stages to maintain cell survival. *J Immunol* **180**(11):7358-7367.

Kim, B. R., Kang, M. H., Kim, J. L., Na, Y. J., Park, S. H., Lee, S. I. *et al.* (2016). RUNX3 inhibits the metastasis and angiogenesis of colorectal cancer. *Oncology Reports* **36**(5):2601-2608.

Kim, B. R., Na, Y. J., Kim, J. L., Jeong, Y. A., Park, S. H., Jo, M. J. *et al.* (2020). RUNX3 suppresses metastasis and stemness by inhibiting Hedgehog signaling in colorectal cancer. *Cell Death Differ* **27**(2):676-694.

Kim, B. R., Park, S. H., Jeong, Y. A., Na, Y. J., Kim, J. L., Jo, M. J. *et al.* (2019). RUNX3 enhances TRAIL-induced apoptosis by upregulating DR5 in colorectal cancer. *Oncogene* **38**(20):3903-3918.

Kim, E. J., Kim, Y. J., Jeong, P., Ha, Y. S., Bae, S. C. and Kim, W. J. (2008a). Methylation of the RUNX3 promoter as a potential prognostic marker for bladder tumor. *Journal of Urology* **180**(3):1141-1145.

Kim, H. R., Oh, B. C., Choi, J. K. and Bae, S. C. (2008b). Pim-1 Kinase Phosphorylates and Stabilizes RUNX3 and Alters Its Subcellular Localization. *Journal of Cellular Biochemistry* **105**(4):1048-1058.

Kim, J. H., Choi, J. K., Cinghu, S., Jang, J. W., Lee, Y. S., Li, Y. H. *et al.* (2009). Jab1/CSN5 Induces the Cytoplasmic Localization and Degradation of RUNX3. *Journal of Cellular Biochemistry* **107**(3):557-565.

Kim, T. Y., Lee, H. J., Hwang, K. S., Lee, M., Kim, J. W., Bang, Y. J. *et al.* (2004). Methylation of RUNX3 in various types of human cancers and premalignant stages of gastric carcinoma. *Laboratory Investigation* **84**(4):479-484.

Kim, W. J., Kim, E. J., Jeong, P. D., Quan, C. Y., Kim, J. Y., Li, Q. L. *et al.* (2005). RUNX3 inactivation by point mutations and aberrant DNA methylation in bladder tumors. *Cancer Research* **65**(20):9347-9354.

Kim, W. J., Lee, J. W., Quan, C., Youn, H. J., Kim, H. M. and Bae, S. C. (2011). Nicotinamide Inhibits Growth of Carcinogen Induced Mouse Bladder Tumor and Human Bladder Tumor Xenograft Through Up-Regulation of RUNX3 and p300. *Journal of Urology* **185**(6):2366-2375.

Kirtane, K. and Lee, S. J. (2017). Racial and ethnic disparities in hematologic malignancies. *Blood* **130**(15):1699-1705.

Kitabayashi, I., Aikawa, Y., Nguyen, L. A., Yokoyama, A. and Ohki, M. (2001). Activation of AML1-mediated transcription by MOZ and inhibition by the MOZ-CBP fusion protein. *EMBO J* **20**(24):7184-7196.

Klunker, S., Chong, M. M. W., Mantel, P. Y., Palomares, O., Bassin, C., Ziegler, M. *et al.* (2009). Transcription factors RUNX1 and RUNX3 in the induction and suppressive function of Foxp3(+) inducible regulatory T cells. *Journal of Experimental Medicine* **206**(12):2701-2715.

Koh, C. P., Wang, C. Q., Ng, C. E., Ito, Y., Araki, M., Tergaonkar, V. *et al.* (2013). RUNX1 meets MLL: epigenetic regulation of hematopoiesis by two leukemia genes. *Leukemia* **27**(9):1793-1802.

Kohlmann, A., Kipps, T. J., Rassenti, L. Z., Downing, J. R., Shurtleff, S. A., Mills, K. I. *et al.* (2008). An international standardization programme towards the application of gene expression profiling in routine leukaemia diagnostics: the Microarray Innovations in LEukemia study prephase. *Br J Haematol* **142**(5):802-807.

Kohu, K., Ohmori, H., Wong, W. F., Onda, D., Wakoh, T., Kon, S. *et al.* (2009). The Runx3 Transcription Factor Augments Th1 and Down-Modulates Th2 Phenotypes by Interacting with and Attenuating GATA3. *Journal of Immunology* **183**(12):7817-7824.

Kohu, K., Sato, T., Ohno, S., Hayashi, K., Uchino, R., Abe, N. *et al.* (2005). Overexpression of the Runx3 transcription factor increases the proportion of mature thymocytes of the CD8 single-positive lineage. *J Immunol* **174**(5):2627-2636.

Komori, T., Yagi, H., Nomura, S., Yamaguchi, A., Sasaki, K., Deguchi, K. *et al.* (1997). Targeted disruption of Cbfa1 results in a complete lack of bone formation owing to maturational arrest of osteoblasts. *Cell* **89**(5):755-764.

Koreth, J., Schlenk, R., Kopecky, K. J., Honda, S., Sierra, J., Djulbegovic, B. J. *et al.* (2009). Allogeneic stem cell transplantation for acute myeloid leukemia in first complete remission: systematic review and meta-analysis of prospective clinical trials. *JAMA* **301**(22):2349-2361.

Kozu, T., Fukuyama, T., Yamami, T., Akagi, K. and Kaneko, Y. (2005). MYND-less splice variants of AML1-MTG8 (RUNX1-CBFA2T1) are expressed in leukemia with t(8;21). *Genes Chromosomes Cancer* **43**(1):45-53.

Kramer, A., Green, J., Pollard, J., Jr. and Tugendreich, S. (2014). Causal analysis approaches in Ingenuity Pathway Analysis. *Bioinformatics* **30**(4):523-530.

Kramer, I., Sigrist, M., de Nooij, J. C., Taniuchi, I., Jessel, T. M. and Arber, S. (2006). A role for Runx transcription factor signaling in dorsal root ganglion sensory neuron diversification. *Neuron* **49**(3):379-393.

Krauth, M. T., Eder, C., Alpermann, T., Bacher, U., Nadarajah, N., Kern, W. *et al.* (2014). High number of additional genetic lesions in acute myeloid leukemia with t(8;21)/RUNX1-RUNX1 T1: frequency and impact on clinical outcome. *Leukemia* **28**(7):1449-1458.

Krygier, A., Szmajda, D., Zebrowska, M., Jelen, A. and Balcerczak, E. (2018). Expression levels of the runt-related transcription factor 1 and 3 genes in the development of acute myeloid leukemia. *Oncol Lett* **15**(5):6733-6738.

Ku, J. L., Kang, S. B., Shin, Y. K., Kang, H. C., Hong, S. H., Kim, I. J. *et al.* (2004). Promoter hypermethylation downregulates RUNX3 gene expression in colorectal cancer cell lines. *Oncogene* **23**(40):6736-6742.

Kueh, H. Y., Champhekar, A., Nutt, S. L., Elowitz, M. B. and Rothenberg, E. V. (2013). Positive feedback between PU.1 and the cell cycle controls myeloid differentiation. *Science* **341**(6146):670-673.

Kulkarni, M., Tan, T. Z., Syed Sulaiman, N. B., Lamar, J. M., Bansal, P., Cui, J. *et al.* (2018). RUNX1 and RUNX3 protect against YAP-mediated EMT, stem-ness and shorter survival outcomes in breast cancer. *Oncotarget* **9**(18):14175-14192.

Kumar, S., Xu, J., Perkins, C., Guo, F., Snapper, S., Finkelman, F. D. *et al.* (2012). Cdc42 regulates neutrophil migration via crosstalk between WASp, CD11b, and microtubules. *Blood* **120**(17):3563-3574.

Kunisaki, Y., Bruns, I., Scheiermann, C., Ahmed, J., Pinho, S., Zhang, D. *et al.* (2013). Arteriolar niches maintain haematopoietic stem cell quiescence. *Nature* **502**(7473):637-643.

Kuo, Y. H., Zaidi, S. K., Gornostaeva, S., Komori, T., Stein, G. S. and Castilla, L. H. (2009). Runx2 induces acute myeloid leukemia in cooperation with Cbfbeta-SMMHC in mice. *Blood* **113**(14):3323-3332.

Kurioka, A., Cosgrove, C., Simoni, Y., van Wilgenburg, B., Geremia, A., Bjorkander, S. *et al.* (2018). CD161 Defines a Functionally Distinct Subset of Pro-Inflammatory Natural Killer Cells. *Front Immunol* **9**:486.

Kusumbe, A. P., Ramasamy, S. K., Itkin, T., Mäe, M. A., Langen, U. H., Betsholtz, C. *et al.* (2016). Age-dependent modulation of vascular niches for haematopoietic stem cells. *Nature* **532**(7599):380-384.

Kuvarina, O. N., Herglotz, J., Kolodziej, S., Kohrs, N., Herkt, S., Wojcik, B. *et al.* (2015). RUNX1 represses the erythroid gene expression program during megakaryocytic differentiation. *Blood* **125**(23):3570-3579.

Kwok, C., Zeisig, B. B., Qiu, J. H., Dong, S. O. and So, C. W. E. (2009). Transforming activity of AML1-ETO is independent of CBF beta and ETO interaction but requires formation of homo-oligomeric complexes. *Proceedings of the National Academy of Sciences of the United States of America* **106**(8):2853-2858.

Lacaud, G. and Kouskoff, V. (2017). Hemangioblast, hemogenic endothelium, and primitive versus definitive hematopoiesis. *Exp Hematol* **49**:19-24.

Lacayo, N. J., Meshinchi, S., Kinnunen, P., Yu, R., Wang, Y., Stuber, C. M. *et al.* (2004). Gene expression profiles at diagnosis in de novo childhood AML patients identify FLT3 mutations with good clinical outcomes. *Blood* **104**(9):2646-2654.

Lachowicz, C. A., Loghavi, S., Kadia, T. M., Daver, N., Borthakur, G., Pemmaraju, N. *et al.* (2020). Outcomes of older patients with NPM1-mutated AML: current treatments and the promise of venetoclax-based regimens. *Blood Adv* **4**(7):1311-1320.

Lacombe, J., Herblot, S., Rojas-Sutterlin, S., Haman, A., Barakat, S., Iscove, N. N. *et al.* (2010). Scl regulates the quiescence and the long-term competence of hematopoietic stem cells. *Blood* **115**(4):792-803.

Lagadinou, E. D., Sach, A., Callahan, K., Rossi, R. M., Neering, S. J., Minhajuddin, M. *et al.* (2013). BCL-2 inhibition targets oxidative phosphorylation and selectively eradicates quiescent human leukemia stem cells. *Cell Stem Cell* **12**(3):329-341.

Laiosa, C. V., Stadtfeld, M., Xie, H., de Andres-Aguayo, L. and Graf, T. (2006). Reprogramming of committed T cell progenitors to macrophages and dendritic cells by C/EBP alpha and PU.1 transcription factors. *Immunity* **25**(5):731-744.

Lam, K. and Zhang, D. E. (2012). RUNX1 and RUNX1-ETO: roles in hematopoiesis and leukemogenesis. *Frontiers in Bioscience-Landmark* **17**:1120-1139.

Landry, J. R., Kinston, S., Knezevic, K., de Bruijn, M. F. T. R., Wilson, N., Nottingham, W. T. *et al.* (2008). Runx genes are direct targets of Scl/Tal1 in the yolk sac and fetal liver. *Blood* **111**(6):3005-3014.

Lapidot, T., Sirard, C., Vormoor, J., Murdoch, B., Hoang, T., Caceres-Cortes, J. *et al.* (1994). A cell initiating human acute myeloid leukaemia after transplantation into SCID mice. *Nature* **367**(6464):645-648.

Lara-Astiaso, D., Weiner, A., Lorenzo-Vivas, E., Zaretzky, I., Jaitin, D. A., David, E. *et al.* (2014). Immunogenetics. Chromatin state dynamics during blood formation. *Science* **345**(6199):943-949.

Larrosa-Garcia, M. and Baer, M. R. (2017). FLT3 Inhibitors in Acute Myeloid Leukemia: Current Status and Future Directions. *Mol Cancer Ther* **16**(6):991-1001.

Lau, Q. C., Raja, E., Salto-Terez, M., Liu, Q., Ito, K., Inoue, M. *et al.* (2006). RUNX3 is frequently inactivated by dual mechanisms of protein mislocalization and promoter hypermethylation in breast cancer. *Cancer Research* **66**(13):6512-6520.

Laurenti, E., Frelin, C., Xie, S., Ferrari, R., Dunant, C. F., Zandi, S. *et al.* (2015). CDK6 levels regulate quiescence exit in human hematopoietic stem cells. *Cell Stem Cell* **16**(3):302-313.

Laurenti, E. and Gottgens, B. (2018). From haematopoietic stem cells to complex differentiation landscapes. *Nature* **553**(7689):418-426.

Laurenti, E., Varnum-Finney, B., Wilson, A., Ferrero, I., Blanco-Bose, W. E., Ehninger, A. *et al.* (2008). Hematopoietic stem cell function and survival depend on c-Myc and N-Myc activity. *Cell Stem Cell* **3**(6):611-624.

Lawrence, S. M., Corriden, R. and Nizet, V. (2018). The Ontogeny of a Neutrophil: Mechanisms of Granulopoiesis and Homeostasis. *Microbiol Mol Biol Rev* **82**(1).

Le, X. F., Groner, Y., Kornblau, S. M., Gu, Y., Hittelman, W. N., Levanon, D. *et al.* (1999). Regulation of AML2/CBFA3 in hematopoietic cells through the retinoic acid receptor alpha-dependent signaling pathway. *J Biol Chem* **274**(31):21651-21658.

Lee, C. W. L., Chuang, L. S. H., Kimura, S., Lai, S. K., Ong, C. W., Yan, B. *et al.* (2011). RUNX3 functions as an oncogene in ovarian cancer. *Gynecologic Oncology* **122**(2):410-417.

Lee, J. W., Kim, D. M., Jang, J. W., Park, T. G., Song, S. H., Lee, Y. S. *et al.* (2019). RUNX3 regulates cell cycle-dependent chromatin dynamics by functioning as a pioneer factor of the restriction-point. *Nat Commun* **10**(1):1897.

Lee, K. S., Lee, Y. S., Lee, J. M., Ito, K., Cinghu, S., Kim, J. H. *et al.* (2010). Runx3 is required for the differentiation of lung epithelial cells and suppression of lung cancer. *Oncogene* **29**(23):3349-3361.

Lee, S. H., Kim, J., Kim, W. H. and Lee, Y. M. (2009). Hypoxic silencing of tumor suppressor RUNX3 by histone modification in gastric cancer cells. *Oncogene* **28**(2):184-194.

Lee, T. I., Jenner, R. G., Boyer, L. A., Guenther, M. G., Levine, S. S., Kumar, R. M. *et al.* (2006). Control of developmental regulators by Polycomb in human embryonic stem cells. *Cell* **125**(2):301-313.

Lee, Y. S., Lee, J. W., Jang, J. W., Chi, X. Z., Kim, J. H., Li, Y. H. *et al.* (2013). Runx3 Inactivation Is a Crucial Early Event in the Development of Lung Adenocarcinoma. *Cancer Cell* **24**(5):603-616.

Leisch, M., Jansko, B., Zaborsky, N., Greil, R. and Pleyer, L. (2019). Next Generation Sequencing in AML-On the Way to Becoming a New Standard for Treatment Initiation and/or Modulation? *Cancers (Basel)* **11**(2).

Levanon, D., Bettoun, D., Harris-Cerruti, C., Woolf, E., Negreanu, V., Eilam, R. *et al.* (2002). The Runx3 transcription factor regulates development and survival of TrkC dorsal root ganglia neurons. *Embo Journal* **21**(13):3454-3463.

Levanon, D., Brenner, O., Negreanu, V., Bettoun, D., Woolf, E., Eilam, R. *et al.* (2001a). Spatial and temporal expression pattern of Runx3 (Aml2) and Runx1 (Aml1) indicates non-redundant functions during mouse embryogenesis. *Mechanisms of Development* **109**(2):413-417.

Levanon, D., Glusman, G., Bangsow, T., Ben-Asher, E., Male, D. A., Avidan, N. *et al.* (2001b). Architecture and anatomy of the genomic locus encoding the human leukemia-associated transcription factor RUNX1/AML1. *Gene* **262**(1-2):23-33.

Levanon, D., Glusman, G., Bettoun, D., Ben-Asher, E., Negreanu, V., Bernstein, Y. *et al.* (2003). Phylogenesis and regulated expression of the RUNT domain transcription factors RUNX1 and RUNX3. *Blood Cells Molecules and Diseases* **30**(2):161-163.

Levanon, D., Goldstein, R. E., Bernstein, Y., Tang, H., Goldenberg, D., Stifani, S. *et al.* (1998). Transcriptional repression by AML1 and LEF-1 is mediated by the TLE/Groucho corepressors. *Proc Natl Acad Sci U S A* **95**(20):11590-11595.

Levanon, D. and Groner, Y. (2004). Structure and regulated expression of mammalian RUNX genes. *Oncogene* **23**(24):4211-4219.

Levanon, D., Negreanu, V., Bernstein, Y., Bar-Am, I., Avivi, L. and Groner, Y. (1994). AML1, AML2, and AML3, the human members of the runt domain gene-family: cDNA structure, expression, and chromosomal localization. *Genomics* **23**(2):425-432.

Levanon, D., Negreanu, V., Lotem, J., Bone, K. R., Brenner, O., Leshkowitz, D. *et al.* (2014). Transcription Factor Runx3 Regulates Interleukin-15-Dependent Natural Killer Cell Activation. *Molecular and Cellular Biology* **34**(6):1158-1169.

Li, Q. L., Ito, K., Sakakura, C., Fukamachi, H., Inoue, K., Chi, X. Z. *et al.* (2002). Causal relationship between the loss of RUNX3 expression and gastric cancer. *Cell* **109**(1):113-124.

Li, Q. L., Kim, H. R., Kim, W. J., Choi, J. K., Lee, Y. H., Kim, H. M. *et al.* (2004). Transcriptional silencing of the RUNX3 gene by CpG hypermethylation is associated with lung cancer. *Biochemical and Biophysical Research Communications* **314**(1):223-228.

Li, Y. Z., Wang, H. W., Wang, X. L., Jin, W., Tan, Y., Fang, H. *et al.* (2016). Genome-wide studies identify a novel interplay between AML1 and AML1/ETO in t(8;21) acute myeloid leukemia. *Blood* **127**(2):233-242.

Liakhovitskaia, A., Lana-Elola, E., Stamateris, E., Rice, D. P., van 't Hof, R. J. and Medvinsky, A. (2010). The essential requirement for Runx1 in the development of the sternum. *Dev Biol* **340**(2):539-546.

Lichtinger, M., Ingram, R., Hannah, R., Muller, D., Clarke, D., Assi, S. A. *et al.* (2012). RUNX1 reshapes the epigenetic landscape at the onset of haematopoiesis. *EMBO J* **31**(22):4318-4333.

Lieschke, G. J., Grail, D., Hodgson, G., Metcalf, D., Stanley, E., Cheers, C. *et al.* (1994). Mice lacking granulocyte colony-stimulating factor have chronic neutropenia, granulocyte and macrophage progenitor cell deficiency, and impaired neutrophil mobilization. *Blood* **84**(6):1737-1746.

Lin, C. S., Lim, S. K., D'Agati, V. and Costantini, F. (1996). Differential effects of an erythropoietin receptor gene disruption on primitive and definitive erythropoiesis. *Genes Dev* **10**(2):154-164.

Lin, S., Mulloy, J. C. and Goyama, S. (2017). RUNX1-ETO Leukemia. *Runx Proteins in Development and Cancer* **962**:151-173.

Lindberg, S. R., Olsson, A., Persson, A. M. and Olsson, I. (2005). The Leukemia-associated ETO homologues are differently expressed during hematopoietic differentiation. *Exp Hematol* **33**(2):189-198.

Ling, G. S., Bennett, J., Woollard, K. J., Szajna, M., Fossati-Jimack, L., Taylor, P. R. *et al.* (2014). Integrin CD11b positively regulates TLR4-induced signalling pathways in dendritic cells but not in macrophages. *Nat Commun* **5**:3039.

Linggi, B., Muller-Tidow, C., van de Locht, L., Hu, M., Nip, J., Serve, H. *et al.* (2002). The t(8;21) fusion protein, AML1-ETO, specifically represses the transcription of the p14(ARF) tumor suppressor in acute myeloid leukemia. *Nature Medicine* **8**(7):743-750.

Link, K. A., Lin, S., Shrestha, M., Bowman, M., Wunderlich, M., Bloomfield, C. D. *et al.* (2016). Supraphysiologic levels of the AML1-ETO isoform AE9a are essential for transformation. *Proceedings of the National Academy of Sciences of the United States of America* **113**(32):9075-9080.

Liu, B., Ma, H., Liu, Q., Xiao, Y., Pan, S., Zhou, H. *et al.* (2019). MiR-29b/Sp1/FUT4 axis modulates the malignancy of leukemia stem cells by regulating fucosylation via Wnt/beta-catenin pathway in acute myeloid leukemia. *J Exp Clin Cancer Res* **38**(1):200.

Liu, F., Wu, H. Y., Wesselschmidt, R., Kornaga, T. and Link, D. C. (1996). Impaired production and increased apoptosis of neutrophils in granulocyte colony-stimulating factor receptor-deficient mice. *Immunity* **5**(5):491-501.

Liu, H., Chen, C., Ma, D., Li, Y., Yin, Q., Li, Q. *et al.* (2020). Inhibition of PIM1 attenuates the stem cell-like traits of breast cancer cells by promoting RUNX3 nuclear retention. *J Cell Mol Med* **24**(11):6308-6323.

Liu, H. P., Cao, A. T., Feng, T., Li, Q., Zhang, W., Yao, S. *et al.* (2015). TGF-beta converts Th1 cells into Th17 cells through stimulation of Runx1 expression. *Eur J Immunol* **45**(4):1010-1018.

Liu, S., Shen, T., Huynh, L., Klisovic, M. I., Rush, L. J., Ford, J. L. *et al.* (2005). Interplay of RUNX1/MTG8 and DNA methyltransferase 1 in acute myeloid leukemia. *Cancer Res* **65**(4):1277-1284.

Liu, Y. Z., Cheney, M. D., Gaudet, J. J., Chruszcz, M., Lukasik, S. M., Sugiyama, D. *et al.* (2006). The tetramer structure of the Neryv homology two domain, NHR2, is critical for AM1/ETO's activity. *Cancer Cell* **9**(4):249-260.

Liu, Z. F., Chen, L., Zhang, X. C., Xu, X., Xing, H. X., Zhang, Y. J. *et al.* (2014a). RUNX3 regulates vimentin expression via miR-30a during epithelial- mesenchymal transition in gastric cancer cells. *Journal of Cellular and Molecular Medicine* **18**(4):610-623.

Liu, Z. F., Xu, X., Chen, L., Li, W. J., Sun, Y. D., Zeng, J. P. *et al.* (2012). Helicobacter pylori CagA inhibits the expression of Runx3 via Src/MEK/ERK and p38 MAPK pathways in gastric epithelial cell. *Journal of Cellular Biochemistry* **113**(3):1080-1086.

Liu, Z. F., Zhang, X. C., Xu, X., Chen, L., Li, W. J., Yu, H. *et al.* (2014b). RUNX3 inhibits survivin expression and induces cell apoptosis in gastric cancer. *European Journal of Cell Biology* **93**(3):118-126.

Lo-Coco, F., Avvisati, G., Vignetti, M., Thiede, C., Orlando, S. M., Iacobelli, S. *et al.* (2013). Retinoic acid and arsenic trioxide for acute promyelocytic leukemia. *N Engl J Med* **369**(2):111-121.

Lo, M. C., Peterson, L. F., Yan, M., Cong, X. L., Jin, F. L., Shia, W. J. *et al.* (2012). Combined gene expression and DNA occupancy profiling identifies potential therapeutic targets of t(8;21) AML. *Blood* **120**(7):1473-1484.

Lobry, C., Ntziachristos, P., Ndiaye-Lobry, D., Oh, P., Cimmino, L., Zhu, N. *et al.* (2013). Notch pathway activation targets AML-initiating cell homeostasis and differentiation. *J Exp Med* **210**(2):301-319.

Lorenz, E., Uphoff, D., Reid, T. R. and Shelton, E. (1951). Modification of irradiation injury in mice and guinea pigs by bone marrow injections. *J Natl Cancer Inst* **12**:197-201.

Lorsbach, R. B., Moore, J., Ang, S. O., Sun, W., Lenny, N. and Downing, J. R. (2004). Role of RUNX1 in adult hematopoiesis: analysis of RUNX1-IRES-GFP knock-in mice reveals differential lineage expression. *Blood* **103**(7):2522-2529.

Lotem, J., Levanon, D., Negreanu, V., Leshkowitz, D., Friedlander, G. and Groner, Y. (2013). Runx3-mediated Transcriptional Program in Cytotoxic Lymphocytes. *Plos One* **8**(11).

Lubbers, R., van Essen, M. F., van Kooten, C. and Trouw, L. A. (2017). Production of complement components by cells of the immune system. *Clin Exp Immunol* **188**(2):183-194.

Lukashev, M., LePage, D., Wilson, C., Bailly, V., Garber, E., Lukashin, A. *et al.* (2006). Targeting the lymphotoxin-beta receptor with agonist antibodies as a potential cancer therapy. *Cancer Res* **66**(19):9617-9624.

Lutterbach, B., Westendorf, J. J., Linggi, B., Isaac, S., Seto, E. and Hiebert, S. W. (2000). A mechanism of repression by acute myeloid leukemia-1, the target of multiple chromosomal translocations in acute leukemia. *J Biol Chem* **275**(1):651-656.

Lutterbach, B., Westendorf, J. J., Linggi, B., Patten, A., Moniwa, M., Davie, J. R. *et al.* (1998). ETO, a target of t(8;21) in acute leukemia, interacts with the N-CoR and mSin3 corepressors. *Molecular and Cellular Biology* **18**(12):7176-7184.

Mach, D. B., Rogers, S. D., Sabino, M. C., Luger, N. M., Schwei, M. J., Pomonis, J. D. *et al.* (2002). Origins of skeletal pain: sensory and sympathetic innervation of the mouse femur. *Neuroscience* **113**(1):155-166.

Maggi, L., Santarlasci, V., Capone, M., Peired, A., Frosali, F., Crome, S. Q. *et al.* (2010). CD161 is a marker of all human IL-17-producing T-cell subsets and is induced by RORC. *Eur J Immunol* **40**(8):2174-2181.

Magor, G. W., Tallack, M. R., Gillinder, K. R., Bell, C. C., McCallum, N., Williams, B. *et al.* (2015). KLF1-null neonates display hydrops fetalis and a deranged erythroid transcriptome. *Blood* **125**(15):2405-2417.

Majeti, R., Becker, M. W., Tian, Q., Lee, T. L., Yan, X., Liu, R. *et al.* (2009). Dysregulated gene expression networks in human acute myelogenous leukemia stem cells. *Proc Natl Acad Sci U S A* **106**(9):3396-3401.

Majeti, R., Park, C. Y. and Weissman, I. L. (2007). Identification of a hierarchy of multipotent hematopoietic progenitors in human cord blood. *Cell Stem Cell* **1**(6):635-645.

Mandoli, A., Singh, A. A., Prange, K. H. M., Tijchon, E., Oerlemans, M., Dirks, R. *et al.* (2016). The Hematopoietic Transcription Factors RUNX1 and ERG Prevent AML1-ETO

Oncogene Overexpression and Onset of the Apoptosis Program in t(8;21) AMLs. *Cell Reports* **17**(8):2087-2100.

Mangan, J. K. and Speck, N. A. (2011). RUNX1 mutations in clonal myeloid disorders: from conventional cytogenetics to next generation sequencing, a story 40 years in the making. *Crit Rev Oncog* **16**(1-2):77-91.

Mao, B., Huang, S., Lu, X., Sun, W., Zhou, Y., Pan, X. *et al.* (2016). Early Development of Definitive Erythroblasts from Human Pluripotent Stem Cells Defined by Expression of Glycophorin A/CD235a, CD34, and CD36. *Stem Cell Reports* **7**(5):869-883.

Martens, J. H. A., Mandoli, A., Simmer, F., Wierenga, B. J., Saeed, S., Singh, A. A. *et al.* (2012). ERG and FLI1 binding sites demarcate targets for aberrant epigenetic regulation by AML1-ETO in acute myeloid leukemia. *Blood* **120**(19):4038-4048.

Martin, J. W., Zielenska, M., Stein, G. S., van Wijnen, A. J. and Squire, J. A. (2011). The Role of RUNX2 in Osteosarcoma Oncogenesis. *Sarcoma* **2011**:282745.

Martinez-Soria, N., McKenzie, L., Draper, J., Ptasinska, A., Issa, H., Potluri, S. *et al.* (2018). The Oncogenic Transcription Factor RUNX1/ETO Corrupts Cell Cycle Regulation to Drive Leukemic Transformation. *Cancer Cell* **34**(4):626-642 e628.

Martinez, M., Hinojosa, M., Trombly, D., Morin, V., Stein, J., Stein, G. *et al.* (2016). Transcriptional Auto-Regulation of RUNX1 P1 Promoter. *PLoS One* **11**(2):e0149119.

Martinez, N., Drescher, B., Riehle, H., Cullmann, C., Vornlocher, H.-P., Ganser, A. *et al.* (2004). The oncogenic fusion protein RUNX1-CBFA2T1 supports proliferation and inhibits senescence in t(8;21)-positive leukaemic cells. *BMC Cancer* **4**(1):44.

Matsuno, N., Osato, M., Yamashita, N., Yanagida, M., Nanri, T., Fukushima, T. *et al.* (2003). Dual mutations in the AML1 and FLT3 genes are associated with leukemogenesis in acute myeloblastic leukemia of the M0 subtype. *Leukemia* **17**(12):2492-2499.

McCune, J. M., Namikawa, R., Kaneshima, H., Shultz, L. D., Lieberman, M. and Weissman, I. L. (1988). The SCID-hu mouse: murine model for the analysis of human hematolymphoid differentiation and function. *Science* **241**(4873):1632-1639.

McKercher, S. R., Torbett, B. E., Anderson, K. L., Henkel, G. W., Vestal, D. J., Baribault, H. *et al.* (1996). Targeted disruption of the PU.1 gene results in multiple hematopoietic abnormalities. *EMBO J* **15**(20):5647-5658.

McNiece, I. K., Langley, K. E. and Zsebo, K. M. (1991). Recombinant human stem cell factor synergises with GM-CSF, G-CSF, IL-3 and epo to stimulate human progenitor cells of the myeloid and erythroid lineages. *Exp Hematol* **19**(3):226-231.

Mei, P. J., Bai, J., Liu, H., Li, C., Wu, Y. P., Yu, Z. Q. *et al.* (2011). RUNX3 expression is lost in glioma and its restoration causes drastic suppression of tumor invasion and migration. *Journal of Cancer Research and Clinical Oncology* **137**(12):1823-1830.

Meier, N., Krpic, S., Rodriguez, P., Strouboulis, J., Monti, M., Krijgsveld, J. *et al.* (2006). Novel binding partners of Ldb1 are required for haematopoietic development. *Development* **133**(24):4913-4923.

Mendelson, A. and Frenette, P. S. (2014). Hematopoietic stem cell niche maintenance during homeostasis and regeneration. *Nat Med* **20**(8):833-846.

Mendez-Ferrer, S., Lucas, D., Battista, M. and Frenette, P. S. (2008). Haematopoietic stem cell release is regulated by circadian oscillations. *Nature* **452**(7186):442-447.

Méndez-Ferrer, S., Michurina, T. V., Ferraro, F., Mazloom, A. R., MacArthur, B. D., Lira, S. A. *et al.* (2010). Mesenchymal and haematopoietic stem cells form a unique bone marrow niche. *Nature* **466**(7308):829-834.

Mendler, J. H., Maharry, K., Radmacher, M. D., Mrozek, K., Becker, H., Metzeler, K. H. *et al.* (2012). RUNX1 mutations are associated with poor outcome in younger and older patients with cytogenetically normal acute myeloid leukemia and with distinct gene and MicroRNA expression signatures. *J Clin Oncol* **30**(25):3109-3118.

Mercer, E. M., Lin, Y. C., Benner, C., Jhunjhunwala, S., Dutkowski, J., Flores, M. *et al.* (2011). Multilineage priming of enhancer repertoires precedes commitment to the B and myeloid cell lineages in hematopoietic progenitors. *Immunity* **35**(3):413-425.

Mercher, T., Cornejo, M. G., Sears, C., Kindler, T., Moore, S. A., Maillard, I. *et al.* (2008). Notch signaling specifies megakaryocyte development from hematopoietic stem cells. *Cell Stem Cell* **3**(3):314-326.

Merika, M. and Orkin, S. H. (1995). Functional synergy and physical interactions of the erythroid transcription factor GATA-1 with the Kruppel family proteins Sp1 and EKLF. *Mol Cell Biol* **15**(5):2437-2447.

Meshinchi, S. and Appelbaum, F. R. (2009). Structural and functional alterations of FLT3 in acute myeloid leukemia. *Clin Cancer Res* **15**(13):4263-4269.

Mevel, R., Draper, J. E., Lie, A. L. M., Kouskoff, V. and Lacaud, G. (2019). RUNX transcription factors: orchestrators of development. *Development* **146**(17).

Meyers, S., Downing, J. R. and Hiebert, S. W. (1993). Identification of AML-1 and the (8;21) translocation protein (AML-1/ETO) as sequence-specific DNA-binding proteins: the runt homology domain is required for DNA binding and protein-protein interactions. *Mol Cell Biol* **13**(10):6336-6345.

Meyers, S., Lenny, N. and Hiebert, S. W. (1995). The t(8;21) fusion protein interferes with AML-1B-dependent transcriptional activation. *Mol Cell Biol* **15**(4):1974-1982.

Meyers, S., Lenny, N., Sun, W. and Hiebert, S. W. (1996). AML-2 is a potential target for transcriptional regulation by the t(8;21) and t(12;21) fusion proteins in acute leukemia. *Oncogene* **13**(2):303-312.

Michaud, J., Wu, F., Osato, M., Cottles, G. M., Yanagida, M., Asou, N. *et al.* (2002). In vitro analyses of known and novel RUNX1/AML1 mutations in dominant familial platelet disorder with predisposition to acute myelogenous leukemia: implications for mechanisms of pathogenesis. *Blood* **99**(4):1364-1372.

Miething, C., Grundler, R., Mugler, C., Brero, S., Hoepfl, J., Geigl, J. *et al.* (2007). Retroviral insertional mutagenesis identifies RUNX genes involved in chronic myeloid leukemia disease persistence under imatinib treatment. *Proceedings of the National Academy of Sciences of the United States of America* **104**(11):4594-4599.

Migliaccio, A. R., Rana, R. A., Sanchez, M., Lorenzini, R., Centurione, L., Bianchi, L. *et al.* (2003). GATA-1 as a regulator of mast cell differentiation revealed by the phenotype of the GATA-1^{low} mouse mutant. *J Exp Med* **197**(3):281-296.

Mikkola, H. K., Klintman, J., Yang, H., Hock, H., Schlaeger, T. M., Fujiwara, Y. *et al.* (2003). Haematopoietic stem cells retain long-term repopulating activity and multipotency in the absence of stem-cell leukaemia SCL/tal-1 gene. *Nature* **421**(6922):547-551.

Miller, J. S., McCullar, V., Punzel, M., Lemischka, I. R. and Moore, K. A. (1999). Single adult human CD34(+)/Lin-/CD38(-) progenitors give rise to natural killer cells, B-lineage cells, dendritic cells, and myeloid cells. *Blood* **93**(1):96-106.

Milner, J. J., Toma, C., Yu, B., Zhang, K., Omilusik, K., Phan, A. T. *et al.* (2017). Runx3 programs CD8(+) T cell residency in non-lymphoid tissues and tumours. *Nature* **552**(7684):253-257.

Ming, Y., Burel, S. A., Peterson, L. F., Kanbe, E., Iwasaki, H., Boyapati, A. *et al.* (2004). Deletion of an AML1-ETO C-terminal NcoR/SMRT-interacting region strongly induces leukemia development. *Proceedings of the National Academy of Sciences of the United States of America* **101**(49):17186-17191.

Miyamoto, T., Nagafuji, K., Akashi, K., Harada, M., Kyo, T., Akashi, T. *et al.* (1996). Persistence of multipotent progenitors expressing AML1/ETO transcripts in long-term remission patients with t(8;21) acute myelogenous leukemia. *Blood* **87**(11):4789-4796.

Miyamoto, T., Weissman, I. L. and Akashi, K. (2000). AML1/ETO-expressing nonleukemic stem cells in acute myelogenous leukemia with 8;21 chromosomal translocation. *Proceedings of the National Academy of Sciences of the United States of America* **97**(13):7521-7526.

Miyoshi, H., Kozu, T., Shimizu, K., Enomoto, K., Maseki, N., Kaneko, Y. *et al.* (1993). The t(8;21) translocation in acute myeloid leukemia results in production of an AML1-MTG8 fusion transcript. *EMBO J* **12**(7):2715-2721.

Miyoshi, H., Ohira, M., Shimizu, K., Mitani, K., Hirai, H., Imai, T. *et al.* (1995). Alternative splicing and genomic structure of the AML1 gene involved in acute myeloid leukemia. *Nucleic Acids Res* **23**(14):2762-2769.

Miyoshi, H., Shimizu, K., Kozu, T., Maseki, N., Kaneko, Y. and Ohki, M. (1991). t(8;21) breakpoints on chromosome 21 in acute myeloid leukemia are clustered within a limited region of a single gene, AML1. *Proc Natl Acad Sci U S A* **88**(23):10431-10434.

Mori, Y., Chen, J. Y., Pluvinaige, J. V., Seita, J. and Weissman, I. L. (2015). Prospective isolation of human erythroid lineage-committed progenitors. *Proc Natl Acad Sci U S A* **112**(31):9638-9643.

Morita, K., Suzuki, K., Maeda, S., Matsuo, A., Mitsuda, Y., Tokushige, C. *et al.* (2017). Genetic regulation of the RUNX transcription factor family has antitumor effects. *Journal of Clinical Investigation* **127**(7):2815-2828.

Motoda, L., Osato, M., Yamashita, N., Jacob, B., Chen, L. Q., Yanagida, M. *et al.* (2007). Runx1 protects hematopoietic stem/progenitor cells from oncogenic insult. *Stem Cells* **25**(12):2976-2986.

Mueller, W., Nutt, C. L., Ehrich, M., Riemenschneider, M. J., von Deimling, A., van den Boom, D. *et al.* (2007). Downregulation of RUNX3 and TES by hypermethylation in glioblastoma. *Oncogene* **26**(4):583-593.

Muller-Tidow, C., Steffen, B., Cauvet, T., Tickenbrock, L., Ji, P., Diederichs, S. *et al.* (2004). Translocation products in acute myeloid leukemia activate the Wnt signaling pathway in hematopoietic cells. *Molecular and Cellular Biology* **24**(7):2890-2904.

Muller, C. I., Luong, Q. T., Shih, L. Y., Jones, L. C., Desmond, J. C., Kawamata, N. *et al.* (2008). Identification of marker genes including RUNX3 (AML2) that discriminate between different myeloproliferative neoplasms and normal individuals. *Leukemia* **22**(9):1773-1778.

Mulloy, J. C., Cammenga, J., Berguido, F. J., Wu, K. D., Zhou, P., Comenzo, R. L. *et al.* (2003). Maintaining the self-renewal and differentiation potential of human CD34(+) hematopoietic cells using a single genetic element. *Blood* **102**(13):4369-4376.

Mulloy, J. C., Cammenga, J., MacKenzie, K. L., Berguido, F. J., Moore, M. A. S. and Nimer, S. D. (2002). The AML1-ETO fusion protein promotes the expansion of human hematopoietic stem cells. *Blood* **99**(1):15-23.

Mulloy, J. C., Jankovic, V., Wunderlich, M., Delwel, R., Cammenga, J., Krejci, O. *et al.* (2005). AML1-ETO fusion protein up-regulates TRKA mRNA expression in human CD34(+) cells, allowing nerve growth factor-induced expansion. *Proceedings of the National Academy of Sciences of the United States of America* **102**(11):4016-4021.

Muta, K., Krantz, S. B., Bondurant, M. C. and Dai, C. H. (1995). Stem cell factor retards differentiation of normal human erythroid progenitor cells while stimulating proliferation. *Blood* **86**(2):572-580.

Nafria, M., Keane, P., Ng, E. S., Stanley, E. G., Elefanty, A. G. and Bonifer, C. (2020). Expression of RUNX1-ETO Rapidly Alters the Chromatin Landscape and Growth of Early Human Myeloid Precursor Cells. *Cell Rep* **31**(8):107691.

Nagahama, Y., Ishimaru, M., Osaki, M., Inoue, T., Maeda, A., Nakada, C. *et al.* (2008). Apoptotic pathway induced by transduction of RUNX3 in the human gastric carcinoma cell line MKN-1. *Cancer Science* **99**(1):23-30.

Nagata, T., Gupta, V., Sorce, D., Kim, W. Y., Sali, A., Chait, B. T. *et al.* (1999). Immunoglobulin motif DNA recognition and heterodimerization of the PEBP2/CBF Runt domain. *Nat Struct Biol* **6**(7):615-619.

Nakagawa, M., Shimabe, M., Watanabe-Okochi, N., Arai, S., Yoshimi, A., Shinohara, A. *et al.* (2011). AML1/RUNX1 functions as a cytoplasmic attenuator of NF-kappaB signaling in the repression of myeloid tumors. *Blood* **118**(25):6626-6637.

Nakamura-Ishizu, A., Takubo, K., Fujioka, M. and Suda, T. (2014). Megakaryocytes are essential for HSC quiescence through the production of thrombopoietin. *Biochem Biophys Res Commun* **454**(2):353-357.

Nakamura, S., Senzaki, K., Yoshikawa, M., Nishimura, M., Inoue, K. I., Ito, Y. *et al.* (2008). Dynamic regulation of the expression of neurotrophin receptors by Runx3. *Development* **135**(9):1703-1711.

Neubauer, A., Fiebeler, A., Graham, D. K., O'Bryan, J. P., Schmidt, C. A., Barckow, P. *et al.* (1994). Expression of axl, a transforming receptor tyrosine kinase, in normal and malignant hematopoiesis. *Blood* **84**(6):1931-1941.

Nevadunsky, N. S., Barbieri, J. S., Kwong, J., Merritt, M. A., Welch, W. R., Berkowitz, R. S. *et al.* (2009). RUNX3 protein is overexpressed in human epithelial ovarian cancer. *Gynecologic Oncology* **112**(2):325-330.

Ng, S. B., Selvarajan, V., Huang, G., Zhou, J., Feldman, A. L., Law, M. *et al.* (2011). Activated oncogenic pathways and therapeutic targets in extranodal nasal-type NK/T cell lymphoma revealed by gene expression profiling. *J Pathol* **223**(4):496-510.

Nick, H. J., Kim, H. G., Chang, C. W., Harris, K. W., Reddy, V. and Klug, C. A. (2012). Distinct classes of c-Kit-activating mutations differ in their ability to promote RUNX1-ETO-associated acute myeloid leukemia. *Blood* **119**(6):1522-1531.

Nishina, S. I., Shiraha, H., Nakanishi, Y., Tanaka, S., Matsubara, M., Takaoka, N. *et al.* (2011). Restored expression of the tumor suppressor gene RUNX3 reduces cancer stem cells in hepatocellular carcinoma by suppressing Jagged1-Notch signaling. *Oncology Reports* **26**(3):523-531.

Nombela-Arrieta, C., Pivarnik, G., Winkel, B., Canty, K. J., Harley, B., Mahoney, J. E. *et al.* (2013). Quantitative imaging of haematopoietic stem and progenitor cell localization and hypoxic status in the bone marrow microenvironment. *Nature Cell Biology* **15**(5):533-543.

Nomoto, S., Kinoshita, T., Mori, T., Kato, K., Sugimoto, H., Kanazumi, N. *et al.* (2008). Adverse prognosis of epigenetic inactivation in RUNX3 gene at 1p36 in human pancreatic cancer. *British Journal of Cancer* **98**(10):1690-1695.

North, T., Gu, T. L., Stacy, T., Wang, Q., Howard, L., Binder, M. *et al.* (1999). Cbfa2 is required for the formation of intra-aortic hematopoietic clusters. *Development* **126**(11):2563-2575.

North, T. E., de Bruijn, M. F., Stacy, T., Talebian, L., Lind, E., Robin, C. *et al.* (2002). Runx1 expression marks long-term repopulating hematopoietic stem cells in the midgestation mouse embryo. *Immunity* **16**(5):661-672.

North, T. E., Stacy, T., Matheny, C. J., Speck, N. A. and de Bruijn, M. F. (2004). Runx1 is expressed in adult mouse hematopoietic stem cells and differentiating myeloid and lymphoid cells, but not in maturing erythroid cells. *Stem Cells* **22**(2):158-168.

Notta, F., Doulatov, S., Laurenti, E., Poepl, A., Jurisica, I. and Dick, J. E. (2011). Isolation of single human hematopoietic stem cells capable of long-term multilineage engraftment. *Science* **333**(6039):218-221.

Novershtern, N., Subramanian, A., Lawton, L. N., Mak, R. H., Haining, W. N., McConkey, M. E. *et al.* (2011). Densely interconnected transcriptional circuits control cell states in human hematopoiesis. *Cell* **144**(2):296-309.

Nucifora, G., Begy, C. R., Kobayashi, H., Roulston, D., Claxton, D., Pedersen-Bjergaard, J. *et al.* (1994). Consistent intergenic splicing and production of multiple transcripts between AML1 at 21q22 and unrelated genes at 3q26 in (3;21)(q26;q22) translocations. *Proc Natl Acad Sci U S A* **91**(9):4004-4008.

Nuez, B., Michalovich, D., Bygrave, A., Ploemacher, R. and Grosveld, F. (1995). Defective haematopoiesis in fetal liver resulting from inactivation of the EKLf gene. *Nature* **375**(6529):316-318.

Nusslein-Volhard, C. and Wieschaus, E. (1980). Mutations affecting segment number and polarity in *Drosophila*. *Nature* **287**(5785):795-801.

Nutt, S. L., Metcalf, D., D'Amico, A., Polli, M. and Wu, L. (2005). Dynamic regulation of PU.1 expression in multipotent hematopoietic progenitors. *J Exp Med* **201**(2):221-231.

O'Bryan, J. P., Frye, R. A., Cogswell, P. C., Neubauer, A., Kitch, B., Prokop, C. *et al.* (1991). axl, a transforming gene isolated from primary human myeloid leukemia cells, encodes a novel receptor tyrosine kinase. *Mol Cell Biol* **11**(10):5016-5031.

Ogawa, E., Inuzuka, M., Maruyama, M., Satake, M., Naito-Fujimoto, M., Ito, Y. *et al.* (1993). Molecular cloning and characterization of PEBP2 beta, the heterodimeric partner of a novel *Drosophila* runt-related DNA binding protein PEBP2 alpha. *Virology* **194**(1):314-331.

Ogawa, S., Satake, M. and Ikuta, K. (2008). Physical and functional interactions between STAT5 and Runx transcription factors. *Journal of Biochemistry* **143**(5):695-709.

Okuda, T., Cai, Z. L., Yang, S. L., Lenny, N., Lyu, C. J., van Deursen, J. M. A. *et al.* (1998). Expression of a knocked-in AML1-ETO leukemia gene inhibits the establishment of normal definitive hematopoiesis and directly generates dysplastic hematopoietic progenitors. *Blood* **91**(9):3134-3143.

Okuda, T., van Deursen, J., Hiebert, S. W., Grosveld, G. and Downing, J. R. (1996). AML1, the target of multiple chromosomal translocations in human leukemia, is essential for normal fetal liver hematopoiesis. *Cell* **84**(2):321-330.

Okumura, N., Tsuji, K. and Nakahata, T. (1992). Changes in cell surface antigen expressions during proliferation and differentiation of human erythroid progenitors. *Blood* **80**(3):642-650.

Osato, M., Asou, N., Abdalla, E., Hoshino, K., Yamasaki, H., Okubo, T. *et al.* (1999). Biallelic and heterozygous point mutations in the runt domain of the AML1/PEBP2alphaB gene associated with myeloblastic leukemias. *Blood* **93**(6):1817-1824.

Oshimo, Y., Oue, N., Mitani, Y., Nakayama, H., Kitadai, Y., Yoshida, K. *et al.* (2004). Frequent loss of RUNX3 expression by promoter hypermethylation in gastric carcinoma. *Pathobiology* **71**(3):137-143.

Otto, F., Stock, M., Fliegau, M., Fenaux, P., Preudhomme, C. and Lubbert, M. (2003). Absence of somatic mutations within the Runt domain of AML2/RUNX3 in acute myeloid leukaemia. *Leukemia* **17**(8):1677-1678.

Otto, F., Thornell, A. P., Crompton, T., Denzel, A., Gilmour, K. C., Rosewell, I. R. *et al.* (1997). Cbfa1, a candidate gene for cleidocranial dysplasia syndrome, is essential for osteoblast differentiation and bone development. *Cell* **89**(5):765-771.

Pabst, T., Mueller, B. U., Harakawa, N., Schoch, C., Haferlach, T., Behre, G. *et al.* (2001). AML1-ETO downregulates the granulocytic differentiation factor C/EBP alpha in t(8;21) myeloid leukemia. *Nature Medicine* **7**(4):444-451.

Panaro, N. J., Yuen, P. K., Sakazume, T., Fortina, P., Kricka, L. J. and Wilding, P. (2000). Evaluation of DNA fragment sizing and quantification by the agilent 2100 bioanalyzer. *Clin Chem* **46**(11):1851-1853.

Pang, S. H. M., de Graaf, C. A., Hilton, D. J., Huntington, N. D., Carotta, S., Wu, L. *et al.* (2018). PU.1 Is Required for the Developmental Progression of Multipotent Progenitors to Common Lymphoid Progenitors. *Front Immunol* **9**:1264.

Papaemmanuil, E., Gerstung, M., Bullinger, L., Gaidzik, V. I., Paschka, P., Roberts, N. D. *et al.* (2016). Genomic Classification and Prognosis in Acute Myeloid Leukemia. *N Engl J Med* **374**(23):2209-2221.

Park, D. J., Kwon, A., Cho, B. S., Kim, H. J., Hwang, K. A., Kim, M. *et al.* (2020). Characteristics of DNMT3A mutations in acute myeloid leukemia. *Blood Res* **55**(1):17-26.

Park, M. H., Shin, H. I., Choi, J. Y., Nam, S. H., Kim, Y. J., Kim, H. J. *et al.* (2001). Differential expression patterns of Runx2 isoforms in cranial suture morphogenesis. *J Bone Miner Res* **16**(5):885-892.

Park, W. S., Cho, Y. G., Kim, C. J., Song, J. H., Lee, Y. S., Kim, S. Y. *et al.* (2005). Hypermethylation of the RUNX3 gene in hepatocellular carcinoma. *Experimental and Molecular Medicine* **37**(4):276-281.

Paschka, P., Marcucci, G., Ruppert, A. S., Mrózek, K., Chen, H., Kittles, R. A. *et al.* (2006). Adverse prognostic significance of KIT mutations in adult acute myeloid leukemia with inv(16) and t(8;21): a Cancer and Leukemia Group B Study. *J Clin Oncol* **24**(24):3904-3911.

Paschka, P., Schlenk, R. F., Weber, D., Benner, A., Bullinger, L., Heuser, M. *et al.* (2018). Adding dasatinib to intensive treatment in core-binding factor acute myeloid leukemia-results of the AMLSG 11-08 trial. *Leukemia* **32**(7):1621-1630.

Passlick, B., Flieger, D. and Ziegler-Heitbrock, H. W. (1989). Identification and characterization of a novel monocyte subpopulation in human peripheral blood. *Blood* **74**(7):2527-2534.

Patterson, L. J., Gering, M., Eckfeldt, C. E., Green, A. R., Verfaillie, C. M., Ekker, S. C. *et al.* (2007). The transcription factors Scl and Lmo2 act together during development of the hemangioblast in zebrafish. *Blood* **109**(6):2389-2398.

Pearn, L., Fisher, J., Burnett, A. K. and Darley, R. L. (2007). The role of PKC and PDK1 in monocyte lineage specification by Ras. *Blood* **109**(10):4461-4469.

Pelletier, N., Champagne, N., Stifani, S. and Yang, X. J. (2002). MOZ and MORF histone acetyltransferases interact with the Runt-domain transcription factor Runx2. *Oncogene* **21**(17):2729-2740.

Pellin, D., Loperfido, M., Baricordi, C., Wolock, S. L., Montepeloso, A., Weinberg, O. K. *et al.* (2019). A comprehensive single cell transcriptional landscape of human hematopoietic progenitors. *Nature Communications* **10**(1):2395.

Pencovich, N., Jaschek, R., Dicken, J., Amit, A., Lotem, J., Tanay, A. *et al.* (2013). Cell-autonomous function of Runx1 transcriptionally regulates mouse megakaryocytic maturation. *PLoS One* **8**(5):e64248.

Pencovich, N., Jaschek, R., Tanay, A. and Groner, Y. (2011). Dynamic combinatorial interactions of RUNX1 and cooperating partners regulates megakaryocytic differentiation in cell line models. *Blood* **117**(1):e1-14.

Peng, Z. H., Wei, D. Y., Wang, L. W., Tang, H. M., Zhang, J., Le, X. D. *et al.* (2006). RUNX3 inhibits the expression of vascular endothelial growth factor and reduces the angiogenesis, growth, and metastasis of human gastric cancer. *Clinical Cancer Research* **12**(21):6386-6394.

Pereira, B., Chin, S. F., Rueda, O. M., Vollan, H. K., Provenzano, E., Bardwell, H. A. *et al.* (2016). The somatic mutation profiles of 2,433 breast cancers refines their genomic and transcriptomic landscapes. *Nat Commun* **7**:11479.

Perkins, A. C., Sharpe, A. H. and Orkin, S. H. (1995). Lethal beta-thalassaemia in mice lacking the erythroid CACCC-transcription factor EKLF. *Nature* **375**(6529):318-322.

Perry, J. M., Harandi, O. F. and Paulson, R. F. (2007). BMP4, SCF, and hypoxia cooperatively regulate the expansion of murine stress erythroid progenitors. *Blood* **109**(10):4494-4502.

Persons, D. A., Allay, J. A., Allay, E. R., Ashmun, R. A., Orlic, D., Jane, S. M. *et al.* (1999). Enforced expression of the GATA-2 transcription factor blocks normal hematopoiesis. *Blood* **93**(2):488-499.

Pesenacker, A. M., Bending, D., Ursu, S., Wu, Q., Nistala, K. and Wedderburn, L. R. (2013). CD161 defines the subset of FoxP3+ T cells capable of producing proinflammatory cytokines. *Blood* **121**(14):2647-2658.

Peterson, L. F., Boyapati, A., Ahn, E. Y., Biggs, J. R., Okumura, A. J., Lo, M. C. *et al.* (2007a). Acute myeloid leukemia with the 8q22;21q22 translocation: secondary mutational events and alternative t(8;21) transcripts. *Blood* **110**(3):799-805.

Peterson, L. F., Yan, M. and Zhang, D. E. (2007b). The p21(Waf1) pathway is involved in blocking leukemogenesis by the t(8;21) fusion protein AML1-ETO. *Blood* **109**(10):4392-4398.

Peterson, L. F. and Zhang, D. E. (2004). The 8;21 translocation in leukemogenesis. *Oncogene* **23**(24):4255-4262.

Pevny, L., Simon, M. C., Robertson, E., Klein, W. H., Tsai, S. F., D'Agati, V. *et al.* (1991). Erythroid differentiation in chimaeric mice blocked by a targeted mutation in the gene for transcription factor GATA-1. *Nature* **349**(6306):257-260.

Pike, B. L. and Robinson, W. A. (1970). Human bone marrow colony growth in agar-gel. *J Cell Physiol* **76**(1):77-84.

Pinho, S. and Frenette, P. S. (2019). Haematopoietic stem cell activity and interactions with the niche. *Nat Rev Mol Cell Biol* **20**(5):303-320.

Pinho, S., Lacombe, J., Hanoun, M., Mizoguchi, T., Bruns, I., Kunisaki, Y. *et al.* (2013). PDGFRalpha and CD51 mark human nestin+ sphere-forming mesenchymal stem cells capable of hematopoietic progenitor cell expansion. *J Exp Med* **210**(7):1351-1367.

Poggi, A., Rubartelli, A., Moretta, L. and Zocchi, M. R. (1997). Expression and function of NKRP1A molecule on human monocytes and dendritic cells. *Eur J Immunol* **27**(11):2965-2970.

Porcher, C., Swat, W., Rockwell, K., Fujiwara, Y., Alt, F. W. and Orkin, S. H. (1996). The T cell leukemia oncoprotein SCL/tal-1 is essential for development of all hematopoietic lineages. *Cell* **86**(1):47-57.

Pozner, A., Goldenberg, D., Negreanu, V., Le, S. Y., Elroy-Stein, O., Levanon, D. *et al.* (2000). Transcription-coupled translation control of AML1/RUNX1 is mediated by cap- and internal ribosome entry site-dependent mechanisms. *Mol Cell Biol* **20**(7):2297-2307.

Pratap, J., Wixted, J. J., Gaur, T., Zaidi, S. K., Dobson, J., Gokul, K. D. *et al.* (2008). Runx2 transcriptional activation of Indian Hedgehog and a downstream bone metastatic pathway in breast cancer cells. *Cancer Res* **68**(19):7795-7802.

Preudhomme, C., Warot-Loze, D., Roumier, C., Gardel-Duflos, N., Garand, R., Lai, J. L. *et al.* (2000). High incidence of biallelic point mutations in the Runt domain of the AML1/PEBP2 alpha B gene in Mo acute myeloid leukemia and in myeloid malignancies with acquired trisomy 21. *Blood* **96**(8):2862-2869.

Ptasinska, A., Assi, S. A., Mannari, D., James, S. R., Williamson, D., Dunne, J. *et al.* (2012). Depletion of RUNX1/ETO in t(8;21) AML cells leads to genome-wide changes in chromatin structure and transcription factor binding. *Leukemia* **26**(8):1829-1841.

Ptasinska, A., Assi, S. A., Martinez-Soria, N., Imperato, M. R., Piper, J., Cauchy, P. *et al.* (2014). Identification of a Dynamic Core Transcriptional Network in t(8;21) AML that Regulates Differentiation Block and Self-Renewal. *Cell Reports* **8**(6):1974-1988.

Ptasinska, A., Pickin, A., Assi, S. A., Chin, P. S., Ames, L., Avellino, R. *et al.* (2019). RUNX1-ETO Depletion in t(8;21) AML Leads to C/EBPalpha- and AP-1-Mediated Alterations in Enhancer-Promoter Interaction. *Cell Rep* **28**(12):3022-3031 e3027.

Puig-Kroger, A., Aguilera-Montilla, N., Martinez-Nunez, R., Dominguez-Soto, A., Sanchez-Cabo, F., Martin-Gayo, E. *et al.* (2010). The novel RUNX3/p33 isoform is induced upon monocyte-derived dendritic cell maturation and downregulates IL-8 expression. *Immunobiology* **215**(9-10):812-820.

Puig-Kroger, A. and Corbi, A. (2006). RUNX3: A new player in myeloid gene expression and immune response. *Journal of Cellular Biochemistry* **98**(4):744-756.

Puig-Kroger, A., Dominguez-Soto, A., Martinez-Munoz, L., Serrano-Gomez, D., Lopez-Bravo, M., Sierra-Filardi, E. *et al.* (2006). RUNX3 negatively regulates CD36 expression in myeloid cell lines. *Journal of Immunology* **177**(4):2107-2114.

Puig-Kroger, A., Sanchez-Elsner, T., Ruiz, N., Andreu, E. J., Prosper, F., Jensen, U. B. *et al.* (2003). RUNX/AML and C/EBP factors regulate CD11a integrin expression in myeloid cells through overlapping regulatory elements. *Blood* **102**(9):3252-3261.

Pulikkan, J. A., Madera, D., Xue, L. T., Bradley, P., Landrette, S. F., Kuo, Y. H. *et al.* (2012). Thrombopoietin/MPL participates in initiating and maintaining RUNX1-ETO acute myeloid leukemia via PI3K/AKT signaling. *Blood* **120**(4):868-879.

Qiao, M., Shapiro, P., Kumar, R. and Passaniti, A. (2004). Insulin-like growth factor-1 regulates endogenous RUNX2 activity in endothelial cells through a phosphatidylinositol 3-kinase/ERK-dependent and Akt-independent signaling pathway. *J Biol Chem* **279**(41):42709-42718.

Qiao, Y., Lin, S. J., Chen, Y., Voon, D. C. C., Zhu, F., Chuang, L. S. H. *et al.* (2016). RUNX3 is a novel negative regulator of oncogenic TEAD-YAP complex in gastric cancer. *Oncogene* **35**(20):2664-2674.

Qin, Y. Z., Wang, Y., Xu, L. P., Zhang, X. H., Chen, H., Han, W. *et al.* (2017). The dynamics of RUNX1-RUNX1T1 transcript levels after allogeneic hematopoietic stem cell transplantation predict relapse in patients with t(8;21) acute myeloid leukemia. *J Hematol Oncol* **10**(1):44.

Radomska, H. S., Huettner, C. S., Zhang, P., Cheng, T., Scadden, D. T. and Tenen, D. G. (1998). CCAAT/enhancer binding protein alpha is a regulatory switch sufficient for induction of granulocytic development from bipotential myeloid progenitors. *Mol Cell Biol* **18**(7):4301-4314.

Ramaswamy, S., Ross, K. N., Lander, E. S. and Golub, T. R. (2003). A molecular signature of metastasis in primary solid tumors. *Nat Genet* **33**(1):49-54.

Ramsey, J., Butnor, K., Peng, Z., Leclair, T., van der Velden, J., Stein, G. *et al.* (2018). Loss of RUNX1 is associated with aggressive lung adenocarcinomas. *J Cell Physiol* **233**(4):3487-3497.

Rapin, N., Bagger, F. O., Jendholm, J., Mora-Jensen, H., Krogh, A., Kohlmann, A. *et al.* (2014). Comparing cancer vs normal gene expression profiles identifies new disease entities and common transcriptional programs in AML patients. *Blood* **123**(6):894-904.

Raveh, E., Cohen, S., Levanon, D., Groner, Y. and Gat, U. (2005). Runx3 is involved in hair shape determination. *Developmental Dynamics* **233**(4):1478-1487.

Regha, K., Assi, S. A., Tsoulaki, O., Gilmour, J., Lacaud, G. and Bonifer, C. (2015). Developmental-stage-dependent transcriptional response to leukaemic oncogene expression. *Nature Communications* **6**.

Reya, T., Morrison, S. J., Clarke, M. F. and Weissman, I. L. (2001). Stem cells, cancer, and cancer stem cells. *Nature* **414**(6859):105-111.

Rhoades, K. L., Hetherington, C. J., Harakawa, N., Yergeau, D. A., Zhou, L. M., Liu, L. Q. *et al.* (2000). Analysis of the role of AML1-ETO in leukemogenesis, using an Inducible transgenic mouse model. *Blood* **96**(6):2108-2115.

Rhodes, J., Hagen, A., Hsu, K., Deng, M., Liu, T. X., Look, A. T. *et al.* (2005). Interplay of pu.1 and gata1 determines myelo-erythroid progenitor cell fate in zebrafish. *Dev Cell* **8**(1):97-108.

Ricklin, D., Reis, E. S. and Lambris, J. D. (2016). Complement in disease: a defence system turning offensive. *Nat Rev Nephrol* **12**(7):383-401.

Rini, D. and Calabi, F. (2001). Identification and comparative analysis of a second rux3 promoter. *Gene* **273**(1):13-22.

Robb, L., Lyons, I., Li, R., Hartley, L., Kontgen, F., Harvey, R. P. *et al.* (1995). Absence of yolk sac hematopoiesis from mice with a targeted disruption of the scl gene. *Proc Natl Acad Sci U S A* **92**(15):7075-7079.

Rodrigues, N. P., Boyd, A. S., Fugazza, C., May, G. E., Guo, Y., Tipping, A. J. *et al.* (2008). GATA-2 regulates granulocyte-macrophage progenitor cell function. *Blood* **112**(13):4862-4873.

Romiguier, J., Ranwez, V., Douzery, E. J. and Galtier, N. (2010). Contrasting GC-content dynamics across 33 mammalian genomes: relationship with life-history traits and chromosome sizes. *Genome Res* **20**(8):1001-1009.

Rongvaux, A., Willinger, T., Takizawa, H., Rathinam, C., Auerbach, W., Murphy, A. J. *et al.* (2011). Human thrombopoietin knockin mice efficiently support human hematopoiesis in vivo. *Proc Natl Acad Sci U S A* **108**(6):2378-2383.

Rosenbauer, F. and Tenen, D. G. (2007). Transcription factors in myeloid development: balancing differentiation with transformation. *Nat Rev Immunol* **7**(2):105-117.

Roudaia, L., Cheney, M. D., Manuylova, E., Chen, W., Morrow, M., Park, S. *et al.* (2009). CBF beta is critical for AML1-ETO and TEL-AML1 activity. *Blood* **113**(13):3070-3079.

Sacchetti, B., Funari, A., Michienzi, S., Di Cesare, S., Piersanti, S., Saggio, I. *et al.* (2007). Self-renewing osteoprogenitors in bone marrow sinusoids can organize a hematopoietic microenvironment. *Cell* **131**(2):324-336.

Sadikovic, B., Thorner, P., Chilton-Macneill, S., Martin, J. W., Cervigne, N. K., Squire, J. *et al.* (2010). Expression analysis of genes associated with human osteosarcoma tumors shows correlation of RUNX2 overexpression with poor response to chemotherapy. *BMC Cancer* **10**:202.

Saia, M., Termanini, A., Rizzi, N., Mazza, M., Barbieri, E., Valli, D. *et al.* (2016). AML1/ETO accelerates cell migration and impairs cell-to-cell adhesion and homing of hematopoietic stem/progenitor cells. *Scientific Reports* **6**.

Saito, Y., Uchida, N., Tanaka, S., Suzuki, N., Tomizawa-Murasawa, M., Sone, A. *et al.* (2010). Induction of cell cycle entry eliminates human leukemia stem cells in a mouse model of AML. *Nature Biotechnology* **28**(3):275-280.

Sakakura, C., Hasegawa, K., Miyagawa, K., Nakashima, S., Yoshikawa, T., Kin, S. *et al.* (2005). Possible involvement of RUNX3 silencing in the peritoneal metastases of gastric cancers. *Clinical Cancer Research* **11**(18):6479-6488.

Sakakura, C., Miyagawa, K., Fukuda, K. I., Nakashima, S., Yoshikawa, T., Kin, S. *et al.* (2007). Frequent silencing of RUNX3 in esophageal squamous cell carcinomas is associated with radioresistance and poor prognosis. *Oncogene* **26**(40):5927-5938.

Salto-Tellez, M., Peh, B. K., Ito, K., Tan, S. H., Chong, P. Y., Han, H. C. *et al.* (2006). RUNX3 protein is overexpressed in human basal cell carcinomas. *Oncogene* **25**(58):7646-7649.

Sanchez-Martin, L., Estechea, A., Samaniego, R., Sanchez-Ramon, S., Vega, M. A. and Sanchez-Mateos, P. (2011). The chemokine CXCL12 regulates monocyte-macrophage differentiation and RUNX3 expression. *Blood* **117**(1):88-97.

Sant, M., Minicozzi, P., Mounier, M., Anderson, L. A., Brenner, H., Holleccek, B. *et al.* (2014). Survival for haematological malignancies in Europe between 1997 and 2008 by region and age: results of EURO CARE-5, a population-based study. *Lancet Oncol* **15**(9):931-942.

Sanz, M. A., Fenaux, P., Tallman, M. S., Estey, E. H., Lowenberg, B., Naoe, T. *et al.* (2019). Management of acute promyelocytic leukemia: updated recommendations from an expert panel of the European LeukemiaNet. *Blood* **133**(15):1630-1643.

Sato, K., Tomizawa, Y., Iijima, H., Saito, R., Ishizuka, T., Nakajima, T. *et al.* (2006). Epigenetic inactivation of the RUNX3 gene in lung cancer. *Oncology Reports* **15**(1):129-135.

Sato, T., Ohno, S., Hayashi, T., Sato, C., Kohu, K., Satake, M. *et al.* (2005). Dual functions of Runx proteins for reactivating CD8 and silencing CD4 at the commitment process into CD8 thymocytes. *Immunity* **22**(3):317-328.

Scheitz, C. J., Lee, T. S., McDermitt, D. J. and Tumber, T. (2012). Defining a tissue stem cell-driven Runx1/Stat3 signalling axis in epithelial cancer. *EMBO J* **31**(21):4124-4139.

Scheller, M., Foerster, J., Heyworth, C. M., Waring, J. F., Lohler, J., Gilmore, G. L. *et al.* (1999). Altered development and cytokine responses of myeloid progenitors in the absence of transcription factor, interferon consensus sequence binding protein. *Blood* **94**(11):3764-3771.

Schessl, C., Rawat, V. P. S., Cusan, M., Deshpande, A., Kohl, T. M., Rosten, P. M. *et al.* (2005). The AML1-ETO fusion gene and the FLT3 length mutation collaborate in inducing acute leukemia in mice. *Journal of Clinical Investigation* **115**(8):2159-2168.

Schnittger, S., Dicker, F., Kern, W., Wendland, N., Sundermann, J., Alpermann, T. *et al.* (2011). RUNX1 mutations are frequent in de novo AML with noncomplex karyotype and confer an unfavorable prognosis. *Blood* **117**(8):2348-2357.

Schnittger, S., Kohl, T. M., Haferlach, T., Kern, W., Hiddemann, W., Spiekermann, K. *et al.* (2006). KIT-D816 mutations in AML1-ETO-positive AML are associated with impaired event-free and overall survival. *Blood* **107**(5):1791-1799.

Schofield, R. (1978). The relationship between the spleen colony-forming cell and the haemopoietic stem cell. *Blood Cells* **4**(1-2):7-25.

Schroeder, A., Mueller, O., Stocker, S., Salowsky, R., Leiber, M., Gassmann, M. *et al.* (2006). The RIN: an RNA integrity number for assigning integrity values to RNA measurements. *BMC Mol Biol* **7**:3.

Schuh, A. H., Tipping, A. J., Clark, A. J., Hamlett, I., Guyot, B., Iborra, F. J. *et al.* (2005). ETO-2 associates with SCL in erythroid cells and megakaryocytes and provides repressor functions in erythropoiesis. *Mol Cell Biol* **25**(23):10235-10250.

Seita, J. and Weissman, I. L. (2010). Hematopoietic stem cell: self-renewal versus differentiation. *Wiley Interdiscip Rev Syst Biol Med* **2**(6):640-653.

Selheim, F., Aasebo, E., Ribas, C. and Aragay, A. M. (2019). An Overview on G Protein-coupled Receptor-induced Signal Transduction in Acute Myeloid Leukemia. *Curr Med Chem* **26**(28):5293-5316.

Selvarajan, V., Osato, M., Nah, G. S. S., Yan, J., Chung, T. H., Voon, D. C. C. *et al.* (2017). RUNX3 is oncogenic in natural killer/T-cell lymphoma and is transcriptionally regulated by MYC. *Leukemia* **31**(10):2219-2227.

Semerad, C. L., Liu, F., Gregory, A. D., Stumpf, K. and Link, D. C. (2002). G-CSF is an essential regulator of neutrophil trafficking from the bone marrow to the blood. *Immunity* **17**(4):413-423.

Seo, W., Ikawa, T., Kawamoto, H. and Taniuchi, I. (2012). Runx1-Cbf beta facilitates early B lymphocyte development by regulating expression of Ebf1. *Journal of Experimental Medicine* **209**(7):1255-1262.

Sharff, K. A., Song, W. X., Luo, X., Tang, N., Luo, J., Chen, J. *et al.* (2009). Hey1 basic helix-loop-helix protein plays an important role in mediating BMP9-induced osteogenic differentiation of mesenchymal progenitor cells. *J Biol Chem* **284**(1):649-659.

Shen, R., Wang, X., Drissi, H., Liu, F., O'Keefe, R. J. and Chen, D. (2006). Cyclin D1-cdk4 induce runx2 ubiquitination and degradation. *J Biol Chem* **281**(24):16347-16353.

Sheng, Q., Vickers, K., Zhao, S., Wang, J., Samuels, D. C., Koues, O. *et al.* (2017). Multi-perspective quality control of Illumina RNA sequencing data analysis. *Brief Funct Genomics* **16**(4):194-204.

Shi, M.-J. and Stavnezer, J. (1998). CBF α 3 (AML2) Is Induced by TGF- β 1 to Bind and Activate the Mouse Germline Ig α Promoter. *The Journal of Immunology* **161**(12):6751-6760.

Shia, W. J., Okumura, A. J., Yan, M., Sarkeshik, A., Lo, M. C., Matsuura, S. *et al.* (2012). PRMT1 interacts with AML1-ETO to promote its transcriptional activation and progenitor cell proliferative potential. *Blood* **119**(21):4953-4962.

Shivdasani, R. A., Fujiwara, Y., McDevitt, M. A. and Orkin, S. H. (1997). A lineage-selective knockout establishes the critical role of transcription factor GATA-1 in megakaryocyte growth and platelet development. *EMBO J* **16**(13):3965-3973.

Shivdasani, R. A., Mayer, E. L. and Orkin, S. H. (1995). Absence of blood formation in mice lacking the T-cell leukaemia oncoprotein tal-1/SCL. *Nature* **373**(6513):432-434.

Shlush, L. I., Zandi, S., Mitchell, A., Chen, W. C., Brandwein, J. M., Gupta, V. *et al.* (2014). Identification of pre-leukaemic haematopoietic stem cells in acute leukaemia. *Nature* **506**(7488):328-333.

Short, N. J., Konopleva, M., Kadia, T. M., Borthakur, G., Ravandi, F., DiNardo, C. D. *et al.* (2020). Advances in the Treatment of Acute Myeloid Leukemia: New Drugs and New Challenges. *Cancer Discov* **10**(4):506-525.

Short, N. J., Rytting, M. E. and Cortes, J. E. (2018). Acute myeloid leukaemia. *Lancet* **392**(10147):593-606.

Shultz, L. D., Lyons, B. L., Burzenski, L. M., Gott, B., Chen, X., Chaleff, S. *et al.* (2005). Human lymphoid and myeloid cell development in NOD/LtSz-scid IL2R gamma null mice engrafted with mobilized human hemopoietic stem cells. *J Immunol* **174**(10):6477-6489.

Shultz, L. D., Schweitzer, P. A., Christianson, S. W., Gott, B., Schweitzer, I. B., Tennent, B. *et al.* (1995). Multiple defects in innate and adaptive immunologic function in NOD/LtSz-scid mice. *J Immunol* **154**(1):180-191.

Sierra, J., Villagra, A., Paredes, R., Cruzat, F., Gutierrez, S., Javed, A. *et al.* (2003). Regulation of the bone-specific osteocalcin gene by p300 requires Runx2/Cbfa1 and the vitamin D3 receptor but not p300 intrinsic histone acetyltransferase activity. *Mol Cell Biol* **23**(9):3339-3351.

Sinha, C., Cunningham, L. C. and Liu, P. P. (2015). Core Binding Factor Acute Myeloid Leukemia: New Prognostic Categories and Therapeutic Opportunities. *Semin Hematol* **52**(3):215-222.

Skokowa, J., Steinemann, D., Katsman-Kuipers, J. E., Zeidler, C., Klimenkova, O., Klimiankou, M. *et al.* (2014). Cooperativity of RUNX1 and CSF3R mutations in severe congenital neutropenia: a unique pathway in myeloid leukemogenesis. *Blood* **123**(14):2229-2237.

Solar, G. P., Kerr, W. G., Zeigler, F. C., Hess, D., Donahue, C., de Sauvage, F. J. *et al.* (1998). Role of c-mpl in early hematopoiesis. *Blood* **92**(1):4-10.

Soler, E., Andrieu-Soler, C., de Boer, E., Bryne, J. C., Thongjuea, S., Stadhouders, R. *et al.* (2010). The genome-wide dynamics of the binding of Ldb1 complexes during erythroid differentiation. *Genes Dev* **24**(3):277-289.

Song, W. J., Sullivan, M. G., Legare, R. D., Hutchings, S., Tan, X., Kufrin, D. *et al.* (1999). Haploinsufficiency of CBFA2 causes familial thrombocytopenia with propensity to develop acute myelogenous leukaemia. *Nat Genet* **23**(2):166-175.

Sontag, S., Forster, M., Qin, J., Wanek, P., Mitzka, S., Schuler, H. M. *et al.* (2017). Modelling IRF8 Deficient Human Hematopoiesis and Dendritic Cell Development with Engineered iPS Cells. *Stem Cells* **35**(4):898-908.

Sood, R., Hansen, N. F., Donovan, F. X., Carrington, B., Bucci, D., Maskeri, B. *et al.* (2016). Somatic mutational landscape of AML with inv(16) or t(8;21) identifies patterns of clonal evolution in relapse leukemia. *Leukemia* **30**(2):501-504.

Sood, R., Kamikubo, Y. and Liu, P. (2017). Role of RUNX1 in hematological malignancies. *Blood* **129**(15):2070-2082.

Soong, R., Shah, N., Peh, B. K., Chong, P. Y., Ng, S. S., Zeps, N. *et al.* (2009). The expression of RUNX3 in colorectal cancer is associated with disease stage and patient outcome. *British Journal of Cancer* **100**(5):676-679.

Souroullas, G. P., Salmon, J. M., Sablitzky, F., Curtis, D. J. and Goodell, M. A. (2009). Adult hematopoietic stem and progenitor cells require either Lyl1 or Scl for survival. *Cell Stem Cell* **4**(2):180-186.

Southwood, C. M., Downs, K. M. and Bieker, J. J. (1996). Erythroid Kruppel-like factor exhibits an early and sequentially localized pattern of expression during mammalian erythroid ontogeny. *Dev Dyn* **206**(3):248-259.

Speck, N. A. and Baltimore, D. (1987). Six distinct nuclear factors interact with the 75-base-pair repeat of the Moloney murine leukemia virus enhancer. *Mol Cell Biol* **7**(3):1101-1110.

Spender, L. C., Cornish, G. H., Sullivan, A. and Farrell, P. J. (2002). Expression of transcription factor AML-2 (RUNX3, CBF alpha-3) is induced by Epstein-Barr virus EBNA-2 and correlates with the B-cell activation phenotype. *Journal of Virology* **76**(10):4919-4927.

Spinello, I., Quaranta, M. T., Pasquini, L., Pelosi, E., Petrucci, E., Pagliuca, A. *et al.* (2009). PLZF-mediated control on c-kit expression in CD34(+) cells and early erythropoiesis. *Oncogene* **28**(23):2276-2288.

Springer, T. A. (1990). Adhesion receptors of the immune system. *Nature* **346**(6283):425-434.

Starck, J., Cohet, N., Gonnet, C., Sarrazin, S., Doubeikovskaia, Z., Doubeikovski, A. *et al.* (2003). Functional cross-antagonism between transcription factors FLI-1 and EKLF. *Mol Cell Biol* **23**(4):1390-1402.

Steinauer, N., Guo, C., Huang, C., Wong, M., Tu, Y., Freter, C. E. *et al.* (2019). Myeloid translocation gene CBFA2T3 directs a relapse gene program and determines patient-specific outcomes in AML. *Blood Adv* **3**(9):1379-1393.

Steinke, F. C., Yu, S. Y., Zhou, X. Y., He, B., Yang, W. J., Zhou, B. *et al.* (2014). TCF-1 and LEF-1 act upstream of Th-POK to promote the CD4(+) T cell fate and interact with Runx3 to silence Cd4 in CD8(+) T cells. *Nature Immunology* **15**(7):646-656.

Stelljes, M., Krug, U., Beelen, D. W., Braess, J., Sauerland, M. C., Heinecke, A. *et al.* (2014). Allogeneic transplantation versus chemotherapy as postremission therapy for acute myeloid leukemia: a prospective matched pairs analysis. *J Clin Oncol* **32**(4):288-296.

Stewart, M., MacKay, N., Cameron, E. R. and Neil, J. C. (2002). The common retroviral insertion locus Dsi1 maps 30 kilobases upstream of the P1 promoter of the murine Runx3/Cbfa3/Aml2 gene. *Journal of Virology* **76**(9):4364-4369.

Stewart, M., Terry, A., Hu, M., O'Hara, M., Blyth, K., Baxter, E. *et al.* (1997). Proviral insertions induce the expression of bone-specific isoforms of PEBP2alphaA (CBFA1): evidence for a new myc collaborating oncogene. *Proc Natl Acad Sci U S A* **94**(16):8646-8651.

Stier, S., Ko, Y., Forkert, R., Lutz, C., Neuhaus, T., Grunewald, E. *et al.* (2005). Osteopontin is a hematopoietic stem cell niche component that negatively regulates stem cell pool size. *J Exp Med* **201**(11):1781-1791.

Stone, R. M., Mandrekar, S. J., Sanford, B. L., Laumann, K., Geyer, S., Bloomfield, C. D. *et al.* (2017). Midostaurin plus Chemotherapy for Acute Myeloid Leukemia with a FLT3 Mutation. *N Engl J Med* **377**(5):454-464.

Subramaniam, M. M., Chan, J. Y., Soong, R., Ito, K., Ito, Y., Yeoh, K. G. *et al.* (2009a). RUNX3 inactivation by frequent promoter hypermethylation and protein mislocalization constitute an early event in breast cancer progression. *Breast Cancer Research and Treatment* **113**(1):113-121.

Subramaniam, M. M., Chan, J. Y., Yeoh, K. G., Quek, T., Ito, K. and Salto-Tellez, M. (2009b). Molecular pathology of RUNX3 in human carcinogenesis. *Biochimica Et Biophysica Acta-Reviews on Cancer* **1796**(2):315-331.

Sugimoto, A., Yamamoto, M., Suzuki, M., Inoue, T., Nakamura, S., Motoda, R. *et al.* (2006). Delta-4 Notch ligand promotes erythroid differentiation of human umbilical cord blood CD34+ cells. *Exp Hematol* **34**(4):424-432.

Sun, C. C., Li, S. J., Chen, Z. L., Li, G., Zhang, Q. and Li, D. J. (2019). Expression and Prognosis Analyses of Runt-Related Transcription Factor Family in Human Leukemia. *Mol Ther Oncolytics* **12**:103-111.

Sun, J., Li, B., Jia, Z., Zhang, A., Wang, G., Chen, Z. *et al.* (2018). RUNX3 inhibits glioma survival and invasion via suppression of the beta-catenin/TCF-4 signaling pathway. *J Neurooncol* **140**(1):15-26.

Sun, X., Zhang, W., Ramdas, L., Stivers, D. N., Jones, D. M., Kantarjian, H. M. *et al.* (2007). Comparative analysis of genes regulated in acute myelomonocytic leukemia with and without inv(16)(p13q22) using microarray techniques, real-time PCR, immunohistochemistry, and flow cytometry immunophenotyping. *Mod Pathol* **20**(8):811-820.

Sun, X. J., Wang, Z. X., Wang, L., Jiang, Y. W., Kost, N., Soong, T. D. *et al.* (2013). A stable transcription factor complex nucleated by oligomeric AML1-ETO controls leukaemogenesis. *Nature* **500**(7460):93-U120.

Suresh, S. and Irvine, A. E. (2015). The NOTCH signaling pathway in normal and malignant blood cell production. *J Cell Commun Signal* **9**(1):5-13.

Sutherland, H. J., Eaves, C. J., Eaves, A. C., Dragowska, W. and Lansdorp, P. M. (1989). Characterization and partial purification of human marrow cells capable of initiating long-term hematopoiesis in vitro. *Blood* **74**(5):1563-1570.

Svendsen, J. B., Baslund, B., Cramer, E. P., Rapin, N., Borregaard, N. and Cowland, J. B. (2016). MicroRNA-941 Expression in Polymorphonuclear Granulocytes Is Not Related to Granulomatosis with Polyangiitis. *PLoS One* **11**(10):e0164985.

Taichman, R. S. and Emerson, S. G. (1994). Human osteoblasts support hematopoiesis through the production of granulocyte colony-stimulating factor. *J Exp Med* **179**(5):1677-1682.

Taichman, R. S., Reilly, M. J. and Emerson, S. G. (1996). Human osteoblasts support human hematopoietic progenitor cells in vitro bone marrow cultures. *Blood* **87**(2):518-524.

Takayama, K., Suzuki, T., Tsutsumi, S., Fujimura, T., Urano, T., Takahashi, S. *et al.* (2015). RUNX1, an androgen- and EZH2-regulated gene, has differential roles in AR-dependent and -independent prostate cancer. *Oncotarget* **6**(4):2263-2276.

Takizawa, H., Regoes, R. R., Boddupalli, C. S., Bonhoeffer, S. and Manz, M. G. (2011). Dynamic variation in cycling of hematopoietic stem cells in steady state and inflammation. *J Exp Med* **208**(2):273-284.

Tallack, M. R., Magor, G. W., Dartigues, B., Sun, L., Huang, S., Fittock, J. M. *et al.* (2012). Novel roles for KLF1 in erythropoiesis revealed by mRNA-seq. *Genome Res* **22**(12):2385-2398.

Tallack, M. R., Whittington, T., Yuen, W. S., Wainwright, E. N., Keys, J. R., Gardiner, B. B. *et al.* (2010). A global role for KLF1 in erythropoiesis revealed by ChIP-seq in primary erythroid cells. *Genome Res* **20**(8):1052-1063.

Tamura, T., Nagamura-Inoue, T., Shmeltzer, Z., Kuwata, T. and Ozato, K. (2000). ICSBP directs bipotential myeloid progenitor cells to differentiate into mature macrophages. *Immunity* **13**(2):155-165.

Tanaka, T., Kurokawa, M., Ueki, K., Tanaka, K., Imai, Y., Mitani, K. *et al.* (1996). The extracellular signal-regulated kinase pathway phosphorylates AML1, an acute myeloid leukemia gene product, and potentially regulates its transactivation ability. *Mol Cell Biol* **16**(7):3967-3979.

Tanaka, T., Tanaka, K., Ogawa, S., Kurokawa, M., Mitani, K., Nishida, J. *et al.* (1995). An acute myeloid leukemia gene, AML1, regulates hemopoietic myeloid cell differentiation and transcriptional activation antagonistically by two alternative spliced forms. *EMBO J* **14**(2):341-350.

Tanaka, Y., Imamura, J., Kanai, F., Ichimura, T., Isobe, T., Koike, M. *et al.* (2007). Runx3 interacts with DNA repair protein Ku70. *Experimental Cell Research* **313**(15):3251-3260.

Tang, H., Chen, S., Wang, H., Wu, H., Lu, Q. and Han, D. (2009a). TAM receptors and the regulation of erythropoiesis in mice. *Haematologica* **94**(3):326-334.

Tang, J. L., Hou, H. A., Chen, C. Y., Liu, C. Y., Chou, W. C., Tseng, M. H. *et al.* (2009b). AML1/RUNX1 mutations in 470 adult patients with de novo acute myeloid leukemia: prognostic implication and interaction with other gene alterations. *Blood* **114**(26):5352-5361.

Tang, Y. Y., Crute, B. E., Kelley, J. J., Huang, X., Yan, J., Shi, J. *et al.* (2000a). Biophysical characterization of interactions between the core binding factor alpha and beta subunits and DNA. *FEBS Lett* **470**(2):167-172.

Tang, Y. Y., Shi, J. X., Zhang, L. N., Davis, A., Bravo, J., Warren, A. J. *et al.* (2000b). Energetic and functional contribution of residues in the core binding factor beta (CBF beta) subunit to heterodimerization with CBF alpha. *Journal of Biological Chemistry* **275**(50):39579-39588.

Taniuchi, I., Osato, M., Egawa, T., Sunshine, M. J., Bae, S. C., Komori, T. *et al.* (2002). Differential requirements for Runx proteins in CD4 repression and epigenetic silencing during T lymphocyte development. *Cell* **111**(5):621-633.

Tao, W., Wang, M., Voss, E. D., Cocklin, R. R., Smith, J. A., Cooper, S. H. *et al.* (2004). Comparative proteomic analysis of human CD34+ stem/progenitor cells and mature CD15+ myeloid cells. *Stem Cells* **22**(6):1003-1014.

Tay, L. S., Krishnan, V., Sankar, H., Chong, Y. L., Chuang, L. S. H., Tan, T. Z. *et al.* (2018). RUNX Poly(ADP-Ribosyl)ation and BLM Interaction Facilitate the Fanconi Anemia Pathway of DNA Repair. *Cell Rep* **24**(7):1747-1755.

Telfer, J. C. and Rothenberg, E. V. (2001). Expression and function of a stem cell promoter for the murine CBFalpha2 gene: distinct roles and regulation in natural killer and T cell development. *Dev Biol* **229**(2):363-382.

Till, J. E. and McCulloch, E. A. (1961). A direct measurement of the radiation sensitivity of normal mouse bone marrow cells. *Radiat Res* **14**:213-222.

Tober, J., Yzaguirre, A. D., Piwarzyk, E. and Speck, N. A. (2013). Distinct temporal requirements for Runx1 in hematopoietic progenitors and stem cells. *Development* **140**(18):3765-3776.

Tomita, A., Kiyoi, H. and Naoe, T. (2013). Mechanisms of action and resistance to all-trans retinoic acid (ATRA) and arsenic trioxide (As₂O₃) in acute promyelocytic leukemia. *International Journal of Hematology* **97**(6):717-725.

Tonks, A., Pearn, L., Musson, M., Gilkes, A., Mills, K. I., Burnett, A. K. *et al.* (2007). Transcriptional dysregulation mediated by RUNX1-RUNX1T1 in normal human progenitor cells and in acute myeloid leukaemia. *Leukemia* **21**(12):2495-2505.

Tonks, A., Pearn, L., Tonks, A. J., Pearce, L., Hoy, T., Phillips, S. *et al.* (2003). The AML1-ETO fusion gene promotes extensive self-renewal of human primary erythroid cells. *Blood* **101**(2):624-632.

Tonks, A., Tonks, A. J., Pearn, L., Mohamad, Z., Burnett, A. K. and Darley, R. L. (2005). Optimized retroviral transduction protocol which preserves the primitive subpopulation of human hematopoietic cells. *Biotechnol Prog* **21**(3):953-958.

Tonks, A., Tonks, A. J., Pearn, L., Pearce, L., Hoy, T., Couzens, S. *et al.* (2004). Expression of AML1-ETO in human myelomonocytic cells selectively inhibits granulocytic differentiation and promotes their self-renewal. *Leukemia* **18**(7):1238-1245.

Trombly, D. J., Whitfield, T. W., Padmanabhan, S., Gordon, J. A. R., Lian, J. B., van Wijnen, A. J. *et al.* (2015). Genome-wide co-occupancy of AML1-ETO and N-CoR defines the t(8;21) AML signature in leukemic cells. *Bmc Genomics* **16**.

Tsai, F. Y., Keller, G., Kuo, F. C., Weiss, M., Chen, J., Rosenblatt, M. *et al.* (1994). An early haematopoietic defect in mice lacking the transcription factor GATA-2. *Nature* **371**(6494):221-226.

Tsapogas, P., Swee, L. K., Nusser, A., Nuber, N., Kreuzaler, M., Capoferri, G. *et al.* (2014). In vivo evidence for an instructive role of fms-like tyrosine kinase-3 (FLT3) ligand in hematopoietic development. *Haematologica* **99**(4):638-646.

Tsujimura, H., Nagamura-Inoue, T., Tamura, T. and Ozato, K. (2002). IFN consensus sequence binding protein/IFN regulatory factor-8 guides bone marrow progenitor cells toward the macrophage lineage. *J Immunol* **169**(3):1261-1269.

Tsunematsu, T., Kudo, Y., Iizuka, S., Ogawa, I., Fujita, T., Kurihara, H. *et al.* (2009). RUNX3 Has an Oncogenic Role in Head and Neck Cancer. *Plos One* **4**(6).

Tsuzuki, S., Hong, D., Gupta, R., Matsuo, K., Seto, M. and Enver, T. (2007). Isoform-specific potentiation of stem and progenitor cell engraftment by AML1/RUNX1. *PLoS Med* **4**(5):e172.

Tsuzuki, S. and Seto, M. (2012). Expansion of functionally defined mouse hematopoietic stem and progenitor cells by a short isoform of RUNX1/AML1. *Blood* **119**(3):727-735.

Uchida, N., Sutton, R. E., Frier, A. M., He, D., Reitsma, M. J., Chang, W. C. *et al.* (1998). HIV, but not murine leukemia virus, vectors mediate high efficiency gene transfer into freshly isolated G0/G1 human hematopoietic stem cells. *Proc Natl Acad Sci U S A* **95**(20):11939-11944.

Ugarte, G. D., Vargas, M. F., Medina, M. A., Leon, P., Necunir, D., Elorza, A. A. *et al.* (2015). Wnt signaling induces transcription, spatial proximity, and translocation of fusion gene partners in human hematopoietic cells. *Blood* **126**(15):1785-1789.

Ulirsch, J. C., Lareau, C. A., Bao, E. L., Ludwig, L. S., Guo, M. H., Benner, C. *et al.* (2019). Interrogation of human hematopoiesis at single-cell and single-variant resolution. *Nat Genet* **51**(4):683-693.

Ussher, J. E., Bilton, M., Attwod, E., Shadwell, J., Richardson, R., de Lara, C. *et al.* (2014). CD161++ CD8+ T cells, including the MAIT cell subset, are specifically activated by IL-12+IL-18 in a TCR-independent manner. *Eur J Immunol* **44**(1):195-203.

Vaillant, F., Blyth, K., Terry, A., Bell, M., Cameron, E. R., Neil, J. *et al.* (1999). A full-length Cbfa1 gene product perturbs T-cell development and promotes lymphomagenesis in synergy with myc. *Oncogene* **18**(50):7124-7134.

Vakoc, C. R., Letting, D. L., Gheldof, N., Sawado, T., Bender, M. A., Groudine, M. *et al.* (2005). Proximity among distant regulatory elements at the beta-globin locus requires GATA-1 and FOG-1. *Mol Cell* **17**(3):453-462.

van Bakel, H., Nislow, C., Blencowe, B. J. and Hughes, T. R. (2010). Most "dark matter" transcripts are associated with known genes. *PLoS Biol* **8**(5):e1000371.

van Galen, P., Kreso, A., Wienholds, E., Laurenti, E., Eppert, K., Lechman, E. R. *et al.* (2014). Reduced lymphoid lineage priming promotes human hematopoietic stem cell expansion. *Cell Stem Cell* **14**(1):94-106.

van Schravendijk, M. R., Handunnetti, S. M., Barnwell, J. W. and Howard, R. J. (1992). Normal human erythrocytes express CD36, an adhesion molecule of monocytes, platelets, and endothelial cells. *Blood* **80**(8):2105-2114.

Vangala, R. K., Heiss-Neumann, M. S., Rangatia, J. S., Singh, S. M., Schoch, C., Tenen, D. G. *et al.* (2003). The myeloid master regulator transcription factor PU.1 is inactivated by AML1-ETO in t(8;21) myeloid leukemia. *Blood* **101**(1):270-277.

Velten, L., Haas, S. F., Raffel, S., Blaszkiewicz, S., Islam, S., Hennig, B. P. *et al.* (2017). Human haematopoietic stem cell lineage commitment is a continuous process. *Nat Cell Biol* **19**(4):271-281.

Vu, L. P., Perna, F., Wang, L., Voza, F., Figueroa, M. E., Tempst, P. *et al.* (2013). PRMT4 blocks myeloid differentiation by assembling a methyl-RUNX1-dependent repressor complex. *Cell Rep* **5**(6):1625-1638.

Wada, M., Yazumi, S., Takaishi, S., Hasegawa, K., Sawada, M., Tanaka, H. *et al.* (2004). Frequent loss of RUNX3 gene expression in human bile duct and pancreatic cancer cell lines. *Oncogene* **23**(13):2401-2407.

Wadman, I. A., Osada, H., Grutz, G. G., Agulnick, A. D., Westphal, H., Forster, A. *et al.* (1997). The LIM-only protein Lmo2 is a bridging molecule assembling an erythroid,

DNA-binding complex which includes the TAL1, E47, GATA-1 and Ldb1/NLI proteins. *EMBO J* **16**(11):3145-3157.

Wang, C. Q., Krishnan, V., Tay, L. S., Chin, D. W. L., Koh, C. P., Chooi, J. Y. *et al.* (2014a). Disruption of Runx1 and Runx3 Leads to Bone Marrow Failure and Leukemia Predisposition due to Transcriptional and DNA Repair Defects. *Cell Reports* **8**(3):767-782.

Wang, C. Q., Motoda, L., Satake, M., Ito, Y., Taniuchi, I., Tergaonkar, V. *et al.* (2013). Runx3 deficiency results in myeloproliferative disorder in aged mice. *Blood* **122**(4):562-566.

Wang, D., Diao, H., Getzler, A. J., Rogal, W., Frederick, M. A., Milner, J. *et al.* (2018a). The Transcription Factor Runx3 Establishes Chromatin Accessibility of cis-Regulatory Landscapes that Drive Memory Cytotoxic T Lymphocyte Formation. *Immunity* **48**(4):659-674 e656.

Wang, H., Chen, S., Chen, Y., Wang, H., Wu, H., Tang, H. *et al.* (2007). The role of Tyro 3 subfamily receptors in the regulation of hemostasis and megakaryocytopoiesis. *Haematologica* **92**(5):643-650.

Wang, H., Yan, M., Sun, J., Jain, S., Yoshimi, R., Abolfath, S. M. *et al.* (2014b). A reporter mouse reveals lineage-specific and heterogeneous expression of IRF8 during lymphoid and myeloid cell differentiation. *J Immunol* **193**(4):1766-1777.

Wang, J. W. and Stifani, S. (2017). Roles of Runx Genes in Nervous System Development. *Runx Proteins in Development and Cancer* **962**:103-116.

Wang, J. X., Hoshino, T., Redner, R. L., Kajigaya, S. and Liu, J. M. (1998). ETO, fusion partner in t(8;21) acute myeloid leukemia, represses transcription by interaction with the human N-CoR/mSin3/HDAC1 complex. *Proceedings of the National Academy of Sciences of the United States of America* **95**(18):10860-10865.

Wang, L., Gural, A., Sun, X. J., Zhao, X. Y., Perna, F., Huang, G. *et al.* (2011a). The Leukemogenicity of AML1-ETO Is Dependent on Site-Specific Lysine Acetylation. *Science* **333**(6043):765-769.

Wang, L., Wang, S. and Li, W. (2012). RSeQC: quality control of RNA-seq experiments. *Bioinformatics* **28**(16):2184-2185.

Wang, Q., Stacy, T., Binder, M., Marin-Padilla, M., Sharpe, A. H. and Speck, N. A. (1996a). Disruption of the Cbfa2 gene causes necrosis and hemorrhaging in the central

nervous system and blocks definitive hematopoiesis. *Proc Natl Acad Sci U S A* **93**(8):3444-3449.

Wang, Q., Stacy, T., Miller, J. D., Lewis, A. F., Gu, T. L., Huang, X. *et al.* (1996b). The CBFbeta subunit is essential for CBFalpha2 (AML1) function in vivo. *Cell* **87**(4):697-708.

Wang, S., Wang, Q., Crute, B. E., Melnikova, I. N., Keller, S. R. and Speck, N. A. (1993). Cloning and characterization of subunits of the T-cell receptor and murine leukemia virus enhancer core-binding factor. *Mol Cell Biol* **13**(6):3324-3339.

Wang, W., Sun, X., Hu, T., Wang, L., Dong, S., Gu, J. *et al.* (2018b). PDK1 regulates definitive HSCs via the FOXO pathway during murine fetal liver hematopoiesis. *Stem Cell Res* **30**:192-200.

Wang, X. P., Aberg, T., James, M. J., Levanon, D., Groner, Y. and Thesleff, I. (2005). Runx2 (Cbfa1) inhibits Shh signaling in the lower but not upper molars of mouse embryos and prevents the budding of putative successional teeth. *J Dent Res* **84**(2):138-143.

Wang, Y. Y., Zhao, L. J., Wu, C. F., Liu, P., Shi, L., Liang, Y. *et al.* (2011b). C-KIT mutation cooperates with full-length AML1-ETO to induce acute myeloid leukemia in mice. *Proceedings of the National Academy of Sciences of the United States of America* **108**(6):2450-2455.

Warren, A. J., Colledge, W. H., Carlton, M. B., Evans, M. J., Smith, A. J. and Rabbits, T. H. (1994). The oncogenic cysteine-rich LIM domain protein rbtn2 is essential for erythroid development. *Cell* **78**(1):45-57.

Weber, J. M. and Calvi, L. M. (2010). Notch signaling and the bone marrow hematopoietic stem cell niche. *Bone* **46**(2):281-285.

Wee, H. J., Huang, G., Shigesada, K. and Ito, Y. (2002). Serine phosphorylation of RUNX2 with novel potential functions as negative regulatory mechanisms. *EMBO Rep* **3**(10):967-974.

Wee, H. J., Voon, D. C., Bae, S. C. and Ito, Y. (2008). PEBP2-beta/CBF-beta-dependent phosphorylation of RUNX1 and p300 by HIPK2: implications for leukemogenesis. *Blood* **112**(9):3777-3787.

Wei, A. H., Strickland, S. A., Jr., Hou, J. Z., Fiedler, W., Lin, T. L., Walter, R. B. *et al.* (2019). Venetoclax Combined With Low-Dose Cytarabine for Previously Untreated

Patients With Acute Myeloid Leukemia: Results From a Phase Ib/II Study. *J Clin Oncol* **37**(15):1277-1284.

Wei, D. Y., Gong, W. D., Oh, S. C., Li, Q., Kim, W. D., Wang, L. W. *et al.* (2005). Loss of RUNX3 expression significantly affects the clinical outcome of gastric cancer patients and its restoration causes drastic suppression of tumor growth and metastasis. *Cancer Research* **65**(11):4809-4816.

Wei, Q. and Frenette, P. S. (2018). Niches for Hematopoietic Stem Cells and Their Progeny. *Immunity* **48**(4):632-648.

Weisenberger, D. J., Siegmund, K. D., Campan, M., Young, J., Long, T. I., Faasse, M. A. *et al.* (2006). CpG island methylator phenotype underlies sporadic microsatellite instability and is tightly associated with BRAF mutation in colorectal cancer. *Nat Genet* **38**(7):787-793.

Weiskopf, K., Schnorr, P. J., Pang, W. W., Chao, M. P., Chhabra, A., Seita, J. *et al.* (2016). Myeloid Cell Origins, Differentiation, and Clinical Implications. *Microbiol Spectr* **4**(5).

Weiss, M. J. and Orkin, S. H. (1995). Transcription factor GATA-1 permits survival and maturation of erythroid precursors by preventing apoptosis. *Proc Natl Acad Sci U S A* **92**(21):9623-9627.

Welch, J. J., Watts, J. A., Vakoc, C. R., Yao, Y., Wang, H., Hardison, R. C. *et al.* (2004). Global regulation of erythroid gene expression by transcription factor GATA-1. *Blood* **104**(10):3136-3147.

Westendorf, J. J., Zaidi, S. K., Cascino, J. E., Kahler, R., van Wijnen, A. J., Lian, J. B. *et al.* (2002). Runx2 (Cbfa1, AML-3) interacts with histone deacetylase 6 and represses the p21(CIP1/WAF1) promoter. *Mol Cell Biol* **22**(22):7982-7992.

Whittle, M. C., Izeradjene, K., Rani, P. G., Feng, L. B., Carlson, M. A., DelGiorno, K. E. *et al.* (2015). RUNX3 Controls a Metastatic Switch in Pancreatic Ductal Adenocarcinoma. *Cell* **161**(6):1345-1360.

Wichmann, C., Quagliano-Lo Coco, I., Yildiz, O., Chen-Wichmann, L., Weber, H., Syzonenko, T. *et al.* (2015). Activating c-KIT mutations confer oncogenic cooperativity and rescue RUNX1/ETO-induced DNA damage and apoptosis in human primary CD34+hematopoietic progenitors. *Leukemia* **29**(2):279-289.

Wildenberg, M. E., van Helden-Meeuwsen, C. G., van de Merwe, J. P., Drexhage, H. A. and Versnel, M. A. (2008). Systemic increase in type I interferon activity in Sjogren's syndrome: a putative role for plasmacytoid dendritic cells. *Eur J Immunol* **38**(7):2024-2033.

Wilson, A., Laurenti, E., Oser, G., van der Wath, R. C., Blanco-Bose, W., Jaworski, M. *et al.* (2008). Hematopoietic stem cells reversibly switch from dormancy to self-renewal during homeostasis and repair. *Cell* **135**(6):1118-1129.

Wilson, N. K., Foster, S. D., Wang, X., Knezevic, K., Schutte, J., Kaimakis, P. *et al.* (2010). Combinatorial transcriptional control in blood stem/progenitor cells: genome-wide analysis of ten major transcriptional regulators. *Cell Stem Cell* **7**(4):532-544.

Winkler, I. G., Sims, N. A., Pettit, A. R., Barbier, V., Nowlan, B., Helwani, F. *et al.* (2010). Bone marrow macrophages maintain hematopoietic stem cell (HSC) niches and their depletion mobilizes HSCs. *Blood* **116**(23):4815-4828.

Wong, W. F., Kohu, K., Chiba, T., Sato, T. and Satake, M. (2011). Interplay of transcription factors in T-cell differentiation and function: the role of Runx. *Immunology* **132**(2):157-164.

Woolf, E., Brenner, O., Goldenberg, D., Levanon, D. and Groner, Y. (2007). Runx3 regulates dendritic epidermal T cell development. *Developmental Biology* **303**(2):703-714.

Woolf, E., Xiao, C. Y., Fainaru, O., Lotem, J., Rosen, D., Negreanu, V. *et al.* (2003). Runx3 and Runx1 are required for CD8 T cell development during thymopoiesis. *Proceedings of the National Academy of Sciences of the United States of America* **100**(13):7731-7736.

Wotton, S., Stewart, M., Blyth, K., Vaillant, F., Kilbey, A., Neil, J. C. *et al.* (2002). Proviral insertion indicates a dominant oncogenic role for Runx1/AML-1 in T-cell lymphoma. *Cancer Res* **62**(24):7181-7185.

Wotton, S., Terry, A., Kilbey, A., Jenkins, A., Herzyk, P., Cameron, E. *et al.* (2008). Gene array analysis reveals a common Runx transcriptional programme controlling cell adhesion and survival. *Oncogene* **27**(44):5856-5866.

Wu, H., Liu, X., Jaenisch, R. and Lodish, H. F. (1995). Generation of committed erythroid BFU-E and CFU-E progenitors does not require erythropoietin or the erythropoietin receptor. *Cell* **83**(1):59-67.

Xiao, W. H. and Liu, W. W. (2004). Hemizygous deletion and hypermethylation of RUNX3 gene in hepatocellular carcinoma. *World Journal of Gastroenterology* **10**(3):376-380.

Xie, H., Ye, M., Feng, R. and Graf, T. (2004). Stepwise reprogramming of B cells into macrophages. *Cell* **117**(5):663-676.

Xie, Y., Shi, X., Sheng, K., Han, G., Li, W., Zhao, Q. *et al.* (2019). PI3K/Akt signaling transduction pathway, erythropoiesis and glycolysis in hypoxia (Review). *Mol Med Rep* **19**(2):783-791.

Yagi, R., Junttila, I. S., Wei, G., Urban, J. F., Zhao, K. J., Paul, W. E. *et al.* (2010). The Transcription Factor GATA3 Actively Represses RUNX3 Protein-Regulated Production of Interferon-gamma. *Immunity* **32**(4):507-517.

Yamada, C., Ozaki, T., Ando, K., Suenaga, Y., Inoue, K., Ito, Y. *et al.* (2010). RUNX3 Modulates DNA Damage-mediated Phosphorylation of Tumor Suppressor p53 at Ser-15 and Acts as a Co-activator for p53. *Journal of Biological Chemistry* **285**(22):16693-16703.

Yamada, Y., Warren, A. J., Dobson, C., Forster, A., Pannell, R. and Rabbitts, T. H. (1998). The T cell leukemia LIM protein Lmo2 is necessary for adult mouse hematopoiesis. *Proc Natl Acad Sci U S A* **95**(7):3890-3895.

Yamaguchi, Y., Kurokawa, M., Imai, Y., Izutsu, K., Asai, T., Ichikawa, M. *et al.* (2004). AML1 is functionally regulated through p300-mediated acetylation on specific lysine residues. *J Biol Chem* **279**(15):15630-15638.

Yamamura, Y., Lee, W. L., Inoue, K., Ida, H. and Ito, Y. (2006). RUNX3 cooperates with FoxO3a to induce apoptosis in gastric cancer cells. *Journal of Biological Chemistry* **281**(8):5267-5276.

Yamanaka, R., Barlow, C., Lekstrom-Himes, J., Castilla, L. H., Liu, P. P., Eckhaus, M. *et al.* (1997). Impaired granulopoiesis, myelodysplasia, and early lethality in CCAAT/enhancer binding protein epsilon-deficient mice. *Proc Natl Acad Sci U S A* **94**(24):13187-13192.

Yamashiro, T., ABerg, T., Levanon, D., Groner, Y. and Thesleff, I. (2002). Expression of Runx1, -2 and -3 during tooth, palate and craniofacial bone development. *Mechanisms of Development* **119**:S107-S110.

Yamazaki, S., Ema, H., Karlsson, G., Yamaguchi, T., Miyoshi, H., Shioda, S. *et al.* (2011). Nonmyelinating Schwann cells maintain hematopoietic stem cell hibernation in the bone marrow niche. *Cell* **147**(5):1146-1158.

Yan, C., Kim, Y. W., Ha, Y. S., Kim, I. Y., Kim, Y. J., Yun, S. J. *et al.* (2012). RUNX3 methylation as a predictor for disease progression in patients with non-muscle-invasive bladder cancer. *Journal of Surgical Oncology* **105**(4):425-430.

Yan, M., Ahn, E. Y., Hiebert, S. W. and Zhang, D. E. (2009). RUNX1/AML1 DNA-binding domain and ETO/MTG8 NHR2-dimerization domain are critical to AML1-ETO9a leukemogenesis. *Blood* **113**(4):883-886.

Yan, M., Kanbe, E., Peterson, L. F., Boyapati, A., Miao, Y., Wang, Y. *et al.* (2006). A previously unidentified alternatively spliced isoform of t(8;21) transcript promotes leukemogenesis. *Nature Medicine* **12**(8):945-949.

Yanada, M., Yaoi, T., Shimada, J., Sakakura, C., Nishimura, M., Ito, K. *et al.* (2005). Frequent hemizygous deletion at 1p36 and hypermethylation downregulate RUNX3 expression in human lung cancer cell lines. *Oncology Reports* **14**(4):817-822.

Yanagawa, N., Tamura, G., Oizumi, H., Kanauchi, N., Endoh, M., Sadahiro, M. *et al.* (2007). Promoter hypermethylation of RASSF1A and RUNX3 genes as an independent prognostic prediction marker in surgically resected non-small cell lung cancers. *Lung Cancer* **58**(1):131-138.

Yang, X., Tan, Y., Wang, P., Zhang, H., Zhao, M., Zhao, X. *et al.* (2018). PML-RARalpha interferes with erythropoiesis by repressing LMO2 in acute promyelocytic leukaemia. *J Cell Mol Med* **22**(12):6275-6284.

Yano, T., Ito, K., Fukamachi, H., Chi, X. Z., Wee, H. J., Inoue, K. *et al.* (2006). The RUNX3 tumor suppressor upregulates Bim in gastric epithelial cells undergoing transforming growth factor beta-induced apoptosis. *Molecular and Cellular Biology* **26**(12):4474-4488.

Yarmus, M., Woolf, E., Bernstein, Y., Fainaru, O., Negreanu, V., Levanon, D. *et al.* (2006). Groucho/transducin-like Enhancer-of-split (TLE)-dependent and -independent transcriptional regulation by Runx3. *Proceedings of the National Academy of Sciences of the United States of America* **103**(19):7384-7389.

Ye, M., Zhang, H., Amabile, G., Yang, H., Staber, P. B., Zhang, P. *et al.* (2013). C/EBPα controls acquisition and maintenance of adult haematopoietic stem cell quiescence. *Nat Cell Biol* **15**(4):385-394.

Ye, Q., Jiang, J., Zhan, G., Yan, W., Huang, L., Hu, Y. *et al.* (2016). Small molecule activation of NOTCH signaling inhibits acute myeloid leukemia. *Sci Rep* **6**:26510.

Yergeau, D. A., Hetherington, C. J., Wang, Q., Zhang, P., Sharpe, A. H., Binder, M. *et al.* (1997). Embryonic lethality and impairment of haematopoiesis in mice heterozygous for an AML1-ETO fusion gene. *Nature Genetics* **15**(3):303-306.

Yokomizo-Nakano, T., Kubota, S., Bai, J., Hamashima, A., Morii, M., Sun, Y. *et al.* (2020). Overexpression of RUNX3 Represses RUNX1 to Drive Transformation of Myelodysplastic Syndrome. *Cancer Res* **80**(12):2523-2536.

Yokomizo, T., Hasegawa, K., Ishitobi, H., Osato, M., Ema, M., Ito, Y. *et al.* (2008). Runx1 is involved in primitive erythropoiesis in the mouse. *Blood* **111**(8):4075-4080.

Yoshida, C. A., Yamamoto, H., Fujita, T., Furuichi, T., Ito, K., Inoue, K. I. *et al.* (2004). Runx2 and Runx3 are essential for chondrocyte maturation, and Runx2 regulates limb growth through induction of Indian hedgehog. *Genes & Development* **18**(8):952-963.

Yoshihara, H., Arai, F., Hosokawa, K., Hagiwara, T., Takubo, K., Nakamura, Y. *et al.* (2007). Thrombopoietin/MPL signaling regulates hematopoietic stem cell quiescence and interaction with the osteoblastic niche. *Cell Stem Cell* **1**(6):685-697.

Yoshimi, M., Goyama, S., Kawazu, M., Nakagawa, M., Ichikawa, M., Imai, Y. *et al.* (2012). Multiple phosphorylation sites are important for RUNX1 activity in early hematopoiesis and T-cell differentiation. *Eur J Immunol* **42**(4):1044-1050.

Yu, C., Cantor, A. B., Yang, H., Browne, C., Wells, R. A., Fujiwara, Y. *et al.* (2002). Targeted deletion of a high-affinity GATA-binding site in the GATA-1 promoter leads to selective loss of the eosinophil lineage in vivo. *J Exp Med* **195**(11):1387-1395.

Yu, F., Gao, W., Yokochi, T., Suenaga, Y., Ando, K., Ohira, M. *et al.* (2014). RUNX3 interacts with MYCN and facilitates protein degradation in neuroblastoma. *Oncogene* **33**(20):2601-2609.

Yu, J., Tian, X., Chang, J., Liu, P. and Zhang, R. (2017). RUNX3 inhibits the proliferation and metastasis of gastric cancer through regulating miR-182/HOXA9. *Biomed Pharmacother* **96**:782-791.

Yuan, Y. Z., Zhou, L. M., Miyamoto, T., Iwasaki, H., Harakawa, N., Hetherington, C. J. *et al.* (2001). AML1-ETO expression is directly involved in the development of acute

myeloid leukemia in the presence of additional mutations. *Proceedings of the National Academy of Sciences of the United States of America* **98**(18):10398-10403.

Zabkiewicz, J., Pearn, L., Hills, R. K., Morgan, R. G., Tonks, A., Burnett, A. K. *et al.* (2014). The PDK1 master kinase is over-expressed in acute myeloid leukemia and promotes PKC-mediated survival of leukemic blasts. *Haematologica* **99**(5):858-864.

Zaidi, S. K., Javed, A., Choi, J. Y., van Wijnen, A. J., Stein, J. L., Lian, J. B. *et al.* (2001). A specific targeting signal directs Runx2/Cbfa1 to subnuclear domains and contributes to transactivation of the osteocalcin gene. *J Cell Sci* **114**(Pt 17):3093-3102.

Zang, C., Luyten, A., Chen, J., Liu, X. S. and Shivdasani, R. A. (2016). NF-E2, FLI1 and RUNX1 collaborate at areas of dynamic chromatin to activate transcription in mature mouse megakaryocytes. *Sci Rep* **6**:30255.

Zeng, C., McNeil, S., Pockwinse, S., Nickerson, J., Shopland, L., Lawrence, J. B. *et al.* (1998). Intranuclear targeting of AML/CBFalpha regulatory factors to nuclear matrix-associated transcriptional domains. *Proc Natl Acad Sci U S A* **95**(4):1585-1589.

Zeuner, A., Francescangeli, F., Signore, M., Venneri, M. A., Pedini, F., Felli, N. *et al.* (2011). The Notch2-Jagged1 interaction mediates stem cell factor signaling in erythropoiesis. *Cell Death Differ* **18**(2):371-380.

Zhang, C. C. and Lodish, H. F. (2008). Cytokines regulating hematopoietic stem cell function. *Curr Opin Hematol* **15**(4):307-311.

Zhang, D. E., Zhang, P., Wang, N. D., Hetherington, C. J., Darlington, G. J. and Tenen, D. G. (1997). Absence of granulocyte colony-stimulating factor signaling and neutrophil development in CCAAT enhancer binding protein alpha-deficient mice. *Proc Natl Acad Sci U S A* **94**(2):569-574.

Zhang, J., Niu, C., Ye, L., Huang, H., He, X., Tong, W. G. *et al.* (2003). Identification of the haematopoietic stem cell niche and control of the niche size. *Nature* **425**(6960):836-841.

Zhang, J. S., Hug, B. A., Huang, E. Y., Chen, C. W., Gelmetti, V., Maccarana, M. *et al.* (2001). Oligomerization of ETO is obligatory for corepressor interaction. *Molecular and Cellular Biology* **21**(1):156-163.

Zhang, L., Fried, F. B., Guo, H. and Friedman, A. D. (2008). Cyclin-dependent kinase phosphorylation of RUNX1/AML1 on 3 sites increases transactivation potency and stimulates cell proliferation. *Blood* **111**(3):1193-1200.

Zhang, P., Iwasaki-Arai, J., Iwasaki, H., Fenyus, M. L., Dayaram, T., Owens, B. M. *et al.* (2004). Enhancement of hematopoietic stem cell repopulating capacity and self-renewal in the absence of the transcription factor C/EBP alpha. *Immunity* **21**(6):853-863.

Zhang, Y., Gao, S., Xia, J. and Liu, F. (2018). Hematopoietic Hierarchy - An Updated Roadmap. *Trends Cell Biol* **28**(12):976-986.

Zhang, Y. Y., Wang, J. F., Wheat, J., Chen, X., Jin, S., Sadrzadeh, H. *et al.* (2013). AML1-ETO mediates hematopoietic self-renewal and leukemogenesis through a COX/beta-catenin signaling pathway. *Blood* **121**(24):4906-4916.

Zhao, M., Perry, J. M., Marshall, H., Venkatraman, A., Qian, P., He, X. C. *et al.* (2014a). Megakaryocytes maintain homeostatic quiescence and promote post-injury regeneration of hematopoietic stem cells. *Nat Med* **20**(11):1321-1326.

Zhao, S. M., Zhang, Y. X., Sha, K., Tang, Q., Yang, X. H., Yu, C. L. *et al.* (2014b). KRAS (G12D) Cooperates with AML1/ETO to Initiate a Mouse Model Mimicking Human Acute Myeloid Leukemia. *Cellular Physiology and Biochemistry* **33**(1):78-87.

Zhao, X., Jankovic, V., Gural, A., Huang, G., Pardanani, A., Menendez, S. *et al.* (2008). Methylation of RUNX1 by PRMT1 abrogates SIN3A binding and potentiates its transcriptional activity. *Genes & Development* **22**(5):640-653.

Zheng, L., Iohara, K., Ishikawa, M., Into, T., Takano-Yamamoto, T., Matsushita, K. *et al.* (2007). Runx3 negatively regulates Osterix expression in dental pulp cells. *Biochemical Journal* **405**:69-75.

Zhu, J. and Emerson, S. G. (2002). Hematopoietic cytokines, transcription factors and lineage commitment. *Oncogene* **21**(21):3295-3313.

Ziegler, B. L., Muller, R., Valtieri, M., Lamping, C. P., Thomas, C. A., Gabbianelli, M. *et al.* (1999). Unicellular-unilineage erythropoietic cultures: molecular analysis of regulatory gene expression at sibling cell level. *Blood* **93**(10):3355-3368.